CONF - 970799

CONF-970799--PROC.

PROCEEDINGS OF THE

1997 DIESEL ENGINE EMISSIONS REDUCTION WORKSHOP

University of California - San Diego
La Jolla, California
July 28-31, 1997

RECEIVED
JUN 0 8 1998
OSTI

Sponsored by:

U.S. Department of Energy
Office of Transportation Technologies
Assistant Secretary for Energy Efficiency and Renewable Energy

DISTRIBUTION OF THIS DOCUMENT IS UNLIMITED

MASTER

This report has been reproduced directly from the best available copy.

Available to DOE and DOE Contractors from the Office of Scientific and Technical Information, P.O. Box 62, Oak Ridge, TN 37831; prices available from (423) 576-8401.

Available to the public from the U.S. Department of Commerce, Technology Administration, National Technical Information Service, Springfield, VA 22161, (703) 487-4650.

Printed with soy ink on recycled paper

CONF - 970799

PROCEEDINGS OF THE

1997 DIESEL ENGINE EMISSIONS REDUCTION WORKSHOP

University of California - San Diego
La Jolla, California
July 28-31, 1997



Sponsored by:

U.S. Department of Energy
Office of Transportation Technologies
Assistant Secretary for Energy Efficiency and Renewable Energy
Washington, DC 20585

Printed with soy ink on recycled paper

DISCLAIMER

This report was prepared as an account of work sponsored by an agency of the United States Government. Neither the United States Government nor any agency thereof, nor any of their employees, makes any warranty, express or implied, or assumes any legal liability or responsibility for the accuracy, completeness, or usefulness of any information, apparatus, product, or process disclosed, or represents that its use would not infringe privately owned rights. Reference herein to any specific commercial product, process, or service by trade name, trademark, manufacturer, or otherwise does not necessarily constitute or imply its endorsement, recommendation, or favoring by the United States Government or any agency thereof. The views and opinions of authors expressed herein do not necessarily state or reflect those of the United States Government or any agency thereof.

DISCLAIMER

Portions of this document may be illegible in electronic image products. Images are produced from the best available original document.

1997 DIESEL ENGINE EMISSIONS REDUCTION WORKSHOP

TABLE OF CONTENTS

Page

Chairman's Overview: vii

SESSION I - Agency Diesel Engine Emissions and Concerns

The Dieselization of America: An Integrated Strategy for Future Transportation Fuels 1

EPA Approaches to Diesel Engine Emissions Controls 9

California 1994 State Implementation Plan for Ozone - Implementation Issues and Strategies for Reducing Emissions from Heavy Duty Vehicles 17

South Coast Air Quality Management District Alternative FuelHeavy Duty Vehicle Projects . . . 25

California's Unique Trucking Problems 31

Locomotive Exhaust Emissions Technology Needs - EPA Exhaust Emissions Regulatory Impacts 33

Ship Air Emissions: Estimation and Regulation 39

SESSION II - Human Health Effects - Diesel Exhaust

Diesel Engine Contributions to Atmospheric Fine Particle Concentrations 45

Particulate Measurement for Health Effects Assessments - Summary of the Health Effects Institute Workshop on Particle Characterization 51

Epidemiological Evidence of Health Effects of Combustion-Source Particulate Air Pollution . . . 61

Cancer Risk from Diesel Exhaust: Evidence from Diesel-Exposed Workers 71

Health Support for Diesel Engine Development: Project Description and Goals 77

Toxicology of Diesel Engine Emissions 81

EPA"s Assessment of Human Health Risk from Exposure to Diesel Engine Emissions 87

SESSION IIIA - Aftertreatment - Non-Thermal Plasma

Fundamental Limits on Gas-Phase Chemical Reduction of NOx in a Plasma 85

Plasma-Assisted Heterogeneous Catalysis for NOx Reduction in Lean-Burn Engine Exhaust . . 101

A Thyratron-Based Pulse Generator for Fundamental Studies of NOx Removal in Non-Thermal Plasmas 109

Vehicle Exhaust Treatment Using Electrical Discharge and Materials Chemistry 115

Effect of Hydrocarbons on Plasma Treatment of NOx 123

Non-Thermal Plasma Exhaust Aftertreatment: Are All Plasmas the Same? 129

Plasma Technology for NOx and Particulate Removal from Heavy Duty Vehicles 137

From Lab to Reality, Plasma Engineering for Pollution Control 139

SESSION IIIB - Aftertreatment - Non-Thermal Plasma

Efficient, Effective, Non-Thermal Plasma Aftertreatment of Diesel Nox 145

Direct Chemical Reduction of NOx in Diesel Exhaust Using Non-Thermal Plasmas and Gas Jet Injection 149

Multi-Stage Selective Catalytic Reduction of NOx in Lean-Burn Engine Exhausts *153*

Application of Advanced Thermoelectric Technology to the Diesel Generator 157

Advanced Turbocharger Rotor for Variable Geometry Turbocharging Systems 163

SESSION IV - Aftertreatment and In-Cylinder Emissions Reduction

Diesel Engines One Option to Power Future Personal Transportation Vehicles 171

Diesel Engine Emissions Reduction History and Future Prospects 201

"Let's Correct the Image of the Diesel, and Let's get Real about the Next 20 Years" 207

Integrated Diesel Engine NOx Reduction Technology Development 215

Direct Injection Diesel Engines: What is the Limit for NOx Reduction? 223

Diesel Engine Emissions Challenges 237

Microwave Regenerated Particulate Trap 247

Commercial Introduction of the Advanced NOxTECH System 253

SESSION V - Combustion, Fuel, and Air Management

Diesel Combustion and Emissions Formation Using Multiple 2-D Imaging Diagnostics 263

Chemical-Kinetic Characterization of Model Fuels Used for Describing Combustion of Diesel- 275

NOx Reduction in Diesel-Fuel Flames by Additions of Water and CO_2 281

Neural Network-Based Intelligent Engine Control for Reducing NOx and PM Emissions from CIDI Engines 293

The Passive Trap, A Means for Meeting Heavy Duty Diesel Emissions Beyond 2004 .(Abstract) 303

Emission Characteristics of a Turbocharged Multi-Cylinder Miller Cycle Diesel Engine 305

Indirect Microwave Treatment of Diesel Exhaust Gases for NOx Control 319

Air Management for Diesel Engines 323

SESSION VIA. - Fuels and Associated Technology

A Review of Current Fuels, Fuel Chemistry, and Fuel Trends 329

Gas Turbine Low NOx Evaluation 339

Commercialization of Heavy Duty Natural Gas Engines 351

U.S. DOE Indirect Coal Liquefaction Program: An Overview 359

A Study of Emission Indices with F76 and Fuel Additives 373

Fuel Additives for In-Cylinder NOx Reduction from Diesel Engines 385

Experimental and Numerical Assessment of On-Road Diesel and Biodiesel Emissions 393

SESSION VIB - Advanced Technology

Details of an Injector Depositing Test for Evaluation of Diesel Quality 403

The Effects of Thermal Barrier Coatings On Diesel Engine Emissions 411

Characterization and Assessment of Diesel Engine Particulate Emission Reduction via Lube-Oil-Consumption Control 423

Modeling Pollution Formation in Diesel Engines 433

Particulate Matter Emission from On-Road Light Duty Vehicles 449

Diesel Engines vs. Spark Ignition Gasoline Engines: Which is Greener? 461

REGISTRATIONS 473

Department of Energy
Washington, DC 20585

CHAIRMAN'S OVERVIEW

This is a very timely Workshop for us to update diesel engine emissions issues. Diesel engine manufacturers in the U.S. have dramatically reduced emissions over the last 12 years. Specifically, oxides of nitrogen (NOx) by 73% and particulates (PM) by about 90% as measured by EPA's Federal Test Cycle for Classes 7 & 8 heavy duty trucks. In an historic agreement between the diesel engine manufacturers, EPA, and CARB, the NO levels for the year 2004 will be essentially 50% of the 1998 standards while PMs will remain unchanged. Recent studies by the human health community indicate that PM size is a far more important criteria than mass. The regulators are reviewing this as we meet. Light trucks are being environmentally challenged. Regulators are considering making diesel engine emissions standards close to those of gasoline engine powered vehicles. Some would have them the same!

The major reductions in diesel engine emissions have been achieved with advanced fuel injection equipment (FIE) and the enhanced understanding of combustion achieved with laser diagnostics. Further emissions will most probably require exhaust gas aftertreatment. The leading candidate in aftertreatment is the non-thermal plasma family of devices to which we have dedicated a full day. These systems have in early stages shown simultaneous reduction of NOx and PM of over 70%. Much of these advances in this technology have been made in the past 18 months. Microwave regenerative particulate traps are over 80% efficient and are getting close to commercial introduction. NOx reducing catalysts for diesel engines still have some challenges.

Currently there is concern about the 4% contribution of carbon dioxide(CO_2) from the combustion of fossil fuels to the atmosphere and its role in the "Greenhouse Effect" for global climate warming. The Department of Energy's Diesel Engine Development for Light Trucks (sport utility vehicles, vans, and pick-up trucks) Program will produce diesel engines that are 70% more fuel efficient than the current gasoline engines in these vehicles and will reduce CO_2 emissions by 60% percent! The challenge is to meet or better the emissions standards.

These are the core activities and their interrelationships that are the focus of this Workshop among the Agencies involved, the engine manufacturers and affiliates, Academia, National Laboratories, and the Health Effects Organizations.

We would like to express our appreciation for the excellent response of the invited speakers and their spirited participation in discussions. Once again Professor Richard Herz of the Department of Chemical Engineering has done an excellent job of coordinating the Workshop with the University of California-San Diego. Greg Gregory did his typical excellent work with all the administrative details and deserves a "BRAVO ZULU" (well done for the land lubbers) along with Rebecca Dyer who earned her share of this award. This is the 5th of our Workshops for which Greg has handled the myriad administrative aspects and done so with the competence one would expect from a West Point Grad, Air Force Officer, and engineer with experience in industry, and the Department of Energy. His efforts have been reflected in the high esteem he is held in by his colleagues.

We are planning to hold a DEER Workshop next summer in Castine, Maine and to return again to the University of California-San Diego in 1999.

Sincerely,

John Fairbanks
Chairman, Diesel Engine
Emissions Reduction Workshop

SESSION I

Agency Diesel Engine Emissions and Concerns

Chairman: Jules Routbort
Argonne National Laboratory

THE DIESELIZATION OF AMERICA: AN INTEGRATED STRATEGY FOR FUTURE TRANSPORTATION FUELS

J.J. Eberhardt
U.S. Department of Energy

BACKGROUND

Recently the spectre of another looming energy crisis has been raised [Hodel 1994, Romm and Curtis 1995]. In addition, there is growing concern about the environmental air quality issues related to vehicle exhaust emissions of criteria pollutants and global climate change from greenhouse gases such as carbon dioxide [Romm and Ervin 1996]. Despite these concerns there still is the economic imperative of continuing to produce and transport goods, and provide services important for economic growth.

Gross domestic product (and hence, economic activity and growth) is directly related to freight transport (in ton-miles of travel) as shown in Figure 1. Meeting energy demand for movement of goods is, therefore, critical to the economy. Since the Arab oil embargo in 1973, essentially all of the increase in highway transportation energy use has been due to trucks because of the continued growth of freight transport provided by heavy duty trucks and more recently, because of the explosive growth in popularity for personal transport of low-mpg (miles per gallon) multi-purpose light trucks such as pickups, vans, and sport utility vehicles (see Figure 2). Data from the Energy Information Administration (EIA) show that by 1995 trucks of all classes consume almost as much fuel as automobiles.

Since commercial truck energy use is less discretionary, even imperative if economic growth is to be maintained, the question then is how can we sustain this continuing expansion of economic activity in an environmentally sound manner. Two issues have to be faced in reducing highway energy of trucks, namely: a) how to meet energy demand for commercial transport to sustain continuing expansion of economic activity in an environmentally sound manner; and b) how to increase the efficiency (without compromising the functionality) of multi-purpose (commercial and personal transport) light trucks such as pickups, vans, and sport

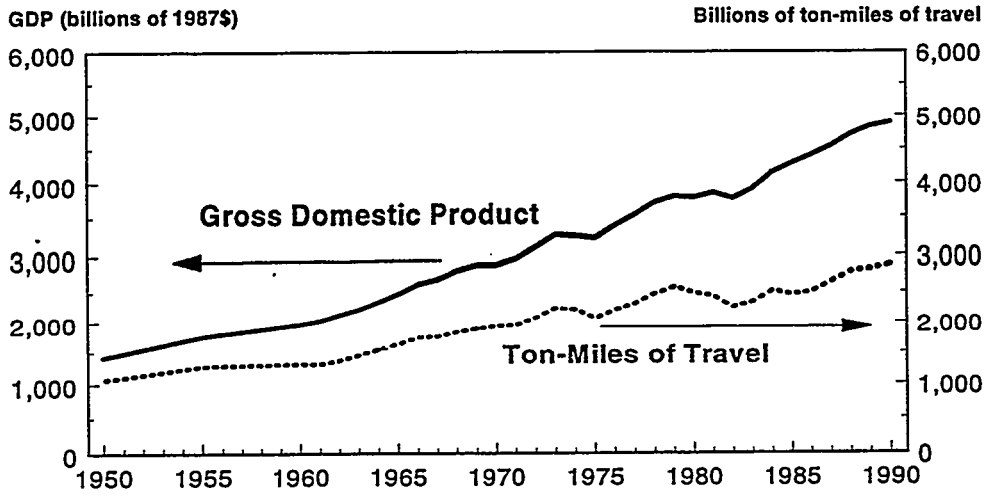


Figure 1. A Healthy Economy is Linked to Efficient Heavy Vehicle Transportation

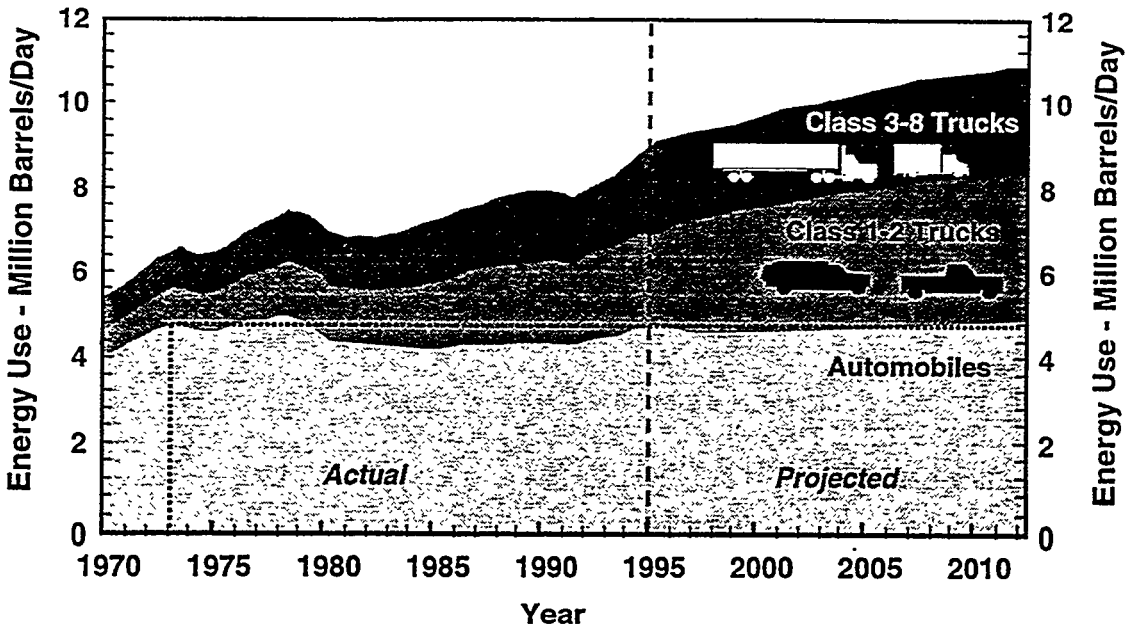


Figure 2. Essentially All of the Increase in Highway Transportation Energy Use Since 1973 Is Due to Trucks

utility vehicles while reducing emissions of exhaust gases to very low levels.

THE DOE HEAVY VEHICLE TECHNOLOGIES R&D PROGRAM

The mission of the DOE Office of Heavy Vehicle Technologies (OHVT) under the Deputy Assistant Secretary for Transportation Technologies, Office of the Assistant Secretary for Energy Efficiency and Renewable Energy is to conduct, in collaboration with its heavy vehicle industry partners and their suppliers, a customer-focused national program to research and develop technologies that will enable trucks and other heavy vehicles to be more energy efficient, able to use alternative fuels, and simultaneously reduce exhaust emissions. The strategy that is both real and viable is to increase the use of the most efficient engine in production today, the Diesel (compression-ignition cycle) engine.

The Case for the Diesel Engine

The Diesel Cycle engine is the engine-of-choice for heavy-duty freight transport where efficiency, low speed power requirements, durability, and reliability are important. It is much more efficient than the Otto cycle gasoline engine, which accounts for its dominance in commercial transport where cost competitiveness is key to staying in business. Truck, rail, and inland marine transport are almost completely diesel powered, and by widespread industry consensus, are expected to remain so in the foreseeable future (for the next 20 years or so). The trend in heavy-duty diesel engine thermal efficiency is shown in Figure 3.

Because of higher efficiency, diesel engines produce lower greenhouse gas emissions than comparable gasoline engines (20 percent less in the 1970s and now over 30 percent due to a widening efficiency gap). With mounting international pressures to reduce greenhouse gas emissions of the U.S. transportation sector, the diesel engine is the technology for doing so rather quickly without adverse economic impacts. The infrastructure for manufacturing and servicing the engine is already in place.

Besides the diesel engine, there are no promising technologies that could radically improve the fuel efficiency of light trucks.

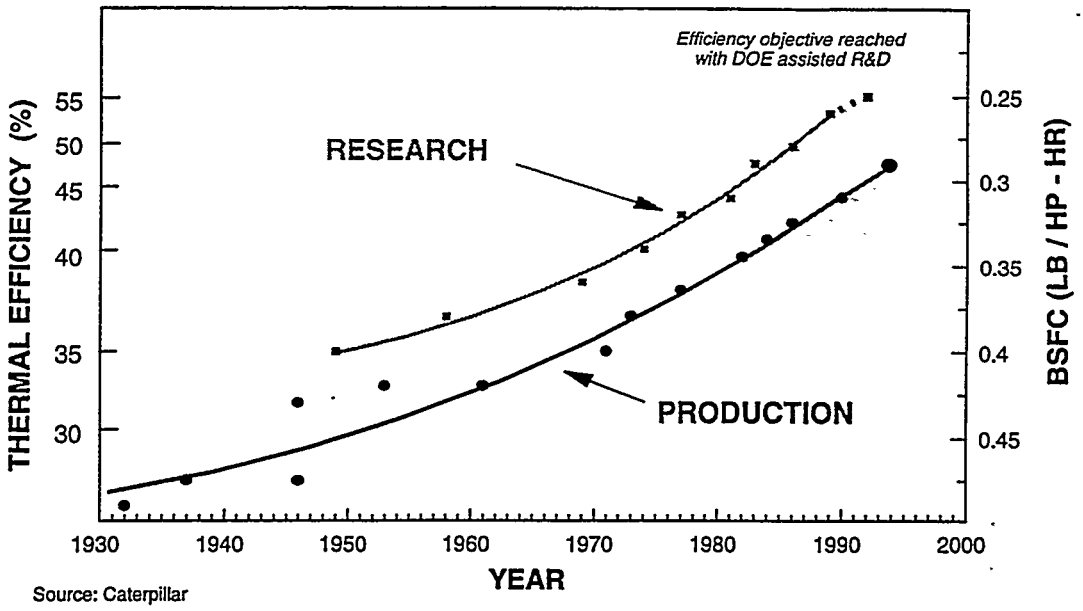


Figure 3. Increasing Diesel Engine Thermal Efficiency

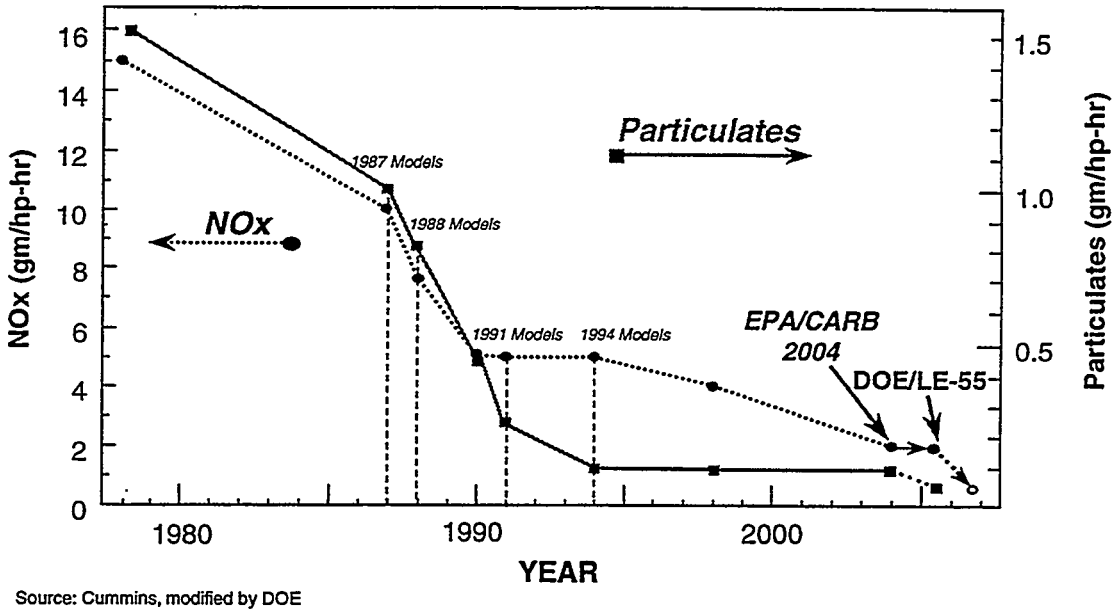
STRATEGY FOR FUTURE FUELS

Perhaps the most significant barrier to the use of alternative, nonpetroleum based fuels for heavy duty trucks is the lack of a fuel production and distribution infrastructure. Commercial transport operators depend on the availability of cost-competitive fuel for continued operation and profitability. In addition, the cost and expected service life of engines in commercial applications (e.g., one million miles or more expected of diesel-fueled engines in tractor trailer combinations) preclude these operators from investing in alternative-fueled engines for which the fuel production and distribution infrastructure is limited or even non-existent. For a future fuels strategy, it would be logical to focus on fuel properties that are suitable for the heavy-duty diesel cycle engine and utilize plentiful feedstocks to produce the fuel with these properties (in contrast to producing a diversity of fuels and forcing them on the engine, and ultimately on the end-users - the truck operators).

What fuel properties are required by the diesel engine? Cetane number has traditionally been an empirical measure of fuel ignitability. Fuels with a cetane number of 50 or higher are suitable for compression ignition in diesel engines. Table I shows the properties of some of the alternative fuels that have been tested as well as those of petroleum based diesel fuel. Comparing cetane numbers, one is led to a reasonable explanation as to why certain fuels do not perform very well in Diesel Cycle engines.

The previous DOE Alternative Fuels Program has demonstrated that Diesel engines can run on fuels that are not compression ignitable (i.e., fuels with very low cetane number such as natural gas, methanol, ethanol) using ignition assist (e.g., spark, glow plug, or pilot injection) but at lower efficiencies than those achieved with petroleum-based conventional diesel fuel. In addition, extensive tuning of the alternative-fueled engines has been necessary. Dimethyl ether, diethyl ether, and biodiesel have suitable cetane numbers and have been run in diesel engines without engine modifications. These alternative fuel-dedicated engines, however, have not made significant penetration into the heavy-duty transport market, for reasons already stated.

A diversity-of-feedstocks strategy as



Source: Cummins, modified by DOE

Figure 4. Decreasing Diesel Engine Emissions

Technologies being developed for the 80 mile per gallon (mpg) car, the third goal of the Partnership for a New Generation of Vehicles (PNGV), e.g., hybrid configuration (possibly turbine with batteries), may be appropriate for automobiles but may be impractical for the multipurpose light trucks. Towing and hauling capacity, torque and power for off-road, are some of the capabilities that account for the popularity of vans, pickups, and sport utility vehicles but which cannot be met by light weight, high mpg autos. The PNGV has recognized the efficiency advantage of Diesel engines over gasoline engines and has identified the fourstroke, direct injection Diesel engine (in stand alone or hybrid-electric configuration) as a principal powertrain candidate for the 80 mpg car. These engines are expected to be 90 horsepower or less, which is not sufficient for the power requirements of multi-purpose vehicles. Direct injection Diesel engines of the approximate power and size for multipurpose pickups, vans, and sport utility vehicles have efficiencies at peak power of 38 to 42 percent compared to gasoline engines at 34 percent. Using Diesel engines in this power range (200 horsepower and greater) can improve light truck fuel economy by as much as 35 percent.

In Europe where fuel prices have always been much higher than the U.S., the Diesel has achieved a substantial measure of acceptance even for personal transportation (14 percent of the passenger car sales in Europe, as much as 35 percent in France, in 1995). In the U.S., Diesel engines have not been popular for passenger cars with the experience with diesel-fueled cars in the mid-70s to early 1980s which were noisy, smokey, not very responsive on hills, and prone to fail due to engineering and design flaws. Also, they were hard to start in cold weather and refueling stations with diesel fuel pumps were very few. In spite of advances in diesel engine technology, the memory of a bad experience lingers and environmental groups continue to foster the image of the Diesel as being a "dirty" engine.

The Emissions Issue

Contrary to the old perception about diesel engines, high efficiency benefits can be obtained without penalizing the environment. Since the 1970s, advances in diesel (compression-ignition cycle) engine

Table 1. Selected Properties of Potential Diesel Engine Fuel(s)

Property	DF-2 Diesel	Fischer-Tropsch	Bio-diesel	CNG	Propane HD-5[h]	Methanol	Ethanol	Di-methyl ether	Di-ethyl ether
Formula	Hydrocarbons ~C10 - ~C21	Principally C_nH_{2n+2} n=10-21	Various oils and esters	Principally CH_4	Principally C_3H_8	CH_3OH	C_2H_5OH	CH_3OCH_3	$C_2H_5OC_2H_5$
Boiling Point, °F	370 - 650	350 - 670	360 - 640	-258.5	-43.9	149	172	-13	94
Vapor Pressure, psi @ 100°F	<0.2	n.a	n.a	n.a.	170	4.6	2.3	116	16.0
Cetane Number	40 - 55	>74	>48	low	low	low	<5[b]	>55	>125[a]
Auto-ignition Temperature, °F	~600	~600	-	990	870	867	793	662	320
Stoichiometric Air - Fuel Ratio, Wt.	15.0	15.2	13.8	16.4	15.7	6.45	9.0	8.9	11.1
Lower Heating Value, Btu/lb	18,500	18,600	16,500	20,750	19,940	8,570	11,500	12,120	14,571
Specific Gravity, 60°F	0.850	0.783	0.880	-	0.506	0.796	0.794	0.66	0.714

technologies have reduced particulate emissions by 95 percent and nitrogen oxide (NOx) emissions by 70 percent (see Figure 4). Today's heavy-duty diesel engines emit just under 5 g/bhp-hr of NOx and 0.10 g1bhp-hr of particulates (<0.05 g1bhp-hr for transit buses). Further reduction of NOx levels to 4 gfbhp-hr by 1998 is mandated by current legislation. In addition, the Environmental Protection Agency (EPA) and major engine manufacturers have issued a "Statement of Principles" that requires, by 2004, further reduction to 0.05 g/bhp-hr particulates and 2.4 g/bhp-hr of NOx plus non-methane hydrocarbons (NMHC) or 2.5 g/bhp-hr of NOx plus NMHC with a maximum of 0.5 gfbhp-hr of NMHC.

In conjunction with industry partners, the DOE Office of Heavy Vehicle Technologies is funding research and development of advanced low-emissions, 55 percent efficient (LE-55) diesel engine technologies to enable heavy-duty trucks to continue to operate efficiently and meet EPA emissions standards proposed for 2004.

Progress of research to date indicates that the heavyduty diesel is well on its way to being an environmentally sound engine for continued economic growth. The question is not if very low levels of emissions can be achieved. but rather, what is cost effective. A three-pronged systems approach that simultaneously addresses fuel formulation, in-cylinder combustion control, and exhaust aftertreatment, is being employed to arrive at the most cost-effective emissions control strategy.

As examples of what can be achieved with alternative fuels, three Cummins diesel engines running on natural gas have been certified as meeting the California Air Resources Board (CARB) and Environmental Protection Agency (EPA) 1998 on-highway heavy duty truck and bus emissions standards without the use of exhaust oxidation catalysts [Cummins 1997]. However, the thermal efficiencies that were achieved were lower than those achievable with conventional petroleum-based diesel fuel. Comparable efficiency and emissions levels have been achieved in diesel engines running on dimethyl ether (DME) with exhaust gas recirculation (EGR) [NREL 1997]. DME is a fuel having excellent compression ignitability (cetane number > 55).

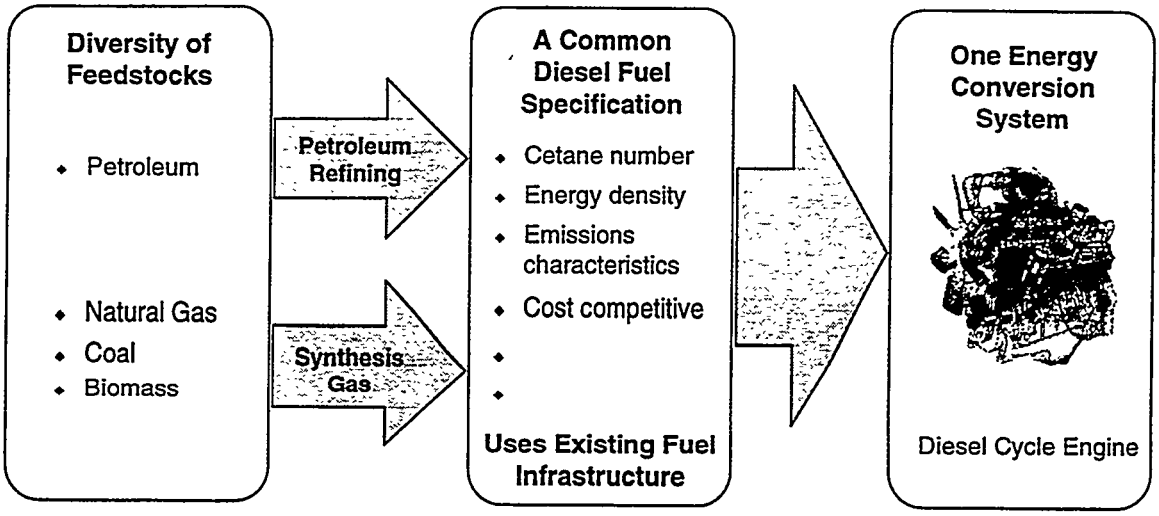


Figure 5. OHVT Future Fuels Strategy

envisioned by the DOE Office of Heavy Vehicle Technologies is shown in Figure 5. The current feedstock is almost exclusively petroleum. However, if other feedstocks such as naturaf gas, coal, and biomass can be converted cost effectively into fuels appropriate for the diesel engine, these fuels can be dispensed using the existing fuel infrastructure, and then utilized by a single energy conversion system, the Diesel Cycle engine. These future fuels from alternative, nonpetroleum resources could then find significant penetration into the heavy duty transport market.

It is possible for the U.S. to take advantage of its indigenous feedstock resources (coal, natural gas, and biomass) to produce high quality fuels for heavy-duty diesel engines. It has been known since World War II that coal can be converted to diesel fuels through the synthesis gas route, commonly called Fischer-Tropsch (F-T) synthesis. What has not been so widely recognized is that the same process can be used to convert methane (natural gas) to F-T diesel fuel as well [Fritsch 1996, Ansell 1994, Tijm 1994, Marriott 1994]. Last but not least, biomass can be "gasified" (i.e., turned into a mixture of carbon monoxide and hydrogen called synthesis gas). From synthesis gas, commonly known as syngas, a number of high quality fuels appropriate for compression ignition engines can be made. These include dimethyl ether and F-T diesel.

Dimethyl ether (DME) has physical properties akin to propane (see Table 1) for which a distribution infrastructure already exists. In Canada, for example, there are significant numbers of propane pumping stations at gasoline retail outlets. F-T diesel is compatible with the current diesel fuel infrastructure. Indeed, the first usage of F-T diesel is as a blend for petroleum-derived diesel fuels to upgrade their cetane number and lower their sulfur and aromatic content. This is already being done in California to a limited extent.

In addition to being gasifiable, the renewable biomass feedstock has two additional routes to provide fuels for heavy duty diesels. Biodiesel can be made from vegetable oils by a simple esterification process. Reaction of soybean or canola oils high in carboxylic acids with methanol (or ethanol) produce the dimethyl or diethyl ester of these dicarboxylic

acids which has good properties for diesel fuel. Indications are that biodiesel formulations may be useful in blends to upgrade petroleum-based diesel fuels or to provide lubrication properties for F-T diesel fuel.

Lastly, much research has been conducted to convert biomass to ethyl alcohol to a point where the cost of production of ethanol is nearly cost competitive with gasoline. However, ethanol has a poor cetane number and is not a suitable Diesel engine fuel. On the other hand, it is easily converted in a one step catalytic process to diethyl ether (DEE) which has extraordinary compression ignition characteristics. Indeed, it is diethyl ether ("e-ther") that is used to start diesel engines in very cold climates. Research is underway to explore the feasibility of using DEE to upgrade the properties of petroleum derived or biodiesel fuels.

CONCLUSION

The Diesel Cycle engine has already established itself as the engine-of-choice for the heavy duty transport industry because of its fuel efficiency, durability, and reliability. In addition, it has also been shown to be capable of using alternative fuels, albeit at efficiencies lower than that achieved with petroleum-derived diesel fuel. Alternative fuel dedicated engines have not made significant penetration of the heavy duty truck market because truck fleet operators need a cost-competitive fuel and reliable supply and fuel-ing infrastructure. In lieu of forcing diverse fuels from many diverse domestic feedstocks onto the end-users, the Office of Heavy Vehicle Technologies envisions that a future fuels strategy for the heavy duty transport sector is one where the diverse feedstocks are utilized to provide a single fuel speci-fication (dispensed from the existing fueling infrastructure) that would run efficiently in a single high efficiency energy conversion device, the Diesel Cycle engine. In so doing, the U.S. commercial transport industry may gain a measure of security from the rapid fuel price increases by relying less on a single feedstock source to meet its increasing fuel requirements.

REFERENCES

I. Hodel, D., Crisis in the Oil Patch, 1994.

2. Romm, J.J. and Curtis, C.B., "Mideast Oil Forever?" The Atlantic Monthly, April 1996.

3. Romm, J.J. and. Ervin, C.A., "How Energy Policies Affect Public Health," Public Health, Reports, September/October 1996.

4. Cummins In the News," Cummins News Releases in the Internet, February 1997.

5. "Development of a Production-Feasible Common Rail Fuel Injection System for Liquid Dimethyl Ether (DME) for Use in Heavy-Duty Vehicles," NREL Fact Sheet, 1997.

6. Fritsch, P., "Exxon Project to Expand Use of Natural Gas," The Wall Street Journal October 30, 1996.

7. Ansell, L.L., Eisenberg, B.,. Bauman, R.F and. Say, G.R "Liquid Fuels from Natural Gas An Update of the Exxon Process," Alternate Energy '94, La Quinta, CA, April 26-29, 1994.

8. Tijm, P.J.A., Marriott, M.M. Senden, M.M.G., and. van Wechem, H.M.H., "Shell Middle Distillate Synthesis -- The Process, the Products, the Plant," Alternate Energy '94, La Quinta, CA, April 26-29, 1994.

9. Marriott, J.N. and Geertsema, A., "Report on the Continuing Progress at Sasol," Alternate Energy '94, La Quinta, CA, April 26-29, 1994.

EPA APPROACHES TO DIESEL ENGINE EMISSIONS CONTROLS

A. Stout
U.S. Environmental Protection Agency

The Environmental Protection Agency (EPA) has several current programs related to diesel engine emission controls, including changes to the National Ambient Air Quality Standards and a variety of proposed and final rules setting new emission standards. If the standards are implemented as proposed, the resulting emission reductions would translate into significant, long-term improvements in air quality in many areas of the U.S. Overall, these programs would provide much-needed assistance to states facing ozone and particulate air quality problems that are causing a range of adverse health effects for their citizens, especially in terms of respiratory impairment and related illnesses.

For current information on several of these and other projects, EPA maintains a large collection of files on its internet home page. This information can be found under http://www.-epa.gov/OMSWWW. EPA also provides a notification service to inform individuals via E-mail messages as new information is posted.

NAAQS

Particulate Matter

EPA finalized new standards for particulate matter (PM) under the national ambient air quality standards (NAAQS). After reviewing hundreds of peer-reviewed scientific studies, the EPA has determined that these changes are necessary to protect public health and the environment. EPA is revising the primary (health-based) PM standards by adding a new annual $PM_{2.5}$ standard set at 15 micrograms per cubic meter ($\mu g/m^{3}$) and a new 24-hour $PM_{2.5}$ standard set at 65 $\mu g/m^3$. EPA is retaining the current annual PM_{10} standard of 50 $\mu g/m^3$ and adjusting the PM_{10} 24-hour standard of 150 $\mu g/m^3$ by changing the form of the standard. EPA is revising the secondary (welfare-based) standards by making them identical to the primary standards. EPA believes that the $PM_{2.5}$ and PM_{10} standards, combined with the Clean Air Act-required regional haze program, will provide protection against the major PM-related welfare effects, including visibility impairment, soiling and materials damage.

EPA is issuing new rules related to PM monitoring requirements under the new standards. One rule addresses the monitoring network design needed for the new $PM_{2.5}$ standards. Other rules establish a new federal reference and equivalent methods for monitoring $PM_{2.5}$. Also, in a separate action, EPA is proposing rules to improve visibility by requiring states to develop programs to help reduce regional haze.

EPA changes the suite of PM_{10} standards by adding two new primary $PM_{2.5}$ standards set at 15 $\mu g/m^3$, annual arithmetic mean, and 65 $\mu g/m^3$, 24-hour average, to provide increased protection against the PM-related health effects found in the community studies. EPA's scientific review concluded that fine particles are a better surrogate for those components of PM most likely linked to mortality and morbidity effects at levels below the previous standards, while high concentrations of coarse fraction particles are linked to effects such as aggravation of asthma. The Clean Air Scientific Advisory Committee made a near unanimous (19 of 21 members) recom-mendation that new standards for $PM_{2.5}$ be added while retaining PM_{10} standards as an indicator for coarse fraction particles.

EPA has set $PM_{2.5}$ standards with 24-hour and annual averaging times to protect against effects from short- and long-term exposure identified in the community studies. In developing a suite of $PM_{2.5}$ standards designed to protect public health, EPA considered the combined effect of the standards rather than an approach that weighed short- and long-term exposure evidence, analyses, and standards independently. EPA concluded that much of the total annual risk associated with short-term exposures is likely to result from days when the PM levels are in the low- to mid-range, below the 24-hour peaks. As a result, lowering a wide range of $PM_{2.5}$ concentrations through an annual standard, as opposed to focusing on controlling peak 24-hour concentrations, is the best way to reduce total $PM_{2.5}$ risk. EPA also believes that the 24-hour standard will provide additional protection for days with high $PM_{2.5}$ concentrations, localized "hot spots," and risks arising from seasonal emissions, such as woodsmoke in the winter.

The final rule establishes a new form for the annual $PM_{2.5}$ standard. Areas will be in compliance with the new annual $PM_{2.5}$ standard when the 3-year average of the annual arithmetic mean $PM_{2.5}$ concentrations, from single or multiple community-oriented monitors, is less than or equal to 15 $\mu g/m^3$. The use of averages from single or multiple community-oriented sites is more closely linked to the underlying health effects information, which relates area wide health statistics to averaged measurements of area wide air quality. EPA believes this more protective annual standard, with the supplemental protection afforded by the 24-hour standard, which is directed at peak concentrations and localized hot spots, will provide a protective target that will reduce area-wide population exposure to fine particles.

For the new 24-hour $PM_{2.5}$ standard, the form is based on the 98th percentile of 24-hour $PM_{2.5}$ concentrations in a year (averaged over 3 years), at the population-oriented monitoring site with the highest measured values in an area. The 24-hour standard will limit peak concentration in areas with high seasonal concentrations and in areas with localized hot spots due to particular sources. This form will reduce the impact of a single high exposure event that may be due to unusual meteorological conditions, and thus would provide a more stable basis for effective control programs. The percentile form compensates for missing data and less-than-every-day monitoring, thereby reducing or eliminating the need for complex procedures previously required for the PM_{10} attainment test. The forms of both the 24-hour and annual standard were adjusted to provide additional protection for community settings with higher than average concentrations within an area.

EPA establishes an annual $PM_{2.5}$ standard level of 15 $\mu g/m^3$, to protect public health with an adequate margin of safety. Although health effects at lower annual concentrations are possible, the evidence for effects at such levels is highly uncertain and the likelihood of significant health risk becomes smaller at concentrations well below the 15 $\mu g/m^3$ level and approaching background levels.

After carefully reviewing public comments on the proposed standards, EPA changed the level of the 24-hour $PM_{2.5}$ standard from 50 $\mu g/m^3$ in the proposal to 65 $\mu g/m^3$. In conjunction with greater protection afforded by the changes to the forms and associated monitoring requirements, EPA believes that a 24-hour $PM_{2.5}$ standard set at 65 $\mu g/m^3$ will provide an appropriate supplement to the annual standard and provides an adequate margin of safety in communities that meet the annual standard, but have infrequent or isolated 24-hour peaks. The resulting suite of PM standards will give greater flexibility to individual sources of pollution while still ensuring that public health is protected.

Based on its assessment of the health and other available information, EPA retains the annual PM_{10} standard of 50 $\mu g/m^3$ to protect against effects from both long- and short-term

exposure to coarse fraction particles.

EPA revises the PM_{10} 24-hour standard of 150 $\mu g/m^3$ by replacing the 1-expected-exceedance form with a 99th percentile form, averaged over 3 years, to protect against short-term exposure to coarse fraction particles. The concentration-based percentile form is a more stable target for control programs and eliminates the need for complex data handling for missing values.

With the addition of fine particle standards, EPA has found that the original quantitative basis for the level of the previous 24-hour PM_{10} standard is no longer appropriate. However, the new health studies and information on coarse particles do not provide a basis for a lower standard level.

Based on careful review of public comments, many of which expressed concern that a 98th percentile might not provide adequate protection against larger particles, EPA changed the form of the PM_{10} 24-hour standard from the 98th percentile to the 99th percentile concentration-based form.

Ozone

EPA has set new national ambient air quality standards for ground-level ozone, the primary constituent of smog. After a lengthy scientific review process, including extensive external scientific review, EPA has determined that these changes are necessary to protect public health and the environment. EPA is phasing out and replacing the previous 1-hour primary ozone standard (health-based) with a new 8-hour standard to protect against longer exposure periods. In establishing the 8-hour standard, EPA is setting the standard at 0.08 parts per million (ppm) and defines the new standard as a "concentration-based" form, specifically the 3-year average of the annual 4th-highest daily maximum 8-hour ozone concentrations.

EPA has also replaced the previous secondary standard (to protect the environment, including agricultural crops, national parks, and forests) with a standard identical to the new primary standard. The 0.12 ppm 1-hour standard will not be revoked in a given area until that area has achieved 3 consecutive years of air quality data meeting the 1-hour standard. The purpose of retaining the current 1-hour standard is to ensure a smooth, legal, and practical transition to the new standard.

EPA concluded that the 1-hour primary standard did not adequately protect the public from adverse health effects. Therefore, EPA replaces the previous standard with an 8-hour standard set at 0.08 ppm; an area will attain the standard when the 3-year average of the annual 4th-highest daily maximum 8-hour concentrations is below 0.08 ppm. As the Clean Air Scientific Advisory Committee unanimously recommended, EPA is changing the ozone standard averaging time to 8-hours. Although 1- to 3-hour and 6- to 8-hour ozone exposures can be addressed through 1-hour or 8-hour standards, the 8-hour standard is more directly associated with the health effects of most concern cited in recent 6- to 8-hour exposure studies. These studies were conducted at more typical exercise levels and at lower exposure levels (0.08 ppm) than the 1-hour studies.

EPA is changing the form of the standard from an expected-exceedance form to a concentration-based form because it more directly relates to ozone concentrations associated with health effects; it avoids exceedances, regardless of size, from being counted equally in the attainment tests. In November 1996, EPA proposed that the annual 3rd-highest daily maximum 8-hour concentrations, averaged over 3 years, be the basis to determine whether or not an area was in attainment with the standards. After carefully examining public comment on the issue, EPA changed the form of the standard from the annual 3rd- to 4th-highest daily maximum concentration. This form will provide greater stability in the designation of areas, consistent with providing

strong public health protections.

In setting the 8-hour standard at 0.08 ppm, the EPA recognizes that since there is no discernible threshold below which no adverse health effects occur, no level would eliminate all risk. Thus, a zero-risk standard is not possible, nor is it required by the Clean Air Act. The selected 0.08 ppm level is based on the judgment that at this level public health will be protected with an adequate margin of safety.

The new 8-hour standard will become effective 60 days after promulgation, while the existing 1-hour standard, for most purposes, will remain in effect until EPA determines that an area has air quality meeting the 1-hour standard.

EPA believes attainment of the new primary standard will substantially protect vegetation. Therefore, EPA is setting the secondary standard identical to the primary standard. Although the Agency is not setting a separate seasonal secondary standard at this time, the Agency is committed to enhancing rural ozone monitoring, working in conjunction with other federal agencies, and considering long-term cumulative effects of ozone on plants as additional information becomes available.

HIGHWAY ENGINE FINAL RULE

EPA is adopting a new combined emission standard for NOx and NMHC for heavy-duty diesel engines used in trucks and buses, beginning in 2004. The new standard represents a NOx level about 50 percent lower than is required for new engines in the 1998 model year, which will significantly assist States in meeting and maintaining National Ambient Air Quality Standards. The consultation and consensus-building activities which EPA undertook in this initiative culminated in widespread support from the engine and trucking industries, States, and the environmental community for the new standard.

In response to the need for additional pollution reduction measures at the national level, EPA held a series of discussions with the California Air Resources Board (CARB) and representatives of the heavy-duty engine manufacturing industry to exchange views on the appropriateness and feasibility of new emission standards for highway and nonroad heavy-duty engines. Based on these discussions, an historic Statement of Principles regarding highway heavy-duty engines was signed by these parties in July 1995. EPA issued an Advance Notice of Proposed Rulemaking on August 31,1995, which requested comment on the Statement of Principles and the Agency's plans to formally propose new heavy-duty engine emission standards consistent with the agreement. EPA formally proposed the standard on June 27, 1996. During the comment period for the rulemaking, stakeholders continued their strong support for the new standards.

The new emission standard is in the form of combined nonmethane hydrocarbons (NMHC) plus NOx and is presented in units of grams emitted per brake horsepower-hour (g/bhp-hr). It applies to diesel engines and becomes effective in model year 2004. Manufacturers have the choice of certifying their engines to either:

2.4 g/bhp-hr NMHC + NOx or
2.5 g/bhp-hr NMHC + NOx with a limit of 0.5 g/bhp-hr on NMHC.

EPA also proposed the above standard for gasoline-fueled engines, but is not finalizing the standard at this time. The Agency is continuing to evaluate new standards for gasoline-fueled engines and is planning a supplemental rulemaking to address gasoline-fueled engines specifically.

EPA is simultaneously adopting provisions to further encourage engine manufacturers to use emission controls that will have a high degree of durability, performing well in use without an unreasonable degree of owner involvement. EPA is finalizing other basic provisions to help encourage the maintenance and repair of emission controls after the end of regulatory

life is reached and to ensure that emission controls are addressed properly during engine rebuilding.

EPA is finalizing changes to the averaging, banking, and trading program to enhance the feasibility and cost-effectiveness of the standards and encourage the early introduction of cleaner engines, thus securing emission benefits earlier than would otherwise be the case.

A technology review will be undertaken in 1999 to assess industry progress and propose changes in the standards if necessary. The potential role of fuels in achieving low heavy-duty engine emissions is being evaluated now as part of a technical working group comprised of representatives from EPA, the engine manufacturers, the oil industry and other stakeholders. The results of these technical evaluations will be considered as a part of the 1999 technology review.

The new standard is expected to reduce NOx emissions from highway heavy-duty engines by 50 percent relative to the 1998 standard. In 2020, EPA projects a reduction of 1,082,000 tons per year in ozone precursors and about 43,000 tons per year of secondary nitrate PM. EPA estimates resulting near-term retail price increases between $260 and $470 per vehicle, with costs decreasing to half that amount in five years. This represents less than one percent of the cost of most new heavy-duty vehicles.

LAND-BASED NONROAD ENGINE PROPOSED RULE

Following the initial effort for highway heavy-duty engines, EPA joined CARB and the engine manufacturers in successfully developing a second Statement of Principles focusing on nonroad engines. EPA issued a Supplemental Advance Notice of Proposed Rulemaking on January 2, 1997 to request comment on the Agency's plans to propose the new emission standards contained in the Nonroad Statement of Principles.

The proposed emission standards for diesel engines include those used in most nonroad applications. The proposal covers nonroad diesel engines and equipment, except for locomotives, commercial marine engines rated above 37 kW (50 hp), and underground mining equipment. The standards, which would be implemented in two tiers over several years (1999-2008), represent a major improvement from the recently implemented first tier of nonroad engine standards and would reduce those standards by up to two-thirds (see Table 1).

The proposal includes many of the provisions developed for the rulemaking for highway engines described above, including requirements related to engine rebuilding, changes to the averaging, banking, and trading program, and a technology review that will be undertaken in 2001.

In addition, EPA is proposing (1) related provisions intended to ensure compliance with the new standards in the field, (2) flexibility provisions to ease compliance for manufacturers of the equipment into which these engines are installed, and (3) a program of voluntary standards for engines with superior control of emissions.

CI MARINE

Compression-ignition marine engines include small auxiliary and propulsion engines, medium-sized propulsion engines on coastal and harbor vessels, and very large propulsion engines on ocean-going vessels. The contribution of this source to the average national mobile source NOx inventory is approximately 2.5 percent, though the contribution is much greater in areas with commercial ports. Emissions from diesel marine engines are virtually unregulated at this time. This will change in the near future, as a result of regulatory efforts at international and national levels.

At the international level, emissions from marine vessels will be regulated by Annex VI of the International Convention on the Prevention of Pollution from Ships (MARPOL). The International Maritime Organization has been working on Nox emission standards from these vessels to be finalized in September 1997. The standards will achieve a 30 percent reduction over uncontrolled levels, and will apply beginning January 1, 2000 to all engines on all vessels used in international voyages, as well as large engines used on marine vessels that operate only domestically. On the national level, smaller domestic vessels not covered by MARPOL will be subject to a new set of CI marine engine regulations currently being developed by EPA.

LOCOMOTIVE PROPOSAL

Since locomotive emissions have not been regulated before, EPA faced the need to create a comprehensive program, including not only emission standards, but also test procedures and a full compliance program. In general terms, the overall program is similar to previously established programs for heavy-duty highway engines and other nonroad engines. One unique feature included for locomotives, however, is the regulation of the engine remanufacturing process, including the remanufacture of locomotives originally manufactured prior to the effective date of this rulemaking. Regulation of the remanufacturing process is critical because locomotives are generally remanufactured 5 to 10 times during their total service lives (typically 40 years or more). Standards that only applied to locomotives originally manufactured after the effective date of the rule would not achieve significant emission reductions in the near term, since those locomotives slowly replace the existing fleet.

Three separate sets of emission standards are proposed, with applicability of the standard dependent on the date a locomotive is first manufactured. The first set of standards (Tier 0) are proposed to apply to locomotives and locomotive engines originally manufactured from 1973 through 1999, any time they are remanufactured in calendar year 2000 or later. The second set of standards (Tier I) apply to locomotives and locomotive engines originally manufactured from 2000 through 2004. These locomotives and locomotive engines would be required to meet the Tier I standards at the time of orginal manufacture and at each subsequent remanufacture. The final set of standards (Tier II) are proposed to apply to locomotives and locomotive engines originally manufactured in 2005 and later. Tier II locomotives and locomotive engines would be required to meet the applicable standards at the time of original manufacture and at each subsequent remanufacture. Electric locomotives, historic steam-powered locomotives, and locomotives originally manufactured before 1973 do not contribute significantly to the emission problem, and thus are not included in this rulemaking.

EPA is proposing a production line testing program that would require manu-facturers and, in some cases, remanufacturers of locomotives to perform production line testing of newly manufactured and remanu-factured locomotives as they leave the point where the manufacturer or remanufacture is completed. The production line testing pro-gram for freshly manufactured units would be based on actual testing, while the program for remanufactured units would be based on an audit of the remanufacture kit's installation, with EPA having the ability to require testing if in-use data indicates a possible problem with production.

A critical element in the success of the proposed locomotive program is ensuring that manufacturers and remanufacturers produce locomotives that continue to meet emission standards beyond certification and production stages, during operation and use in the field. EPA is proposing to adopt an in-use compliance program with two distinct components. The first program would require the manufacturers and remanufacturers to test representative locomotives from all engine families using the full Federal Test Procedure. This testing would

occur at about 75 percent of useful life. Actual repair in the event of a determination of noncompliance or recall action, however, would apply to all locomotives of that family, regardless of whether the locomotives have exceeded their useful lives. Second, EPA is proposing to require that Class I railroads annually test 10 perrcent of their locomotives which have met or exceeded their useful lives using a modified version of the Federal Test Procedure.

EPA is proposing averaging, banking, and trading provisions to allow manufacturers and remanufacturers the flexibility to meet overall missions goals at the lowest cost, while allowing EPA to set emission standards at levels more stringent than they would be if each and every engine family had to comply with the standards. Averaging, banking, and trading is also designed to encourage early introduction of cleaner engines, which would secure emission benefits earlier than would otherwise be the case.

EPA is proposing regulation that would codify and clarify Clean Air Act preemption of certain state and local requirements relating to the control of emissions from new locomotives and new locomotive engines. This preemption was included in the Clean Air Act because of the inherent interstate nature of the railroad industry. Moreover, EPA believes that a strong federal program that addresses manufacturing, remanufacturing, and in-use compliance is the best way to achieve the necessary emission reductions.

The primary focus of this rulemaking is on reducing NOx and PM emissions, although there are also reductions in HC and CO. NOx emis-sions from locomotives will be reduced almost 60 percent by 2040, compared to 1990 baseline levels. This would be about 600,000 tons per year. Most of these reductions will come early in the program (e.g., 39 percent reduction by 2010), due to the standards that apply to pre-2000 locomotives when they are remanufactured. In addition to the NOx benefits of the proposed rule, the proposal will provide some PM benefits through the Tier II standards. A PM reduction of 42 percent is expected by 2040, compared to 1994 baseline levels. This reduction is over 10,000 tons per year, and amounts to over one percent of national PM emissions from mobile sources.

LIGHT-DUTY VEHICLES

The Clean Air Act directs EPA to set new emission standards for light-duty vehicles (or passenger cars) and light-duty trucks. Federal Tier 1 emission standards were established for 1994 model year vehicles. Table 2 shows the current Tier 1 and projected Tier 2 emission standards for the various classes of light-duty vehicles and trucks.

The Clean Air Act is very specific for passenger cars and the LDT1 category of light-duty trucks. The Act set the current Tier 1 numbers, which provide a substantial break for diesel engines. The Act also strongly suggests that diesel vehicles meet the same standards as for gasoline starting in the 2004 model year. In separate language, the Act lays out presumptive Tier 2 standards for this category, which would take effect unless EPA justifies some other le. While EPA intends to conduct the study to evaluate the appropriate Tier 2 standards, the language in the Act sets a clear guideline for targeting emission reductions. This study will include considera-tion of the energy and global warming benefits of diesel engines.

The Clean Air Act is less specific about emission standards for the bigger light trucks. Analysis has shown, though, that 70% of light-duty NOx emissions come from light-duty trucks in the LDT2, LDT3, and LDT4 categories. The dominant emission contribution of these ve-hicles can be attributed partly to the less stringent standards and partly to the big increase in population in recent years. For any effective emission reductions, then, EPA will need to focus on

setting more stringent standards for these light trucks.

Table 1
Proposed Land-Based Nonroad Diesel
Engine Emission Standards in g/kW-hr (g/hp-hr)

Engine Power	Tier	Model Year	NMHC + NOx	CO	PM
kW<8 (hp<11)	Tier 1	2000	10.5 (7.8)	8.0 (6.0)	1.0 (0.75)
	Tier 2	2005	7.5 (5.6)	8.0 (6.0)	0.80 (0.60)
8≤kW<19 (11≤hp<25)	Tier 1	2000	9.5 (7.1)	6.6 (4.9)	0.80 (0.60)
	Tier 2	2005	7.5 (5.6)	6.6 (4.9)	0.80 (0.60)
19≤kW<37 (25≤hp<50)	Tier 1	1999	9.5 (7.1)	5.5 (4.1)	0.80 (0.60)
	Tier 2	2004	7.5 (5.6)	5.5 (4.1)	0.60 (0.45)
37≤kW<75 (50≤hp<100)	Tier 2	2004	7.5 (5.6)	5.0 (3.7)	0.40 (0.30)
	Tier 3	2008	4.7 (3.5)	5.0 (3.7)	—
75≤kW<130 (100≤hp<175)	Tier 2	2003	6.6 (4.9)	5.0 (3.7)	0.30 (0.22)
	Tier 3	2007	4.0 (3.0)	5.0 (3.7)	—
130≤kW<225 (175≤hp<300)	Tier 2	2003	6.6 (4.9)	3.5 (2.6)	0.20 (0.15)
	Tier 3	2006	4.0 (3.0)	3.5 (2.6)	—
225≤kW<450 (300≤hp<600)	Tier 2	2001	6.4 (4.8)	3.5 (2.6)	0.20 (0.15)
	Tier 3	2006	4.0 (3.0)	3.5 (2.6)	—
450≤kW<560 (600≤hp<750)	Tier 2	2002	6.4 (4.8)	3.5 (2.6)	0.20 (0.15)
	Tier 3	2006	4.0 (3.0)	3.5 (2.6)	—
kW≥560 (hp≥750)	Tier 2	2006	6.4 (4.8)	3.5 (2.6)	0.20 (0.15)

Table 2
Full Life NOx Standards (g/mi)

Category	Fuel	Current Tier 1	Presumptive Tier 2
LDV, LDT1	gasoline	0.6	0.2
	diesel	1.25	0.2
LDT2, LDT3	gas/diesel	1.0	—
LDT4	gas/diesel	1.5	—

CALIFORNIA 1994 STATE IMPLEMENTATION PROGRAM FOR OZONE IMPLEMENTATION ISSUES AND STRATEGIES FOR REDUCING EMISSIONS FROM HEAVY DUTY DIESEL VEHICLES

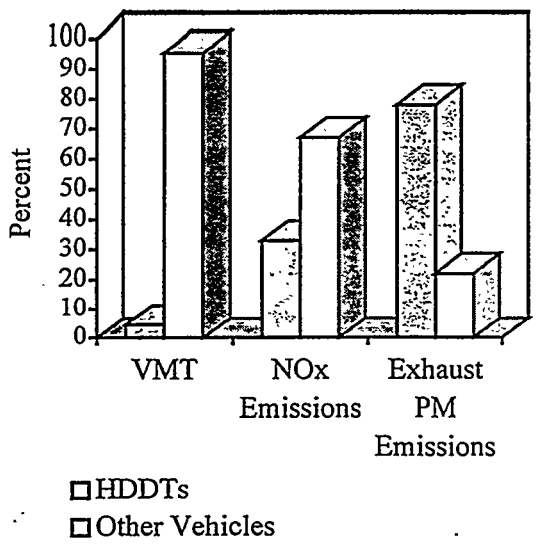
R. Nguyen
California Air Resources Board

BACKGROUND

Heavy-duty vehicles carry over 60 percent of the transported goods, by weight, in California. The majority of these vehicles are powered by diesel engines. Because of their efficiency, reliability, and durability, diesel engines are expected to continue to be the engine of choice for the freight transport industry. The preference for diesel engines gives rise to an air quality challenge since emissions from diesel engines have not been controlled to the same extent as gasoline vehicles, particularly light- and medium-duty vehicles. Whereas emissions from light-duty vehicles have been reduced to greater than 95 percent compared to uncontrolled levels, existing control requirements for heavy duty diesel vehicles have only resulted in approximately 70 percent reductions of oxides of nitrogen (NOx) compared to uncontrolled levels. Furthermore, heavy duty diesel vehicles involved in goods movement applications typically accrue higher annual mileage than other vehicles. Consequently, the emissions, particularly of NOx and particulate matter (PM), from heavy duty diesel vehicles are disproportionately high compared to their population or vehicle miles traveled (VMT). In the SCAB, even though heavy duty diesel trucks accounted for about five percent of the VMT for all on-road vehicles in 1995, they emitted about 30 percent of the NOx emissions and almost 80 percent of the exhaust PM emissions from all on-road vehicles. Figure 1 shows the VMT and emission contributions of heavy duty diesel trucks compared to the total vehicle population. In addition, heavy duty vehicle VMT are projected to increase nearly 50 percent from 1995 to 2010. Thus, it is clear that emissions from heavy duty diesel vehicles have to be reduced further if air quality goals are to be achieved.

Figure 1

Percent of Vehicle Miles Traveled and Emissions from Heavy Duty Diesel Trucks in SCAB--1995

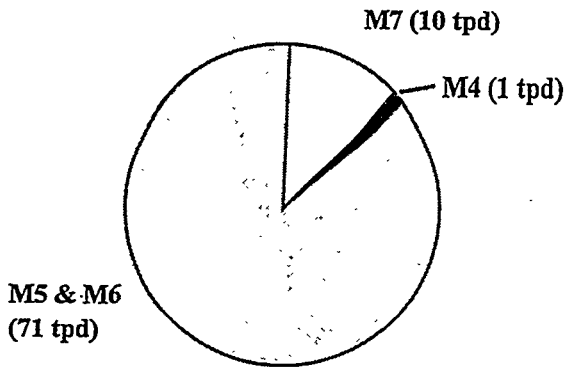


The ARB adopted the SIP in November 1994, in compliance with the requirements of the 1990 Clean Air Act Amendments. The SIP is a comprehensive effort aimed at reducing emissions from all sources, both mobile and stationary. It contains plans and strategies for non-attainment areas to achieve the Federal ambient air quality standards for ozone by the specified dates. A key focus is strategies to reduce emissions from on-road heavy duty diesel vehicles. The emphasis on heavy duty diesel vehicles comes directly from the magnitude of emissions from this source and the potential to further reduce these emissions.

The 1994 California SIP contains four measures specifically designed to reduce emissions from on-road heavy duty vehicles. Measure M4 is an incentive-based program to encourage the early introduction of reduced-emission heavy duty engines into fleets. Measure M5 calls for the adoption by ARB of a 2.0 grams per brake horsepower hour (g/bhp-hr) NOx emission standard for new heavy duty engines sold in California, or alternative measures, beginning in 2002. Measure M6 calls for Federal adoption of nationwide emission standards for heavy duty engines, equivalent to that proposed for M5, beginning in 2004. Measure M7 is an accelerated retirement program for heavy duty vehicles. Altogether, these SIP measures were designed to reduce over 80 tpd (40 percent) of Nox emissions from on-road heavy duty vehicles in 2010 in the South Coast Air Basin (SCAB). Figure 2 shows the heavy duty NOx emission reductions in the SCAB for these measures.

Figure 2

Anticipated NOx Emission Reductions Measures M4, M5, M6, M7, SCAB--2010



STATUS OF SIP MEASURES FOR HEAVY DUTY VEHICLES

Since the 1994 California SIP was adopted, ARB staff has participated in a number of efforts to further develop and implement these SIP measures for on-road heavy duty vehicles. While SIP measure M7, early retirement of heavy duty vehicles, does not appear to be able to achieve the desired emission reductions, notable successes were achieved for SIP measures M5 and M6 with the signing of the Statement of Principles (SOP), discussed below, with heavy duty engine manufacturers. Efforts to implement SIP measure M4 are ongoing. ARB staff is currently exploring options to increase implementation of SIP measure M4. The status of each of these four SIP measures is presented below.

MEASURES M5 AND M6

SIP measures M5 and M6 are the cornerstones of California's strategy to further reduce emissions from on-road heavy duty engines. Measures M5 and M6 call for the adoption, at the state and Federal levels, respectively, of an emission standard equivalent to 2.0 g/bhp-hr of NOx.

In 1995, heavy duty engine manufacturers, U.S. EPA, and ARB signed the SOP with the goal of reducing emissions from on-road heavy duty vehicles. Included in the SOP is a provision specifying national emission standards for on-road heavy duty engines. Heavy duty engine manufacturer signatories to the SOP are committed to developing on-road heavy duty engines capable of meeting a NOx emission level of approximately 2.0 g/bhp-hr beginning in 2004. The SOP provides manufacturers with the flexibility to choose between two different options: a) a combined non-methane hydrocarbon (NMHC) plus NOx standard of 2.4 g/bhp-hr; or b) a combined NMHC plus NOx standard of 2.5 g/bhp-hr with an NMHC cap of 0.5 g/bhp-hr. It is expected that these emission levels will be equivalent to the 2.0 g/bhp-hr NOx-only standard as proposed in the 1994 California SIP. With the implementation of the SOP through Federal and California rulemaking, NOx emissions from on-road heavy duty engines will be reduced by half while PM emission levels are maintained. A final Federal rule incorporating the SOP agreements is expected in August 1997.

The U.S. EPA is required to make a determi-

nation of feasibility in 1999 to assess the progress of engine manufacturers in meeting the 2004 emission standards for on-road heavy duty engines. Depending on the status of heavy duty engine technology at that time and on projections of future technology development, revisions to the standards could be considered. Assuming no revisions are necessary, on-road heavy duty diesel engines would be required to comply with the reduced emission standards by 2004. Thus, all but 6 tpd of the SIP emission reductions assigned for M5 and M6 would be fully realized. The unrealized 6 tpd are those emission reductions that would be achieved from a California-only standard for NOx emissions, effective in the 2002 and 2003 model years. For a number of reasons, ARB would prefer that the emissions from California-only standards in 2002 and 2003 could be obtained from alternative strategies. Due to the interstate nature of the trucking industry, a California-only emission standard could create a situation where California-based truck operators could be put at a competitive disadvantage if they have to buy more expensive engines compared to out-of-state truck operators. In addition, the time frame of a California-only standard, 2002 and 2003, in light of the upcoming national emission standard in 2004, could cause some truck operators to delay purchasing newer engines until 2004.

However, ARB has obligations to meet for reducing emissions, and we are committed to obtaining the emission reductions identified in the SIP. The major beneficiaries of the 2002 and 2003 emission reduction benefits from measure M5 are those districts that have 2005 attainment dates, although those emission reduc-tions are also important in the SCAB for attainment in 2010. Ensuring that reduced-emission engines are on the road before 2004 is an important heavy duty vehicle strategy. One provision of the upcoming Federal and California heavy duty vehicle emission requirements for 2004 is the averaging, banking, and trading (ABT) program. As discussed later in this paper, the ABT program may provide some benefits for certain areas in California, but may also result in some disbenefits for other areas, depending upon an area's attainment date. Another means of reducing emissions in the pre-2004 time frame is the use of incentives to place reduced-emission heavy duty vehicles in the fleet. This strategy is presented in the following section describing SIP measure M4.

MEASURE M4

SIP measure M4 relies on the early introduction of reduced emission heavy duty engines/-vehicles to achieve near-term emission reductions necessary in some non-attainment areas. This is to be accomplished through the use of incentives to encourage fleet operators to purchase reduced-emission heavy duty engines/vehicles. Incentives are necessary to partially or wholly offset the higher costs of heavy duty engines capable of meeting NOx emission levels much lower than required. At the present time, these are only alternative fuel engines. Although there may be reduced-emission diesel engines available before 2004, the emission reduction benefits from these engines will likely be retained by the engine manufacturers as ABT credits. In any case, it is unlikely that there will be diesel engines that can match the performance of alternative fuel engines over the next four years. Alternative fuel heavy duty engines have the potential to meet significantly lower NOx levels in the near term. In fact, some alternative fuel heavy duty engines are already meeting these much-lower emission levels. But limited availability and higher costs of these engines compared to diesel engines have so far limited their market appeal and have constrained their commercial penetration to only a few specialized applications, such as urban buses.

Ongoing efforts aimed at creating incentives that would be attractive to engine manufacturers, fleet operators, and fuel providers have not had the desired results. Cost has been the most basic of several obstacles that have, thus far, discouraged fleet operators from purchasing alternative fuel heavy duty engines. The approaches that have been considered to implement measure M4, therefore, share a common goal of reducing the higher cost to the operators of alternative fuel heavy duty engines so as to make them more economically

competitive with conventional diesel engines. The following discussion summarizes efforts to promote the more widespread use of reduced-emission heavy duty engines/vehicles, both alternative fuel and diesel, through incentives.

U.S. EPA's Averaging, Banking, & Trading Program

The ABT program provides that engines produced before 2004 and that are below the NOx standard that applies through 2003 (4.0 g/bhp-hr) earn credits that can be used after 2004. That is, if a manufacturer produces a cleaner engine than required before 2004, that manufacturer can produce a "dirtier" engine than is required after 2004. If a substantial number of manufacturers take advantage of the ABT provision, significant emission reduction benefits will accrue to those districts that have 2005 attainment dates because the pre-2004 heavy duty fleet will be cleaner that it would have been otherwise. However, because a greater number of "dirtier" engines could be produced than would otherwise be required after 2004, the emissions in 2010 would be more than if there were no ABT program.

Incentive Programs

In the effort to develop a strategy to implement measure M4, ARB has maintained a technology-neutral position regarding the choice of powerplants for on-road heavy duty vehicles. Our emphasis is to obtain the emission reductions for this measure as early as possible by encouraging the deployment of engines with emission characteristics as close to the SOP 2004 NOx emission levels as practicable. Only alternative fuel heavy duty engines have the potential to meet these low emission levels in the near term. Consequently, efforts to implement measure M4 have focused on providing incentives to make it more attractive for fleets to purchase alternative fuel heavy duty engines.

Various groups have focused on creating incentives via legislation that would provide financial assistance to offset the higher cost of reduced-emission heavy duty engines. The general approach with these legislative efforts has been to attempt to provide some tax relief for purchasers of reduced-emission heavy duty engines so that the cost of these engines is more competitive with conventional diesel engines. These efforts are still being pursued in the current legislative session.

A different approach to increase the number of reduced-emission on-road heavy duty vehicles involves the corridor concept. This approach attempts to reduce the cost of on-road alternative fuel heavy duty vehicles and make them more attractive to fleets by increasing purchasing power, sharing refueling infrastructure, and financial assistance. Two different, but potentially complementary, corridor projects are underway: the Interstate Clean Transportation Corridor (ICTC) project and the District Corridor Program.

Interstate Clean Transportation Corridor

The ICTC project is a public/private effort to develop an economically sustainable alternative fuel infrastructure along the western states interstate highways. This infrastructure would support on-road alternative fuel heavy duty vehicles in the transportation of goods throughout the region. ARB is one of several co-funders for the ICTC project and ARB staff also participates as a Steering Committee member of the ICTC. The goals of the ICTC project are to deploy 250 on-road alternative fuel heavy duty vehicles and to establish ten alternative fuel refueling and service stations along a triangulated interstate corridor connecting California, Nevada, and Utah. Phase I of the ICTC project began in January 1996 and ended on March 31, 1997. Phase II, which will focus on achieving the numerical vehicle and fueling station targets, is scheduled to begin in mid-1997.

District Corridor Program

The District Corridor Program is an effort by public agencies to develop an incentive-based program having uniform criteria that would apply to all participating air pollution control

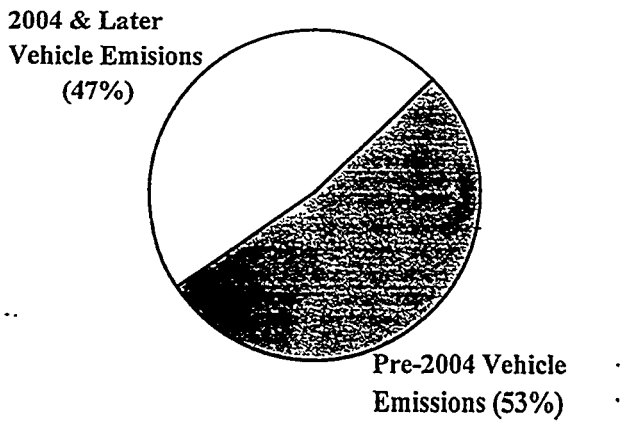
and air quality management districts that would assist in the deployment of reduced-emission heavy duty vehicles in California. ARB staff is working with air district staff, in the framework of the District Corridor Group, to formulate strategies and options for this inter-district program. The District Corridor Group is made up of representatives from ARB and air districts located along the Interstate 5 and Highway 99 corridors from Sacramento to Los Angeles. These two corridors are the principal north-south throughways for the commercial transport of goods in California. Since inter-district heavy duty vehicles typically would cross air district boundaries along these corridors, any emission benefits from reduced-emission heavy duty vehicles would be distributed among different districts as a direct result of those vehicles being driven within the district boundaries. The corridor project would establish funding criteria for reduced-emission projects and would provide for a way to distribute the cost of the projects among participating districts, based on the estimated share of emission reductions a particular district would receive from those projects. The money to fund this program would come from vehicle registration surcharge fees and other sources. In addition to cost sharing, another goal of the corridor project is to create a streamlined and uniform application process for truck operators, regardless of where their business is located or where they apply for project funding. The District Corridor Group is currently evaluating various options to implement this corridor program.

MEASURE M7

A particular attribute of heavy duty diesel engines is that they can be rebuilt many times during their lifetimes. This characteristic is one of the factors that results in diesel engines being the engine of choice when many hours of operation and high mileage are expected. However, this desirable characteristic of heavy duty diesel engines, from a fleet operation point of view, turns into a potential liability from an air quality perspective. Because of their long operating life, which could be extended considerably through rebuilds, older diesel engines with less effective emission control technology can continue operating well past the years they were originally manufactured. These older engines can continue to emit more pollutants per hour of operation than newer, cleaner engines. ARB staff estimates that, upon implementation of the 2004 emission standards, in the SCAB in 2010 trucks older than seven years will contribute over 50 percent of all on-road diesel truck NOx emissions for that region. This is shown graphically in Figure 3.

Figure 3

Contribution of Pre-2004 Vehicles to NOx Emissions from Heavy Duty Diesel Trucks -- SCAB in 2010



To reduce emissions from these older vehicles, SIP measure M7 called for the annual retirement (scrapping or removal) of about 1,600 of the oldest, high-emitting trucks in the SCAB, beginning in 1999 until 2010. As proposed in the SIP, incentives would be provided to operators of older trucks to purchase newer, lower-emitting vehicles in return for the retirement of the older models. This measure was estimated to result in a reduction of NOx emissions by 10 tpd in 2010 in the SCAB. Although ARB staff worked closely with the trucking industry to investigate possible ways to implement this measure, it is not likely that

this measure would be able to get the emission reductions anticipated in the SIP. To obtain the anticipated emission reductions, the scope of the program would have to be greatly expanded to include newer vehicles, as well as a much greater number of vehicles than anticipated in the SIP. The greatly expanded scope of an M7-type program would negatively impact its implementation feasibility since it is unlikely that sufficient money would be available to fully implement an expanded M7 program. Given the uncertainty in implementing measure M7, the emission reductions expected for M7 will have to be achieved through other means.

ISSUES AND STRATEGIES

From the foregoing discussion, a number of observations can be made. First, efforts to implement the SIP measures for heavy duty vehicles have had mixed results. Substantial strides were made in the implementation process of SIP measures M5 and M6 by the signing of the SOP and the soon-to-be-promulgated U.S. EPA rulemaking for on-road heavy duty engines. Successful implemen-tation of the 2004 standards will address a large portion, about 80 percent, of the emission reduction obligations assigned to on-road heavy duty vehicles. As discussed previously, the emission reductions from the other heavy duty vehicle measures may need to be achieved through alternative means. Continuing efforts to develop incentive-based programs to encourage the early introduction of reduced-emission heavy duty vehicles, if successful, would assist in that effort.

A second observation is the increased importance of incentive-based programs for heavy duty vehicles, especially for the near-term attainment strategies of some non-attainment areas. While much cleaner heavy duty diesel engines will be available in 2004, they will provide little assistance for areas that have to demonstrate attainment with the Federal ambient air quality standards for ozone by 2005. The only remaining viable option is to push for the rapid deployment of alternative fuel heavy duty vehicles so that they would be bought, instead of diesel vehicles, when fleets are replacing their older diesel vehicles. The emission reduction benefits of this strategy are obvious but the higher cost of these cleaner alternative fuel heavy duty engines remains the stumbling block that has prevented the penetration of these engines into the commercial freight transport market.

Diesel heavy duty engines will likely retain their prominent position in the industry, at least through the dates by which California must attain the air quality standards. Emissions from older diesel vehicles in both 2005 and 2010 will still be substantial despite efforts to reduce emissions from this source. As pointed out previously, emissions from trucks older than seven years will account for over 50 percent of the on-road heavy duty truck emissions in 2010 in the SCAB. If the emissions from those trucks in the total emission inventory could be reduced further, that would benefit California's SIP attainment efforts.

Reducing emissions from heavy duty vehicles to meet the SIP goals remains a challenge. ARB is balancing several strategies to achieve these goals. ARB plans to adopt U.S. EPA's 2004 emission standards for on-road heavy duty vehicles once the Federal regulation is promulgated. ARB also plans to participate with U.S. EPA in the research and development of even lower emission heavy duty diesel engines that would be capable of meeting a NOx emission level of approximately 50 percent of the 2004 standards. To address emissions from pre-2004 trucks, there is a need to phase in reduced emission engines expeditiously. To achieve this objective, incentives for heavy duty engine manufacturers need to be sufficiently attractive for them to produce en-gines capable of emitting sub-4.0 g/bhp-hr of NOx prior to 2004. The ABT component of the U.S. EPA's proposed regulation for on-road heavy duty vehicles may provide some of that incentive. ARB also plans to accelerate the efforts to encourage the deployment of alter-native fuel heavy duty vehicles through the ICTC and the District Corridor programs. However, the funding available for these programs is not

expected to be sufficient to meet the SIP goals unless efforts to seek legislation to support these types of programs are successful. If those efforts are successful, they could greatly accelerate the implement-ation of the incentive-based SIP programs.

CONCLUSIONS

Reducing emissions from heavy duty vehicles must remain a focus of the overall SIP strategy. Due to the nature of the trucking industry, the emission targets, and varied attainment dates, a successful strategy must necessarily be flexible. It would be impractical to favor a diesel-only approach since that would not yield sufficient emission reductions for areas that have near-term attainment dates. It would be as impractical to embrace an alternative-fuel only approach since the technology is not mature enough to meet the needs of the trucking industry. Accordingly, ARB plans to pursue strategies to realize near-term emission benefits offered by alternative fuel heavy duty engines while continuing to push for cleaner heavy duty diesel engines to ensure that longer-term attainment targets are met.

REFERENCES

1. California Air Resources Board, The California State Implementation Plan for Ozone, Sacramento, California, November 15, 1994.

2. California Air Resources Board, Methodology for Estimating Emissions from On-Road Motor Vehicles, Sacramento, California, November 1996.

3. United States Environmental Protection Agency, Notice of Proposed Rulemaking for the Control of Air Pollution from Heavy-Duty Engines, July 1996.

SOUTH COAST AIR QUALITY MANAGEMENT DISTRICT ALTERNATIVE FUEL HEAVY DUTY VEHICLE PROJECTS

C. Sullivan
South Coast Air Quality Management District

Heavy duty trucks account for 4 percent of the vehicle population in California, but contribute nearly 50 percent of the oxides of nitrogen (No_x) and over 70 percent of the on-road particulate mat-ter (PM). The majority of these trucks are powered by diesel fuel. Diesel exhaust is considered a potential or probable human carcinogen by several health agencies, including the Na-tional Institute of Occupational Safety and Health and the International Agency for Research on Cancer. The California Office of Environmental Health and Hazard As-sessment (OEHHA) and the Air Resources Board (ARB) have initiated the process of identifying diesel exhaust as a Toxic Air Contaminant,

Alternative fuel heavy duty engines cur-rently produce one-half or less the NOx of their diesel counterparts. The South Coast Air Quality Management District's Technol-ogy Advancement Office manages projects for the development and demonstration of alternative fuels in heavy duty engines. Fuels and technologies demonstrated in-clude methanol, natural gas, propane,. hybrid-electric, and fuel cells.

This presentation provides an overview of alternative fuel heavy duty vehicle demon-stration programs completed or underway, in addition to a discussion of planned ac-tivities with other local and State agencies in California.

WHY EMPHASIZE HEAVY DUTY VEHICLES

- NO_x and particulate emissions from heavy duty vehicles are a concern both from an air quality and health impact aspects

NO_x EMISSIONS

- Although heavy duty vehicles do not account for the largest contribution to the NO_x emissions inventory; their contribution is very high for the vehicle population

CARS VS. TRUCK$

- In other words one truck has the NO_x emissions of 15 cars.

SIP MEASURES

- Recognizing the challenging of meeting Federal standards for NO_x, the State has incorporated several measures into the State Implementation Plan directed specifically at heavy duty vehicles. The AQMD has incorporated these measures into its Air Quality Management Plan. These measures do not specifically require the use of alternative fuels.

- Measure M4 - Early Introduction of 2.0 gram NO_x engines

This measure projects a 5% sales penetration of 2.0 gram engines between 1996 and 1999; and 10% between 20000-2002.

- Measure M5 - Additional NO_x Reductions in 2002

Although directed to attainment in Sacramento and Ventura, this measure is certainly supported by the AQMD as a NO_x reduction strategy for the Basin. The measure proposes adoption by the ARB of a 2.0 gram NO_x emission standard for new engines sold in California beginning in 2002.

- Measure M6 - 2.0 gram NO_x Federal Standard in 2004. Many heavy duty trucks travel into California from other States. Without a national emission standard, the emissions impact of California regulations will be limited.

AQMD FUNDING PROGRAMS

- Technology Advancement
- Discretionary Funds
- Air Quality ~Investment Program

TECHNOLOGY ADVANCEMENT

- Established by AQMD in 1988

- Funded by $1 fee on vehicles registered in Basin
- Clean fuel development and demonstration projects

DISCRETIONARY FUNDS

$4/Vehicle/Year--Divided:
- 30% to SCAQMD
- 40% to Local Governments
- 30% to Discretionary Fund

- Focus on Near-term Emission Benefits

AIR QUALITY INVESTMENT PROGRAM

- Voluntary Program
- Evaluation Criteria relies heavily on cost-effectiveness
- Not easy for vehicle implementation programs to meet cost-effectiveness criteria

NATURAL GAS ENGINE TECHNOLOGY

AQMD has co-funded a number of demonstrations of natural gas engine technology; host sites include Wal-Mart and Unocal.

LA TIMES TRUCK

We are continuing a demonstration of the DDC Series 60 natural gas engine with the LA Times. The initial demonstration utilized CNG. Future plans are to convert the engine to LNG operation and continue demonstration and further engine refinement.

PIMA GRO TRUCK

Technology Advancement is funding the demonstration of the Caterpillar pilot ignition technology. The application is a long-haul truck, hauling bio-solids from the Orange County Sanitation District to a site near Bakersfield. The project uses the 3406 engine in a CNG configuration.

ARROWHEAD WATER TRUCK

There are several other demonstrations of the Caterpillar/Clean Air Partners/Power Systems natural gas technology in both CNG and LNG configurations. Applications include delivery trucks such as this and refuse transfer trucks operating in various locations in the Basin

ATA PROGRAM

- AQMD has entered into a partnership with DOE and GRI to fund natural gas engine

efficiency projects

- Initial Funding is $1.2 million; $400,000 from each partner; it is anticipated that further funding will be available in the future
- Program Administrator is the American Trucking Associations
- Initially, John Deere, Cummins, and Mack will receive awards

PROPANE

OCTA

- AQMD is currently funding development and demonstration of a DDC Series 50 propane engine for transit applications. The project is currently in the early demonstration stage. The objective is to certify the engine for transit applications.

CITY OF PASADENA

- Technology Advancement is funding the development and demonstration of a Cummins B Series propane engine. The engine is operating in two City of Pasadena shuttle buses. The engine is expected to be certified to ARB medium duty ULEV standards.

ELECTRIC AND HYBRID TECHNOLOGIES

Although we do not traditionally think of electric vehicle technology having application in the trucking sector, there may be several niche applications. TAO is funding several projects in this area

ELECTRIC CONVERSION OF USPS LONG-LIFE VEHICLES (LLV)

- Contractor: TransMotive Technologies, Santa Rosa
- Vehicles have 24 year life; overhaul gasoline engines after 12 yrs
- Developing electric drive train conversion with US Electricar
- 80 HP (peak) AC Induction motor/controller from Systronics
- 336 V DC nominal 28 Optima sealed lead-acid batteries
- Minimum Electric LLV range of 40 miles

HYBRID-ELECTRIC TRUCK

- ISE was initially funded through the Discretionary Funds Program to perform a research study on the feasibility of electric hybrid technology in trucking applications. This project, fielded by TAO, applies that study in a practical application.
- Demonstrated in a commercial refuse hauling application
- Kenworth T-800 Class-8 Truck/Tractor
  - New 386 HP (peak) AC-Induction Motor/Controller
  - 105 HP (continuous) Clean Air Partners/GM CNG APU (4.3L)
  - 672 VDC nominal 2x56 sealed lead-acid battery pack (VRLA)

Status: APU CNG tanks installed in chassis and functional

Differential assembly being modified
Motor/controller under development in cooperation with United Defense LP and Siemens

ELECTRIC WATER DELIVERY TRUCK

McKesson Water Products - Delivers Sparklettes Bottled Water
Up to 200 engine start-stops per day
Class 7 FWD cab~chassis
312 hp (peak) ISE Research AC induction motor/controller
Sealed lead-acid battery pack
Expected range 70 miles

Status:
Cab-chassis complete
Hackney Bros. water body to be installed
Propulsion system under development
Truck operational 1/98

FUEL CELL TECHNOLOGY

BALLARD FUEL CELL ENGINE

The 250 kW (275 hp) Ballard proton exchange membrane (PEM) fuel cell engine fits within a normal transit bus engine compartment

The engine can provide comparable performance, with reduced range AQMD has been a strong supporter of fuel cells - contributed $1 million to development of the technology.
This 40 ft. bus is the most advanced fuel cell bus in the world.
Chicago Transit will be receiving 3 advanced technology Ballard buses in late 1997.
Ballard's agreement with Daimler-Benz will mean aggressive commercialization of PEMFC: buses and automobiles.

Biggest Remaining Issues:
- fuel logistics (reform HC such as MeOH, or use pure H_2?)
- Availability and cost of fuel
- Need volume production of stocks to reduce cost

GAS RAIL USA - 16 CYLINDER TEST ENGINE

Development of LNG combustion technology at SWRI
Development of pilot diesel ingestion for LNG
Achieved a 75% reduction in NOx
Also has low PM without an increase in CO and HC
The EMD F59PH locomotive is being converted to LNG
To be demonstrated in LA passenger rail application in 1998

CALIFORNIA'S UNIQUE TRUCKING PROBLEMS

S. Williams
California Trucking Association

The trucking industry is extremely com-petitive and trucking companies located in California are finding it increasingly difficult to compete its carriers located outside the state. California-only environmental regulations adopted without consideration for competition from within the national and international freight movement system penalize California-based trucking companies. To sustain California's transportation market share and obtain forecasted emission reductions immediate action must be taken to level the playing field for California truckers. The most threatening air quality issues that separate California from the rest of the nation are: 1) a single-state fuel, 2) implementation of Proposition 65, and 3) proposed labeling of diesel fuel as a toxic air contaminant.

SINGLE-STATE FUEL

Since the introduction of the California-only diesel fuel in 1993, diesel users have been forced to operate with uncertainty, market instability, and severe price spikes seen only in the golden state. California is no longer a free market for diesel fuel. The state has sacrificed competition in oil refining by requiring an exotic fuel that only a handful of companies can produce. All but 11 of the 30 refineries once competing in California were forced out of the market when the California-only regulations for diesel fuel were adopted. The remaining refineries are owned by five companies.

By limiting the number of producers, California has created a fuel island for purchase-but not for use. The State permits use of noncomplying fuel in the State by national and international carriers. A heavy duty truck operates up to 1800 miles with-out refueling, so that buying fuel outside California and burning it in the State is not only possible but now is the norm: Diesel sales in California dropped significantly when the cost differential jumped so high. Shippers choose their freight provider primarily by a single factor...cost per mile. The shipper is not concerned with Cali-fornia-only market problems.

It is no coincidence that California has the oldest fleet in the nation and recently the worst new truck sales in history. The California Air Resources Board claimed a 7 percent reduction in oxides of nitrogen from the introduction of CARB fuel. Compared with an x-year-old vehicle, a new truck reduces those pollutants by 70 percent. If the playing field for freight were level, trucking companies would have purchased the newer technology and the benefits to the air would be enormous. Instead, evasion of the state fuel is rampant and California businesses are forced to delay equipment purchases to make up for operating at a competitive disadvan-tage. The result? Both methods of reducing NO_x are slower and less effective than forecasted.

PROPOSITION 65

Proposition 65, otherwise known as the Sate Drinking and Water Act, is another threat to the California trucking company. The Office of Environmental Health Hazard Assessment, a part of the California Environmental Protection Agency, is respons- ible for implementation of the Safe Drinking and Water Act. Proposition 65 requires the governor to publish a list of chemicals known to the State of California to cause cancer, birth defects or other reproductive harm. Only the chemicals on the list are regulated under law. Businesses that produce, use, release, or otherwise engage in activities involving those chemicals must comply with requirements for clear and reasonable warnings and prohibition from

discharging into drinking water.

Diesel exhaust was added to the governor's list In 1991. Federal EPA and other States do not find diesel exhaust cancer-causing and have no requirements for regulating diesel exhaust. In California, though, more than 70 carriers have been sued for emitting diesel exhaust while driving on the state's roads and not giving pedestrians clear and reasonable warning. The same carriers held hostage by California-only fuel are held liable for using it. The California Air Resources Board certifies all on-road engines for use in California and every formulation of diesel fuel used in the State.

The California Air Resources Board certifies more than 20 different formulations (mixtures) of diesel fuel for sale in California. Diesel exhaust cannot be eliminated, but constituent parts of the mixture can be reduced. By inaccurately listing diesel exhaust as a chemical, future technologies with zero emissions would be considered cancer-causing to the State. For example, a fuel truck fueled by diesel and emitting only water and carbon dioxides as constituents in the exhaust would be considered by the State of California to cause cancer because the exhaust, not its specific chemical components, is what has been listed.

DIESEL AS A TOXIC AIR CONTAMINANT

Beyond Proposition 65, OEHHA has proposed to list diesel exhaust as a toxic air contaminant. No other state considers diesel exhaust a toxic air contaminant. If diesel exhaust is labeled by the State as a toxic air contaminant, the public must be notified that the industrial fuel used for commerce worldwide causes cancer. Then, trucking companies in California would be liable for citizen suits claiming any exposure becomes a threat to the public health. Additional regulations will be required for employees exposed to diesel exhaust and associated California-only costs.

The economic impact of California-only regulations places regulatory burden on businesses in California, causing companies to relocate to more business-friendly bordering States to avoid excess regulation. A method to measure the effectiveness of government regulations is necessary to avoid unnecessarily penalizing those companies attempting to comply with environmental regulations

LOCOMOTIVE EXHAUST EMISSIONS TECHNOLOGY NEEDS EPA EXHAUST EMISSIONS REGULATORY IMPACTS

R. Cataldi
Association of American Railroads

The U.S. Environmental Protection Agency is close to finalizing rules for locomotive emissions that will affect nearly all locomotives owned by the major railroads after the year 2000. Not only will the OEMs have to meet typical mobile source standards on their newly manufactured engines; but the railroads will have to retrofit most of their existing fleets to meet emissions limits that reduce oxides of nitrogen by approximately 35% from the current unregulated fleet.

The proposed rule (A Notice of Proposed Rulemaking or NPRM was published by EPA on January 31, 1997) would have an immediate impact on locomotive engine manufacturers as well as almost everyone who performs heavy overhauls on locomotive engines. These engines will then have to be maintained properly throughout their lives. Proper maintenance will not necessarily be defined by the locomotive operator — a railroad — but by whoever holds the EPA certificate on the engine family.

The proposed rule would separate locomotives into four groups:

- "Tier 0" where the engine was originally manufactured from January 1, 1973 through December 31, 2001
- "Tier I" where the engine was originally manufactured from January 1, 2002 through December 31, 2004
- "Tier II" where the engine was originally manufactured on January 1, 2005 or later
- Pre-Tier 0 engines, which are not covered by the rule unless the owner upgrades them to Tier 0 standards

The proposed gaseous and particulate matter emisssions standards for Tiers 0, 1, and II are given in Table 1, with weighting factors for determining the emissions level shown in Table 2. Every locomotive must meet both the line-haul and switcher standards. Passenger locomotives would be weighted differently than freight locomotives, as shown. Smoke standards are given in Table 3. EPA developed these standards by calculating reductions in oxides of nitrogen (NO_x) of 33%, 45% and 60% respectively for Tiers 0, I, and II compared to mid 1990s national fleet averages. Tiers I and II have some tightening of particulate matter, hydrocarbons, and carbon-dioxide compared to the baseline, while Tier 0 locomotives do not have to make any reductions in these emittants. The smoke standards are similar to those for truck and off-highway engines.

It seems likely that OEMs and other suppliers will be able to develop kits to meet the retrofit needs. Further it is likely that the OEMs will have little difficulty meeting the new engine Tier I standards that will go into effect in 2002. The Phase II standards that go into effect January 1, 2005 are where the challenge arises. The Phase II limits include 5.5 g/hp-hr NO_x and 0.2 g/hp-hr particulate matter. While onhighway engines will be meeting more stringent standards before 2005, those engines are installed in vehicles which have an order of-magnitude smaller power density and considerably more air cooling potential than locomotives have. Both EPA and the OEMs believe that present technology will only bring locomotive engines down to approximately 6.5 g/hp-hr NO_x. Also, the test procedure for on-highway engines is quite different from the proposed locomotive test procedure. While it is difficult to compare the two tests, in general the locomotive test procedure is more stringent.

Besides high power density and limited cooling potential, locomotive engines have tight overhead clearances which limit stack lengths to mere inches leave little room for exhaust treatment devices. This does not mean that exhaust

treatment cannot be done; but considerable engineering would be necessary to make it fit.

We expect the OEMs to use the normal bag of tricks on engine design features to meet emissions limits, especially for the "Phase I" standards. Improved fuel injection systems tied to electronic engine control is probably the key to any future engine design. The turbocharging will likely be improved upon to match the engine's needed fuel-air mixture needs better, while intercooler-aftercooler equipment will be further refined from today's levels to lower the inlet air temperature.

The locomotive regulations will allow the higher sulfur off-highway fuel that railroads currently use. So, the OEMs need to plan for approximately 0.2% sulfur in the fuel while meeting the 0.2 g/hp-hr particulate limit.

EPA recognized that some engine models may not make the standards without massive redesign that would be unreasonably expensive, so they proposed that manufacturers can average, bank, and trade emissions credits to meet the standards on a fleet-wise basis. This could be especially useful for Tier 0 locomotives that were never designed to meet any emissions standards and which are all over the map on their baseline emissions levels. "Banking" means that a manufacturer can earn a credit for having an engine family under the emissions limits in one year and hold those credits for up to 3 years and then offset any engine family that exceed the limits. "Trading" allows manufacturers to give their credits to other manufacturers. Compensation is set by the marketplace and is of no concern to EPA.

Locomotives will have to be "remanufactured" (using a certified "kit") at the time that the owner performs an overhaul on the diesel engine. For Tier 0, this will go into effect on January 1, 2000 for locomotives originally manufactured starting on January 1, 1994 and January 1, 2002 for locomotives originally manufactured from 1973 through 1993. No owner is required to do these remanufacturing events any sooner than he would normally perform an overhaul. EPA expects that nearly all linehaul locomotives will be remanufactured by the end of 2006. Switchers will take much longer, though no one knows today how long it will take to bring all of them into compliance.

Any entity that wishes to may obtain a certificate. The likely cast of certificate holders (EPA calls them "remanufacturers") will include the OEMs (General Electric Transportation Systems, General Motors Locomotive Group, and Caterpillar); some aftermarket suppliers; some non-railroad, non-OEM locomotive engine rebuilders; and possibly one or more railroads. The certificate basically covers an engine family that the remanufacturer defines by engine specifications and that has a certified level of emissions determined through an EPA "Federal Test Procedure" or FTP. The remanufacturer defines a "kit" that is installed in the engine family by an installer at the time of a top-end overhaul. The installer may be a railroad, the remanufacturer, or a third party engine shop. While we expect that the installer will not have to hold the EPA certificate, he must obtain the use of it for every Tier 0 and later engine he overhauls starting in 2000.

What will constitute a "kit" could vary quite a bit. It must include installation instructions and instructions for inspection, maintenance, and repairs for the life of the engine. Some kits may include parts, while others may include specific parts lists for the installer to buy. Other remanufacturers may take a less specific approach to the parts and leave it to the installer to select parts and components that meet performance parameters or there may be a list of acceptable parts from different suppliers. The marketplace will determine the contents of kits. Installers can expect to pay something to remanufacturers for the license to use the certified kits. Again, the marketplace will determine the price. Remanufacturers will spend hundreds of thousands of dollars per engine family to develop and certify their kits and they will assume considerable liability for auditing installers, conducting in-use testing of the engines, and solving any in-use problems that are identified by in-use tests. So a remanufacturer will expect to recover that investment either in license fees or in the sale of parts.

EPA's NPRM includes an estimate that the incremental cost of the license, parts, and labor

for Tier 0 remanufacturing will be approximately $80,000 per locomotive. This is a cost that would be incurred at the time of an engine overhaul and assumes the incremental is above and beyond what it would cost to replace all of the engine power assemblies and fuel injectors and resetting of engine timing. For the engines that will be built new to meet the Tier II standards, EPA estimates that there will be no incremental cost passed on to the railroads.

EPA didn't give much documentation of how they reached the $80,000 and $0 figures, citing proprietary information obtained from the OEMs. In extreme examples, some "kits" may involve nothing more than resetting fuel injection timing at the time of a heavy overhaul while others could entail replacing mechanical engine governors and fuel injection equipment with electronically controlled equipment; rematching turbochargers; changing the design of pistons, cylinder liners, and heads; adding additional radiators; and repiping the entire cooling system. Even without a license fee, the latter kit would result in an incremental cost well over $80,000, while the former kit would cost nothing at the time of an overhaul other than the license fee.

Remanufacturers will have to conduct market research to determine what the railroads want in these kits. An option is to make a fairly advanced technology kit that does not cause any fuel penalty and that improves engine performance and reliability. Such a kit would cost more, but presumably it would have a positive rate-of-return on the investment. Another option for the same engine family might be an inexpensive kit that causes a fuel penalty and does nothing to improve performance and reliability.

At about three-quarters of what EPA calls the "useful life" of engines, the manufacturers/ remanufacturers will be required to conduct in-use FTP emissions tests of a small sample of engines. If the engines do not exceed the emissions levels that the remanufacturer specified in his certification, the engines "pass" the test. If they exceed those levels, the remanufacturer must determine the reason for it. If the reason is because the owner or operator of the locomotive did not follow the remanufacturer's inspection, maintenance, and repairs recommendations, the remanufacturer is not liable for the results (and neither is the owner/operator, as long as he used reasonable judgement in maintaining his locomotive). If the problem is due to the design of the kit or a part or to workmanship of a part or component, the remanufacturer must develop a fix for the problem. These fixes would be agreed upon between the remanufacturer and EPA and would be provided to the railroads with the expectation that the fixes would be done during regularly scheduled maintenance. EPA has not proposed mandatory recalls with locomotives taken out of service.

Useful life was defined as 7.5 times the horsepower rating to obtain megaWatt-hours. A 4000 horsepower locomotive would have a useful life of 30,000 megaWatt-hours. Three quarters of that would be 22,500 megaWatt-hours. For Tier 0 locomotives lacking Watt-hour meters, the useful life would be 750,000 miles.

There is an "antitampering" provision in the NPRM that is common to all EPA rules. If a railroad or other engine maintainer knowingly changes the emissions characteristics of the engine (through changes in engine set-up, removing emissions control devices, or replacing a part with another part known to alter the emis-sions characteristics), the maintainer has com-mitted a Federal crime. The civil penalties were not spelled out in the NPRM, but will probably be the same as for other mobile sources.

The anti-tampering provision and the remanufacturer's maintenance instructions will change locomotive maintenance. These rules apply to newly manufactured locomotive engines too.

The certificate holders will provide recommended inspection and maintenance intervals and will recommend what specific parts should be replaced or requalified at these intervals. The NPRM does not say that the railroad or other engine maintainer must follow those recommendations exactly. The railroad or maintainer may use its own experienced judgement, as they do today. Unacceptable maintenance is knowingly installing parts that affect the emissions level. That would include parts that might even "improve" emissions.

TABLE 1. SUMMARY OF EPA PROPOSED LOCOMOTIVE EMISSIONS LIMITS
(Units are grams per brake horsepower-hour)

Type of Service:	Line-Haul Duty Cycle			Switcher Duty Cycle		
Year Originally Built:	1973-99	2000-04	2005-??	1973-99	2000-04	2005-??
Tier:	0	I	II	0	I	II
Hydrocarbons HC	1.0	0.55	0.3	2.1	1.2	0.6
Carbon Monoxide CO	5.0	2.2	1.5	8.0	2.5	2.4
Oxides of Nitrogen Nox	9.5	7.4	5.5	14.0	11.0	8.1
Particulate Matter PM	0.6	0.45	0.2	0.72	0.54	0.24

Notes:
1. These are the limits for engines operating on diesel fuel oil. Different limits are proposed for CO from natural gas engines. Aldehyde limits are proposed for alcohol-fueled engines.
2. EPA has proposed individual throttle position limits for each emittant in addition to the duty cycle weighted limits.

TABLE 2. EPA PROPOSED ENGINE DUTY CYCLES FOR CERTIFICATION

Duty Cycle:	Freight	Passenger	Switcher
Throttle Notch			
Idle	38.0	47.4	59.8%
1	6.5	7.0	12.4
2	6.5	5.1	12.3
3	5.2	5.7	5.8
4	4.4	4.7	3.6
5	3.8	4.0	3.6
6	3.9	2.9	1.5
7	3.0	1.4	0.2
8	16.2	15.6	0.8
Dynamic Brake	12.5	6.2	0.0

TABLE 3. SMOKE STANDARDS[1]
(Units are % Opacity)

Number of stacks	Exhaust Diameter	Examined Plume Section	Steady-State	30-sec Peak	3-sec Peak
Single	12" or less	Total	20	35	50
	More than 12"	Each 6" Segment, or	10	15	20
		Total[2]	30	40	55
Multiple	12" or less	Any One	20	35	50
		Sum of Stacks	30	40	55
	More than 12"	Each 6" Segment, or	10	15	20
		Total for any One	30	40	55
		Sum of Stacks	40	50	60

SHIP AIR EMISSIONS: ESTIMATION AND REGULATION

J.J. Corbett and P.S. Fischbeck
Carnegie Mellon University

Diesel engines power 95% of the world's oceangoing ships. The global and regional impact of air pollution from ship engines not been addressed until quite recently. The fact that international ship emissions contribute approximately 2% of carbon emissions from human activity has veiled their greater contribution to global pollution of nitrogen and sulfur. Ship engine emissions contribute approximately 14% of nitrogen emissions from all fossil fuel, and approximately 16% of sulfur emissions from all petroleum sources (5% of sulfur from all fossil fuels including coal). Current policy efforts by International Maritime Organization (IMO) provide the first attempts to limit air pollution from ships involved in international trade. This summary presents current work in this area that updates the science available to global change researchers, international policy makers, and industry stakeholders.

INTRODUCTION

Study of air pollution from shipping has typically been limited to its impact on local air pollution in busy ports suffering significant air quality challenges, such as Los Angeles and Yokohama. Additionally, concern has focused on visible emissions until recently. With our growing understanding of the role of aerosols in climate change, it is important to study the scale and geographic pattern of ship emissions globally. Prior to this study, fuel inventories used for generating maps of global areosol concentrations assigned ship emissions to land masses where the ships are fueled – thus failing to take appropriate account of ship emissions. As a result, the information describing the impact of shipping both globally and locally has not been available to policy makers or global change researchers.

Currently, many U.S. states regulate opacity (smoke) emissions from international and domestic ships while transiting coastal or port waters. However, nitrogen and sulfur pollution from ship propulsion remains uncontrolled globally. The IMO plans to vote on proposed limits during their fall 1997 diplomatic session and the U.S. Environmental Protection Agency will develop regulations following international action. Similar to other precedent-setting environmental policy measures, the debate over ship air pollution has suffered from the inadequacy of available science regarding global ship emissions. Without an analysis of global ship emissions and their relative importance compared to other sources, policy makers are limited to a handful of port and regional studies that at their best evaluate the efficacy of regulation locally, and at worst skew the discussion by choosing small scales (in horizontal and vertical extent) to argue insignificant impacts from ship propulsion emissions.

Ship emissions are significantly larger than previously considered – on the order of domestic nitrogen and sulfur emissions inventories from the largest emitting nations. Moreover, these emissions are not constrained to remote ocean regions or distributed homogeneously; rather ship emissions are concentrated along well-defined trade routes between highly populated regions where regional air quality is a prime concern. In assessing the global inventory of ship emissions, we used current emission test data for ships. As shown in Table 1, approximately 55% of the registered vessels use slow speed diesel propulsion. Medium speed diesel engines power another 40% of the world's registered ships, either in diesel-gear or diesel-electric propulsion. All other types of ship propulsion account for 5%, the

most common non-diesel propulsion being steam turbine technology.

Table 1. World Ship Engine Profile

Engine Types	Military Fleet	Commercial Fleet	Total Fleet
Slow Speed Diesel	1,289 (7%)	56,628 (66%)	58,287 (55%)
Medium Speed Diesel	14,940 (76%)	27,758 (32%)	41,894 (40%)
Steam and Others	3,417 (17%)	1,820 (2%)	5,673 (5%)
Total Vessels	19,646	86,206	105,854

We estimated the global annual nitrogen and sulfur emissions from ships to be 3.2 million metric tons and 4.2 million metric tons, respectively. Not only are these values equivalent to nitrogen and sulfur emissions from the largest energy-consuming nations; they represent more than 14% of nitrogen emissions from global fuel combustion sources and more than 16% of sulfur emissions from world petroleum use.

COMPARISON AND POTENTIAL IMPACT

Figure 1 compares ship nitrogen emissions with domestic nitrogen emissions reported for several OECD nations and with global inventories. Figure 2 compares ship sulfur emissions with domestic and global sulfur inventories. Worldwide ship nitrogen emissions are equal to 42% of nitrogen emissions from North America, nearly half of the total emissions from the U.S., 74% from OECD Europe, and 1.9 times that of East and West Germany (1) They are equal to 87% of nitrogen emissions from U.S. stationary sources and equal to of those from U.S. mobile sources. Ship sulfur emissions equal 35% of sulfur emissions from North America, 43% of total sulfur emissions from the U.S., 53% from OECD Europe, and 178% from Germany. Most of the continental sulfur emissions are from stationary sources.

Ship emissions account for 14% of nitrogen emissions from fossil fuels (2) and 16% of all sulfur from petroleum uses. Ship sulfur accounts for 5% of sulfur emitted by all fuel combustion sources. This is equivalent to 10% of sulfur from hard coal combustion and 45% from lignite combustion. Carbon dioxide emissions from ships are only 2% of the 6000 Tg carbon emitted from fossil fuel use (3). Ship engines are thus among the world's highest polluting combustion sources per ton fuel consumed.

Moreover, these emissions are not constrained to remote ocean regions or distributed homogeneously; rather ship emissions are concentrated along well-defined trade routes between highly populated regions where regional air quality is a prime concern. This was confirmed by developing a ship emission density profile using the *Comprehensive Ocean-Atmosphere Data Set (COADS), Standard 1a*, from the National Center for Atmospheric Research (NCAR) and the National Oceanic and Atmosphere Administration (NOAA) (4). "The Comprehensive Ocean-Atmosphere Data Set (COADS) is the most extensive collection of surface marine data available for the world ocean over the past century and a half" (5). *COADS Standard 1a* is a subset of one of the longest continuous climate records in existence, begun in 1854 by international agreement of the world maritime nations. The *Standard 1a* data set summarizes on a 2° latitude by 2° longitude (2° x 2°) resolution ship location and weather observations taken by merchant and naval mariners covering the period of 1980-93. By dividing the global sulfur emissions by the traffic density derived from COADS, we characterized the emissions density geographically.

While we have not yet modeled transport distances explicitly for ship emissions, initial review of the literature suggests "that the median transport velocity is about 400 km per day. Emitted SO_2 and NO and their atmospheric oxidation products are thought to have mean residence times of ~1 to ~3 days, indicating mean transport distances of ~400 to

~1200 km" (6). More recent studies demonstrate that while the characteristic transport distance over the North Atlantic region depends on direction, "the minimum value of the average is 900 km and the minimum values for the 10th and 90th percentiles are 400 and 1,700 km" (7). Based on this literature, 400 km appears to be a lower-bound transport distance in regions where the wind direction may transport ship emissions toward land..

POLICY ISSUES

Global emission limits proposed by the IMO may soon be enacted. NOx regulations will apply only to new ships or major ship conversions on or after 1 January 2000. For a yearly fleet replacement rate of 1.5% of 106,000 ships (8) after the year 2000, measurable reduction in global nitrogen emissions from ships will not occur for many years. For NOx controls that reduce emissions by 30% to 50%, IMO regulations would reduce emissions by less than 1% per year. Current IMO language limits fuel-sulfur levels to 5% (9). This provides little reduction if any, and practically codifies the status quo, since International Organization for Standardization fuel standards set a 5% sulfur limit in 1987. However, both of these global limits are valuable, because adoption of the IMO regulation means multinational consensus on the principles of emission control. Under IMO criteria, regional efforts must include trade-off considerations to determine the utility of more stringent regulation.

Two policy domains must be considered: (i) nations providing international marine fuel to ships; and (ii) nations registering commercial vessels. International fuel provided by the top 20 nations accounts for 82% of global ship emissions, using the Energy Information Agency international marine-fuel data (10). The top 20 of 206 nations with registered vessels account for 56% of the world ships. Ships registered to these top 20 nations emit between 55% and 65% of global ship nitrogen and sulfur emissions. However, ten of these nations are considered foreign registers (sometimes referred to as "flags of convenience"), since vessel ownership is in another nation. Foreign flag registry has increased recently (8). In other words, emissions from ships attributed to nations of registry would be significantly different than emissions from ships attributed to nations of ownership. Strict enforcement policies aimed at registering nations may inadvertently shift which foreign nation registries are selected by vessel owners, instead of achieving emission reduction goals.

Another problem is that open-market interests and treaty commitments may limit strict emission control strategies for ships. Moreover, in most cases, cargo transport by ship produces lower emissions than other modes of transport. Without attention to these policy issues, the potential exists to affect the flow of trade in unplanned ways (e.g., by creating incentives for developing port areas to adopt less stringent requirements than current shipping destinations). This could increase environmental emissions from cargo transport, especially if modes with higher emissions per ton cargo (such as rail or truck) become substitutes for ship transport.

However, the policy horizon is even more complex than these characterizations suggest. Individual nations and regional interests (such as the U.S. EPA and the Baltic states) can be expected to adopt more stringent emission controls than the IMO language provides. Motivation for this will be the contribution from ship emissions to regional air quality problems, including other pollutants such as particulate matter. Reducing ship propulsion emissions with minimum trade-off in engine operation, cost, etc., can best be implemented in new engine design. With the low replacement rate for ships and ship engines, regulations limiting pollution from existing engines may be developed. Developing effective control strategies will require that three criteria are balanced: 1) Technologies controlling emissions need to preserve fuel economies; 2) Policy strategies must ensure that controls can be implemented via international companies without negatively affecting trade; and 3) Compliance and/or

enforcement of emission controls must be verifiable by those communities most affected by pollution from ship traffic

CONCLUSIONS

International ship nitrogen and sulfur emissions are larger than previously considered, with estimates on the order of the largest nations' domestic emissions. Characterizing these emissions geographically, they are concentrated in the northern hemisphere, particularly along heavily traded routes. Current IMO policy provides an extremely important international framework for control of ship emissions, although the current regulatory provisions may not reduce global emissions until well into the 21st century, except in areas of stricter control. Increased policy focus will result from improved understanding of the science of marine diesel emissions, although it may be limited by economic and environmental trade-offs. Manufacturers and operators of large marine engines need to maintain the dialogue with pollution scientists and policy makers to ensure that emissions control strategies for ships balance the complex criteria motivating (and constraining) action.

This DEER paper (and presentation) summarizes the following article: J. J. Corbett, P. S. Fischbeck,*"Emissions From Ships"*,. Science, Volume 278, Number 5339, 31 October 1997, pages 823-824.

REFERENCES

1. OECD, "OECD Environmental Data: Compendium 1995" *97 95 16 3* (Organisation for Economic Co-Operation and Development (OECD), 1995).

2. Middleton, P., in *Composition, Chemistry, and Climate of the Atmosphere* H. B. Singh, Ed. (Van Nostrand Reinhold, New York, NY, 1995) pp. 88-119.

3. Khalil, M. A.K.., Rasmussen, R. A., in *Composition, Chemistry,and Climate of the Atmosphere* H. B. Singh, Ed. (Van Nostrand Reinhold, New York, NY, 1995) pp. 50-87.

4. Woodruff, S., (National Oceanic and Atmospheric Administration (NOAA), and National Center for Atmospheric Research (NCAR), Boulder, CO, 1996).

5. Woodruff, S. D., Lubker, S. J.,. Wolter, K., Worley, S., J., Elms, J. D.,. *Earth System Monitor* 4 (1993).

6.. Schwartz, S. E., *Science* 243, 753-763 (1989).

7. Benkovitz, C. M., et al., *Journal of Geophysical Research* 99, 20,725-20,756 (1994).

8. UNCTAD, "Review of Maritime Transport 1994" *TD/B/CN.4/49* (United Nations, 1995).

9. IMO, M. 39/6, Ed. (International Maritime Organization, London, UK, 1996).

10. Maloney, M. J., (Energy Information Administration (EIA), Washington, D.C., 1996).

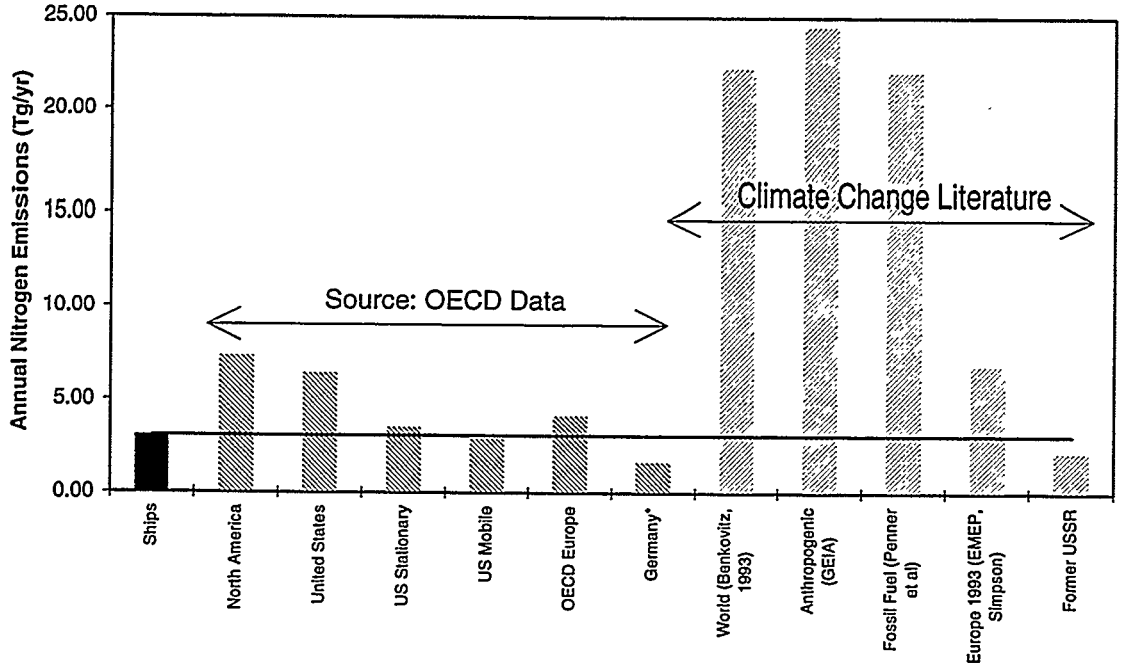


Figure 1. Comparison of Ship Nitrogen Emissions with Other Global Source Inventories

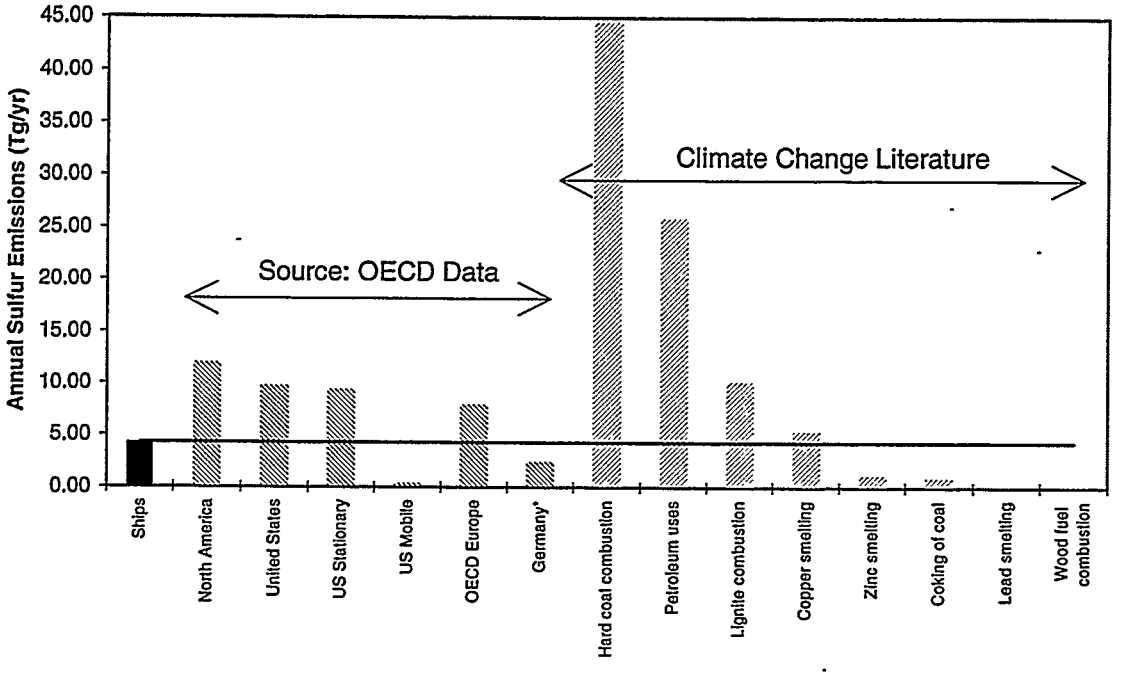


Figure 2. Comparison of Ship Sulfur Emissions with Other Global Source Inventories

SESSION II

Human Health Effects - Diesel Exhaust

Chairman: Joe Mauderly
Lovelace Respiratory Research Institute

DIESEL ENGINE CONTRIBUTIONS TO ATMOSPHERIC FINE PARTICLE CONCENTRATIONS

J.J. Schauer and G.R. Cass
California Institute of Technology

INTRODUCTION

Urban and regional air pollution problems in densely populated areas arise from the combined effects of the emissions from hundreds of different types of air pollution sources. Emissions from stationary fuel combustion sources combine in the atmosphere with the emissions from motor vehicles, including diesel engine exhaust. To these combustion source effluents are added the emissions from widely dispersed small-scale activities in the community such as emissions from food cooking, and the generation of paved road dust as vehicle traffic moves over the streets. As the emissions from these sources mix in the atmosphere and are transported downwind, atmospheric chemical reactions take place. The secondary air pollutants that are formed by atmospheric chemical reactions include secondary particulate sulfates, nitrates and organics that are formed from the low vapor pressure reaction products of directly emitted pollutant gases. This mixture of directly emitted particles and gases, combined with their secondary atmospheric reaction products can adversely affect human health and damage materials. Fine particle air pollutants scatter and absorb light and thus lead to visibility reduction.

In this paper, methods for the characterization of fine particle concentrations in the atmos-phere and fine particle emissions from sour-ces first will be described. Then air quality modeling methods will be discussed that can be used to determine how the various emissions sources present in a city combine to produce the observed airborne particle mix-ture. From these models, the contribution that diesel engine exhaust makes to ambient fine particle concentrations can be determined.

ATMOSPHERIC MONITORING

Fine particle concentrations in the atmosphere can be characterized at community air monitoring stations using the methods described by Gray et al. (1). Fine particle samples collected downstream of cyclone separators are analyzed to determine fine particle mass concentration, organic carbon and elemental carbon (2), ionic species including sulfates, nitrates, chlorides, ammonium ion and sodium, and trace elements by X-ray fluorescence. From these measurements, a material balance can be constructed on the chemical composition of the atmospheric particle mixture that sheds considerable light on the sources that contribute to the atmospheric samples. Of particular importance to the current discussion, the black elemental carbon particle concentrations in cities are often dominated by emissions from diesel engines and thus an ability to account for black carbon particles in the atmosphere is often a key test of various air quality modeling methods that might be applied to study diesel engine exhaust in the atmos-phere. Atmospheric fine particle samples also can be extracted in organic solvents, and from these solvent extracts, the individual organic compounds present in the particles can be determined by gas chromatography/mass spectrometry (3). Among the organic com-pounds that can be quantified are the series of the hopanes and steranes. These are petroleum biomarkers that are present in motor vehicle exhaust that are useful in tracking the quantity of motor vehicle exhaust aerosol in the atmosphere.

MEASUREMENT OF EMISSIONS FROM SOURCES

Use of mathematical models that can reveal

source contributions to atmospheric fine particle concentrations requires that the characteristics of the particle emissions at the most important urban sources be understood. Particulate matter emissions from combustion sources are difficult to measure, in part because organic compounds that form particulate matter at ambient temperature and pressure are often still in the vapor phase at elevated stack temperatures and thus will pass through a particulate matter filter if care is not taken to bring the stack gases to ambient conditions before sampling. The solution to this problem is to employ a dilution source sampling system that cools the source samples by mixing with cooled purified dilution air prior to filtration. Such a source sampling system that can be used to measure the emissions from both stationary and mobile sources has been described by Hildemann et al. (4). This source sampling system has been used to characterize the mass emissions rate and chemical composition of the fine particles released from catalyst and non-catalyst equipped automobiles, heavy duty diesel trucks, oil-fired boilers, natural gas home appliances, meat cooking operations, fireplace combustion of wood, asphalt roofing tar pots, cigarette smoke, paved road dust, plant fragments, tire dust, and brake lining wear dust (5), as well as the particle size distribution of the emissions from many of these sources (6).

Fine particle samples collected during the source testing program of Hildemann et al. (5) have been subjected to solvent extraction and have been analyzed by GC/MS to determine the mass emissions rate of hundreds of or-ganic compounds that are emitted from the source types mentioned above (7-15). Many of these organic compounds are diagnostic for the presence of the emissions from spe-cific sources and can be used to determine source contributions to atmospheric particle concentrations by organic molecular tracer techniques, as will be explained shortly.

MODELING THE EFFECT OF EMISSIONS SOURCES ON AMBIENT AIR QUALITY

Two approaches can be employed to compute the contribution that specific emissions sources make to the atmospheric fine particle burden. In the source-oriented modeling approach, an atmospheric transport model is used to track pollutant emissions through a simulation of atmospheric fluid motion (and possibly chemical reaction) as the pollutants are transported from their sources to community air monitoring sites. To use this method, a grid system is first laid down over the urban area of interest. The spatial and temporal distribution of fine particle emissions from each of the major emissions sources to be studied is inventoried within each of these grid cells. Then these particle emissions are released into a simulation of atmospheric transport and dilution that is driven by historically measured meteorological data. Pollutant concentrations predicted to result from this atmospheric transport process are then compared to ambient measurements made at community air monitoring stations. Examples of diesel engine contributions to atmospheric carbon particle concentrations in the 1980's in the Los Ange-les area have been computed by Gray and Cass (16). Related transport models also have been developed that can predict the source contributions to the individual organic com-pounds present in the atmospheric particles (17) and that can predict the evolution of the size distribution of the chemical composition of the atmospheric fine particle complex (18,19).

In the second modeling approach, particulate organic compounds that act as tracers for the presence of the effluent from particular sources are used to determine the relative importance of the many sources that contribute to an atmospheric fine particle sample. Source profiles, first, are constructed that describe the relative distribution of organic compounds plus silicon, aluminum and elemental carbon in the direct particle emissions from the urban sources tested by Hildemann et al. (5) and Rogge et al. (7-15). Then, the best

linear combination of those source profiles required to reconstruct the distribution of organic compounds measured in atmospheric particle samples is determined by least squares regression techniques (20). From this analysis, the absolute magnitude of up to nine different source types that contribute to the atmospheric fine particle burden can be dis-tinguished, apart from the sulfates, nitrates and ammonium ion that are present in the particle samples due to gas-to-particle con-version processes in the atmosphere (20). An example of such an organic chemical tracer analysis of source contributions to the fine particle concentrations in the Los Angeles area in the early 1980's is given in Figure 1 from the study by Schauer et al. (20). Figure 1 shows that diesel engine emissions were among the most important fine particle sources in Los Angeles at that time. In more recent years as new fuels and engine technologies have been introduced into the vehicle fleet, elemental carbon concentrations in the Los Angeles atmosphere have declined to about half of the concentrations measured during the 1982 period represented in Figure 1, suggesting that diesel engine contributions to ambient fine particle concentrations probably have declined significantly over the last 15 years (21).

REFERENCES

1. Gray, H.A., Cass, G.R. (1986) Characteristics of Atmospheric Organic and Elemen-tal Carbon Particle Concentrations in Los Angeles. Environmental Science and Technology, 20,1567-1582.

2. Birch, M.E., and Cary, R.A., (1996) Elemental Carbon-Based Method for Monitoring Occupational Exposures to Particulate Diesel Exhaust, Aerosol Science and Technology, 25, 221-241.

3. Rogge, W.F., Mazurek, M.A., Hildemann, L.M., Cass, G.R., and Simoneit, B.R.T. (1993) Quantification of Urban Organic Aerosols at a Molecular Level: Identification, Abundance and Seasonal Variation, Atmospheric Environment 27, 1309 1330.

4. Hildemann, L.M., Cass, G.R., and Markowski, G.R., (1989) A Dilution Stack Sampler for Collection of Organic Aerosol Emissions: Design, Characterization and Field Tests, Aerosol Science and Technology, 10, 193-204.

5. Hildemann, L.M., Markowski, G.R., and Cass, G.R. (1991) Chemical Composition of Emissions from Urban Sources of Fine Organic Aerosol, Environmental Science and Technology, 25, 744-759.

6. Hildemann, L.M., Markowski, G.R., and Cass, G.R. (1991) Submicrometer Aerosol Mass Distributions of Emissions from Boilers, Fireplaces, Automobiles, Diesel Trucks, and Meat-Cooking Operations, Aerosol Science and Technology, 14,138-152.

7. Rogge, W.F., Hildemann, L.M., Mazurek, M.A., Cass, G.R., and Simoneit, B.R.T. (1991) Sources of Fine Organic Aerosol. 1. Charbroilers and Meat Cooking Operations. Environmental Science and Technology 25,1112-1125.

8. Rogge, W. F., Hildemann, L. M., Mazurek, M. A., Cass, G. R., and Simoneit, B. R. T. (1993) Sources of Fine Organic Aerosol. 2. Noncatalyst and Catalyst-equipped Automobiles and Heavy Duty Diesel Trucks. Environmental Science and Technology 27, 636-651.

9. Rogge, W.F., Hildemann, L.M., Mazurek, M.A., Cass, G.R., and Simoneit, B.R.T. (1993) Sources of Fine Organic Aerosol. 3. Road Dust, Tire Debris, and Organometallic Brake Lining Dust: Roads as Sources and Sinks. Environmental Science and Technology 27, 1892-1904.

10. Rogge, W.F., Hildemann, L.M., Mazurek, M.A., Cass, G.R., and Simoneit, B.R.T. (1993) Sources of Fine Organic Aerosol. 4 Particulate Abrasion Products from Surfaces of Urban Plants. Environmental Science and Technology 27, 2700-2711.

11. Rogge, W.F., Hildemann, L.M., Mazurek,

M.A., Cass, G.R., and Simoneit, B.R.T. (1993) Sources of Fine Organic Aerosol. 5. Natural Gas Home Appliances. Environmental Science and Technology 27, 2736-2744.

12. Rogge, W.F., Hildemann, L.M., Mazurek, M.A., Cass, G.R., and Simoneit, B.R.T. (1994) Sources of Fine Organic Aerosol. 6. Cigarette Smoke in the Urban Atmosphere. Environmental Science and Technology 28,1375-1388.

13. Rogge, W.F., Hildemann, L.M., Mazurek, M.A., Cass, G.R., and Simoneit, B.R.T. (1997) Sources of Fine Organic Aerosol. 7. Hot Asphalt RoofingTarpot Fumes. Environmental Science and Technology 31, 2726-2730.

14. Rogge, W.F., Hildemann, L.M., Mazurek, M.A., Cass, G.R., and Simoneit, B.R.T. (1997) Sources of Fine Organic Aerosol. 8. Boilers Burning No. 2 Distillate Fuel Oil. Environmental Science and Technology 31, 2731-2737.

15. Rogge, W.F., Hildemann, L.M., Mazurek, M.A., Cass, G.R., and Simoneit, B.R.T. (1997) Sources of Fine Organic Aerosol. 9. Pine , Oak, and Synthetic Log Combustion in Residential Fireplaces. Environmental Science and Technology, in press.

16 Gray, H.A., and Cass, G.R. (1997) Source Contributions to Atmospheric Fine Carbon Particle Concentrations, accepted for publication in Atmospheric Environment

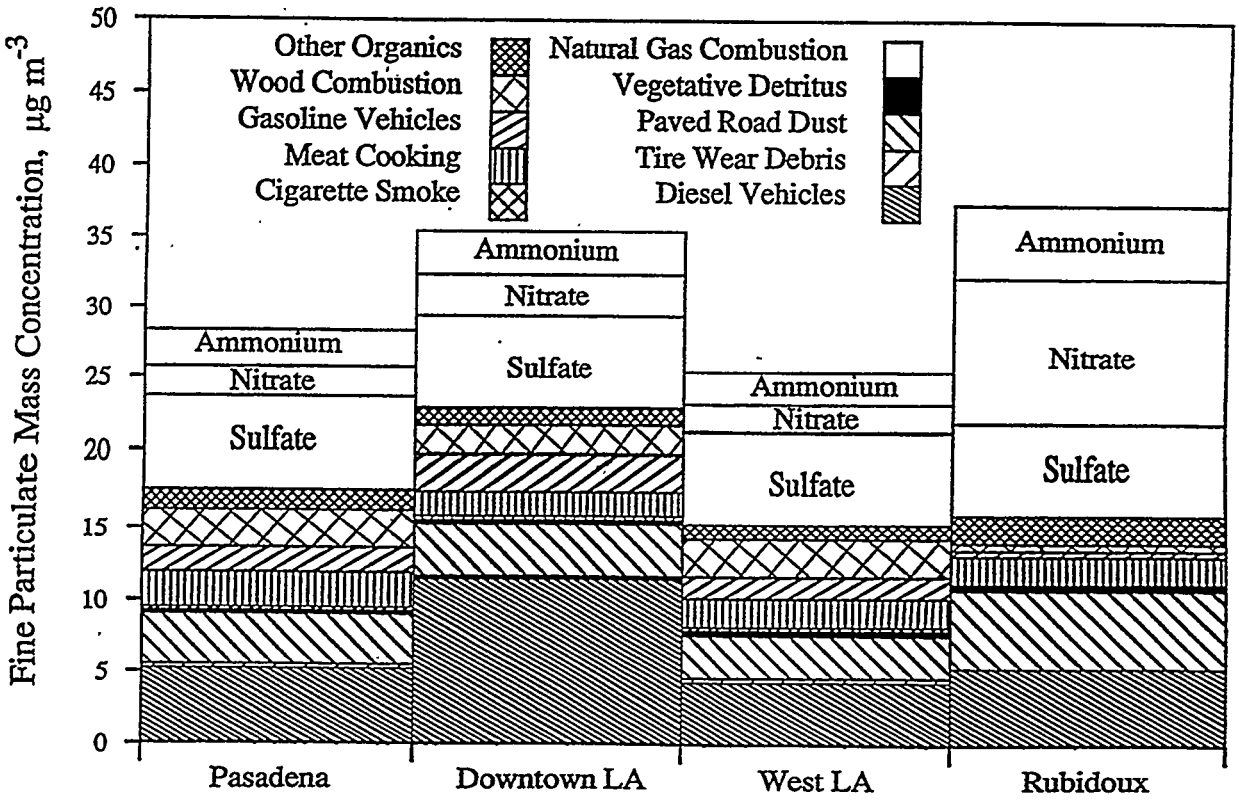
17 Rogge, W. F., Hildemann, L.M., Mazurek, M.A., Cass, G.R., and Simoneit, B.R.T. (1996) Mathematical Modeling of Atmospheric Fine Particle-associated Primary Organic Com-pound Concentrations. Journal of Geophysi-cal Research Atmospheres 101 (D1 4), 19379-19394.

18. Eldering, A., and Cass, G.R. (1996) A Source-Oriented Model for Air Pollutant Effects on Visibility, Journal of Geophysical Research -Atmospheres, 101,19,343-19,369.

19. Kleeman, M.J., Cass, G.R., and Eldering, A. (1997) Modeling the Airborne Particle Complex as a Source-Oriented External Mixture, Journal of *Geophysical Research-Atmospheres, 102, 21,355-21,372.*

20. Schauer, J.J., Rogge, W.F., Hildemann, L.M., Mazurek, M.A., Cass, G.R. and B.R.T. Simoneit (1996) Source Apportionment of Air-borne Particulate Matter Using Organic Com-pounds as Tracers, *Atmospheric Environ-ment, 30, 3837-3855.*

21. Christoforou, C.S., Salmon, L.G., Hannigan, M.P., Solomon, P. A., and Cass, G.R. (1997) Trends in Fine Particle Concentration and Chemical Composition in Southern California, submitted to *Journal of the Air and Waste Management Association.*



Source apportionment of fine mass concentrations — annual average.

Figure 1.

PARTICULATE MEASUREMENT FOR HEALTH EFFECTS ASSESSMENTS

Summary of the Health Effects Institute Workshop on Particle Characterization

R. Sawyer, University of California at Berkeley,
M. Costantini, The Health Effects Institute

Airborne particulate has long been associated with adverse health effects, including death, especially at high concentrations. Historically, concerns for diesel particulate has been primarily associated with carcinogenic compounds attached to the particulate. More recently, epidemiological studies suggest an association between low levels of fine particulate, 2.5 μm or less, and both acute and long term adverse health effects, including mortality and morbidity. While the mechanisms by which fine particulate may cause adverse health effects are not currently understood, it is likely that the size distribution and chemical composition of the particulate are important characteristics. Motor vehicles are important contributors to fine ambient particulate, both as primary (direct) and secondary (indirect) sources. Diesel engines emit fine particulate (soot) and oxides of nitrogen which are precursors to photochemical nitrate particulate. Information on the size distribution and chemical composition of fine particulate, both primary and secondary is limited. The Health Effects Institute recently conducted a workshop on particle characterization with the objective of bringing health effects, atmospheric, and engine researchers together to discuss the needs for particulate characterization and the current understanding of how particles are formed and the methodologies for their characterization.

At the workshop the relation between atmospheric particulate and adverse health effects was reviewed. Hypothesized mechanisms of these effects were summarized. The physical and chemical processes leading to combustion generated particulate were explained. Engine particulate primarily has been measured in terms of mass emission rates, because this is what is currently regulated. From a laboratory study the reduction in mass emissions from some modern diesel engines appears to have been accompanied by a large increase in the numbers of fine particles emitted. The consequences of this change could prove adverse if the health effects turn out to be associated with particle numbers or surface area rather than mass, as suggested by some investigators. Laboratory, on-road, tunnel, and ambient measurements all provide insight into the characteristics of motor vehicle generated particulate. Both emitted and secondary particulate are subject to atmospheric transformations which affect both size distributions and compositions. Health effects researchers face problems in generating and characterizing particulate for animal experiments. The researchers from the diverse fields share common problems in characterizing fine particulate.

The HEI Workshop on Particle Characterization is reported in more detail in the publication: "Formation and Characterization of Particles in Emissions: Summary of the 1996 HEI Workshop," Health Effects Institute Communications Number 5, August 1997, which can be obtained from the Health Effects Institute, 955 Massachusetts Ave., Cambridge MA 02139.

Robert F. Sawyer
University of California at Berkeley

1997 Diesel Engine Emissions Reduction Workshop--Session II
Human Health Effects of Diesel Exhaust

PARTICULATE MEASUREMENT FOR HEALTH EFFECTS ASSESSMENTS--

Summary of the Health Effects Institute Workshop on Particle Characterization

Robert F. Sawyer
Professor, University of California at Berkeley
Research Committee, Health Effects Institute
Maria Costantini
Senior Scientist, Health Effects Institute

San Diego, 28 July 1997

UCB/LBNL COMBUSTION

HEI PARTICLE CHARACTERIZATION WORKSHOP

- Cambridge MA, 3-4 December 1996
- Bring together workers in
  - Health effects
  - Atmospheric chemistry and physics
  - Engine emissions
- Review current understanding, characterization methodology, research needs

UCB/LBNL COMBUSTION

HEI WORKSHOP REPORT

HEI Communications, Number 5, August 1997, *Formation and Characterization of Particles in Emissions: Summary of the 1996 HEI Workshop*

- Current understanding of the health effects of particles and the characteristics that determine dose or effect, *J. Mauderly and G. Oberdorster*
- Particle formation in combustion, *J. Howard and G. Hunter*
- The EPA particle emission testing procedure, *J. Somers*

HEI WORKSHOP REPORT

- Results of characterization of particulate matter and vapor-phase organic compounds from motor vehicles exhaust

  Diesel and gasoline engines, *D. Kittelson, J. Johnson, K. Schindler, M. Maricq, M. Hawkins*

  Motor vehicles in-use, *G. Cass, W. Pierson, S. Cadle*
- Atmospheric aerosol transformation, *S. Pandis*
- Generating particles for experimental Studies, *Y.-S. Cheng, and P. Koutrakis*
- Summary, *R. Sawyer and M. Costantini*
- Issues and research needs for particle characterization

Robert F. Sawyer
University of California at Berkeley

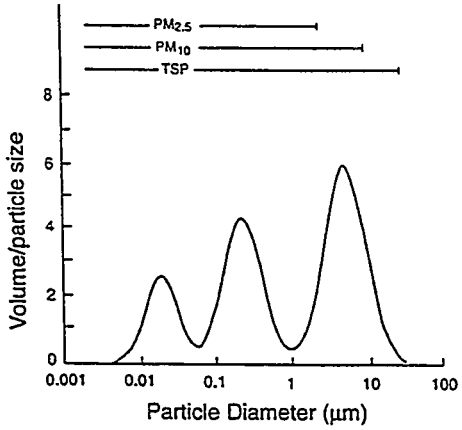
HEALTH EFFECTS OF PARTICLES

- Epidemiology establishes an association between acute and chronic mortality, morbidity and particles
- Mechanism not known
- Important particle characteristics not known--mass, size, surface area, number, chemical composition, physical shape?

UCB/LBNL COMBUSTION

PARTICLE AREA DISTRIBUTION BY AERODYNAMIC DIAMETER,

USEPA Air Quality Criteria Document, 1996



UCB/LBNL COMBUSTION

PARTICLE FORMATION

- Laboratory combustion of pure hydrocarbons, *Howard*
  - Condensation
  - Accumulation
  - Oxidation
  - Fragmentation
- Engine combustion of real fuels, *Hunter*
  - Pyrolysis, condensation, accumulation to carbonaceous particles (soot)
  - Sulfates, ash (metal oxides), adsorbed hydrocarbons
  - Particle burnout--NO_x tradeoff

UCB/LBNL COMBUSTION

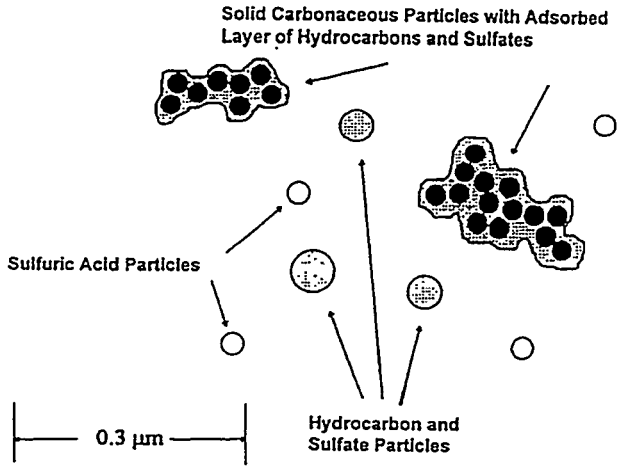
EPA PARTICLE EMISSION TESTING PROCEDURE, *Somers*

- Light duty--FTP cycle
- Heavy duty--transient engine dynamometer
- Off-road--8 mode steady state
- Dilution tunnel, 125°C, fluorocarbon filter
- Total mass

UCB/LBNL COMBUSTION

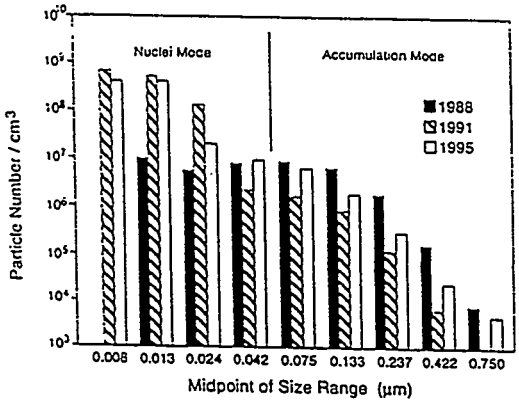
Robert F. Sawyer
University of California at Berkeley

CHARACTERISTICS OF ENGINE EMITTED PARTICLES, *Kittelson*



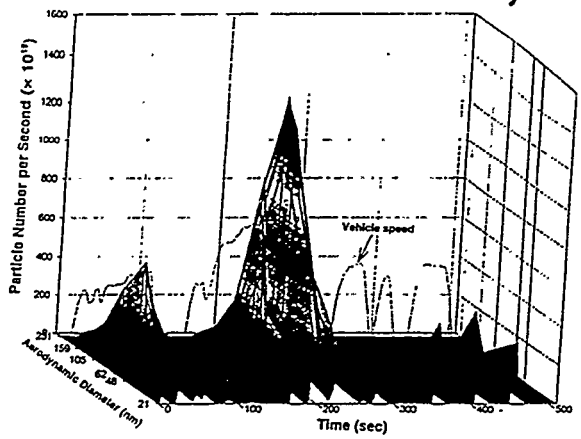
UCB/LBNL COMBUSTION

DIESEL ENGINE PARTICLE SIZE DISTRIBUTION, STEADY STATE TESTING, *Johnston, et al.*



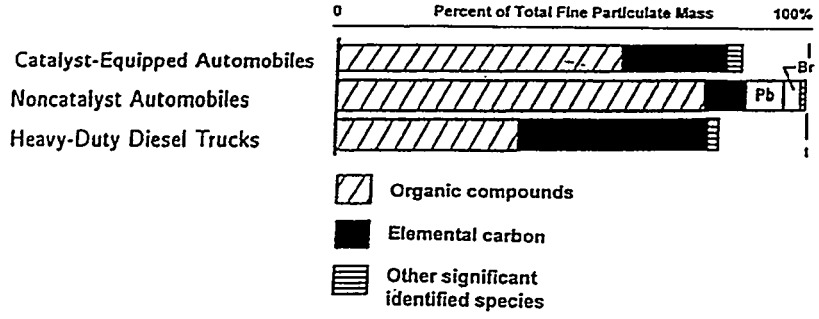
UCB/LBNL COMBUSTION

GASOLINE ENGINE PARTICLE SIZE DISTRIBUTION, BAG 1, TRANSIENT TESTING, *Maricq*



UCB/LBNL COMBUSTION

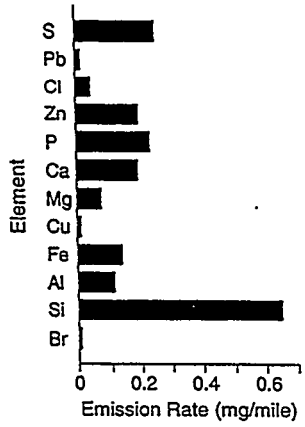
PARTICLE COMPOSITION, DIFFERENT ENGINES, 1980s, *Cass*



UCB/LBNL COMBUSTION

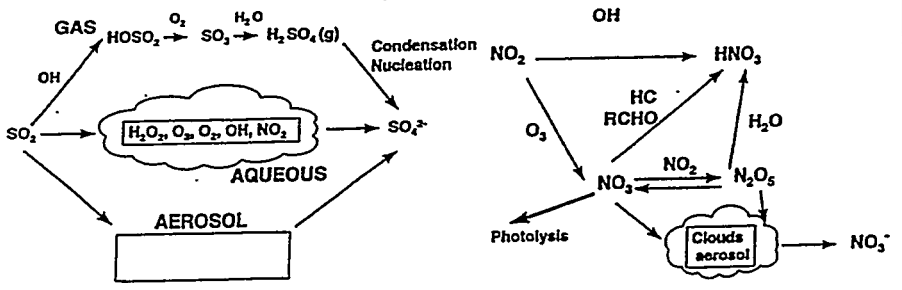
Robert F. Sawyer
University of California at Berkeley

METALS FROM HIGH EMITTING AUTOMOBILES, *Cadle, et. al.*



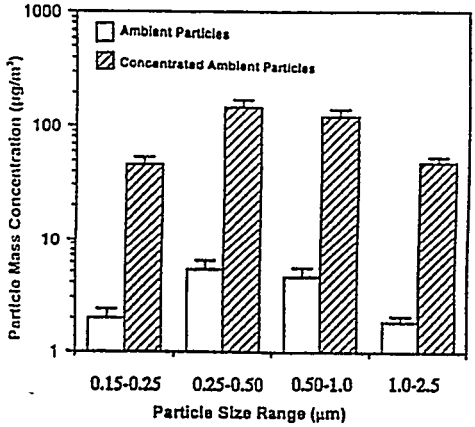
UCB/LBNL COMBUSTION

SULFATE AND NITRATE FORMATION, *Pandis*



UCB/LBNL COMBUSTION

CONCENTRATED AMBIENT PARTICLES FOR ANIMAL EXPOSURES, *Godleski, et al.*



UCB/LBNL COMBUSTION

RESEARCH NEEDS FOR PARTICLE CHARACTERIZATION

- Ambient particles: size distribution, chemical and physical properties
  - to assist epidemiology
  - to identify sources
- Indoor and outdoor particle characteristics
  - to aid in estimating exposure
- Atmospheric generation and transformation processes
  - modification of primary particles
  - formation of secondary particles

UCB/LBNL COMBUSTION

Robert F. Sawyer
University of California at Berkeley

RESEARCH NEEDS FOR PARTICLE CHARACTERIZATION

- Chemical and physical properties by size of emitted particles under real-world appropriate conditions
- Equivalency or relationship of different particle sampling methods
- Equivalency or relationship of different particle sizing methods
- Methods of generating, delivering, and characterizing particles for animal and human clinical studies relevant to real- world conditions

UCB/LBNL COMBUSTION

SOME OBSERVATIONS AND COMMENTS, *Sawyer*

- $PM_{2.5}$ air quality standard may be changed before controls are implemented
- Engineers need to follow particle health research to ensure they are measuring and controlling particles appropriately
- The current EPA specified engine particle measurements are probably not appropriate
- Need particle number--size distributions; chemical and physical characteristics by particle size

UCB/LBNL COMBUSTION

EPIDEMIOLOGICAL EVIDENCE OF HEALTH EFFECTS OF COMBUSTION-SOURCE PARTICULATE AIR POLLUTION

C.A. Pope III
Brigham Young University

INTRODUCTION

Many epidemiological studies have investigated the health effects of particulate air pollution. Various researchers with differing training, interests, and research skills have conducted a wide variety of studies. This paper provides a simple framework to catagorize the basic study designs of most of the currently available epidemiological studies of the health effects of particulate air pollution and reviews the basic results of these studies. Currently there are nearly 100 relevant and published epidemiological studies on particulate air pollution. All of these studies cannot be referenced in this brief paper, but there have been several recent reviews of many of these studies. (1-12). In this paper, key studies will be referred to in parentheses by author and year of publication. For more detailed discussions and full references, see Dockery and Pope 1996, and Pope and Dockery 1996 (11, 12).

BASIC STUDY DESIGNS

Currently available studies typically fall within two broad classifications: 1) acute exposure studies, and 2) chronic exposure studies (See Figure 1). The acute exposure studies use short-term temporal changes in pollution as their source of exposure variability. These studies evaluate short-term changes in health endpoints associated with short-term changes in pollution. These studies may be as simple as observing changes in health over a pollution episode that lasts for one or more days, or they may be highly formal daily time-series studies. Because these studies typically evaluate only short-term temporal relationships (usually 1-5 days), the observed pollution effects are typically interpreted as the health effects of acute exposure.

Available chronic exposure studies primarily use spatial differences in pollution as their source of exposure variability. Chronic exposure studies, therefore, compare various health outcomes across communities or neighborhoods with different levels of pollution. These studies are principally cross-sectional in design and use longer-term pollution data (usually one year or more). These studies are often interpreted as evaluating the chronic and/or cumulative effects of exposure.

Nearly all of the currently published acute and chronic exposure studies can also be subdivided as population-based studies or cohort-based studies. The population-based studies are often referred to as ecological studies where the units of comparison are entire populations of communities or neighborhoods. The cohort-based studies include studies descriptively referred to as panel studies or sample-based studies. Although, central-site community-based monitoring is typically used to estimate pollution exposure in the cohort-based studies, the units of comparison for health outcomes and co-risk factors are individuals enrolled in a well-defined cohort, panel, or sample.

These studies can be further subdivided by the specific health outcomes evaluated. An appraisal of the strength of the overall epidemiological evidence of health effects of air pollution requires an evaluation of coherency. Effects of pollution should be evaluated across a range of related health outcomes. Cardiopulmonary health outcomes that have been evaluated include mortality, hospitalizations or health care visits for respiratory and/or cardiovascular disease, respiratory symptoms, measures of lung function, and restricted activity due to illness.

ACUTE EXPOSURE, POPULATION-BASED, MORTALITY STUDIES

Early studies focused on severe air pollution episodes, often in narrow industrial valleys such as the Meuse River in Belgium (Firket 1931) and Donora, PA (Ciocco & Thompson 1961). The most dramatic of these documented air pollution episodes occurred in London, England (Logan 1953). Several later studies in London reported associations between daily mortality air pollution at much lower pollution levels (Ostro 1984, Schwartz and Marcus 1990, Ito et al. 1993). Elevated respiratory and cardiovascular disease morbidity and mortality have also been reported for a more moderate increase in pollution in the North Rhine--Westfalia area of Germany (Wichmann et al. 1989).

The severe air pollution episodes have been frequently reviewed (Ellison & Waller 1978, Holland et al. 1979, Shy 1979, Bates 1980). They demonstrated an important link between cardiopulmonary disease mortality and morbidity with extremely elevated concentrations of particulate and/or sulfur oxide air pollution. They also suggested effects at lower levels. Although the biological mechanisms involved were poorly understood, there remained little disagreement that, at very high levels, ambient air pollution can be an important risk factor associated with increased cardiopulmonary disease and early mortality.

A series of recent studies analyzed the temporal distribution of deaths and particulate air pollution at current levels. The U.S. EPA has reviewed these studies in the recent criteria document on the health affects of particulate air pollution and other reviews of these studies have been made (1-12). These studies observed changes in daily death counts associated with short-term changes in particulate air pollution. A particulate pollution threshold was not generally observed in these studies. The relative risk of mortality increased monotonically with particulate concentrations--usually in a near linear fashion.

These studies have observed similar particulate air pollution effects in varied locations. Because various measurements of particulate pollution were used, precise comparisons between studies are difficult. But when particulate measurements are converted to PM_{10}, there is remarkable consistency in the estimated effect of PM10 across these studies. The esimated effect ranges between a 0.5 percent and 1.6 percent in daily mortality for each 10 $\mu g/m^3$ increase in PM_{10} concentration with a weighted mean of about 0.8 percent.

Several studies also provided a breakdown of mortality by broad cause-of-death categories. Particulate air pollution generally had the largest effect on respiratory disease mortality but effects on cardiovascular mortality were also observed. An examination of cardiovascular deaths in Philadelphia reported that on days with high particulate air pollution there was a substantial increase in respiratory factors as contributing causes for death, with cardiovascular disease reported as the underlying cause of death.

ACUTE EXPOSURE, POPULATION-BASED, HOSPITALIZATION STUDIES

The results of a unique natural experiment that occurred in the Utah Valley have been reported (Pope 1989, 1991). During the winter of 1986-1987 a labor dispute resulted in the closure of the local steel mill, the largest single source of particulate air pollution in the valley. During this winter, PM_{10} concentrations averaged 51 $\mu g/m^3$ with a high of 113 $\mu g/m^3$ compared with a mean of 90 $\mu g/m^3$ with a high of 365 $\mu g/m^3$ during the previous winter. During this winter, children's hospital admissions for respiratory disease dropped by more than 50 percent, compared with adjacent years. Regression analysis estimated a 4.2 percent decrease in asthma and bronchitis admissions of children associated with a 10 $\mu g/m^3$ increase in 2-month mean PM_{10}.

Several studies have found that increased rates of respiratory hospital admissions in southern

Ontario are associated with increased sulfate and ozone concentrations (Bates and Sizto 1987, 1989; Burnett et al. 1994). Burnett et al (1995) also evaluated hospital admissions data for 168 hospitals in Ontario and observed significant positive associations between respiratory and cardiac hospital admissions and sulfate concentrations. Thurston and colleagues have reported similar associations in Toronto, Ontario (Thurston et al. 1993) and for several cities in New York State (Thurston et al. 1992). The focus of these studies was the effects of acid aerosols, but estimates were reported for various measures of particle exposure. Taken together, these studies found an increase in hospital admissions for respiratory diagnoses ranging from approximately 0.8 percent to 3.4 percent for each 10 $\mu g/m^3$ increase in daily mean PM_{10}.

Several studies have also analyzed emergency department visits and found them to be associated with particulate air pollution. For example, particulate air pollution was associated with emergency department visits for asthma in Seattle, WA (Schwartz et al. 1993), emergency department visits for chronic obstructive pulmonary disease in Barcelona (Sunyer et al. 1991, 1993), and emergency department visits in Steubenville, OH (Samet et al. 1981). The estimated percent increase in emergency visits associated with a 10 $\mu g/m^3$ increase in PM_{10} ranged from 0.5 percent to 3.4 percent with a weighted mean of approximately 1.0 percent.

Given the associations between particulate pollution and emergency department visits, it would be expected that associations would also be observed for outpatient visits for respiratory illness. There is less availability of outpatient data to researchers than there is for hospitalization data. However, based on a limited study of outpatient data from a clinic in Salt Lake City, UT, Lutz (1983) reported that strong positive associations were observed between weekly particulate pollution levels and the percentage of patients with a diagnosis of respiratory tract or cardiac illness.

ACUTE EXPOSURE, COHORT-BASED, SYMPTOM/DISEASE STUDIES

Studies of upper and lower respiratory symptoms have been conducted in the Utah Valley (Pope et al. 1991, Pope and Dockery 1992), the Netherlands (Hoek & Brunekreef 1993, 1994), a study of six U.S. cities (Schwartz et al. 1994), and Southern California (Ostro et al. 1993). Very small, often statistically insignificant associations between particulate pollution and upper respiratory symptoms were observed. Association with lower respiratory disease were larger and usually statistically significant. Based on these studies, the estimated percent increase in reported lower respiratory symptoms associated with a 10 $\mu g/m^3$ increase in PM_{10} was as high as 15 percent, but the weighted mean was approximately 3.0 percent.

Cough was analyzed separately in three of these studies as well as in another diary study in the Netherlands (Roemer et al. 1993), a study of two Swiss cities (Braun-Fahrlander et al. 1992), and a study in Uniontown, Pennsylvania (Neas et al. 1992). Cough was typically associated with particulate pollution, with the estimated percent increase in reported cough associated with a 10 $\mu g/m^3$ increase in PM_{10} as high as 28 percent but with a weighted mean of approximately 1.2 percent

Evidence from hospital admissions and emergency visit studies suggests that exposures to particulate air pollution may be directly associated with asthma attacks. Several investigators have considered less severe asthmatic attacks as reported by panels of asthma patients. Winter studies of asthmatic children with chronic respiratory symptoms in The Netherlands (Roemer et al. 1993) and of asthmatic adults in Denver, Colorado, (Ostro et al. 1991) both found substantial increases in reported asthmatic attacks associated with particle exposures. An earlier study in the Los Angeles area (Whittemore and Korn 1980) reported increased attacks associated with particle exposures but the effect was much

lower than in the more recent studies. The weighted mean of these three studies gives an effect estimate of 3 percent increase in asthmatic attacks associated with 10 $\mu g/m^3$ increase in PM_{10}.

Bronchodilator use has also been evaluated as a measure of exacerbation of asthma in a panel of asthmatics in the Netherlands (Roemer et al. 1993) and in the Utah Valley (Pope et al. 1991). Based on the reported results of these studies, the estimated percent increase in asthma attacks or use of bronchodilator associated with a 10 $\mu g/m^3$ increase in PM_{10} range from 1.1 percent to 12 percent with a weighted mean of approximately 3.0 percent.

Associations between particulate air pollution and more general measures of acute disease have also been observed. For example, Ostro (1983, 1987, 1990) and Ostro and Rothschild (1989) evaluated the timing of restricted activity days of U.S. adult workers. Restricted activity due to respiratory morbidity was consistently associated with particulate pollution. Morbidity was often more strongly associated with the fine, respirable, or sulfate component of particulate pollution. Ransom and Pope (1992) reported similar associations between PM_{10} and grade-school absences in children in the Utah Valley, Utah. Lagged pollution effects of up to several weeks were observed for both restricted activity in adults and in school absences.

ACUTE EXPOSURE, COHORT-BASED, LUNG FUNCTION STUDIES

Several studies have observed negative associations between particulate pollution and lung function. Panels of elementary school children in Steubenville, OH had their lung function measured weekly before, during, and after particulate and sulfur oxide episodes during four periods in 1978 through 1980 (Dockery et al. 1982). Declines in forced expired volume in 0.75 seconds ($FEV_{.75}$) were observed following these episodes. In a re-analysis of the Steubenville data, Brunekreef et al. (1991) found the strongest association with the mean particle concentrations over the previous 5 days. Similar decreases in forced expired volume in 1 second (FEV_1) were observed in school children following a particulate and sulfur oxide pollution episode in January 1985 in the Netherlands (Dassen et al. 1986). Subsequent studies of panels of school children in the Netherlands with weekly lung function measurements (Hoek & Brunekreef 1993, 1994) have also shown decreased FEV_1 associated with daily PM_{10} concentrations. Lagged effects of up to seven days were observed.

Pope and Kanner (1993) analyzed repeated FEV_1 measurements in a panel of adults with chronic pulmonary disease who were participating in the Lung Health Study. Measurements were taken 10 to 90 days apart. FEV_1 levels were found to be associated with PM_{10} concentrations. Koenig and colleagues (1993) studied the lung function [forced vital capacity (FVC) and FEV_1] of children in Seattle, WA with relatively low particulate air pollution levels. Lung function declines were associated with fine particulate air pollution for asthmatic children, but not for non-asthmatic children. Overall, these studies generally observed a decrease of up to 0.35 percent in FEV_1 associated with each 10 $\mu g/m^3$ increase in daily mean PM_{10}, with a weighted average of 0.15 percent.

Several studies have used peak flow measurements as an indicator of acute changes in lung function including studies in the Netherlands (Hoek and Brunekreef 1993, 1994; Roemer et al. 1993), the Utah Valley (Pope et al., 1991; Pope and Dockery 1992), and Uniontown, PA (Neas et al. 1992). In these studies a 10 $\mu g/m^3$ increase in PM_{10} was associated with a 0.04 percent to 0.25 percent decreases in peak flow measurements. As with FEV_1, the strongest associations with peak flow included particulate pollution over the previous several days, allowing for a lag in effect.

CHRONIC EXPOSURE, POPULATION-BASED MORTALITY STUDIES

There have been many studies that have suggested mortality effects of chronic exposure to air pollution. Martin (1964) reported that in the Greater London region overall annual respiratory mortality (as opposed to episodic mortality) was significantly related to smoke (or particulate pollution) levels. In 1970 Lave and Seskin reported the results of one of the first serious attempts to measure the long-term mortality effects of air pollution in the U.S. The work of Lave and Seskin has been followed by many other similar studies that have tried to replicate or refine their use of population-based (ecologic) cross-sectional study designs. Most of these studies observed that mortality rates tended to be higher in cities with higher fine or sulfate particulate pollution levels. Formal regression modeling techniques to evaluate cross-sectional differences in air pollution and mortality and to control for other ecological variables were used. In an attempt to control for other risk factors, population average values for demographic variables and other factors such as smoking rates, education levels, income levels, poverty rates, housing density, and others were often included in the regression models. The basic conclusions from the population-based cross-sectional studies include: 1) Mortality rates are associated with air pollution; 2) Mortality rates are most strongly associated with fine or sulfate particulate matter; and 3) An average mortality effect of 3 to 9 percent of total mortality can be estimated.

Although these population-based cross-sectional studies suggest that air pollution contributes to human mortality, these studies have severe limitations and have been largely discounted for several reasons. An overriding concern of these studies was that these population-based cross-sectional studies could not directly control for individual differences in cigarette smoking and other risk factors. They could only try to control for them by using population-based averages --making potential confounding a concern.

CHRONIC EXPOSURE, COHORT-BASED MORTALITY STUDIES

Recently the results of two prospective cohort mortality studies have been reported. Because of their improved study design these studies brought some of the most compelling evidence about mortality effects of chronic exposure to air pollution. The first of these recently reported prospective-cohort mortality studies was the "Six Cities study" (Dockery et al. 1993). This study involved a 14-16 year prospective follow-up of 8,111 adults living in 6 U.S. cities. The data were then analyzed using survival analysis, including multivariate Cox proportional hazards regression modeling. Although TSP concentrations dropped over the study periods, fine particulate and sulfate pollution concentrations were relatively constant. Mortality risks were most strongly associated with cigarette smoking, but after controlling for individual differences in age, sex, cigarette smoking, body mass index, education, and occupational exposure, differences in relative mortality risks across the six cities were strongly associated with pollution levels in those cities. Associations between mortality risk and air pollution were stronger for respirable particles and sulfates, as measured by PM_{10}, $PM_{2.5}$, and SO_4, than for TSP, SO_2, acidity (H^+), or ozone. The association between mortality risk and fine particulate air pollution was consistent and nearly linear, with no apparent "no effects" threshold level above the ambient level in the least polluted city (Portage). The adjusted total mortality-rate ratio for the most polluted of the cities compared with the least polluted was 1.26 with 95% confidence interval (CI) from 1.08 to 1.47. Fine particulate pollution was associated with cardiopulmonary mortality and lung cancer mortality (not statistically significant) but not with the mortality due to other causes analyzed as a group.

Similar results were observed in a much larger prospective cohort study (Pope et al. 1995). In this study approximately 500,000 adults drawn from the American Cancer Society (ACS) Cancer Prevention Study II (CPS-II) who lived in 151 different U.S. metropolitan areas

were followed prospectively from 1982 through 1989. Individual risk-factor data and 8 years of vital status data were collected. Ambient concentrations of sulfates and fine particles, were used as indices of exposure to combustion-source ambient particulate air pollution. Exposure was estimated from national data bases. Pollution exposure also was assessed for a time period just prior to entry into the cohort. An association between mortality and air pollution was observed after adjusting for age, sex, race, cigarette smoking, pipe and cigar smoking, exposure to passive cigarette smoke, occupational exposure, education, body mass index, and alcohol use. Mortality-rate ratios (and 95 percent confidence intervals) of total mortality for the most polluted areas compared with the least polluted equaled 1.15 (1.09-1.22) and 1.17 (1.09-1.26) when using sulfate and fine particulate measures, respectively. For total, cardiopulmonary, and lung cancer mortality, the associations with sulfate particles were highly statistically significant ($P < 0.01$). For total and cardiopulmonary mortality, significant associations were also found using fine particulate matter as the index of air pollution levels. The association between air pollution and all-cause and cardiopulmonary mortality was observed for both men and women and for smokers and nonsmokers.

CHRONIC EXPOSURE, COHORT-BASED, SYMPTOMS/DISEASE STUDIES

There have been several studies that have evaluated associations between particulate air pollution and chronic respiratory symptoms and disease. These studies include the Harvard six-cities study (Dockery et al 1989), analysis of chronic obstructive pulmonary disease (COPD) symptoms of never-smoking Seventh-Day Adventists in California (Euler et al., 1987), analysis of data from the 1979 version of the U.S. National Health Interview Survey (NHIS) (Portney and Mullahy, 1990), analysis using data from the first National Health and Nutrition Examination Survey (NHANES I) (Schwartz 1993), and analysis of the symptoms data from the 24-cities study (Dockery et al, 1993). The effects of air pollution on respiratory disease or symptoms were estimated while adjusting for individual differences in various other risk factors. In all of these studies, statistically significant associations were observed between particulate air pollution and respiratory symptoms. Particulate air pollution was most consistently associated with bronchitic symptoms. The results suggest that a 10 $\mu g/m^3$ increase in PM_{10} was typically associated with a 10 to 25 percent increase in bronchitis or chronic cough.

CHRONIC EXPOSURE, COHORT-BASED, LUNG FUNCTION STUDIES

Holland and Reid (1965) made a cross-sectional comparison of British male postal employees in London and in smaller country towns, where levels of SO_2 and particulate pollution were about half of those in the metropolis. Accounting for cigarette smoking levels, significant decrements of FEV_1 in London employees compared to those in the provinces were reported. There have been several more recent studies that have evaluated associations between measures of lung function (FVC, FEV_1, PEF) and particulate pollution levels in the U.S. These studies include analysis of children's lung function data from the Harvard six-city study (Dockery et al, 1989), analysis of data from both the first and second National Health and Nutrition Examination Surveys (NHANES I and NHANES II) (Chestnut et al, 1991 and Schwartz, 1989), analysis of children's lung function from 24 U.S. cities (Raizenne et al, 1993) and analysis from eight different areas in Switzerland (Ackermann-Liebrich et al, 1987). Each of these studies had information on individual persons in the samples. The effects of air pollution on lung function were estimated after adjusting for individual differences in age, race, sex, height, and weight and controlling for smoking or restricting the analysis to never-smokers.

All of these studies observed small negative associations between lung function and particulate air pollution. In the six-cities study, which had the least statistical power, the association was very weak and statistically

insignificant. In each of the other studies, the association was small, but statistically significant. The results suggest that a 10 $\mu g/m^3$ positive difference in PM_{10} was typically associated with less than a two percent decline in lung function. However, lung function measures have been shown to be important measures of health with remarkable predictive capacity for survival (Bates 1989). Furthermore, as reported in the 24-city study, the risk of relatively large deficits in lung function (15 percent or more) was much higher in the more polluted cities, suggesting detrimental effects of respirable particulates or particulate acidity on normal lung growth and development.

SUMMARY AND CONCLUSIONS

Table 1 presents ranges of effect estimates relating particulate exposure to various health end points. Although the biological linkages remain poorly understood, the results of the acute and chronic exposure studies are complementary. The current epidemiologic evidence suggests that respirable particulate air pollution, at levels common to many urban and industrial areas in the United States, contributes to human morbidity and mortality. Long-term, repeated exposure increases the risk of chronic respiratory disease and the risk of cardiorespiratory mortality. Short-term exposures can exacerbate existing cardiovascular and pulmonary disease and increase the number of persons in a population who become symptomatic, require medical attention, or die. The pattern of cardiopulmonary health effects associated with particulate air pollution that has been observed by epidemiological studies is the strongest evidence of the health effects of this pollution. Nevertheless, the epidemiological studies have important limitations that stem largely from the use of people who are living in uncontrolled environments, and who are exposed to complex mixtures of particulate air pollution.

In addition to providing limited information about biological mechanisms, current epidemiological studies provide relatively meager information regarding linkages between ambient and personal exposures, and are unable to fully explore the relative health impacts of various constituents of air pollution. Furthermore, the relationships between chronic versus acute exposures remain unclear. Much of the recent epidemiological effort has focused on effects of acute exposure, primarily because of the relative availability of relevant time-series data sets. However, the effects of chronic exposure may be more important in terms of overall public health relevance.

REFERENCES

1. Bates, D.V.: Health Indices of the Adverse Effects of Air Pollution: The Question of Coherence. Environ. Res. 59:336-349 (1992).

2. Ostro, B.: The Association of Air Pollution and Mortality: Examining the Case for Inference. Arch. Environ. Health 48:336-342 (1993).

3. Lipfert, F.W.: Air Pollution and Community Health: A Critical Review and Data Sourcebook. Van Nostrand Reinhold, New York, NY (1994).

4. Dockery, D.W.; Pope, C.A. III: Acute Respiratory Effects of Particulate Air Pollution. Annu. Rev. Public Health. 15:107-132 (1994).

5. Schwartz, J.: Air Pollution and Daily Mortality: A Review and Meta Analysis. Environ. Res. 64:36-52 (1994).

6. Pope, C.A. III; Dockery, D.W.; Schwartz, J.: Review of Epidemiological Evidence of Health Effects of Particulate Air Pollution. Inhalation Toxicology 7:1-18 (1995).

7. Pope, C.A. III; Bates, D.V.; Raizenne, M.E.: Health Effects of Particulate Air Pollution: Time for Reassessment? Environ. Health Persp. 103:472-480 (1995).

8. Jedrychowski, W.: Review of Recent Studies from Central and Eastern Europe Associating Respiratory Health Effects with High Levels of Exposure to

"Traditional" Air Pollutants. Environ. Health Perspect. 103(S2):15-21(1995).

9. Folinsbee, L.J.: Human Health Effects of Air Pollution. Environ. Health Perspect. 100:45-56(1995).

10. Brunekreef, B.; Dockery, D.W.; Krzyzanowski, M.: Epidemiological Studies of Health Effects of Low Levels of Major Ambient Air Pollution Components. Environ. Health Perspect. 103(S2):3-13(1995).

11. Dockery, D.W.; Pope, C.A., III: Epidemiology of Acute Health Effects: Summary of Time-Series Studies. Particles in Our Air: Concentrations and Health Effects Eds. Richard Wilson and John D. Spengler. Harvard University Press, 1996, pp. 123-147.

12. Pope, C.A., III; Dockery, D.W.: Epidemiology of Chronic Health Effects: Summary of Cross-Sectional Studies. Particles in Our Air: Concentrations and Health Effects Eds. Richard Wilson and John D. Spengler. Harvard University Press, 1996, pp. 149-167.

Figure 1: Basic Study Designs of Currently Published Studies of Health Effects of Particulate Air Pollution

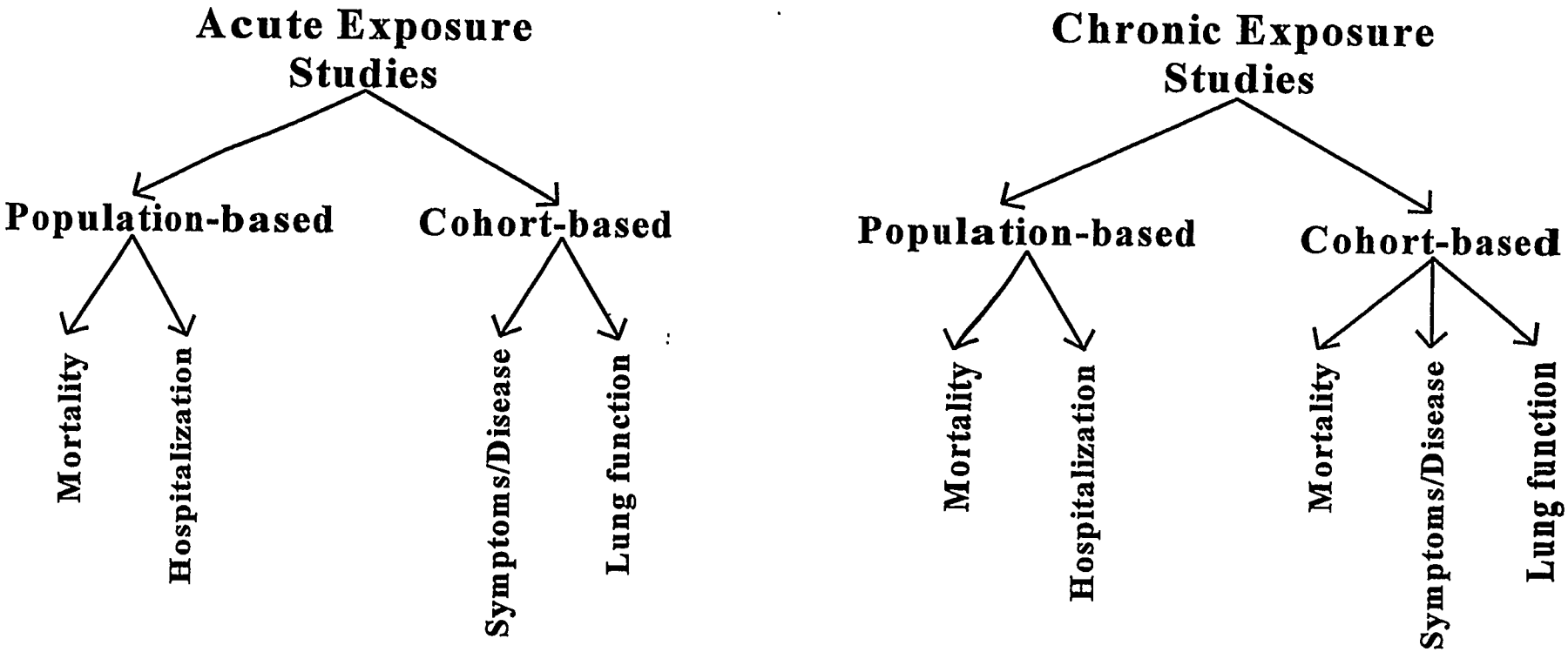


Table 1. Approximate range of estimated effects measure as percent change in health endpoint per 10 $\mu g/m^3$ increase in PM_{10} for the different basic study designs.

Health Endpoints	Acute Exposure		Chronic Exposure	
	Population-Based	**Cohort-Based**	**Population-Based**	**Cohort- or Sample-Based**
Mortality	Total: 0.5 - 1.5 Resp: 1.5 - 4.0 Cardio: 0.5 - 2.0		Total: 0 - 5	Total: 3 - 6 Cardiopulmonary: 5 - 9 Lung cancer: 0 - 9
Respiratory Health Care	Hospit. Admit: 0.5 - 4.0 Emergency Visits: 0.5 - 3.5			
Decrease in Lung Function		FEV_1: 0.05 - 0.35 PEF: 0.04 - 0.25		Lung function 0 - 2
Respiratory Symptoms, Disease		Lower: 0 - 15 Upper: 0 - 7 Cough: 0 - 25 Asthmatic attacks: 1 - 12		Emphysema, Chronic bronchitis or cough 10 - 25
Restricted Activity	Grade school absences: 1.0 - 4.0	Restricted activity days: 1.0 - 5.0		

CANCER RISK FROM DIESEL EXHAUST: EVIDENCE FROM DIESEL-EXPOSED WORKERS

D. S. Greenbaum
The Health Effects Institute

The assessment of the health risks from exposure to diesel exhaust has relied on toxicological studies, and on epidemiological studies of health effects in workers exposed to diesel exhaust. Although a variety of health effects have been investigated, the focus of most research and risk assessments has been on cancer, with a particular emphasis on lung cancer. Toxicology studies have found evidence of increased lung cancer in rats at high levels of exposure, most likely due to a biological mechanism related to the inability of the rat lung to clear high doses of particles. This leaves open the question of whether humans, exposed at lower levels, might still be subject to increased risk based on a different, perhaps genotoxic, mechanism related to the chemicals adsorbed on diesel particulate matter.

In 1995, the Health Effects Institute published *Diesel Exhaust: A Critical Analysis of Emissions, Exposure, and Health Effects,* which summarized and analyzed the toxicologic and epidemiologic research on diesel exhaust. In January, 1996, HEI sponsored, along with the California Environmental Protection Agency, U.S. EPA, World Health Organization, and National Institute of Occupational Safety and Health, a public workshop on the use of diesel epidemiologic data in risk assessment. The following summarizes the results of the HEI review, and places it in the context of the workshop's discussions, and of recent developments on the use of epidemiology studies of diesel exhaust in risk assessment.

OCCUPATIONAL STUDIES

To date, over thirty epidemiological studies have investigated the relative risk of lung and other cancers among railroad workers, truckers, dock workers, and others. These studies have focused exclusively on male workers exposed to diesel emissions after 1950, when these industries widely converted to diesel engines. Two types of studies have been conducted: (1) studies of occupational cohorts exposed to relatively high concentrations of diesel emissions, and (2) studies that used interviews or questionnaires to identify individuals from the general population who had received occupational exposures to diesel exhaust. The occupational cohorts studied most extensively include railroad, dock, trucking industry, and bus garage workers. Underground miners are also exposed to diesel exhaust; however, they have not historically been targeted for epidemiologic studies of diesel emissions because they are often exposed to other pollutants such as radon, asbestos, dust, and metals. (A long-delayed study of miners is just now beginning to get underway). No data are available on the effects of diesel exposure on women, children, or individuals with cardiovascular or respiratory disease.

The results of the occupational cohort and case-control studies of diesel exhaust, especially those published in the last fifteen years, are generally consistent in showing a weak association between exposure to diesel exhaust and lung cancer. They suggest that prolonged exposure to diesel exhaust over many years is associated with a 1.2 to 1.5 times increase in the relative risk of lung cancer incidence or mortality in workers. Figures 1 and 2 summarize the relative risks and confidence intervals for railroad workers and truckers respectively. In all studies, the incidence rate for lung cancer was higher in workers classified as "exposed to diesel exhaust" than in workers classified as "unexposed." However, as illustrated in Figures 1 and 2, the increase in the relative risk of lung cancer was generally small, and many of the

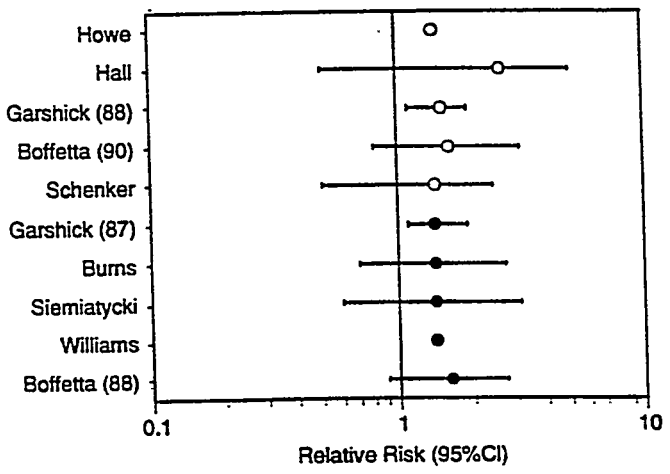


Figure 1. Lung cancer and exposure to diesel exhaust in railroad workers. ● = RR adjusted for cigarette smoking; ○ = RR not adjusted for cigarette smoking. For the two studies by Howe and Williams, CIs were not reported and could not be calculated.

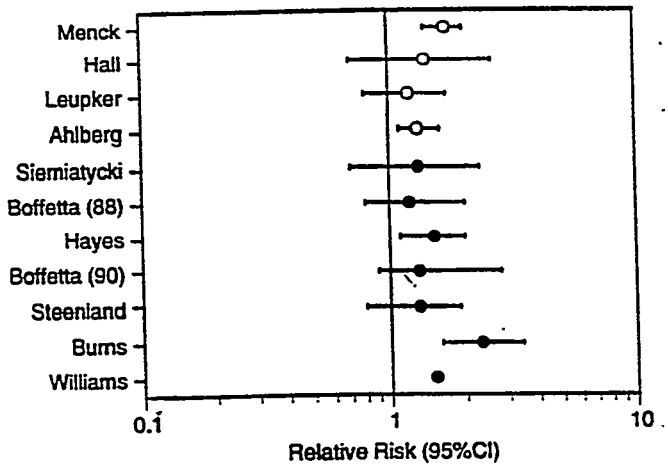


Figure 2. Lung cancer and exposure to diesel exhaust in truck drivers. ● = RR adjusted for cigarette smoking; ○ = RR not adjusted for cigarette smoking. For the study by Williams, CIs were not reported and could not be calculated. For the Steenland study, the data were gathered from union reports of long-haul truckers; for the Boffetta (1988) study, the data were self-reported by diesel truck drivers; and for the Siemiatycki study, they were self-reported by heavy-duty truck drivers (personal communication).

measurements were imprecise; thus the results of most of the studies were not statistically significant. However, the results of the studies with larger populations were statistically significant, which increases confidence in interpreting the positive lung cancer data in occupational cohorts. Moreover, in some of the studies, the largest relative risks were seen in the categories expected to have the greatest cumulative exposure to diesel exhaust (Garshick et al. 1987,1988; Gustavsson, et al. 1990; Steenland et al. 1992, Emmelin et al. 1993). The general population studies also indicate small elevations in lung cancer rates among workers in similar occupational groups such as truckers, railroad workers , mechanics, and dock workers; however, these estimates are based on small numbers of exposed subjects.

In addition to lung cancer, some epidemiologic studies suggest that an elevated risk of bladder cancer may be linked to diesel exhaust exposure in occupational settings. The evidence for bladder cancer, however, is not as consistent as that for lung cancer.

LIMITATIONS

The epidemiologic studies of diesel exhaust have been criticized on two fronts. First, many of the studies did not control for possible confounding factors which might also be linked to elevated lung cancer, such as cigarette smoking, environmental tobacco smoke, nondiesel particulate matter, diet, socioeconomic factors, or exposures to other air pollutants. Controlling for such factors is a common methodologic challenge for epidemiologists. Cigarette smoking is particularly important because it is the dominant cause of lung cancer, and failure to control for its effects can seriously compromise any epidemiologic study of lung cancer risks. An analysis by Cohen and Higgins (Health Effects Institute, 1995) indicates that controlling for smoking, which reduces the risks in some studies, could not fully explain the associations between exposure to diesel exhaust and lung cancer. Also, when Cohen and Higgins estimated the impact of hypothetical differences in cigarette smoking prevalence on the lung cancer rates observed in two studies of emissions that did not control for smoking, their estimate supports the idea that cigarette smoking cannot fully explain the observed increases in lung cancer in railroad workers (Garshick, et al. 1987) or

bus garage workers (Gustavsson et al. 1990).

Only a few epidemiological studies considered other potential confounders such as asbestos exposure, environmental tobacco smoke, diet, and socioeconomic factors. No study has addressed possible confounding due to exposure to nondiesel particles, which are possibly important in light of recent animal studies that demonstrate that, at high concentrations, many poorly soluble particles cause lung tumors in rats.

The second criticism of the epidemiologic studies of diesel exhaust is that none included measurements of any constituent of diesel emissions during the time the study population was actually exposed. Instead, exposure classification was based on self-reported work histories or company records and on the investigator's or the industrial hygienists' opinions about whether the reported job or occupation entailed exposure to diesel exhaust. Although these approaches are probably sensitive to diesel exhaust exposure (i.e. they tend to identify most truly exposed subjects), they are not specific (i.e., they tend to classify some unexposed subjects as exposed). Misclassification of exposures can cause spurious increases or decreases in estimates of effects depending on whether the misclassification differs between subjects with and without disease.

Another complicating factor is that the diesel exhaust to which the populations were actually exposed were never fully characterized. This information gap cannot be filled by using later characterizations of diesel exhaust because the characteristics of emissions depend greatly on factors such as the type of engine, how it is operated ; and the specific fuel used. For example, diesel fuel for locomotives has a higher content of aromatic hydrocarbons than the diesel fuel used in truck engines (Sawyer and Johnson, in Health Effects Institute, 1995). Therefore, the PAH content of locomotive exhaust is probably higher than that of exhaust from trucks and other diesel engines that use diesel fuels - a factor that needs to be considered if data obtained in railroad worker studies are extrapolated to the general population. Furthermore, both the particulate and the PAH content of diesel emissions have decreased dramatically over the last two decades. Therefore, large uncertainties are associated with applying emissions or exposure data from one type of engine during a specific time period to risk assessments for other populations and time periods. These uncertainties limit the use of the epidemiologic data for quantitative risk assessments.

HEI CONCLUSIONS

Based on its review of the epidemiologic and exposure data, HEI drew the following conclusions about the epidemiologic data:

- The epidemiologic data show that long-term exposure to diesel exhaust in a variety of occupations is associated with small increases (in the 1.2 - 1.5-fold range) in the relative risk of lung cancer occurrence, or mortality, or both. The epidemiologic studies are consistent in showing weak associations between exposure to diesel exhaust and lung cancer, but vary in the strength of the statistical association; only a few studies showed relative risks that were statistically significant.

- The absence of exposure measurements in the study populations is the main methodologic problem limiting interpretation of the epidemiologic data and its use in quantitative risk assessments. None of the published studies measured actual levels of exposure to diesel exhaust or characterized the actual emissions from the exposure source.

- The issue of confounding is difficult to assess. Cigarette smoke is a major potential confounder in lung cancer studies. Most studies that controlled for cigarette smoking found that the association of lung cancer with exposure to diesel

exhaust persisted after such controls were applied, although in some cases the risks were lower. Only a few epidemiologic studies considered other potential confounders such as nondiesel particles, environmental tobacco smoke, asbestos exposure,, diet, and socioeconomic factors. At present there is insufficient evidence to conclude whether confounding by these factors influenced the results.

- The above conclusions are based on studies of male workers. None of the epidemiologic studies conducted to date examined the risk of diesel exhaust exposure for women or potentially susceptible populations such as infants, children, or people with health disorders.

WORKER STUDIES AND RISK ASSESSMENT

A variety of State, Federal, and international agencies have considered the question of whether the epidemiologic evidence on diesel exhaust is adequate to support quantitative risk assessment and determinations of whether or not diesel exhaust is a human carcinogen. A summary of those reviews is presented below:

- In 1989, the *International Agency for Research on Cancer* reviewed the data, and concluded that there is "limited human evidence" for carcinogenicity in humans of diesel exhaust. (IARC, 1989)

- In 1994, The *U.S. Environmental Protection Agency*, in its draft risk assessment for diesel, concluded that there was limited evidence for carcinogenicity in humans and that, given conflicting dose/response analyses of the Garshick study, the data was insufficient for quantitative risk assessment (EPA,1994)

- In 1996, the *World Health Organization* concluded that the "results of the available epidemiological studies were considered inadequate for a quantitative estimate of human risk." (IPCS, 1996)

- In 1997, the *California Environmental Protection Agency*, in its draft identification of diesel exhaust as a Toxic Air Contaminant, concluded that a "causal association of diesel exhaust exposure and lung cancer" was "a reasonable and likely explanation for the increased rates of lung cancer observed in the epidemiological studies," and found the data adequate to make a quantitative estimate of cancer risk. (CALEPA, 1997)

SUMMARY

To date, over thirty studies have investigated the relative risk of lung and other cancers among railroad workers, truckers, dock workers, and others. These studies suggest that the risk of lung cancer among workers classified as having been exposed to diesel exhaust is approximately 1.2 to 1.5 times the risk in those workers classified as unexposed. Although the data appear consistent, the association is weakened because the reported effects were small, and the absence of concurrent exposure information limits the interpretation of the epidemiologic studies and the use of these data for quantitative estimates of cancer risk. However, the association of increased lung cancer at levels of exposure which appear to be below those to which animals have been exposed (i.e. 100 μ/m^3 vs. 2,000μ/m^3) suggests that a biological mechanism based on the chemicals carried by diesel exhaust particles cannot be excluded.

In reviewing this data, risk assessment agencies have generally not found that the epidemiologic data are adequate to produce a quantitative estimate of cancer risk for humans exposed to diesel exhaust in ambient settings. The one exception to this is the DRAFT risk assessment produced by the California Environmental Protection Agency, which is currently undergoing public and scientific review.

REFERENCES

California Environmental Protection Agency. Proposed identification of diesel exhaust as a toxic air contaminant. May, 1997 Public Comment and SRP Version. California EPA. Sacramento, California.

Emmelin A, Nystrom L, Wall S. 1993. Diesel exhaust exposure and smoking: A case-referent study of lung cancer among Swedish dock workers Epidemiology 4:237-244

Garshick E., Schenker MB, Munoz A, Segal M, Smith TJ, Woskie SR, Hammond SK, Speizer FE. 1987. A case-control study of lung cancer and diesel exhaust exposure in railroad workers. Am Rev Respir Dis 135:1242-1248

Garshick E., Schenker MB, Munoz A, Segal M, Smith TJ, Woskie SR, Hammond SK, Speizer FE. 1988. A retrospective cohort study of lung cancer and diesel exhaust exposure in railroad workers. Am Rev Respir Dis 137:820-825

Gustavsson P, Plato N, Lidstrom EB, Hogstedt C. 1990. Lung cancer and exposure to diesel exhaust among bus garage workers. Scand J Work Environ Health 16:348-354

Health Effects Institute. 1995. Diesel exhaust: a critical analysis of emissions, exposure, and health effects. Health Effects Institute Special Report. Cambridge, MA.

International Agency for Research on Cancer. 1989. Diesel and gasoline engine exhausts and some nitroarenes. In: Monographs on the Evaluation Of Carcinogenic Risks to Humans, Vol. 46. World Health Organization, IARC, Lyon, France

International Programme on Chemical Safety. 1996. Diesel fuel and exhaust emissions. Environmental Health Criteria 171, World Health Organization, IPCS, Geneva, Switzerland

Steenland K, Silverman D, Zaebst D. 1992. Exposures to diesel exhaust in the trucking industry and possible relationships with lung cancer. Am J Ind Med 21:887-890.

U.S. Environmental Protection Agency. 1994 Health Assessment Document for Diesel Emissions: External Review Draft. EPA 600/8-90/057. Office of Research and Development, Washington, D.C.

HEALTH SUPPORT FOR DIESEL ENGINE DEVELOPMENT PROJECT DESCRIPTION AND GOALS

J.L. Mauderly
Lovelace Respiratory Research Institute

INTRODUCTION

The Office of Heavy Vehicle Technologies within the Office of Energy Efficiency and Renewable Energy (the "Office") has responsibility for fostering the improvement of motive power to meet the nation's heavy-duty transportation needs. It is clear that, for at least the next few decades, compression ignition (diesel) engines will continue to be the technology of choice for the majority of heavy-duty motive power in the U.S. New generation diesels have potential for substantial penetration into me-dium and light-duty applications as well. It is the purpose of this project to ensure that the remarkable, rapid engineering developments in diesel technology are not thwarted by a lack of understanding of critical health issues or a lack of health-related information for guiding engineering choices.

The advancement of diesel engine technology requires successfully meeting two engineering and public relations challenges: 1) Improving energy efficiency and cost-effectiveness of operation; and 2) reducing potential adverse impacts on health. There is a growing international concern for the health impacts of fine particulate air pollution, and the U.S. Environmental Protection Agency (EPA) is implementing a new National Ambient Air Quality Standard (NAAQS) for fine particulate matter ($PM_{2.5}$). Diesel soot, like particulate emissions from all internal combustion engines and most other combustion sources, falls within the $PM_{2.5}$ size range and contributes a variable portion of the fine PM in ambient air. There are also concerns for non-particulate emissions of diesel engines, such as nitrogen oxides and aldehydes. Thus, the potential health impacts of diesel engine emissions are under intense scrutiny, and there are pressures from groups with extreme views to eliminate the use of diesel engines alto-gether. To be successful in meeting both na-tional energy strategy goals and corporate fi-nancial goals, diesel engine manufacturers must take a proactive stance in understanding and addressing health issues, and fostering an appropriate view of diesel technology in the public mind.

This project was initiated to ensure that concerns for health were appropriately integrated into the Office's diesel engine development program. The purposes of this project are two-fold: 1) to ensure that the Office and developers of diesel engine, fuel, and emis-sions control technologies are aware of current health issues by serving as an information, interpretation, and communication resource; and 2) to provide the diesel technology community with an iterative feedback loop for assessment of the potential health impacts of alternate engineering choices. The overall goal of this project is to facilitate an appropriate future role for diesel engine technology by supporting the mitigation of health risks in parallel with the increases in utility and energy efficiency.

HEALTH INFORMATION SUPPORT

This project provides the Office with a readily available single point-of-contact resource for health information related to diesel technology. The Principal Investigator, Dr. Joe L. Mauderly, and other staff of the Lovelace Respiratory Research Institute, have been closely involved in both diesel health research and research on other airborne particle issues for many years, and are involved in numerous related activities of other DOE Offices, other agencies, government-industry working groups, industry associations, and individual engine manu-facturers. There is no other health research organization with broader involvement and perspective

regarding basic health research, interpretive, and regulatory issues concerning diesel emissions. Lovelace maintains an awareness of relevant meetings, presentations, publications, controversies, and regulatory actions and provides this information to the Program Office on a proactive basis.

This project coordinates health-related presentations and sessions at workshops and meetings sponsored by the Office, or other meetings in which the Office chooses to participate. This project also provides partici-pation, either electronically or in person, by appropriate health experts in discussions, briefings, or testimonies internal and external to DOE. This project also provides health-related information and briefing materials to meet the Office's communication needs.

It is the intent of this project to extend its information and communications support services to the Office's other contractors. The infor-mation transfer will be conducted through several avenues. First, this project plan and subsequent updates will be disseminated to appropriate individuals in the Office's contracting organizations to provide current background information and make them aware of the availability of the resources of this project. Second, the Principal Investigator or other appropriate experts will contact other contractors at the Office's request to address key issues related to the individual contractor's work. Third, this project will serve as an information, discussion, and briefing resource to contractors as requested, in much the same manner that it supports the Program Office.

TARGETED HEALTH RESEARCH

Identification of Critical Research Needs

This project will conduct research targeting specific information needs critical to the mission of the Office's diesel engine program. This effort differs from, and complements, those of other organizations in that it will be focused on, and limited to, laboratory and risk assessment activities directly addressing key contemporary issues facing the Office and its other contractors in the refinement of diesel technology.

A key function of this project is to identify health information needs critical to the Office's work by maintaining a current awareness of medical and regulatory issues impacting the future of diesel technology and influencing technological choices, reviewing current research sponsored by other organizations to identify information needs that are not being met, and developing and prioritizing focused research strategies to meet those needs. Awareness is maintained by attending scientific meetings and regulatory discussions involving diesel health issues and by keeping abreast of current literature. Project staff have been closely involved in these activities on a routine basis for many years. Project staff will work with the Office to identify appropriate fuel, engine, and emissions control technology meetings and discussions in which to participate, in order to identify critical linkages between health issues and technological choices.

Critical health issues amenable to research will be identified and prioritized on a continuing basis. Issues to be addressed under this project and their priorities will be proposed by this Institute and research will be initiated in consultation with the Office. An awareness will be maintained of the issues being addressed by other organizations, to avoid duplication of effort. Opportunities for the Program Office to partner with other organizations to accomplish needed research will be identified and brought to the Office's attention.

Research Currently Underway

1. Development of Standardized Soot Toxicity Assays

There is a need for standardized cell or tissue culture assays for rapid, inexpensive screening for differences in the toxicity of soot due to changes in size and composition. Several potential assays are available, but none have been evaluated, optimized, and standardized as a first-line screen for the effect of subtle

differences in soot characteristics on cellular toxicity. The first laboratory effort initiated in this project was aimed at meeting this need. The responses of candidate assays to test particles are being compared. The principal challenge is to establish an assay system and measurable response indicators having sufficient sensitivity to reflect subtle differences in soot, which is a material of low acute toxicity.

A suitable assay would have two purposes: 1) for use in other toxicological research planned under this project; and 2) to screen the toxicity of soot generated by the Program's other participants. When the assays are adequately developed, this project will provide direct support to other contractors by making the screening capability available on request. It is envisioned that samples sent by other contractors will be analyzed at this Institute, and that the assays may also be applied in "real time" at other sites.

2. Determination of the Health Impacts of Reduced Soot Size

Current soot emissions standards are based on mass, and remarkable progress has been made in reducing mass emissions. However, some approaches to reducing mass concurrently reduce soot particle size and can result in a net increase in the number of particles emitted. There is growing scientific, regulatory, and public interest in the health significance of ultra fine particles, but there is a paucity of actual data. There are a few toxicological data sup-porting the plausibility of concerns that reduc-ing soot size may increase its toxicity by reducing its clearance from the lung, increasing its penetration into lung tissues, increasing its distribution to sites outside the lung, and increasing the bioavailability of soot-associated toxic compounds. At present, there is broad speculation that reducing soot size would increase its toxicity and perhaps even offset health gains made by reducing mass, but there have been no comparative studies and no data exist on which to judge whether toxicity would be reduced, unchanged, or increased. Although the present mass-based emissions standards are not driving expenditures to reduce particle numbers, it is rapidly becoming critical for the diesel technology community to determine whether or not soot size is likely to become a critical health and regulatory issue.

This project is initiating experiments to generate information, as rapidly as possible, on the potential health importance of reduced soot size. The studies will use both the cell and tissue culture test systems described above, and studies of animals inhaling particles of different size. The experiments will use soot, carbon particles to which specific organic and inorganic compounds can be adsorbed, and noncarbonaceous radiolabeled particles, to answer key questions.

The most important issue, and the first to be examined, is the extent to which the penetration and distribution of ultra fine particles after deposition in the respiratory tract differ from those of larger respirable particles. Solid particles larger than 0.1 μm are generally scavenged by alveolar macrophages after deposition on the lung surface. Small amounts can penetrate through the surface cell layer, but largely stay within the lung interstitium and lymph nodes. There is anecdotal evidence suggesting that smaller particles may escape collection and clearance via the macrophage system, penetrate readily into and through surface cells, and distribute throughout the body via the blood. This will be determined first using radioactive silver particles that can be located and counted in other tissues. If size-related differences in dosimetry are found, it will be determined if soot-like carbon particles behave similarly.

Both cell systems and animals will be used to determine if toxicity and bioavailability are important issues. The relative cytotoxicity and inflammatory potential of fine and ultrafine soot will be compared by measuring cell damage, the production of chemical mediators of in-flammation, and pathological responses of intact lungs. Animals and cells will be exposed to carbon particles coated with specific compounds by vapor adsorption and soot generated from burners or engines burning fuel with radio labeled constituents to compare the

bioavailability of soot-associated organics and metals. Release from the soot will be determined by measuring the desorbed compounds in cells and fluids after removal of particles, and by measuring the production of metabolites.

3. Comparative Life-Cycle Risk Assessments

There is inadequate information on the comparative "life cycle" health risks of diesel and competing technologies. A comprehensive view of health risks includes not only tailpipe emissions, but also fuel production and transport, evaporative emissions, collision-related explosions, and fires, etc. Diesel engine technology has advantages over gasoline engine technology in all of these facets of risk, but the comparative risks have not been adequately estimated and communicated. If ultra fine particle number proves to have health signifi-cance, the generally unrecognized fact that contemporary gasoline engines contribute heavily to the ambient ultra fine particle load through tailpipe and evaporative emissions would be another point of comparison. Opportunities for comparative life-cycle risk assessments will be explored and if feasible, such assessments will be coordinated or performed under this project.

SUMMARY

This project will provide the Office, participants in its diesel technology development programs, and the diesel fuel, engine, and emissions control technology community with dedicated support focused on identifying and resolving, in a proactive and objective manner, critical path health issues. This support has already proven useful to the Office, and should prove increasingly useful to its other program participants.

TOXICOLOGY OF DIESEL ENGINE EMISSIONS

J.L. Mauderly
Lovelace Respiratory Research Institute

INTRODUCTION

Diesel engine exhaust is a complex mixture of gases, vapors, and particles (soot), each consisting of a large number of compounds (1). Concern for health risks from diesel exhaust has focused primarily on the potential lung carcinogenicity of inhaled diesel soot, because of its respirability and its content of mutagenic organic compounds. Research on the potential lung cancer risk from inhaled diesel exhaust has taken three forms (2). First, researchers at tempted to identify the compounds responsible for its mutagenicity in cultured bacteria and mammalian cells, and to estimate cancer risk by comparing the mutagenicity of diesel exhaust to those of known human lung carcinogens. Second, several long-term inhalation studies in rats, mice and Syrian hamsters were conducted in the U.S., Europe, and Japan, followed by additional studies to determine the interpretive value of the results from rats. Third, epidemiological studies of occupational populations thought to have high diesel exhaust exposure were conducted. This paper reviews laboratory studies of the mutagenicity and carcinogenicity of diesel exhaust, and sum-marizes our present interpretation of the re-sults.

GENOTOXICITY OF DIESEL SOOT

Recognition of the potential carcinogenicity of diesel soot occurred in 1955, when Kotin et al. demonstrated that solvent extracts of soot caused cancer when applied to mouse skin (3). Concern was elevated in the late 1970s when U.S. Environmental Protection Agency researchers reported that soot extract was a direct-acting mutagen in bacteria (4), concurrently with a predicted increase of diesel engines among the U.S. light-duty fleet. The majority of the mutagenic activity in bacteria and mammalian cells was subsequently found to be attributable to polycyclic aromatic hydrocarbon (PAH) compounds, and especially the nitro-PAHs (5).

The extent to which the soot-associated organic mutagens are released after deposition in the lung remains unclear (2,6). Because the aqueous lung environment is quite different from the strong solvents, heat, and ultrasonic energy typical of laboratory extractions, it is extremely unlikely that the entire organic fraction would be released *in vivo*. Extractions using lung fluid simulants remove little mutagenic activity; however, some mutagenic activity is released from soot by lung macrophages (mobile scavenger cells) in culture. Mutagenic activity has been identified in the urine of rodents exposed to diesel soot by the intragastric, intraperitoneal, and subcutaneous routes, but no urinary mutagenic activity has been observed following exposure of rodents to soot by inhalation. Increases in the levels of DNA adducts (foreign molecules attached to DNA) have been detected in lungs of rats exposed by inhalation to high concentrations of diesel exhaust (6), but this finding is difficult to interpret. Similar increases in adducts have been observed in parallel groups exposed to carbon black and other particles having very little mutagenic activity (6-8). In addition, the increases occur primarily in adducts that also occur in unexposed rats (7). Finally, the increases in lung DNA adducts do not appear to progress during long-term exposures (7).

CARCINOGENICITY IN ANIMALS EXPOSED TO DIESEL EXHAUST BY INHALATION

By the mid-1980s, several long-term studies of rodents exposed by inhalation to whole, diluted diesel exhaust had been conducted. These initial studies included 11 studies of rats

conducted in nine laboratories, five studies of Syrian hamsters conducted in four laboratories, and five studies of mice conducted in five laboratories (2,9). Although the studies used different strains of animals, engines and operating conditions, fuels, exposure concentrations, weekly exposure patterns, and total lengths of exposure, a consistent pattern of results emerged.

Whole diesel exhaust, inhaled repeatedly at high concentrations for 24 mo or longer, caused increased incidences of lung tumors in rats. The tumors were located in peripheral lung tissue, were of epithelial (air space lining cell) origin, and consisted of both benign and malignant types. Another lesion, keratin cysts, also occurred at the higher exposure levels and were reported as benign tumors by some groups; however, these cysts are not currently considered "tumors" in the U.S. The tumor response did not appear to be influenced strongly by the strain of rat or by engine type, fuel type, or engine operating condition, but the response was consistently greater in females than in males.

The results of the most comparable and robust studies, all involving exposures of substantial numbers of rats for 30 months or longer, are presented graphically in Figure 1. The tumor response clearly demonstrated an exposure-response relationship, and was approximately proportional in a nonlinear manner to the exposure rate expressed as the weekly soot concen-tration x time product. The lowest exposure rate causing a significant increase in lung tu-mors in rats exposed for 30 months or longer was approximately 122.5 $mg \cdot h \cdot m^{-3}$, or 3,500 $\mu g/m^3$ x 7 h/d x 5 d/wk. Lower exposure rates did not cause significant carcinogenicity. Tu-mors were observed late in the life span, most near or after 24 months of exposure. Studies containing no groups with significant increases either involved only exposure rates below 120 $mg \cdot h \cdot m^{-3}$ or

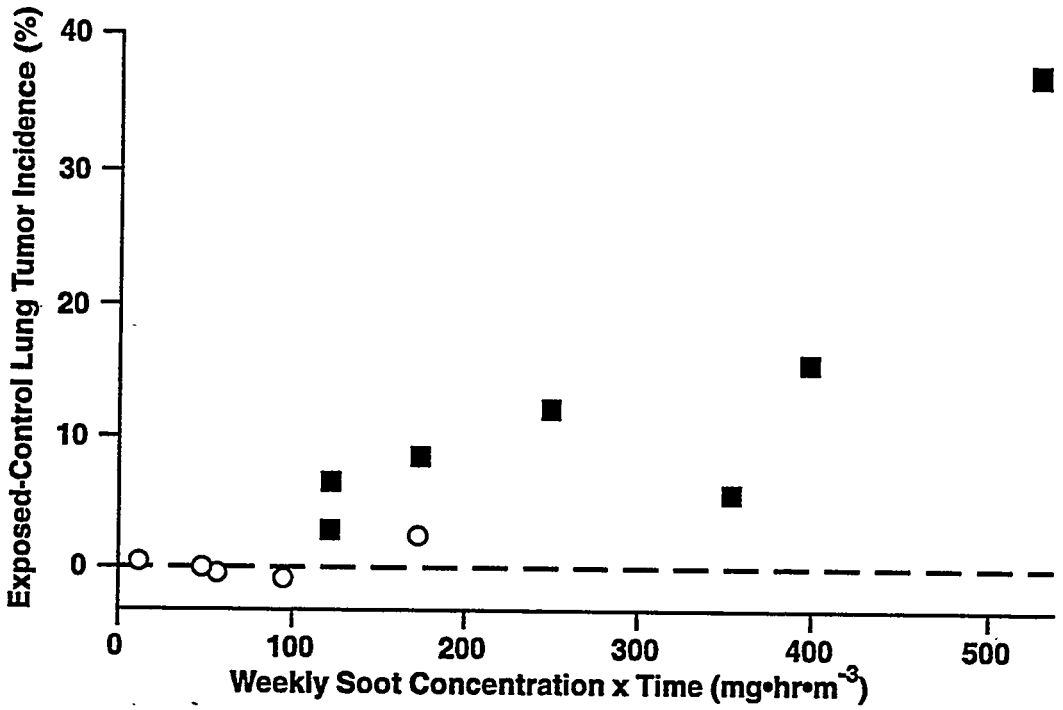


Figure 1. Relationship between diesel exhaust exposure and lung tumor response in rats exposed for a minimum of 30 months. Lung tumor response is expressed as the net (exposed -control) incidence, with the dashed line indicating zero net response. Exposure is expressed as the weekly concentration x time product. Filled squares represent groups with stati-stically significant increases in lung tumor incidence. Open circles represent exposed groups without significant increases in lung tumor incidence. Reproduced from reference (2).

exposures and observations of rats for less than 24 months. There was no evi-dence of a carcinogenic effect in other organs of rats. Exhaust filtered to remove soot did not cause tumors.

Exposures causing lung tumors in rats resulted in deposition of soot in the lung at rates exceeding the capacity of normal particle clearance, causing a slowing of clearance and a progressively increasing lung burden of soot (10). Exposures causing tumors also caused a progressive pneumoconiosis consisting of inflammation, fibrosis, hyperplasia (increased cell numbers) of alveolar and terminal bronchiolar epithelium, and epithelial metaplasia (altered cell types) (11). Conversely, exposures that did not cause substantial build-up of soot in the lung and progressive pneumoconiosis did not increase the incidence of lung tumors.

Parallel studies of mice and rats produced mixed results. Increased incidences of lung tumors were produced in a few groups of mice of strains that are genetically sensitive to chemical carcinogenesis, but results were equivocal or negative in ordinary strains (2,12). Soot accumulated in lungs of mice in amounts equivalent on a size basis to the accumulations in rats, and mice also developed chronic inflammation and fibrosis (13); however, mice had little epithelial hyperplasia and metaplasia.

Parallel studies of rats and Syrian hamsters demonstrated that soot exposure rates causing lung tumors in rats did not increase the lung tumor incidence in hamsters. Soot accumulated in the hamster lungs and caused lung pathology, but no increases in lung tumors were reported.

INTERPRETATION OF CARCINOGENICITY RESULTS FROM ANIMALS

By the late 1980s, data accumulated suggesting that lungs of rats respond similarly to heavy loading with diverse types of poorly soluble, nonfibrous particles (14). Several particles, including some with no organic mutagens, caused a similar syndrome of inflammation, fibrosis, epithelial hyperplasia and metaplasia, and epithelial tumors of the same type induced by diesel soot. Carcinogenesis by particles with no organic mutagens raised doubts that the diesel soot-associated organic mutagens were responsible for the pulmonary carcino-genicity of diesel exhaust in rats. The impor-tance of the soot-associated organic mutagens in the rat lung tumor response to diesel soot was tested in two studies. Nikula et al. (15) exposed rats 6 h/d, 5 d/wk for 2 y to either diesel exhaust at 2.5 or 6.5 mg/m^3 soot or identical concentrations of similar-sized carbon black having negligible mutagenic content. The diesel soot and carbon black exposures caused essentially identical lung tumor re-sponses, despite the large difference in muta-genicity of the two materials. Heinrich et al. (16) exposed rats to multiple concentrations of diesel soot, to mutagen-poor carbon black or to titanium dioxide, and found that the three materials had equal carcinogenic potency. These results demonstrated that the soot-associated organic mutagens, which were the principal concern for potential human cancer risk, are not important in causing the lung tumors in rats exposed to diesel exhaust.

The difference between lung tumor responses of rats and other rodents is not unique to diesel soot (17). Ten particles of different types have been shown to cause lung tumors in rats, but not mice, exposed by inhalation. Six of these materials have also been shown to be negative in hamsters, and four have not been tested in that species. In addition, beryllium metal and nickel oxide, like diesel soot, are lung carcin-ogens in rats exposed by inhalation, but only produce equivocal results in mice. The difference between rats and mice is not consistent for all particulate materials however; cadmium oxide, calcium chromate, coal tar aerosol, and cobalt sulfate cause lung tumors in both rats and mice exposed by inhalation.

Little is known about the long-term responses of non-rodent animal species to chronic, heavy particle exposure. Snipes (18) reviewed the scanty information available for non-rodent species and drew the tentative conclusions that particles tend to accumulate differently in

rats and non-rodent species and that the cellular responses of non-rodent species to deposited particles are typically less than that of rats. Nikula et al. (19) recently provided support for this conclusion by demonstrating that diesel soot and respirable coal dust accumulate in different preferential locations in lungs of rats and non-human primates exposed in parallel by inhalation. These materials accumulated primarily in alveoli in rats, but largely in the interstitium in monkeys. Also, in contrast to rats, monkeys had little epithelial proliferative re-sponse to either material.

CONCLUSIONS

There is a large amount of laboratory data on the toxicology of diesel emissions. Laboratory studies have shown clearly that diesel emissions contain toxic materials, but laboratory data do not allow confident prediction of the existence, nature, or magnitude of the potential human health risks. Attention has been focus-ed largely on lung cancer risk. The present laboratory evidence indicates that the lung tumor response of rats to heavy, chronic exposures to diesel soot should not be used to develop quantitative estimates of lung cancer risk in humans exposed to environmental levels. The tumor response of rats occurs only at high exposure concentrations, and has an apparent exposure threshold. The tumor response of rats can not be extrapolated to other rodents. Monkeys do not develop the epithelial proliferative response to diesel soot that occurs in rats. Moreover, there is no evidence that the lung epithelial cell proliferation and tumor development observed in rats is characteristic of the response of human lungs to heavy particle loading.

The inapplicability of the rat results to quantitative estimates of human lung cancer risk does not prove that diesel exhaust presents no risk to humans. The toxicological results give no strong basis for excluding diesel exhaust when considering the total exposure of humans to inhaled mutagens in the workplace or general environment. On the other hand, our present knowledge of the toxicology of diesel exhaust does not provide a basis for assigning any unique human lung cancer risk to diesel exhaust other than that presented by any material containing similar types of mutagenic activity.

REFERENCES

1. International Agency for Research on Cancer; *Monographs on the Evaluation of Carcinogenic Risks to Humans, Vol 46, Diesel and Gasoline Engine Exhausts and Some Nitroarenes*, IARC, Lyon, 1989.

2. Mauderly, J; *Environmental Toxicants;* M. Lippmann, Ed.; Van Nostrand Reinhold, New York, 1992; pp 119-162.

3. Kotin, P.; Falk, H.; Thomas, M. Arch. Ind. Health 1955 11 113-120.

4. Huisingh, J.; Bradow, R.; Jungers, R; et al.; *Application of Short-Term Bioassays in the Fractionation and Analysis of Complex Environmental Mixtures*; Waters M., Nesnow, S., Huisingh, J., Sandhu, S., Claxton, Eds L.; Plenum Press, New York, 1978; pp 381-418.

5. Rosenkranz, H.; *Diesel Exhaust: A Critical Analysis of Emissions, Exposure, and Health Effects*; Health Effects Institute, Cambridge, MA, 1995; pp 243-250.

6. Shirname-More, L.; *Diesel Exhaust: A Critical Analysis of Emissions, Exposure, and Health Effects*; Health Effects Institute, Cambridge, MA, 1995; pp 221-242.

7. Randerath, K.; Putnam, K.; Mauderly, J., et al.; *Pulmonary Toxicity of Inhaled Diesel Exhaust and Carbon Black in Chronically Exposed Rats, Part II: Diesel Exhaust and DNA Damage*; Health Effects Institute, Cambridge, MA, 1996.

8. Gallagher, J.; Heinrich, U.; George, M., et al.; Carcinogenesis 1994 15 1291-1299.

9. Busby, W.; Newburne, P.; *Diesel Exhaust: A Critical Analysis of Emissions, Exposure, and Health Effects*; Health Effects Institute, Cambridge, MA, 1995; pp 185-220.

10. Wolff, R.; Henderson, R.; Snipes, M., et al.; Fundam. Appl. Toxicol. 1987 9 154-166.

11. Mauderly, J.; Jones, R.; Griffith, W., et al.; Fundam. Appl. Toxicol. 1987 9 208-221.

12. Mauderly, J.; Banas, D.; Griffith, W., et al.; Fundam. Appl. Toxicol. 1996 30 233-242.

13. Henderson, R.; Pickrell, J. Jones, R., et al.; Fundam. Appl. Toxicol. 1988 11 546-567.

14. Mauderly J.; *Toxic and Carcinogenic Effects of Solid Particles in the Respiratory Tract*; Mohr, U., Dungworth, D., Mauderly, J., Ober-dörster, G., Eds; ILSI Press, Washington, 1994; pp 355-366.

15. Nikula, K.; Snipes, M.; Barr, E., et al.; Fundam. Appl. Toxicol. 1995 25 80-94.

16. Heinrich, U.; Fuhst, R.; Rittinghausen, S., et al.; Inhal. Toxicol. 1995 7 553-556.

17. Mauderly, J.L. Environ. Health Perspect. 1997 (in press).

18. Snipes, M. Inhal. Toxicol. 1996 8S 91-109.

19. Nikula, K.; Avila, K.; Griffith, W., et al.; Fundam. Appl. Toxicol. 1997 36 (in press).

EPA'S ASSESSMENT OF HUMAN HEALTH RISK FROM EXPOSURE TO DIESEL ENGINE EMISSIONS

W.E. Pepelko
U.S. Environmental Protection Agency

INTRODUCTION

EPA's concerns regarding the possible health effects of diesel engine emissions arose in the mid to late 1970s as a result of the energy crisis and the accompanying belief that the number of diesel equipped passenger automobiles would increase greatly with accompanying increases in particulate matter pollution. This concern was enhanced by the possibility that diesel exhaust may be carcinogenic. Although the ability of diesel particle extracts to induce skin cancer had been reported in an early study by Kotin et al. (1955), the carcinogenic potential of diesel exhaust received little notice until publication of a report by Huisingh et al. (1978). This report indicated that organic extracts of diesel particulate matter are mutagenic. Furthering this interest was the knowledge that organic extracts of diesel particles contain compounds such as benzo(*a*)-pyrene, albeit at very low concentrations, that are well known for their ability to cause cancer.

The increase in diesel engine equipped automobiles did not occur due to the initial low quality of diesel engines available for passenger cars; decreasing fuel costs with the passing of the energy crisis; and the fact that diesel engines lacked wide appeal because of noisiness, greater purchase costs, slow acceleration, and unpleasant odors. While the number of diesel engine equipped automobiles has remained low, however, diesel engine usage has steadily increased in trucks, construction and mining equipment, locomotives, and ships. The potential threat to human health due to increased diesel usage is at least partially offset by improved engine design resulting in increased engine efficiency and decreased emissions. Nevertheless, because chronic exposure to diesel exhaust (DE) has been shown to induce adverse health effects, interest in further evaluation of the nature as well as the degree of human susceptibility to these effects has remained high.

EVALUATION OF NONCANCER HEALTH EFFECTS

Acute toxicity The most readily identified acute effects of diesel exhaust in humans are subjective complaints of eye, throat, and bronchial irritation and neuropsychological symptoms such as headache, lightheadedness, nausea, vomiting, numbness, and tingling of extremities. Diesel odors are also considered to be noxious. Over the course of workshifts in studies of underground miners, bus garage workers, dock workers, and locomotive repairmen, decrements in lung function occasionally have been reported (Cohen and Higgins, 1995). The only evidence of permanent harm from acute exposure, however, is an unpublished case report (private communication from EPA Office of Mobile Sources) of a mechanic suffering from severe and disabling lung damage following a brief exposure to a very high concentration of diesel exhaust.

Exposures of 5 hours duration to pure diesel exhaust from an engine running under a heavy load resulted in 100% mortality in guinea pigs, rabbits and mice. Lighter loads resulted in progressively lower mortality rates (Pattle et al., 1957). Exposure of laboratory animals for several days to diesel particle concentrations of up to about 6 mg/m^3 induced an inflammatory response as indicated by alveolar macrophage (AM) aggregation near the terminal bronchioles, Type II cell proliferation, and the thickening of alveolar walls adjacent to AM aggregations. Lung function decrements, however, were generally minimal and overall impairment of health was not reported (Watson

and Green, 1995).

Dose-response for acute exposure. Lung pathology was the primary effect reported in experimental animals acutely exposed to concentrations of several mg/m^3. Adverse clinical effects in humans, on the other hand, noxious odor, headache, and mucous membrane irritation occurred at considerably lower concentrations. In clinical trials a threshold for odor detection of diesel exhaust diluted as much as 475-fold with clean air (i.e. estimated to equal a particle concentration of about about 200 *u*g/m^3) was reported (Linnell and Scott, 1962). Although a formal determination of safe acute exposure levels have not been determined, concentrations greater than 200 *u*g/m^3 may be noxious and even lower concentrations may induce adverse effects in sensitive individuals.

Chronic toxicity. Epidemiologic evidence from chronic exposure to Diesel exhaust is conflicting. Although effects in occupationally exposed workers have generally been quite limited, indications of obstructive or restrictive lung disease have occasionally been reported. Many of these studies are difficult to interpret because they suffer from methodological problems including incomplete information on DE concentrations, the presence of confounding variables such as smoking or concomitant exposure to other toxic substances, as well as short duration and low intensity of exposure. Moreover, definitive data regarding possible pathologicial effects from autopsies or lung biopsies are generally unavailable (Cohen and Higgins, 1995). Information regarding effects in other organ systems are limited

An extensive database on animal studies (rats, mice, hamsters, cats, and monkeys) is available. The study results are consistent among all species in that the critical target site is the deep lung. Long-term exposure to a DE particulate matter concentration of 2 mg/m^3 and above have typically resulted in restrictive lung disease. Histopathological findings included alveolar histiocytosis, macrophage aggregation, tissue inflammation, increases in polymorphonuclear leukocytes, hyperplasia of bronchiolar and alveolar Type II cells, thickened alveolar septa, edema, fibrosis, and emphysema. The severity of these inflammatory responses were directly related to exposure levels. Decreased rates of particle clearance were noted at exposure concentrations greater than 1 mg/m^3. Behavioral effects were also reported in rats exposed from birth to 28 days of age These included a decrease in spontaneous locomotor activity and a detrimental effect on learning during adulthood. These studies, however, were only conducted at exposure concentrations of several mg/m^3. For further details regarding noncancer health effects see Watson and Green (1995).

Dose-response for chronic toxicity. The determination of safe levels for chronic noncancer effects was carried out by the development of a reference concentration (RfC). An RfC is defined as an estimate (with uncertainty spanning perhaps an order of magnitude of a continuous inhalation exposure to the human population, including sensitive subgroups) that is likely to be without appreciable risks of deleterious effects during a lifetime. Two studies of rats exposed for 2 years or longer to particle concentrations ranging from 0.11 to 7.1 mg/m^3, and having measurements of a large number of endpoints, were used for the development of the RfC (Ishinishi et al., 1986; Mauderly et al., 1987).

An RfC is derived from the highest no-observable-effect-level (NOAEL). Based on the Ishinish et al. (1986) study, the NOAEL was determined to be 460 *u*g per m^3 with lung pathology the critical endpoint. Since the animals were exposed 16 hours/day, 6 days/-week, an adjustment to continuous exposure of 0.57 (16/24 x 6/7) was made. A dosimetry model developed by Yu et al. (1991) was used to extrapolate concentration from animals to humans. According to this model, which accounted for rat to human differences in respiratory exchange rates, particle deposition efficiency, particle clearance rates, and transport of particles from lung associated lymph nodes, an adjustment of 0.57 is appropriate. After these adjustments and division by an uncertainty factor of 30, 10 for varia-

tions in human sensitivity and 3 for possible differences in sensitivity of rats and humans, an RfC of 5 ug/m^3 was derived.

The RfC is considered to be sufficiently protective even for sensitive populations. Lower thresholds for adverse health effects have not been noted in a variety of other species tested. Effects from DE exposure were only noted in occupationally exposed humans at concentrations considerably greater than the RfC. Although sensitive humans are unlikely to be found among this group, addition of a 30-fold uncertainty factor should protect sensitive individuals.

EVALUATION OF CARCINOGENICITY

Qualitative assessment of carcinogenicity. The possible carcinogenic effects of DE in humans have been reviewed by Cohen and Higgins (1995). The studies suggest that exposure to diesel exhaust in a variety of occupational circumstances is associated with small to moderate increases in relative risk of lung cancer mortality. These elevations do not appear to be fully explicable by confounding due to cigarette smoking or other sources of bias. DE exposure, therefore, provides the most reasonable explanation for these elevations. Cohen and Higgins (1995), however, have cautioned that risk elevations of the magnitude reported (20%-40%) should not be overinterpreted. For example, inaccuracies of exposure measurement could either spuriously elevate or underestimate risk.

Animal carcinogenicity studies have been reviewed by Busby and Newberne (1995) and Mauderly (1992). The carcinogenicity of DE has been confirmed in two strains of rats in at least five different laboratories. The data for mice are equivocal. Lung cancer studies were generally negative in common laboratory strains of mice. However, increases were noted on the Sencar strain which is very sensitive to cancer induction in epithelial tissue (Pepelko and Peirano, 1983). Syrian hamsters have not developed lung tumors in any of the studies reported thus far.

Under EPA's 1986 Cancer Risk Assessment Guidelines (U.S. EPA, 1986), DE is tentatively considered to be a probable human carcinogen. According to EPA's Proposed Guidelines for Carcinogen Risk Assessment (U.S. EPA, 1996), diesel exhaust is considered "highly likely" to be carcinogenic in humans by the inhalation route of exposure. These classifications are based primarily on reported increases in lung cancer mortality in a number of occupational exposure studies. The conclusion that DE is a "probable" or a "highly likely" rather than a "known" carcinogen is due to lack of specific DE exposure data in human studies. The exposure data limitations include an inability to completely eliminate confounding factors such as exposure to other pollutants, especially tobacco smoke. Strong support for the conclusion that DE is "highly likely" to be a human carcinogen is provided by positive cancer data in bioassays with rats, positive genotoxicity data, and the knowledge that diesel exhaust contains carcinogenic compounds.

Dose response assessment. Cancer potency estimates for inhaled agents are published as unit risks. The unit risk for DE is defined as the estimated 95% upper bound of the lifetime risk of cancer from continuous lifetime exposure to 1 ug/m^3 of diesel particulate matter. Estimates are based upon particle concentration because few effects have been noted following exposure to the vapor phase of DE, intratracheal instillation of DE particles is capable of inducing lung cancer, and particle concentration is the most practicle dosimeter. A variety of approaches for estimating cancer potency have been attempted for DE utilizing data from epidemiology studies, laboratory animal bioassays, and in vitro studies.

The earliest attempts to determine the carcinogenic potency of DE were based upon the so called "comparative potency" method. This method was developed because of a lack of either human cancer epidemiology studies or animal cancer bioassays for DE exposure. It is based upon the belief that the carcinogenic effects are due to the organic constituents of the particles and that these constituents in various combustion products acted by similar

mechanisms. In this approach, the potency of DE particle extracts were compared in a variety of short-term tests such as skin painting, mutagenicity, sister chromatid exchange, etc. to related combustion or pyrolysis products, roofing tar, cigarette smoke condensate, and coke oven emissions. The ratio of the potency of DE paarticle extracts to each of these pollutants was then multiplied by the epidemiology based unit risk estimate for each of these agents. Using this method, Albert et al. (1983) derived unit risk estimates for DE averaging near 3×10^{-5} per ug/m^3.

Pike and Henderson (1981) found good agreement between lung cancer risk and concentration of benzo(*a*)pyrene [B(*a*)P] in the inspired air of smokers, British gas workers, U.S. coke oven workers, U.S. hot pitch workers, and when comparing residents of rural and urban locations. Based upon an estimated lung cancer risk of 1/1500 per ng/m^3 B(*a*)P and B(*a*)P concentration in particles from a Volkswagen engine (Heinrich et al.,1995), a unit risk estimate of about 1×10^{-5} per ug/m^3 particulate matter can be derived. Which is essentiall equivalent to Albert et al. (1983).

During the mid to late 1980s, several long-term animal cancer bioassays including those by Brightwell et al. (1989), Ishinishi et al. (1986), and Mauderly et al. (1987) were published. As a result, a number of cancer risk estimates based upon experimental tumor data in rats were derived (Albert and Chen, 1986; Pott and Heinrich, 1987; McClellan et al., 1989; Smith and Stayner, 1990; Pepelko and Chen, 1993; and Chen and Oberdoerster, 1996). A variety of low-dose extrapolation models were used, although none departed significantly from linearity. The more recent ones, such as those derived by Pepelko and Chen (1993) used a detailed dosimetry model to more accurately extrapolate dose from animals to humans. These unit risk estimates ranged from about 1.6×10^{-5} to 1.2×10^{-4} per ug/m^3.

During this period, a number of epidemiologic studies were also reported. A case-control study of railroad workers published by Garshick et al. (1987) was the most useful for quantitating cancer risk. Using this study McClellan et al. (1989) estimated the annual number of lung cancer deaths due to DE exposure in the United States. From these mortality estimates and assuming a mean exposure concentration of 500 ug/m^3, a unit risk estimate of 6×10^{-4} per ug/m^3 could be derived.

Each of these approaches has strengths as well as uncertainties. Well controlled epidemiology studies are preferable for assessing human risk. Human data eliminates uncertainties due to dose extrapolation and possible differences in sensitivity between experimental animals and humans. Human exposures also are usually at lower concentrations than those used in animal bioassays and thus require a shorter extrapolation to ambient levels. The greatest uncertainty in use of human data is accurate determination of exposure levels. Although recent measurements for occupationally exposed groups are generally available, historic exposure measurements are very limited. Because of the long induction time for carcinogenesis, lack of accurate historic exposure data increases uncertainty considerably. Also, there is a chance for error due to small increases in relative risk coupled with an inability to completely eliminate confounding variables such as smoking and exposure to other chemicals.

In the comparative potency method it is assumed that carcinogenic effects are due to the organic matter constituents of diesel particles. Laboratory studies, however, show that carbon black, which is similar to the carbon core of diesel particles, is capable of inducing lung cancer in experimental animals (Heinrich et al., 1995). Failure to account for particle effects increases the uncertainty of using this approach. This approach, however, still deserves consideration since lung cancer induction at low doses is more likely to be induced by the organic fraction.

A strength of the biomarker approach is the fact that the risk estimates for a variety of the related pollutants compared are derived from human data. On the other hand, particles from

other combustion and pyrolysis products consist of, to a large extent, organic compounds, with little or no elemental, insoluble carbon core. Differences in the composition of the particle core increases uncertainty since particle effects may be minimal with soluble particles.

In estimating risk based upon chronic animal bioassays, actual tumor counts are available and exposure conditions are usually quite well defined. Some uncertainty occurs in extrapolating dose from animals to humans, but this can usually be minimized by the use of a suitable dosimetry model. Greater uncertainty occurs during low-dose extrapolation. There is at least some evidence suggesting that the mode of action of lung tumor induction in rats exposed at high doses may be related to lung pathology associated lung particle overload. If so, the dose response curve may be nonlinear. Another source of uncertainty is the suitability of the rat model for assessing human risk from exposure to particulate matter (Mauderly, 1996).

Each of the above approaches for estimating human lung cancer risk from DE exposure has uncertainties of sufficient magnitude to preclude selecting one as the "most scientifically valid." As a result, a single point estimate of risk, at least tentatively, is not proposed. Collectively, however, the various estimates are considered to be adequate for bounding risk. The estimate of 6×10^{-4} per ug/m^3 derived from the Garshick et al. (1987) case-control study of railroad workers provides a reasonable upper bound. Because few of the the relative risk ratios reported in other studies exceeded that reported by Garshick et al. and because exposure estimates were quite conservative, risk is unlikely to be underestimated. Risk estimates using the comparative potency or B(*a*)P method were lower, ranging from as little as 1×10^{-5} per *u*g/m^3. Since they are based primarily upon the organic fraction of DE, risk is unlikely to be underestimated because of the possibility that particles also may play a role in tumor induction. Risk estimates derived from animal bioassays also fall within this range. For these reasons upper confidences limits of lung cancer risk are considered to be bounded by a range of 1×10^{-5} to 6×10^{-4} per *u*g/m^3 of diesel particulate matter. It should be noted, however, that this recommendation has not been approved as official EPA policy and is subject to revision. No endorsement by EPA is intended.

SUMMARY

DE is considered to be a probable human carcinogen under EPA's 1986 cancer risk assessment guidelines and highly likely to be carcinogenic under EPA's 1996 proposed guidelines for cancer risk assessment. The 95% upper confidence limit for cancer potency is tentatively determined to be bounded by a range of 6×10^{-4} to 1×10^{-5} per *u*g/m^3. The critical target organ for noncancer health effects is the lung. An RfC of 5 *u*g/m^3 is recommended.

REFERENCES

1. Albert, R.E; Chen, C. (1986) U.S. EPA studies on inhalation hazards. In: Ishinishi, N., Koizumi, A., McClellan, R.O., and Stober, W., eds., Carcinogenicity and mutagenicity of diesel engine exhaust. Elsevier Science Publishers, Amsterdam: pp.411-419.

2. Albert, R.E.; Lewtas, J.; Nesnow, S.; Thorslund, T.W.; Anderson, E. (1983) Comparative potency method for cancer risk assessment. Application to diesel particle emissions. Risk Anal. 3:101-117.

3. Brightwell, J.; Fouillet, X.; Cassano-Zoppi, A.L.; Bernstein, D.; Crawley, F.; Duchosal, F.; Gatz, R.; Perczel, S.; Pfeifer, H. (1989) Tumours of the respiratory tract in rats and hamsters following chronic inhalation of engine exhaust emissions. J. Appl. Toxicol. 9:23-31.

4. Busby, W.F.; Newberne, P.M. (1995) Diesel emissions and other substances associated with animal carcinogenicity. In: Diesel Exhaust: A Critical Analysis of Emissions, Exposure, and Health Effects. Health Effects Institute, Cambridge, MA: pp. 185-220.

5. Busby, W.F. Jr.; Watson, A.Y. (1995) Noncancer effects of diesel emissions. In: Diesel Exhaust: A Critical Analysis of Emissions, Exposure, and Health Effects. Health Effects Institute,

Cambridge, MA: pp. 139-164.

6. Chen, C.; Oberdoerster, G. (1996) Selection of models for assessing dose-response relationships for particle-induced lung cancer. Inhal. Toxicol. 8(Suppl) : 259-278.

7. Cohen, A.J.; Higgins, M.W.P. (1995) Health effects of diesel exhaust: Epidemiology. In: Diesel Exhaust: A Critical Analysis of Emissions, Exposure, and Health Effects. Health Effects Institute. Cambridge, MA: pp. 251-292.

8. Garshick, E.; Schenker, M.B.; Munoz, A.; Segal, M.; Smith, T.J.; Woskie, S.R.; Hammond, S.K.; Speizer, F.E. (1987) A case-control study of lung cancer and diesel exhaust exposure in railroad workers. Am. Rev. Respir. Dis.135: 1242-1248.

9. Heinrich, U.; Fuhst, R.; Rittinghausen, S.; Creutzenberg, O.; Bellmann, B.; Koch, W.; Levsen, K. (1995) Chronic inhalation exposure of Wistar rats and two different strains of mice to diesel engine exhaust, carbon black and titanium dioxide. Inhal. Toxicol. 7:553-556.

10. Huisingh, J.; Bradow, R.; Jungers, R.; Claxton, L.; Zweidinger, R.; Tejada, S.; Baumgarner, J.; Duffield, F.; Waters, M.; Simmon, V.F.; Hare, C.; Rodriguez, C.; Snow, L. (1978) Application of bioassays to the characterization of diesel particle emissions. In: Waters, M.; Nesnow, S.; Huisingh, J.; Sandhu, S.; Claxton, L.; eds. Applications of Short-Term Bioassays in the Fractionation and Analysis of Complex Environmental Mixtures. Plenum Press, New, York: pp. 348-418.

11. Ishinishi, N.; Kuwabara, N.; Nagase, S.; Suzuki, T.; Ishiwata, S.; Kohno, T. (1986) Long-term inhalation studies on effects of exhaust from heavy and light duty engines on F344 rats. In: Ishinishi, N.; Koizumi, A.; McClellan, R.O.; Stober, W. eds. Carcinogenic and Mutagenic Effects of Diesel Engine Exhaust. Elsevier, Amsterdam: pp. 329-348.

12. Kotin, P.; Falk, H.L.; Thomas, M. (1955) Aromatic hydrocarbons: III. Presence in the particulate phase of diesel-engine exhausts and the carcinogenicity of exhaust extracts. AMA Arch. Ind. Health 11:113-120.

13. Linnell, R.H.;Scott, W.E. (1962) Diesel exhaust composition and odor studies. J. Air Pollution Control Assoc. 12:510-515

14. Mauderly, J.L.; Jones, R.K.; Griffith, W.C.; Henderson, R.F. (1987) Diesel exhaust is a pulmonary carcinogen in rats exposed chronically by inhalation. Fundam. Appl. Toxicol. 9:208-221.

15. Mauderly, J.L. (1992) Diesel exhaust. In: Lippman, M., ed. Environmental Toxicants--Human Exposure and Their Health Effects. Van Nostrand Reinhold, New York, NY:pp. 119-162.

16. Mauderly, J.L. (1996) Lung overload: The dilemma and opportunities for resolution. Inhal. Toxicol. 8, Suppl: 1-28.

17. McClellan, R.O.; Cuddihy, R.G.; Griffith, W.C.; Mauderly, J.L (1989) Integrating diverse data sets to assess risks of airborne pollutants. In: Mohr, U.; Bates, D.V.; Dungworth, D.L.;. McClellan, R.O., Roe, F.J.C, eds. Assessment of Inhalation Hazards. Springer Verlag, Berlin:pp. 3-22.

18. Pattle, R.E.; Stretch, H.; Burgess, F.; Sinclair, K.; Edgington, J.A.G. (1957) The toxicity of fumes from a diesel engine under four different running conditions. Br. J. Ind. Med. 14:47-55.

19. Pepelko, W.E.; Chen, C. (1993) Quantitative assessment of cancer risk from exposure to diesel engine emissions. Regul. Toxicol. Pharmacol. 17:52-65.

20. Pepelko, W.E.; Peirano, B. (1983) Health effects of exposure to diesel engine emissions: a summary of animal studies conducted by the U.S. Environmental Protection Agency's Health Effects Research Laboratories at Cincinnati, Ohio. J. Am. Coll. Toxicol. 2:253-306.

21. Pike, M.E.; Henderson, B.E. (1981) Epidemiology of polycylic aromatic hydrocarbons: quantifying the cancer risk from cigarette smoking and air pollution. In: Gellbond, H.V.; Tso, P.O.P, eds. Polycyclic Hydrocarbons and Cancer. Academic Press, New York:pp. 317-334.

22. Pott, F.; Heinrich, U. (1987) Dieselmotorabgas und Lungenk auf die Gefahrdung des Menschen. Umwelhygiene (Dusseldorf). 19:130-167.

23. Smith, R.A.; Stayner, L. (1990) An exploratory assessment of the risk of lung cancer associated with exposure to diesel exhaust based on a study with rats (final report). National Institute for Occupational Safety and Health, Division of Standards Developement and Technology Transfer.

24. U.S. Environmental Protection Agency. (1986) Guidelines for carcinogen risk assessment. Federal Register 51 (185):3392-34003.

25. U.S. Environmental protectionAgency. (1996) Proposed guidelines for carcinogen risk assessment. Federal Register 61(79):17960-18011.

26. Watson, A.; Green, G. (1995) Noncancer effects of diesel emissions. In: Diesel Exhaust: A Critical Analysis of Emissions, Exposure, and Health Effects. Health Effects Instute, Cambridge MA:pp. 139-185.

27. Yu, C.P.; Yoon, K.J.; Chen, Y.K. (1991) Retention modeling of diesel exhaust particles in rats and humans. J. Aerosol Med. 4:79-115.

SESSION IIIA

Aftertreatment - Non-Thermal Plasma

Chairman: Ron Graves
Oak Ridge National Laboratory

sociation of NO molecules. However, because of the relatively low concentration of NO in the exhaust gas, direct dissociation of NO by the electrons is not probable. The kinetic energy of the electrons is deposited primarily into the major exhaust gas components, N_2 and O_2.

The physics of electron collisions with the N_2 and O_2 molecules determines the electrical energy cost for the NOx conversion chemistry. The chemistry in the plasma always start with electron-impact dissociation of the abundant molecules. The efficiency for dissociation of various molecules is determined by the average kinetic energy of the electrons. The average electron kinetic energy is determined by the electron-molecule collision cross section and the electric field experienced by the el

The electrons could lose considerable kinetic energy through reactions, such as the vibrational excitation of N_2, which heats up the N_2 molecule but does not promote the conversion of NOx. The most useful deposition of electron kinetic energy into N_2 and O_2 is associated with the production of N and O radicals through electron-impact dissociation:

$$e + N_2 \rightarrow e + N(^4S) + N(^4S,^2D) \quad (1)$$
$$e + O_2. \rightarrow e + O(^3P) + O(^3P,^1 D) \quad (2)$$

where $N(^4S)$ and $N(^2D)$ are ground-state and metastable excited-state nitrogen atoms, respectively, and $O(^3P)$ and $O(^1D)$ are ground state and metastable excited-state oxygen atoms, respectively.

The NOx in the engine exhaust gas initially consist mostly of NO. The ground state atomic nitrogen, $N(^4S)$, is the only species produced by the plasma that can lead to the gas-phase chemical reduction of NO:

$$N(^4S) + NO \rightarrow N_2 + O \quad (3)$$

The gas-phase chemical reduction of NOx is therefore determined by the electron-impact dissociation of N_2.

COLLISION CROSS SECTION

The electron-molecule collision cross section represents the probability that the molecule will undergo a specific reaction (for example, dissociation) when hit by an electron. The collision cross section is expressed in units of a geometrical cross sectional area, typically on the order of 10^{16} cm^2. If the electron hits a circular target of this size perpendicular to its path and centered at the molecule, then the reaction occurs. If it misses that area, then the reaction does not occur.

The collision cross section is a fundamental quantity that has been measured by atomic physicists. The cross section for electron collision with a particular molecule is independent of the composition of the exhaust gas. The cross section for electron-impact dissociation of N_2 has a maximum that cannot be exceeded regardless of the plasma reactor design or the way the electrical voltage is delivered to the plasma reactor.

Figure 1 shows the cross section for electron impact on N_2 leading to neutral atomic nitrogen products [1].

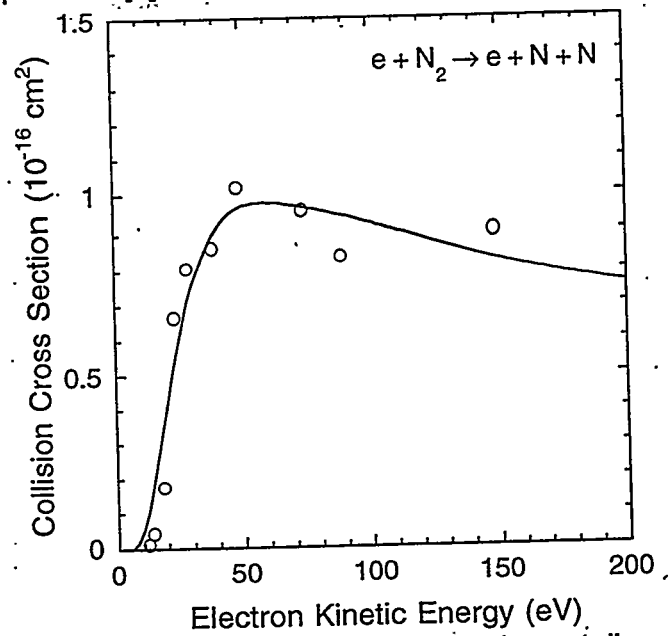


Figure 1. Cross section for electron-impact dissociation of N_2.

ELECTRIC FIELD

There are basically only two types of non-thermal plasma reactors: discharge and electron beam. Discharge plasma reactors are those reactors in which the high voltage elec-

trodes are immersed in the atmospheric-pressure gas stream. The attainable electron kinetic energy in this kind of reactor is very limited. The electrons collide rapidly with the background gas molecules and therefore cannot be accelerated to very high kinetic energies. Electron beam plasma reactors are those reactors in which the high voltage electrodes are in vacuum. The electrons are accelerated in thevacuum region before they are injected into the exhaust gas stream.

The electric field in a discharge plasma is determined largely by the electrical breakdown threshold. Under atmospheric-pressure conditions, the electric field experienced by the discharge plasma is between 30 and 60 kWcm [2], as shown in Figure 2.

Because of the limited range of electric fields that the electrons experience inside a discharge plasma, the average kinetic enrgy that the electrons can attain is also very limited.

Figure 3 shows the average electron kinetic energy as a function of the electric field. All discharge plasma reactors have average electron kinetic energies of 3 to 6 eV [3].

ELECTRICAL ENERGY COST

For now let us assume an ideal condition in which the plasma is not producing oxidative radicals. Let us further assume that all nitrogen atoms (labeled simply as N) are used entirely for the reduction of NO:

$$N + NO \rightarrow N_2 + O$$

In this case the electrical energy required to reduce NO is simply determined by the electrical energy required to produce N from the electron-impact dissociation of N_2. What is the energy required to implement this reduction scheme?

The electrical energy cost for the dissociation of N_2 is proportional to the average electron speed and inversely proportional to the dissociation rate. The average electron speed, known as the electron drift velocity, is a balance between energy gain because of electron acceleration

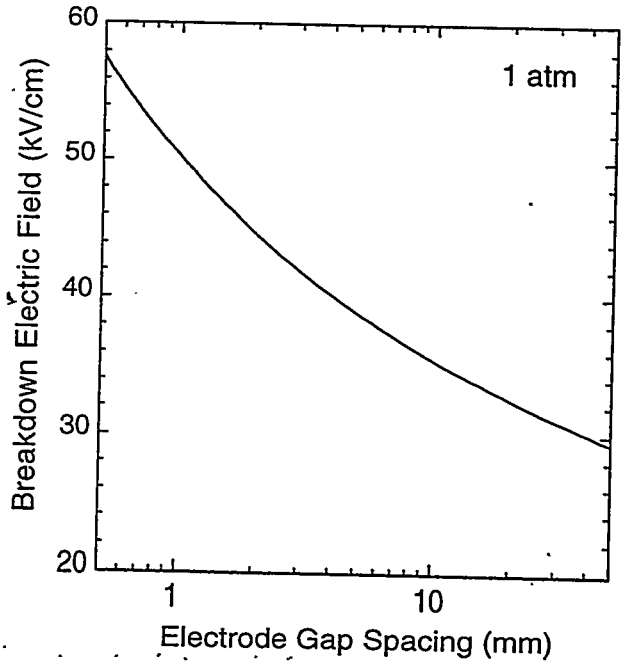


Figure 2: . Breakdown electric field in an atmospheric-pressure discharge plasma.

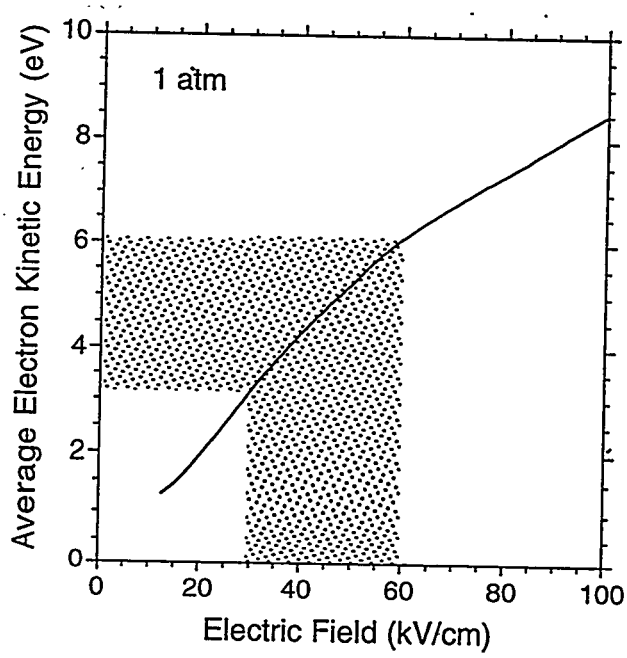


Figure 3. Average electron kinetic energy as a function of the electric field in an atmosphericpressure discharge plasma.

by the electric field and energy loss because of electron collisions with the molecules. Like the average kinetic energy, the drift velocity is determined by the electron-molecule collision cross sections and the electric field.

To minimize the electrical energy cost, one would like to have the highest dissociation rate. The dissociation rate is proportional to the dissociation cross section. The rate for dissociation of N_2 has a maximum because of the maximum in the cross section for electron-impact dissociation of N_2. The minimum electrical energy consumption for dissociation is determined by the maximum rate for dissociation.

The electrical energy cost can be expressed as a function of the electric field or the average kinetic energy of the electrons in the plasma. Figure 4 shows the electrical 'energy cost for N atom production as a function of the average electron kinetic energy. The electrical energy cost for NOx reduction by reaction (4) is equal to that for N atom production.

The electrical energy cost is very sensitive to the speed of the electrons. For most discharge plasma reactors the average electron kinetic energy is 4 eV [3]. In this case the electrical energy cost for NOx reduction is around 240 eV per NOx molecule. This means that if the plasma uses 5% of the engine energy output, then the amount of NOx that can be removed is $[0.05 / (240 \times 7.8\times10^{-4})] = 0.27$g(NOx)/bhp-hr. To remove 2g(NOx)/bhp-hr, the plasma would need at least 37% of the engine's output energy!

Fast electrons are required to minimize the electrical energy cost for NOx reduction. There are many proposals on how the electron kinetic energy can be increased. For the sake of establishing a fundamental limit, let us assume that a very high electron kinetic energy can be achieved in practice. As shown in Figure 4, the minimum electrical energy cost is 40 eV per NOx molecule [4]. Under this condition, the plasma can chemically reduce 1.6g(NOx)/bhp-hr when 5% of the engine output energy is delivered to the plasma.

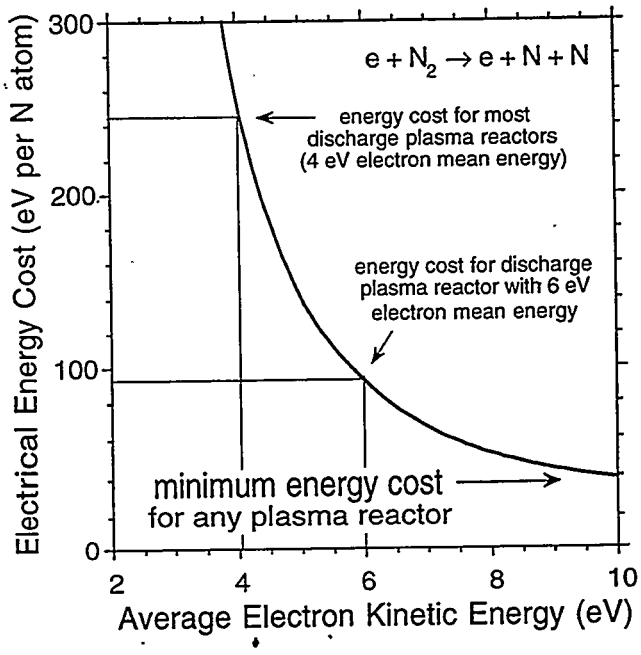


Figure 4. Electrical energy cost for N atom production as a function of the average electron kinetic energy.

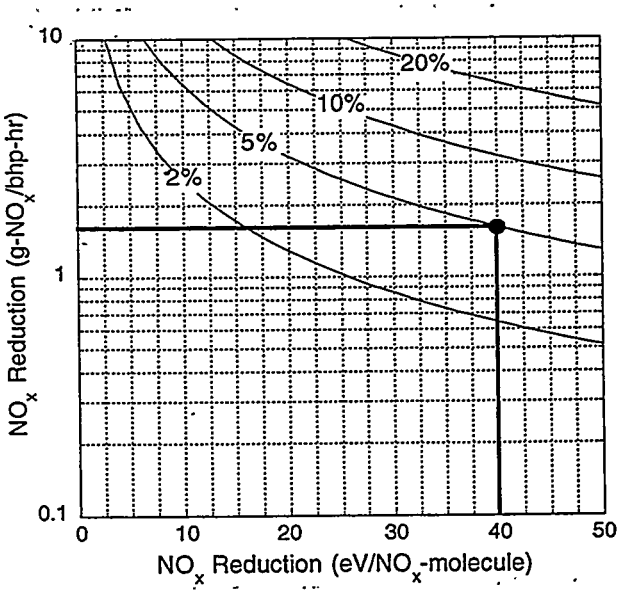


Figure 5: Conversion curves between eV per Nox molecule to give g(NOx)bhp-hr. The curves correspond to different percents of engine output energy aplied to the plasma. The value of 40 eV per NOx molecule is the minimum electrical energy cost for gas-phase chemical reduction of NOx in a plasma. This energy cost corresponds to a maximum NOx reduction of 1.6 g(NOx)bhp-hr when 5% of the engine output energy is applied to the plasma.

EFFECT OF OXYGEN

It is much easier and cheaper for the electrons to dissociate O_2 compared to N_2. The dissociation of O_2 will produce only oxidative radicals. With O_2 concentrations of 5% or more, a significant fraction of the electrical energy delivered to the plasma is dissipated in the dissociation Of O_2. The ground state oxygen atoms, 0(3P), convert NO to NO_2:

$$O(^3P) + NO + M \rightarrow NO_2 + M \quad (5)$$
$$O(^3P) + O_2 + M \rightarrow O_3 + M \quad (6a)$$
$$O_3 + NO \rightarrow NO_2 + O_2 \quad (6b)$$

Reactions (5) and (6) convert NO to NO_2 and leave the same amount of NOx.

During the dissociation of O_2, a significant fraction of the atomic oxygen products is in the excited state. This metastable excited-state atomic oxygen, $O(^1D)$, reacts with H_2O to produce OH radicals. The OH radicals convert NO and NO_2 to nitrous acid and nitric acid, respectively. Acid products in the plasma can easily get adsorbed on surfaces in the plasma reactor and in the pipes. When undetected, the absence of these oxidation products is often mistaken for chemical reduction of NOx.

In the presence Of O_2, not all of the N atoms resulting from the dissociation of N_2 lead to the reduction of NO. Dissociative excitation of N_2 contributes a large fraction to the total N_2 dissociation [5]. A significant species produced by dissociative excitation of N_2 is the long-lived metastable, $N(^2D)$. For fast electrons, over half of the total N atoms produced are in the excited metastable states. The rate constants characterizing the interaction of the metastable species N(2D) with various gases are large [6]. In the treatment of NO, there are two competing reactions involving the N(2D) metastable species:

$$N(^2D) + NO \rightarrow N_2 + O \quad (7)$$
$$N(^2D) + O_2 \rightarrow NO + O \quad (8)$$

With 500 ppm NO and 10% O_2, the N(2D) species is twenty times more likely to react with O_2 than with NO. This means that N(2D) is consumed in the production of NO rather than in the reduction of NO. Whereas the reaction of ground state N atoms, N(4S)' with O_2 can proceed only at very high temperatures, the reaction of excited N atoms, N(2D), with O_2 can proceed even at room temperature. Since almost half of the total N atoms produced in the plasma are in this excited state, the reduction of NO by the ground state N atoms is almost completely counterbalanced by the production of NO by the excited N atoms. What is left in terms of NOx conversion chemistry is the oxidation of NO to NO_2

HETEROGENEOUS REACTIONS

What we have examined in this paper is the gas-phase chemical reduction of NOx. Heterogeneous reactions in the plasma reactor can also take place. Absorption of NO_2 and nitric acid on particulates and reactor walls are often mistaken for gas-phase chemical reduction. There may be conditions in which one can take advantage of plasma oxidation products as intermediaries for the heterogeneous chemical reduction of NOx.

CONCLUSIONS

The gas-phase chemical reduction of NOx in a plasma can be accomplished via reaction with atomic nitrogen. Under the best condition, the plasma can chemically reduce 1.6 grams of NOx per brake- horsepower-hour when 5% of the engine output energy is delivered to the plasma. This NOx reduction efficiency is a fundamental limit that cannot be exceeded in the absence of heterogeneous reactions or chemical additives.

Fast electrons are required to optimize the production of atomic nitrogen from electron-impact dissociation of N_2- Unfortunately, a large fraction of the atomic nitrogen produced by the fast electrons are in the excited state. In the presence of O_2, the excited-state nitrogen atoms lead to the production of NO. Thus the development of plasma reactors that can produce fast electrons is not the key to achieving high NOx reduction efficiency when O_2 is present in the exhaust gas.
With the O_2 concentrations present in diesel and lean-burn engine exhausts, the dissociation of O_2 is the most dominant

dissociation reaction that takes place in the plasma. The dissociation Of O_2 promotes the gas-phase oxidation of NO to NO_2 and nitric acid, but not the gas-phase reduction of NOx to N_2. Absorption of NO_2 and nitric acid on particulates and reactor walls are often mistaken for gas-phase chemical reduction of NOx,

ACKNOWLEDGMENTS

This work was performed at Lawrence Livermore National Laboratory under the auspices of the U.S. Department of Energy under Contract Number W-7405-ENG-48, with support from the Chemical Sciences Division of the Office of Basic Energy Sciences and a Cooperative Research and Development Agreement with Cummins Engine Company.

REFERENCES

1.. Cosby, P.C:, *Journal of Chemical Physics* 98
(1993)9544.

2.. Raizer, Y.P,: *Gas Discharge Physics* (Springer-Verlag, New York, 1991).

3. Penetrante,B.M., Hsiao, M.C., Merritt, B.T., Vogtlin, G.E. Wallman, P.H., Neiger,M., Wolf, O., Hammer, T., and Broer, S., *Applied Physics Letters* 68(1996)3719.

4. Penetrante,B.M., Hsiao, M.C., Merritt, B.T., Vogtlin, G.E., Wallman, P.H., Kuthi, A.,. Burkhart, C.P., and Bayless,J.R:, *Applied Physics Letters* 67 (1995) 3096.

5. Zipf, E.C.. in *Electron-Molecule Interactions and their Applications* ed. L. Christophorou, Vol. 1 (Academic Press, New York, 1984) pp. 335401.

6. Schofield,:K., *Journal of Physical and Chemical Reference Data* 8 (1979) 723.

PLASMA-ASSISTED HETEROGENEOUS CATALYSIS FOR NO_x REDUCTION IN LEAN-BURN ENGINE EXHAUST

B.M. Penetrante, M.C. Hsaio, B.T. Merritt, and G.E. Vogtlin
Lawrence Livermore National Laboratory
C.Z. Wan, G.W. Rice, and K.E. Voss
Engelhard Corporation

INTRODUCTION

The NO_x in engine exhausts is composed primarily of NO. Consequently, aftertreatment schemes have focused a great deal on the reduction of NO. Recent developments in catalytic control of NO_x are revealing the significance of NO_2 as an intermediary for achieving higher NO_x removal efficiencies.

The leading catalytic technologies for removal of NO_x from lean-burn engine exhausts are the lean-NO_x SCR catalyst [1-2] and the lean-NO_x trap [3-5].

Selective catalytic reduction (SCR) is based on the reaction of NO with hydrocarbon species activated on the catalyst surface. Many studies now suggest that the conversion of NO to NO_2 is an important intermediate step in the reduction of NO_x to N_2[6-10]. The formation of NO_2 has been found to be a necessary but not a sufficient condition for the SCR of NO.

The lean-NO_x trap involves the catalytic oxidation of NO to NO, followed by the formation of a nitrate on the surface. The nitrate stored on the surface is decomposed by periodically operating under rich-burn condition and so the released NO_x is reduced.

Both lean-NO_x SCR and lean-NO_x trap technologies require low sulfur fuel because catalysts that are active in converting NO to NO_2 are also active in converting SO_2 to SO_3- SO_3 leads to the formation of sulfuric acid and sulfates that increase the particulates in the exhaust and poison the active sites on the catalyst.

This paper discusses the combination of a plasma with a catalyst to improve the reduction of NO_x under lean-burn conditions. We have been investigating the effects of a plasma on the NO_x reduction activity and temperature operating window of various catalytic materials. One of our goals is to develop a fundamental understanding of the interaction between the gas-phase plasma chemistry and the heterogeneous chemistry on the catalyst surface. We have observed that plasma assisted heterogeneous catalysis can facilitate NO_x reduction under conditions that normally make it difficult for either the plasma or the catalyst to function by itself. By systematically varying the plasma electrode and catalyst configuration, we have been able to elucidate the process by which the plasma chemistry af-fects the chemical reduction of NO_x on the cata-lyst surface.

We have discovered that the main effect of the plasma is to induce the gas-phase oxidation of NO to NO_2. The reduction of NO_x to N_2 is then accomplished by heterogeneous reaction of O with activated hydrocarbons on the catalyst surface. The use of a plasma opens the opportunity for a new class of catalysts that are potentially more durable, more active, more selective and more sulfur-tolerant compared to conventional lean-NO_x catalysts.

TEST SETUP

Figure 1 shows one of the possible embodiments of the plasma-assisted catalyst processor. In this setup the plasma reactor is located upstream of the catalyst reactor. The same result is achieved if the catalyst is placed inside the plasma reactor.

The plasma reactor used in our study is a pulsed corona discharge reactor consisting of a metal wire inside a metal cylinder. The power supply is a magnetic pulse compression system that delivers up to 3O kV output into 100 ns pulses at repetition rates up to the kilohertz range. The catalyst structures we have investigated consisted of either a pellet bed or a monolith.

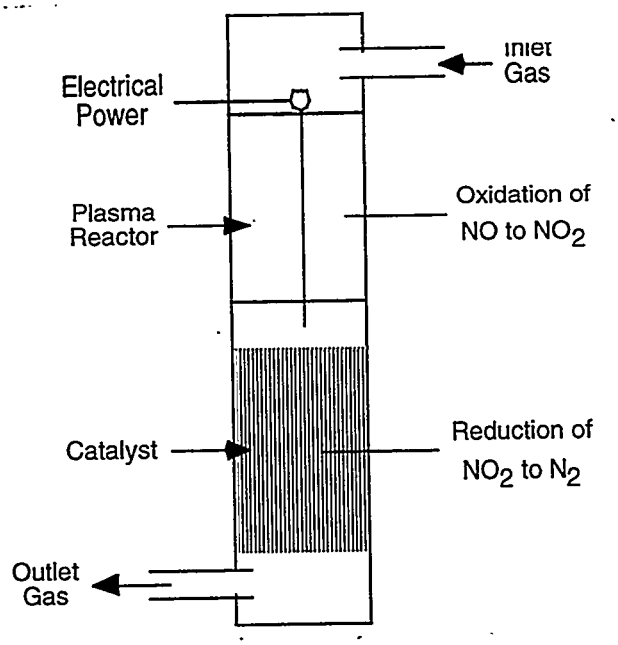


Figure 1. An embodiment of the plasma-assisted SCR process. The same result is achieved if the catalyst is placed inside the plasma reactor.

Heater bands and thermocouples are used to provide active control of the plasma/catalyst processor temperature. The processor temperature can be adjusted from room temperature up to 5000C. This has been used to investigate the operating temperature window of the process.

The separate plasma/catalyst configuration in Figure 1 is very flexible. Although we have used a pulsed corona reactor, this type of reactor is not necessarily the only type that produces the same effect. It can be used with any type of plasma reactor and does not require a specific type of high-voltage power supply. All electrical discharge plasma reactors accomplish essentially the same gas-phase plasma chemistry for the same gas mixture [11-12].

The separate plasma/catalyst configuration is also very flexible with respect to the catalyst support structure. It can be used with a bed of catalyst pellets or a monolith. For monolith structures, any L/D (length/diameter) ratio can be accommodated.

Tests of the plasma/catalyst processor have been done using both a simulated exhaust gas mixture and a real diesel engine exhaust. A gas blending manifold is used to custom make gas streams consisting of N_2, O_2, H_2O, CO_2, hydrocarbons, and NO_x. These gases are metered through mass flow controllers which permit exact control of the flow rate. After mixing in the manifold, the gas then passes through a temperature controlled heater which preheats the gas to the processor temperature. The use of custom-made gas mixtures is necessary for studying the effect of the gas composition on the gas-phase plasma chemistry and the activity of the catalyst. The effect of various gas components on the process products and process efficiency can thus be studied.

The plasma/catalyst processor is also connected to a generator set consisting of a Cummins B5.9 diesel engine. This enables us to test the process on a real diesel exhaust.

HOW THE PROCESS WORKS

The plasma-assisted catalytic reduction of NO_x is accomplished in essentially two steps. First, the plasma oxidizes NO to NO_2 in the presence of a hydrocarbon:

plasma + NO + HC +O_2 → NO_2 + HC-products

where HC refers to a hydrocarbon and HC-products refers to partially oxidized hydrocarbons. Second, the catalyst reduces NO_2 to N_2 by selective reduction using the hydrocarbons:

catalyst + NO_2 + HC → N_2 + CO_2 +H_2O-

Figure 2 shows the FTIR spectra of the process for a model exhaust gas consisting of 500 ppm NO, 1000 PPM (C_3) propene, 10%O_2 and balance N_2. The plasma/catalyst processor temperature is 3000C.

The spectrum of the inlet gas is shown in the top box of Figure 2. When the electrical power to the plasma reactor is turned off and this gas mixture is passed through the catalyst, the efficiencies for both the NO_x reduction and the hydrocarbon oxidation are very low, as shown in the second box ("catalyst only"). The NO_x reduction at this temperature is very low in spite of the relatively large amount of hydrocarbons available for the catalyst to do SCR.

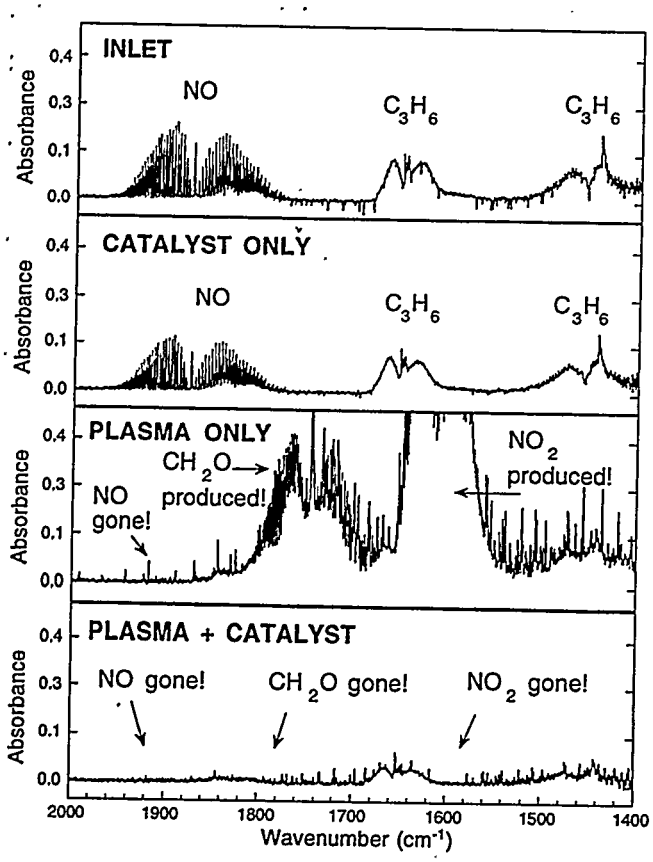


Figure 2. FTIR spectra showing the plasma-assited catalytic reduction of NO_x.

When the electrical power to the plasma reactor is turned on, the NO is oxidized to NO_2 and the propene is partially oxidized to formaldehyde, as shown in the third box ("plasma only"). The NO_x reduction is still very low. The same amount of total NO_x (NO +NO_2) is left in the gas stream.

When the NO_2-containing gas stream from the plasma is then passed through the same catalyst, both the NO_x and the hydrocarbons are eliminated, as shown in the bottom box ("plasma + catalyst"). This is true chemical reduction of NO_2 to N_2, and not just absorption of NO_2 on the catalyst surface. Both the original hydrocarbon and the partially oxidized hydrocarbons are eliminated in the process of reducing NO_2 to N_2.

KEY FEATURES

There are three key features in the plasma-assisted catalytic reduction of NO_x.

First, the plasma oxidation process is partial. This means the plasma oxidizes NO to NO_2 but does not further oxidize NO_2 to nitric acid. The plasma also produces some partially oxygenated hydrocarbons, but does not completely oxidize the hydrocarbons to CO_2 and H_2O.

Second, the plasma oxidation process is selective. This means the plasma oxidizes NO to NO_2, but does not oxidize SO_2 to SO_3. This makes the plasma-assisted process more tolerant to the sulfur content of fuel compared to conventional lean-NO_x technologies.

Third, by using a plasma to change the composition of NO_x from NO to NO_2, one can take advantage of a new class of catalysts that are potentially more durable and more active than conventional lean-NO_x catalysts.

ROLE OF HYDROCARBONS IN THE PLASMA

The use of a plasma does not automatically guarantee the efficient oxidation of NO to NO_2.

In exhausts containing both O_2 and H_2O, the plasma produces not only O radicals but also O H radicals. The O radical can be effective in oxidizing NO to NO_2. However, the OH radical can further oxidize NO_2 to nitric acid. This acid formation is not a desired part of the plasma process and has to be prevented.

The production of O radicals from electron-impact dissociation of O_2 has an associated cost in electrical energy. The oxidation of one NO molecule will require at least one O radical:

$$O + NO \rightarrow NO_2 \qquad (1)$$

For temperatures typical of engine exhausts, the oxidation of NO to NO_2 by the O radical becomes very inefficient. At high temperatures (for example, 3000C), the NO to NO_2 reaction is counteracted by the reduction reaction

$$O + NO_2 \rightarrow NO + O_2 \qquad (2)$$

The OH radical can prevent the back conversion reaction (2), but does this at the expense of converting NO_2 to nitric acid.

The hydrocarbon plays several important roles in

the plasma. The presence of the hydrocarbon prevents the formation of acid products and increases the efficiency for NO to NO_2 oxidation.

The hydrocarbon promotes the selective partial oxidation of NO to NO_2- Instead of reacting with NO and NO_2, the O and OH radicals preferentially react with the hydrocarbons. The hydrocarbons react with O and OH to produce HO_2 and RO_2, where R is a hydrocarbon radical such as HCO and CH3O- It is then the HO_2 and RO_2 radicals that oxidize NO to NO_2. For instance,

$$HO_2 + NO \rightarrow NO_2 + OH. \quad (3)$$

The OH radical is reproduced when NO is oxidized by HO_2. This OH radical will in turn decompose another hydrocarbon molecule and lead to the production of more HO_2 and RO_2 radicals. The decomposition of one hydrocarbon molecule leads to the oxidation of several NO molecules. The electrical energy requirement for conversion of NO to NO_2 is therefore decreased significantly.

Because the OH radical reacts preferentially with the hydrocarbon, the oxidation of NO_2 to nitric acid is prevented. If SO_2 is present in the exhaust, scav-enging of the O and OH radicals by the hydrocar-bons will also prevent the oxidation of SO_2 to SO_3-

The hydrocarbon serves important roles not only on the catalyst, but also in the plasma. For lean burn gasoline engine exhausts, the hydrocarbons are al-ready present - mostly in the form of propene - typically at C_3 concentrations about twice that of NO. For diesel exhausts, the emitted gaseous hydrocarbon levels are much lower. However, the volatile organic fraction of the particulates could be a useful source of additional hydrocarbons.

PROCESS PRODUCTS

Conventional low-temperature lean-NO_x catalysts, such as those based on Pt, can achieve NO_x reduction at the expense of producing N_2O.

Figure 3 shows the concentrations of the N_xO_y species after the plasma/catalyst processor as a function of the input electrical energy density in the plasma. Without the plasma (energy density = O), only 20%NO_x reduction is achieved by the catalyst. This is shown by the decrease in NO concentration, from 500 down to 400 ppm. This NO removal is true chemical reduction of NO to N_2. Both the NO_2 and N_2O concentrations are negligible.

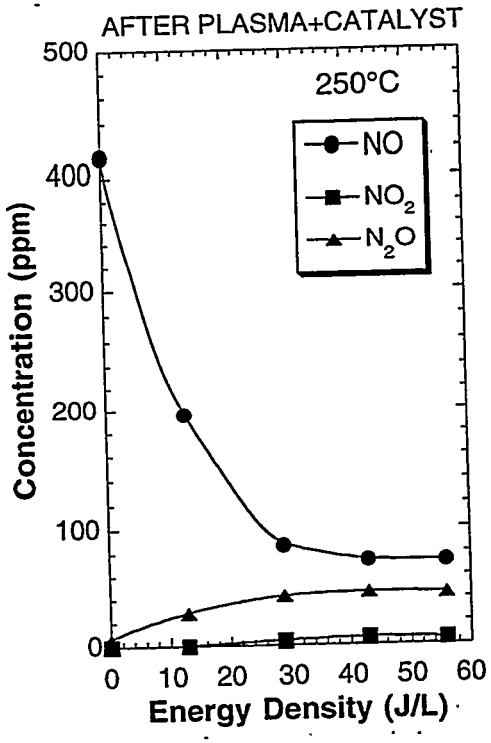


Figure 3. Plasma-assisted catalytic reduction of NO_x in a model exhaust gas at 2500C.

As the electrical energy density input to the plasma is increased, more NO is removed by conversion to NO_2. As the NO_2-containing stream goes through the catalyst, the NO_2 is reduced, mostly to N_2. As shown in Figure 3, the NO_2 concentration is very low after the plasma + catalyst. Also, only a relatively small amount of N_2O is produced at 250'C and below, even when the overall NO_x removal efficiency is high. At temperatures of 3000C and above, the formation of N_2O is negligible.

As mentioned previously, the presence of hydrocarbons prevents the formation of nitric acid and SO_3 in the plasma.

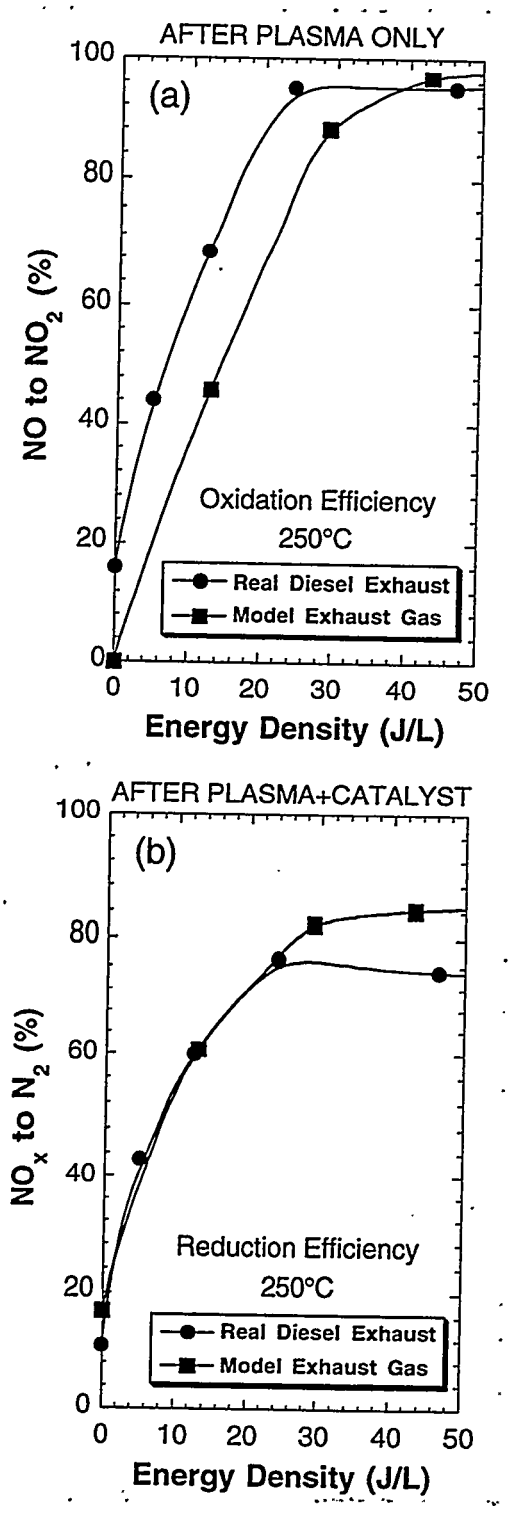


Figure 4. (a) Plasma oxidation efficiency and (b) NO_x reduction efficiency, in a real diesel exhaust compared to those in the model exhaust gas.

TREATMENT OF REAL DIESEL EXHAUST

Figure 4(a) shows the efficiency for plasma oxidation of NO to NO_2, presented as a function of the electrical energy density in the plasma. Figure 4(b) shows the efficiency for reduction of NO_x to N_2, after the plasma and catalyst.

The results using the exhaust from a Cummins diesel engine are compared to those taken using the model exhaust gas. The processing of the real diesel exhaust and the simulated exhaust show very similar results in both the plasma and the catalyst.

CONCLUSIONS

Plasma-assisted heterogeneous catalysis can enhance the NO_x reduction under conditions that normally make it difficult for either the plasma or the catalyst to function by itself. By systematically varying the plasma electrode and catalyst configuration, we have been able to elucidate the process by which the gas-phase plasma chemistry affects the chemical reduction of NO_x on the catalyst surface. Our results are consistent with recent studies that reveal the significance of NO_2 as an intermediary for achieving higher NO_x removal efficiencies. We have shown that the main effect of the plasma is to enhance the gas-phase oxidation of NO to NO_2. The reduction of NO_x to N_2 is then accomplished by the heterogeneous reaction of NO_2 with activated hydrocarbons on the catalyst surface. The use of a plasma opens the opportunity for a new class of catalysts that are potentially more durable, more active, more selective, and more sulfur-tolerant compared to conventional lean-NO_x catalysts.

Lean-NO_x catalysts are inherently multi-functional when targeted towards NO. Recent studies have been devoted to separating the oxidative and reductive functions of the catalyst in a multi-stage system [13]. This method works fine for systems that require hydrocarbon addition; the hydrocarbon can be injected between the oxidation catalyst and the reduction catalyst. For a lean-burn exhaust that already has a significant amount of hydrocarbons, the oxidation catalyst for NO is also active for the oxidation of the hydrocarbon; this results in a decrease in the

efficiency of the hydrocarbon reductant. With plasma-assisted catalysis there is no longer a need to develop catalysts that can oxidize NO to NO_2 but not oxidize the hydrocarbon reductant. This method is also more tolerant to the sulfur content of the fuel because it will not oxidize SO_2. The function of the catalyst can be greatly simplified by focusing on the reduction of NO_2. Plasma-assisted NO_x reduction can also work with both lean-NO_x SC R and lean-NO_x trap technologies:

The plasma-assisted catalytic reduction process is very flexible. It can be implemented with any type of plasma reactor and does not require a specific type of electrical power supply. This flexibility gives us the freedom to choose the least expensive and most durable plasma reactor power supply combination. The process can also accommodate any catalyst support structure. We can choose to put a bed of catalyst pellets inside the plasma reactor, or put a catalyst monolith downstream of the plasma reactor. In the latter case, the volumes of the plasma and the catalyst can be optimized separately.

ACKNOWLEDGMENTS

The work at Lawrence Livermore National Laboratory was performed under the auspices of the US Department of Energy under Contract Number W-7405-ENG-48, with support from the Chemical Sciences Division of the DOE Office of Basic Energy Sciences, the Environmental Technologies Program of the DOE Office of Fossil Energy, and a Cooperative Research and Development Agreement with Cummins Engine Company.

REFERENCES

1. Hamada, H., "Selective Reduction of NO by Hydrocarbons and Oxygenated Hydrocarbons over Metal Oxide Catalysts", *Catalysis Today* 22-(1994)21.

2. Shelef, M., "Selective Catalytic Reduction of NO_x With N-Free Reductants", Chemical Reviews 95 (1995) 209.

3. Matsumoto, S., Watanabe, H., Tanaka, T., Isogai, A., et al., "Development of NO_x Storage Reduction Catalyst for Automotive Lean-Burn Engine", Nippon Kagaku Kaishi 12 (1996) 997.

4. Takahashi, N., Shinjoh, H., Iijima, T., Suzuki, T., et al., "The New Concept 3-Way Catalyst for Auto-motive Lean-Burn Engine -NO_x Storage and Reduction Catalyst", *Catalysis Today* 27 (1996)63.

5. Jewell, L., Sokolovskii, V.D., Coville, N.J., Glasser, D., et al., "A Catalytic Trap for Low Temperature Complete NO Reduction in Oxygen-Rich Media", *Chemical Communications* Sep 7 (1996) 2081.

6. Shelef, M., Montreuil, C.N., and Jen, C.W., "NO_2 Formation Over Cu-ZSM-5 and the Selective Catalytic Reduction of NO", *Catalysis Letters* 26(1994)277.

7.. Bethke, K.A., Li, C., Kung, M.C., Yang, B., et al.,"The Role of NO_2 in the Reduction of NO by Hydrocarbon over Cu-ZrO_2 and Cu-ZSM-5 Catalysts", *Catalysis Letters* 31 (1995), 287.

8. Yokoyama, C. and Misono, M., "Catalytic Reduction of Nitrogen Oxides by Propene in the Presence of Oxygen over Cerium IonExchanged Zeolites: 2. Mechanistic Study of Roles of Oxygen and Doped Metals", *Journal of Catalysis* 150 (1994) 9.

9.. Lukyanov, D.B., Sill, G.,. Ditri, G.L., and Hall, W.K., "Comparison of Catalyzed and Homogeneous Reactions of Hydrocarbons for Selective Catalytic Reduction (SCR) of NO_x", *Journal of Catalysis* 153 (1995) 265.

10. Beutel, T., Adelman, B.J., Lei, G.D., and Sachtler, "W.M.H., Potential Reaction Intermediates of NO_x Reduction with Propane over Cu/ZSM-5", *Catalysis Letters* 32 (1995) 83.

11. B.M. Penetrante, M.C. Hsiao, B.T. Merritt;G.E. Vogtlin and P. H. Wallman, "Comparison of Electrical Discharge Techniques for NonThermal Plasma Processing of NO in N_2", *IEEE Transactions on Plasma Science* 23 (1995) 679.

12. Penetrante, B.M.. Hsiao, M.C., Merritt, Vogtlin, G.E., et al., "Pulsed Corona and Dielectric-Barrier

Discharge Processing of NO in N_2", *Applied Physics Letters* 68 (1996) 3719.

13. Iwamoto, M., Hernandez, A.M., and Zengyo, T., "Oxidation of NO to NO_2 on a Pt-MFI Zeolite and Subsequent Reduction of NO_x by C21-14 on an In-MFI Zeolite: a Novel De-NO_x Strategy in Excess Oxygen", *Chemical Communications* Jan 7 (1997) 37.

A THYRATRON-BASED PULSE GENERATOR FOR FUNDAMENTAL STUDIES OF NO_x REMOVAL IN NONTHERMAL PLASMAS

R.A. Korzekwa and L.A Rosocha
Los Alamos National Laboratory

INTRODUCTION

Nonthermal plasmas, generated by electric discharges and electron beams, have previously been used in the investigation of NO_x removal as well as the removal of other unwanted pollutants [1-5]. Although most pulsed corona discharges are driven by relatively fast risetime pulse generators (typically 10 ns or greater), most dielectric-barrier discharges have been driven with low frequency (a few to tens of kilohertz) ac power circuits or inverters. For a given gap spacing in dielectric barrier cell, the breakdown voltage of a cell driven by a fast pulse generator can be several times higher than that of a low frequency driven cell. A fast-risetime thyratron switched pulse generator circuit and dielectric-barrier discharge cell has been developed to investigate the effect on NO_x reduction of the higher breakdown voltage and resulting reduced electric field strength, E/N, at breakdown. This fast pulsed nonthermal plasma generator was also designed to provide a low temporal and spacial jitter for the investigation of the plasma chemistry properties by laser induced fluorescence (LIF) and tunable diode laser absorption spectroscopy (TDLAS). The initial results presented here include 1) a comparison of the removal efficiency of NO in nitrogen between the pulsed dielectric-barrier discharge and a pulsed corona discharge and, as another point of reference, 2) a comparison of the removal efficiency of an example chlorinated hydrocarbon trichloroethylene (TCE), in dry air between the pulsed dielectric-barrier discharge and an ac-driven dielectric-barrier discharge.

EXPERIMENTAL SETUP

Pulse Generator

A low power, high-voltage pulse generator capable of driving a small dielectric-barrier discharge cell was designed to meet specifications for low temporal jitter required by plasma chemistry diagnostic systems, such as LIF [6]. Figure 1 shows a schematic diagram of the high-voltage pulse generating circuit. To

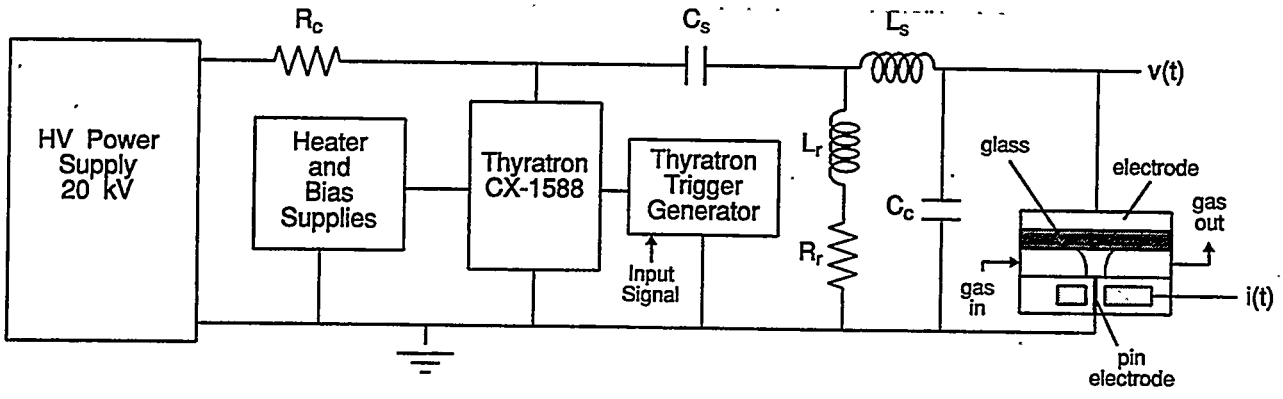


Figure 1. The thyratron-based high-voltage pulse circuit with dielectric-barrier discharge cell.

obtain a temporal jitter of less than 5 ns, a commercially available fast-risetime hydrogen thyratron tube (CX-1588, EEV Inc.) was used to switch the high-voltage pulse circuit. This low pressure hydrogen thyratron tetrode requires heater supplies for both the cathode and the hydrogen reservoir as well as bias supplies for the two grids. A positive bias voltage (50 V), with a current limiting resistor, creates a low current discharge between grid1 and the cathode. A negative bias voltage (-100 V) was supplied to the grid2 with respect to the cathode to prevent triode firing of the tube. A trigger generator (Northstar Research Corp., Model TT-18-V) was capacitively coupled to grid2 to trigger the thyratron. A low voltage pulse (5V peak with a <10 ns risetime) was used as the input to the trigger generator. A positive 20 kV dc high-voltage power supply (Plastic Capacitors, Inc., Model HV200-152M) was used to charge a storage capacitor, C_s, through a current limiting resistor, R_c = 25 MW. the slow charging process, the "ringout" inductance, L_r = 3 mH, and resistance, R_r = 50 W, effectively grounds the other side of C_s. The thyratron tube was used to switch the positively charged storage capacitor to ground which produces a negative pulse across L_r, R_r and the rest of the circuit. The risetime of the high-voltage pulse produced at the cell is set by the series resonant frequency of the combination of C_s, the stray inductance (L_s), and the high-voltage output cable capacitance (C_c). For proper circuit operation, the conditions $L_r >> L_s$ and C_c much greater than the cell capacitance must be met. In this case, C_s = 1.2 nF, L_s = 90 nH, and C_c = 150 pF (150 cm of RG-217 coaxial cable) which gives a risetime of 6.5 ns. The maximum cell capacitance without a discharge was approximately 15 pF. For a series resonant circuit, when $C_s >> C_c$ the peak voltage produced at the cell is a factor of two greater than the initial voltage on C_s. Therefore, for this pulse generator, the peak voltage is variable up to 40 kV. The dielectric-barrier discharge occurs on the risetime of the output voltage pulse. After the discharge occurs, the low frequency resonant circuit composed primarily of C_s, L_r and R_r slowly "rings out" and dissipates the remaining energy stored in the circuit in R_r so that another charge/-discharge cycle can be initiated after an appropriate delay set by the desired repetition frequency. The repetition frequency for this configuration is limited to 20 Hz. The maximum temporal jitter between the trigger input signal and the initiation of the dielectric-barrier discharge was 4 ns.

Voltage and current diagnostics were used to measure the associated waveforms which provide a measurement of the energy dissipated in the discharge plasma. The voltage, V(t), was measured using a high-voltage probe (Tektronix, model P6015A) and the current I(t) is measured using a current probe (Pearson, model 2877) as seen in Fig. 1. Both probes were calibrated before use to ensure accuracy at these frequencies and to ensure that the delays of the signal cables from the probes to the oscilloscope were equal. Typical voltage and current waveforms are shown in Fig. 2.

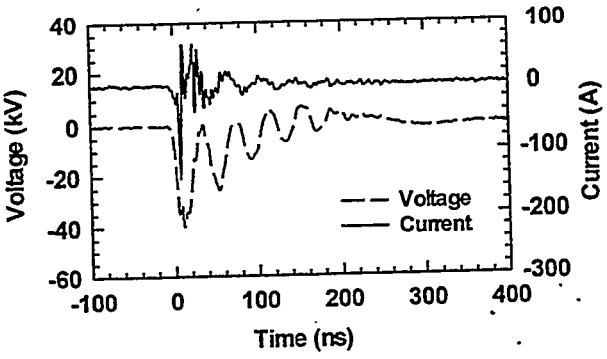


Figure 2. Typical voltage and current versus time waveforms produced at the dielectric-barrier discharge cell.

The series resonant charging of C_c is seen in the voltage waveform and is associated with the high-frequency oscillation. A lower frequency oscillation, ~7 MHZ, is associated with the "ringout" circuit components described above. The discharges occur at the large negative peak on the current waveform (approximately 5 ns wide). The subsequent fast oscillations are the result of the voltage collapse across the air gap when the micro discharges occur and the decay of the associated resonant energy stored locally in the

low inductance cell geometry. Only a small percentage, 2% to 4%, of the energy stored in C_s is dissipated in the discharge. This can be understood by recognizing that only the energy stored locally in the air gap is available to the discharge, while most of the initial stored energy sent to the load is used to charge the comparatively large cable capacitance. This energy and remaining energy in C_s is dissipated in R_r to prepare the system for another negative pulse.

B. Dielectric-Barrier Discharge Cell

A small single dielectric-barrier discharge cell was constructed for use in these low power "bench-top" experiments. Figure 3 provides an illustration of the cell showing the two possible discharge modes. The nylon insulating housing has two gas ports and four window ports (not shown). The upper high-voltage electrode disk is imbedded in the housing and a Pyrex disk, which provides the single dielectric barrier, is bonded to the housing underneath the electrode. The cell could be configured in two ways, 1) a single-barrier/pin arrangement in Fig. 3a or 2) a single-barrier/flat electrode arrangement in Fig. 3b. In Fig. 3a, a 1.5 mm diameter stainless steel pin is used as the lower electrode and is surrounded by a nylon spacer to provide a flat surface at the bottom of the air gap. The advantage of this arrangement is that a micro discharge (lasting less than ten nanoseconds) is produced at the location of the pin with a low temporal jitter which makes it possible to use a short laser pulse to probe the plasma. Also the time evolution and decay of chemical species can be observed using this configuration. The disadvantage of this elec-trode arrangement is that removal efficiency measurements cannot be obtained since the plasma does not fill the whole volume. The electrode arrangement in Fig. 3b, however, can be used to measure the removal efficiency since a flat stainless steel disk is used as the lower electrode enabling the volume between the plates to be filled with micro discharges. The complete assembly, cell and electrical diagnostic probes, were mounted in an alumi-num enclosure to reduce the inductance at the cell and provide shielding. The high-voltage feedthrough connects the cable ground to the enclosure and the center conductor of the cable to the high-voltage electrode of the cell. A picture of the micro discharge in nitrogen using the barrier/pin

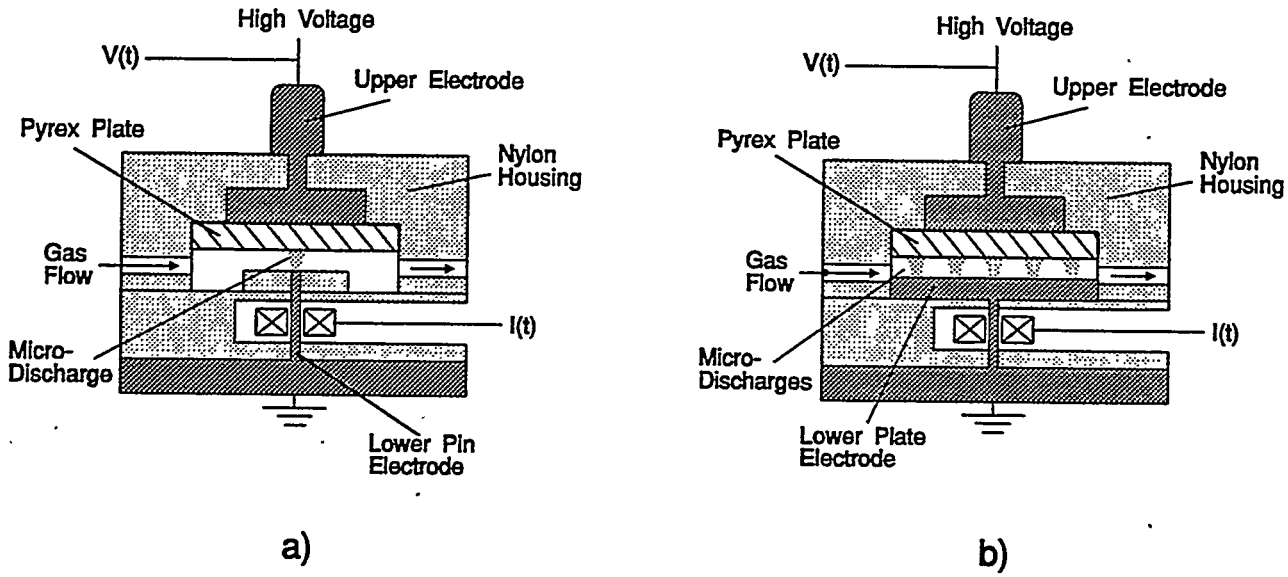


Figure 3. A diagram of the dielectric-barrier discharge cell where a) is the single-barrier/pin arrangement and b) is the single-barrier/plane electrode arrangement.

arrangement is shown in Fig. 4. In this picture the "footprint" of the region of charge extracted from the glass plate is approximately four times larger than the pin diameter.

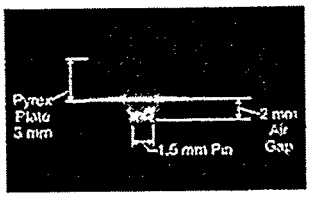


Figure 4. A photograph of the discharge produced in the single-barrier/pin arrangement in nitrogen.

C. Chemical Diagnostics

A gas bottle was filled to a high pressure with either a mixture of dry air and TCE or a mixture of NO in dry nitrogen as seen in Fig. 5. A gas regulator and mass flow controller were used to set the flow through the discharge cell before entering the vent (for TCE) or the gas bag (for NO). The method for measuring the reduction of TCE used a gas-tight syringe to extract a sample at a known volume from the gas output line which was then injected into a gas chromatograph with a sample concentrator (Varian model Star 3400CX GC and OI Corp. - model 4460A sample concentrator). To measure the reduction of NO in dry nitrogen at the low flow rates (50 mL/min) needed to achieve an energy density, E, up to 100 J/l, a gas bag was filled slowly over 40 minutes at a partic-ular energy density setting and then pumped through the chemiluminescent gas analyzer (California Analytical Instruments, model 240-CLD) at 1.5 L/min.

III. EXPERIMENTAL RESULTS

The removal efficiency of NO in nitrogen using a pulsed dielectric barrier discharge was compared to that previously obtained from a peak voltage of 30 kV [7]. The pulsed corona tube (90 cm long) was constructed using a 500 μm diameter stainless steel wire center conductor with a 2.4 cm diameter stainless steel tube as the outer conductor. The E/N at breakdown of both discharges was approximately 500 Td (at room temperature and pressure). A comparison of the removal efficiency for the two discharge types is shown in Fig. 6. The removal efficiency is close to the same between the pulsed dielectric-barrier and corona discharges indicating that the gaseous electronics occurring in the discharges and the resulting chemistry are similar.

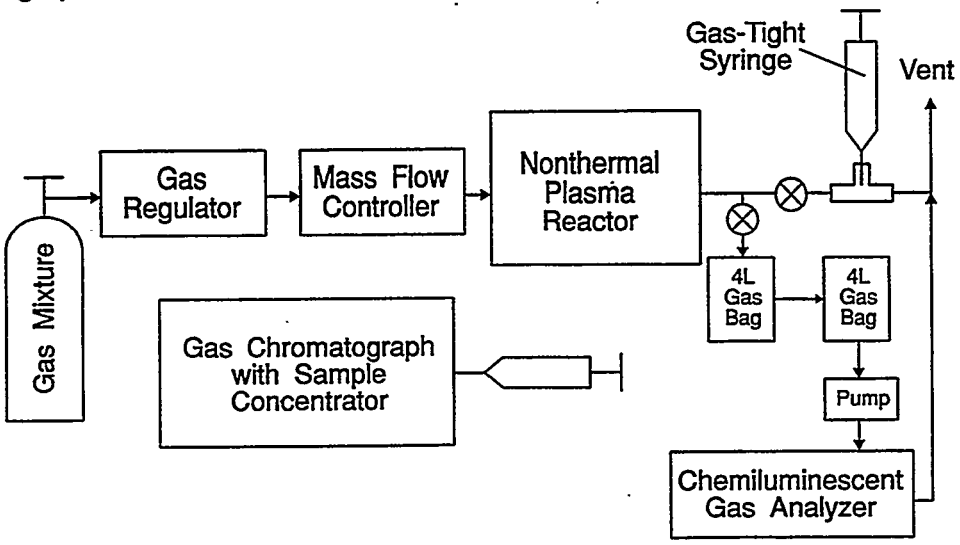


Figure 5. The chemical diagnostics setup used to obtain removal efficiency data for TCE (gas tight syringe) and for NO in Nitrogen (Teflon gas bag).

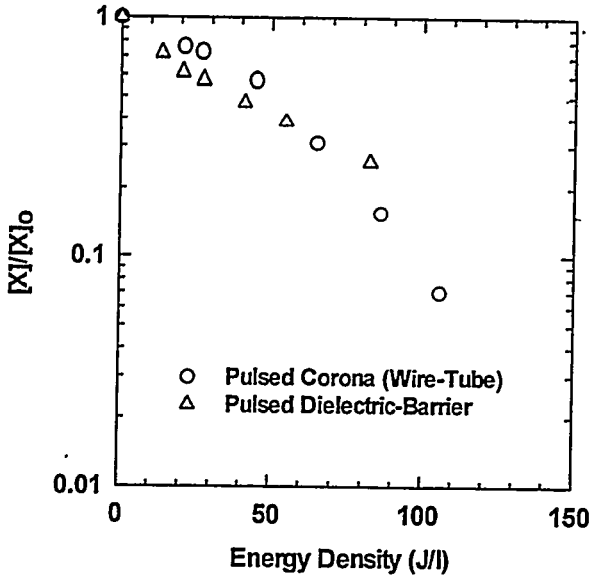


Figure 6. The removal efficiency, $[X]/[X]_o$, versus energy density for 500 ppm of NO in nitrogen using both pulsed corona and pulsed dielectric-barrier discharges.

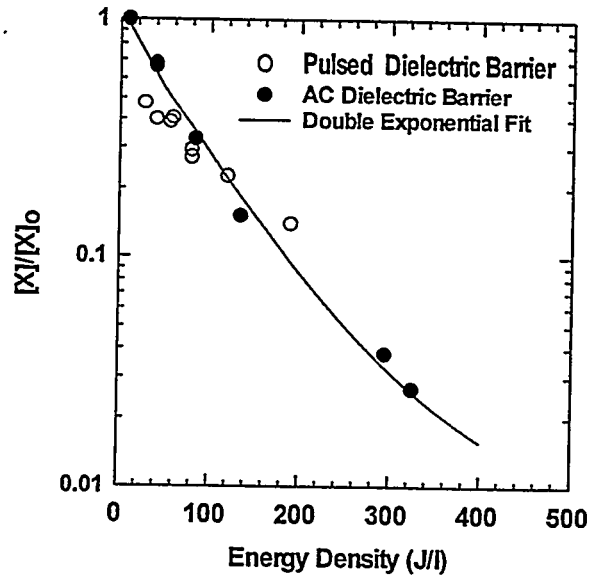


Figure 7. The removal efficiency, $[X]/[X]_o$, versus energy density for 200 ppm of TCE in dry air using both pulsed and ac-driven dielectric-barrier discharges.

The removal efficiency of TCE in dry air using a pulsed dielectric barrier discharge was compared to that previously obtained from an ac-driven dielectric-barrier discharge. The ac-driven dielectric-barrier discharge was powered by a sinusoidal power supply at a frequency of 1.2 kHz with a peak voltage of 25 kV [7]. The discharge cell was constructed in a flat-plate geometry using two 0.3 cm x 38 cm x 70 cm Pyrex plates with a gap spacing of 3.5 mm and an active discharge area of 1800 cm^2. Two aluminum electrode plates were pressed to each side of the cell with a charge measuring capacitor between the low voltage plate and ground. The E/N at breakdown of the pulsed dielectric-barrier discharge was much larger than that of the ac-driven discharge, 500 Td for the pulsed discharge and 80 Td for the ac-driven discharge. A comparison of the removal efficiency for the two discharge types is shown in Fig. 7. Even with the large difference in E/N at breakdown between the two differently-driven discharges, the removal efficiency was close to the same between the pulsed and ac-driven discharges. In this case it is known that the primary decomposition-initiating chemical reaction is between $O(^3P)$ and TCE. The results in Fig. 7 indicate that the generation of $O(^3P)$ radicals is similar between the two types of barrier discharges.

IV. SUMMARY

A small, single dielectric-barrier discharge cell driven by a fast risetime pulse generator circuit has been constructed to investigate NO_x reduction. The thyratron switched fast-pulse circuit used to drive the dielectric-barrier discharge had a risetime of 6.5 ns, a maximum peak output voltage of 40 kV, a maximum repetition rate of 20 Hz, and a temporal jitter of 4 ns. This pulsed dielectric-barrier discharge and a pulsed corona discharge were compared in terms of the removal efficiency of 500 ppm of NO in nitrogen. The removal efficiency of 200 ppm of TCE in dry air has been compared between this pulsed dielectric-barrier discharge and an ac-driven dielectric-barrier discharge.

REFERENCES

1. Non-Thermal Plasma Techniques for Pollution Control, edited by B.M. Penetrante

and S.E. Schultheis, Part A and Part B (Springer-Verlag, Berlin Heidelberg, 1993).

2. J.J. Coogan and A.D. Sappey, "Distribution of OH Within Silent Discharge Plasma Reactors, IEEE Trans. Plasma Sci., Vol. 24, No. 1, pp. 91-92, 1993.

3. D. Evans, L.A. Rosocha, G.K. Anderson, J.J. Coogan, and M.J. Kushner, Plasma Remediation of Trichloroethylene in Silent Discharge Plasmas," J. Appl. Phys., Vol. 74, No. 9, pp. 5378-5386, 1993.

4. B.M. Penetrante, M.C. Hsiao, B.T. Merritt, GE. Vogtlin, and P.H. Wallman, "Comparison of Electrical Discharge Techniques for Nonthermal Plasma Processing of NO in N2," IEEE Trans. Plasma Sci. Vol. 23, No. 4, p. 679-687, 1995.

5. P.H. Wallman, M.C. Hsiao, B.T. Merritt, B.M. Penetrante, and G.E. Vogtlin, "Nonthermal Aftertreatment of Diesel Engine Exhaust," Proceedings of the 1995 Diesel Engine Emissions Reduction Workshop, La Jolla, California, July 24-27, 1995.

6. M.J. Nusca, P.A. Sagear, andA.W. Miziolek, "Experimental and CFD Studies of Non-Thermal Plasmas for NOx Control," Proceedings of the 2nd International Symposium on Non-Thermal Plasma Technology for Pollution Control, Salvador, Brazil, August 11-15, 1997.

7, R.A. Korzekwa and L.A. Rosocha, "Experimental Results Comparing Pulsed Corona and Dielectric Barrier Discharges for Pollution Control," Presented at the 11th IEEE International Pulsed Power Conference, Baltimore, Maryland, June 29 - July 2, 1997.

VEHICLE EXHAUST TREATMENT USING ELECTRICAL DISCHARGE AND MATERIALS CHEMISTRY

R.G. Tonkyn, M.L. Balmer, S.E. Barlow,and T.M. Orlando
Pacific Northwest National Laboratory
D. Goulette, Delphi Energy and Engine Management Systems
J.Hoard, Ford Research Laboratory

INTRODUCTION

Current "3-way" catalytic converters have proven quite effective at removing NO_x from the exhaust of spark ignition vehicles operating near stoichiometric air-to-fuel ratios. However, diesel engines typically operate at very high air-to-fuel ratios. Under such lean burn conditions current catalytic converters are ineffective for NO_x removal. As a result, considerable effort has been made to develop a viable "lean"NO_x catalyst. Although some materials have been shown to reduce NO_x under lean burn conditions, none exhibit the necessary activity and stability at the high temperatures and humidities found in typical engine exhaust. As a result, alternative technologies are being explored in an effort to solve the so-called "lean NO_x problem".

Theoretical [1,2] and experimental work [1-11] has shown that non-thermal discharges can effectively lower concentrations of both hydrocarbons and NO in gas streams, though successful treatment over the wide range of gas compositions and temperatures present in typical engine exhaust streams has yet to be demonstrated. Modeling and current experimental efforts suggest that homogeneous, gas phase remediation by discharge technology will not have the necessary energy efficiency to be practical However, techniques that combine discharges with surface chemistry may have this potential--a fact that has recently attracted attention in the United States, Europe and Japan. Packed-bed barrier discharge systems are well suited to take advantage of plasma-surface interactions due to the large number of contaminant surface collisions in the bed. The close proximity of the active surface to transient species produced by the plasma may lead to favorable chemistry at considerably lower temperatures than required by thermal catalysts.

We present data in this paper illustrating that the identity and surface properties of the packing material can alter the discharge-driven chemistry in synthetic leanburn exhaust mixtures. Results using non-porous glass beads as the packing material suggest the limits of NO_x reduction using purely gas phase discharge chemistry. By comparison, encouraging results are reported for several alternative packing materials.

EXPERIMENTAL

A typical dielectric barrier, packedbed reactor consists of three elements that can be assembled in a variety of ways. Two electrodes are required to create the high electric fields necessary to form a discharge at atmospheric pressure. One or both of the electrodes must be electrically isolated by a dielectric barrier to prevent direct arcing between the electrodes. In a packed-bed reactor, the volume between the electrodes is filled with a non-conductive, dielectric packing material. The packing material serves two purposes. By virtue of its shape and dielectric constant a packed bed creates numerous regions of highly amplified electric field. These regions will go into discharge at a relatively low applied voltage, and the large number of such regions helps spread the discharge throughout the entire volume of the reactor. Also, the tortuous path required for gases to traverse the bed ensures multiple contaminant-surface collisions, enhancing the possibility of favorable surface chemistry.

We utilized a cylindrical geometry reactor, consisting of a 25 mm Vycor tube, a 3.2 mm diameter stainless steel central electrode, and an outer electrode made of stainless steel tape or screen affixed tightly to the exterior of the

tube. The outer electrode was 5 cm high, giving a reactor volume of roughly 20 cm^3. The position and height of the outer electrode defined the active volume, as there was no corona generated elsewhere in the reactor. The packing material of interest filled only the volume inside the outer electrode. It was held in place by a porous ceramic "washer" which rested on top of a 10 cm bed of glass beads. Electrical heating tape heated the region containing the glass beads to 10°C below the desired reaction temperature. A separate heating tape surrounded the outer electrode to maintain the desired temperature in the active portion of the reactor. Two thermocouples affixed to the outside of the reactor were used with feedback to control the bed temperature. A schematic view of our reactor is given in Figure 1.

The discharge was driven by AC voltage from a high voltage transformer (30kV/30mA). Either a variable output transformer (0 to 110 volt) operating on 60 cycle room power, or a high power audio amplifier (0-70 V, 60-20,000 Hz) was used to drive the transformer.

Our discharge diagnostic system consisted of extensive gas handling facilities, power, temperature and relative humidity measurement instrumentation, a differentially pumped mass spectrometer and a chemiluminescent NO_x analyzer. For safety considerations, the reactor and high voltage power supply were housed in a vented steel cabinet. For some benchmark experiments we utilize a GC-Mass spectrometer and an FTIR spectrometer for analysis.

Accurate measurements of the power consumption in the corona reactor are critical to understanding the mechanisms of NO_x/-hydrocarbon removal as well as for evaluating efficiencies and economic feasibilities. The power deposited into a barrier discharge reactor can be measured with a capacitive circuit. [12] A high voltage probe is used to measure the input voltage, and a large capacitor on the low voltage side integrates the charge transferred across the reactor per cycle.

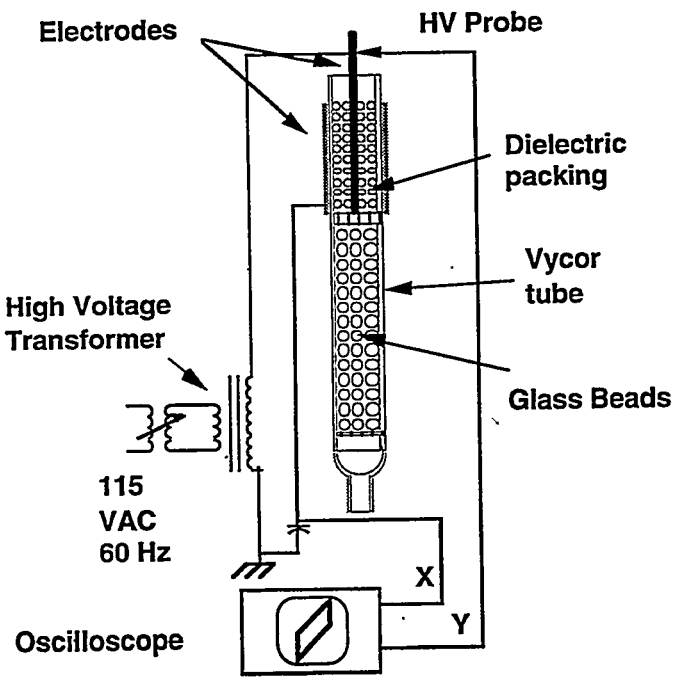


Figure 1: Schematic view of reactor and power measurement circuit. The energy per cycle is proportional to the area inside an x-y plot of the input high voltage vs. the voltage across a series capacitor.

The energy dissipated per cycle is given by:

$$E = \int_0^\tau P(t)dt = \int_0^\tau V(t)i(t)dt = \int_0^\tau V(t)dq(t) = C\oint_\tau V(t)dV_C(t)$$

Here τ is the period of the driving wave form, P is the delivered power, V is the input high voltage, I is the current flow., q is the charge transported across the reactor, C is the capacitance of the series capacitor and Vc is the voltage across that capacitor. The integral on the right was calculated from the area inside an x-y plot of V vs. Vc over 1 period. This yielded the energy deposited in the reactor per cycle, which was converted to the average power consumption.

For most of the experiments described the simulated lean exhaust mix consisted of 7.5% oxygen, 4% CO_2, 2% H_2O, 0.2% CO, 750 ppm C_3H_6 and 270 ppm NO. The balance was nitrogen. For some experiments nonane was used (200 ppm) instead of propane. The water content was kept at a moderate level to prevent condensation in the exhaust line or NO_x meter.

RESULTS AND DISCUSSION

Both NO and NO_x were monitored with a chemiluminescent NOX detector, with the difference attributed to NO_2 in the gas stream. In order to simplify comparisons between packing materials, the data were normalized to the inlet concentration. The data were fit assuming that the NO loss rate was first order in the energy deposited in the reactor per liter (at 298 K) of gas flow. The removal of NO_x was also assumed to be exponential, but with a non-zero final value, consistent with our observation that NO_x always appears to approach a limiting value at high energy. The equations used are as follows:

$$[NO]=[NO]_0 * e^{-E/\beta}$$

$$[NOx]=[NOx]_F+([NOx]_0-[NOx]_F)*e^{-E/\beta}$$

Here β is the first order decay parameter, typically in units of Joules/liter, which is commonly used to characterize and compare the energy efficiency of discharge treatment technologies. We stress that although the NO decay is first order in energy at fixed inlet conditions, the overall reaction kinetics is quite complicated. As we show below, the measured energy dependence varies with NO_x concentration. We have also observed strong dependence of β on the temperature and humidity in the gas stream.

Some plots include a line labeled "fraction reduced." What this represents is the fraction of NO loss which is not due simply to oxidation to NO_2, and is calculated by dividing the NO_x loss by the NO loss.

$$f=\frac{[NOx]_0-[NOx]}{[NO]_0-[NO]}$$

Since molecular nitrogen product was not detected due to the excess of N_2 in the gas stream, this fraction is an upper limit to the amount of NO which has been chemically reduced to nitrogen.

We have investigated the possible production of other oxidative products. For example, if nitric acid were formed, we would expect a reasonable fraction to be found in water condensed from the exhaust stream. However we typically find the water to be only slightly acidic. We have found no evidence of organo-nitrate products, either with a mass spectrometer or an FTIR spectrometer. The production of N_2O is also possible, but is difficult to detect with a mass spectrometer due to the background (and product) CO_2 present. However without added CO_2 in the buffer gas, increases in the mass 44 signal appear to be correlated with the loss of propene signal (at mass 41) rather than with the NO or NO_x signal. This suggests that most of the product mass 44 arises from oxidation of propene to CO_2. In agreement with this observation, little or no N_2O was detected with the FTIR. Finally, we have looked for surface bound nitrates in post-experiment thermal analyses of our packing material. Although some nitrates are invariably observed, the amount detected is too small to explain the time-integrated quantity of NO_x which disappears.

For a limited number of experiments at a second facility we utilized an FTIR and GC-mass spectrometer to analyze the exhaust. Under typical operating conditions we saw little or no evidence of organo-nitrates, N_2O or nitric acid production. We did see a noticeable increase in CO, suggesting incomplete oxidation of the added propene. Interestingly, over a short period at least, the addition of 15 ppm SO_2 had no noticeable effect on the NO_x chemistry.

MATERIALS EFFECTS

We have investigated many different materials in our reactor, with varying results. A general observation is that there is not necessarily a good correlation between thermal activity and discharge driven activity. Figures 2a and 2b show our results for 3 separate materials in both thermal activation and in the reactor. As can be seen, the most effective material in the plasma was completely inactive for lean NO_x reduction from 100 to 500° C. This suggests that in some cases at least, the mechanism for discharge driven chemistry can be quite

different from that observed in thermal catalysis.

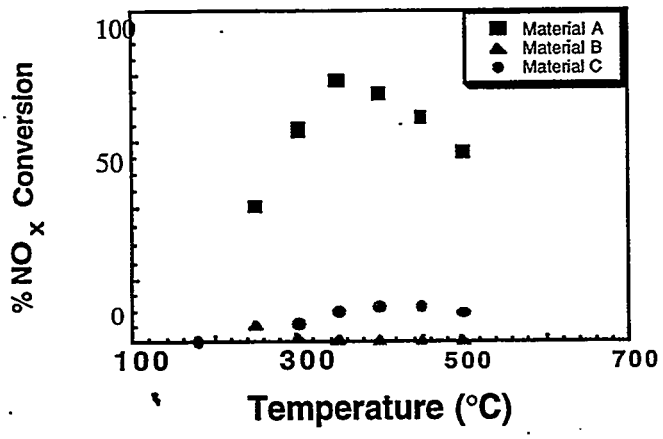


Figure 2a: Plot of the thermal activity of 3 separate materials for NO_x conversion.

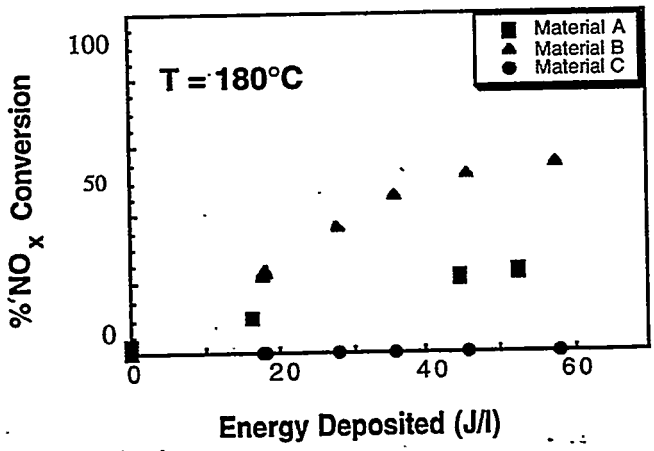


Figure 2b: Activity of the same three materials towards lean NO_x reduction in a packed bed corona reactor.

GLASS BEADS

We used non-porous glass beads as a packing material in order to study the gas phase discharge chemistry. We did not expect much, if any discharge driven surface chemistry to occur in this case, and in fact saw no evidence for it. Figures 3 and 4 illustrate our results. In Figure 3 we show a decay curve for both NO and NO_x in simulated lean exhaust as a function of the discharge energy. As can be seen, NO disappears readily, but almost all of the disappearance can be explained as oxidation of NO to NO_2. At best only 10 to 15% of the NO loss is due to chemical reduction.

In Figure 4 we show the variation in ~ with the initial concentration of NO. The balance gas composition and temperature were held constant with the exception that the ratio propene to NO was held constant. The NO_x decay was limited to a few percent loss in each case. The decay of NO appears first order in energy, but the decay constant increases linearly with the concentration of NO as shown. Extrapolation of the data to low concentrations suggests a minimum value of ~7 J/l at extremely low concentrations. Although this result pertains only to the gas phase oxidation of NO, it illustrates the importance of characterizing energy costs under a variety of conditions. In an actual vehicle, not only the NO_x concentration but the humidity, temperature and flow velocity will be continually changing. In the long run, only tests on actual exhaust are likely to yield accurate estimates of the energy costs of discharge driven exhaust remediation.

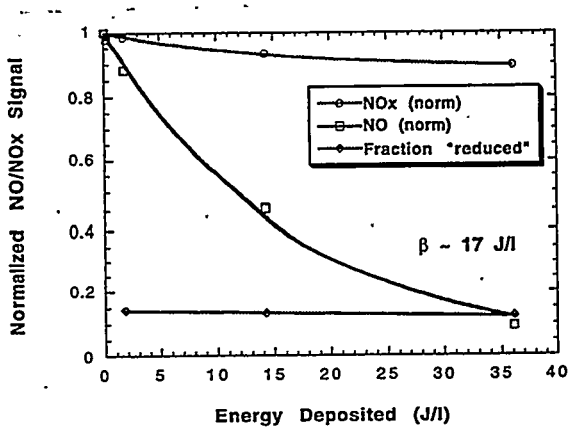


Figure 3: Plot of the normalized NO and NO_x concentrations vs energy density in Joules per liter of flow for 3 mm glass beads.

ZEOLITE MATERIALS

In general, zeolites performed well in producing clean, reproducible discharges in our reactor. For many packing materials we observe an increasing number of large voltage spikes at higher input voltages, indicative of the onset of long scale arcing between the electrode and the dielectric barrier. These spikes, which limit

the attainable energy density, are not only dangerous to the instrumentation and the reactor; they are also inefficient in creating reactive species. With zeolite packings we observed many small scale discharges, even at high input voltages, consistent with small scale surface roughness resulting in multiple high field regions near the beads.

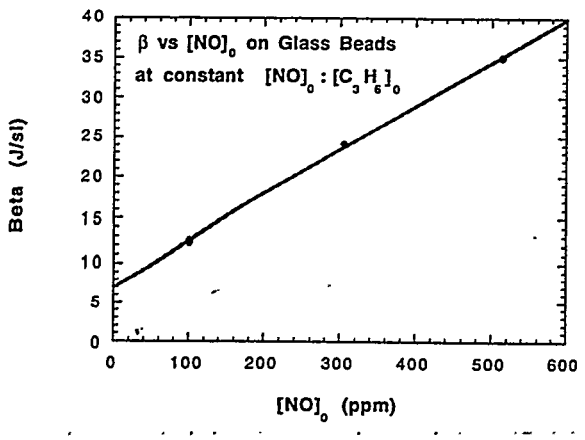


Figure 4: Variation of Beta with initial NO concentration at constant propane to NO ratio. Balance gas is simulated lean exhaust.

We report here on three different commercially available zeolites. They are labeled simply as materials A, B and C to protect their exact identity for proprietary reasons. Figure 5 illustrates data taken with material B. the most efficient material found so far. As is evident, a significant increase in the "reductive" channel was observed over that seen with glass bead packing. This is an indication that the overall chemistry has changed. Both the fraction reduced and the energy efficiency varied between the three zeolites, but their general behavior was similar. The maximum fraction of NO we have been able to "reduce" is approximately 50%, which suggests the possibility that the net reaction is a disproportionation of NO into N_2 and NO_2. Our results for three materials are summarized in Table 1.

Examination of the energy efficiency for NO loss for many different materials indicates that the rate sometimes approaches but never exceeds that found for the (presumed) gas phase oxidation with glass beads. Furthermore, on one occasion we managed to increase the

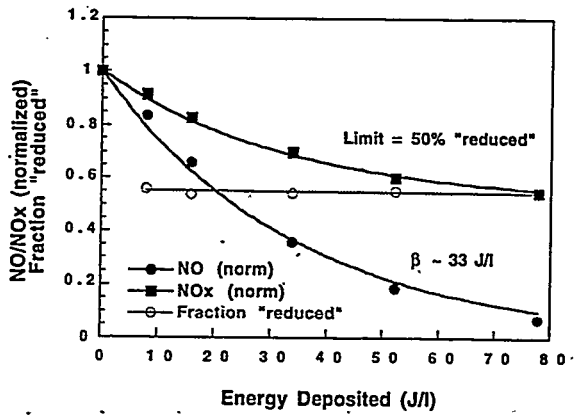


Figure 5: Plot of the normalized NO and NO_x concentrations vs. energy deposited for material B at 180°C. Approximately 45% of the NO is converted to NO_2.

	Temp (°C)	$[NO_X]_0$ (ppm)	$\%[O_2]_0$ (ppm)	$[C_3H_6]_0$ (ppm)	β (J/l)	$[NO_X]_{t=\infty}$ (fraction)
A	160	250	5.5	780	57	0.63
B	180	270	7.3	760	34	0.5
C	180	270	7.3	760	48	0.52

Table 1: Destruction of NO in lean exhaust with Materials A, B and C.

energy beyond that required to drop the NO concentration to our detection limit. No further change was observed in the NO_x concentration at higher energies. As shown in Figure 6, oxygen enhances both the NO and NO_x decay channels, suggesting that oxidation of NO, perhaps in the gas phase, is a necessary first step in the overall discharge chemistry. A similar result is shown for the effect of added propane at constant energy in Figure 7. Interestingly, the calculated fraction of NO_x to NO loss did not vary with either added oxygen or propene. These results are similar to those observed in NO_x selective catalytic reduction studies of thermally active zeolites. [13,14] In those studies the evidence suggested that the production of N_2 from NO_x was driven by reaction of NO_2 with methane to yield both NO and N_2 product. Added oxygen enhanced the oxidation of NO to NO_2, and added methane enhanced the subsequent reduction step.

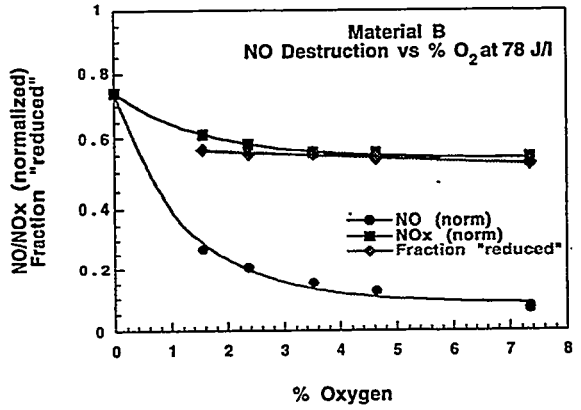


Figure 6: Plot of the normalized NO and NO_x concentrations as a function of added oxygen at constant energy on material B. The data were taken with 270 ppm NO at 180°C, with the concentrations of the other constituents held fixed

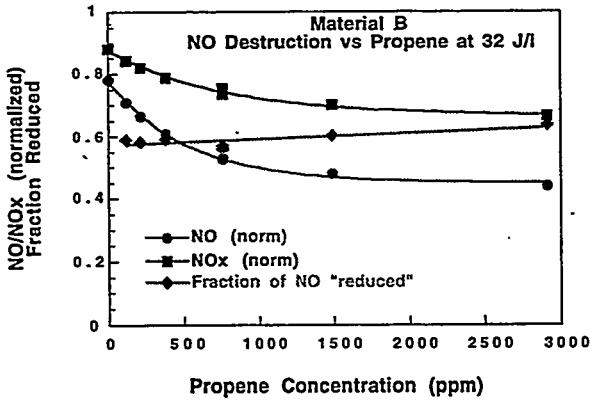


Figure 7: Plot of the normalized NO and NO_x concentrations vs. propane at constant energy on material B. The data were taken with 270 ppm NO at 215 °C, with the concentrations of the other constituents held fixed.

An obvious aspect of utilizing zeolites as a packing material is the huge available surface area. In order to investigate the effect of surface area we sintered a sample of material B for 1 hour at 800 °C. This treatment reduced the BET surface area to near zero by collapsing the pores and also changing the phase. As can be seen in Figure 8, the observed chemistry looks quite similar to that found for glass beads. The energy efficiency for NO loss did *not* change, although the observed products did. A similar test at 700 °C only reduced the surface area by 7% without a phase change and had little effect on the chemistry.

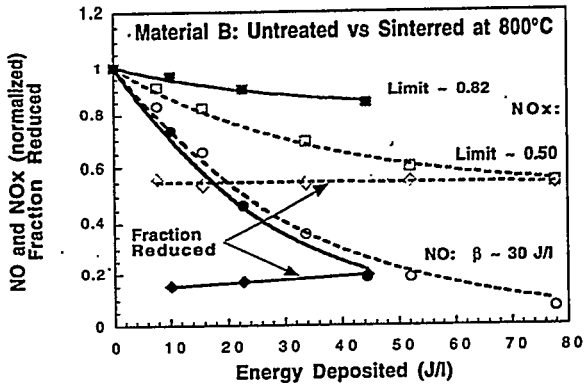


Figure 8: Comparison of material B performance before and after sintering at 800°C. The dashed lines represent the untreated material; solid lines the treated material. The loss of NO is identical, but the NO_x behavior changes considerably.

The hydrocarbons found in normal diesel exhaust tend to include higher molecular weight species than for automobile exhaust. We ran tests to determine whether a higher weight hydrocarbon would react significantly differently from propene. Figure 9 shows a comparison of the NO chemistry when we substituted ~200 ppm of nonane for 700 ppm of propene. If anything, the results for nonane are slightly better than for propane, even when considered on the basis of the carbon to NO ratio.

The increased loss of NO_x found for zeolite pack-ings could be due to plasma-assisted deposition of nitrates, nitrites or organo nitrites onto the zeolites. This has been reported to occur on γ alumina beads[15]. Certainly deposition occurs to some extent, as an excess of NO_2 is commonly observed after turning off the discharge, or upon additional heating of the

packing material. However the observed excess does not appear to be enough to explain the time-integrated loss in NO_x signal. In one experiment on material B. the time integrated loss of NO_x was measured for 13 hours of reactor op-elation. The beads were then removed and an-alysed for adsorbed nitrates by temperature programmed decoration (100-600° C). The observed NO + NO_2 could only explain roughly 15% of the NO_x loss. Finally, we have never seen evidence of NO or NO_2 breakthrough.

Not all zeolites tested worked as well in the plasma reactor as the ones illustrated here. Some zeolites were not at all effective at reducing NO_x, and in fact tended to promote coke formation in the reactor, suggesting that the discharge led to surface bound graphite.

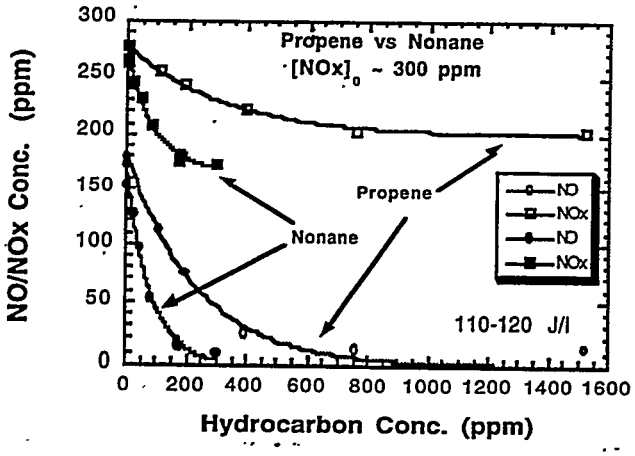


Figure 9: Comparison of the effect of added propane vs added nonane on the activity of material D for lean NO_x reduction at fixed energy

CONCLUSION

Our data indicate that the identity of the packing material in a packed-bed dielectric barrier reactor can strongly affect the chemistry observed in the low-temperature plasma treatMERT of lean NO_x exhaust streams. With inactive glass beads in the reactor we show that our gas phases discharge chemistry heavily favors oxidation of NO to NO_2 over reduction. However we have found that certain zeolite materials increase what we have labeled the "reductive" channel up to 50%, a marked improvement from glass beads. It is plausible, but by no means proven, that this channel is indeed reduction to N_2. We have looked for but not seen significant production of N_2 O, nitric oxide or organo-nitrates in the exhaust stream. While some surface bound nitrates are seen in post-experiment analysis of the packing materials, the amount is not large enough to explain our data. The observed energy efficiency improves with increased oxygen and propene, but the branching ratio between oxidation and reduction is unchanged. Although these results are promising, progress in increasing both the energy efficiency and the fraction reduced will be necessary before a practical device can be produced.

ACKNOWLEDGMENTS

This work was supported by a Cooperative Research and Development Agreement with the Low Emissions Technology Research and Development Partnership. Pacific Northwest National Laboratory is operated for the U.S. Department of Energy by Battelle Memorial Institute under Contract No. DE-AC0676RLO 1831.

REFERENCES

(1) Gentile, A. C.; Kushner, M. J. J. *App. Phys.* 1995, 78, 2074.

(2) Penetrante, B. M.; Hsiao, M. C.; Merritt, B. T.; Vogtlin, G. E.; Wallman, P. H.; Kuthi, A.; Burkhart, C. P.; Bayless, J. R., *Appl. Phys.* Lett. 1995, 67, 3096.

(3) Hsaio, M. C.; Merritt, B. T.; Penetrante, B. M.;. Tonkyn, R. G.; Orlando, T. M., J. *Adv. Oxid. Tech.* 1996, 1, 79.

(4) Hsiao, M. C.; Merritt, B. T.; Penetrante, B. M.; Vogtlin, G. E.; Wallman, P. H., J. *Appl. Phys,* 1995, 78, 1.

(5) Tonkyn, R. G.; Barlow, S. E.; Orlando, T. M. J. *Appl. Phys.* 1996, 80, 4877.

(6) Rosocha, L. A.; Anderson, G. K.; Bechtold, L. A.; Coogan, J. J.; Heck, H. G.; Kang, M.;

McCulla, W. H.; Tennant, R. A.; Wantuck, P. J. . In *Non-Thermal PlasmaTechniques for Pollution Control Part B:Electron Beam and Electrical Discharge Processing;* Penetrante, B. M., Schulthies, S. E., Eds.; Springer-Verlag: Heidelberg, 1993; pp 281.

(7) Lerner, B.; Birmingham, J.; Tonkyn, R. G.; Barlow, S. E.; Orlando, T. M. *12th. Int. Symp. on Plasma Chemistry,* 1995, Minneapolis, MN.

(8) Chan, M. B.; Lee, C. C. *Environ. Sci. Technol.* 1995, *29,* 181.

(9) Evans, D.; Rosocha, L. A.; Anderson, G. K.; Coogan, J. J.; Kushner, M. J. J. *Appl. Phys.* 1993, 74, 5378.

(10) Virden, J. W.; Heath, W. O.;.Goheen, S.C.; Miller, M. C.; Mong, G. M.; Richardson, R. L., *"Proceedings of the Int Topical Meeting on Nuclear and Hazardous Waste Management";* Spectrum 92, 1992, Boise, Idaho.

(11) Chang, M. B.; Kushner, M. J.; Rood, M. J., *Environ.Sci. Technol.* 1992, 777.

(12) Rosenthal, L. A.; Davis, D. A., *IEEE Trans. Ind., Appl.* 1975, *I*-5, 328.

(13) Lukyanov, D. B.; Lombardo, E. A.; Sill, G. A.; d'Itri, J. L.; Hall, W. K. *J. Cat.* **in press.**

(14) Lukyanov, D. B.; Sill, G.; d'Itri, J. L.; Hall, W. K. J. *Cat.* 1995, 153, 265.

(15) Tas, M. A.; Hardeveld, R. v.; Veldhuizen, E. M. V. van Santen, R.A, *12th International Symposium on Plasma Chemistry,* 1995, Minneapolis, MN.

EFFECT OF HYDROCARBONS ON PLASMA TREATMENT OF NO_x

B.M. Penetrante, W.J. Pitz, M.C. Hsaio, B.T. Merritt, and G.E. Vogtlin
Lawrence Livermore National Laboratory

INTRODUCTION

Lean burn gasoline engine exhausts contain a significant amount of hydrocarbons in the form of propene. Diesel engine exhausts contain little gaseous hydrocarbon; however, they contain a significant amount of liquid-phase hydrocarbons (known as the volatile organic fraction) in the particulates.

The objective of this paper is to examine the fate of NO_x when an exhaust gas mixture that contains hydrocarbons is subjected to a plasma. We will show that the hydrocarbons promote the oxidation of NO to NO_2, but not the reduction of NO to N_2. The oxidation of NO to NO_2 is strongly coupled with the hydrocarbon oxidation chemistry. This result suggests that gas-phase reactions in the plasma alone cannot lead to the chemical reduction of NO_x. Any reduction of NO_x to N_2 can only be accomplished through heterogeneous reactions of NO_2 with surfaces or particulates.

TEST SETUP

Previous studies [1-3] have shown that all electrical discharge plasma reactors produce a plasma with an average electron kinetic energy of around 3-6 eV. The plasma chemistry in discharge plasma reactors is therefore very similar regardless of electrode structure or the way the voltage is delivered to the reactor.

The plasma reactor used this study is a pulsed corona consisting of a 1.5 mm diameter wire in a 60 mm diameter metal tube 300 mm long. Heater bands and thermocouples provide active control of the processor temperature. The power supply is a magnetic pulse compression system capable of delivering up to 30 kV output into 100 ns pulses at variablerepetition rates to the kilohertz range. The electrical energy deposition into the gas was determined by monitoring the electrical parameters associated with the discharge.

The experiments were performed in a flow-through configuration. We prepared a mixture containing trace amounts of NO and hydrocarbons and recorded the composition of the effluent gas as a function of input electrical energy density. The input energy density, Joules per standard liter (J/L), is the ratio of discharge power to gas flow rate at standard conditions (25° C and 1 atm). The gas blending manifold allowed us to custom make gas streams consisting of N_2, O_2, propene, and NO_x. We metered these gases through mass flow controllers which permited exact control of flow rate. We used calibrated gas mixtures of either hydrocarbons or NO in N_2. This arrangement allowed us to blend in small concentrations of the trace components using mass flow controllers. After mixing in the manifold, the gas then passed through a temperature controlled heater which preheated the gas to the processor temperature. We monitored the outlet gas composition with a Fourier Transform Infrared (FTIR) spectrometer. We heated the absorption cell to 120° C to avoid condensation of any water byproduct.

PLASMA PROCESS WITHOUT HYDROCARBONS

Lean burn engine exhausts contain high concentrations of oxygen, rendering conventional catalytic converters ineffective for the treatment of NO_x. A critical issue in the application of plasmabased methods to cars and trucks is whether the NO is removed by reduction to benign gases such as N_2, or by oxidation to NO_2 and nitric acid. To avoid the need for scrubbing of process products, the desired method of NO removal is by chemical reduction to N_2.

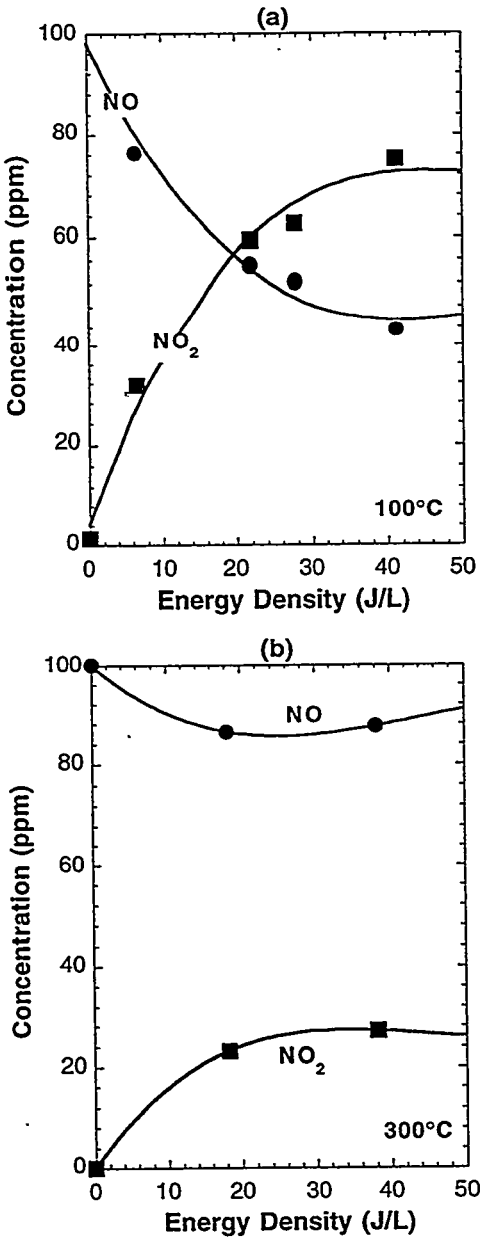


Figure 1. Effect of temperature on the plasma oxidation of NO in the absence of hydrocarbons. Plasma processing of 100 ppm NO in 10% O_2, balance N_2, at (a) 100° C and (b) 300° C.

Oxidation is the dominant process for exhausts containing dilute concentrations of NO in mixtures of N_2, O_2 and H_2O, particularly when the O_2 concentration is 5% or higher. The kinetic energy of the electrons is deposited primarily into the major gas components, N_2 and O_2. The most useful deposition of energy is associated with the production of N and O radicals through electronimpact dissociation:

$$e + N_2 \rightarrow e + N(^4S) + N(^4S, ^2D) \quad (1)$$

$$e + O_2 \rightarrow e + O(^3P) + O(^3P, ^1D) \quad (2)$$

where $N(^4S)$ and $N(^2D)$ are ground-state and metastable excited-state nitrogen atoms, respectively, and $O(^3P)$ (simply referred to as O) and $O(^1D)$ are ground-state, and metastable excited-state oxygen atoms, respectively. The $N(^4S)$ is the only plasma-produced species that could lead to the chemical reduction of NO:

$$N(^4S) + NO \rightarrow N_2 + O \quad (3)$$

In the presence of O_2, the oxidation pathway becomes dominant for two reasons:

(a) The dissociation energy of O_2 is smaller than that of N_2. For electrical discharge plasma reactors, the average electron kinetic energy is low, around 3-6 eV.[1-3] Under this condition the rate for dissociation of O_2 is much higher compared to the dissociation of N_2 [4]. The dissociation of O_2 will produce only oxidative radicals. The ground-state oxygen atom, $O(^3p)$, will convert NO to NO_2 via

$$O(^3P) + NO + M \rightarrow NO_2 + M \quad (4)$$
$$O(3P) + O_2 + M \rightarrow O_3 + M \quad (5a)$$
$$O_3 + NO \rightarrow NO_2 + O_2 \quad (5\,b)$$

The metastable oxygen atom, $O(^1D)$, will react with H_2O to produce OH radicals:

$$O(^1D) + H_2O \rightarrow 2OH \quad (6)$$

The OH radicals will convert NO and NO_2 to nitrous and nitric acid, respectively.

(b) Under conditions optimum for the dissociation of N_2, the production of the reducing species, $N(^4S)$, also leads to the production of the metastable atomic nitrogen, $N(^2D)$.[5] The $N(^2D)$ species can lead to undesired reactions in the presence of O_2. Rather than reducing NO, the $N(^2D)$ species would react with O_2 to produce NO:

$$N\,N(^2D) + O_2 \rightarrow NO + O \quad (7)$$

The production of NO by $N(^2D)$ will counterbalance the reduction of NO by $N(^4S)$, thus effectively leaving oxidation as the only

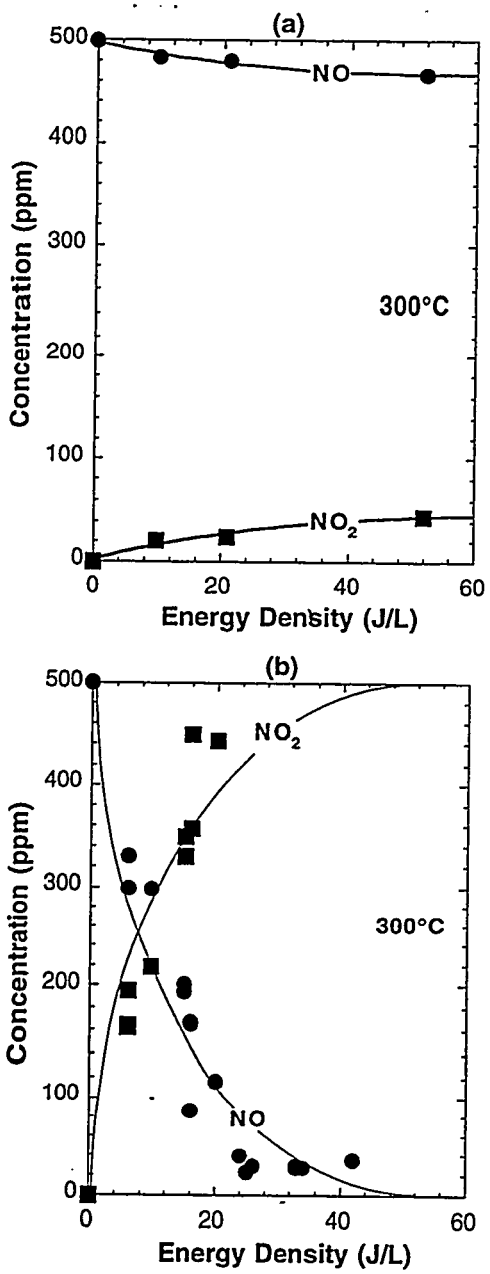


Figure 2. Effect of propene on the plasma oxidation of NO at 300° C. Plasma processing of 500 ppm NO in 10% O_2, balance N_2, (a) without propene, and (b) with 1000 ppm propene.

pathway for NO conversion.

We examined the plasma processing of 100 ppm NO in 10%O_2 and balance N_2, without hydrocarbons. The NO_x concentrations for the cases at 100° C and 300° C are shown in Figures 1(a) and 1(b), respectively. They are plotted as a function of electrical energy density (J/L). For the 100° C case, about 60% of the NO is converted to NO_2 at energy densities of 40 J/L and above. For the 300° C case, the conversion of NO to NO_2 is only around 20% even at the high energy densities.

The efficiency for oxidation of NO to NO_2 drops as the temperature is increased. At high temperatures, the NO to NO_2 oxidation reactions are counteracted by the reduction reaction:

$$O+NO_2 \rightarrow NO+O_2 \qquad (8)$$

Without hydrocarbons the oxidation of NO by the O radical is not efficient at high temperatures.

PLASMA PROCESS WITH HYDROCARBONS

We next examined the effect of hydrocarbons on the plasma processing of NO. Propene was used as a representative hydrocarbon. The gas mixture contained 500 ppm NO in 10% O_2 and balance N_2. The NO_x concentrations for the cases without propene and with 1000 ppm propene are shown in Figures 2(a) and 2(b), respectively, for processing at 300° C. For the case without propene (Figure 2(a)), less than 20% of the NO is converted to NO_2 even at the high energy densities. This is consistent with the previous observation shown in Figure 1 (b). At high temperatures, the efficiency for conversion of NO to NO_2 is poor in the absence of hydrocarbons in the gas stream. Figure 2(b) shows the NO_x concentrations when 1000 ppm of propene is added to this gas stream. The main fate of NO in the plasma in the presence of hydrocarbons is the oxidation of NO to NO_2.

The oxidation of NO to NO_2 is coupled with the hydrocarbon oxidation chemistry and will be discussed in the following section.

OXIDATION CHEMISTRY

This section will discuss the hydrocarbon oxidation chemistry, using propene as the representative hydrocarbon.

In the very early stages of reaction the propene is mainly consumed by the O atom:

$$C_3H_6+O \rightarrow C_2H_5+HCO \qquad (9)$$
$$C_3H_6+O \rightarrow CH_2CO+CH_3+H \qquad (10)$$
$$C_3H_6+O \rightarrow CH_3CHCO+H+H \qquad (11)$$

Of the total reaction with O atom, reaction (9) contributes 50%, and reactions (10) and (11) contribute 25% each. The O atoms are consumed more effectively by reactions (9)-(11) than reactions (4) and (5): $O+NO \rightarrow NO_2$.

At 300° C and early in the reaction, about 98% of the O atoms react with propene compared to 2% with NO. The rate constants for propene + O are much faster than that of NO +O. This result means that the propene consumes most of the O atoms that might otherwise react with NO to form NO_2-

After the initial stages of reaction, the OH radical rather than O atom becomes the main radical consuming propene:

$$C_3H_6+OH \rightarrow C_3H_6OH \quad (12)$$
$$C_3H_6+OH \rightarrow C_3H_5+H_2O \quad (13)$$

where C_3H_5 radical symbolized all three isomers, which were distinguished individually in the reaction mechanism. The switch from O atom reactions to OH reactions is mainly due to OH being produced by the reaction

$$NO+HO_2 \rightarrow NO_2 + OH \quad (14)$$

This is also the main reaction that converts NO to NO_2. The HO_2 radicals are also produced from reactions involving hydrocarbon intermediates of propene oxidation:

$$CH_2OH+O_2 \rightarrow CH_2O+HO_2 \quad (15)$$
$$CH_3O+O_2 \rightarrow CH_2O+HO_2 \quad (16)$$
$$HCO+O_2 \rightarrow CO+HO_2 \quad (17)$$
$$H+O_2 \rightarrow HO_2 \quad (18)$$

Therefore, the propene supplies HO_2 radicals which convert NO to NO_2. Without the propene, the main reaction to convert NO to NO_2 are reactions (4) and (5): $O+ NO \rightarrow NO_2$.

Nearly all the O atoms for conversion are supplied by electron impact, which has an associated cost in electrical energy. The propene lowers the energy requirement by production of HO_2 radicals which then become the main radical for conversion of NO to NO_2.

The OH produced from reaction (6) can also react with NO and NO_2 to form their related acids:

$$NO+OH \rightarrow HONO \quad (19)$$
$$NO_2+OH \rightarrow HONO_2 \quad (20)$$

At 300° C, during the time when the propene is being consumed most rapidly, only about 6% of the OH is reacting with NO and NO_2 while the remainder is reacting mostly with propene and its aldehydic intermediate products. At 100° C 15% of the OH is reacting with NO and NO_2, while the remainder reacting mostly with propene and aldehydic intermediates. The rate constants for these reactions are much slower than for propene+OH reactions, so that OH reacts mainly with propene rather than NO and NO_2.

CONCLUSIONS

The objective of this paper was to examine the fate of NO when a lean burn exhaust gas that contains hydrocarbons is subjected to a non-thermal plasma. We have found that the NO is mainly oxidized to NO_2 by

$$NO+HO_2 \rightarrow NO_2+OH$$
$$NO+RO_2 \rightarrow NO_2+RO$$

where R is a hydrocarbon radical. The oxidation of NO to NO_2 is coupled with the hydrocarbon oxidation chemistry. The O and OH radicals are consumed mainly by reactions with the hydrocarbons rather than with NO. Only oxidizing radicals in the form of HO_2 and RO_2 are produced during the breakup of the hydrocarbons. The hydrocarbons lower the energy cost for the oxidation of NO by converting O and OH to HO_2; the OH radical is then reproduced when NO is oxidized by HO_2. This cyclic process leads to a very efficient utilization of the plasma-produced radicals for the selective partial oxidation of NO to NO_2. This result suggests that gas-phase reactions in the plasma alone cannot lead to the chemical reduction of NO_x. Any reduction of NO_x to N_2 can only be accomplished through heterogeneous reactions of NO_2 with surfaces or particulates.

ACKNOWLEDGMENTS

This work was performed at Lawrence Livermore National Laboratory under the auspices of the U.S. Department of Energy under Contract Number W-7405-ENG-48, with support from the Chemical Sciences Division of the Office of Basic Energy Sciences and a Cooperative Research and Development Agreement with Cummins Engine Company.

REFERENCES

1. Penetrante, B.M., Hsiao, M.C., Merritt, B.T., Vogtlin, G.E., Wallman, P.H., Neiger, M., Wolf, O., Hammer, T., and Broer, S.,: *Applied Physics Letters* 68(1996)3719.

2. Penetrante, B.M., Hsiao, M.C., Merritt, B.T., Vogtlin, G.E., Wallman, P.H., Kuthi, A., Burkhart C.P., and Bayless, J.R.,: *Applied Physics Letters* 67 (1995) 3096.

3. Penetrante, B.M., Hsiao, M.C., Merritt, B.T., Vogtlin, G.E., and Wallman, P.H.: *IEEE Transactions on Plasma Science* 23 (1995) 679.

4. Penetrante, B.M., in *Non-Thermal Plasma Techniques for Pollution Control - Part A: Overview, Fundamentals and Supporting Technologies,* edited by B. M. Penetrante and S. E. Schultheis (Springer-Verlag, Berlin Heidelberg New York, 1993) pp. 65-90.

5. Penetrante, B.M., Bardsley, J.N., and Hsiao, M.C., *Japanese Journal of Appied Physics* 36 (1997)5007.

NON-THERMAL PLASMA EXHAUST AFTERTREATMENT : ARE ALL PLASMAS THE SAME?

J.H. Whealton, G.R. Hanson, J.M. Storey, R.J. Raridon,
J.S. Armfield, T.S. Bigelow, and R.L. Graves
Oak Ridge National Laboratory

BACKGROUND

Plasma aftertreatments have been identified as a possible exhaust remediation technique since non-thermal plasma (NTP) can induce a host of new chemical reactions due to electron excitation resulting in the abundant production of radicals and excited state molecules. Present plasma aftertreatments rely on high local electric fields which directly produce energetic electrons. These energetic electrons can influence the chemistry, even in the collision dominated regime, because they do not lose much energy in elastic collision due to their small mass, but instead bounce around and transfer most of their energy to molecules; either dissociating, ionizing, or otherwise exciting them. The excitation and radical production can cause vast changes in reaction rates (as much as a hundred thousand-fold increase in some instances). Oxidation and reduction reaction pathways are possible for the dissociation of NO_x. Oxidation leads to the production of such compounds as N_2O and nitric acid. Nitric acid is toxic and is to be avoided in mobile applications. Reduction, on the other hand, leads to dissociative attachment eventually forming N_2.

To explore excited state chemistry, it is desirable to produce as high an electric field as possible. This would at first seem to entail applying high enough voltages to a suitably arranged configuration of electrodes. However, for plasma densities of interest, there is considerable plasma shielding of the applied fields even in the collision dominated regime and field limits due to low impedance arcing (Ref. 1). This space charge shielding is due to the charge imbalances arising within the plasma because of the higher mobility of electrons compared to the positive ions.

PROPOSED TECHNOLOGY

The efficiency of NTP is limited by several factors as indicated in Ref. 2. One limitation is that the electric fields are generally limited by high voltage breakdown which leads to a low impedance discharge. Significant increases in this arc transition electric field should be possible by incorporating high frequency power (5Ghz) implying 40 ps risetime. Another problem, probably not incorporated into the analysis of Ref. 2, is that plasma shielding effects take place for fields at frequencies below the electron plasma frequency. As a result of plasma shielding, the volume of the plasma where high field enhanced reduction reactions is reduced to within a few Debye lengths or an electron energy relaxation distance of the plasma edge which can reduce the high field reaction volume by orders of magnitude. This plasma shielding effect is significantly reduced by using high frequency power. Resonance cavities enable an efficient coupling of high frequency power to produce high electric fields. Surface charging of dielectrics, to the extent it occurs at all at high frequencies, will likely enhance rather than diminish (as occurs for low frequency) the fields in the next (reverse field) half cycle. Better chemistry (reduction as opposed to oxidation) is obtained by having the electric fields ramp up so fast

Based on work performed at the Oak Ridge National Laboratory, managed by Lockheed Martin Energy Research Corporation for the U.S. Department of Energy under contract number DE-AC05-960R22464.
The submitted manuscript has been authored by a contractor of the U.S. Government under contract No. DE-AC05- 960R22464. Accordingly. the U.S. Government retains a nonexclusive, royalty free license to publish or reproduce the published form of this contribution, or allow others to do so, for U.S. Government purposes.

(~40ps) that the probability of the discharge initiating near threshold is substantially reduced.

There are two issues which inhibit development of plasma discharge aftertreatment, undesirable chemistry path and low electrical efficiency. Both of these issues are addressed in the proposed technology.

Chemistry Path: The difficulty of reaching high E/N in the existing embodiments of the above mentioned discharges has resulted in an inability for a plasma aftertreatment device to achieve a high fraction of reduction of NO_x as opposed to oxidation. To enable much higher E/N, and a continuous production of atomic Nitrogen, we propose to employ bursts of high frequency ac electric fields with fast risetimes and many cycles per burst. Specifically, high-power microsecond bursts of 5GHz microwaves will be used which have a risetime of ~40ps (100 times shorter than present state-of-the-art pulse risetimes in this application) and allow thousands of electric field oscillations per burst of microwave power.

The net benefit of this approach in producing the best chemistry is as follows:

(A) For 40ps risetime, the fields turn on with a time scale short compared with the time an electron drifts toward the edge of the plasma; strict space charge neutrality is achieved in the plasma preventing field reduction due to plasma shielding; (B) Atomic nitrogen will be produced and available during the entire treatment since the time between microwave bursts is small compared to the recombination time; (C) Surface charging of dielectrics, to the extent it occurs at all, will enhance the fields in the next (reverse field) half cycle; (D) Field limits due to arc breakdowns (e.g., Paschen limit) will be significantly increased due to the high frequency; (E) Higher fields by having the electric fields ramp up so fast that the probability of the discharge initiating near threshold is substantially reduced.

These improvements should allow a substantial increase in the strength/efficacy of the applied fields and result in a tilt of the reaction pathway toward the desirable reduction of NO_x to N_2. This technology is intended to be used in conjunction with solid catalyst surfaces in proximity to the plasma. For a certain class of such catalysts, the surface reactivity can be enhanced by the microwave fields in addition to the effect of higher reactivity in the plasma itself.

In some cases, it could be desirable to heat the catalyst to increase its reactivity only very locally in places just where the reactions are taking place. One of the features of the proposed technology is to introduce such a scheme of controlled and highly localized enhanced catalyst reactivity.

Consider an inhomogeneous high dielectric material in the presence of low dielectric voids. If an oscillating electric field is applied to such a mixture, the potential distribution could look something like that shown in Fig.2 at an instant of time. Notice the concentration of equipotentials at certain points on the surface of the dielectric indicating the presence of high fields. The heating rate of the dielectric is dependent on these field strengths and so would be very localized even if the absorption of the electric field was uniform; however, the power absorbed is proportional to the square of the electric field. The field absorption at the edges of the dielectric is in fact made greater than that within the bulk of the dielectric by considering the polarizability catastrophe. The polarizability catastrophe occurs in the transition between vibrational excitation (small displacement and, therefore, small field absorption) and rotational excitation (large displacement and, therefore, large field absorption). When a material gets hot enough, lattice excursions become sufficiently frequent so that there is occasionally room for a rotational excitation. When this happens, the heating rate increases a hundredfold and produces more excursions producing yet more rotational excitation and so on. Unless one turns off the rf power quickly enough, a nonlinear catastrophe occurs - hence the name (effect discovered by Debye). The reason for mentioning this bit of historical trivia here is that on the edge of the dielectric, rotational excitation can always occur even at low temperatures since there is no lattice

to get in the way. Therefore, even if the electric field was uniform there could be preferential heating at the very edge of the dielectric. Figure 2a shows that this heating would become even more preferential since that is exactly the place where the electric field is strongest.

EXPERIMENTAL DETERMINATIONS

We describe initial experiments employing 5.5GHz pulsed microwave power, which should result in enhanced chemistry compared to present state-of-the-art plasma aftertreatments by; reducing plasma electric field shielding, increasing availability of atomic nitrogen, exploiting surface charging of dielectrics, avoiding (low field) threshold initiated discharges, and achieving a higher high energy tail on the electron distribution function. As an example, we decided to test for NO reduction in N_2. While this reaction is not a complete description of the exhaust issues by any means, we thought it would demonstrate the technology proposed.

PROCESS

The fast rise time non-thermal plasma NO_x control reactor uses a 5.5 GHz pulsed microwave source to generate a DBD with electric field rise times of less than 50 ps. A gas mixture is fed to the reactor from a flow bench that can mix up to eight gases and cycle certain gases with time. The microwave source is a magnetron tube and power supply with a frequency output tunable from 5.3 GHz to 5.8 GHz, a peak output power of 200 kW, and an average power output of 200 W. The output pulse widths can be 0.5, 1.5, and 2.25 μs with a duty factor up to 0.001. The microwave applicator or reactor, see Fig. 1, consists of a 43 cm length of WR-187 waveguide with a 16 mm OD, 14 mm ID quartz tube penetrating through the wave guide at a 15° angle. The microwave electric field is generated between the top and bottom walls of the waveguide and thus passes through the quartz tube in the region where the tube is within the waveguide. The tube is angled to provide a slow change in dielectric constant in the waveguide. The outlet end of the waveguide, as shown in Fig. 2, is shorted with a plate to reflect any power not absorbed in the first pass back into the reaction volume. The waveguide is pressurized with sulfur-hexaflouride to prevent breakdown around the outside of the quartz tube, rather than inside the tube. The quartz tube is filled with 4 mm dielectric beads to provide electric field enhancement and electrical breakdown. A DBD is generated when an arc is initiated between dielectric surfaces. The electrons at the leading edge of the arc are trapped on the surface of the dielectric, locally canceling out the electric field and extinguishing the arc. A new arc is then immediately formed but intersecting the dielectric surface at a different location. Figure 2 shows the basic waveguide layout from the microwave source to the reactor. A signal sampling coupler is used with coaxial detectors is used to measure the applied and reflected power levels at the reactor.

Gas concentrations of NO_x were determined by chemiluminescence (Rosemount model 951) operated in the NO_x mode. No attempt was made to quantify O3 and N_2O, although this capability will be available for future efforts.

EXPERIMENTAL RESULTS AND DISCUSSION

The set of experiments performed with the described setup involved a simple mixture of NO in N_2. Initial concentrations of NO were set at 1000 ppm and 2000 ppm with flow rates of 4.6 lpm and 10.6 lpm. This gave a residence time of 100 ms and 44 ms respectively in the active zone of the discharge, or space velocities of 36,000 h^{-1} and 83,000 h^{-1}. Because no H_2O was present, the outlet of the reactor was fed directly into the analyzers.

For these experiments, an average pulse width of 1.5 ps and period of 3 ms were used resulting in a duty factor of 0.0005 to 0.001. Several different power levels were investigated resulting in peak transmitted powers of 22 to 150 kW and average transmitted powers of 3 to 100 W. Transmitted and reflected powers were monitored using a calibrated waveguide signal sampler with coaxial detectors. The absorbed power was taken as the difference of applied and reflected power. This is an upper bound for absorbed power because other losses are neglected. Input energy density in joules/liter is calculated from the absorbed power and the flow rate. To put the results in perspective of others'

work, the results are scaled linearly to 100 ppm input NO concentration and the input energy densities are plotted vs ppm NO in Figure 3. Penetrante et al. presented modeling and experimental results on similar axes for pulsed corona discharge generated electrons.[ref]. The resulting energy per molecule NO converted was found to be 238 eVmolecules. The microwave generated plasma is converting at a lower energy per molecule.

The high peak power, low repetition rate data appears to indicate a high efficiency of conversion with low energy densities. This is explained perhaps by the efficiency at which microwave energy can penetrate a plasma and heat the electrons as long as the microwave frequency remains higher than the characteristic electron plasma frequency (cutoff is avoided). For the 5.5GHz typically used in these experiments, the corresponding electron cutoff density is approximately 3.5 x 10-11 cm-3.

DISCUSSION OF ERRORS

The errors in these data have three contributions: NO concentration measurements, gas flow measurements, and microwave power measurements. The transmitted and reflected microwave powers are measured by means of coaxial detectors on a signal sampling coupler in the waveguide system. Random uncertainties in the power measurements result from the reading of the detector voltages, the pulse width and the pulse period are estimated to be ± 15% in the average absorbed power (transmitted power - reflected power). The power measurements are also subject to systematic errors resulting from the signal sampler and coaxial detector calibration. These errors are estimated to be >10% and would offset all of the data in the same way and so not affect any trends displayed in the data here.

The errors in the measurement of NO and NO_2 are small relative to the errors in power measurement. The particular chemiluminescence instrument used for this study drifts less than 1% in a day and was spanned before each set of runs. Similarly, NO_2 response was checked with a standard mixture. The standard deviation over the ten samples taken for each run is also incorporated into the error, for an overall error of concentration of ± 7%. The errors in flow measurement, which is incorporated into the input energy density determination is also small. The mass flow controllers are specified at ± 2% accuracy. The contribution of this error to the overall error in calculating the input energy density is negligible.

CONCLUSIONS

As an illustration, this plasma generator was applied to the removal of NO in N_2. Instead of the usual 238 eV per removed NO obtained with other slower rise time plasmas, a 70% reduction (75 eV per removed NO) was obtained.

The electron temperature was 6.5 eV vs the usual 4 eV, see Fig. 4 [3].

A new plasma generator for NTP treatment of exhaust gases was investigated. It features a fast rise time (40 ps) discharge which is comparable to electron transport times in the plasma. This is obtained from a 5.5GHz microwave generator coupled to a suitable resonance cavity. Thus, plasma shielding is reduced and a higher E/N in the bulk of the plasma achievable. This may reduce the N_2 vibrational excitation risk and allow for high electron temperatures. As an illustration, this plasma generator was applied to the removal of NO in N_2. Instead of the usual 238 eV per removed NO obtained with other slower rise time plasmas, a 25% reduction (167 eV per removed NO) was obtained. This improvement is in and of itself hardly sufficient to admit the stand alone commercial feasibility of the technique, but offers possibilities when combined with smart catalytic converters. With such catalytic converters, the higher electron temperature and concomitant different reaction kinetics (enhanced excited state molecular production) offer a synergistic and enhanced improvement in exhaust remediation. This is in addition to the expected enhanced reactivity of the catalyst itself due to the microwave induced rotational excitation at the catalyst surface edges.

REFERENCES

1. J. H. WHEALTON AND R. L. GRAVES, "EX-

HAUST REMEDIATION USING NON-THERMAL (PLASMA) AFTERTREATMENT: A REVIEW," *PROCEEDINGS OF THE 1995 DIESEL ENGINE EM/SS/ONS REDUCTION WORKSHOP,* V-25, LAJOLLA.

2. B. M. PENETRANTE ET AL., "COMPARISON OF ELECTRICAL DISCHARGE TECHNIQUES FOR NONTHERMAL PLASMA PROCESSING OF NO IN N_2," PP. 679 - 687 IN *IEEE TRANSACTIONS IN PLASMA SCIENCE,* VOL. 23, NO. 4, 1995.

3. B.M. PENETRANTE, PREVIOUS PAPER DEER '97

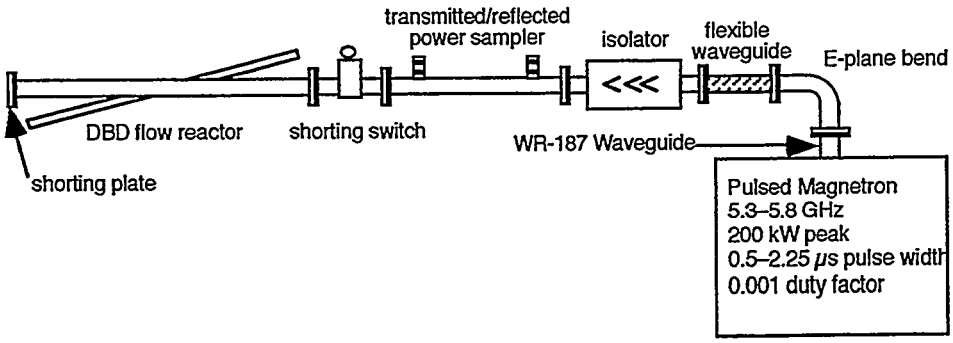


Fig. 1. Waveguide reactor for microwave generated DBD non-thermal plasma treatment of exhaust gases. The microwave energy causes breakdown in the portion of the quartz tube within the waveguide. The quartz tube is filled with dielectric beads through which the gases flow. Electric field enhancement along the surfaces of the dielectric beads leads to the DBD.

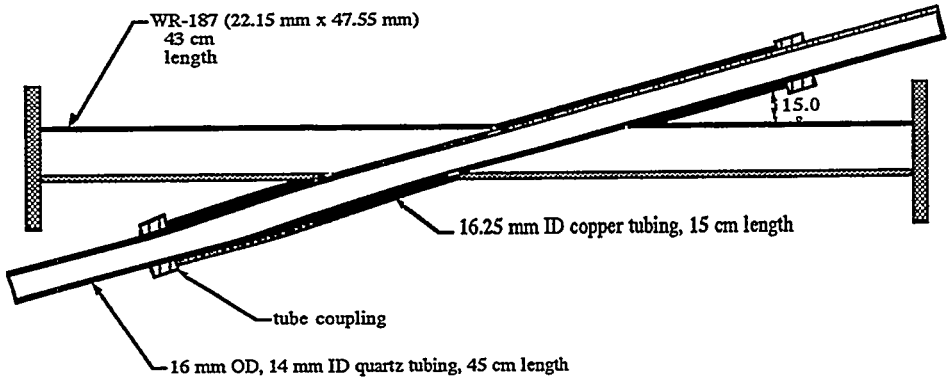


Fig. 2. Microwave generated DBD flow reactor waveguide layout. The microwave energy is generated by a pulsed magnetron tube and conveyed to the waveguide reactor by WR-187 waveguide.

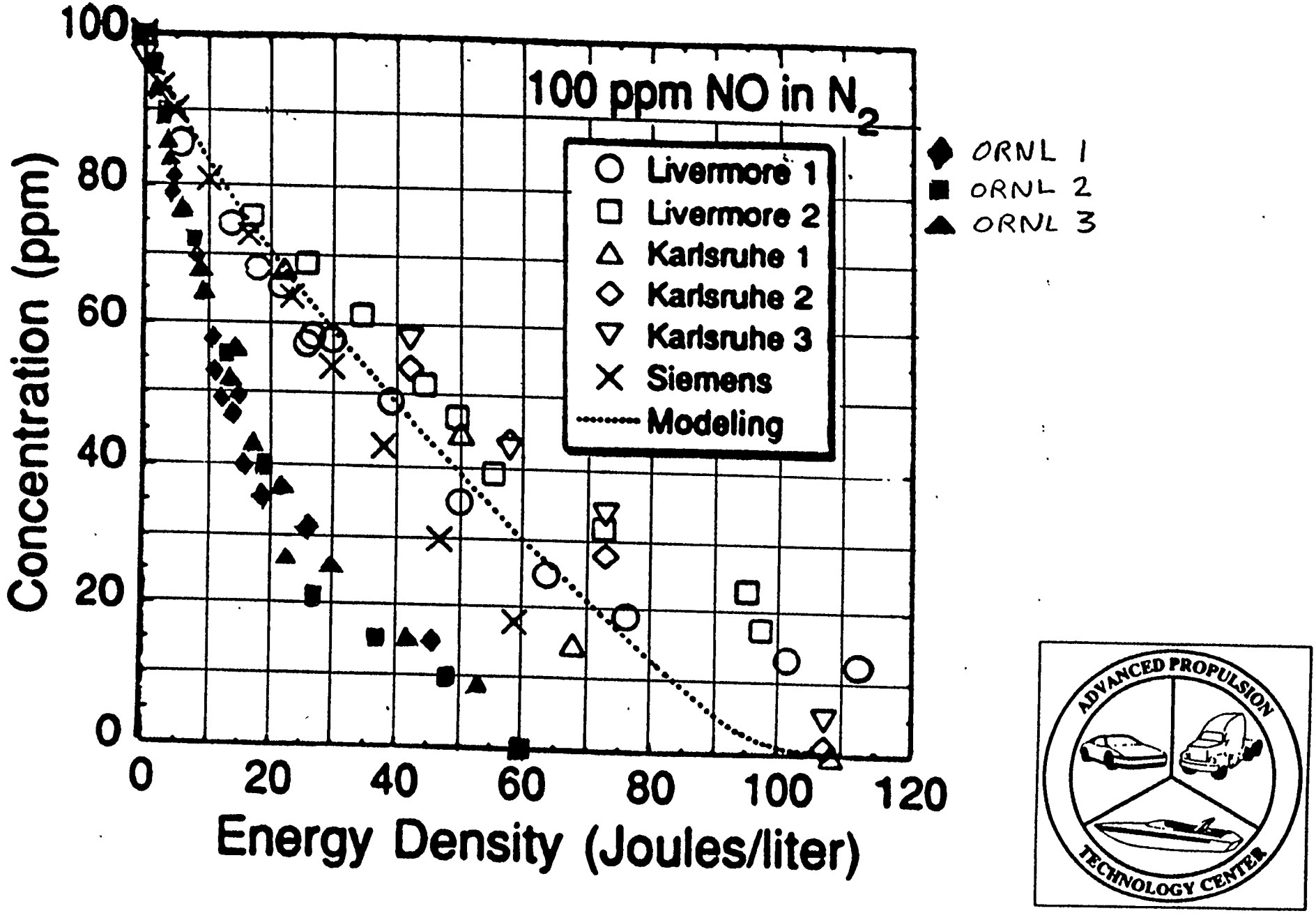
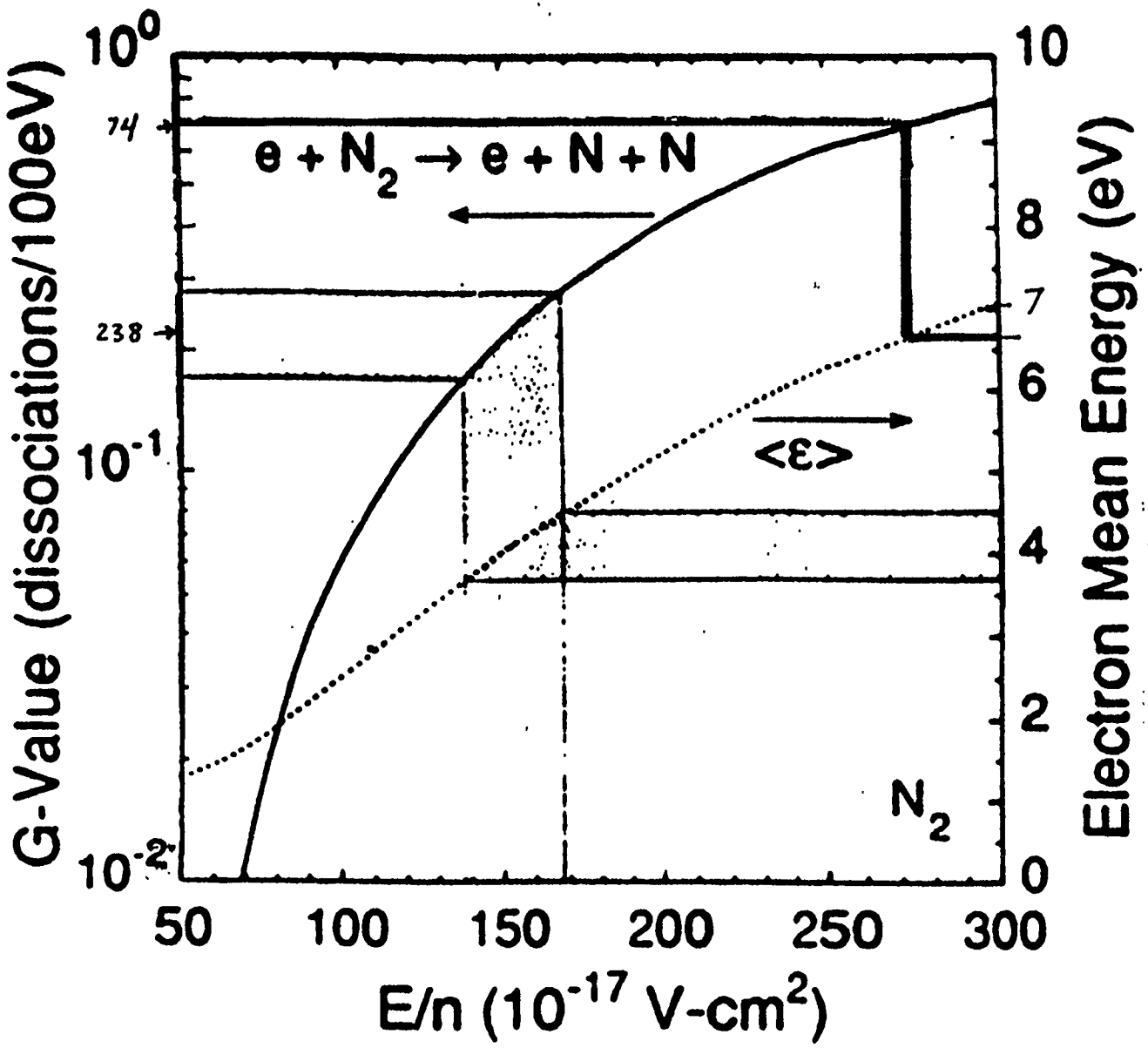


FIG. 3. Pulsed corona and dielectric-barrier discharge processing of 100 ppm NO in N_2.



	$\bar{\varepsilon}$
ORNL	6.6
LIVERMORE	4.2
KARLSRUHE	4.2
Siemens	4.2

FIG. 4. Calculated G value (number of dissociations per 100 eV of energy input) for electron-impact dissociation of N_2, and electron mean energy, as functions of the reduced electric field E/n.

PLASMA TECHNOLOGY FOR NO_x AND PARTICULATE REMOVAL FROM HEAVY DUTY VEHICLES

V. Palekar, M. Ramavajjala, and R. Slone
NOxTECH, INC.

Federal and State emission standards for heavy duty diesel engines have resulted in the evaluation of various engine modification (in-cylinder and EGR) and aftertreatment strategies to reduce NO_x and particulates from stationary and mobile diesel engines. Past emissions requirements have been achieved by controlling engine combustion parameters. Mandates on extremely low NO_x and particulate levels such as potential 2004 EPA regulations may require an external aftertreatment device downstream of the engine.

Modern diesel engines employ stratified charge combustion with air/fuel ratios of ≈ 20, that produce lean exhausts (high O_2 levels) in the temperature range of 250°-850° F. Conventional thermal and catalyst technologies, such as three-way catalysts, have been found to be ineffective under these high O_2 conditions. The use of non-thermal plasmas offer the potential to selectively reduce NO_x and oxidize particulates in such high O_2 exhausts without the need for supplemental scavengers or additives.

This paper focuses on the non-thermal plasma technologies being developed at NOxTECH, Inc. for heavy-duty vehicles. Specifically, progress made on a gas phase pulsed power system and a plasma assisted catalyst system is reviewed with performance data on diesel exhaust for NO_x and particulate removal.

Non-thermal plasma technology involves the in-situ production of the desired active radicals and ionic species at low temperatures. The plasma environment consists of a number of highly energetic electrons which collide with the predominant molecules, viz. N_2, O_2, H_2O and CO_2 to form N, O and OH radicals. The two main reactions involved are:

$$NO + N \rightarrow N_2 + O \quad (1)$$
$$NO + O \rightarrow NO_2 \quad (2)$$

Reaction 1 results in the desired product N_2 while reaction 2 results in the undesired NO_2.

Figure 1 shows the NO_x reduction for the gas phase pulsed power system. This test was conducted on a slipstream from a 4 kW diesel engine with a baseline NO/NO_x concentration of 200/245 ppm, 13% O_2, 5% H_2O and particulates. Greater than 60%NO_x reduction was obtained at less than 5% energy. This performance was found to be better at higher baseline NO_x conditions. The selectivity ($\Delta NO_x/\Delta NO_2$) was found to be consistently higher than 3 and the NO_x removal efficiency was found to vary between 30 and 60 eV/molecule. Under these conditions, greater than 50% particulate removal was simultaneously obtained. The removal of NO_x was found to be largely invariable with respect to temperature up to 500° F. Additional data at higher temperature is being obtained.

Figure 2 shows a pictorial view of the second system, namely the plasma assisted catalyst system. This system also selectively reduces NO_x to N_2 and oxidizes particulates to CO_2 without the use of additives. In this system, the plasma is generated across a catalytic packed bed. Greater than 70%NO_x reduction at less than 5% energy was obtained on a slipstream of a 60 kW diesel genset with a baseline of 183/192 NO/NO_x, 17% O_2 and 8% H_2O. This is shown in Figure 3. The nature of the catalyst beads seemed to have a considerable influence on system performance. Similar to the gas phase system, a selectivity ($\Delta NO_x/\Delta NO_2$) of greater than 3 was obtained. Also, greater than 50% simultaneous removal of particulates was obtained.

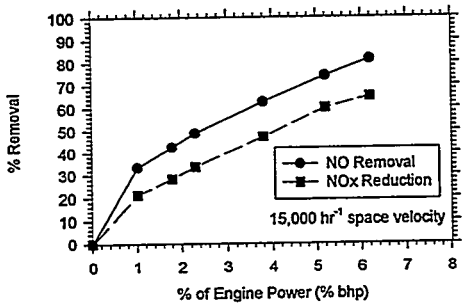


Fig. 1: NO Removal and NO_x Reduction for the Gas Phase Pulsed Power Plasma System

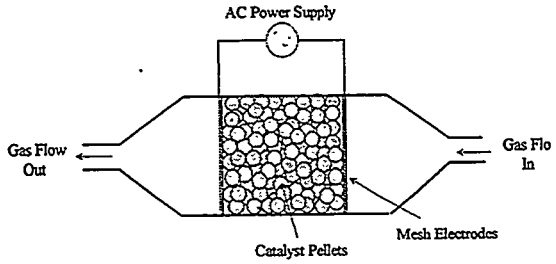


Fig 2: Simplified Schematic of the Plasma Assisted Catalyst System

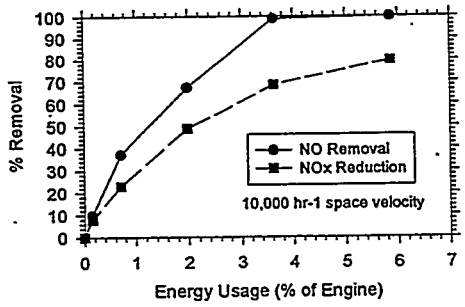


Fig 3: NO Removal and NO_x Reduction for the Plasma Assisted Catalyst System

Byproduct measurements showed no N_2O and less than 2 ppm HNO_3 under all conditions.

Also, the gas phase system was found to be insensitive to sulfur levels while additional work is needed to determine the sensitivity of the plasma assisted catalyst system to fuel sulfur levels.

NOxTECH is targeting a device that will allow engine manufacturers to meet 2004 regulations. Continuing development efforts are targeting greater than 80%NO_x and 70% particulate emissions at or below engine exhaust temperatures with less than 5% parasitic load on engine. A prototype system for an 80 hp diesel engine is planned for early 1998.

Present-day diesel engines are optimized for emissions and performance instead of performance and economy. The use of a cost effective plasma emissions reduction device will help boost combustion efficiency and may offer the potential for substantial reduction in engine cost.

FROM LAB TO REALITY, PLASMA ENGINEERING FOR POLLUTION CONTROL

S. Hall
AEA Technology pic

INTRODUCTION

AEA Technology has engineered laboratory scale non-thermal plasma technologies into commercially successful systems and processes which are the subject of extensive patents worldwide..For example, systems have been developed for the sterilisation of medical equipment and the removal of volatile organics in the pharmaceutical industry. This paper presents a series of case studies which demonstrate the importance of applications engineering and understanding product requirements in the development of laboratory scale science into plasma-based products.

In the laboratory almost any plasma generating technique can be used to demonstrate the effectiveness or otherwise of a proposed process. However, when attempts are made to scale up and engineer a product to a specification it becomes clear that the plasma generation technique and the associated hardware are key factors in arriving at a commercially viable solution.

Examples of how the product specification influences the choice of the plasma generation technique are illustrated in the following case studies.

INCINERATOR OFF-GAS TREATMENT

Product specification

Figure 1.1 illustrates the client's product specification for incinerator off-gas treatment. The overriding specification requirements are for a rugged system capable of reducing dioxins and furans to <0.1 ng/m 3 (ITEQ) under high gas throug-hput and low pressure drop conditions. These process requirements, which force the downselection of the plasma generation method, are inherent properties of a wire to cylinder corona reactor design. Issues associated with the complexity and size of corona power supply technology (especially in pulsed mode) are minimised in this ground based environment which already employs high voltage electrostatic precipitation.

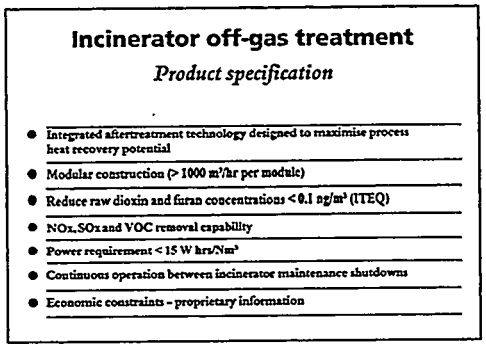


Figure 1.1

© AEA Technology plc

Scaling up issues

Initial trials were performed by applying a short-pulse of high voltage to the inner wire electrode of a wire to cylinder geometry reactor, resulting in the formation of small streamers of ionised gas which propagate towards the outer earth electrode. The electrons and ions in these streamers, and free radicals which are formed, process the gas stream. The stability and efficiency of the pulsed corona system is achieved by short high voltage pulses having rapid rise time at high frequency.

The initial laboratory reactor had an inner electrode wire with a diameter of 0.5 mm and an outer electrode cylinder with a 50 mm diameter and length of 100 mm. An immediate challenge was the accurate centering of the wire, as misaligned electrodes had a tendency to arc before peak generation was achieved thus absorbing power and reducing process efficiency.

Pilot scale prototype

The product specification demands high gas throughput with low pressure drop. The impact of scaling the corona reactor to meet these requirements introduces a wide range of design considerations.

Scaling the outer electrode diameter increases the distance between electrodes, resulting in higher operating voltages which raise further issues such as safety and electrical insulation. Non-uniform plasma distribution between electrodes is of concern. In order to ensure efficient energy transfer it is important that the reactor and power supply are considered in combination.

These considerations have resulted in the development of a patented 7.5 liter volume geometry system. A bank of four such reactors has been successfully demonstrated at a domestic waste incinerator in the UK. Confirmation of the corona reactor's performance during this demonstration is illustrated in Figure 1.2. This shows typical reactor performance data. The data was recorded just after a truckload of hospital waste had been delivered for incineration. The data shows a background VOC emissions spike from the burn. Note the reduction in VOC when the plasma is applied at t = 4 minutes and t = 20 minutes.

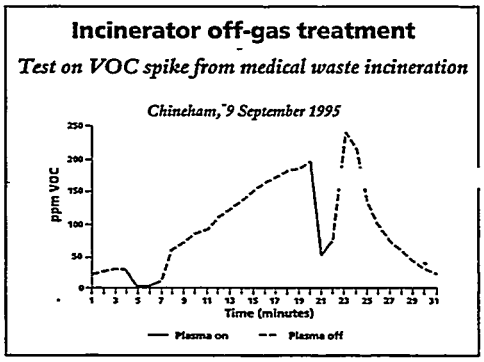


Figure 1.2 © AEA Technology plc

Final product modular design

Further scaling up of both the corona reactors and power supply was necessary to achieve the requirements laid down in the product specification. Taking into consideration firstly, the product specification and secondly, the valuable

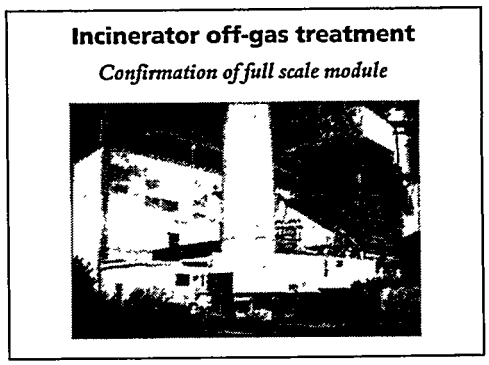


Figure 1.3 © AEA Technology plc

lessons learnt under real world conditions by operating the pilot scale system at the incinerator (in particular, differential thermal expansion and the corrosive nature of incinerator off gas), a 1000 nm³/h modular system has been developed. Figure 1.3 shows the AEA Technology corona system undergoing trials in the UK. The system met the demands laid down in the product specification. Figure 1.4 illustrates typical experimental data, confirming the reactor's performance in meeting the required emissions target.

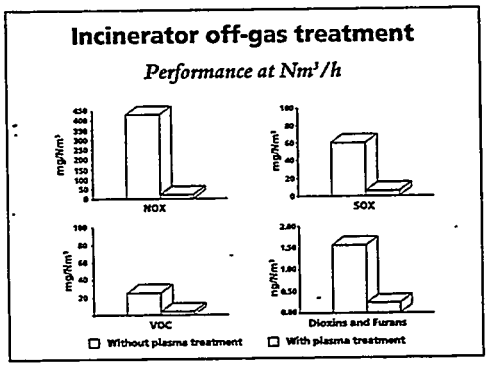


Figure 1.4 © AEA Technology plc

VOC REMOVAL IN PROCESS INDUSTRY

Product specification

The second case study examined is that of microwave plasma technology for application to VOC removal in the process industry. Figure 2.1 illustrates the product specification set out by the customer.

In this instance the client was looking for an economic and practical alternative to incineration, which could be integrated into the existing solvent management system. Cost is the determining factor governing the engineered

solution. Utilising off the-shelf 2.45 GHz microwave magnetron technology provides both a cost effective and efficient means of generating a plasma. The 2.45 GHz magnetron is a continuous wave generator. It's disadvantage is a tendency to form a thermal plasma and this represented a significant engineering challenge.

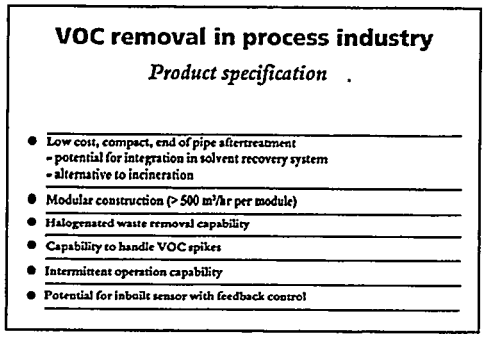


Figure 2.1 © AEA Technology plc

Scale up issues

The tendency to form a thermal plasma can be overcome with high gas flows. However, it is generally difficult to initiate and stabilise atmospheric discharges at high gas flows utilising microwave technology. The challenge was to design and develop a reactor capable of both initiating and producing a stable non-thermal discharge. The reactor electrode geometry is illustrated in figure 2.2A. The plasma is generated using field enhancing electrodes each of which has a radial gas passage. An annular gap between the electrodes serves to generate the plasma. This gas processing region is a hostile environment in which corrosive gases form rapid wear conditions and where temperatures under low flows can rise to in excess of 1500 K. Meeting the demands of the final product specification also represents a significant metallurgical challenge, and a wide range of transitional materials have been evaluated to improve the operational lifetime of the electrode.

Pilot scale prototype

The engineering challenge in scaling up the microwave reactors is to satisfy the conflicting requirements of higher gas throughput whilst achieving a stable plasma. The development of the patented microwave reactor illustrated in Figure 2.3 utilises a PTFE cassette which forces the process gas to rotate around the electrode knife edges, as shown in figure 2.2A. This helps to achieve increased residence time and plasma stability. It is essential that the cassette is manufactured from a material that is microwave transparent, such as PTFE. However, the introduction of a PTFE cassette distorts the microwave wave front resulting in a less than optimum

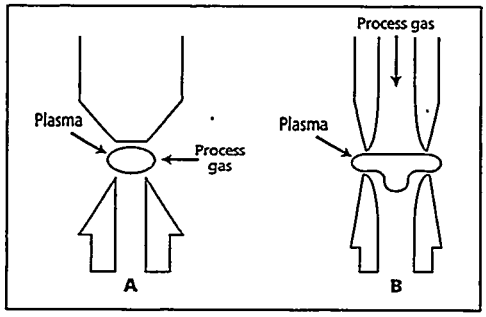


Figure 2.2A and B © AEA Technology plc

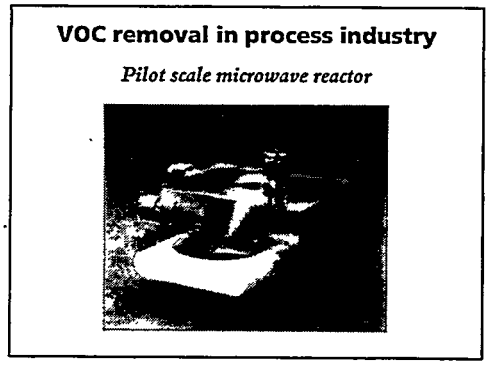


Figure 2.3 © AEA Technology plc

transfer of power. The engineering solution to overcome this inherent problem was to devel-op and incorporate a low cost wave-guide transformer tuning mechanism into the design of the reactor. Figure 2.4 shows the system's ability to convert hydrocarbons,such as clichloromethane, into soluble hydrogen halide. The soluble gas can then be processed using existing solvent management recovery systems.

The final product specification requires a cost effective end product, capable of processing high gas throughput with low pressure drop. In order to achieve the latter it was necessary to develop the axial flow electrode geometry illustrated in figure 2.2B. Process gas flows of 1000 slm through a single reactor have been achieved in this way.

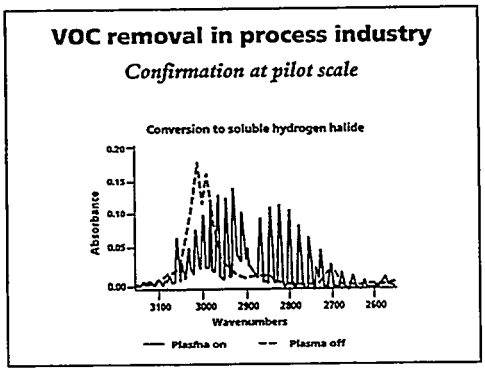


Figure 2.4 © AEA Technology plc

Final product design

To achieve efficient energy distribution at high gas flows electrode arrays were considered, utilising a single magnetron. However, the cost driver dictated the development of a close coupled magnetron assembly. Figure 2.5 illustrates the final patented product design, which meets the product specification.

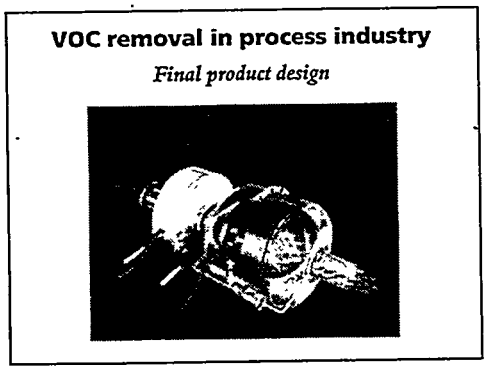


Figure 2.5 © AEA Technology plc

EMISSIONS CONTROL FOR IC ENGINES

Market specification

The third case study is surface discharge plasma technology applied to automotive exhaust aftertreatment. Health issues and public opinion are forcing legislators to introduce tighter emissions standards. The stringent legislation earmarked for the new millennium both in North America and Europe requires an effective, affordable solution in a single aftertreatment package to meet the specification set out in figure 3.1.

AEA Technology is addressing this requirement with the development of the ELECTROCAT™ Clean Emissions System, a patented plasma catalyst which has the capability of simultaneous

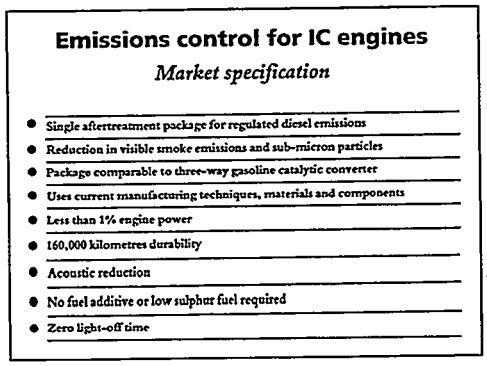


Figure 3.1 © AEA Technology plc

particulate removal and NO. reduction. Again, the demands for cost, durability and efficiency forced the downselection of the plasma generation technique, which in this case requires the production of the plasma without elaborate expensive power supplies.

Confirmation at lab scale

The original lab scale device is shown in figure 3.2. Early trials of this device were carried out at Southwest Research Institute (SwRI), processing diesel exhaust from Dodge and Toyota diesel pickup trucks. The glass-tube reactor used in these trials consisted of an A.C. voltage applied across ceramic packing material. The material can be modified to assist catalytic activity to further enhance the performance of the discharge reactor.

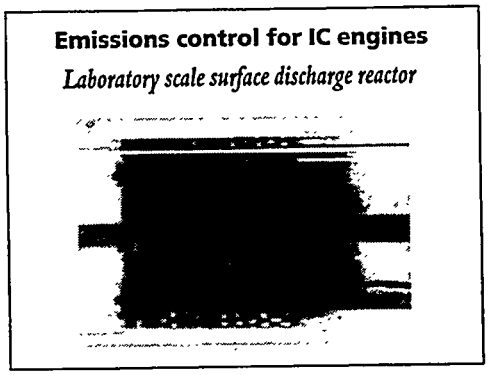


Figure 3.2 © AEA Technology plc

Figure 3.3 illustrates typical test data recorded at SwRI and confirms the simultaneous particulate removal and NOx reduction efficiencies (of up to 90% and 70% respectively) which were achieved with the lab scale device.

Full scale prototype

AEA Technology has continued to develop and

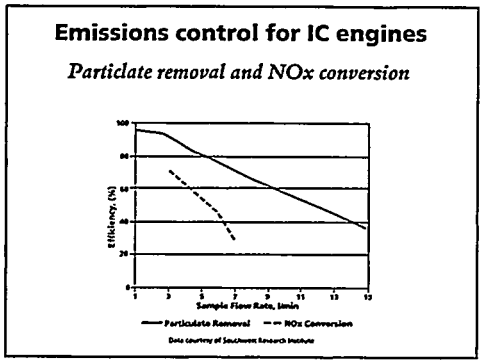


Figure 3.3 © AEA Technology plc

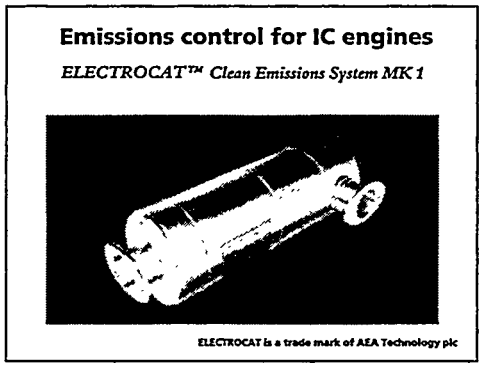


Figure 3.5 © AEA Technology plc

engineer the ELECTROCAT™ since these early trials, and has designed and manufactured full scale plasma reactor systems, the designs of which are proprietary and subject to patent filings. Testing of these prototypes has provided verification of the SwRI laboratory scale data at full scale. ELECTROCAT™'s performance data base has been extended to include European regulatory drive cycles (ESE+EDUC.) modified with Year 2000 test protocol, and confirmation of the removal of ultra-fine sub-micron particulate, as illustrated in Figure 3.4.

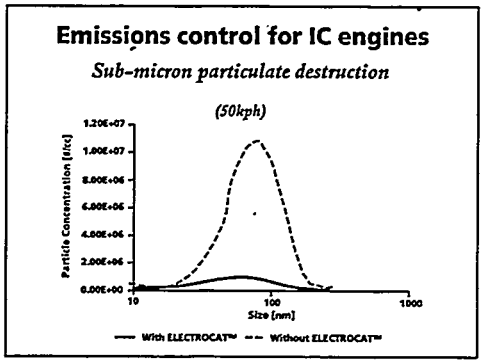


Figure 3.4 © AEA Technology plc

Final product design

Further development programmes and trials are now focused on production engineering the device to meet the market specification. Figure 3.5 illustrates one of the first engineered prototypes, which are scheduled to undergo tests in 1998.

Conclusion

An understanding of plasma technology and the final product requirements are fundamental to developing a successful product. No one plasma generation technique offers a universal panacea for emissions control, and, irrespective of what can be demonstrated in the laboratory, it is the applications engineering and system integration of the right plasma technology which will determine the successful product. By understanding and following these principles, a correctly engineered and integrated plasma technology can provide effective and commercially desirable solutions to meet a range of emissions targets.

Background Sources

1. Process Engineering, Miller House Publishing, London, March 1997.

2. The Engineer, Miller House Publishing, London, 13 March 1997.

3. Semiconductor International, Cahners International Publishing Company, October 1997.

4. Industrial Environmental Management, Faversham House Group, July 1997.

5. Shawcross, J. T., PhD thesis entitled *The Application of Non-thermal Plasmas to the After-treatment of Diesel Engine Exhaust*, September 1996, and references therein.

6. Penetrante B.M, Schultheis S.E., *Non-thermal plasma* techniques for pollution control, Springer-Verlag, 1993.

Acknowledgments and Thanks

The author wishes to thank Bob Fanick and Bruce Bykowski of the Southwest Research Institute, Texas. The author also thanks Dave Ray-

bone, Fiona Winterbottom, and all his colleagues involved in the development of plasma processing products at AEA Technology.

For further information about plasma processing at AEA Technology or enquiries about copyright and reproduction of any part of this paper, please write to Yvonne Zaslawska, Information Manager, Environmental Technologies, at AEA Technology plc, F4 Culham Science Centre, Abingdon, Oxfordshire OX14 3DB, United Kingdom or e-mail yvonne.zaslawska@aeat.co.uk

ELECTROCAT is a trade mark of AEA Technology
AEA Technology is the trading name of AEA Technology plc

SESSION IIIB

Aftertreatment - Non-Thermal Plasma

Chairman: John Garbak
U.S. Department of Energy

EFFICIENT, EFFECTIVE, NON-THERMAL PLASMA AFTERTREATMENT OF DIESEL NOx

M. Gundersen, V. Puchkarev, and G. Roth
University of Southern California

INTRODUCTION

Plasma processing for control of effluents from many different sources including diesel engines, incinerators, and power plants is currently receiving considerable attention because these approaches have potentially broad impact on the reduction of harmful gaseous pollutants. For example, the removal of nitrogen oxides (NO_x) is an important problem, and has led to rigid regulation on the level of NO_x emission[1]. E-beam, pulsed corona, surface and silent discharges have been implemented to study efficiency of NO_x removal in many experiments[2]. In this project we are studying underlying physics issues, and limitations to practical applications. We have obtained data showing that advanced pulsed modulator technology used in conjunction with pulsed plasma devices can be used to initiate favorable plasma chemistry to reduce emittants for a variety of these applications.

There are several issues that affect the practical application of pulsed plasma devices including: i) energy cost, ii) by-products emission, iii) pulsed power implementation, and iv) reactor design.

Energy costs that have been reported vary considerably - for example, in terms of energy cost per treated molecule from Å3 to 500 eV/molecule (this approach to calculating energy costs is discussed in ref. 2). To be competitive for remediation of diesel engine emission, the energy cost should be <10-20 eV per NO molecule for concentrations Å1000 ppm, which would correspond to an overall power consumption < 5% of the total engine power, although power requirements will depend on the application. Electron beam processing has been reported to have low energy cost following injection of highly energetic electrons requiring, however, a level of sophistication in implementation that is impractical at present for diesel exhaust treatment. Reactors based on corona and silent discharges have the advantages of relative simplicity, scalability, and lower capital cost than existing e-beam technology. Thus it is of interest to understand the physical mechanisms and practical limits to energy cost for this competing, simpler technology. Here we report evidence that plasma processing with a corona discharge can be applied to the problem of NO_x reduction with an energy cost previously considered attainable only by sophisticated electron beam methods.

APPROACH

The experimental apparatus reported here incorporated discharge chambers, pulsed power modulator, and gas manifold with controller gauges and emission analyzer. A number of reactors were studied; a typical pulsed corona reactor consisted of a cylindrical chamber length of 0.4 m and varying diameter inner electrode 2-34 mm and outer electrode 20-62 mm. It was possible to vary the current density and "active" plasma volume by varying the electrode surface area. The reactor cathode surface was typically threaded to ensure a high local electric field with increasing radius. The current density entering the plasma volume was estimated for a nominal cylinder surface 1 mm above the surface of central electrode. The term "active" plasma volume is used to mean the volume which is within this cylindrical surface (e.g. volume enclosing the maximum electric field).

A pulse generator supplied high voltage pulses with amplitude ²40 kV, pulse duration of 50-100 ns (rise time 20 ns), and repetition rate up to 1 kHz.

Pulses reflected from an unmatched load (the reactor and discharge) were absorbed in a matched pulse generator load. By monitoring voltage and current signals related to the discharge it was possible to determine the energy deposition into the gas. The total current contains both the discharge current and the current associated with charging the capacitance of the reactor. The product of the discharge current and voltage during the corona discharge yields the pulse energy, so that the displacement current is not included in the energy delivered to the gas (although it is included in the overall energy expended). This is an important effect at low current density because for short pulse conditions, which are important for this work, the displacement current is larger (typically 3-6 times) than the conduction current.

The power input into the discharge was varied as a function of pulse length, voltage amplitude and repetition rate. Two types of diesel engines were used: a) 60 kW (Volkswagen Rabbit), b) 300 kW Cummins. Typical data were obtained with the 60 kW engine operated at idle speed and NO emission concentrations of 100-130 ppm. Here the exhaust temperature was 40-50° C. We monitored the outlet gas composition using a NO analyzer (Bacharach, Nonoxor II). The 300 kW engine was operated under load with NO emission (600-1000) ppm. The exhaust temperature was varied from 85 to 180° C. A Horiba analyzer was used for emission monitoring. This system allowed detection of the following components: NO, NO2, HC, CO, CO2, SO2. The flow rate through the reactors was varied between 100 and 1500 standard liters per minute (flow velocity was from 1 to 10 m/s).

On varying discharge parameters (pulse width, voltage amplitude, frequency, pulse polarity) it was found that the energy cost changes considerably, and that short pulses (50 ns) are more advantageous in energy cost than longer pulses, in part because short pulses allow operation with a higher pulse voltage during the time of treatment of the effluent. We found that the energy cost for NO removal is affected by pulse polarity. The energy cost for positive corona (plus at the central electrode) is 1.5-2 times that for negative charging of the central electrode. This difference is even more pronounced at higher repetition rates over Å1000 Hz. This is because positive corona carry higher current at a given pulse voltage than negative, and current is found here to be a crucial parameter for determination of energy cost. Data hereafter refer to negative corona and a pulse duration of 50 ns.

ACCOMPLISHMENTS:

We performed experiments to compare the efficiency of pulsed corona discharges with and without a dielectric insert under otherwise identical experimental conditions, in order to compare barrier discharge efficiencies with corona discharges. Previous studies under this project had shown surface discharges to be less efficient. The voltage amplitude and the frequency were adjusted in such a way that these approaches could be compared for the same level of NO reduction. It was found that a dielectric insert results in higher current and current density. Reduction of NO is approximately equal, but energy cost with the dielectric insert is 2-3 times greater than for the discharge without dielectric. A high repetition rate regime is found to be advantageous for both cases. It was also found in our data that the energy cost decreases with increasing frequency. Energy cost lowering occurs basically due to the decrease of energy per pulse with increasing of repetition rate. To increase NO removal by increasing voltage and current results in a growth of energy cost. For example, almost the same NO removal -- 55 and 65 ppm -- can be obtained at 8 and 30 eV/molecule respectively; however, in the first case, the current Å15 A and the repetition rate is 1000 Hz, while in the latter case Å200 A, and f=300 Hz, with a voltage drop across the discharge Å15 kV in both experiments.

Plasma aftertreatment of diesel exhaust principally relies on the removal of nitrogen oxides (NO_x) and other hazardous components by highly reactive radicals produced in corona discharge by energetic electrons. During the high voltage short pulse, energetic electrons

and radicals are generated and subsequently initiate chemical reactions. For this, pulsed parameters (voltage amplitude and pulse width) must be optimized in accordance with the reactor design, and it is observed that these depend in subtle ways on small variations in design. Short pulse excitation is followed by a post-pulse period which lasts from 10s of microseconds to 100s of ms or longer.[4] During this time various remediation and oxidation reactions occur, which are as yet not well characterized, although calculated optimal time intervals for post-pulse chemical reactions are Å1 ms.

The chemical reactions occur mainly in the gas phase, but the plasma composition and characteristics can be affected by heterogeneous reac-tions of ions, electrons, and radicals. These reac-tions can considerably decrease the energy cost. For example, the lowest energy cost of several eV per molecule has been measured using e-beam for SO_2 decomposition[5,6]. The authors found that the energy consumption is affected by pulse durations and current density[6], decreasing with decreasing current density. Further, Deminskii et. al. dis- cussed the kinetics of a heterogeneous oxidation process which involves chemical reactions between gas and aerosol particles with consider-ation of dissolved components, transfer processes in gas and the dynamics of the formation and decay of aerosol particles. They found good agree-ment with experimental data and predicted even less energy cost ~0.3 eV/molecule. In this work we attempted to study the relation between cur-rent density and energy cost for corona discharge-based reactors. The energy cost of NO removal by pulsed corona discharge is also driven by current density similar to e-beam processing of SO_2. A reactor with a dielectric insert exhibits however much higher energy cost. We had anticipated increased NO reduction with low energy cost be-cause this reactor had a large plasma volume and large area cathode: the ratio of inner-to-outer elec-trode diameter was 0.58 (34 - 58 mm). Here the dielectric barrier was supposed to prevent arcing. Despite that we found that the discharge trends to contract into bright filaments at high repetition rates. One should note that a homogeneous plas-ma is a major problem for the use of a corona discharge. Due to a strong nonlinear dependence of field emission on the local electric field the number of starting streamers is an extremely sensitive function of electric field and cathode micro geometry, which is hard to control. It may be that at high currents, the current is carried by a finite number of filaments, rather than equally distributed over the cathode surface. The high repetition rate and flow appears to help smoothing the current irregularities. This result is still the subject of further study.

In a pulsed corona discharge NO is partly converted into NO_2. The production of NO_2 was found to vary with current density, and be minimal at a low current density ~0.2 A/cm^2, correspond-ing also to energy efficient operation of the reactor. It was found that NO_2 production drops with decreasing of current: at current density 2 A/cm^2 the ratio of NO_x reduction to NO_2 production NO_x/ NO_2 =1.2, and at current density 0.2 A/cm NO_x/ NO_2 =1.4.

Chemistry in heterogeneous media may also have beneficial effects. It was found that there is a higher energy cost for hot exhaust - 180° C, above the vaporization temperature for water, corre-sponding to elimination of droplets. A similar result was previously re-ported.

Energy cost measurements of NO removal from diesel exhaust with a pulsed corona discharge have been experimentally studied. After optimiza-tion of pulsed parameters (polarity, pulse width) we found that the energy cost is driven by current decreasing with corresponding current density de-crease. Best efficiency (< 10 eV/mol) is obtained at current density <0.2 A/cm^2 and repetition rate (~1 kHz). With increasing current density (energy deposition into gas) the removal efficiency decreases. Our results indicate that a pulsed coro-na discharge provides effective NO remediation with energy cost comparable to e-beam proces-sing. The cost effective

regime was realized, however, at low NO concentration (100 ppm), and it was seen that the spatial and temporal charac-teristics of streamer discharge impose limitations on the removal efficiency at high NO concentration so that reactor design is an important consider-ation

CONCLUSION

Efficient reduction of NO emission with a transient, non-equilibrium plasma created by pulsed corona discharge was shown to be energy efficient. The transient plasma (Å50 ns) is found to reduce NO emission by 50% in a flow of 2-25 liters/second with energy cost Å10-20 eV/molecule, corresponding to a fraction of source power of As %. The efficiency of NO_x reduction is a complex function of parameters that include pulse width, pulse polarity, current density, repetition rate, and reactor design. It was found that best efficiencies are correlated with a low current density (0.2A/-cm^2) and high repetition rate (1 kHz) under high flow rate. Careful optimization of all these parameters is required to reach cost effective NO_x reduction.

REFERENCES

1. Experiments with 300 kW engine and emission analysis were performed under the direction of D. Walker at the Diesel Technology Laboratory, Golden West College, Huntington Beach, CA.

2. A. C. Gentile and M. J. Kushner, J. Appl. Phys, 78, 2074, (1995).

3. D L Kuzuetsov, G.A.Mesyats and Yu. N. Novoselov, Tech. Phys. Lett. 20, 269, (1994).

4. A. Deminskii, B.V. Potapkin, V. D. Rusanov, and A. A. Fridman, High Energy Chemistry 28, 304, (1994)

5. E. M. van Veldhuizen, W. R. Rutgers, and V. A. Bityurin, Plasma Chemistry and Plasma Processing 16, 227, (1996).

6. M. Gundersen, V. Puchkarev, I Yampolsky, US Patent #5 603 893 (1997).

DIRECT CHEMICAL REDUCTION OF NOx IN DIESEL EHAUST USING NONTHERMAL PLASMAS AND GAS JET INJECTION

S. Bittenson and F. Becker
Thermo Power Corporation

BACKGROUND

The control of NO_x in diesel engines is of increasing concern as regulatory restrictions on emissions continue to tighten. Conventional catalytic materials are unsuitable for diesel NO_x aftertreatment due to limitations associated with combustion stoichiometry, particulate contamination, and exhaust temperature control. Nonthermal plasma technology is widely considered to have the potential to control NO_x in combustion exhaust without these restrictions, by electrically inducing the thermodynamically unstable NO_x species to decompose into nitrogen and oxygen. The principal chemical mechanism targeted for this process is the reaction of exhaust nitric oxide (NO) with ground state atomic nitrogen, reaction (1). The atomic nitrogen reactant is generated by dissociative collisions of electrons in the nonthermal plasma with molecular nitrogen, the majority chemical species in exhaust.

$$N + NO \rightarrow N_2 + O \qquad (1)$$

Many researchers worldwide have been working toward this end, but a practical diesel NO_x reduction system has yet to be introduced. The principal technological issue working against the success of nonthermal plasmas for NO_x chemical reduction has been that the electric discharges that generate atomic nitrogen for chemical reduction of NO_x also generate atomic oxygen and hydroxyl, which drive chemical processes to oxidize NO_x.

The cross section for dissociating molecular nitrogen in a nonthermal plasma discharge is lower than that for oxygen at typical electron collision energies of ~4.5 eV (dissociation energy 9.7 eV for N_2 compared with 5.2 eV for O_2). In addition to the resulting prevalence of oxidizing species in the discharge, nearly gas kinetic rates of some of the subsequent gas phase oxidation reactions results in the overall chemistry being dominated by NO oxidation to nitrogen dioxide (NO_2) and nitric acid (HNO_3). This chemical outcome is unacceptable for diesel engine NO_x removal.

In addition to the chemical problems described above, most nonthermal plasma devices are subject to serious performance problems when operated in the harsh environment of diesel exhaust. Any commercially viable NO_x reduction technology for mobile diesel engines must tolerate regular exposure to particulates (soot) and water condensation. It must also operate over a wide range of oxygen concentrations, exhaust flow velocities, and temperatures from near ambient up to several hundred degrees Celsius. Meeting these environ-mental operating requirements has been found by many researchers to be as much of a challenge as establishing the appro-priate chemical processes for chemical reduction.

Recent efforts have been made to develop two-step processes which first oxidize NO to NO_2, followed by catalytic reduction of NO_2 to nitrogen and oxygen,[1] but even if such processes succeed chemically, other less positive aspects of catalytic exhaust treatment technology will likely carry forward with the new approach.

NITROGEN JET INJECTION

Since 1989, Thermo Power has demonstrated ever more efficient and reliable technology for generating homogeneously volume-filling nonthermal plasmas for combustion gas treatment, culminating in the engineering of its barrier-discharge based *TecoLytic*[2] nonthermal plasma technology for utility-scale oxidative NO_x

removal. It became clear during this development work that the direct plasma treatment approach would not be commercially viable for the chemical reduction of NO_x particularly in the diesel exhaust environment discussed above. The principal factors contributing to this conclusion were:

1. Non-selective reactant generation
Relatively inefficient production by the discharge of atomic nitrogen compared with oxidizing species.

2. Kinetic competition
Very fast oxidative kinetics dominate over reductive chemical paths. Even if the electron energy distribution in the discharge could be skewed to higher energies to favor nitrogen dissociation, many oxidative reactions are faster than the reductive analogs.

3. Variable operating conditions
Nonthermal plasma discharge properties are dependent on gas composition, humidity and temperature.

4. Fouling
Dielectric barrier electrodes immersed in sooty exhaust are readily fouled by the deposition of a conductive surface layer.

Thermo Power addresses all of these technical problems with its *TecoJet* approach by generating atomic nitrogen external to the exhaust stream, followed by rapid injection and mixing to achieve chemical NO_x reduction.

The persistent yellow-orange glow of "active nitrogen" has been recognized for decades to be emission from electronically excited molecular nitrogen which has only slowly recombined from atomic nitrogen generated in a low-pressure electric discharge.[3] Of particular interest to gas-phase chemists is active nitrogen's extreme reactivity with other chemical species despite multi-second stability in isolation.

Although most work with active nitrogen in the past was done in vacuum vessels, the property of relatively long recombination time coexisting with very high reactivity continues to hold true at higher pressures. Atomic nitrogen recombines to form N_2 on the timescale of a few milliseconds at atmospheric pressure, but the reaction of atomic nitrogen with NO is one to two orders of magnitude faster than recombination, so external generation of atomic nitrogen followed by rapid mixing with exhaust gas can yield useful quantities of chemical reduction.

To deliver atomic nitrogen rapidly and efficiently, the dissociating discharge is located immediately adjacent, but not directly exposed to the exhaust stream. Isolation of the discharge from the exhaust eliminates the direct dissociation of oxygen and other exhaust gases, and practical delivery times on the order of 10-50 μs followed by turbulent mixing in the exhaust stream largely preserves the nascent atomic nitrogen concentration for NO_x reduction. We have observed the characteristic light emission from nitrogen recombination to extend as far as 7 cm beyond a 1 mm diameter jet orifice in a laminar treatment stream containing no NO. The physical extent of the light emission in such a stream is reduced dramatically by the addition of NO. Optimum mixing for diesel NO_x treatment is achieved by using multiple jets injected into a turbulent exhaust stream. The jet injectors themselves need not physically penetrate into the exhaust channel, facilitating the design of NO_x reactors with unobstructed exhaust flow and very small pressure drops.

The *TecoJet* approach specifically addresses each of the concerns listed above for nonthermal plasma techniques:

1. Selectivity in reactant generation
The use of nitrogen jets to generate atomic nitrogen eliminates issues regarding the relative efficiency of nitrogen and oxygen dissociation.

2. Reduced kinetic competition
With nitrogen as the only molecular species dissociated in the discharge, chemical reduction of NO by atomic nitrogen can dominate the chemistry. The relatively small quantity of atomic oxygen produced by

reaction (1) does not contribute significantly to oxidation of NO. Measurements in diesel fuel combustion exhaust have demonstrated >80% of the chemical reaction achieved going to chemical reduction of NO_x. Our measurements of the action of conventional nonthermal plasma methods to treat diesel exhaust yield no significant chemical reduction: nitrogen dioxide and nitric acid are the principal products.

3. Stable operating conditions

The *TecoJet* discharge external to the exhaust stream is not affected by the chemical composition of the stream. Discharge properties are no longer dependent on gas composition, humidity or exhaust temperature.

4. Non-fouling electrodes

The discharge electrodes are isolated from the exhaust stream, making them inherently non-fouling. *TecoJet* reactors operate successfully in wet and sooty environments.

FACILITY

Initial laboratory tests of *TecoJet* were performed using a diesel fuel fired combustor. to provide an exhaust stream of up to 60 scfm. Exhaust from the combustor could be diverted through a heat exchanger to control the working temperature at the *TecoJet* reactor, which was comprised of up to 24 indiviually adjustable jets. Firgure 1 shows an operating 18 jet *TecoJet reactor*. NO could be added to the exhaust stream to extend the test range to high NO_x conditions (typically 60-600 ppmv NO). Exhaust gas composition was monitored at locations before and after the *TecoJet* reactor. Particular attention was paid to measuring nitric acid and nitrogen dioxide formation relative to chemical reduction of NO. Additional analytical capabilities included measure-Mert of oxygen, carbon dioxide, carbon monoxide, total hydrocarbons, and sulfur dioxide.

DISCUSSION

Modeling of the nitrogen jet injection technique for NO_x reduction suggests ultimate attainable overall efficiencies (parasitic power) on the

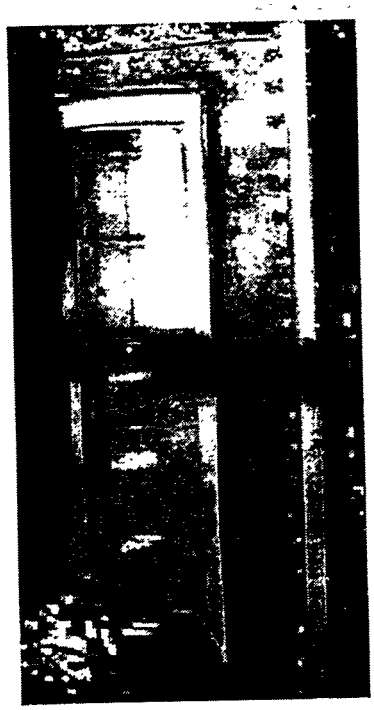


Figure 1. 18-jet *TecoJet* reactor with observation window

order of 1.2% of the output of the engine for each g/bhp-h of NO_x removed. This includes power required to separate nitrogen from air or exhaust gas. Work has begun to evaluate practical tradeoffs among nitrogen preparation methods, purity, and the efficiency of the chemical reduction process.

While external production of atomic nitrogen for NO_x chemical reduction with *TecoJet* dramatically reduces competition from most NO_x oxidation processes, some kinetic competition with reaction (1) remains at high temperatures and high exhaust oxygen concentrations from the reaction of atomic nitrogen with exhaust oxygen, reaction (2).

$$N + O_2 \rightarrow NO + O \qquad (2)$$

Temperature dependent competition between these reactions arises because the rate of reaction (1) varies only slightly with temperature (very low activation energy) while that of reaction (2) increases with temperature (activation energy approximately 7 kcal/mole #). To date, Thermo Power has measured chemical reduction of NO in diesel fuel combustion exhaust at temperatures up to approximately

210°C, and work is in progress to extend these measurements toward an estimated practical limit of 500-600°C.

SUMMARY

TecoJet is the first nonthermal plasma method to achieve practical quantities of chemical reduction of NO_x in diesel exhaust. It achieves this by isolating the plasma from the exhaust stream while maintaining the chemical activity of discharge-generated free radicals. *TecoJet* is inherently non-fouling and has been demonstrated to operate in wet and sooty exhaust. Further qualification of the process is in progress, to validate the performance and economics for mobile diesel engines.

---

1. [1]B. Penetrante, "Plasma-Assisted Heterogeneous Catalysis for No_x Reduction in Lean-Burn Engine Exhausts," Proceedings of the 1997 Diesel Engine Emissions Reduction Workshop, July 27-31-1997.

2. T. Orlando, "Vehicle Exhaust Treatment Using Electrical Discharge and Materials Chemistry," Proceedings of the 1997 Diesel Engine Emissions Reduction Workshop, July 27-31-1997.

3. [2]R.W. Breault, C.R. McClarnon, F.E. Becker, "Coronal-Catalytic Apparatus and Method for No_x Reduction," U.S. Patent #5,458,748, 1995.

4. [3]Discussed in many spectroscopic and chemistry texts, e.g., F.A. Cotton and G.W. Wilkinson, Advanced Inorganic Chemistry, John Wiley & Sons, 1966.

5. [4]F. Westley, D.H. Frizzell, J.T. Herron, R.F. Hampson, and W.G. Mallard, Editors, "NIST Chemical Kinetics Database," U.S. Department of Commerce, 1994.

MULTI-STAGE SELECTIVE CATALYTIC REDUCTION OF NO_x IN LEAN BURN ENGINE EXHAUST

B.M. Penetrante, M.C. Hsaio, B.T. Merritt, and G.E. Vogtlin
Lawrence Livermore National Laboratory

INTRODUCTION

Many studies suggest that the conversion of NO to NO_2 is an important intermediate step in the selective catalytic reduction (SCR) of NO_x to N_2 [1 -5]. Some effort has been devoted to separating the oxidative and reductive functions of the catalyst in a multi-stage system [6]. This method works fine for systems that require hydrocarbon addition. The hydrocarbon has to be injected between the NO oxidation catalyst and the NO_2 reduction catalyst, as shown in Figure 1; otherwise, the first-stage oxidation catalyst will also oxidize the hydro-carbon and decrease its effectiveness as a reductant. The multi-stage catalytic scheme is appropriate for diesel engine exhausts since they contain insufficient hydrocarbons for SCR, and the hydrocarbons can be added at the desired location. For lean-burn gasoline engine exhausts, the hydrocarbons already present in the exhausts will make it necessary to find an oxidation catalyst that can oxidize NO to NO_2 but not oxidize the hydrocarbon.

A plasma can also be used to oxidize NO to NO_2 Plasma oxidation has several advantages over catalytic oxidation. Plasma-assisted catalysis work can well for both diesel engine and lean-burn gasoline engine exhausts. This is because the plasma can oxidize NO in the presence of hydrocarbons without degrading the effectiveness of the hydrocarbon as a reductant for SCR. In the plasma, the hydrocarbon enhances the oxidation of NO, minimizes the electrical energy requirement, and prevents the oxidation Of SO_2-

This paper discusses the use of multi-stage systems for selective catalytic reduction of NO_x. The multi-stage catalytic scheme is compared to the plasma-assisted catalytic scheme.

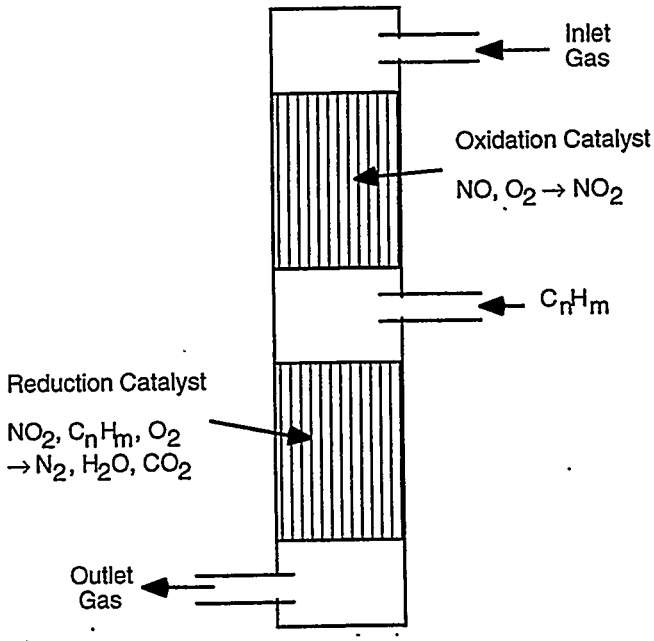


Figure 1. Multi-stage SCR scheme using an oxidation catalyst to convert NO to NO_2 and then a reduction catalyst to convert NO_2 to N_2.

MULTI-STAGE CATALYTIC SCHEME

The multi-stage selective catalytic reduction of NO_x is accomplished in two steps. First, an oxidation catalyst converts NO to NO_2 in the absence of a hydrocarbon:

oxidation catalyst+NO+$O_2 \rightarrow NO_2$

Then, a reduction catalyst reduces NO_2 to N_2 by selective reduction using hydrocarbons:

reduction catalyst+NO_2 +HC $\rightarrow$ N_2+CO_2+H_2O-

Multi-stage SCR has several advantages over conventional SCR. First, the multi-stage scheme offers high NO_x reduction efficiency from catalysts that, separately, are not very active for reduction of NO. Second, the multi-stage scheme alleviates the problem of

selectivity between NO reduction and hydrocarbon oxidation. The important NO_2 intermediate is formed without consuming the hydrocarbon reductant.

Figure 2 shows the FTIR spectra of the process for a model exhaust gas consisting of 500 ppm NO, 10% O_2 and balance N_2. The first-stage oxidation catalyst is Pt-based. The second-stage catalyst is essentially the same material but without the Pt. The hydrocarbon, 500 ppm (C_3) propene, is injected between the oxidation catalyst and the reduction catalyst. The temperature of both catalysts is 3000C.

The spectrum of the inlet gas is shown in the top box ("inlet") of Figure 2. Without the oxidation catalyst (i.e., first stage is removed), the NO_x reduction efficiency is very low, as shown in the second box ("outlet without oxidation catalyst"). The NO_x reduction at this temperature is very low even in the presence of a hydrocarbon reductant.

When the gas stream is first passed through the oxidation catalyst, the NO is oxidized to NO_2, as shown in the third box ("after first catalyst"). The NO_x reduction is still very low. The same amount of total NO_x ($NO + NO_2$) is left in the gas stream.

When the NO_2-containing gas stream from the first catalyst is mixed with the hydrocarbon reductant and then passed through the second catalyst, both the NO_x and the hydrocarbons are eliminated, as shown in the bottom box ("after second catalyst"). The NO_2 is chemically reduced to N_2 on the second catalyst.

PLASMA-ASSISTED CATALYTIC SCHEME

The oxidation of NO to NO_2 can also be accomplished with a plasma. The chemistry behind the plasma oxidation of NO is presented in an accompanying paper in this proceedings [7].

This section will present the advantages of plasma oxidation over catalytic oxidation.

The multi-stage catalytic scheme requires the injection of hydrocarbon between the NO

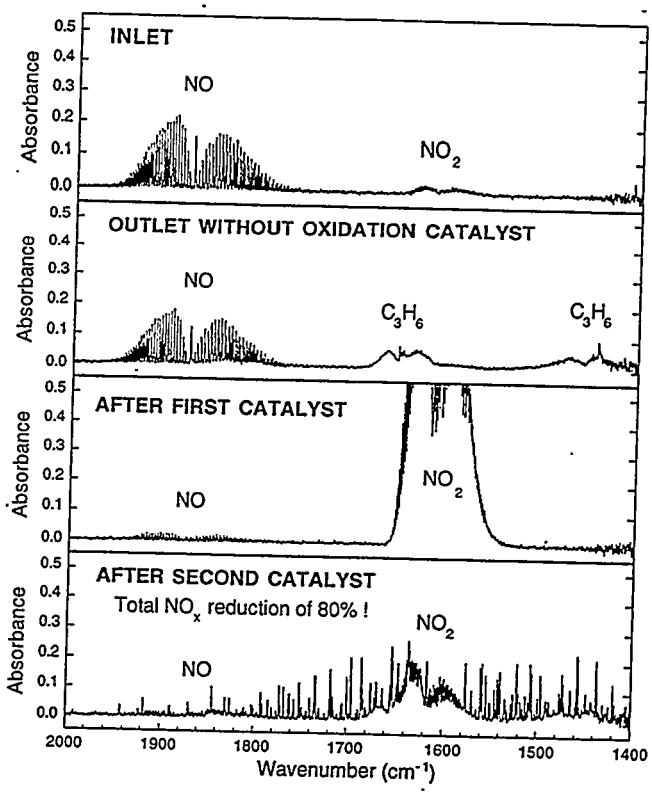


Figure 2. FTIR spectra showing the multi-stage selective catalytic reduction of No_x

oxidation catalyst and the NO_2 reduction catalyst. This is necessary because the oxidation catalyst will also oxidize the hydrocarbon and decrease its effectiveness as a reductant. The plasma can oxidize NO in the presence of hydrocarbons without degrading the effectiveness of the hydrocarbon as a reductant for SCR. Plasma assisted catalysis therefore works well for both diesel engine and lean-burn gasoline engine exhausts. The hydrocarbon in the plasma is actually beneficial. In the plasma, the hydrocarbon enhances the oxidation of NO, minimizes the electrical energy requirement of the plasma reactor, and prevents the oxidation of SO_2. During the oxidation of NO to NO_2, the plasma oxidizes a fraction of the hydrocarbons, but leaves partially oxygenated hydrocarbon products that are as least as effective as the original hydrocarbons.

Catalytic oxidation has a limited temperature operating range. Figure 3 shows the efficiency for oxidation of NO to NO_2 by a Pt-based catalyst in a model exhaust gas consisting of 500 ppm NO, 10% O_2, and balance N_2. The

oxidation efficiency maximizes at 2500C. The efficiency drops substantially at temperatures below 2000C. The efficiency also drops substantially at temperatures above 4000C. It is therefore important to match the temperature operating condition of the oxidation catalyst with that of the reduction catalyst.

Plasma oxidation of NO in the presence of hydrocarbons can have high efficiency over a wide range of temperatures. Figure 4 shows the efficiency for plasma oxidation of NO to N O_2 in a model exhaust gas consisting of 500 ppm NO, 1000 PPm (C_3) propene, 10% O_2 and balance N_2.

CONCLUSIONS

Multi-stage SCR offers high NO_x reduction efficiency from catalysts that, separately, are not very active for reduction of NO, and alleviates the problem of selectivity between NO reduction and hydrocarbon oxidation. In multi-stage SCR, either an oxidation catalyst or a plasma can be used to convert NO to NO_2, followed by a reduction catalyst to convert NO_2 to N_2. The use of a plasma for the oxidation of NO offers several advantages over catalytic oxidation. The plasma method works well for both diesel engine and lean burn gasoline engine exhausts. The plasma can oxidize NO in the presence of hydrocarbons without degrading the effectiveness of the hydrocarbon as a reductant for SCR.

ACKNOWLEDGMENTS

This work was performed at Lawrence Livermore National Laboratory under the auspices of the U.S. Department of Energy under Contract Number W-7405-ENG-48, with support from the Chemical Sciences Division of the Office of Basic Energy Sciences, and a Cooperative Research and Development Agreement with Cummins Engine Company.

REFERENCES

1. Shelef, M., Montreuil, C.N., and Jen, H.W., *Catalysis Letters* 26 (1994) 277.

2. Bethke, K..A., Li, C., Kung, M.C., Yang, B., et al., *Catalysis Letters* 31 (1995) 287.

3. Yokoyama C., and Misono, M., *Journal of Catalysis* 150 (1994) 9.

4. Lukyanov, D.B., Sill, G., Ditri, J.L., and Hall, W.K., *Journal of Catalysis* 153 (1995) 265.

5. Beutel, T., Adelman, B.J., Lei, G.D., and Sachtler, W.M.H., *Catalysis Letters* 32 (1995) 83.

6. Iwamoto, M., Hernandez, A.M., and Zengyo, T., Chemical Communications Jan 7 (1997) 37.

7. Penetrante, B.M., et al., "Effect of Hydrocarbons on Plasma Treatment of NO_x", Proceedings of the 1997 Diesel Engine Emissions Reduction Workshop.

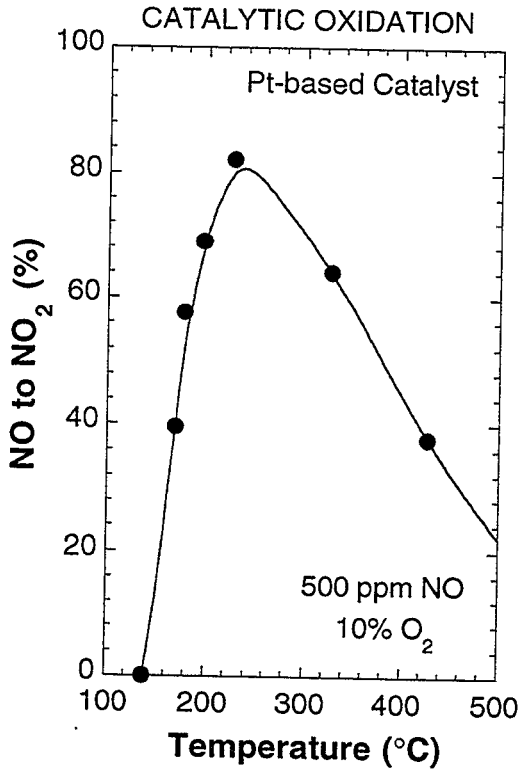


Figure 3. NO to NO_2 oxidation efficiency of a Pt-based catalyst for a model exhaust gas.

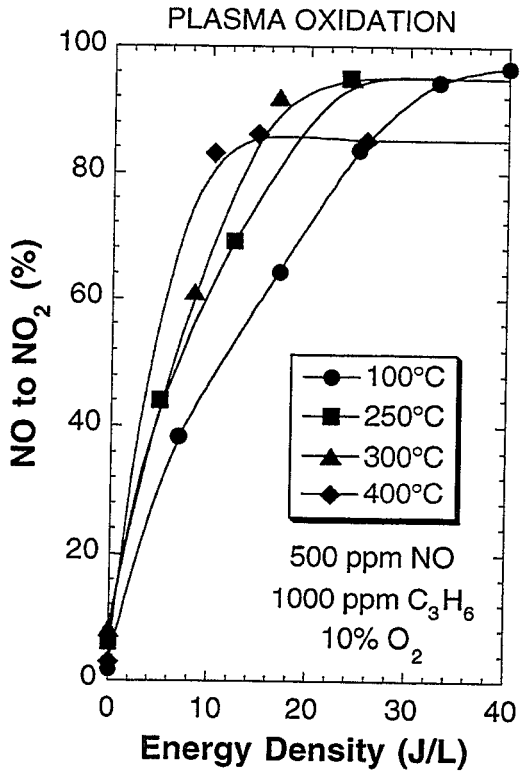


Figure 4. Effect of temperature and input electrical energy density on the efficiency for plasma oxidation of NO to NO_2 in a model exhaust gas.

APPLICATION OF ADVANCED THERMOELECTRIC TECHNOLOGY TO THE DIESEL GENERATOR

J.C. Bass, N.B. Elsner, and S. Ghamaty
Hi-Z Technology, Inc.

The auxiliary power requirements for heavy-duty trucks continue to increase. This will be particularly true when the power required to operate systems to reduce NO_x and particulates are introduced. If something is not done to reduce the engine auxiliary power load, these cleanup systems could essentially double the auxiliary power requirements which will result in a significant increase fuel consumption.

Hi-Z has been working for several years to develop a system that can reuse the waste energy available in the engine's exhaust to provide the auxiliary power for the truck[1]. The system we are currently testing is shown in Figure 1 mounted on a class 8 truck in place of the muffler. This generator uses thermoelectric modules made of bismuth-telluride to convert the exhaust heat directly to 1kW of electricity with an efficiency of about 5%. A study of replacing the alternator with a 1kW thermoelectric generator completed in 1992[2] showed that while the projected cost at the 1kW thermoelectric generator is more than a comparable alternator, the break even time for a class eight truck using such a system should be about two years in the United States and about eight months overseas.

This study only considered replacing the alternator. However, there are gains in fuel economy to be made if some of the other engine driven auxiliaries can be replaced by electric driven components whose power is derived from waste heat rather than from the engine shaft. These auxiliary devices could include the fan, power steering, power brakes, air compressor, NO_x and particulate cleanup systems, and possibly air conditioning.

Figure 2 is an energy diagram for a typical present-day (96) Diesel engine. Figure 3

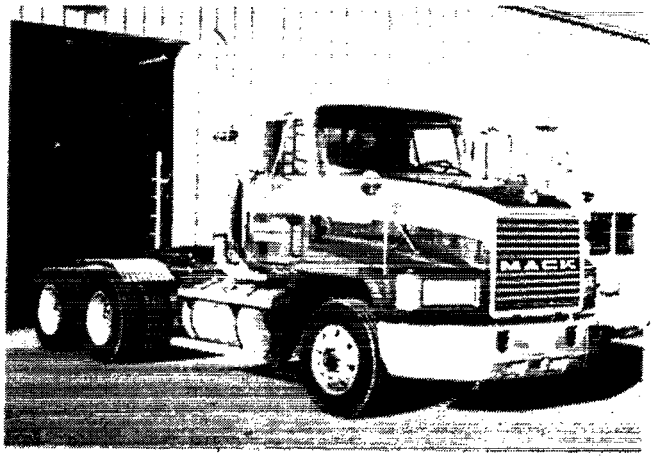


Figure 1: 1kW Thermoelectric Generator Installed on a Class 8 Truck

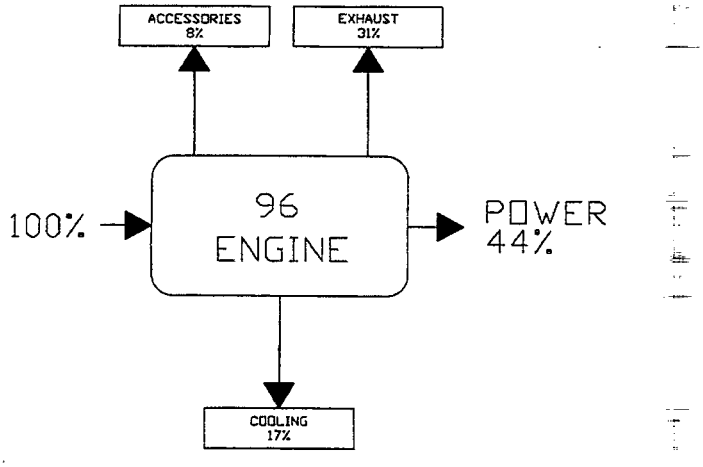


Figure 2: Energy Diagram for 96 Diesel Engine

shows the same engine with a 5% efficient thermoelectric generator. One sees that the efficiency of the engine is increased almost two percentage points or 4.4% using the thermoelectric generator.

One has two choices to reduce the breakeven times. The first is to reduce the cost of the

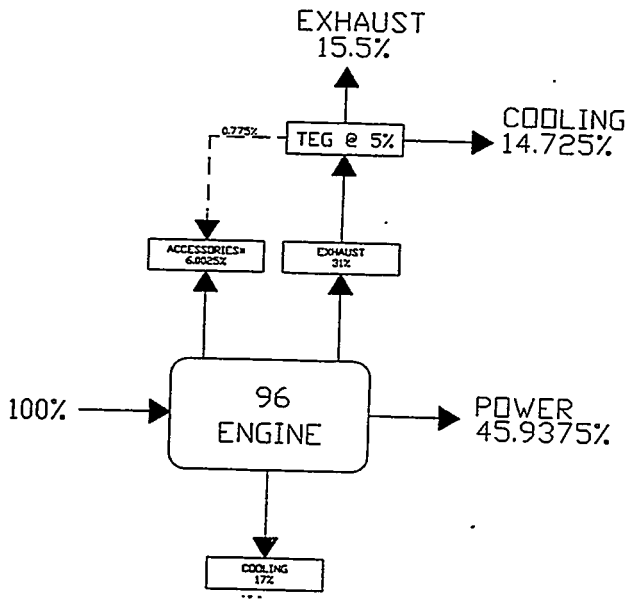


Figure 3: Energy Diagram for 96 Engine with 5% Thermoelectric Generator

generator components and the second is to increase the system conversion efficiency.

Reducing component cost is difficult to do by itself. It can be more easily achieved, however, when the conversion efficiency is increased because one needs to transfer and convert less energy to provide the same output power. This results in fewer, smaller, and, therefore, cheaper components being required which should result in a lower cost and, therefore, a shorter breakeven time.

Hi-Z is approaching the problem of increasing system efficiency in two ways. The first is a near term program which should bear fruit within the next few months and the second is a long term program which may require several years to complete.

NEAR TERM

The Jet Propulsion Laboratory in Pasadena recently announced[3] the development of zinc-antimonide (βZn_4Sb_3). The figure of merit (Z) for several conventional P-type thermoelectric materials including zinc-antimonide are shown as a function of temperature in Figure 4. One can see that the Z for zinc-antimonide is higher than that for bismuth telluride above about 125°C. Since the energy conversion is proportional to the area under the ZT curve, the use of a P-type thermoelectric element made of a combination of bismuth-telluride on the cold end and zinc-antimonide on the hot end holds promise for a higher, greater conversion efficiency than using P-type bismuth-telluride alone in the 250 to 300° C range.

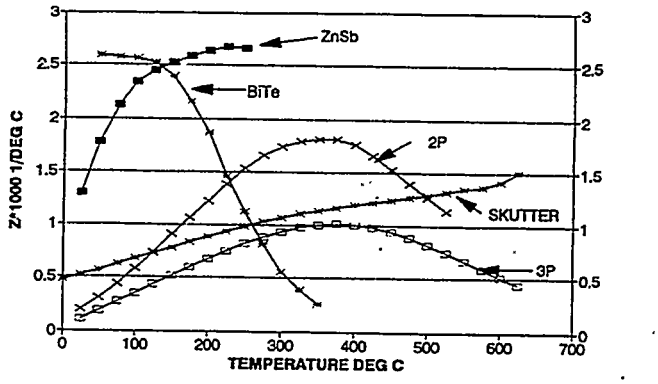


Figure 4: Figure of Merit Vs. Temperature for Several Thermoelectric Methods

Hi-Z and JPL are currently working on a program funded by DARPA to segment P-type zinc-antimonide and P-type bismuth-telluride to optimize the system conversion efficiency. If this program is successful, the module conversion efficiency will increase from 5% to about 7% which represents a 40% increase.

Figure 5 is an energy diagram for a conventional (96) engine with a 7% efficient thermoelectric generator showing where the energy goes in percentages. In this case the engine efficiency is increased by 2.7 percentage points or 6.16%.

LONG TERM

Hi-Z has been developing multilayer quantum well (MLQW) thermoelectrics for several years. These materials consist of very thin (100Å) alternating layers of materials with two different electron band gaps. When properly fabricated, the resulting material has very much improved thermoelectric properties compared to the same basic material made by conventional bulk methods.

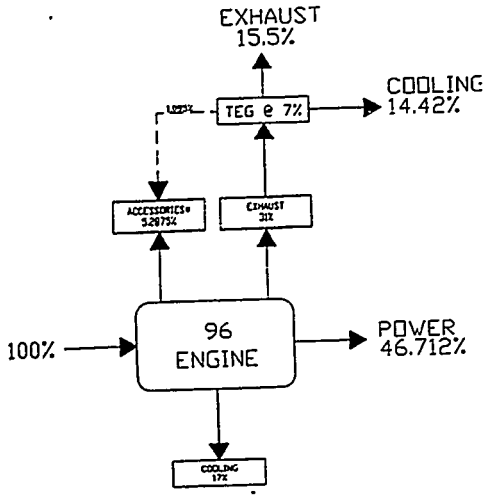


Figure 5: Energy Diagram for 96 Engine with 7% Thermoelectric Generator

Two types of MLQW systems have been discovered to date and both are now being developed under contracts to DoE. These systems are the silicon-germanium MLQW[4] and the boron carbon MLQW[5]. The silicon-germanium MLQW data indicate they will be used for cooling applications while boron carbon MLQW indicate they are good for power production. The boron carbon MLQW will be discussed first.

One of the problems that remain to be solved with the boron-carbon MLQW is that it can only be made as a P-type material. We are currently investigating other materials systems to see if we can develop an N-type MLQW material with high temperature capability similar to that of the boron-carbon MLQW.

A conventional N-type bulk alloy such as bismuth-telluride can be used with the P-type boron-carbon MLQW materials to form the required couples. This will not result in conversion efficiencies as high as a system which uses both N- and P-type MLQW, however, the theoretical conversion efficiencies are still significantly higher than those provided by a system which uses only conventional bulk alloys. The current estimate is that a thermoelectric conversion system which uses a boron-carbon MLQW for the P legs and conventional bismuth-telluride for the N leg will have a conversion efficiency of about 20%.

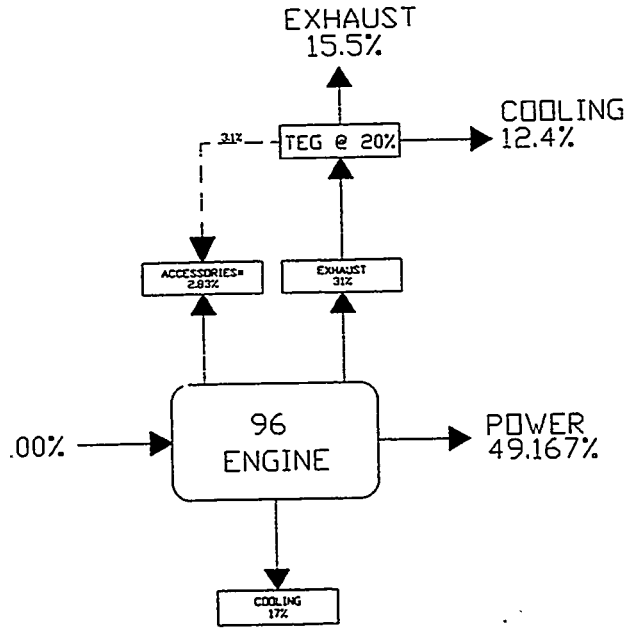


Figure 6: Energy Diagram of 96 Engine with 20% Thermoelectric Generator

The energy balance diagram shown in Figure 6 is for a present day (96) engine and a thermoelectric generator with a 20% energy conversion efficiency which can be achieved using the MLQW technology. In this case the overall energy efficiency is improved by a little over 5 percentage points or 11.1% compared to the standard engine.

Figure 7 shows the energy diagram for a conventional LE 55 engine. Since there is less energy content in the exhaust of the LE 55 than the present day (96) engine, less energy is available for conversion. However, the inclusion of a thermoelectric generator with 20% efficiency would still improve the efficiency of the LE 55 by over 3 percentage points or 6%, as shown in Figure 8.

It appears possible that the conversion efficiency of a MLQW device could be as high as 40% if a high temperature N-type material can be identified. If that does happen, then the energy balance for the LE 55 with an advanced thermoelectric generator could be as shown in Figure 9. This energy balance shows a potential efficiency improvement of almost 8.5 percentage points or 15.4% over the LE 55's nominal 55 percent efficiency.

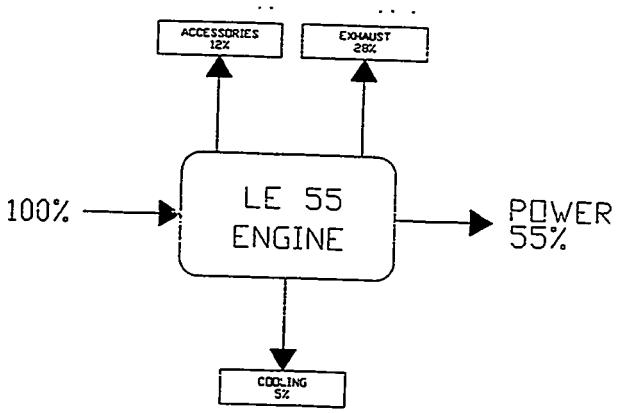


Figure 7: Energy Diagram of LE 55 Engine

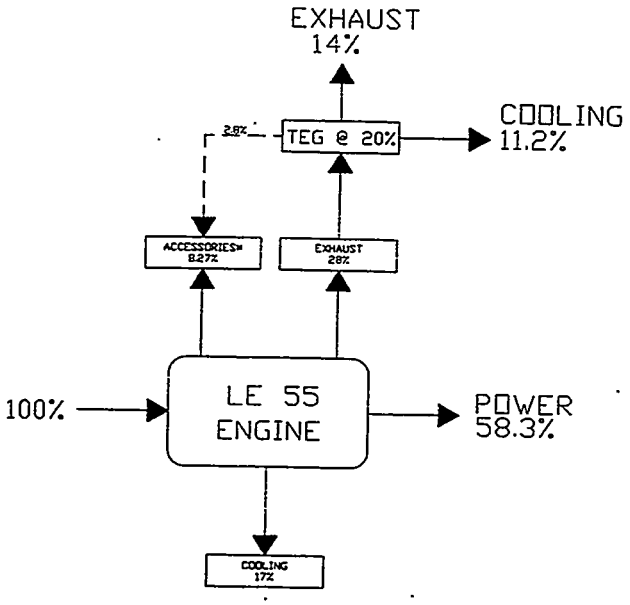


Figure 8: Energy Diagram of LE 55 Engine with 20% Thermoelectric Generator

CONCLUSION

The overall engine efficiency of large Diesel engines can be improved by adding a thermoelectric generator to convert some of the energy available in the exhaust to useful electric energy. The overall percentage improvements which can be expected from current materials is low. However, new materials are being developed which can lead to significant improvements in overall engine efficiency over the next several years. Some of these materials will be available within a few months while more advanced materials

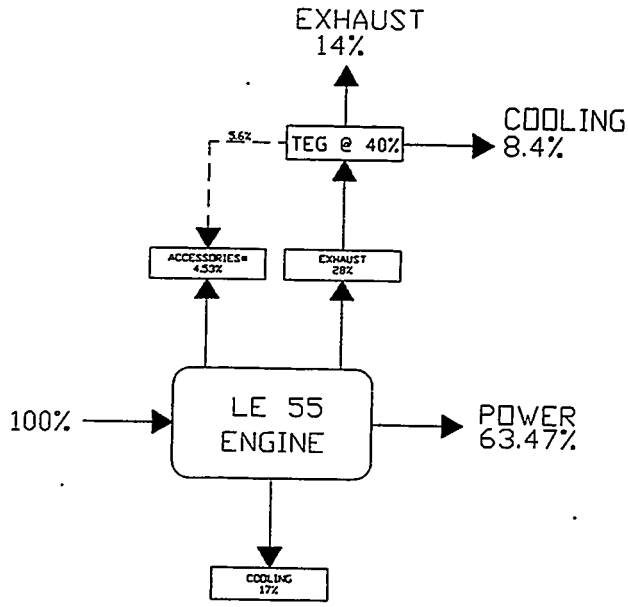


Figure 9: Energy Diagram of LE 55 Engine with 40% Thermoelectric Generator

will require several years of development. Incorporation of these new thermoelectric materials should lead to a significant improvement in overall engine efficiency as well as a shorter break-even time. While the improvements expected are greater when thermoelectrics are applied to present day engines, it will also significantly improve the efficiency of the advanced LE 55 engine.

REFERENCES

1. Bass, J.C., "Proof-of-Principle Test for Thermoelectric Generator for Diesel Engines", Final Report HZ72691-1, Hi-Z Technology, Inc., July, 1991.

2. Bass, J.C., R.J. Campana, and N.B. Elsner, "Evaluation of Novel Waste Heat Recovery concepts for Heavy Duty Diesel Engines", Final Report, HZ021191-1, Hi-Z Technology, Inc., February, 1991.

3. Caillot, T., J.P. Fleurial, and A. Borshchevsky, "Preparation and Thermoelectric Properties of Semiconducting Zn_4Sb_3", Journal of the Physics and Chemistry of Solids, V58, No. 7, Pp 1119-1125, Pergarmon Press, 1977, Great Britain.

4. N.B.Elsner, et al "Thermoelectric Performance of $Si_{0.8}Ge_{0.2}$/Si Heterostructures Synthesized by MBE and Sputtering", Proceedings of XIII International Conference on Thermoelectrics, Kansas City, Mo August, 1994.

5. S. Ghamaty, N.B.Elsner, K.Wang, and Qi Xiang, "Thermoelectric Performance of B_4C/B_9C Heterostructures", Proceedings XIV International Conference on Thermoelectrics, Pasadena, California, March, 1996.

ADVANCED TURBOCHARGER ROTOR FOR VARIABLE GEOMETRY TURBOCHARGING SYSTEMS

R.J. Stafford, J.M. Mulloy, T.M. Yonushonis, H.G. Weber, and M.J. Patel
Cummins Engine Company, Inc,

INTRODUCTION

Turbocharging of diesel engines has enhanced fuel economy and reduced diesel engine emissions. The initial applications of turbochargers to heavy duty diesel engines during the early 1970's reduced Bosch smoke (a measure of particulate matter used at the time) from 2.4 to 0.6 units. At the same time, engine specific fuel consumption was reduced from 0.36 lb./bhp-hr to 0.35 lb./bhp-hr. Since that time, a variety of improvements including further advances in turbocharger technology have reduced particulates to the level that they are below 0.1 Bosch units (the bottom of the scale) while specific fuel consumption is at the 0.32 lb./bhp-hr level. At optimum conditions, modern diesel engines can achieve in excess of 42% thermal efficiency which is competitive with stationary power plant efficiencies. One hundred percent (100%) of Cummins heavy duty diesel and medium duty diesel engines are turbocharged. Current turbochargers are optimized at one set of engine conditions and by necessity, at the off-design conditions or transient conditions the fuel economy and emissions performance are penalized.

Cummins and Holset, a Cummins subsidiary, have been working together on development of an advanced variable geometry turbocharger system for heavy duty diesel engines to improve off-design conditions. Variable geometry turbocharging provides an additional control of the turbocharger and assists in low speed response by modifying the inlet area to the turbine rotor. Cummins has also investigated modified radial rotors to improve off-design turbocharger performance. We believe that these new rotor designs coupled with variable geometry control systems can improve turbocharger efficiency by up to 15% at off-design points, which would result in particulate reductions of up to 40% and engine fuel economy improvements of 2 to 4 %. These improvements represent major advances for state-of-the-art diesel engines.

The current variable geometry turbines utilize existing turbine rotor or impeller designs. To be successful, the variable geometry turbine must provide acceptable efficiency over a 2:1 or 3:1 range in turbine flow at a given pressure ratio. The typical turbine has great difficulty in doing this, because the current impeller designs cannot efficiently accommodate such a wide range of flow conditions. Figure 1 shows the Dry Particulate versus Response curves for standard Fixed and Variable Geometry turbine wheels.

A rotor was designed and a prototype fabricated which showed as much as a 10% efficiency improvement at off-design conditions (1, 2). The leading edges are blunt and rounded to accept the flow from the turbine nozzles at a variety of inlet conditions with a minimum of losses. Photographs of this prototype are shown in Figure 2. The rotor efficiency is better at all conditions and the advantage improves as it operates at conditions further from the design point. Unfortunately, the conventional materials from which this turbine rotor was constructed had inadequate strength to allow its use on engines, and had such high rotational inertia that transient response would have been severely compromised.

MODELING

With the introduction of high strength, light weight materials, such as silicon nitride (Si_3N_4) and titanium aluminide (TiAl), the rotor design with blunt, rounded leading edges was revisited. The original design was used as a baseline design. Stress

modeling of the baseline design predicted peak stresses of 280,000 psi for TiAl and 225,000 psi for Si_3N_4. These stresses greatly exceed the yield stress for both materials.

A series of design iterations was conducted which minimized the peak stresses while providing a shape which could be manufactured. Two dimensional stress analysis of this design predicted peak stresses of 49,000 psi for TiAl. Three dimensional stress analysis and minor design optimization resulted in a final design with peak stresses of 70,000 psi for TiAl. The finite element stress comparison from the original design to final optimized design for the TiAl rotor is shown in Figure 3. Stress modeling was not conducted for Si_3N_4 because the rotor shape was considered too complex to be produced by currently available ceramic manufacturing methods. Photographs of the optimized rotor design are shown in Figure 4.

MANUFACTURING

The turbocharger rotors for testing were manufactured using production shell casting methods with a TiAl alloy. After metal casting and solidification, the rotors were chemically cleaned to remove the ceramic shell. The rotors were then hot isostatic pressed to densify the component and heat treated to develop the optimal material properties for the TiAl alloy.

The rotors were machined to develop the blade tip profiles and a shaft bore through the center. The wheels were then attached to production-like shafts using a locking nut and set of shims to set the correct operating height within the turbo-charger shroud.

TESTING

Performance testing was conducted at the Cummins Turbine Mapping Facility. This facility determines the turbine stage efficiency by measur-ing the compressor and bearing system work as well as the turbine mass flow and pressure ratio. The

Figure 1

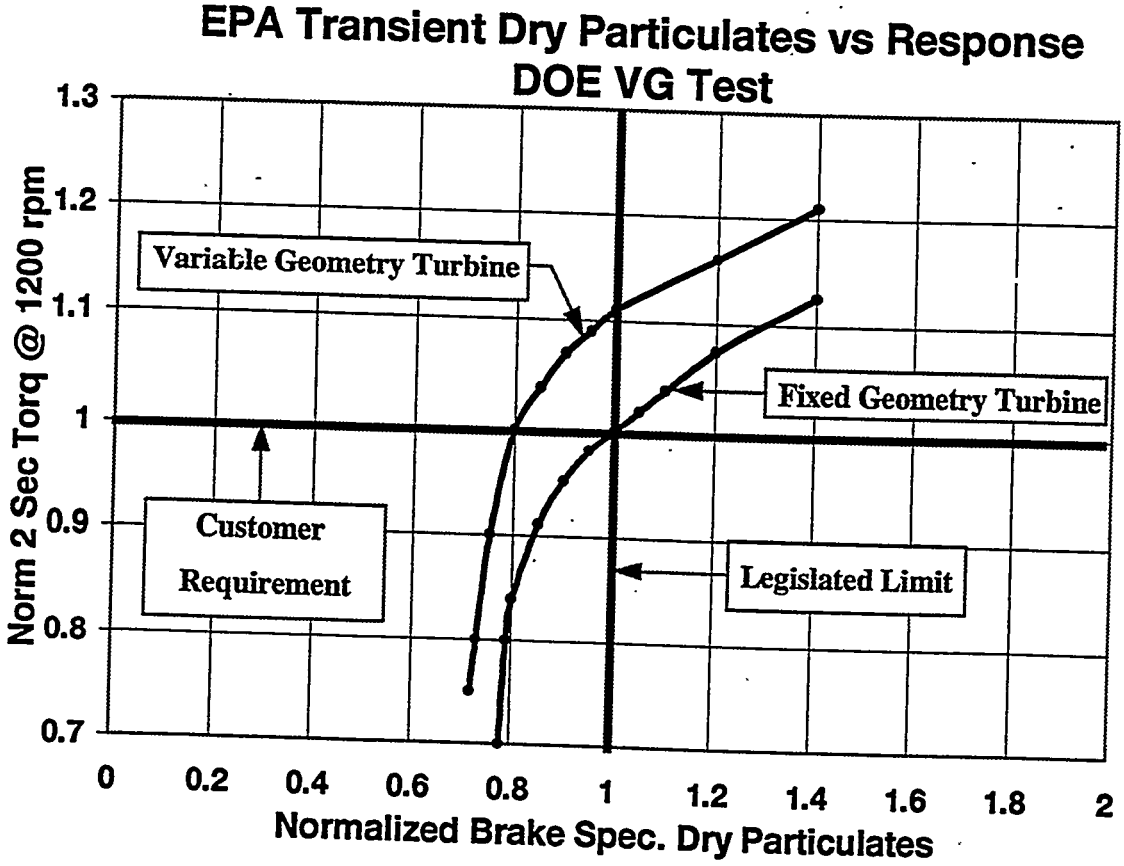
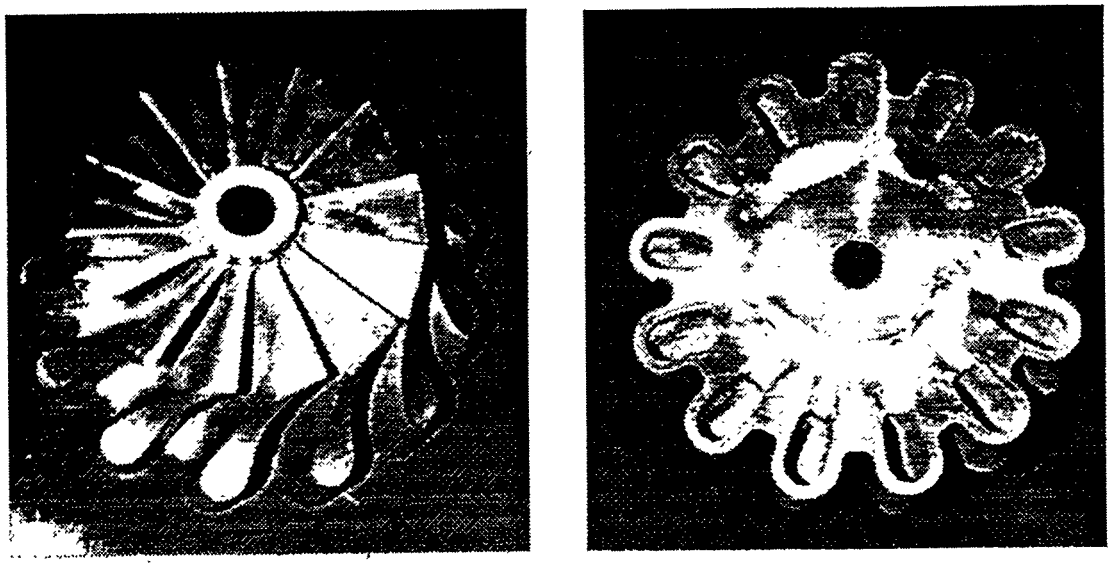


Figure 2 - Original Prototype Airfoil-style Rotor

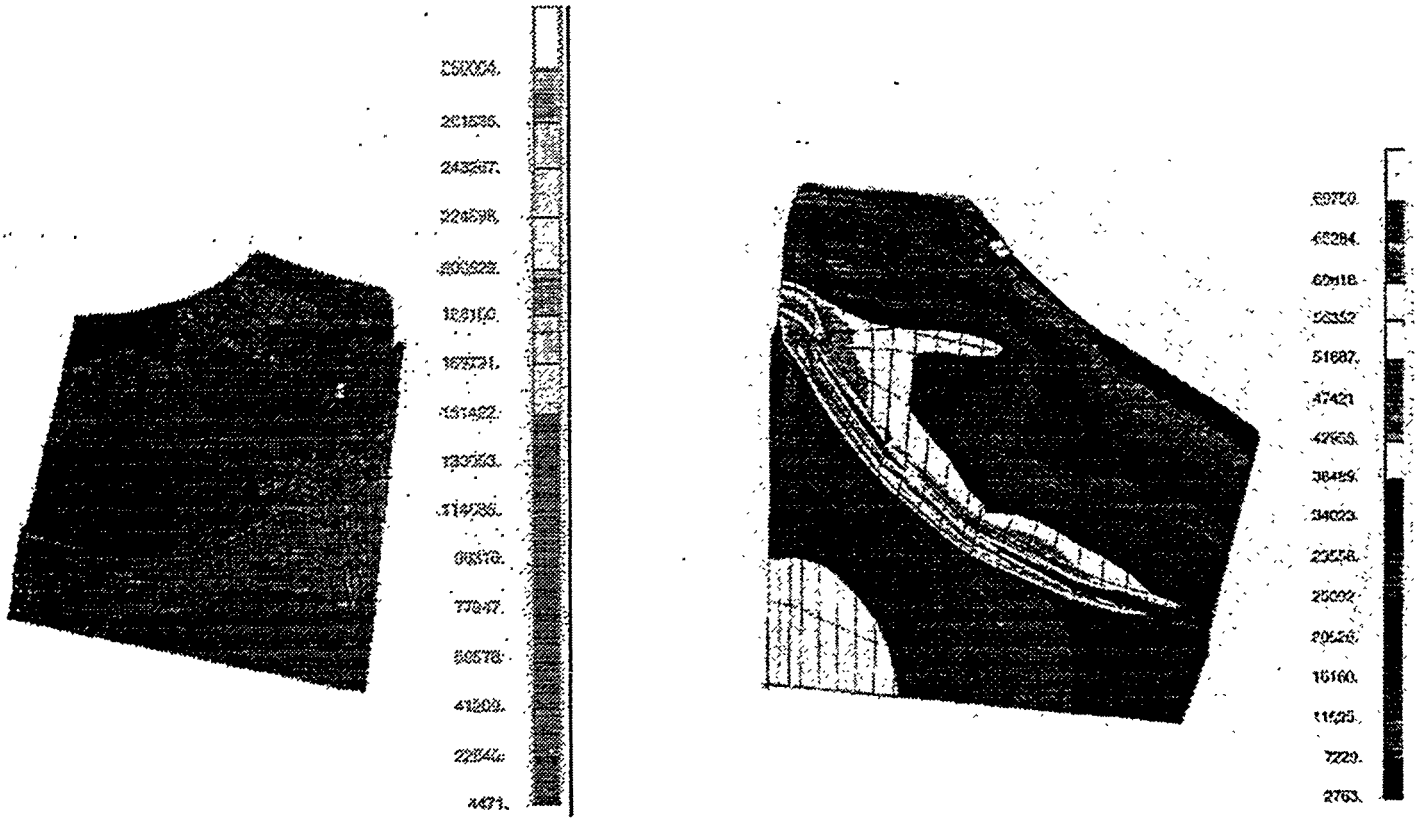


test facility measures turbine efficiency as Total to Static, meaning the turbine stage effici-ency is reduced by the kinetic energy left in the gas as it exits the turbine. This efficiency measurement represents the single staged diesel engine turbocharger efficiency.

Performance Mapping

To determine the performance characteristics of the experimental rotor in a variable geometry turbocharger (VGT) system, a Holset HX75 turbocharger unit was selected

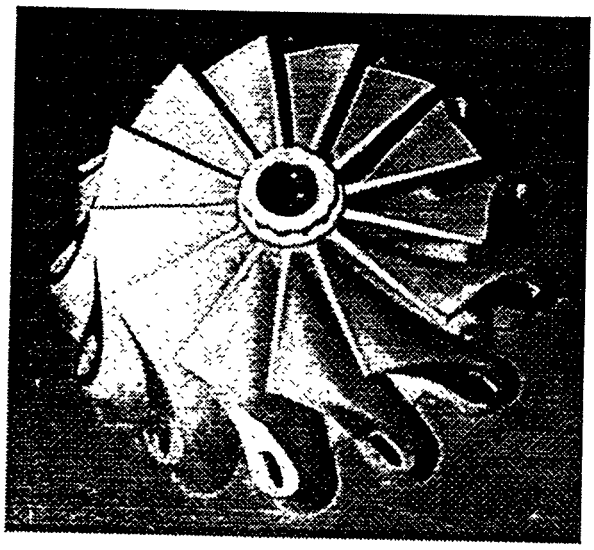
Figure 3 - Finite Element Stress Analysis Comparison

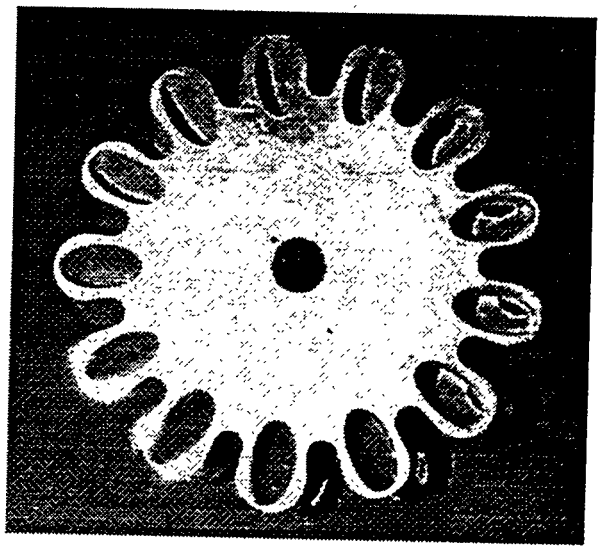


Original Design, 280 Ksi

Final Optimized Design, 70 Ksi

Figure 4 - Optimized Final Design





and nozzle rings were machined to expedite the testing. Four nozzle ring vane designs were made, one curved and three straight. The three straight vane designs had dif-ferent critical areas (variations in nozzle throat areas) to increase actual air flow rates. All the nozzle rings were originally machined to 15 mm vane height to fit the HX75 unit baseline and then machined down between maps to the next desired nozzle vane height. The assembled turbo-charger rotor and nozzle ring are shown in Figure 5.

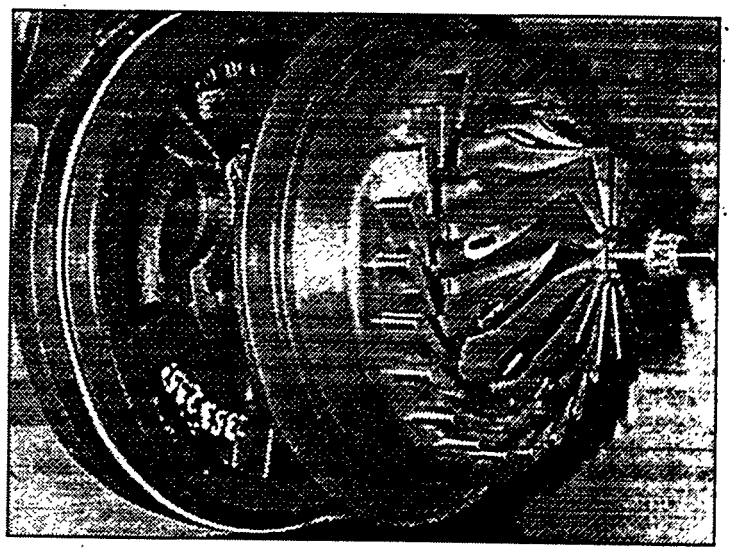
The testing was conducted using standard test procedures. During mapping, we had two major rotor bursts which destroyed the nozzle rings (see detail in Burst Testing). Once the cause of the failures was deter-mined to be related to defects in the wheel, the mapping proceeded without incident. The initial testing showed that the curved nozzle vane gave the slightly better perform-ance. Therefore, we mapped the HX75 unit using the curved nozzle vanes with vane heights of 15, 13, 11, 9, 7, 5, 3, and 2 mm. Then, in order to obtain data with higher flow rates, two of the straight vaned, increased throat area nozzle rings were mapped at a vane height of 15 mm.

Performance Comparison of the Experimental Rotor to a Conventional Rotor

The purpose of this effort was to improve the low flow efficiency of the VGT turbine which would then increase acceleration capabilities therby reducing particulate emis-sion and improve overall trip fuel economy. Figure 6 shows the comparison of the experimental rotor and two standard rotors in VGT systems. Since all the units had different mass flow capacities it was necessary to evaluate at the data on a non-dimensional basis. To determine the non-dimensional mass flow ba-sis, the mass flow point of peak turbine efficiency (where the nozzle vane height was equal to the rotor inlet tip height) was used as the 100% point. All other mass flows were divided by this value.

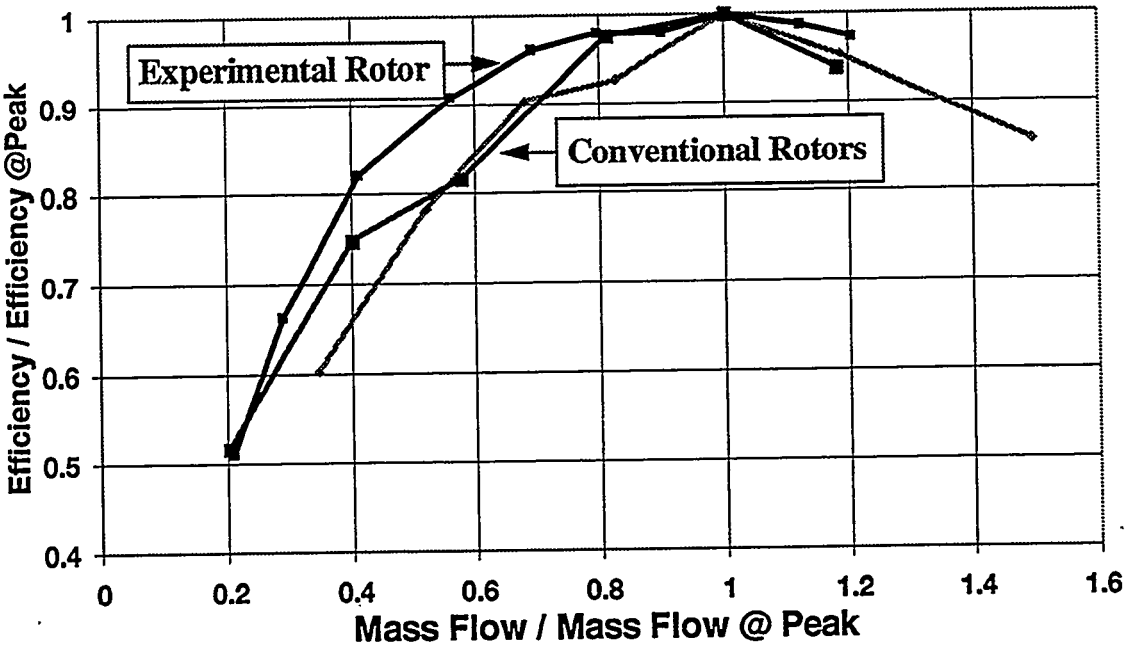
Figure 5

Assembled Turbocharger Rotor and Nozzle Ring



Firgure 6

Variable Geometry Turbine Comparison



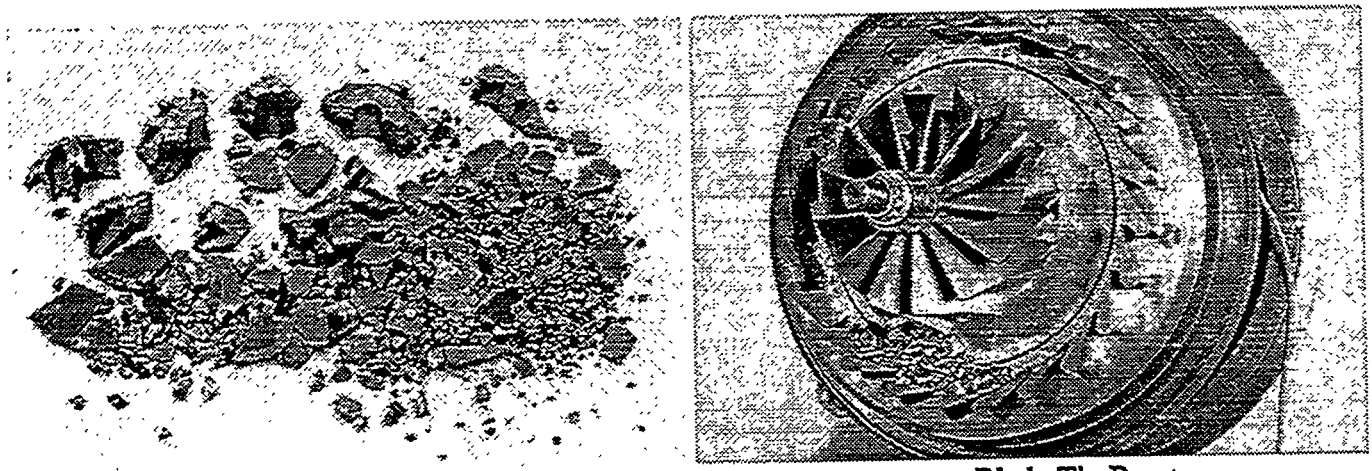
All the data points shown in Figure 6 are raw data without any curve fitting. As can be seen, the experimental rotor has significantly improved the turbine stage efficiency over the 0.30 to 0.80 range as well as showing improvement in the 1.10 to 1.20 range.

Burst Testing

The TiAl rotor was inadvertently accelerated to high speed conditions when a hose in the load absorption system which controls the rotor speed ruptured. The rotor was operating at 65,000 rpm at the time the hose ruptured, and immediately spun up to a speed which caused a hub burst of the rotor.

The TiAl rotor fragments were contained completely within the housing of the turbocharger which was a successful result. The TiAl fragments were generally small granular pieces with the largest fragments measuring less than 1 in. by 2 in. by 1 in. Analysis of the fragments did not reveal any

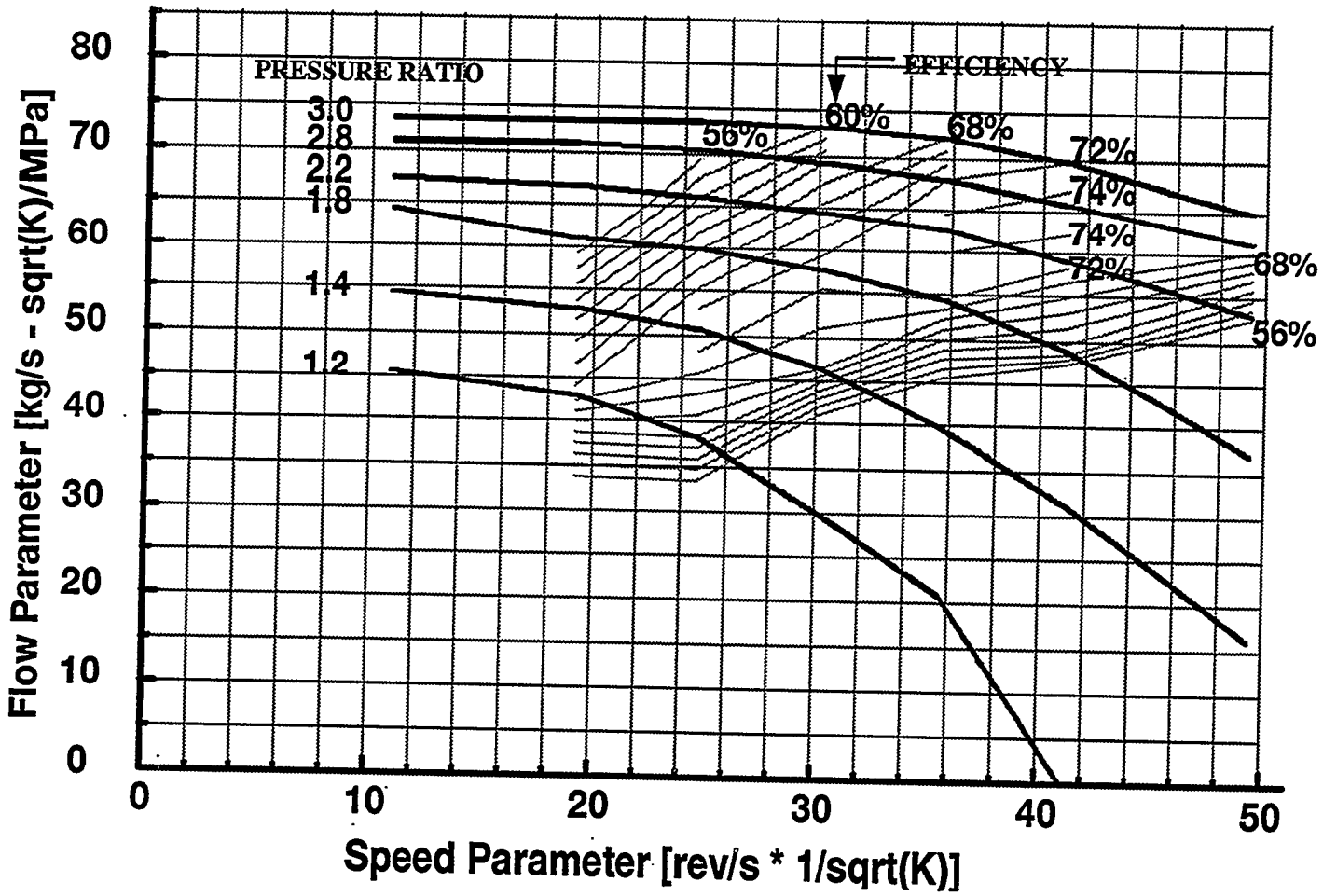
Figure 7 - Burst Test



Hub Burst

Blade Tip Burst

Figure 8 - Typical Turbine Map



mechanism for the fracture, however, dye penetrant examination of the remaining rotors showed small cracks in the machined bore on two rotors. A crack may have been present in the shaft bore causing the hub burst fracture when the rotor made a rapid change in speed.

A second TiAl rotor fractured during testing with the blade tips being removed from the hub. The blade tips again fragmented into small granular pieces and were contained completely within the housing. Examination and analysis of the hub and fragments did not reveal any mechanism for the fracture. However, based on the condition of the remaining rotors, it was suspected that a small pre-existing surface defect or crack caused one blade tip to fracture. The fracture caused rapid progressive damage of the other blade tips in the tightly toleranced space. The hub burst and blade tip burst are shown in Figure 7.

Demonstration of Advanced Turbocharger System

The objective was to evaluate the novel rotor geometry in a variable geometry

turbocharger system and compare the operation to the operation of a conventional design rotor in a variable geometry turbocharger system.

In order to compare the novel geometry turbine rotor to a standard rotor, Cummins used in-house engine simulation and vehicle simulations pro-grams. These programs are computer simulations of engine conditions which have been modeled and verified through comparison with engine performance data.

To complete this evaluation and comparison, engineers matched the engine simulation program conditions to an experimental data set which used the standard rotor in a variable geometry turbine. Then the simulation was run and used to predict the experimental system performance over the operating range. This simulation process is a standard operating procedure at Cummins and the results for various comparisons have consistently shown excellent agreement with experimental testing. For the simulation to work correctly the subsystem component maps must be supplied as input. These maps were available for the standard rotor in the variable geometry turbine but had to be generated for the experimental rotor.

For a variable geometry turbine several turbine maps must be generated to show the overall capability of the unit. Each map consists of running the unit at a constant pressure ratio while varying the rotor speed to determine the flow capacity and efficiency. This must be done at several pressure ratios since the engine will drive the turbomachinery to operate at pressure ratios from 1.0 to approximately 4.0. A typical map will include data for 1.1, 1.2, 1.4, 1.8, 2.2, 2.6 and 3.0 pressure ratios. Figure 8 is a sample turbine map showing rotor speed vs. efficiency and mass flow at different pressure ratios. For the variable geometry unit with the novel wheel, eight maps were generated at different nozzle vane heights to simulate what would be required during an actual engine test.

Once the mapping was completed, a valid comparison could be made with Cummins engine simulation programs. This comparison was accomplished by running the simulation at various operating conditions which have been determined to be major contributors to the system fuel consumption by engine measurements over a standard driving route on the highway. A different set of operating conditions, determined by engine measurements, was used for emissions reduction predictions.

The final results of the comparison after analysis with the simulation programs showed predicted improvements in cycle fuel consumption of 2 to 3 % and reduction in particulate emissions of approximately 30%.

CONCLUSIONS

The demonstrated performance of the experimental rotor in the VGT has provided the means to reduce particulate by approximately 30% and improved cycle fuel consumption by 2 to 3%. The basis for these results is a comparison to previous engine testing and cycle simulation modeling on the original prototype rotor. These results showed additional improvements in the cycle simulation model which predicts the above overall improvements compared to conventional designed rotors.

ACKNOWLEDGMENTS

This work was funded in part by the California Energy Commission, contract 500-92-042, and by the U. S. Department of Energy, contract DEN3-373. Technical review of the work was provided by Dr. Jim Patten and the senior management of the Cummins Technical Center. The oversight of Mr. John Fairbanks at the U. S. Department of Energy and Dr. Gary Yowell and his colleagues at the California Energy Commission was also greatly appreciated. Completion of this work required the efforts of many people and these people are listed below:

Holset Turbocharger
Jacqueline Kearney
MacNeal-Schwendler Corporation, PDA Division
Dr. J. G. Crose, Robert Holman, David Bremmer, Ernie Julian, John Norman and Robert Schindler
Consultant to MSC, PDA Division
Douglas Marx
Cummins Engine Company, Inc.
George Delay, Paul Park, Scott Kronhart, Stanley Bishop, Roger England, Mike Goble, Bob Gray and Scott Sims
Precision Castparts Company
Jim Barrett, Srivats Ram and Dave Harmon
Port City Machine and Tool Company
Doug Hartman

REFERENCES

1. Mulloy, J. M. and Weber, H. G., "A Ra-dial Inflow Turbine Impeller for Improved Off-Design Performance", ASME Paper No. 82-GT-101

2. Flynn, P. F., Weber, H. G. and Mulloy, J. M., U.S. Patent No. 4243357, Jan. 6, 1981.

SESSION IV

Aftertreatment and In-Cylinder Emissions Reduction

Chairman: Gary Yowell
California Energy Commission

DIESEL ENGINES: ONE OPTION TO POWER FUTURE PERSONAL TRANSPORTATION VEHICLES

R.B. Krieger, R.M. Stewart, J.A. Pinson, N.E. Gallopoulos, D.L. Hilden, D.R. Monroe,
R.B. Rask, A.S.P. Solomon, General Motors Research and Development Center
P.Zima, General Motors Technical Center Europe

INTRODUCTION

As we stand at the threshold of a new millennium, we wonder about the shape of personal transportation beyond 2000 AD. To start, we consider the societal, environmental, economic, and technological forces that are constantly applying pressure for change. These forces are not numerous, but they are powerful: the explosion in world population and its ravenous appetite for improved living standards are straining the earth's natural resources, its urban and agricultural space, and its environmental health. Translated into terms germane to automotive transportation, the most important forces are urban congestion, air pollution, global warming, and petroleum depletion. Responses to these driving forces can be considered in terms of scenarios [1], an artifice that distances the engineer from prediction while allowing contemplation of a wide range of alternatives without embarrassment. Such an analysis has led us to the conclusion "that the ultimate goals for personal transportation would be zero vehicle emissions in polluted areas and zero fossil fuel consumption, if the most dire predictions of climatologists and resource experts materialize" [2].

To move from the present toward these ultimate goals, a number of pathways involving various technologies exist. A useful schematic representation of this journey from the present into the future is shown in Figure 1, where various technologies are positioned with respect to their effects on fossil fuel consumption and vehicle emissions (in terms of U.S. and California standards). A third, and very important dimension, cost, is not shown, but generally, cost would increase as we move from the technologies of the present to those of the future. Note also, that as a benchmark, Figure 1 shows the position of the Honda Civic equipped with a VTEC engine.

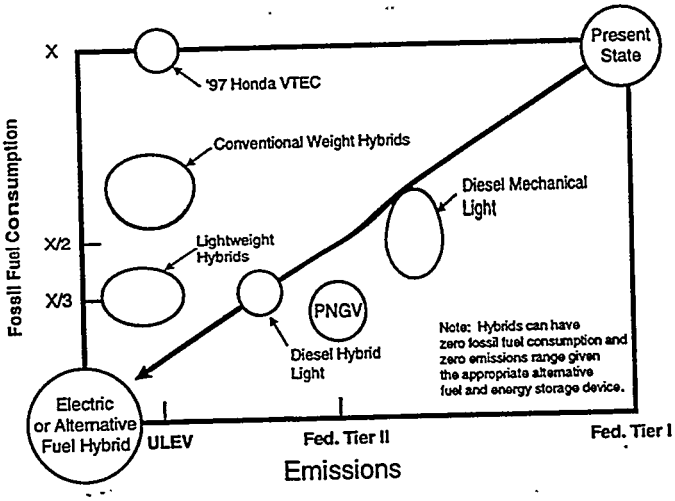


Figure 1. Options for Approaching Fuel Consumption and Emissions Goals.

Figure 1 is not a prediction. Rather, it helps organize the technological direction in personal transportation and it illustrates some important points: there are no silver bullets; many options and their combinations can be used to construct alternative pathways to the future; all aspects of transportation vehicles must be addressed (mass, resistance to motion, powertrains, fuels, and exhaust aftertreatment where applicable). Furthermore, Figure 1 illustrates that despite many years of research and the big push for development that resulted from the two petroleum crises of the 70's, the auto industry is still dealing with an undiminished range of options for meeting future challenges, options that span a broad spectrum of technological and commercial maturity.

Gasoline engines, diesel engines, fuel cells, electric vehicles, hybrid vehicles, and an assortment of alternative fuels still populate both the imagination and continuing research and development. These options are actively pursued by automakers worldwide, as well as by governmental and academic laboratories. Over the years, more and more of the technologies

are being tried out in demonstration or limited market situations. Witness the General Motors electric vehicle EV-1, the PNGV program in the U.S., the BMW hydrogen-fueled car, and the Honda CNG Civic, as a few examples. No clear choice exists as yet, and even the diesel engine, which some had written off years ago, remains as one of the options.

Figure 1 also shows that diesel engines, either as stand-alone vehicle powerplants or as auxiliary power units in hybrid vehicles, could be viable choices for meeting future needs, depending on the requirements that must be satisfied and on progress in diesel technology compared to progress in the other technologies depicted in the figure.

Figure 1 suggests that some of the other options depicted are much preferable to the diesel engine. Such a conclusion, however, ignores two additional important dimensions not included in this two-dimensional figure: demonstrated technological performance and cost. In theory, more efficient powerplants than the diesel engine exist, but no powerplant has the demonstrated high efficiency of the diesel engine. The diesel engine's cost is higher than that of a comparable gasoline engine, but this cost is known and it is likely to be considerably smaller than that of some of the more exotic solutions suggested in Figure 1.

The Achilles' heel of diesel engines is exhaust emissions. If engine-out emissions could be reduced and if exhaust aftertreatment devices could be developed to further reduce emissions, the position of the diesel engine options in Figure 1 would be improved dramatically. Efforts to do both are under way in industrial, academic, and governmental laboratories worldwide. This paper will describe recent efforts in our laboratory, which have concentrated primarily on reducing engine-out emissions without sacrificing efficiency while using conventional diesel fuel. On our way to describing this work, however, we will also touch upon a number of related subjects. We will start by placing the diesel engine in perspective with respect to other powerplants, so as to add some detail to the broad outline already presented and summarized in Figure 1. This broadly based material will be expanded with detailed accounts of the following: the efficiency and emissions of state-of-the-art diesel engines; the research that we have done to advance the state of the art; and the technologies that, based on our work and that of others, could improve diesel engines. We will illustrate some of these technologies using examples taken from the new General Motors ECOTEC diesel engine. The topics of alternative fuels, exhaust aftertreatment devices, and application of diesels to hybrids will also be covered, but in a more general way, as they have not been our prime research areas in the recent past. For extensive research on some of these topics we rely more on the appropriate supplier industry, academia, and government. Furthermore, as our concern is personal transportation, we will limit the scope of this paper to light-duty vehicles.

We are not prepared to declare the diesel engine either the winner of the race to the future or a last-place finisher. We believe it to be one of the still open options, and we are intrigued by its technological challenges. Consequently, it is but one of several technologies that we are actively pursuing within our R&D portfolio.

THE DIESEL IN PERSPECTIVE

In North America, the contact of the public with diesel engines is largely through trucks, buses, and locomotives, many of which are older designs. Thus, the image of diesel engines in the minds of much of this public, and perhaps the public of other parts of the world as well, is of engines that are slow to start, slowly accelerating, noisy, and dirty. In the 1970's, two "energy crises" led to the introduction of new diesel powered passenger cars into the North American market and to a surge in their sales. Following a return to pre-energy crises levels of fuel availability and prices, diesel passenger car sales fell again to very low levels. In Europe on the other hand, where public policy has kept fuel prices high through taxes, diesels have historically captured a more substantial market share. In some countries, favorable diesel-to-gasoline price ratios have further contributed to high diesel sales. Motivated by the steadier market, auto manufacturers and en-

gine consulting firms have worked continuously on the shortcomings of diesel engines and have made tremendous progress in correcting them. As a result of these efforts, contemporary European diesel passenger cars are difficult to distinguish from those with gasoline engines. These latest European diesel cars start nearly as rapidly, have similar noise characteristics, emit no visible exhaust smoke or perceptible exhaust odor, and provide equal or better acceleration, especially in traffic, compared to their gasoline-engined brethren. The effect of these improvements on the market has been a dramatic increase in diesel market share for new vehicles in the European Union (EU) from about 14% in 1990 to about 27% in 1996.

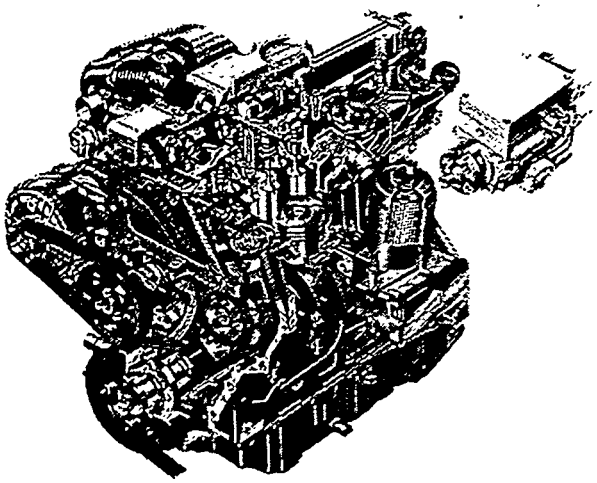


Figure 2. ECOTEC 2.0-L DI Diesel Engine [3].

Recent advanced engine development in Europe has focused on high-speed direct-injection (HSDI) configurations. For example, General Motors Europe introduced for the 1997 model year [3] a new four-valve per-cylinder HSDI diesel engine of 2.0-L displacement called the ECOTEC DI (see Figure 2). This engine is the first to reach the market of an expected wave of new HSDI diesel engines that combine a number of attributes: four valves per cylinder, high-pressure electronically controlled fuel injection, and high levels of EGR (exhaust gas recirculation). The motivation for choosing these attributes is that they are enablers for minimizing exhaust emissions from HSDI diesel engines. These and other enablers will be discussed in more detail later.

To place the diesel in perspective, we must compare it to other available options or competitive technologies.

COMPETITIVE TECHNOLOGIES

The baseline engine that new engine technologies are compared to is the SI (spark ignition) piston engine. Its most common form is port fuel injected, homogeneous stoichiometric charge with modest EGR, and a three-way-catalyst exhaust-aftertreatment system. While this engine has been the "standard" for several years, it is being continually improved in all its aspects including efficiency and emissions.

For all engines, minimizing heat transfer losses helps to improve engine efficiency. Changes that lower the combustion chamber temperature or minimize the surface area exposed to hot gases will reduce the fraction of fuel energy lost as heat. However, attempts to simply insulate engines have not been successful. Various characteristics of the engine cycle also influence efficiency, and engine modifications that improve the cycle efficiency are used (e.g. increased compression ratio). Anything that influences the efficiency of the combustion process, either in the fraction of fuel burned usefully or in optimizing the times and phasings of the combustion event, is a target for improvement. Minimizing losses due to friction is also sought during the evolution of the standard PFI (port fuel injection) engine.

Efficiency also depends on how the engine is operated. The baseline engine is less efficient at converting fuel into mechanical energy at light load than it is at heavy load. Load is controlled by throttling the flow of inlet air, and energy is dissipated to pump the inlet air across this pressure drop. Anything that increases the average loading (increased BMEP) during a typical driving cycle (the FTP cycles are of prime concern) will increase the fuel economy of the vehicle. This leads to strategies involving engine downsizing, perhaps accompanied by boost devices, cylinder deactivation, variable displacement, etc. The alternative to changing the operating range is to broaden the efficiency islands (i.e., contour islands of constant efficiency when plotted on a load-

TABLE 1. Qualitative Comparison of Light Duty Vehicle Engines

	Fuel Economy	Emissions	Cost	Comments
SI Piston Engine				
Baseline PFI engine	0	0	0	Homogeneous stoichiometric, modest EGR, 3-way catalyst
Variable Valve Timing (VVT)				Many mechanizations possible
Performance enhancing	+	+	-	Broader torque curve, more power, internal EGR
Load control	++	0	--	Elimination of throttle and consequent losses
Cylinder deactivation	++	-	--	Operates on fewer cylinders to increase load
Enhanced Dilution PFI				Basically homogeneous operation, improved combustion stability
EGR	+	+	0	Uses three-way catalyst
Lean	+	-	-	Probably needs lean NOx catalyst
EGR and Lean	+	0	0	Mixture of above two strategies
Direct Injection Stratified	+++	-	--	Dilution enhancement obtained with stratified operation. Operate with both EGR and air (lean) dilution. Will need lean NOx catalyst.
Downsized boosted				With intercooler
Turbocharged	++	0	---	Mostly used today as a power enhancement.
Supercharged	++	0	---	Probably will evolve towards Miller cycle.
Modified Cycles				
Overexpansion	++	0	---,U	Needs a viable mechanism. (Except for Miller cycle as above)
2-stroke cycle	+	-	0	May end up in niche markets.
SI Engine With Different Mechanization	0	0	U	Examples are Wankel and swash plate designs. Gains must be in areas of more compact/lightweight design, cheaper, and less friction. Surface to volume ratio influences combustion performance. Likely requires major tooling investment.
DI Diesel Engine	+35%	-	---	Turbocharged and intercooled with lean NOx aftertreatment. The only engine with demonstrated large fuel economy gains.
Stirling Engine	U	+	---,U	Not a likely near term contender; considerable demonstration/ development work needed. Most suitable for hybrids.
Gas Turbine	U	+	---,U	Not a likely near term contender; considerable demonstration/development work needed. Most suitable for hybrids. Low cost ceramics probably needed to make it viable.

+ = better, 0 = baseline, - = worse; U = unknown (speculative). The number of +'s and -'s indicates a rough measure of the advantage or disadvantage respectively.

speed graph) shifting larger portions of a driving cycle to high efficiency locations on the engine load-speed map. These changes typically involve operation with greater charge dilution using air, EGR, or both.

Table 1 lists some engine types/features that will provide competition to the **DI Diesel Engine** in delivering value to the customer. The taxonomy must always be arbitrary, and the listing is not exhaustive, but the table provides an overview of the engine types that many people believe (or wish) will be available in the near future. Many variations are shown for the baseline **SI Piston Engine** because improved versions of the baseline engine will likely be the most viable light duty vehicle engines for many years to come. Many of the SI Piston Engine features act to control losses from throttling and heat transfer. Hence, one cannot view the list as a "shopping cart" and simply sum up the features.

The fuel economy potentials of the **Stirling Engine** and **Gas Turbine** options are listed in the table as "Unknown" even though there are many numbers available from developers of these engines. As there are no demonstrated, viable, automotive Stirling engines or gas turbines, their efficiency gains are highly speculative. Peak thermodynamic efficiencies of a refined Stirling engine could approach 50%, and those for a high temperature (i.e., ceramic) gas turbine could be in the range of 40%. The thermodynamic efficiency for converting fuel into mechanical energy of a good, contemporary baseline SI engine is approximately 35% at its best operating condition. This compares to approximately 42% for a diesel engine. Obviously, operation away from the peak efficiency point degrades efficiency, and average efficiencies over a driving cycle are less than the maximum efficiency. In hybrid vehicle operation, the power range over which the engine oper-ates is reduced, but it seems very unlikely that any hybrid will operate only at the engine's peak efficiency. Efficiencies and operating characteristics of all components of the hybrid vehicle system will dictate the optimum strategy for engine operation and for overall vehicle efficiency.

Fuel cells have not been added to this chart as information about them would be even more speculative than that of gas turbines or Stirling engines. However, fuel cells are clearly a long-time-frame contender, as they offer great potential for both fuel efficiency and emissions. Fuel cells need breakthroughs in both technol.-go capability and costs in order to achieve commercial success. They would be incorporated into an electric hybrid drive train.

Table 1 shows that there are no clear winners among these engines and that the diesel faces several challengers.

DIESEL ATTRIBUTES AND CHALLENGES

The major challenges for continued growth of diesel engines in the market, as already noted, are exhaust emissions and cost. The exhaust emissions challenge derives from current and future exhaust emissions standards shown in Table 2.

TABLE 2. Future Diesel Light Duty Vehicle Emissions Standards

		Emissions - g/mi			
US	**Year**	**NOx**	**CO**	**NMHC or NMOG**	**PM**
Federal Tier I	Current	0.4	3.4	0.25	0.08
Federal Tier II	2004	0.2	1.7	0.125	0.08
California* LEV	--	0.2	3.4	0.075	0.08
California* ULEV	--	0.2	1.7	0.04	0.04

		Emissions - g/km			
EUROPE		**NOx**	**CO**	**HC+ NOx**	**PM**
Stage III	2000	0.5	0.64	0.56	0.05
Stage IV	2005	0.25	0.5	0.30	0.025

*California standards are for the fleet average and they are phased in over a period of 10 years (1993-2003).

For light-duty vehicles, compliance with expecked U.S. Federal standards (Federal Tier II) following expiration of the current diesel NOx emissions exemption of 1.0 g/mi will require intensive efforts. The most difficult to achieve standards are NOx and particulate matter (PM), which tend to trade off with each other. Compliance with HC (i.e., NMHC or NMOG) and CO emissions will be challenging as well, but less so than for NOx/PM. On the bright side, the long standing unregulated emissions issue of

diesel exhaust odor has been virtually eliminated by the use of exhaust oxidation catalysts.

Other challenges for diesel engine developers are cost, vehicle mass increase, and both the characteristics and the quality of fuels. Diesel engines are more costly to produce than gasoline engines due primarily to the high-pressure electronically controlled fuel injection systems required. These systems can approach half the cost of the engine. Additional expenses also come from higher cylinder pressures and the need for intake boosting. Higher cyfinder pressures require stronger and, therefore, more costly reciprocating parts (e.g., piston, connecting rod, bearings, crankshaft, etc.). Boosting, which is also required to provide acceptable performance, needs turbochargers (in most cases) and intercoolers (in some cases), both of which add cost. High output current and future diesels also require oil coolers. Vehicle costs also increase due to requirements for increased battery power (for cold cranking against high compression ratios).

The increased engine strength required to control high cylinder pressures without NVH (noise, vibration, and harshness) problems contributes to increased vehicle weight as do the boost and intercooler devices. Diesel fuel characteristics influence cold startability, combustion noise, and exhaust emissions as will be noted later.

Against these challenges, diesels offer the highest proven fuel economy of any engine, performance advantages (due to their torque characteristics), and increased vehicle driving range. From an environmental point of view, diesels offer CO_2 reductions proportional to their energy efficiency gains and minimal organic emissions from evaporative losses, running losses, and refueling. These issues will be addressed in more detail with focus on the HSDI diesel. To do this, however, we need to examine data that will help project the characteristics of future diesel engines. Such characteristics include performance, efficiency, and emissions.

PERFORMANCE AND EFFICIENCY OF FUTURE DIESELS

POWER DENSITY AND PERFORMANCE

The peak power density of diesel engines has been increasing steadily. A snapshot of data from a group of current and advanced development engines is shown in Figure 3. On the left is data from a group of IDI (indirect injection) and DI turbo diesels with power densities ranging from 35 to 50 kW/L. Also shown are spark ignition (SI) engine data from a two-valve engine in NA (naturally aspirated) and boosted form (33 to 44 kW/L, respectively), and a group of NA four-valve SI engines (42 to 46 kW/L). A high-performance four-valve gasoline SI engine is also shown with 72 kW/L. In spite of having the lowest peak power engine speeds, the diesel engines have comparable power density to the supercharged two-valve SI engine and only slightly lower values than the typical NA four-valve SI engines.

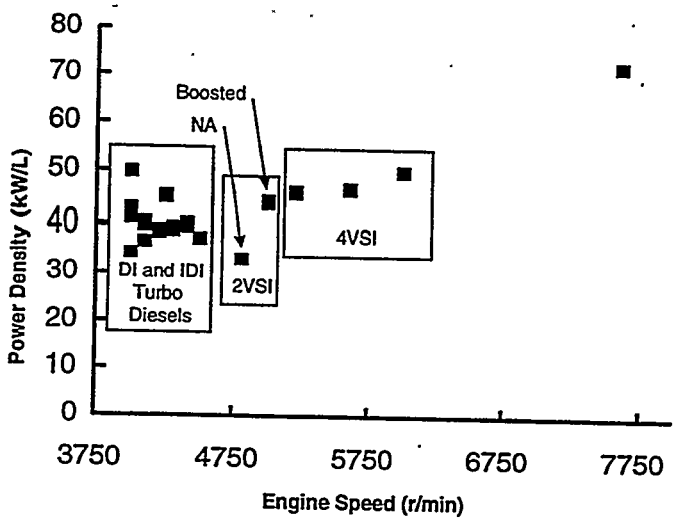


Figure 3. Peak Power Density for DI Diesel, IDI Diesel, and SI PFI Engines.

However, vehicle performance depends not only on peak power, but also on the peak torque and torque curve shape. The peak torque density values corresponding to the data of Figure 3 are shown in Figure 4, which shows that the diesels have the highest peak torque densities and their peak torque values occur at lower engine speeds than those for the SI engines. This characteristic results from the shape of the diesel torque-speed (or BMEP-speed) curve, as

shown in Figure 5.

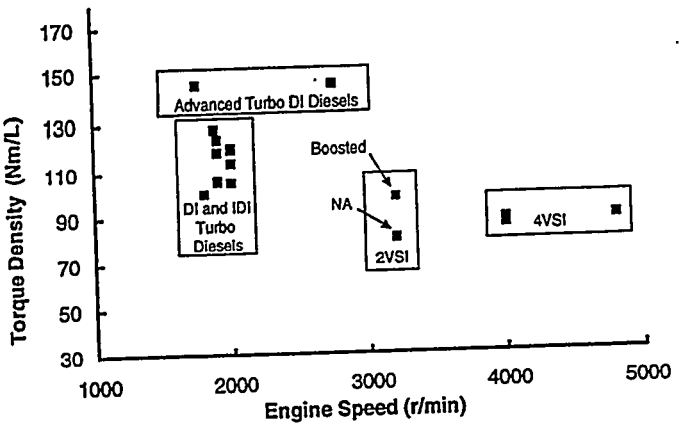


Figure 4. Peak Torque Density for DI Diesel, IDI Diesel and Spark Ignited Engines.

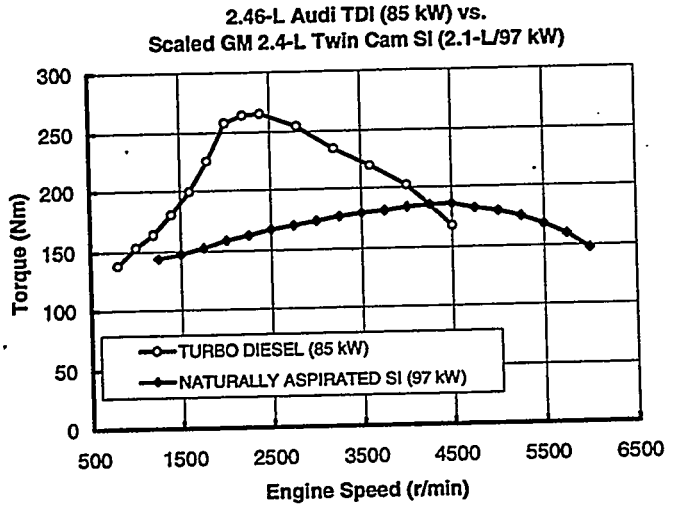


Figure 5. Torque Versus Eengine Speed for HSDI and Four Vlve P.F.I. SI.

The effect of these high torque values and low peak torque speeds is to provide vehicle accelerations equivalent to SI engine vehicles with higher peak power, as expected from the following equation, which provides a crude estimate of the relationship between maximum engine power and vehicle acceleration [4]

$$Peak\,Power\,(kW) = C \cdot \frac{Vehicle\,Mass\,(kg)}{Acceleration\ (0-60(s))} \qquad (1)$$

The coefficient C depends primarily on three things, the shape of the torque curve, the final drive ratio, and the transmission ratio range. Based on comparisons of Equation 1 with simulation calculations for a vehicle with a 2.1-L L-4 SI engine with a four-speed automatic transmis-sion, the coefficient value is 0.75. For a 2.46-L turbo HSDI diesel with the same transmission, the coefficient for the diesel is 0.64. Thus, because of the torque-curve shape and peak torque value of the diesel engine, the maximum power required is about 14% less than that for a SI engine for equal vehicle mass and equal 0-60 mph performance. In addition, because the diesel peak torque speed occurs at 1800-2500 r/min compared with 3500-5000 for the SI en-gine, diesel powered vehicles respond well to traffic speed variation, thus requiring fewer transmissiбn shifts for equivalent vehicle performance in urban and suburban traffic.

TABLE 3. Comparison of VW (Passat) TDI Vehicles - Variable Nozzle Turbocharger (VNT) vs. Conventional Wastegate Turbocharger [5]

	Wastegated Turbo	VNT Turbo
Displacement	1896 cm^3	1896 cm^3
Nominal Power	66 kW	81 kW
Nominal Speed	4000 r/min	4150 r/min
Specific Power	34.8 kW/L	42.7 kW/L
Maximum Torque	202 Nm @ 1900 r/min	235 Nm @ 1900 r/min
Maximum BMEP	1.34 Mpa	1.56 MPa
Euromix* Fuel Consumption	5.4L/100 km	5.2L/100 km
0-100 km/h	14.4 s	12.1 s
Maximum Speed	173 km/h	188 km/h

*Euromix fuel consumption is the average of that for Euro city cycle, that for a steady 90 km/h and that for a steady 120 km/h, all equally weighted.

One enabler for high power density is a variable geometry turbocharger, which is now being used on production HSDI diesel vehicles. VW and Audi both offer versions of their TDI engines with conventional wastegate turbochargers and also versions with VNT's (variable nozzle turbochargers). Relative performance data for the VW 1.9 TDI engines is shown in Table 3 [5].

FUEL EFFICIENCY

It is clear from Table 3 that the VNT provides not only improved performance, but also re-

duced vehicle fuel consumption. As would be expected, the VNT is more costly than the conventional turbocharger. Nonetheless, it is likely that future vehicles will make greater use of this technology, particularly in premium vehicle packages.

From an efficiency point of view, HSDI diesels currently offer around 35% lower volumetric fuel consumption than equivalent performance SI engines as shown in Table 4 below.

Table 4. Fuel Consumption and Performance of Opel Vectra Vehicles with Gasoline and DI Diesel Engines.

Engine	Gasoline x16 XEL	Diesel x20 DTL
Top Speed (km/h)	175	178
Acceleration, sec. (0-100 km/h)	15.5	15.5
Fuel Cons. (L/100km)		
City	9.0	6.0
90 km/h	4.8	3.8
120 km/h	6.1	5.0
Euromix	6.6	4.9

From Table 4 it can be seen that an Opel Vectra vehicle with a gasoline engine consumes 35% more fuel than one with a 2.0-L low charge (i.e., non-intercooled) ECOTEC diesel on the Euromix test cycle for equivalent performance. On an energy basis, the consumption increase is about 23% for the gasoline vehicle with an equal increase in CO_2 emissions. These differences in consumption and CO_2 emissions are caused by the roughly 12% volumetric energy difference between diesel and gasoline fuels.

Fuel efficiency for future HSDI diesels may not improve significantly due to combustion modifications that will be required to meet future exhaust emissions standards. Nonetheless, as was noted earlier in comparing HSDI diesel technologies with competing technologies, HSDI diesel engines offer the highest fuel econ-omy alternative among piston engine candi-dates and the highest demonstrated fuel econ-omy among the other engine alternatives.

HYBRIDIZATION

Currently, a number of development efforts are being pursued jointly by the Big 3 U.S.' automakers through USCAR and the Federal Department of Energy to exploit the potential of hybrid drive trains [6]. Many options exist to configure hybrid power trains. These range from a power boost parallel hybrid with a small amount of hybridization at one end of the spectrum to a series hybrid at the other end. Various power sources can be used among these choices ranging from near-term piston engines, such as the HSDI diesel, to mid-term technologies, such as gas turbine and Stirling engines, to long-range technologies, such as fuel cells.

Since the focus of this paper is on the HSDI diesel engine as an option, it is worth considering what hybrid configurations make the most sense with HSDI diesel engines. The efficient operation over broad load and speed ranges, which is characteristic of the HSDI diesel, makes it well suited for parallel hybrid applications, although series configurations are also an option. One such parallel hybrid approach would involve a flywheel alternator-starter placed between the engine and transmission, which would facilitate packaging a parallel hybrid with relatively small modifications to current powertrain packaging layouts. The potential efficiency gains that might be achievable from an HSDI diesel hybrid would depend on the details of the powertrain configuration, operational strategy, and the efficiency of the system for energy storage and withdrawal [6].

EMISSIONS CHALLENGES AND OPPORTUNITIES

PROJECTIONS BASED ON VEHICLE DATA

Currently, HSDI diesel-powered passenger cars have been certified for emissions compliance in both the U.S. and Europe. However, as was noted earlier in Table 2, future emissions standards are tightening. The next tightening comes with the Euro Stage III standards in the year 2000, which require a 36% reduction in CO, a 38% reduction in NOx + H2, and a 50% reduction in PM from Stage II levels. In addition to

compliance with the legislated exhaust constituents shown in Table 2, there is a strong interest in Europe for reducing CO_2 emissions to address global climate change concerns. The European Union (EU) has proposed an emissions target for the 2005/2010 time frame of 120 g/km CO_2- In addition, there is a German target involving tax incentives to encourage CO_2 emissions below 90 g/km. In recognition of the low fuel consumption of diesel engines and their corresponding low CO_2 emissions. European emissions targets in Stage III and Stage IV are less stringent for diesel engines than for gasoline engines. This approach reflects the European view that local pollution issues must be balanced with global issues like climate change and energy conservation.

Current production vehicles in Europe have some margin relative to Stage II compliance, which takes them toward Stage III compliance. For example, the ECOTEC diesel vehicle egis-Zions are compared to the standards in Table 5 [3].

TABLE 5. ECOTEC Diesel Vectra Emissions, g/km

	CO	NOx	HC+NOx	PM
ECOTEC Diesel	0.37		0.71	0.039
Stage II Stds	1.0	0.5	0.9	0.1
Stage III Stds	0.64	0.25	0.56	0.05

However, in spite of already achieving future CO and PM emissions levels with the ECOTEC engine, considerable additional effort is required to meet the H2+NO_x goals. Auto manufacturers, independent engine manufacturers, and engine consulting firms are working on roughly the same set of technologies to achieve NOx control. For example, vehicles with advanced prototype four-valve HSDI diesel engines in vehicles of different inertia weights have achieved emissions below the Stage III values as shown in Figure 6. In this case, the values for the 1400 kg vehicle (7] were achieved with a 2.2-L four-cylinder engine, while the results for 1590 kg and 1810 kg were achieved with a 3.0-L V6 [8]. Both of these engines were equipped with advanced high-pressure electronic radial distributor pump type injection systems with two-stage injection nozzles. The 2.2-L engine was also equipped with a VNT and a fresh passive (i.e., no extra fuel added to the exhaust stream) lean NOx catalyst.

The more challenging Euro Stage IV values proposed for NOx/PM in 2005 are also shown in Figure 6. The NOx/PM values are one half

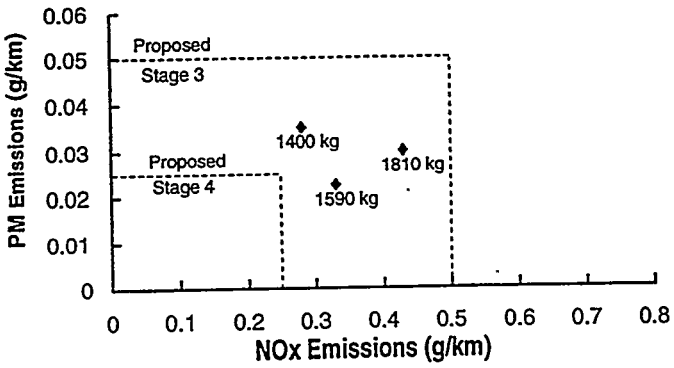


Figure 6. Development Status Toward Achiev ing Euro Stage III Emissions for 1400 kg [7], 1590 kg [81 and 1810 kg [8] Vehicles.

those for Stage III. The final values enacted will be based on progress demonstrated before the end of 1998. At the present time, some of the technology development for Stage IV tar-gets is being conducted on single-cylinder en-gines. For example, we have been trying to develop combustion system technologies to achieve the future emissions standards such as U.S. Tier 2 and ULEV as well as the Euro Stage IV values. Some of these efforts are described next.

SINGLE-CYLINDER ENGINE STUDIES AND PROJECTIONS OF FUTURE HSDI ENGINES

Single-cylinder engine studies are convenient tools in efforts to improve combustion systems. They yield the data on which projections of full-scale engine performance can be made, thereby providing the information required to decide on the extent of a developmental program. In this section, after describing our single-cylinder engine studies, we will use results of these studies to assess the future potential of HSDI engines.

Engine and Injection System Description

Small-bore, high speed HSDI diesel engine combustion was studied using a single-cylinder

engine with a high-pressure common-rail fuel injection system.

Figure 7 shows the significant features of the combustion system. The cylinder head had four vertical valves actuated by dual overhead camshafts. The fuel injector was vertical and centrally located. The combustion chamber was formed by the re-entrant bowl in the piston and received the multiple sprays from the fuel injector. Swirl was promoted by the use of one tangential and one helical intake port. Cylinder heads having two different swirl levels were available (i.e., values of 1.1 and 1.7). Swirl was further increased for some cases by closing the inlet to either intake port. The cylinder liner and head were mounted on an AVL 528 single-cylinder research engine.

To meet power and emission requirements, turbocharging and/or supercharging to boost intake manifold pressure above atmospheric pressure is required for HSDI diesels at high load conditions. For the single-cylinder engine, such boosting was simulated by raising inlet and exhaust pressures to appropriate values.

Exhaust gas recirculation (EGR) was accomplished by drawing exhaust gas from the exhaust plenum and introducing it into the intake plenum through an external pipe, where it mixed with the inlet airflow regulated by a critical airflow system. Temperature of the inlet charge was regulated independently by heating the inlet air.

Cylinder pressure was measured and recorded using a conventional water-cooled piezoelectric pressure transducer surface mounted in the combustion chamber.

Table 6 contains an abbreviated list of key engine specifications:

An experimental high-pressure common-rail system consisting of an electronically controlled high-pressure fuel rail, continuous high pressure pump, and a rateshape controllable injector from Ganser-Hydromag of Zürich [9] was used. Fuel was spilled from the high pressure common-rail to obtain the desired rail

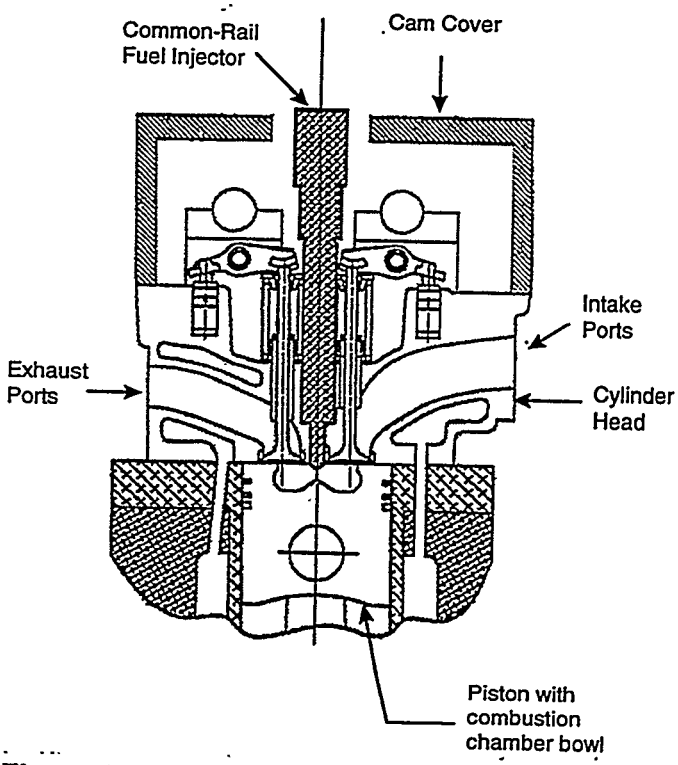


Figure 7. Single-Cylinder Engine Combustion System.

TABLE 6. Single-Cylinder Engine Specifications

Bore	76	mm
Stroke	94	mm
Compression Ratio	18.7	--
Squish Distance	0.7	mm
Bowl Depth	11	mm
Bowl Entrance Diameter	40	mm
Maximum Bowl Diameter	45	mm
Diameter of Intake Valves	24	mm
Diameter of Exhaust Valves	22	mm
Swirl Ratios	1.1, 1.7	--

The engine was run on Amoco Premium low sulfur diesel fuel with key properties listed in Table 7.

TABLE 7. Diesel Fuel Properties for Single-Cylinder Experiments

Specific gravity	0.83	-
Hydrogen/Carbon ratio	1.93	-
Stoichiometric mass A/F	14.6	-
Lower Heating Value	42.8	MJ/kg
Cetane Number	53	-
Aromatics	22	%
T95	321	C
Sulfur	<0.05	% wt

pressure. That pressure was limited to a maximum of 120.0 MPa (1200 bar) with the current hardware. The injector was actuated with single or multiple control pulses, the latter allowing pilot or post injection to be investigated. A needle lift sensor gave information on actual opening and closing timings.

A multi-hole valve-covered-orifice (VCO) spray tip was used. For the tests reported, nozzle tips were used having five spray holes ranging in diameter from 0.16 to 0.19 mm. Spray angles of 135° to 160° were used. Protrusion of the injector tip into the chamber was controlled with shims at the seat and was set to give maxi-mum smoke-limited power.

Fuel injection rate was controlled primarily by selection of rail pressure, as injection rate varies in proportion to rail pressure. The injector also has an internal adjustment allowing different slopes of needle lift opening that additionally influence the overall rate of injection for a given control pulse and rail pressure. Needle closing rate, however, is independent of rail pressure or opening rate settings. Closing occurs rapidly, but without needle bounce.

More information on the engine test procedures used can be found in the Appendix.

Combustion System Parameter Effects

Examples of tests exploring some of the important parameters controlling combustion and emissions are discussed in this section.

Rail Pressure and Pilot Injection

Rail pressure was varied from 500 to 1000 bar and tests were run with and without pilot injection. Engine speed was 1200 r/min, IMEP 575 kPa, and injection pulse timing was set to 3.50 btdc. The pilot pulse of 0.4ms was at 7.5° btdc, introducing about 10% of the fuel in advance of main injection. These tests were run without EGR, and naturally aspirated (NA) inlet conditions were maintained.

Rail pressure and pilot injection each affect average injection rate -- the injected fuel quantity divided by injection duration as observed from needle lift measurements. As one would imagine, injection rate increases with increasing rail pressure and decreases with pilot injection as noted in Figure 8.

In the following discussion, exhaust emission results are reported as emissions index, which is defined as ratio of the mass of emissions in grams to the engine fuel mass in kilograms. Smoke emissions are reported as smoke number, which is proportional to the concentration of carbon particles in the exhaust. A smoke number of two is considered the visibility limit.

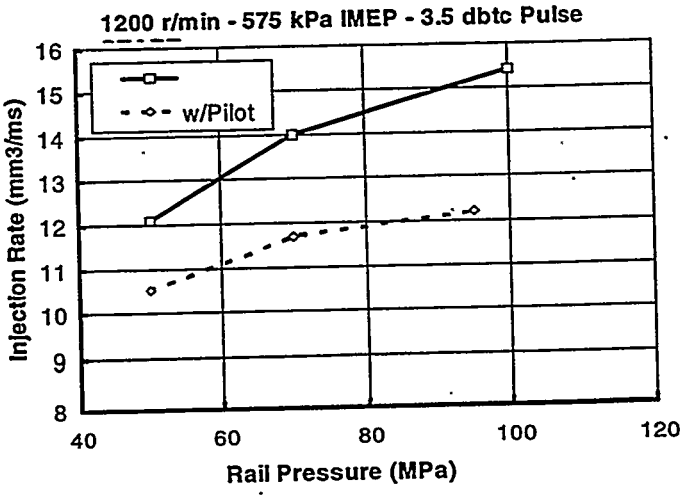


Figure 8. Effects of Rail Pessure and Pilot on Injection Rate.

NOx emission index (EI) increases with increasing rail pressure; and slightly higher values were reached with pilot injection (Figure 9). NOx typically will increase with faster burning rates and/or more advanced combustion timings. Pilot injection reduces injection rate by extending the time over which fuel is injected, which tends to lower NOx. For this example, however, the advanced timing of the pilot offset the rate effect, resulting in higher NOx.

Smoke emissions decreased with increasing rail pressure but levels were significantly higher with pilot injection (Figure 10). Increased injection rate, with its attendant increase in burning rate, is expected to reduce smoke emissions. The increase in smoke with pilot injection is typical and likely due to such details as shifting to more diffusion burning and reduced pre-mixed burning. Also, the main injected fuel will overtake that from pilot injection, so combustion

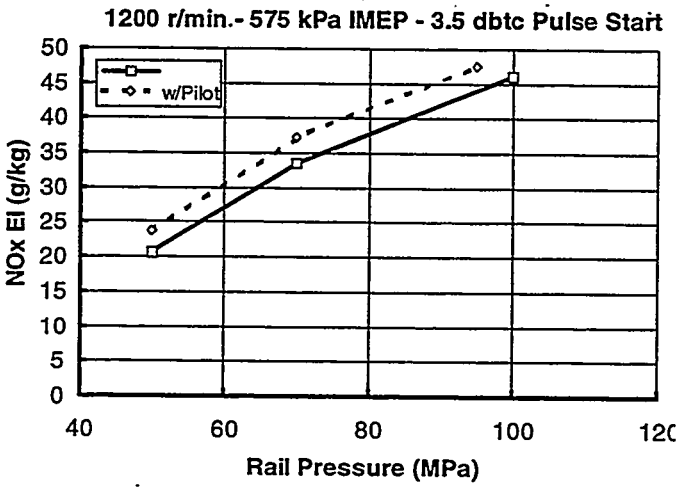


Figure 9. Effects of Rail Pressure and Pilot Injection on NOx Emissions.

could occur in areas already depleted of oxygen from combustion of the pilot.

The response of smoke to rail pressure noted in Figure 10 is a key feature of common-rail fuel injection that has great significance for both emissions and maximum torque at low engine speed operation, since in principle, high injection pressures can be achieved independent of engine speed. However, these advantages must be weighed against the disadvantages of common-rail systems. This topic will be discussed in more detail later under Enabling Technologies, Fuel Injection.

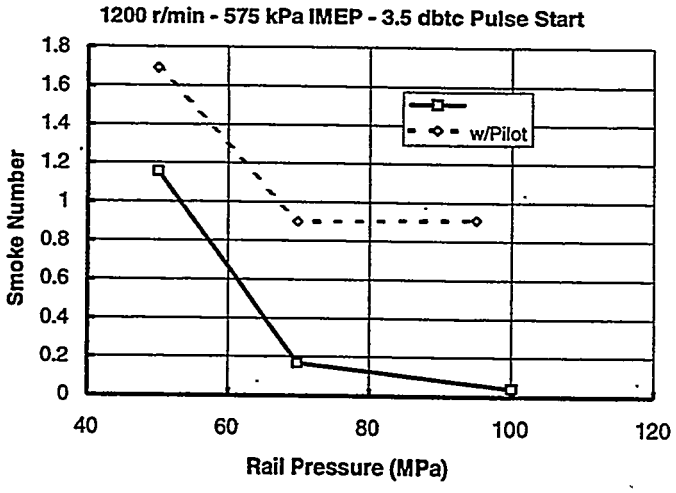


Figure 10. Effects of Rail Pressure and Pilot Injection on Smoke Emissions.

The high injection rates at the high rail pressures increased the maximum burn rate. Figure 11, which increased the rates of cylinder pressure rise (Figure 12). Pilot injection is shown to significantly reduce maximum burn rate and pressure rise rate since less fuel is injected prior to ignition, limiting the amount of rapid, pre-mixed burning. Because maximum cylinder pressure rise is a primary indicator of combustion generated noise, techniques such as pilot injection are desirable for reducing combustion noise.

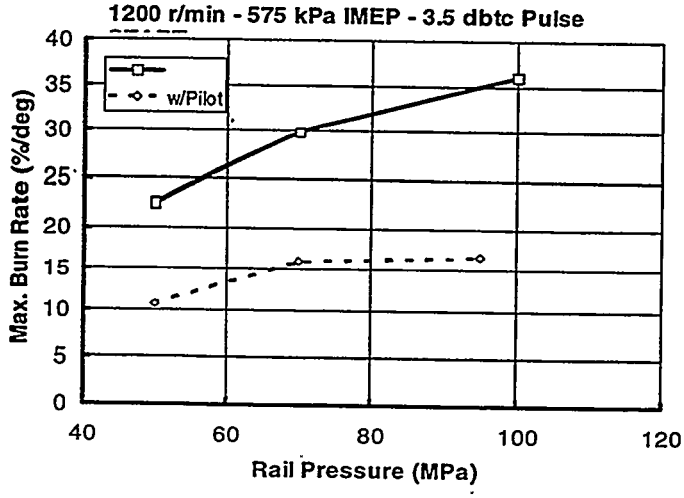


Figure 11. Effects of Rail Pressure and Pilot Injection on Maximum Burn Rate.

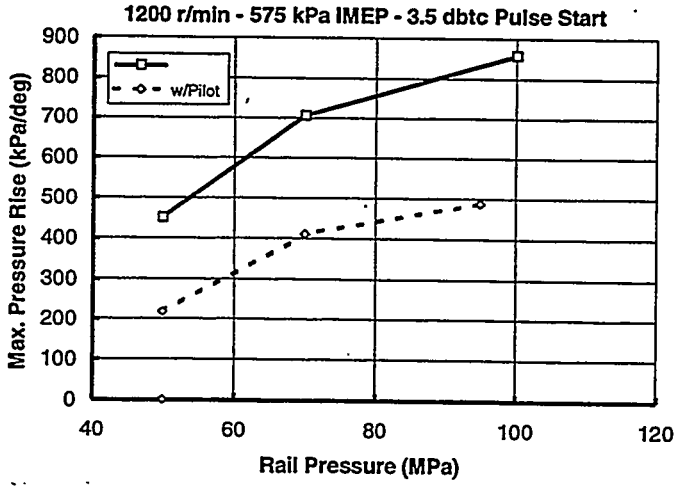


Figure 12. Effects of Rail Pressure and Pilot Injection on Maximum Rate of Pressure Rise.

EGR and Injection Timing

At a rail pressure of 700 bar and with pilot

injection, EGR was increased to near the maximum amount for stable combustion. Injection timing was then progressively retarded at the high EGR condition by delaying the pilot and main pulse timings. As EGR increases, Figure 13, NOx decreases substantially, while smoke increases. However, a small amount of injection retard (4.50) lowered smoke to the no-EGR levels, with little effect on NOx. The effect of SOI (start of injection) timing on smoke is believed due to subtle changes in the details of the spray and bowl interactions to which smoke can show high sensitivity, such as in this example. Supporting evidence for this supposition was found when a small additional injection timing retard of only 0.50 caused a five-fold increase in smoke compared the level at 4.5° of retard.

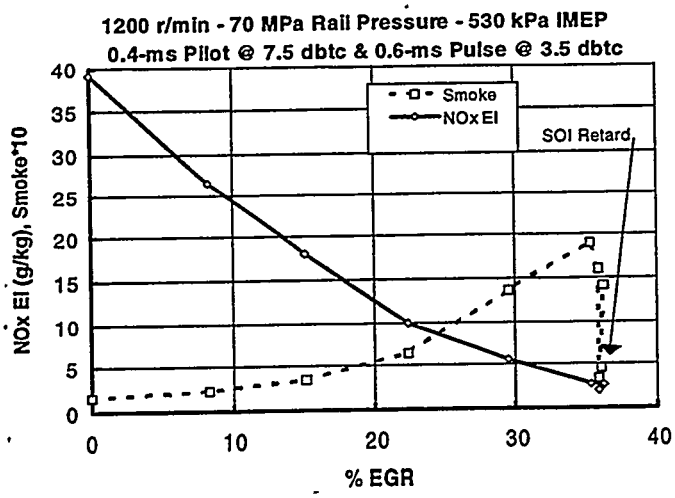


Figure 13. Variation of NOx and Smoke Emissions with Exhaust Gas Recirculation.

The air-fuel ratio for this particular test is shown in Figure 14. As EGR increases, air-fuel ratio decreases since exhaust gas is simply displacing inlet air. For this example, the air-fuel ratio decreases

The amount of EGR that may be applied to decrease NOx is dictated by the magnitude of the air-fuel ratio with no EGR and the minimum acceptable air-fuel ratio with maximum EGR. At light loads, such as idle where air-fuel ratio may be in the order of 100:1, more EGR can be used than for a heavy load condition, where the air-fuel ratio without EGR may be on the order of 25:1. At heavy loads, however, boosting intake pressure, as with a turbocharger, increases air-fuel ratio, also allowing more EGR to be used. In most cases, the minimum acceptable air-fuel ratio at heavy loads will be determined by the allowable smoke limit. At light loads, combustion instability or an abrupt increase in gaseous emissions or particulates will be the likely limitations.

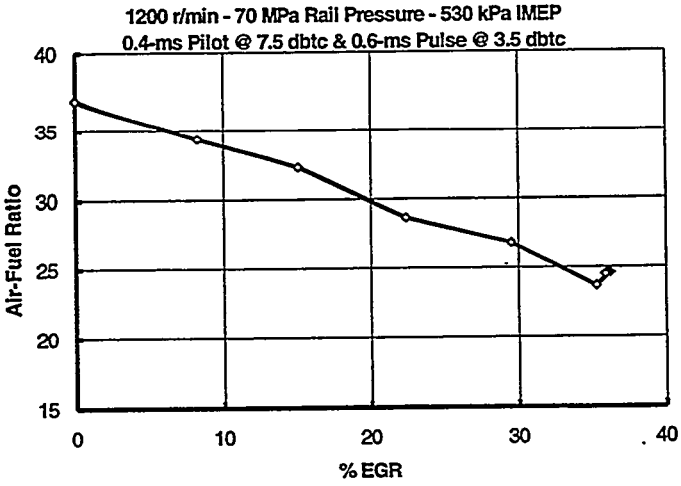


Figure 14. Variation of Air-Fuel-Ratio With Exhaust Gas Recirculation.

Port Throttling (Increased Swirl)

Inlet port throttling tests were run at 2400 r/min, 600 kPa IMEP, 700 bar rail pressure using pilot injection while closing either the throttle to the tangential port or to the helical port. Naturally aspirated inlet conditions were maintained and no EGR was used. With both port throttles open, the computed swirl ratio is 1.1 (determined by using experimental port-flow data and an engine simulation computer program). Closing the tangential port forces all the airflow through the helical port, resulting in a modest increase in swirl ratio to about 1.4. For this particular set of ports, closing the helical port and forcing all the airflow through the tangential port results in a larger calculated swirl ratio of 1.75. These tests were repeated with a high swirl head which had a base swirl ratio of 1.7, increasing to 2.2 and 2.8 as either the tangential or the helical port, respectively, was fully closed. Data also are included for the case without pilot injection for the high-swirl head.

As shown in Figure 15, the effect of swirl on

smoke depended upon which port was throttled. At this particular operating condition, throttling the helical port increased smoke, whereas the opposite effect occurred with throttling the tangential port. The high swirl head produced lower levels of smoke as did the elimination of pilot injection. Obviously, the in-cylinder air motion affects smoke, but this effect cannot be correlated by a single parameter as simple as the swirl number.

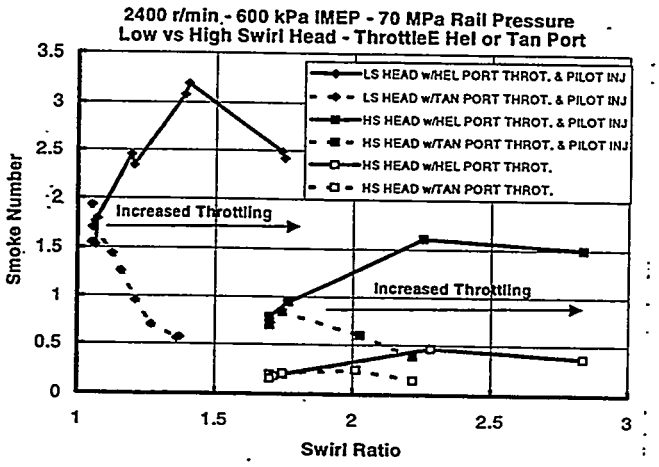


Figure 15. Effects of Intake Swirl on Smoke Emissions. LS and HS Denote Low and High Swirl, Respectively.

Increased swirl in general accelerates combustion as evidenced by reduced combustion durations, increased peak burn rates, and increased maximum cylinder pressure-rise rates. As shown in Figure 16, combustion duration decreased or increased swirl by throttling either port for both cylinder heads with and without pilot injection.

The influences of fuel injection rail pressure, use of pilot injection, amount of EGR, and intake flow swirl ratio, whose individual effects on emissions indices at one fixed operating condition for a single-cylinder engine have just been discussed, represent some of the major parameter effects that are used to optimize HSDI diesel combustion. Now, with these influences as a guide to the choice of the best values for these parameters, we will estimate the overall emissions performance of a six cylinder version of the single-cylinder engine

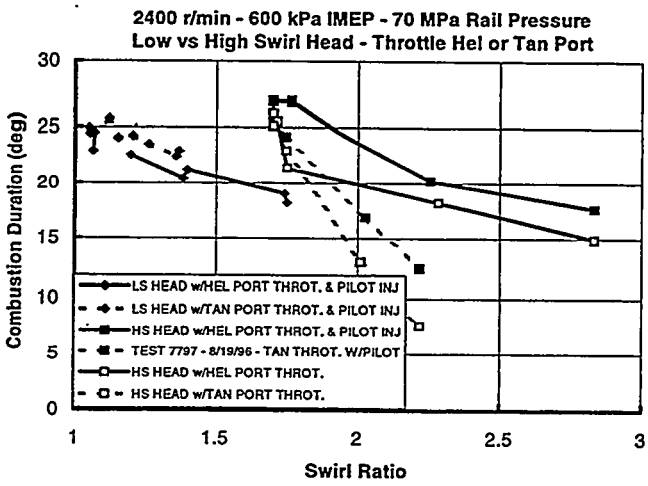


Figure 16. Effects of Intake Swirl on the Combustion Duration. LS and HS Denote Low and High Swirl, Respectively.

operating in a vehicle over the FTP driving cycle. The results will be expressed not as emissions indices, but as vehicle emissions in grams per mile.

Projections for NOx and PM During the FTP

Steady-state tests were run for multiple speed-load conditions to simulate operation on the U.S. FTP test schedule for the 2.56-L engine powering a 1588-kg test weight vehicle. Although such a simulation neglects warm-up and transient effects, those effects are generally less significant for an engine using direct fuel injection (diesel or gasoline). The emissions results are indicative of engine-out emissions as no catalyst or aftertreatment was used. The qualitative trend data generated by such tests provide valuable insights, and the quantitative information shows if one is "in the ball park".

To obtain the test points, first a vehicle simulation computer program called "GPSIM" [10] is run for the desired powertrain and specified transient test cycle. Multiple steady-state test points (e.g., seven) are then chosen after analysis of the resulting engine speed and brake torque histogram. Motoring data from a multi-cylinder HSDI engine having an engine-driven rotary injection pump, expressed as MMEP (motoring mean effective pressure) are then used to convert BMEP values derived from the

speed and torque histogram to IMEP (i.e., IMEP = BMEP + MMEP). The single-cylinder engine is then run at these seven settings of speed and IMEP.

Combined Effects: Based on the parameter effects described earlier, a combination of measures can be chosen that demonstrates the NOx/PM emissions capability of this particular combustion system. To demonstrate this, a strategy was chosen that employs: high rail pressure to decrease smoke and particulate emissions; high levels of EGR to decrease NOx; and significant (simulated) turbocharger boost at high loads to decrease smoke and particulate emissions while enabling even higher EGR levels. Specifically, the highest available rail pressure of 1200 bar was used, except at light loads and idle, where rail pressure was reduced to 900 bar. Pilot injection was used at light loads for reductions in gaseous emissions with little particulate penalty and for a noise benefit. Boost levels were the maximum consistent with state-of-the-art turbochargers for light-duty vehicle size engines. The high swirl head was used for these tests, but without port throttling. With this strategy, the single-cylinder engine was then operated at each of the seven test points with EGR and injection timing adjusted to drive NOx and PM emissions as close to the Tier 2 standards as possible.

Figure 17 gives total and dry PM versus NOx results as EGR is increased. In this case, the total particulate and dry particulate mass values were determined from filter measurements.

After weighing for total particulates, the filters were vacuum baked to drive off the volatile material and re-weighed to determine the dry quantity. The dry particulate indicates the minimum particulates possible assuming an ideal oxidation catalyst that removes all the volatile material from the particulate.

U.S. Federal emissions standards for particulates and NOx from passenger car diesel vehicles are shown as boxes in Figure 17. Results for the maximum EGR level (54% averaged over 7 test points) suggest that it might be possible to achieve Tier 2 emissions

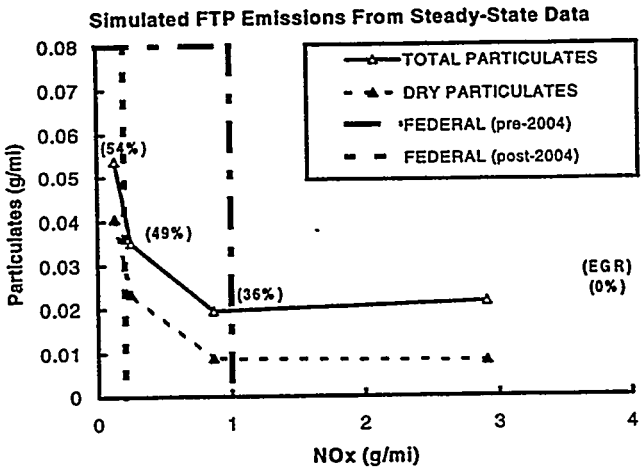


Figure 17. Potential for Meeting Future Standards of the Combustion System Evaluated in the Single Cylinder Tests Based on FTP Simulation.

levels with this combustion system. This suggestion is somewhat misleading since it would not be possible to calibrate a multi-cylinder engine using this combustion system and the high EGR levels for each of the seven test points that make up each data point on Figure 17: practical EGR systems would not provide the uniform cylinder-to-cylinder EGR distribution required. If one cylinder exceeded the EGR level used for these single-cylinder experiments, then that cylinder would contribute more PM emissions than the other cylinders, possibly pushing the engine emissions too high. Similarly, during an engine transient, the EGR level called for by the engine control system may be exceeded by the actual amount of EGR received by the cylinder due to any number of reasons (e.g., engine manifold pressure wave dynamics, EGR valve transient response, turbocharger and/or wastegate response, etc.). Thus, to avoid exceeding the chosen EGR limit for the combustion system, the multi-cylinder engine would have to be calibrated with lower levels of EGR, thereby producing higher levels of NOx than those obtained in the single-cylinder engine tests.

ENABLING TECHNOLOGIES FOR EMISSIONS CONTROL

Based on the single-cylinder work described above as well as on other HSDI work going on

throughout the industry [4,6-7,11-13], it is clear that a number of enabling technologies will be required to provide the best opportunity for achieving the most stringent emissions standards. The following list identifies the major technologies.

COMBUSTION SYSTEM

In order to maximize fuel economy thereby, minimizing CO_2 emissions, a direct-injection combustion system will be required. Four valves per cylinder should be used to allow placing the fuel injector in a central, vertical position as shown in Figure 18. This positioning improves the symmetry of the combustion chamber and spray, thereby reducing smoke and PM emissions [11]. However, the use of four valves complicates the choice of intake and exhaust port arrangement since both helical and tangential port types can be arranged in different combinations and in different locations. These port choices all influence and are influenced by valve train preferences as well. Figure 19 shows the intake port arrangement of the single-cylinder engine used for the work reported above, which combined a helical and a tangential port. Figure 20 illustrates an alternative arrangement of two tangential ports, which is similar to that used on the ECOTEC engine. These two port arrangements require different valve placement as shown in Figure 21.

Two intake ports enable the use of port throttling to vary inlet swirl (Figure 22). Inlet swirl is an important parameter for matching flows with fuel spray characteristics over the engine speed range. An example of how the port flow coefficients and in-cylinder swirl parameters trade off is shown in Figure 23. Effects of port throttling on combustion were evaluated with the single-cylinder tests. As was noted, swirl level alone is not an adequate descriptor of the inlet and in-cylinder flow.

Ultimately, the interaction between the flowfield in the piston bowl combustion chamber near top dead center and the fuel spray must be optimized. This optimization involves the fuel spray characteristics, the inlet flow, and the piston bowl shape. A number of piston bowls

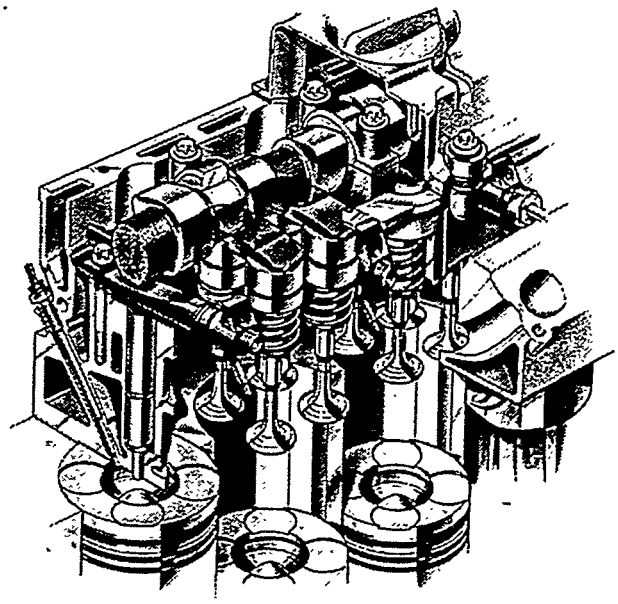


Figure 18. Cutaway of the ECOTEC 2.0 Cylinder Head [3].

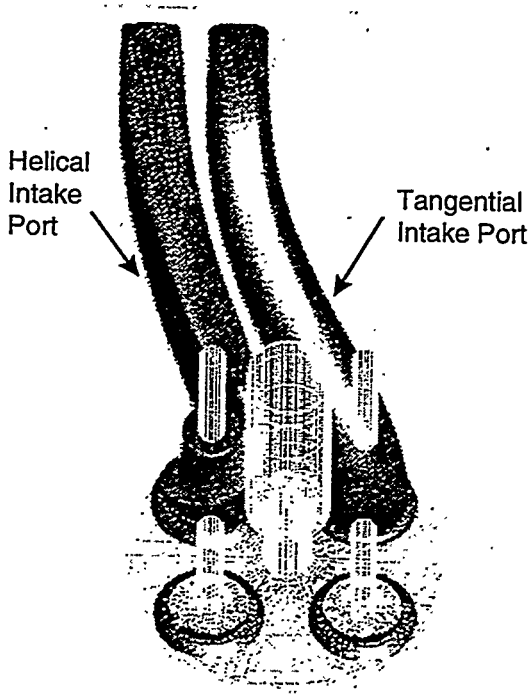


Figure 19. Intake Port Arrangement for the Single-Cylinder Test Engine.

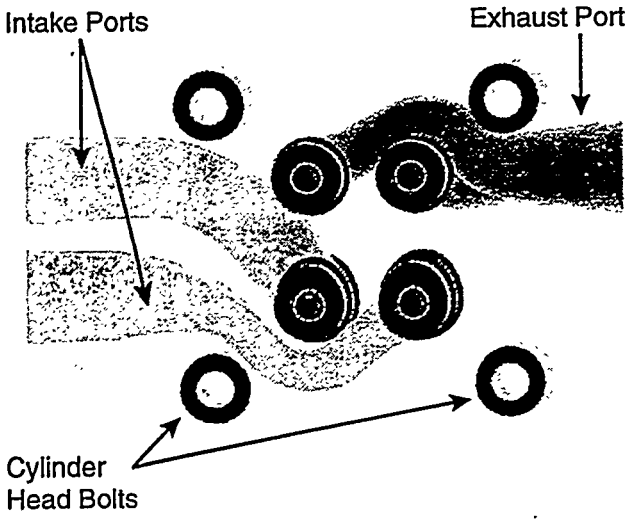


Figure 20. Alternative Intake Port Arrangement.

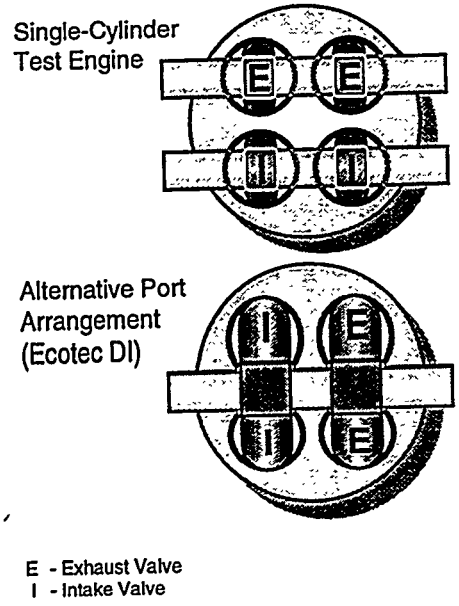


Figure 21. Two Valve Placement Alternatives

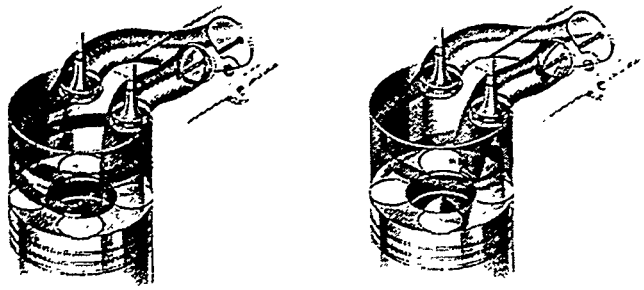


Figure 22. Port Throttling Arrangement Used on the ECOTEC DI Engine [3].

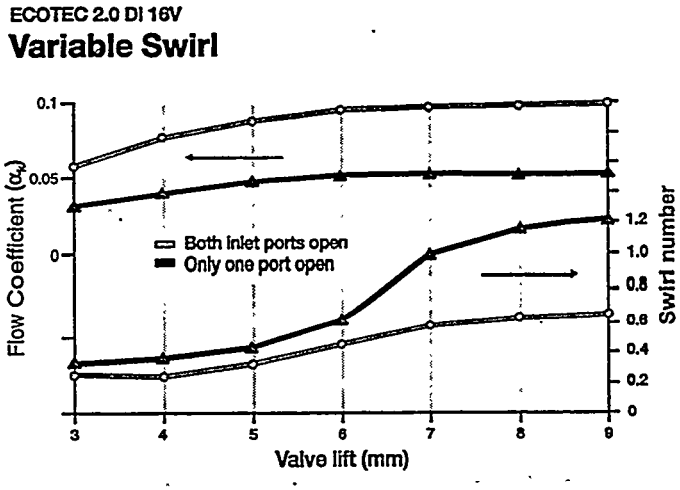


Figure 23. Effect of Port Throttling on Port Flow Coefficients and Swirl at Various Intake Valve Lifts [3].

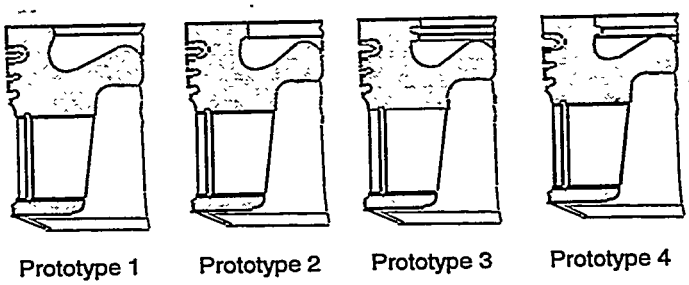


Figure 24. Combustion Chamber Design for the ECOTEC 2.0 Engine [3].

studied during the development of the ECOTEC engine are shown in Figure 24. The critical parameters in piston bowl design are the squish ratio (i.e., ratio of bowl throat area to cylinder bore area), the re-entrancy (i.e., ratio of bowl throat diameter to maximum bowl diameter), bowl lip shape, bowl depth, and bowl interior shape. However, influence of piston bowl geometry on combustion must be balanced with its influence on piston temperature distribution to assure long-term durability of the piston.

EGR SYSTEM

It is clear from the single-cylinder results shown earlier that EGR is a major enabler for NOx emissions control. Figure 25 shows the EGR map for the ECOTEC engine as it is currently calibrated for Euro Stage II emissions standards where EGR levels up to 30% are used. Considerably higher EGR levels will be required to achieve future emissions standards

as seen from Figure 17. Configuring an EGR system for a multi-cylinder HSDI diesel engine to deliver such high levels involves consideration of numerous issues. First, there are tradeoffs associated with obtaining good cylinder-to-cylinder distribution versus good transient response. For example, if the EGR is delivered to the engine close to the inlet ports, transient response is enhanced, but obtaining good cylinder-to-cylinder distribution is more challenging. On the other hand, if EGR is delivered far upstream of the inlet manifold, mixture uniformity (and, therefore, cylinder-to-cylinder uniformity) is enhanced, but transient response is more difficult to maximize because EGR must be cleared out of a larger volume before a full air charge can be delivered to the cylinders.

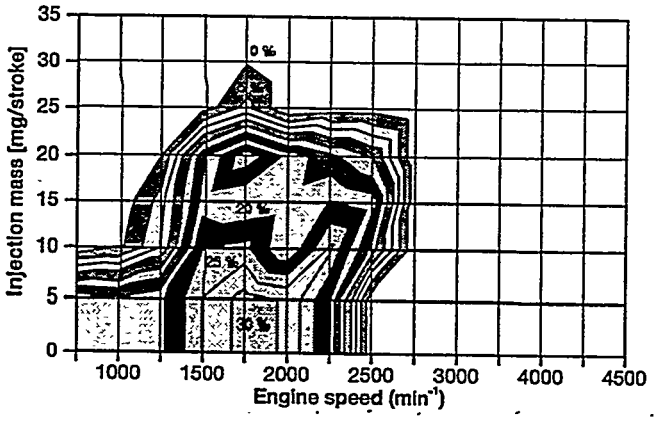


Figure 25. EGR Map as a Function of Fueling Level and Engine Speed for ECOTEC 2.0 DI Engine [3].

A second issue with EGR is cooling. Cooled EGR reduces NOx emissions by lowering charge temperature. However, depending on the system routing used, providing cooling for EGR can add complexity to the engine plumbing and create packaging challenges. One solution to this dilemma is to deliver the EGR using cooled passages internal to the cylinder head. Such an approach was used on the ECOTEC engine and is shown in Figure 26. During cold start, this EGR routing also enhances coolant warm-up and, therefore, passenger compartment heating, which is more of a challenge with HSDI diesel engines because of their low heat rejection.

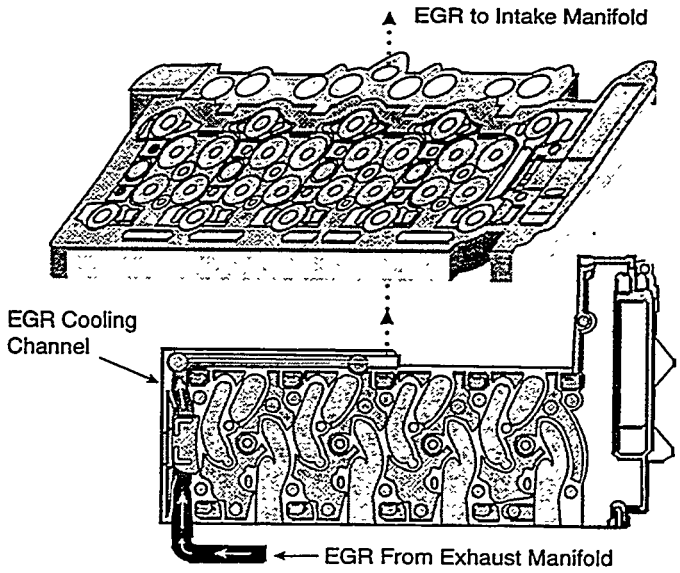


Figure 26. Exhaust Gas Recirculation Channel for the ECOTEC 2.0 Engine [3]. (shown are two horizontal slices thorough cylinder head. Lower slice shows routing of internal EGR passage through cylinder head from exhaust side to intake side. Upper slice shows exit of EGR passage after EGR passes through upper slice)

To reach minimum NOx emissions within these system constraints, EGR flow rates must be provided by the EGR system at levels that are as near to maximum combustion tolerance as cylinder-to-cylinder variation and transient response error allow.

With a typical HSDI diesel engine system, EGR is taken from the exhaust upstream of the turbocharger turbine, and it is delivered downstream of the turbocharger compressor and intercooler to avoid deposit build up in the compressor and intercooler. Depending on the turbocharger and engine characteristics, insufficient pressure difference may exist between exhaust and intake to provide sufficiently high EGR rates. One solution to this problem is to utilize an air inlet throttle, which adds some throttling losses to the engine, but may be a more practical approach than routing EGR upstream of the compressor with its system fouling and transient response shortcomings. Another approach may be possible if a VNT is used. By controlling the turbine nozzle area, exhaust back pressure could be controlled, thus providing additional means of controlling

EGR flow rate.

Needless to say, integrating the control requirements of all these functions to achieve optimum engine system performance will require extensive effort, but it will be essential to achieving emissions targets.

FUEL INJECTION SYSTEMS

The fuel injection system (FIS) is the most critical element of the combustion system of HSDI diesels, and it is a major enabler for combustion modifications to achieve optimum emissions control. For future HSDI diesel engines, the following key criteria must be met by a FIS to be a candidate for selection:

- Sufficiently high injection pressure
- Sufficiently flexible injection rate shape
- Small enough to be packaged in small-bore, four-valve cylinder head designs
- Cost competitive with electronic distributor pump systems
- Parasitic losses equal to or below those of electronic distributor pump systems
- Acceptable durability, reliability, etc.

First let us consider injection pressure. There is a well known link between smoke and particulate emissions and injection pressure (see Figure 10). In recognition of this relationship, injection pressures have been rising as illustrated by Figure 27 where maximum injection pressures or pressure ranges versus engine speed are shown for three injection systems: an older distributor-pump-based injection system (Bosch VP-37); a new distributor-pump-based system (Bosch VP-44); and a future Bosch common-rail system [14]. The expected pressure range potential of common-rail systems is also shown. The VP-37 system generates about 90 MPa at the nozzle. The Bosch VP-44 system, which was first introduced on the GM ECOTEC DI, generates about 130 MPa at the nozzle in its current form, although higher pressure versions are expected in the future.

The common-rail pressure characteristic curve shown is for a suggested calibration [14] for a

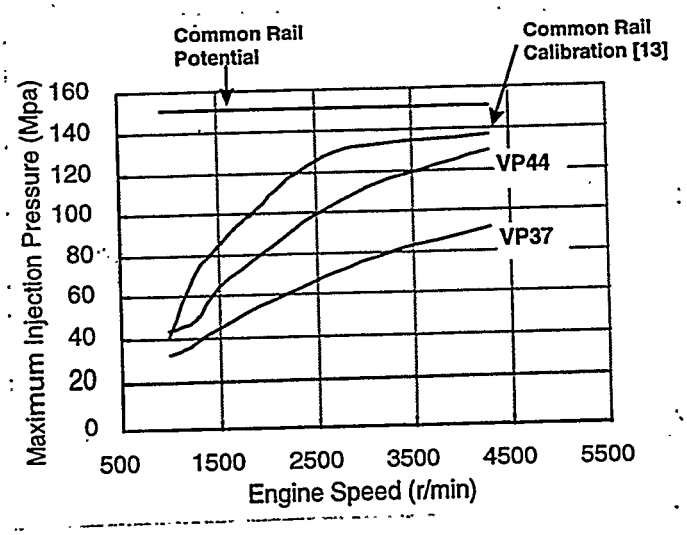


Figure 27. Injection Pressure Calibration Curves for the VP37, VP44 [3], and Common Rail Injection System [14].

future Bosch common rail system expected to be in production soon. However, as shown by the "common-rail potential" range, common-rail systems can generate higher pressures at low engine speeds and there are two potential benefits from this capability. First, high injection pressures allow increased smoke-limited peak torque due to the beneficial effect of such pressures on particulate formation. Second, we saw earlier from the single-cylinder results that higher injection pressures can be beneficial for minimizing NOx/PM emissions at low-speed part-load conditions. However, the emissions benefit of higher pressures at low engine speeds and part loads must be balanced against higher parasitic losses from increased fuel-injection pump work, which increases fuel consumption. In any event, to meet future needs for small HSDI's, a FIS should be capable of 150 MPA maximum injection pressure at as low an engine speed as possible.

Next, let us consider rate shape flexibility. Future injection systems should provide the capability for multiple injection events per combustion event. Figure 28 illustrates the needle lift versus time characteristics which may be required to optimize emissions control. The pilot pulse must reliably inject small quantities of fuel (e.g., 1-5 mm^3) at any crank angle right up to the main injection pulse. This pilot capability is important for control of emissions and noise as

shown earlier with the single-cylinder results and as shown by others [15]. But pilot capability is also important for improved starting and emissions performance at low ambient temperatures [16]. When the pilot event occurs just before the main pulse, this capability is similar to that provided by dual-spring injectors, which are used with good effect on current passenger HSDI diesels with distributor pump FISs. The influence of dual-spring nozzles on the lift curve is illustrated in Figure 28 by the "boot toe" portion of the needle-lift curve.

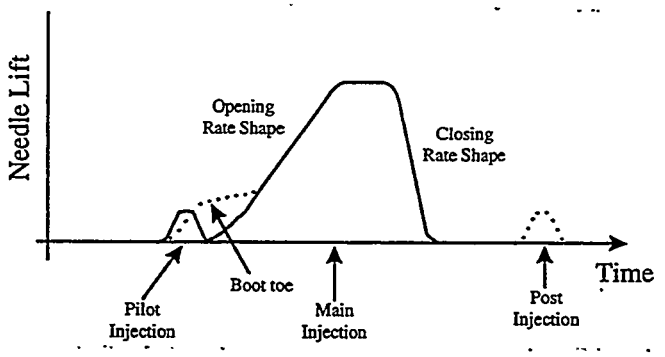


Figure 28. Flexible Needle Lift Profiles Needed for Future Injection Systems.

Accurate control of the opening rate shape is important for controlling combustion noise and NOx emissions. Injection systems such as the Ganser system used in our studies provide a means for adjusting the opening rate as shown in Figure 29. For ultimate injection control, the main injection event should have an electronically controllable opening rise rate with a rapid and repeatable closing event with no needle bounce or after injections. Finally, the FIS should be capable of injecting pilot-like quantities (i.e., as small as 1-2 mm^3) after the main injection (post injection) for two possible benefits. First, it has been shown that carefully scheduled post injections can improve the NOx/PM tradeoff in heavy duty engines [17] and reduce smoke in HSDI's [18]. Second, there are potential benefits from injection either during expansion or exhaust to provide additional exhaust hydrocarbons for use with a lean NOx catalyst.

In addition to functional requirements, there are also packaging constraints on fuel injectors

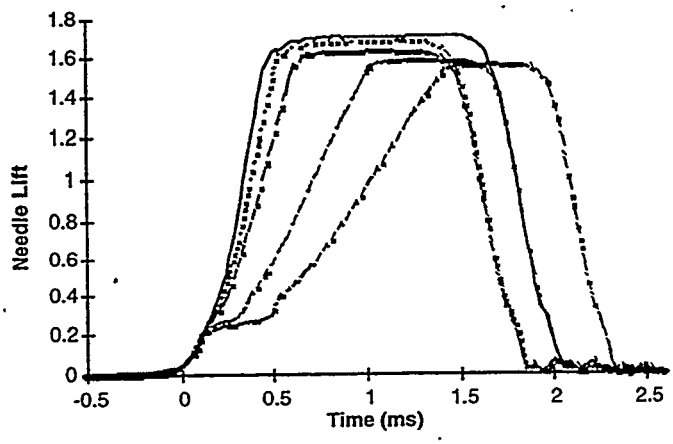


Figure 29. Needle Lift Profiles with Different Opening Rate Settings.

imposed by valve train components. These components can interfere with the top of the fuel injectors and can constrain the size of the bottom end of injectors by the need to maximize valve size while still maintaining adequate coolant flow within the cylinder head to cool exhaust ports, fuel injectors, fire deck, etc. This problem is particularly difficult for smaller bore engines (i.e., less than 80 mm bore), which are being studied for the European market [191 as well as for application to PNGV (Partnership for a New Generation of Vehicles) in the U.S.[20]

New developments in some other fuel injection system aspects could also be beneficial. Examples of such developments are the capability to manufacture smaller injector hole sizes or injector designs with variable nozzle hole area. At the present time, the practical lower bound for production nozzle hole sizes is in the range of 0.16 to 0.18 mm. This lower bound is determined by manufacturing constraints. Recent engine experiments with micro-hole nozzles that were 0.06 mm in size have demonstrated significantly shorter ignition delays and lower particulate emissions than with larger holes [21,22]. In practice, smaller holes are preferred at low load and speed to control engine noise and particulates. There is some evidence that small holes limit the maximum penetration of the liquid core of the spray jets independent of injection pressure [19]. Whereas small holes are beneficial to low load and speed conditions, more holes or larger holes are required at full load and speed conditions to deliver sufficient

fuel in a short enough time. The normal increase in injection pressure between low and high speed helps, but even more flexibility is desirable.

Variable flow area injector nozzles have long captured the imagination of DI injector designers. One approach to variable area nozzle tips is the poppet-covered orifice design which incorporates two sets of holes that are progressively uncovered with increasing needle lift [23]. An alternate approach relies on the alignment of a control surface and the nozzle hole to control the effective nozzle flow area [24]. Performance of both of these injector designs has shown promise, but neither concept has been put into production.

FUEL CHARACTERISTICS

Another potential enabler for minimizing emissions is modification of the fuel characteristics.

Reformulated Diesel Fuel

Beginning in October 1993, a low-sulfur reformulated diesel fuel was required for all on-highway use in the 49 states excluding California. Specifically, this fuel has the following limits: 0.05 weight percent sulfur maximum, 40 cetane number minimum, and 35 volume percent aromatics maximum. At the same time, California required all vehicular diesel fuel to meet the same sulfur requirement and an aromatics limit of only 10 volume per-cent maximum. Alternatively, in California, diesel fuel demonstrating equivalent or lower emissions as a reference fuel in a specific heavy-duty diesel engine test procedure could be sold [25].

The California diesel fuels are generally blended to achieve the equivalent emissions option [26,27]. Aromatic content of commercial diesel fuels in California may exceed 27% [27], but this, combined with very low fuel sulfur and high cetane number, still meets the emissions requirements. Such fuels can be expected to produce significant HC and CO reductions along with some particulate emissions advantage. However, the effect on NOx emission is minimal [26). NOx has generally proven the most difficult of all the regulated emissions to alter by fuel reformulation.

The recently completed European Auto/Oil study (EPEFE) considered the effects of fuel properties (i.e., density, polyaromatics, cetane number, and T95 distillation point) on the emissions from 19 light-duty diesel vehicles. These vehicles included 17 passenger cars and two trucks. Fourteen of them used indirect injection (1131) combustion systems and the remaining five used direct injection (DI). All of them were fitted with oxidation catalysts [28]. The vehicles were tested using the European MEG test cycle which combines urban and extra-urban test cycles. Linear regression equations were developed to show the effects of fuel properties on the exhaust emissions averaged over the test fleet [29]. Table 8 shows the reductions in exhaust emissions predicted when all four fuel properties were changed simultaneously as indicated.

TABLE 8. Predicted Emission Reductions (%) As Fuel Properties Are Changed [29]

HC	CO	NOx	PM
34	42	-3	24

Based on the following simultaneous changes in fuel properties:

Density, kg/m3	Polyaromatics, %mass	Cetane no.	T95, °C
855 → 826	8 → 1	50 → 58	370 → 325

Interestingly, the NOx emissions increased slightly. These results were dominated by the IDI vehicles, which generally showed an increase in NOx as cetane number increased. On the other hand, the DI vehicles generally emitted lower NOx as cetane number increased. Other studies on reformulated diesel fuels with reduced density, polyaromatic, and T95 (and increased cetane number) have reported NOx reductions (e.g., [30]). In any case, the effect of moderate diesel fuel reformulation on NOx emissions appears to be small. However, in those cases where NOx is the critical emission in achieving emissions compliance, it may be found that reduction of other regulated emissions (i.e., HC, CO, and PM) via fuel composition changes will provide an

opportunity to recalibrate the vehicle's emission control system for reduced NOx without increasing the other emissions above their original values. Further, substantial reductions in unregulated emissions (e.g., the mutagenicity of particulate soluble organic fraction and formaldehyde emissions) have been reported with reformulated diesel fuels [31].

Studies are currently under way to determine the emissions effects with more aggressively reformulated diesel fuels. Perhaps, the ultimate possible reformulated hydrocarbon-based diesel fuel is represented, not by a petroleum-derived fuel, but, rather, by fuels now being produced in pilot plant operations using the Fischer-Tropsch (F-T) process with natural gas as the starting material [32]. For example, Sasol has reported that diesel fuels with over 70 cetane number, less than 0.1% aromatics, and less than 10 ppm sulfur can be produced using their "Slurry Phase Distillate" version of the F-T process [33].

Beyond hydrocarbon-based reformulated diesel fuel, oxygenated hydrocarbons have been the most commonly suggested blending components for the purpose of reformulation. Alcohols have been used for this purpose, but their high octane numbers and correspondingly low cetane numbers have generally made them more attractive for use in reformulated gasoline. Oxygenated diesel fuel produced by the addition of modified vegetable oils (e.g., esterified rapeseed and soy) to diesel fuel appears to be a better choice, since the vegetable oils generally exhibit relatively high cetane numbers [34]. Their high viscosities, relatively poor low temperature properties (e.g., pour point) and decreased stability dictate that these oils be used as blending components (e.g., 20%) in diesel fuel rather than neat. An EMA (Engine Manufacturers Association) paper on the use of biofuels [34] concluded that they may be beneficial for reducing PM. Although engines fueled with these blends demonstrated reduced particulate and CO emissions, they also tended toward increased NOx emissions [34]. In addition, these fuels have typically been quite expensive compared to conventional diesel fuel, and it is not clear that they will be cost competitive for some time into the future.

Regardless of which advanced processes ultimately provide reformulated diesel fuels with the greatest value, it seems clear that the trend toward extremely low sulfur will continue. When sulfur is reduced, the possibility of catalyst poisoning is also reduced, and both oxidation and lean NOx exhaust converters become possible. Volkswagen was first to market an HSDI diesel passenger car that included a lean NOx converter, but others are likely to follow in an effort to take advantage of the outstanding fuel economy of the light-duty HSDI diesel engine while still achieving stringent emissions reductions. It remains to be shown how fuel reformulation will affect the performance of these converters.

Alternative Fuels

Many alternative fuels have been proposed for diesel engines over the years, including pulverized coal, neat alcohols, diesel fuel-water emulsions, and, more recently, "designer fuels" - materials specifically synthesized for use as diesel fuels. For the purposes of this discussion, emulsified fuels and dimethyl ether (one of the designer fuels) will be discussed, as they are currently of the most interest. A wealth of literature exists on the various other alternative diesel fuels, but a review of these other alternatives is beyond the scope of this paper.

Diesel/water emulsions have been suggested repeatedly as a practical means to simultaneously reduce particulate and NOx emissions. The addition of water or any diluent (e.g., EGR) is expected to reduce the combustion temperature and, thereby, decrease the formation of NOx [35]. The presence of water also decreases overall particulate emission in most cases. Indeed, studies of the effect of emulsified diesel/water fuels (typically 10 to 50% water) have shown that it is possible to simultaneously reduce NOx and smoke compared to a baseline diesel fuel [36,37]. Recently, Caterpillar participated in a joint venture to develop proprietary diesel/water emulsions for reduced emissions. Although the joint venture has been dissolved, Caterpillar's work continues, and significant benefits in both particulate and NOx emissions have been reported [38] along with some disadvantages (e.g., higher HC

emission). Further reports on emulsified diesel fuel performance from Caterpillar and other companies are expected. Even if successful in reducing emissions, these fuels will need to overcome major barriers to their widespread use in the form of higher cost, inadequate infrastructure development, and fuel system incompatibilities.

Dimethyl ether (DME) consists of two methyl groups chemically bonded to a central oxygen atom. It is currently produced from natural gas, and it is used as a propellant for cosmetics aerosols sold in Europe. As with methanol, since the fuel is partially oxidized and it contains no carbon-carbon bonds, the possibility of forming carbonaceous particulate emissions during combustion of DME is essentially eliminated. However, unlike methanol, DME has a high enough cetane number - >55 [391 - to perform well as a compression-ignition fuel. Also, unlike methanol, DME is a gas at ambient temperature and pressure, so it must be stored under pressure as a liquid similar to LPG (liquefied petroleum gas). Its physical properties (e.g., density, viscosity, lubricity, etc.) are so different from diesel fuel that the entire fuel system must be redesigned [40]. Preliminary studies have concluded that it should be possible to just achieve ULEV emissions using a properly designed DME-based fuel injection system with an HSDI engine and an oxidizing catalytic converter in a passenger car [39].

It seems clear that DME and, perhaps, other fuels will be able to produce much larger emissions reductions than will be possible with diesel fuel for a specific level of complexity of the fuel storage and injection system. However, it is not clear that this apparently inherent emissions advantage can offset the fuel's lack of established supply infrastructure and the need to distribute and carry a pressurized fuel onboard the vehicle. Before DME or other alternative fuels become used extensively in compression ignition engines, the tradeoff between the complexity of engine and fuel system development with reformulated (liquid) fuels and their emission performance must be established. If emissions targets can be achieved with liquid fuels that can be distributed and handled by the existing diesel fuel infrastructure, it is unlikely that alternative compression ignition fuels will play a significant role.

EXHAUST AFTERTREATMENT

As noted earlier, two exhaust constituents pose the greatest challenge in meeting future diesel emission standards: NOx and particulates. Given the interrelationship that exists between the engine-out levels of these two, any aftertreatment that reduces the emissions of one will allow the other to be reduced by engine calibration. The approaches currently offering the greatest hope of reducing exhaust NOx concentrations are the selective reduction of the NOx by either a catalyst or by a catalyst working in conjunction with a plasma discharge in the exhaust. The approaches currently offering the greatest hope of reducing exhaust particulate mass are particulate filters, an exhaust plasma (which is reported to reduce NOx as well), and catalysts to oxidize the heavy hydrocarbons before they condense on the soot to become the soluble oil fraction (SOF).

NOx Reduction

Lean NOx catalysts have received a great deal of attention in the 1990's. These catalysts are designed to react HC's present in the exhaust selectively with NOx rather than with oxygen. Figure 30 shows the HC and NOx conversions as a function of temperature for one such catalyst developed by the USCAR Lean NOx CRADA [41]. Typical of all such catalysts, NOx conversion is poor at low temperature, the conversion rises to a maximum at an intermediate temperature, and then it falls as the temperature increases further. The maximum NOx conversion generally takes place close to the temperature at which the HC lights off. The temperature at which the maximum NOx conversion occurs is a function of the active metals used, with the maximum for Pt-containing catalysts in the 200-250 C range, while the maximum for Cu-containing catalysts is in the 450-500 C range. The activity-temperature characteristics of the Pt-based catalyst are most compatible with diesel exhaust, the temperature of which ranges between 150 C and 400 C in the Euro or U.S. test cycles. The major problems faced by lean NOx catalysts

are: the narrowness of the temperature window; the limited NOx conversion, even at the optimal temperature; and the need for HC's for the selective reduction of NOx. The inherently low level of HC's in the exhaust from direct-injection diesels will require that the exhaust HC's be enhanced by the addition of fuel during either the expansion or exhaust strokes, as was suggested above in the Fuel Injection discussion. The Pt catalysts face the additional shortcomings of being highly active for sulfate formation and for forming N_20, a principal NOx reduction product, which is a potent greenhouse gas.

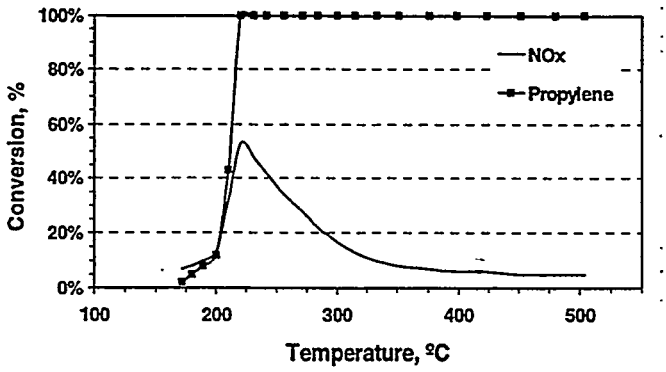


Figure 30. HC and NOx Conversions with a Pt-Containing Lean-NOx Catalyst.

The concept of using a nonthermal plasma to remove NOx has been discussed for a long time but has generally been dismissed as impractical. Penetrante et al [42] have shown that the minimum electrical energy to remove 100 ppm of NO from a gas by plasma-induced gas-phase reactions is 15 Joules per liter of exhaust treated (6.5 ppm NOx/Joule/L,), a value too high to be of interest for automotive applications. Recently, though, coupling the plasma approach with a catalyst to reduce the energy requirement of the system has been considered. Most of the work in this area is proprietary, and while many claims abound, little information exists in the technical literature. NOxTECH, a firm that plans to commercialize the plasma-catalyst system for NOx removal, has reported that they obtain greater than 70% removal of both NOx and particulates from diesel exhaust with less than a 7% fuel economy penalty [43].

Particulate Reduction

The amount of particulates in diesel engine exhaust can be reduced by filtering, and this approach has been investigated extensively. The primary difficulty is not the filtration (or trapping), but the regeneration of the trap by burning off the collected soot. The combustion temperature of soot can vary but generally begins at about 500° C [44], a temperature that is not encountered often in the exhaust of a light-duty direct-injection diesel. The ignition of the soot can be initiated by a burner or by electrical heat. The ignition temperature of the soot can also be lowered by the addition of iron, copper, or cerium additives to the fuel. Pattas et al. [45] were able to induce trap regeneration at 300° C by doping the fuel with 100 ppm of cerium, but they found that the increased back pressure due to the soot accumulation could result in as much as a 15% fuel economy penalty.

As mentioned previously, the nonthermal plasmas that are reported to reduce NOx are also reported to reduce particulates, but such claims have not been verified. Measuring the impact of catalysts on particulates can be difficult, since catalyst beds can retain particulates for extended periods of time.

Heavy HC's that are present in diesel exhaust will condense on the particulates, thereby increasing the mass of the particulates. Oxidation catalysts have been used for a number of years to oxidize some of the HC's in diesel exhaust, reducing both the HC and particulate emissions. However, catalysts that are highly active for HC oxidation also tend to be active for oxidizing $S0_2$ to $S0_3$, which collects on particulates, also increasing the mass of the particulates. Catalysts can be designed to offer reasonable HC oxidation performance without excessive levels Of $S0_2$ oxidation activity [46]. Hammerle et a[. [47] recently showed an 18% reduction in the particulate emissions from an HSDI diesel engine during an FTP test using such an oxidation catalyst.

Exhaust aftertreatment for diesel engines is a critical technological area to the ability of diesel engines to meet future emissions standards.

Despite much progress in this area, many challenges remain that offer opportunities for progress.

ENGINE CONTROLS

Another important enabler for emissions control is highly capable engine controls.

The high EGR tolerance and low NOx/PM trade-off observed in the single-cylinder engine tests cannot be exploited in a multi-cylinder engine without a capable emissions control system. With the enabling technologies listed above, the emissions control system must manage control of the fuel injection process, which, for a common-rail system, involves numerous parameters such as pilot injection, rail pressure, injection rate, and post injection during the expansion or exhaust strokes to provide HC for a lean NOx catalyst. In addition to fuel injection, the control system must manage the actuation and modulation of port throttles (if used), EGR valve, inlet throttle (if used), turbocharger (either wastegate or VNT control), and possibly a separate catalyst fuel system, if a common-rail injection system is not used. One capability that would be useful for meeting future emissions standards is closed-loop control of EGR, which would not only enable more aggressive EGR calibrations, but also compensate for changes in engine and EGR system components over the life of the vehicle.

HYBRIDIZATION TO ENABLE EMISSIONS CONTROL

Although hybridization was discussed earlier with regard to performance and efficiency, hybridization also offers opportunities as an emissions control enabler to help achieve Tier 2, ULEV, and Euro Stage IV emissions standards with HSDI diesel engines. For example, emissions occurring during engine transients could possibly be reduced through hybridization by applying stored energy to shave transient change rates. Also, during more steady-state operation, there may be opportunities to modify exhaust temperature by modulating energy storage system charging or withdrawal rates to enable more optimum exhaust gas aftertreatment. However, the extent to which such opportunities exist or can be effectively exploited remains to be determined.

CLOSURE

Today's HSDI diesel engine offers demonstrated fuel economy advantages unmatched by any other engine. HSDI diesels are also proven and, in their latest implementations, offer similar pleasability to that of the SI engine. However, to remain a contender in the future, HSDI diesels must meet the challenges posed by tighter emissions standards and tighter competition for product value (i.e., "value" standards). Because HSDI diesels are more costly to produce than SI engines, future value standards will be most easily met by HSDI diesels for customers for whom fuel costs are an important part of the cost of vehicle ownership, thus allowing recovery of the higher initial purchase price. Stringent value competition will continue to be provided by technologies based on the SI engine, particularly for customers with lower fuel costs. In addition, evolutions of the conventional SI engine are expected to meet the future emissions standards with much less difficulty than for HSDI diesels. Hybrid drivetrains offer an opportunity and a challenge for HSDI diesels -- an opportunity for the use of diesels as part of such drivetrains and competition for diesels when other fuel-driven power sources are used.

Thus, HSDI diesels are one option for future personal transportation powertrains whose attributes must be weighed against the different attribute sets of other technologies as we configure powertrains and vehicles for the next century for differing markets throughout the world.

ACKNOWLEDGMENTS

The authors would like to thank Jim Cauley and Gerry Malta for their support of the single-cylinder engine work as well as the other members of the diesel engine team in the Engine Research Department.

REFERENCES

1. Gallopoulos, N.E.,"Bridging the Present to the Future in Personal Transportation - The Role of Internal Combustion Engines," SAE Paper 920721, 1992.

2. Gallopoulos, N.E.,"Don't Hurry to Write the Epitaph of the Internal Combustion Engine," GM R&D Publication R&D-8466, January 22-23, 1996.

3. Zima, P., Steiger, W., "Opel's New Two Liter 4-Valve DI Diesel Engine," 8' International Conference CONAT 96,13-15 Nov. 1996, Brasov

4. Malliaris, A.C., Hsia, H., Gould, H.,"Concise Description of Auto Fuel Economy and Performance in Recent Years, SAE Paper 760045, 1976.

5. Rhode, W. and Jeckel, D. "Le Nouveau Moteur 1,9 L TDI 81 KW Developpe par Volkswagen," S.I.A. Conference, (Le Moteur Diesel: Evolutions et Mutations), Ecole Centrale de Lyon, April 10-11, 1996.

6. Asmus, T. Belaire, R., Skellenger, G. "Energy Converters for the PNGV Vehicle," SAE Paper to be Presented at Future Transportation Technology Conference, SAE, August 6-9, 1997.

7. Edwards, S.P. Penny, I.J., and Ross-Martin, T.J., "The Development of the Ricardo CERES HSDI Diesel Engined Passenger Car for Euro 3 and Beyond," 4th International Conference on The Automotive Industry and the Environment, Session 3, Paper 5, Brussels, September 17-18, 1996.

8. Faulkner, S.A., Perkins Technology Consultancy presentation to PNGV 4SDI Technical Team, February 28, 1997.

9. Ganser, M.A., "Operating Characteristics of a Common-Rail Type Fuel Injector for Passenger Car and Light-Duty Truck DI-Diesel Engines," SIA Paper 9506A12, European Automobile Engine Cooperation, 5th International Congress, Strasbourg, 21-23 June 1995.

10. Waters, W.C., "General Purpose Automotive Vehicle Performance and Economy Simulator," SAE Paper 720043,1972.

11. Herrmann, H.O., and Dürnholz, M., "Development of a DI-Diesel Engine with Four Valves for Passenger Cars," SAE Paper 950808,1995.

12. Wünsche, P., König, F., "AVL Leader - The Development of a New High-Speed DI Diesel Engine Generation," Automotive Design Yearbook, 1995.

13. Menne, R.J. et al., "Ford 4-Valve Light Duty DI Diesel Development," SAE Paper 9419-26,1994.

14. Stumpp. G., and Ricco, M., "Common Rail - An Attractive Fuel Injection System for Passenger Car DI Diesel Engines," SAE Paper 960870,1996.

15. Dürnholz, M., Endres, H., and Frisse, P. "Preinjection a Measure to Optimize the Emission Behavior of a DI-Diesel Engine," SAE Paper 940647, 1994.

16. Osuka, I., Nishimura, M., Tanaka, Y., and Miyaki, M., "Benefits of New Fuel Injection System Technology on Cold Startability of Diesel Engines - Improvement of Cold Startability and White Smoke Reduction by Means of Multi-Injection with Common Rail Fuel System (ECD-U2)," SAE Paper 940586,1994.

17. Pierpont, D.A., Montgomery, D.T., and Reitz, R.D., "Reducing Particulate and NOx Using Multiple Injections and EGR in a D.I. Diesel," SAE Paper 950217,1995.

18. Ishida, S., Ichimasa, T., Sano, T., Sato, K.. "Isuzu's Approach to Small DI Diesel Engines," Symposium on Newly Developed Diesel Engines, JSAE Tokyo, March 8,1997, Symposium Number 9703.

19. Abthoff, J., Duvinage, F., Pischinger, Weber, S., 'The Potential of Small DI-Diesel Engines with 250 cm^3/cylinder for Passenger Car Drive Trains," SAE 970838,1997.

20. Boggs, D.L., Belaire, R.C., Bartunek, B.,

Dürnholz, Ecker, H.J., "A Small Displacement DI Diesel Engine Concept for High Fuel Economy Vehicles," SAE 97FTT-65,1997.

21. Kobori, S., Kamimoto, T., and Kosaka, H., "Ignition, Combustion and Emissions in a DI Diesel Engine Equipped with a Micro-Hole Nozzle," SAE Paper 960312,1996.

22. Iida, N., Nishimura, H., Kotsuji, T., Yoshida, Y., and Hosonuma, S., "Effects of High-Pressure Fuel Injection and a Micro-Hole Nozzle on Combustion in a Rapid Compression Machine," SAE Paper 970893,1997.

23. Sczomak, D.P., "The Poppet Covered Orifice Fuel Injection Nozzle," SAE Paper 900821, 1990.

24. Potz, D., Kreh, A., and Warga, J., "Variable Orifice Geometry Verified on the Two-Phase Nozzle (VRD)," SAE Paper 950081, 1995.

25. SAE J313, "Surface Vehicle Recommended Practice Diesel Fuels," proposed draft, January 1997.

26. Nikanjam, M., "Development of the First CARB Certified California Alternative Diesel Fuel," SAE Paper 930723,1993.

27. American Automobile Manufacturers Association, "International Fuel Survey - Diesel Fuel," Summer 1996.

28. Steinbrink, R., Cahill, G., Signer, M., and Smith, G., "European Programmes on Emissions, Fuels and Engine Technologies (EPEFE) - Vehicle/Engine Technology," SAE Paper 961067,1996.

29. Hublin, M., Gadd, P., Hall, D., and Schindler, K., "European Programmes on Emissions, Fuels, and Engine Technologies (EPEFE) - Light Duty Diesel Study," SAE Paper 961073, 1996.

30. Rantanen, L., Mikkonen, S., Nylund, L., Kociba, P., Lappi, M., and Nylund, N., "Effect of Fuel on the Regulated, Unregulated and Mutagenic Emissions of DI Diesel Engines," SAE Paper 932686, 1993.

31. Rantanen, L., Juva, A., Niemi, A., Mikkonen, S., Aakko, P., and Lappi, M., "Effect of Reformulated Diesel Fuel on Unregulated Emissions of Light Duty Vehicles," SAE Paper No. 961970, 1996.

32. Salomon Brothers, "Gas-to-Liquids Technology -Dawning of New Era for Global Natural Gas," November 6, 1996.

33. SASOL, http://www.sasol.com/textonly/Tslurry4.htm.

34. Engine Manufacturers Association, "Biodiesel Fuels and Their Use in Diesel Engine Applications," EMA, Chicago, August 1995.

35. Ahmad, T., and Plee, S., "Application of Flame Temperature Correlations to Emissions from a Direct-Injection Diesel Engine," SAE Transactions, 92, SAE Paper 831734,1983.

36. Odaka, M., Koike, N., and Tsukamoto, Y. "Reduction Effect of Emulsified Fuel on NOx and Smoke Emissions from Direct Injection Diesel Engines," JSAE Review, 14 (2), 1993, 85.

37. Tsukahara, M., Yoshimoto, Y., "Reduction of NOx, Smoke, BSFC, and Maximum Combustion Pressure by Low Compression Ratios in a Diesel Engine Fuelled by Emulsified Fuel," SAE Paper 920464, 1992.

38. Personal Communication from Richard Cemenska, November 22,1996.

39. Kapus, P., and Cartellieri, W., "ULEV Potential of a DI/TCI Diesel Passenger Car Engine Operated on Dimethyl Ether," SAE Paper 952754, 1995.

40. McCandless, J., and Li, S., "Development of a Novel Fuel Injection System (NFIS) for Dimethyl Ether -and Other Clean Alternative Fuels," SAE Paper 970220,1997.

41. Gardner, T.J., Presentation to Pacific Coast Regional Meeting of The American Ceramics Soc., Seattle, WA, November 1995.

42. Penetrante, B.M., Hsiao, M.C., Merritt, B.T., and Vogtlin, G.E., "Fundamental Limits on NOx

Reduction by Plasma," SAE Paper 97FL-258,1997.

43. Personal Communication, V. Palekar, NOx-TECH, Irvine, CA. March 19,1997.

44. Otto, K., Sieg, M.H., Zinbo, M., and Bartosiewicz, L., "The Oxidation of Soot Deposits from Diesel Engines," SAE Paper 8003-36,1980.

45. Pattas, K., Kyriakis, N., Samaras, Z., Mustel, W., and Rouveirolles, P., "The Effect of Size and Positioning of Ceramic DPFs on Regeneration Induced by a Cerium Based Additive," SAE Paper 970184, 1997.

46. Wyatt, M., Manning, W.A., Roth, S.A., D'Aniello, Jr., M.J., Andersson, E.s., and Fredholm, S.C.G., "The Design of Flow-Through Diesel Oxidation Catalysts," SAE Paper 930130,1993.

47. Hammerle, R.H., Ketcher, D., Horrocks, R.W., Lepperhoff, G., Huthwohl, G., and Luers, B., "Emissions from Diesel Vehicles With and Without Lean NOx and Oxidation Catalysts and Particulate Traps," SAE Paper 952391, 1995.

48. MacDonald, J.S., Plee, S.L., D'Arcy, J.B., and Schreck, R.M., "Experimental Measurements of the Independent Effects of Dilution Ratio and Filter Temperature on Diesel Exhaust Particulate Samples," SAE Paper 800185, 1980.

APPENDIX - SINGLE-CYLINDER ENGINE INSTRUMENTATION AND TEST PROCEDURES

A brief description of test measurements and procedures is given in this appendix for the single cylinder engine-dynamometer studies reported in this paper.

GASEOUS EXHAUST EMISSION MEASUREMENTS

Gaseous exhaust emissions measurements were made as listed in Table A-1. An additional $C0_2$ analyzer was used to sample $C0_2$ concentrations in the intake plenum to calculate EGR or in the dilution mini-tunnel to calculate dilution ratio for calculation of particulate mass.

TABLE A-1

Component	Units	Analyzer Type
HC	ppm C_3	Heated Flame Ionization Detector
CO	ppm	Infrared Analyzer
CO_2	%	Infrared Analyzer
O_2	%	Magneto-Pneumatic Analyzer
NOx	ppm	Chemiluminescence Analyzer using NO_2 to NO Converter

EXHAUST PARTICULATES

Actual particulate mass measurements were made on a more selective basis due to the time and effort required for collection and analysis. Particulate emissions were measured on a filter using a dilution mini-tunnel [48]. A small fraction of the exhaust is extracted and diluted within the tunnel. A portion of the diluted exhaust is then drawn though the filter.

Prior to test, new filters (47-mm diameter Pallflex Fiberfilm T60A20) were baked in a vacuum oven for 4 hours at 210°C while maintaining a vacuum of 88 kPa. Following stabilization for at least one hour in a temperature- and humidity-controlled room, the filters were weighed using a micro-balance before and after collection to determine the total particulate mass. Then, to drive off the volatile particulate material; the filters were baked in the vacuum oven again, using the same procedure as for new filters. Re-weighing the baked filters after stabilization gave the dry particulate mass.

During collection, a filter temperature of 50° C and a face velocity of 0.7 m/s were maintained. Dilution ratio was controlled within the range of 5 to 8:1.

OTHER MEASUREMENTS AND CALCULATIONS

The data for each test point were acquired every half second and averaged over a 90-s period. Fuel injected quantities and timing were specified with control pulses to the fuel injector. Fuel rail pressure was controlled independently to alter injection rate. The resulting fuel flow was measured with a constant volume flow me-

ter that outputs 110 pulses per cm^3 of fuel. Airflow was controlled and measured by varying the upstream pressure to four critical flow nozzles of different sizes that can be selected in any combination. Measured air-fuel ratio was checked with that from exhaust gas analysis using both carbon-balance and oxygen-balance calculations. Exhaust gas analysis also was used to convert raw emission concentration measurements to emission index (mass emissions in grams per kg of fuel). By controlling airflow and exhaust pressure, inlet and exhaust pressure levels were set to simulate naturally aspirated or turbocharged operating conditions.

Cylinder pressure was measured with an AVL QC32C water-cooled piezoelectric pressure transducer mounted flush in the cylinder head. The common rail fuel injector included a needle-lift sensor. For routine testing, cylinder pressure and needle lift were digitized every 1.0 crank angle degree using an engine-driven shaft encoder and digital oscilloscope, producing a data file averaging 64 non-consecutive cycles. Post processing included pressure analysis and a simple heat release analysis of that average file. More detailed analysis, when warranted, was accomplished by digitizing 64 consecutive cycles of cylinder pressure and needle lift every 0.2° crank angle using a dedicated high-speed data acquisition system and post-processing the individual cy-cles with a rigorous pressure and heat release analysis.

MULTIPLE-POINT OPERATING CONDITIONS FOR SIMULATION OF FTP

Table A-2 gives the seven steady-state test conditions used in this paper to project emissions on the urban test cycle (FTP) from single-cylinder engine data. The modeled powertrain includes a 2.56-L DI diesel engine with a 5-speed manual transmission powering a 1588-kg test weight vehicle. The single-cylinder engine is run at each speed and IMEP (dynamometer indicated, not cylinder-pressure based) listed in Table A-2. That IMEP gives the required BMEP when using motoring mean effective pressures (MMEP) typical of multi-cylinder engines. The equation for MMEP given in Table A-2 is a correlation of passenger car size DI diesel engines having rotary injection pumps.

For each test point, the fuel rate times the ratio of the multi-cylinder to single-cylinder engine displacement (2.56/0.426) gives the projected multi-cylinder fuel rate. The product of that fuel rate (kg/s), the pollutant emission index (g/kg), and time (s) gives the pollutant mass emissions (g) for each test point. Then the sum of pollutant mass for all test points divided by the FTP cycle distance (7.44 miles) gives the projected g/mi values.

TABLE A-2

Point #	Schedule	Engine Speed (rpm)	Brake Torque (Nm)	BMEP (kPa)	IMEP* (kPa)	Time (s)	Energy (kWh)
7-POINT FTP							
1	FTP	800	2.0	10	181	363.5	0.3117
2	FTP	1714	122.9	604	793	62.2	0.5007
3	FTP	2296	85.3	419	633	67.8	0.5835
4	FTP	2215	24.4	120	330	212.0	0.9177
5	FTP	1731	7.33	36	226	279.9	0.6485
6	FTP	1706	57.6	283	472	216.5	1.032
7	FTP	1027	18.9	93	266	62.2	0.1006
					SUM =	1264.1	
					(TOT. FTP =	1372.1)	

* MMEP = 176.4 -1.880E-2*(rpm) +1.526E-5*$(r/min)^2$

DIESEL ENGINE EMISSIONS REDUCTION HISTORY AND FUTURE PROSPECTS

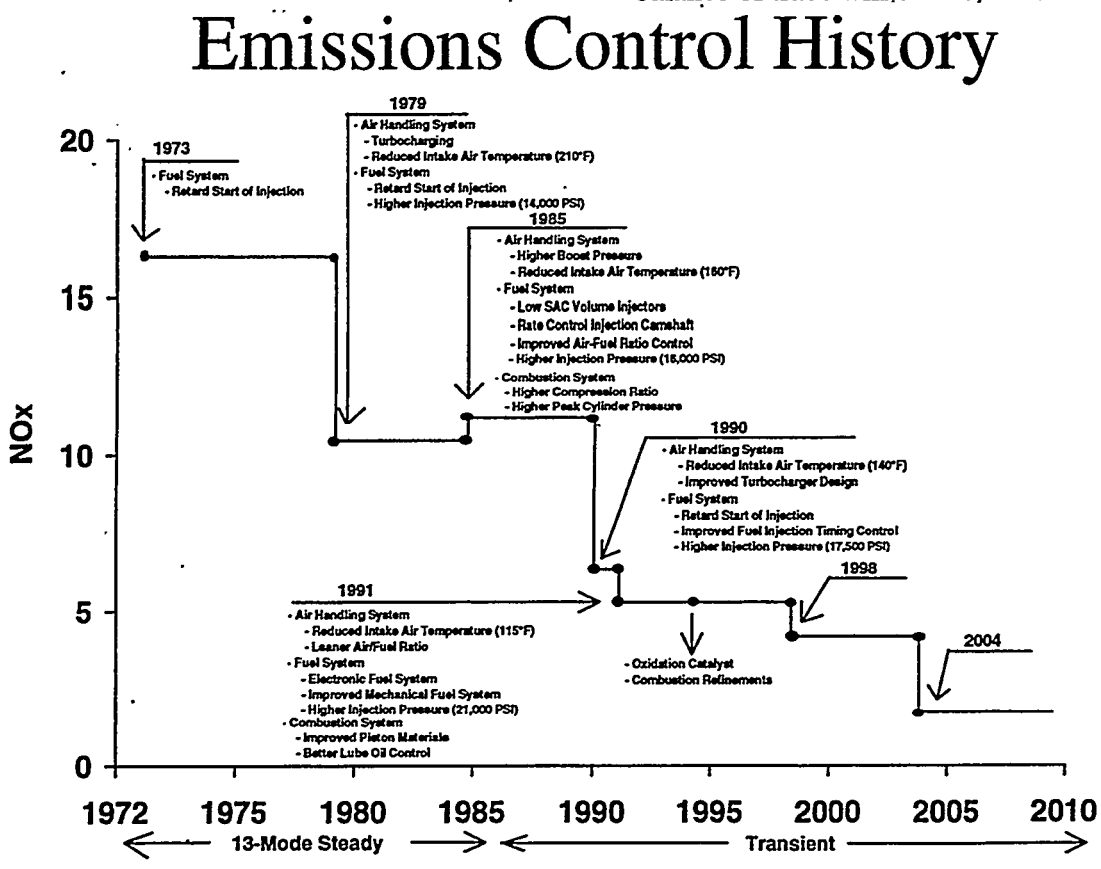
J.W. Patten
Cummins Engine Company, Inc.

Heavy Duty trucks now achieve about 8-10 mgp, or about 1/2 to 1/3 the vehicle fuel economy of a current full size automobile and 1/8 to 1/10 the vehicle fuel economy of a PNGV automobile. However, on a weigh-specific basis, heavy duty trucks are 4 times more efficient than a PNGV automobile and, on a cargo specific basis, they are 5 to 10 times more fuel efficient.
The Heavy Duty transportation community is driven by economics = fuel consumption.

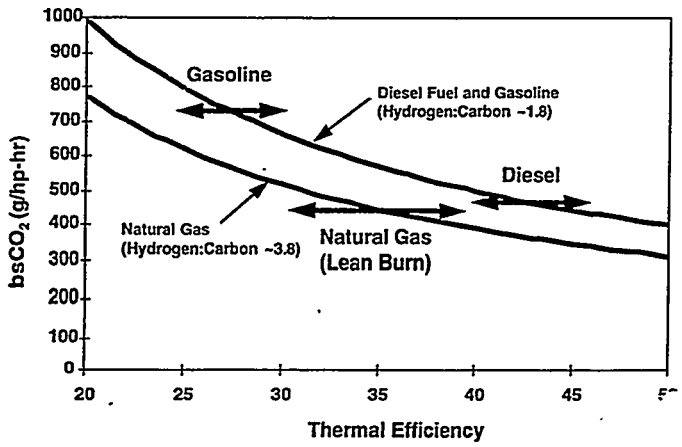
Heavy Duty trucks are 80,000 lb. vehicles, or about 40 times as heavy as a PNGV automobile (at 2000 lbs.).

Heavy Duty trucks carry about 55,000 lbs., or about 50-100 times the cargo of a full size automobile.

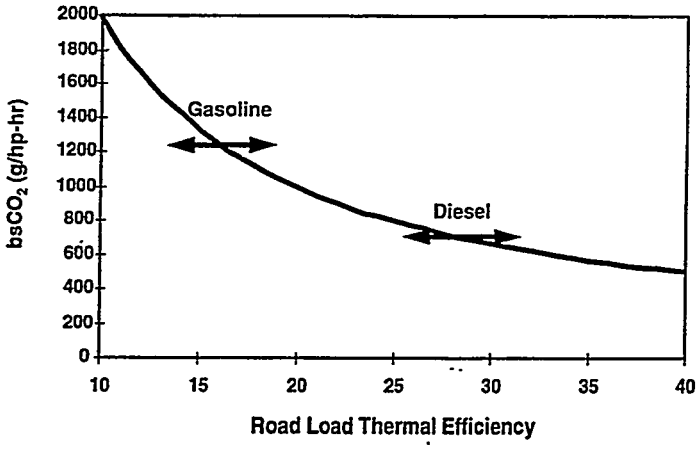
Heavy Duty trucks have become this efficient by very aggressively pursuing the most fuel efficient technology available, and virtually all such trucks are now diesel powered. Diesel emissions reductions from state-of-the-art heavy trucks have directly tracked fuel economy improvements, so that today's diesel engines are very clean. Furthermore, new diesel emissions technology developments are emerging at a rapid rate, and the potential for continued reductions in heavy duty diesel emissions are very good.
Cummins Engine Company believes that our heavy duty diesel technology can be applied to personal transportation vehicles, beginning with sport utility vehicles (now 42% of all new personal transportation), and perhaps extending to PNGV vehicles. If this can be accomplished, the improvements in emissions/air quality, fuel consumption, petroleum independence, and the balance of trade will be very worthwhile.



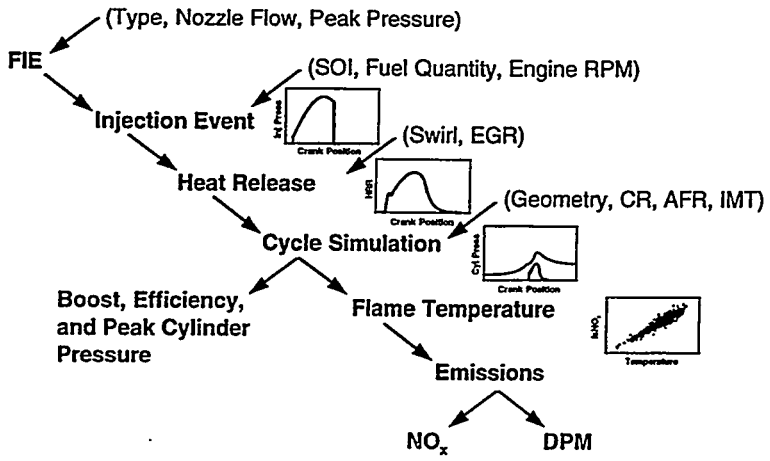
$bsCO_2$ Emissions @ Peak Efficiency



bsCO2 Emissions @ Road Load



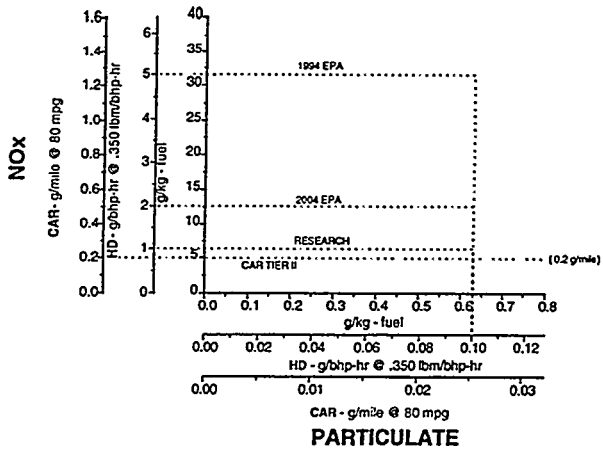
Combustion Modeling Capabilities



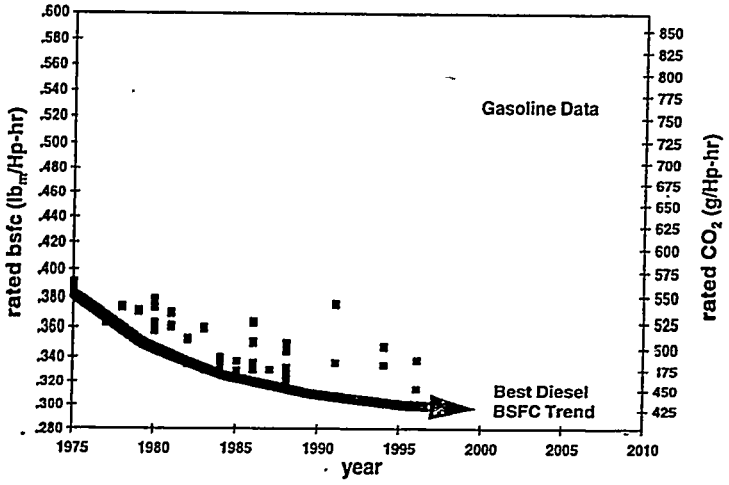
Emission and Performance Goals:

- Exhaust Emission Requirements
  - CO
  - HC
  - NOx
  - Particulate
- Fuel Economy
- Low Noise
- Drivability and Transient Response
- Off Design Performance

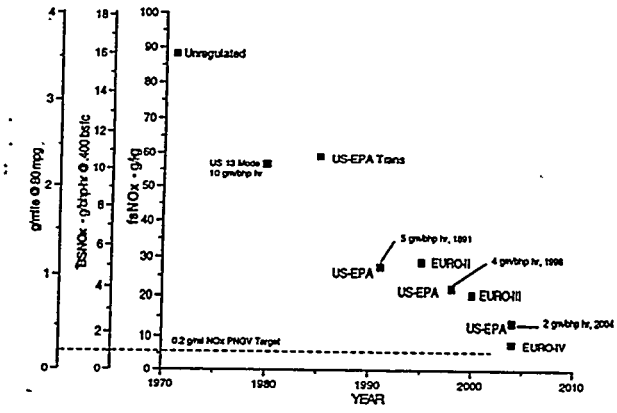
DIESEL EMISSIONS



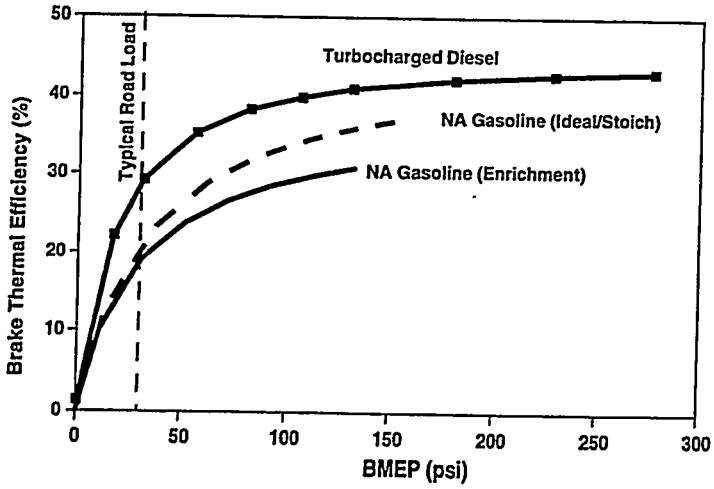
Rated bsfc History



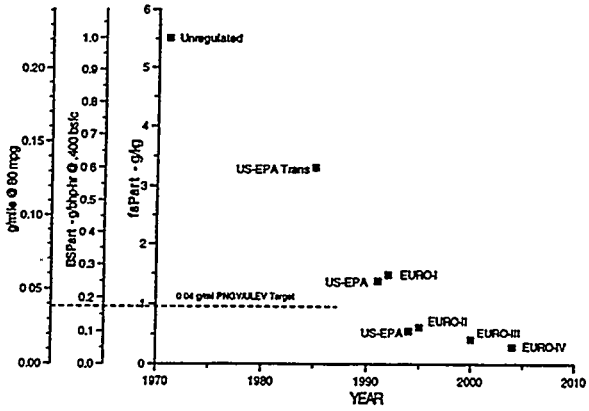
HDD NOx History/Targets



Brake Thermal Efficiency Comparison

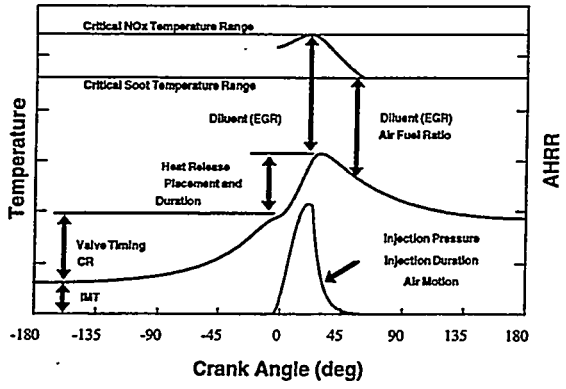


HDD Particulate History/Targets

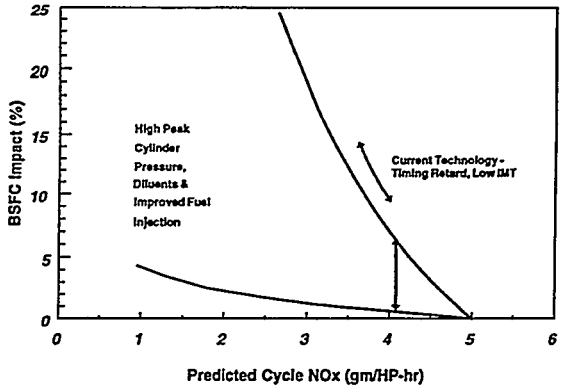


Design Space:

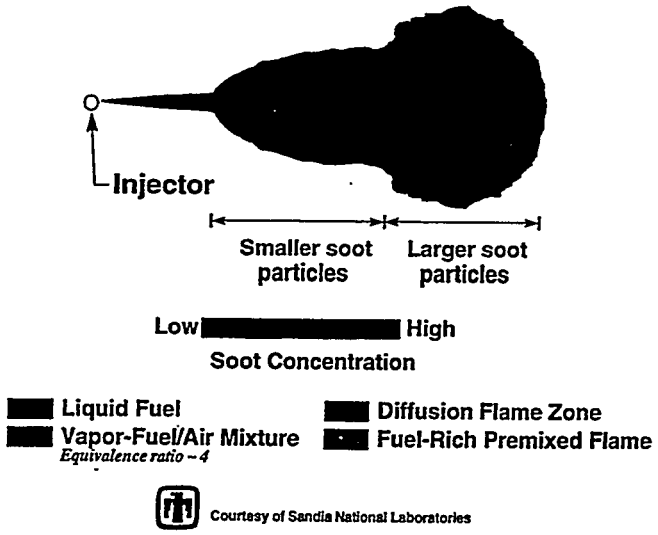
Impact on NOx, Particulate



Application of Technologies:



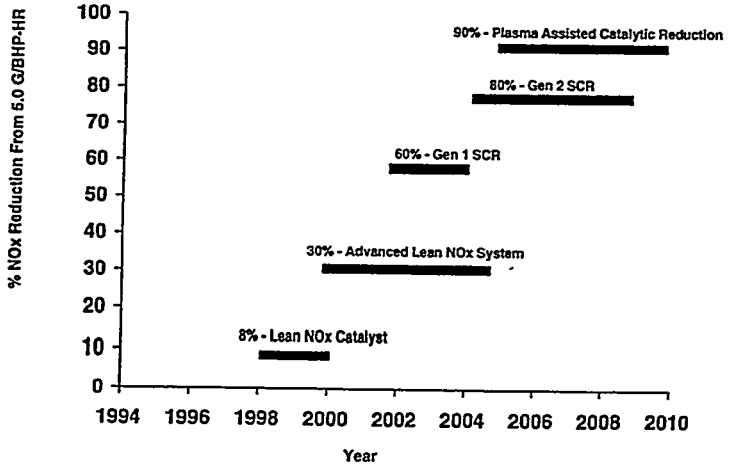
New Conceptual Model of Diesel Combustion



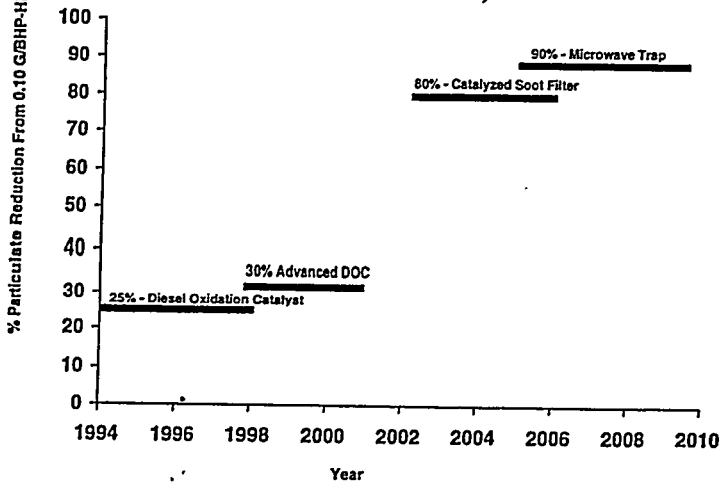
Courtesy of Sandia National Laboratories

Projected NOx Reduction

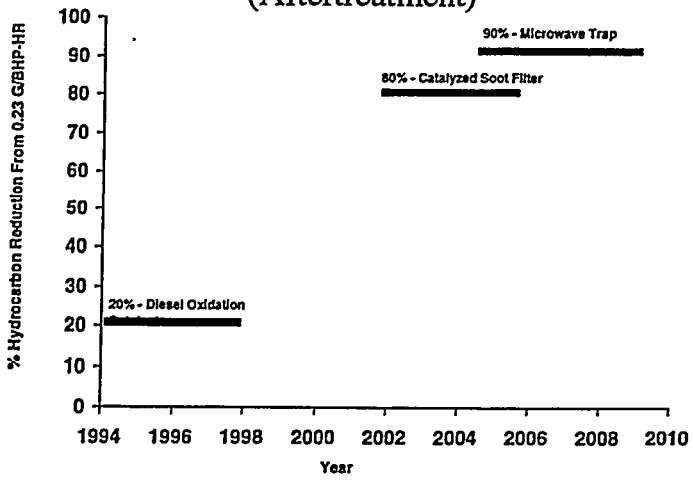
(Aftertreatment)



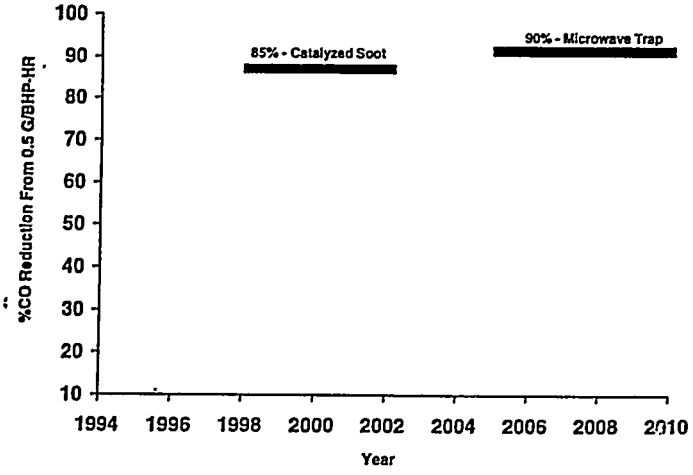
Projected Particulate Reduction
(Aftertreatment)



Projected Hydrocarbon Reduction
(Aftertreatment)



Projected CO Reduction
(Aftertreatment)



Other Technology Opportunities With Diesel Engines

Alternate Fuels

Reformulated Diesel

F.T. Diesel (natural gas and biofuel feed stocks)

CNG

DME

Lean Homogenous Charge Compression Ignition

"LET'S CORRECT THE IMAGE OF THE DIESEL AND LET'S GET REAL ABOUT THE NEXT 20 YEARS"

T. Vachon
Caterpillar Inc.

To appreciate the diesel cycle engine and its future potential, one must first get beyond the traditional image. Societal cost/benefit summaries for the current populations of both gasoline and diesel powered vehicles are given. The benefits in terms of the transportation work performed, and the costs are in terms of the fuel energy consumed plus the emissions of criteria air pollutants, toxins, and greenhouse gases.

Reducing the total societal cost of transportation is an important national need. DOE's OTT understands this and has addressed the problem by helping to set the stage and provide the handwriting on the wall:

The stage is set with the unprecedented industry/government transportation R&D collaborations managed by OAAT and OHVT.

The handwriting on the wall is the new information that these programs have already produced.

In the big picture, the new information from OAAT is simply that the longer range technologies are further out than many thought. From OHVT, it is the recognition that development of advanced HSDI (high speed direct injection) diesel engines for light trucks provides the greatest potential for major reductions in fuel use and CO_2 emissions. In this year of the PNGV technology downselect, and DOE's reorganization to better effect real world change, we must make best use of this valuable new information. Best use is simply accepting all the facts and better predictions we now have regarding new technologies, required infra-structures, market demands, future oil price, tax policy, regulations, etc. This collective new, and better informed, view of the future strongly suggests:

1. We can make a significant impact on the social cost of transportation within the next 20 years.

2. The critical enabler will be a much cleaner and user friendly generation of diesel cycle engines.

HOW BAD ARE DIESEL EMISSIONS ?

WHAT ABOUT THE CO2, FUEL EFFICIENCY AND FLASHPOINT ADVANTAGE ?

WE NEED A FAIR MEANS OF COMPARISON.

WE NEED TO GET CALIBRATED.

CAN WE ESTIMATE A TOTAL SOCIETAL COST WITH A LOGICAL COMMON DENOMINATOR ?

COST/BENEFIT ANALYSIS ?

ON-ROAD VEHICLE EMISSIONS

DIESEL VS. GASOLINE

Ref.: EPA National Air Pollutant Emission Trends, Oct. 1996, etc.

	GASOLINE % SHARE	DIESEL % SHARE	
ENERGY USE			
% Trans. Oil Energy	81	19	
TRANS WORK (ton-miles)			
% Trans. Work	**45**	**55**	
SMOG, O_3			
% VOC,NMHC, tailpipe+evap.	95	5	(x 0.56 POCP **)
	(97)	(3)	
% NO_x	73	27	
TOXINS (known)			
% CO	98	2	
% NH_3	100	0	
% Benzene,	97	3	
% 1,3 Butadiene	(95)	(5)***	
% Acetaldehyde	(95)	(5)***	
% Formaldehyde	(95)	(5)***	
GREENHOUSE GASES			
% CO_2	81	19	
% N_2O	99	1	

* Trans. work = overall average thermal efficiency x fuel energy use

** POCP = photochemical ozone creation potential, R.G. Derwent, Photochemical Ozone Creation Potentials ....., *Atmospheric Environment*, 30(2): 181-199, 1996.

***For lack of data, assumed (as other studies have) that the sourcing of these three toxics is apportioned the same as the VOC's.

emisimag

	GASOLINE VEHICLES %SHARE	DIESEL VEHICLES % SHARE	
PARTICULATES ("probable toxins")	NATL	NATL	SCAB
DIRECT			
% PM_{10} (exhaust + other*)	34	66	62
% PM_{10} (exh.+ other weighted at 1/2 of exh.**)	29	71	67
% PM_{10} (exh. + other weighted at 1/2 of exh. & catalyst at 3X direct exh.*3)	49	51	46
SECONDARY			
Inorganic			
% Nitrate PM_{10} (NO_x+NH_3)	73	27	26
% Sulfate PM_{10} (SO_x+NH_3)	74	26	43
Organic			
% PM_{10} Org. Aerosols (tailpipe+evap.)	95	5	4
Overall weighted*4 secondary PM_{10}	78	22	27
TOTAL (contribution weighted*4 for worst areas, 2/3 secondary, 1/3 direct; exh. + other)	63	37	39
(2/3 secondary, 1/3 direct , exh. + other weighted at 1/2 exh.)	62	38	40
(2/3 secondary, 1/3 direct; exh. + other weighted at 1/2 of exh.; catalyst at 3X direct exh.)	68	32	33

* other = tire, brake and road dust

** assuming 50% of gasoline vehicle PM_{10} is exhaust & 50% tire, brake and road dust
" 85% " diesel " " " " " 15% " " " " "
" other PM_{10} is 1/2 as harmful as exhaust PM_{10}

*3 " PM10 from catalyst equipped gasoline vehicles has 3 times the unit risk of PM10 from non-catalyst equipped gasoline or diesel vehicles. EPA 420-R-93-005

*4 contribution allocation as given in "The Social Cost of the Health Effects of Motor Vehicle Air Pollution", Report # 11, UC Davis, pg. 246.

TABLE S.1 Estimated Emission Values for 17 U.S. Regions

Area	Emission Value ($/ton, 1989 dollars)				
	NO_x	ROG	PM_{10}	SO_x	CO
	Damage-Based				
Atlanta	4,330	2,150	5,170	2,720	N/A
Baltimore	4,430	2,210	4,520	2,620	N/A
Boston	4,120	2,030	5,090	2,820	N/A
Chicago	5,380	2,700	10,840	3,600	N/A
Denver	2,840	1,350	3,390	2,330	N/A
Houston	6,890	3,540	5,190	2,910	N/A
Las Vegas	910	320	2,450	N/A[a]	N/A
Los Angeles	9,800	5,110	17,200	3,970	N/A
Milwaukee	3,890	1,930	2,960	2,210	N/A
New Orleans	3,880	1,910	3,600	2,471	N/A
New York	7,130	3,650	15,130	4,030	N/A
Philadelphia	5,940	3,010	8,360	3,340	N/A
Sacramento	3,870	1,920	3,150	2,190	N/A
San Diego	5,510	2,800	4,800	2,600	N/A
San Francisco Area	3,730	1,810	5,970	2,970	N/A
San Joaquin Valley	4,490	2,240	6,550	2,610	N/A
Wash., D.C.	4,900	2,450	6,260	3,070	N/A
	Control-Cost-Based				
Atlanta	9,190	8,780	3,460	6,420	2,280
Baltimore	10,310	9,620	3,170	5,600	2,490
Boston	7,980	7,850	3,120	5,060	1,610
Chicago	7,990	8,150	4,660	9,120	2,440
Denver	6,660	6,590	2,790	4,900	2,960
Houston	17,150	15,160	2,780	3,590	2,680
Las Vegas	5,220	5,100	4,190	11,650	2,770
Los Angeles	21,850	19,250	6,060	13,480	4,840
Milwaukee	11,350	10,250	2,560	4,380	1,590
New Orleans	9,190	8,670	2,400	3,130	1,410
New York	12,340	11,720	5,390	11,090	3,910
Philadelphia	11,360	10,730	4,040	7,330	3,160
Sacramento	11,350	10,240	2,950	5,800	3,040
San Diego	14,110	12,630	3,460	6,640	2,740
San Francisco Area	5,230	5,760	3,200	4,900	2,460
San Joaquin Valley	10,310	9,630	5,110	12,480	2,750
Wash., D.C.	9,190	8,910	3,340	5,320	3010

[a] N/A = not available.

TABLE 11-A.35. COST OF AIR POLLUTION ATTRIBUTABLE TO A 10% REDUCTION IN MOTOR VEHICLE EMISSIONS, BY EMISSION-POLLUTANT PATHWAY AND HEALTH EFFECT, $/1000 VMT (URBAN U.S. TOTAL 1990) (LOWER BOUN

Emission	Ambient pollutant	Health effect	LDGVs			LDGTs			HDGTs			Total gasoline vehicles			LDDVs			LDDTs			HDDVs			Total diesel vehicles			Total all vehicles		
			V	V+U	V+U+RD	V	V+U	V+U+RD	V	V+U	V+U+RD	V	V+U	V+U+RD	V	V+U	V+U+RD	V	V+U	V+U+RD	V	V+U	V+U+RD	V	V+U	V+U+RD	V	V+U	V+U+RD
CO	CO	mortality	023	023	023	035	035	035	091	091	091	026	026	026	001	001	001	000	000	000	004	004	004	003	003	003	024	024	024
		hospitalization	004	004	004	006	006	006	014	014	014	004	004	004	000	000	000	000	000	000	001	001	001	000	000	000	004	004	004
		headaches	024	024	024	037	037	037	096	096	096	027	027	027	001	001	001	000	000	000	004	004	004	003	003	003	026	026	026
NOx	NO2	sore throat	028	028	028	044	044	044	087	088	088	032	032	032	016	016	016	006	006	006	111	112	112	087	087	087	036	036	036
		excess phlegm	012	013	013	019	020	020	038	039	039	014	014	014	007	007	007	002	003	003	049	049	049	038	039	039	016	016	016
		eye irritation	011	011	011	018	018	018	035	035	035	013	013	013	007	007	007	002	002	002	045	045	045	035	035	035	014	015	015
NOx, NH3	nitrate PM10	mortality	277	279	279	428	433	433	856	865	865	312	315	315	159	160	160	055	057	057	1093	1102	1102	853	860	860	351	355	355
		chronic illness	079	080	080	122	123	123	248	251	251	089	090	090	046	046	046	016	016	016	315	318	318	246	248	248	101	102	102
		asthma attacks	000	000	000	000	000	000	001	001	001	000	000	000	000	000	000	000	000	000	001	001	001	001	001	001	000	000	000
		RRAD	014	014	016	021	021	021	042	043	043	015	016	016	008	008	008	003	003	003	054	055	055	042	043	043	017	018	018
Total for NOx and NH3 emissions			422	426	426	651	659	659	1308	1321	1321	475	480	480	243	245	245	084	087	087	1668	1681	1681	1302	1313	1313	535	540	540
PM2.5	PM2.5	mortality	055	062	075	119	134	152	357	379	425	071	079	093	712	714	724	229	234	250	1946	1974	2098	1599	1621	1717	182	192	212
		chronic illness	016	018	021	035	039	044	103	109	121	021	023	027	211	212	214	067	069	073	556	564	595	458	464	488	053	056	061
		asthma attacks	000	000	000	000	000	000	000	000	000	000	000	000	001	001	001	000	000	000	002	002	002	001	001	001	000	000	000
		RRAD	003	003	004	006	007	008	018	019	021	003	004	005	035	035	036	011	012	012	097	098	104	079	080	085	009	010	010
		lung cancer	001	001	001	002	002	002	007	007	007	001	001	001	007	007	007	002	002	002	021	021	021	017	017	017	002	002	002
Coarse PM10	coarse PM10	mortality	018	020	084	032	036	129	092	097	336	021	024	096	045	046	096	014	016	097	101	108	747	085	090	587	026	029	131
		chronic illness	005	006	022	009	010	033	027	028	087	006	007	025	013	014	026	004	005	025	029	031	188	024	026	148	008	008	034
		asthma attacks	000	000	000	000	000	000	000	000	000	000	000	000	000	000	000	000	000	000	000	000	001	000	000	000	000	000	000
		RRAD	001	001	004	002	002	006	005	005	017	001	001	005	002	002	005	001	001	005	005	005	037	004	004	029	001	001	007
Total for direct PM10 emissions			099	111	211	205	230	376	608	645	1013	125	140	251	1027	1031	1109	329	338	463	2757	2803	3793	2269	2305	3074	282	298	457
SOx, NH3	sulfate PM10	mortality	082	135	135	133	246	246	221	394	394	093	159	159	463	484	484	172	216	216	1221	1421	1421	1008	1166	1166	160	233	233
		chronic illness	023	036	036	037	066	066	060	103	103	026	043	043	131	135	135	048	059	059	329	379	379	273	312	312	044	062	062
		asthma attacks	000	000	000	000	000	000	000	000	000	000	000	000	000	000	000	000	000	000	001	001	001	001	001	001	000	000	000
		RRAD	004	007	007	007	012	012	011	019	019	005	008	008	023	024	024	009	011	011	061	071	071	050	058	058	008	011	011
Total for SOx and NH3 emissions			110	179	179	177	324	324	293	517	517	124	210	210	617	643	643	228	285	285	1612	1871	1871	1332	1537	1537	213	307	307
VOCs	organic PM10 (SOA)	mortality	024	035	035	041	060	060	126	160	160	028	041	041	004	008	008	002	008	008	048	083	083	037	064	064	029	043	043
		chronic illness	007	009	009	012	016	016	037	044	044	008	011	011	001	002	002	000	002	002	014	021	021	010	017	017	008	012	012
		asthma attacks	000	000	000	000	000	000	000	000	000	000	000	000	000	000	000	000	000	000	000	000	000	000	000	000	000	000	000
		RRAD	001	002	002	002	003	003	006	008	008	001	002	002	000	000	000	000	000	000	002	004	004	002	003	003	001	002	002
	acetaldehyde	oral cancer	000	000	000	000	000	000	000	000	000	000	000	000	000	000	000	000	000	000	000	000	000	000	000	000	000	000	000
	benzene	leukemia	000	000	000	001	001	001	002	002	002	001	001	001	000	000	000	000	000	000	000	000	000	000	000	000	001	001	001
	1,3-butadiene	cancer all sites	002	002	002	003	003	003	007	007	007	002	002	002	000	000	000	000	000	000	000	000	000	000	000	000	002	002	002
	formaldehyde	oral cancer	000	000	000	000	000	000	000	000	000	000	000	000	000	000	000	000	000	000	000	000	000	000	000	000	000	000	000
Sub-total for VOC emissions			035	048	048	058	083	083	177	221	221	041	057	057	006	010	010	002	011	011	064	109	109	050	085	085	041	059	059
VOCs, NOx	O3	asthma attacks	001	001	001	002	002	002	004	004	004	001	001	001	000	000	000	000	000	000	002	003	003	002	002	002	001	001	001
		lower resp illness	004	004	004	006	007	007	014	015	015	005	005	005	001	002	002	001	001	001	009	010	010	007	008	008	005	005	005
		upper resp illness	001	001	001	002	002	002	004	005	005	001	001	001	000	000	000	000	000	000	003	003	003	002	002	002	001	002	002
		eye irritation	004	005	005	007	008	008	015	017	017	005	005	005	002	002	002	001	001	001	010	011	011	008	009	009	005	005	005
Subtotal mortality effects			480	555	631	787	944	1055	1742	1986	2271	551	644	729	1385	1412	1472	472	531	628	4412	4691	5454	3585	3805	4397	773	875	998
Subtotal cancer effects			003	003	003	006	006	006	015	015	015	004	004	004	007	007	007	002	003	003	022	022	022	018	018	018	005	005	005
Subtotal chronic morbidity effects			131	150	169	215	255	282	475	536	606	151	174	195	403	409	424	136	150	174	1243	1312	1500	1012	1067	1213	214	239	270
Subtotal acute morbidity effects			113	118	122	178	188	194	390	408	423	128	134	139	104	106	109	036	040	045	456	474	513	363	377	408	145	152	158
Subtotal ambient PM10			612	709	809	1007	1211	1355	2216	2534	2902	704	824	935	1863	1899	1977	634	710	835	5095	6257	7247	4792	5077	5846	1003	1135	1294
Subtotal ambient O3			010	011	011	017	018	018	037	041	041	012	013	013	004	004	004	001	002	002	025	027	027	019	021	021	012	013	013
Subtotal ambient NO2			052	052	052	080	082	082	160	162	162	058	059	059	030	030	030	010	011	011	205	207	207	160	161	161	066	066	066
Subtotal ambient CO			051	051	051	078	078	078	201	201	201	057	057	057	002	002	002	001	001	001	008	008	008	006	007	007	054	054	054
Total all emissions, pollutants, effects			727	826	926	1186	1393	1537	2623	2946	3315	834	956	1067	1899	1935	2013	646	724	869	6133	6500	7490	4978	5267	6036	1137	1271	1431

PRELIMINARY EFFORT AT DETERMINING

THE SOCIAL COST PER TON-MILE

OF ON-ROAD GASOLINE AND DIESEL VEHICLES

Vehicle Plus Upsteam Emissions, Health Risk Cost, $'s/1000 mi.
Criteria pollutant cost as per UC Davis Report #11 (high emphasis on PM, low emphasis on CO)
CO_2 @ $15 / short ton
Gasoline/Diesel @ $1.25/gal. and $1.15/gal.

	LDGC	LDDC	LDGT	*LDDT**	HDGT	HDDT
Criteria Emis. $/1000 mi.	8.26	19.35	13.93	*13.93*	29.46	65.00
CO_2 $/1000 mi.	6.5	6.3	8.7	*5.2*	22.9	25.3
	(28mpg)	(28mpg)	(21mpg)	*(31mpg)*	(8mpg)	(7mpg)
Fuel $/1000 mi.	45	41	60	*37*	156	164
Ton Miles/ 1000 mi.	1580	1800	2100	*2100*	8000	30000
Emis. Cost $/Ton Mile	.009	.014	.011	*.009*	.007	.003
Social Cost (Emis. + Fuel) $/Ton Mile	.038	.037	.039	*.027*	.026	.008

* Potential commercial result of DOE's "Light Truck Clean Diesel" technology development program.

INTEGRATED DIESEL ENGINE NOx REDUCTION TECHNOLOGY DEVELOPMENT

J. Hoelzer, J. Zhu, and C.L. Savonen
Detroit Diesel Corporation

K.C.C. Kharas, O.H. Bailey, M. Miller, and J. Vuichard
Allied Signal Environmental Catalysts

INTRODUCTION

The primary purpose of current production diesel catalyst has been HC, CO, and SOF (soluble organic fraction) oxidation as typically needed for vehicles operating in congested urban areas and in underground mining operations. More stringent air quality standards will require significant NOx reduction as well. New lean NOx catalyst tech-nology is being developed for this purpose.

Figure I illustrates that current production diesel engines require development to meet the projected environmental requirements. Passenger car and heavy duty diesel engines require a factor of two or more NOx reduction relative to existing production emission levels.

TECHNICAL APPROACH

Project activity flow is diagrammed in Figure 2. The interdependent systems include the engine, catalyst, and fuel. Key technologies and develop-ment interactions are also implied in the diagram. The primary thrust of in-cylinder management of NOx control is to reduce the peak temperature of combustion while minimizing fuel consumption penalties and/or particulate generation.

New catalyst formulations are developed at bench levels with simulated diesel exhaust before scaling to sizes required for engine assessment. Exhaust gas hydrocarbon speciation studies are aiding design of a reductant system which meets cataly-sis requirements. System design will ultimately be refined in full scale system testing.

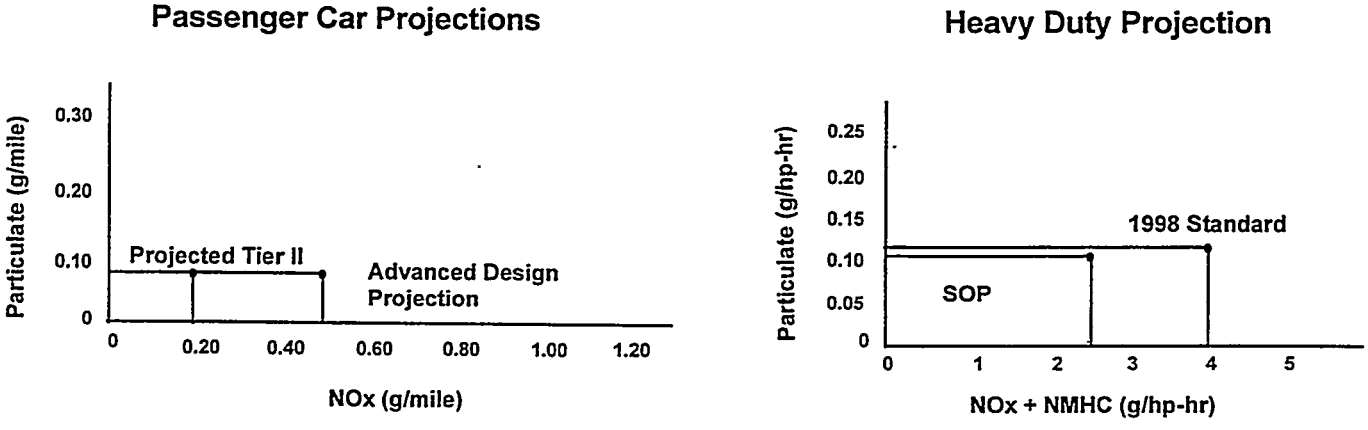


Figure 1 - Proposed NOx and Particulate Standards for HD and Passenger Car Engines

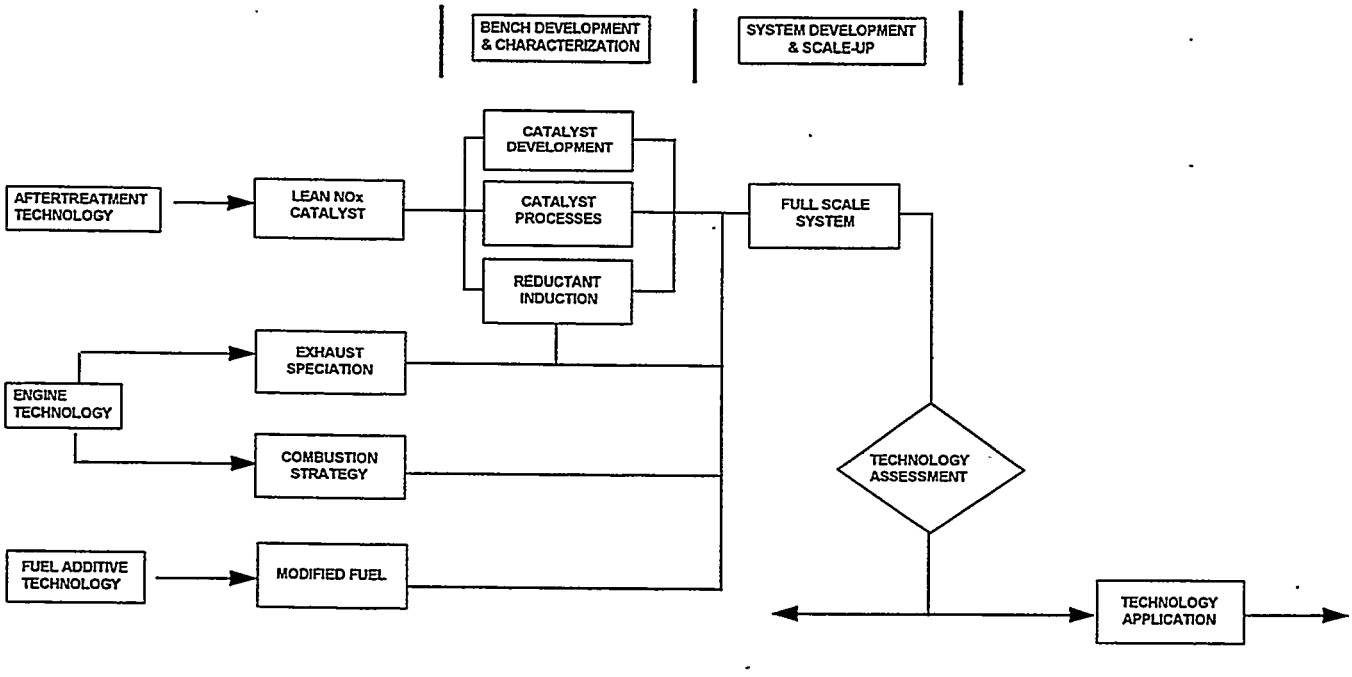


Figure 2 - Integrated Engine-Catalyst-Fuel Development Approach

Related fuel studies are a key feature of the integrated strategy. Production viability requires understanding of in-cylinder NOx forming chemi-stry but also whether and how intermediate spe-cies formation may facilitate NOx catalytic reduc-tion. Sulfur content is a significant challenge to the applicability of lean NOx catalyst systems. Sulfur removal is not so much a technical barrier, but a key variable of a complex technology-economics-infrastructure equation.

IN-CYLINDER MANAGEMENT - ANALYTICAL STUDIES

Analytical computational studies are contributing to better understanding of the complex combus-tion system interactions and their influence on real-time exhaust gas behavior. Computer assisted diesel combustion modeling continues to produce valuable development guidance. For engine-after-treatment systems, models provide insight to the complex balance of in-cylinder and aftertreatment mechanisms that influence the total emission signature. The use of super computer based KIVA modeling supports this need.

Figure 3, results from a KIVA study, are snapshots of in-cylinder temperature late in the power stroke. It is a three dimensional, one eighth segment with the apex of the 'pie slice' at the cylinder centerline. The piston is near bottom dead center. In the plan view, the segment is centered on an injector plume.

Given the direct correlation between temperature and NOx formation, knowledge of the temperature distribution provides valuable in-cylinder NOx reduction information which can be weighed against emission control strategies external to the combustion event. This iso-temperature profile provides the engine engineer with four-dimensional feed-back (including time) on potential changes to reduce local high temperature regions while maintaining the high mass average temperature needed for then notorious high thermal efficiency of a diesel engine. Iso-thermal, iso-CO, and iso-NOx contours are illustrated in Figure 3.

A related mixing challenge is shown in the iso-CO contour. This indication of incomplete combustion suggests local regions in-cylinder during the cycle where the opportunity for HC

and particulate management exist

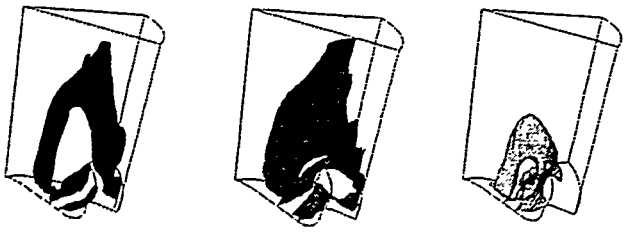


Figure 3 - Late Cycle In-cylinder Contours of Temperature, CO, and NOx

BASE ENGfNE R&D STATUS

Figure 4 tracks progress that has been made in the past ten years for the high speed direct injection (HSDI) engine. Changes in the basic engine design description and Tier II emission requirements are included for context. Combustion strategies, shown as a key element of new designs, continue to be developed based on the direct injection (DI) system, with key features being refined in-cylinder airflow structure and more tightly controlled injection spray orifice designs. Increased injection pressure and rate shaping capabilities allow for exploration of advanced fuel-air mix strategies.

Hardware and software evolution of injection system technology has provided increased precision of injection patterns over a broader range of engine operating conditions. The combination of cooled EGR, variable valve timing, variable swirl, variable turbine geometry, and low turbine wheel inertia provide engine breathing improvements, and extend the benefits over a larger engine operating range. Similar technology mix and emission reduction progress has been achieved on the heavy duty engine.

In addition to the base engine improvement described above, the application of diesel catalysts may play a key role in achieving future emission control compliance. Lean NOx catalysts activities associated with this IER program are detailed below.

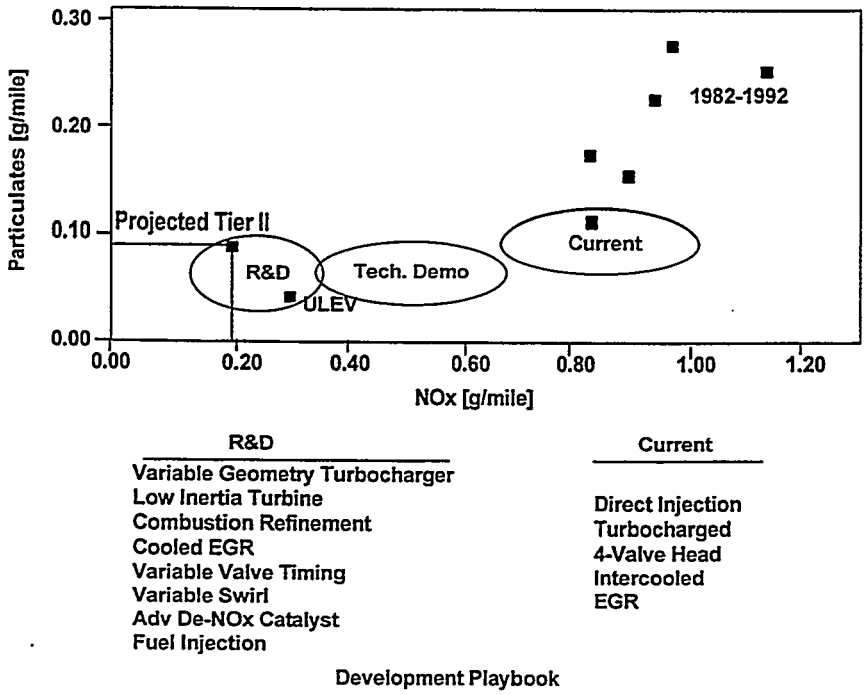


Figure 4 - HSDI Diesel Technology Advancements

LEAN NOx CATALYST DEVELOPMENT

Lean NOx catalysts may be categorized into two groups with respect to operating temperatures. We consider first the technology status of those catalysts designed for operating at higher temperatures (Figure 5). These catalysts usually exhibit onset of NOx conversion at temperatures greater than 300'C and the more intriguing ones continue to reduce NOx at temperatures over 500'C.

- Onset of NOx conversion occurs at 300-400°C.
- High NOx conversion achieved to temperatures > 500°C, given sufficient HC/NOx ratio.
- A wide variety of hydrocarbons including diesel fuel, paraffins, olefins, and oxygenates sustain NOx reduction.
- Durability has been demonstrated after high temperature catalysis.
- NOx conversion > 80% demonstrated both using synthetic gas and in engine tests.

Figure 5 - High Temperature Lean NOx Catalysts Characteristics

Concentrating on high temperature Allied Signal Environmental Catalysts (ASEC) R&D catalysts, there is ability to use a wide variety of hydrocar-bons as reductants. NOx reduction efficiency varies among the classes of hydrocarbons men-tioned, but encouragingly good performance is observed. With alcohols or heavy alkanes, broad ternperature windows with NOx conversion > 90% at HC/NOx = 4 can be observed.

As will be shown, thermal durability under catalytic conditions is demonstrated for these catalysts.

In Figure 6, NOx conversion of ASEC LNX-28 catalysts is plotted as a function of catalyst inlet temperature. The octane-containing gas is made synthetically in a laboratory scale reactor system and contains 4000 ppm C_1 as octane, 1000 ppmv NOx, 300 ppmv CO, 20 ppmv SO_2, 12% O_2, 8% H_2O, 8% CO_2, and balance N_2. NOx reduction exhibits a sharp onset at temperatures of about 340°C.

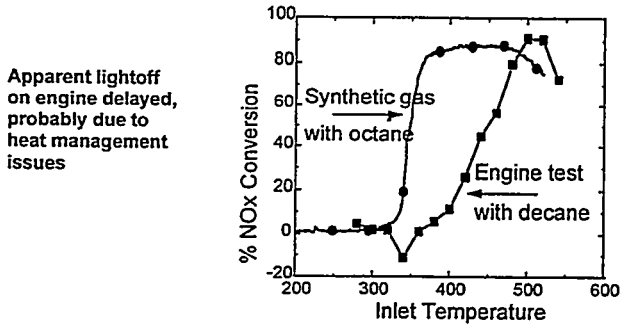


Figure 6 - LNX-28 Shows Interesting NOx Conversion Using Both Synthetic Exhaust and Engine Exhaust

NOx conversion is also plotted as a function of catalyst inlet temperature for a similar catalyst. These results were obtained using diesel exhaust from a 1.9 liter light duty diesel engine at constant speed and load. Temperature variation was introduced by passing the exhaust gas through a heat exchanger. Decane was introduced as a reductant at a constant rate using a Hewlett-Packard Liquid Chromatography pump/fuel injector assembly. The inlet NOx concentration was about 500 ppmv and inlet HC about 4500 ppm C_1.

The origins of the difference in NOx lightoff in the two environments were investigated. Issues relating to effective heating and vaporization of reductants injected into diesel exhaust are believed to account for part of the difference between the synthetic gas and the engine test results.

Catalytic performance of lean NOx catalysts is generally sensitive to the relative amount of HC present. This is specifically true for the current generation of LNX-28.

The left-hand panel in Figure 7 shows dynamometer data of the same catalyst for nominal HC I /NOx ratios of either 6 or 9. The catalyst shows better performance at the higher C/N ratio.

The right-hand panel in Figure 7 shows performance in a laboratory testing plant when octane is used as the reductant. We find that this catalyst reduces NOx over greater temperature ranges in a laboratory testing plant than it does over the dynamometer.

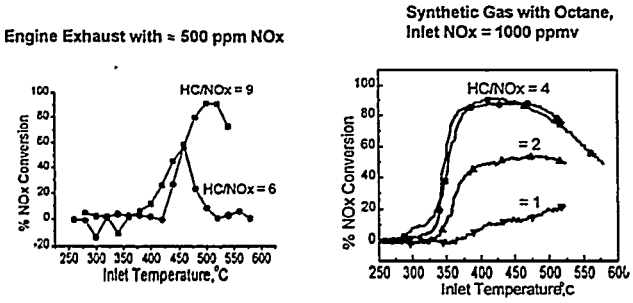


Figure 7 - NOx Reduction Performance is Sensitive to HC/NOx

Figure 8 dernonstrates a degree of catalytic durability that is encouraging for a base metal catalyst. The data were acquired using a laboratory reactor system. A synthetic gas mixture was used that includes components that are often poisons or inhibitors for base metal catalysts, such as SO_2 and H_20, which inevitably reside in diesel emissions. Aging conditions involved an inlet temperature of 550°C in a full complement of simulated exhaust gas. We have found that many other base-metal catalysts are more subject to thermal deactivation under catalytic conditions than under conditions that simply involve a stated temperature, air, and steam.

Benchmark lean NOx catalysts, such as CuZSM-5, degrade precipitously under these conditions. Generally speaking, catalysts susceptible to thermal degradation will show this susceptibility after short times on stream. LNX-28 shows no degradation after 50 hours onstream, leading to the expectation that this catalyst will provide good thermal durability for extended times. This is a necessary but only partial condition for demonstration as a practically useful catalyst.

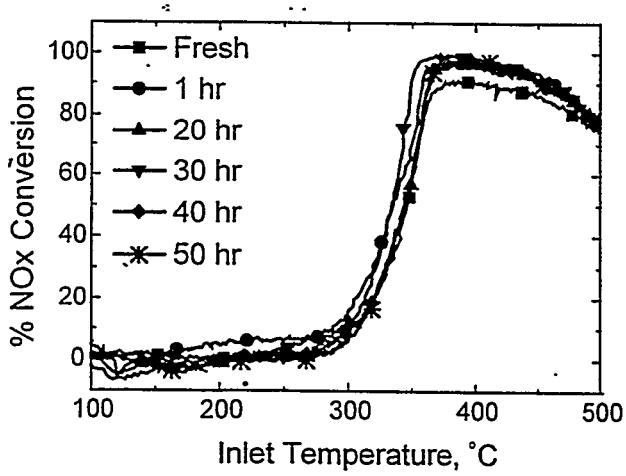


Figure 8 - LNX-28 Does Not Thermally Deactivate After Extended Catalysis

- Selective catalytic reduction using hydrocarbons
- Moderate NOx reduction activity at very low HC/NOx (<1 on average)
- Noble metal based
- Operating range below 150°C to about 300°C
- Low temperatures allow integration of hydrocarbon storage & release components with lean NOx reduction components
- Demonstrated NOx reduction on vehicles range from 20-35%

Figure 9 - Characteristics of Low Temperature Lean NOx Catalysts

As summarized in Figure 9, various catalysts employing noble metals, often platinum, can reduce NOx at lower temperatures between about 125-300°C. At temperatures below 100°C, these catalysts are not very active. At temperatures above 300°C these catalysts are quite active, and oxidize hydrocarbons very rapidly. But unfortunately, they have low selectivity for using HC species as the reductant, and the fraction of HC oxidized by atmospheric

02 becomes high. Hence, at higher temperatures, these catalysts cannot be considered to be lean NOx catalysts.

Noble metal catalysts can also contain a hydrocarbon storage and release component (or more than one such component) to help manage HC utilization, minimize HC breakthrough, and improve HC-NOx reactivity.

Demonstrated NOx reduction, exemplified here by use of the European test cycle, ranges frorn 20%35%, for advanced lean NOx catalysts, depending on the design of the overall vehicular emissions control system.

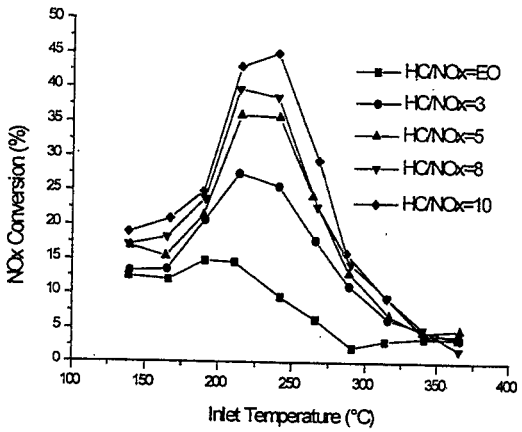


Figure 10 - Pt-Based Lean NOx Catalysts such as LNX-16.1B Utilize HC for the Reduction of NOx

As is the normal case for lean NOx catalysts, Pt-based catalysts such as ASEC LNX- 16.1 B exhibit sensitivity to the overall HC/NOx ratio. This sensitivity was assessed on a dynamometer, at various temperatures and steady state, and is shown in Figure 10. By operating at steady state, only catalytic efficiency is evaluated, and coupling between transient HC ad sorption/re lease is not probed.

Figure 11 shows tailpipe emissions of a diesel passenger car equipped with a similar ASEC Ptbased lean NOx catalyst. A fair HC, CO, NOx, and PM 4-way control is demonstrated. High degrees of HC conversion are obtained due in part to good HC storage/release management. The storage/release is well coupled with NOx reduction, leading to fair levels of NOx control in spite of very low HC/NOx values maintained over most of the evaluation. CO is adequately controlled. Only a portion of the PM is converted, but most of the unconverted PM occurs as solid, soot-like particulate that is not amenable to catalytic oxidation with flow-through devices. Very high levels of oxidation of the SOF portion of particulate are realized.

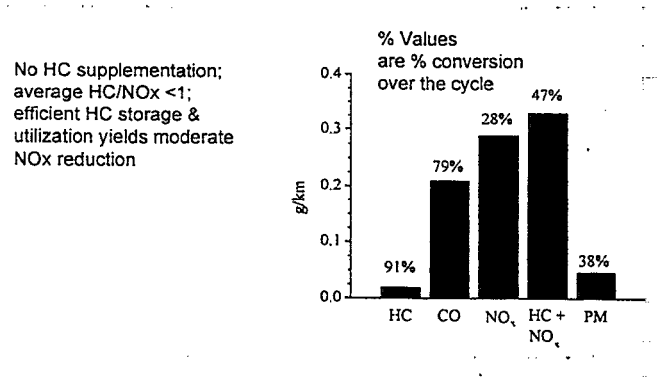


Figure 11 - Test Results Representing State-of-theArt Diesel Passenger Car Lean NOx Control

Several decision points regarding integration of catalyst and systems designs lie ahead, as outlined in Figure 12. It is not clear whether both high temperature and low temperature catalyst technologies will be needed for HD or LD NOx control. Many issues regarding method and strategy of HC provision, in-cylinder late injection versus in-exhaust injection, remain open and may be influenced by multiple catalyst technologies.

- Integration of catalyst and system designs
- Increased performance from both high tem-perature and low temperature catalysts
- Improved materials and systems designs will probably contribute

Figure 12 - Future Targets, Prospects

Desired levels of catalytic NOx control range from

30%-80%, depending on the nature of the engine-vehicle system and its intended application. Higher performance frorn low-ternperature catalysts is needed, since moderate conversion levels of less than 50% require unacceptable fuel economy penalties. Although durable high temperature catalysts appear to offer high performance, this performance must be moved to lower temperatures. This is especially true since many engine-vehicle systems create a large fraction of total NOx emitted at catalyst inlet temperatures of 300-400'C

REDUCTANT SYSTEM DESIGN ENGINE/-CATALYST INTEGRATION

Although a number of reductants are more effective in the NOx reduction processes, diesel fuel is preferred. While there are many possible approaches to the system design, the system must deliver uniformly distributed, vaporized reductant of the preferred species to the catalyst. Oxidation of the reductant prior to the catalyst must be minimized to maintain superior diesel engine fuel economy. Control logic should integrate the other engine systems such as those being considered for advanced HSDI engines (Figure 4).

DDC has embarked on an exhaust gas speciation study to help verify reductant system design choice. The approach is detailed in Figure 13.

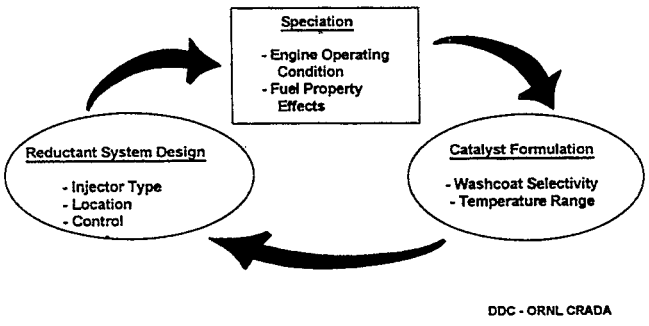


Figure 13 - Exhaust Speciation

Independent variables in the matrix include engine design, reductant system design, reductant system control logic, and fuels. The effectiveness of an advanced lean NOx catalyst will be studied as the independent variables are changed. Major promoting and inhibiting HC species for NOx reduction will be identified. This study will provide valuable information for the final integrated NOx reduction system.

SUMMARY

The effectiveness of catalyst performance is a function of the inlet exhaust gas temperature, gas flow rate, concentration of NOx and oxygen, and reductant quantity and species. Given this interrelationship, it becomes immediately clear that an integrated development approach is necessary. Such an approach is taken in this project. As such, the systern development path is directed by an engine-catalyst engineering team.

Of the tools at the engine engineer's disposal the real-time aspects of computer assisted subsystem modeling is valuable. It will continue to be the case as ever more subtle improvements are needed to meet competitive performance, durability, and emission challenges. A review of recent prototype engines has shown that considerable improvements to base diesel engine technology are being made. For example, HSDI NOx has been reduced by a factor of two within the past ten years. However, additional substantial NOx/PM reduction is still required for the future. A viable lean NOx catalyst would be an attractive solution to this end.

Tile results of recent high and low temperature catalyst developments were presented. High temperature base metal catalysts have been formulated to produce very good conversion efficiency and good thermal stability, albeit at temperatures near the upper range of diesel engine operation. Low temperature noble metal catalysts have been developed to provide performance of promising 4-way control but need increased NOx reduction efficiency.

ACKNOWLEDGMENTS

The authors gratefully acknowledge the primary sponsor, the Department of Energy, and the prograrn manager, Dr. Ron Graves of Oak Ridge National Laboratory, Lockheed Martin Energy Systems, Inc. The co-sponsorship of Detroit Diesel Corporation and Allied Signal Environmental Catalysts, and guidance of Drs. Nabil Hakim and Heinz Robota are also acknowledged.

02 becomes high. Hence, at higher temperatures, these catalysts cannot be considered to be lean NOx catalysts.

Noble metal catalysts can also contain a hydrocarbon storage and release component (or more than one such component) to help manage HC utilization, minimize HC breakthrough, and improve HC-NOx reactivity.

Demonstrated NOx reduction, exemplified here

with NOx reduction, leading to fair levels of NOx control in spite of very low HC/NOx values maintained over most of the evaluation. CO is adequately controlled. Only a portion of the PM is converted, but most of the unconverted PM occurs as solid, soot-like particulate that is not amenable to catalytic oxidation with flow-through devices. Very high levels of oxidation of the SOF portion of particulate are realized.

DIRECT INJECTION DIESEL ENGINES: WHAT IS THE LIMIT FOR NOx REDUCTION?

D.W. Dickey and T. Ryan
Southwest Research Institute

INTRODUCTION

The purpose of this paper is to review in-cylinder NO_x reduction strategies and to investigate the lower limit for NO_x emissions for a direct-injected diesel engine. NO_x and particulate emissions have decreased steadily for the past decade while engine thermal efficiency has simultaneously increased. The question is, how long can we continue to refine the current direct injection combustion system and still realize further reductions in NO_x emissions? Is there some fundamental limit to in-cylinder NO_x reduction, and if so, what is it?

In the United States, the Statement of Principles (SOP) agrees to NO_x emissions of 2.0 g/hp-hr in the year 2004 for on-highway heavy-duty engines. At the same time, the SOP research goals are 1.0 g/hp-hr. Engine manufacturers can refine current technology to meet the 2.0 g/hp-hr NO_x level for 2004. The research goal of 1.0 g/hp-hr NO_x is much more challenging. There are potentially two options to meet the 1.0 g/hp-hr level. One option is to use NO_x aftertreatment which is now the subject of intense research. Lean NO_x catalysis, $DeNO_x$ systems, and thermal plasmas are some of the technologies being studied. The other option is to attack the problem at the source (i.e., in-cylinder). It will be shown in this paper that if we change the combustion process in the diesel engine from a diffusion flame to a premixed lean combustion system, then orders of magnitude reduction in NO_x are possible.

BACKGROUND

In the late 1980's, meeting the 1991 and 1994 U.S. NO_x standard of 5.0 g/hp-hr was viewed as a real challenge. Now just a few short years later we are faced with meeting 4.0 g/hp in 1998 and 2.0 g/hp in 2004 with SOP research goals of 1.0 gram NO_x. The 1991 and 1994 5.0 gram levels were easily met using turbocharging with intercooling, higher injection pressures, combustion system optimization, and injection timing retard. The 1998 standard of 4.0 g/hp will be met with the addition of injection rate shaping. The 2004 NO_x level of 2.0 g/hp can be demonstrated using the above technology plus the use of exhaust gas recirculation. Unfortunately, EGR has an adverse effect on particulates so careful attention must be paid to developing an EGR system to optimize the NO_x-Particulate-BSFC tradeoffs while not sacrificing engine durability.

Historically then, we have been able to meet future NO_x standards by advancing the state-of-the-art for the diffusion flame combustion system. Now, to meet NO_x emissions standards beyond 2004, we may have to take a more radical approach. We should begin to think about changing the mode of combustion in order to get significant reductions in NO_x without resorting to aftertreatment systems.

IN-CYLINDER NO_x REDUCTION STRATEGIES

NO_x is formed in the combustion chamber when nitrogen and oxygen are present in a high temperature region. In a diesel engine, the adiabatic, stoichiometric, flame temperature is used as the characteristic temperature for a diffusion-controlled combustion process. Fuel mixes with entrained air in the fuel jet and burns near stoichiometry. Correlations between this calculated flame temperature and NO_x emission formation are common in the literature.[1]* Methods to reduce NO_x then focus on reducing peak flame temperature and\or reducing the oxygen concentration.

Numbers in parentheses designate entries in the Reference List

Strategies used to reduce NO_x emissions include:

- Injection Timing Retard
- Injection Rate Shaping
- Charge Air Chilling
- Water Fuel Emulsions
- Exhaust Gas Recirculation (EGR)

The effect of injection timing retard is shown in Figure 1. Injection timing retard can be used to reduce peak flame temperature and NO_x emissions but at the expense of fuel consumption. Injection timing retard was important to meet the U.S. 1994 NO_x level but by 1998, the benefit was depleted because further retarding of injection timing can result in poor combustion. The ability to change injection timing as a function of engine speed and load is also important.

Injection rate shaping can be used to tailor the injection event to reduce peak flame temperature. Hydraulic intensifiers and some common rail fuel systems have the capability to change injection rate shape as a function of speed and load as shown in Figure 2 (Herzog, P., IMECHE Conference 1989). Rate shaping can also be accomplished by changing the injection cam profile for in-line pumps and unit injector engines.

Special cases of rate shaping include pilot injection and split injection. The effect of pilot injection on NO_x and BSFC is shown in Figure 3[2]. In this case, the pilot injection event has a main injection that is retarded four degrees (compared to the no pilot case) with a pilot that leads the main injection by 15 degrees crank angle. As shown in Figure 3, NO_x is reduced at this 50 percent load condition by 16 percent with no effect on BSFC.

Split injections are another possibility to reduce NO_x emissions. Split injections are compared with a single injection in Figure 4[3]. The split injection provides a lower particulate level at retarded injection timings which allows the engine to operate at a lower NO_x level. Note that the improvements shown in Figure 4 were accomplished on an engine that may not be representative of more advanced technology engines. The objective of split and pilot injection is to tailor the heat release to minimize peak combustion temperature where NO_x is formed.

Air-to-air intercooling was effectively used in 1991 to reduce NO_x emissions. Charge air chilling is an extension of this same principle. A vapor cycle refrigeration system was added to the engine intake to lower intake manifold temperature well below the 40°C level used for conventional intercooling. The effect of manifold temperature on NO_x emissions is shown in Figure 5. NO_x reduction varied from 0.5 - 0.67 percent per °C reduction in intake manifold temperature. Unfortunately, chilling the intake air is not a viable solution due to the large BSFC penalty (shown in Figure 6) and the increase in cost and package size.

Water fuel emulsions are another technology used to reduce NO_x emissions. Water fuel emulsions are somewhat unique because they also have the potential to reduce particulates and fuel consumption. The effect of water content in the fuel on NO_x emission is shown in Figure 7. At a high load, the NO_x reduction is 1.0 - 1.3 percent per 1 percent water by volume in the fuel. A production water emulsion system must have the ability to control the water content in the fuel as a function of engine speed and load on a cycle-by-cycle basis.

EGR is now the most popular technology being investigated to meet the 2004 NO_x level of 2.0 g/hp-hr. A well-developed EGR system can reduce NO_x by 40 percent or more over the U.S. transient cycle. EGR can also be used to improve engine fuel consumption at intermediate NO_x levels by substituting EGR for injection timing retard. The effect of EGR on NO_x emissions is shown in Figure 8. EGR reduces NO_x by diluting the fuel air mixture with inert mass which has the effect of limiting peak flame temperatures. Unfortunately, EGR also increases particulates (except at idle where EGR reduces particulates) by lowering the temperature late in the combustion cycle where particulate matter is oxidized.

EGR SYSTEM DEVELOPMENT

The development of an EGR system will briefly be described in this section. The EGR system

was used as a tool to investigate the lower NO_x limit.

A high pressure loop (HPL) EGR system was developed and installed on a 1991, 11.1 liter, Detroit Diesel, Series 60 engine. A schematic of the HPL EGR system is shown in Figure 9. A unique HPL EGR valve was designed, fabricated, and installed between the exhaust manifold and turbine housing as shown in Figure 10. A unique throttle blade located in the valve simultaneously opened the EGR passage and applied backpressure to drive EGR. Under non EGR conditions, the EGR passage was closed to preserve turbocharger pulse energy. A schematic drawing of the valve and photographs of the valve in the full open and closed positions are shown in Figures 11-13.

The effect of EGR on steady-state NO_x and particulates at rated power is shown in Figure 14. EGR rates are selected to provide the best NO_x-PM tradeoff. As shown in Figure 14, about 8 percent EGR can be used at rated power to reduce NO_x by 40-50 percent with minimal impact on particulate. Steady-state mapping can be used to derive an EGR strategy for the U.S. FTP as shown in Figure 15. No EGR is used at low speed high load due to the air-fuel ratio deficit. Fifty percent EGR is used at idle to reduce both NO_x and PM. At part load, 10-30 percent EGR is used.

An EGR control system is required to make the transition between EGR regions as well as to handle extreme transients. The transient EGR strategy turns off EGR during severe "up-transients". A step transient shown in Figure 16 (taken from a portion of the FTP) was used to tune the transient control parameters. The effect of the transient control strategy on opacity is shown in Figure 17. The opacity with EGR and transient control approaches the no EGR level. Turning off EGR during up transients also has an impact on NO_x emissions as shown in Figure 18.

Several U.S. transient tests were then conducted with the Series 60 engine. Real time NO_x and particulate emissions for the third section (600-900 seconds) of the transient test are shown in Figures 19 and 20. The emissions for the engine with and without EGR are similar during up transients because EGR was turned off during severe up transients. At the other conditions, EGR generally lowers NO_x and increases particulates.

The effect of several different EGR strategies on transient NO_x and particulates is shown in Figure 21. A curve is drawn through the data showing the best tradeoff. The best EGR strategy for this engine produces about a 40 percent reduction in NO_x with a 20 percent increase in particulate. EGR was gradually added until the engine began to fail the transient test statistics due to poor engine performance. It is interesting to note that the curve asymptotically approaches 2 g/hp-hr NO_x at high EGR levels for this 1991 engine. Modern engines with more refined combustion systems can achieve NO_x levels below 2 g/hp-hr with EGR using today's diesel fuel. The question remains, what is the lower limit for NO_x? Can the SOP research goal of 1 g/hp-hr NO_x be acheived?

LIMIT FOR NO_x REDUCTION

What keeps us from reducing NO_x even further? A list of potential factors that limit NO_x reduction are listed below:

- Fuel Composition
- Fuel Injection System
- EGR System
- **Diesel Engine Combustion**

Fuel composition has a definite effect on NO_x emissions. Generally fuels with a higher H/C such as methane produce lower NO_x due to their lower flame temperatures. But for the sake of this argument we will assume that we will use diesel fuel. Advances in fuel injection systems have resulted in lower NO_x emissions through rate shaping and injection timing control. Further advancements in fuel systems will likely result in lower particulates but the NO_x benefit is probably already saturated. EGR systems that are perfectly matched and have perfect transient control could result in an additional 15 percent reduction in NO_x but again this parameter's effect is already saturated. The real limit to further NO_x

reduction is the direct-injection diesel engine combustion process itself.

Diesel engine combustion is shown pictorially in Figure 22. A high pressure fuel jet entrains air during injection into the combustion chamber. While this nonhomogeneous mixture has high global air fuel ratios (ranging from 20 - 120:1) combustion occurs locally near stoichiometry. This localized, stoichiometric, diffusion controlled combustion process results in high peak flame temperatures and high NO_x. The basic problem with the diffusion controlled combustion process is that the combustion zone temperature is much higher than the bulk gas temperature.

The bulk gas temperature is compared with a calculated combustion zone temperature for a diesel engine in Figure 23. The combustion zone temperature is much higher than the bulk gas temperature because of the nonhomogeneous localized burning that takes place with diffusion controlled combustion surrounding the individual fuel jets. NO_x is formed in this high temperature combustion zone. The best we could do to reduce NO_x emissions would be to burn the fuel everywhere in the combustion chamber at the global air fuel ratio. For this combustion scenario, the two curves in Figure 23 would converge; the combustion zone temperature would approach the bulk gas temperature.

Returning to the original question, what is the limit for NO_x reduction? The limit is diesel engine combustion. Stoichiometric diffusion combustion produces high flame temperatures and high NO_x. Diluents can be added to reduce flame temperature up to the point where combustion begins to deteriorate. If the diesel combustion could be changed from a stoichiometric, diffusion flame to a homogeneous, lean mixture combustion, significant reductions in NO_x emissions are possible.

The other important question is what is the lowest engine-out NO_x that can be obtained using the diesel engine? A "NO_x Boundary" is shown in Figure 24 along with the future NO_x and particulate standards for the U.S. The NO_x Boundary is defined as the minimum NO_x that the diesel engine can emit. While the exact value of the NO_x Boundary is not known; it is shown as 1.5 g/hp-hr in Figure 24 assuming today's diesel fuel and current diesel technology. The value of 1.5 was chosen based on experience. Certainly, most engine manufactures have demonstrated engine out NO_x values near or just below this value. The exact value of the NO_x Boundary is not as important as the overall concept that a lower limit exists due to the fundamental limits of diffusion flame combustion. Showing the NO_x Boundary at 1.5 g/hp-hr does however raise the question, can we get to the SOP research goal of 1.0 g/hp-hr without aftertreatment?

The conventional diesel engine (stoichiometric diffusion flame) produces NO_x values above the NO_x Boundary as shown in Figure 24. Retarding the injection timing, injection rate shaping, chilling the intake air, and adding diluents such as EGR or water can only reduce the NO_x to the NO_x Boundary. There are three possible ways to jump over this NO_x Boundary:

- Change the fuel
- Use NO_x aftertreatment
- Change the diesel combustion process

The first two approaches are not considered in this paper. If the diesel combustion process is changed from a stoichiometric diffusion flame to a lean premixed type of combustion system, the flame temperature and NO_x can be reduced. In fact, the area below the NO_x Boundary represents the ideal combustion where the combustion temperature approaches the bulk gas temperature.

A SwRI NO_x model called ALAMO_ENGINE[1] was used to estimate the value of the NO_x Boundary as an analytical check on our experimental observation. First, ALAMO_ENGINE results were compared with experimental data from a Caterpillar 3176 engine equipped with an EGR system, as shown in Figure 25. The air-fuel ratio and EGR rates were measured for an 8-mode cycle. The measured NO_x agreed well with the ALAMO_ENGINE result. More aggressive EGR schedules were then applied using the model while maintaining a minimum air-fuel ratio as

shown in Figures 26-29. Finally, the most aggressive EGR schedule was selected as shown in Figure 29 in an effort to determine the NO_x Boundary. The results in Figures 28 and 29 indicate that the NO_x Boundary is somewhere between 1.0 and 1.5 g/hp-hr. Note that this is a best case scenario because the model does not account for combustion deterioration with EGR.

HOMOGENEOUS CHARGE DIESEL ENGINE

As mentioned above, one method to go below the NO_x Boundary is to change the diesel combustion process from a diffusion flame to a lean premixed combustion. SwRI has conducted research with a Homogeneous Charge Compression Ignition (HCCI) combustion system [4]. The HCCI system is shown schematically in Figure 30. Diesel fuel is port injected using an air assist injector into a heated intake air stream. The homogeneous charge is then compression ignited creating many ignition sites throughout the lean mixture. The multiple lean ignition sites produce low peak flame temperatures and extremely low NO_x emissions. HCCI combustion approaches the ideal combustion (below the NO_x Boundary) where the combustion zone temperature approaches the bulk gas temperature.

The NO_x and particulate emissions from a single cylinder diesel engine operating in conventional diesel and HCCI combustion mode are compared in Figure 31. The HCCI engine produces NO_x values that are 98 percent lower than the conventional diesel engine. The particulates for HCCI combustion should also be very low. The particulates for both the diesel and HCCI engine are relatively high in Figure 31 because of the use of a small, single-cylinder, variable-compression-ratio, research engine. In addition, characterization of the particulate emissions obtained during HCCI operations indicted that the particulate was predominantly volatile organic material. A comparison between the heat release rate and cylinder pressure for the diesel and HCCI engines are shown in Figures 32 and 33. HCCI combustion heat release always has a characteristic precombustion, or cool flame reaction, before the main combustion event, as shown in Figure 32.

HCCI engines produce extremely low NO_x emissions compared to the conventional diesel engine, as shown in Figure 31. So when will all the diesel engine manufacturers convert to HCCI combustion? Well there are some technical challenges that must be overcome before HCCI combustion engines are adopted for use in trucks. The main challenge with HCCI combustion is to control the start of combustion. HCCI combustion occurs between limits of misfire on one side and engine knock on the other side. It is also difficult to get the engine to operate in HCCI mode over all of the engine speed and load range. The efficiency of current HCCI engines is not as good as diesel engines because of a lower compression ratio (10-11:1) required to eliminate knock and early start of combustion resulting in poor cycle efficiency. To eliminate the problem with limited speed and load operating range, the first HCCI engines will probably show up as dual-combustion mode engines. The engine would start as a conventional diesel engine and then switch over to HCCI operation (by turning on a port injector and turning off the in-cylinder injector) at predefined speeds and loads. The conventional diesel engine could have a HCCI operating regime that produces extremely low emissions. The "Dual Combustion Mode Engine" would improve the emissions of the conventional diesel engine while solving the limited operating range problem of the HCCI engine[5]. The ultimate goal is to have a diesel engine that operates over the full operating range with HCCI combustion. The "complete HCCI engine" can then eliminate the expensive direct injection fuel system and replace it with a relatively inexpensive port fuel injection system.

CONCLUSIONS

In-cylinder NO_x reduction may be limited by diffusion flame combustion in the direct-injected diesel engine.

- With today's diesel fuel and current technology, the observed NO_x limit appears to be around 1.0-1.5 g/hp-hr over the U.S. transient cycle.

- The ALAMO_ENGINE NO_x model predicts a NO_x limit of 1.2 g/hp-hr over a simulated transient cycle. The NO_x model assumes no deterioration in combustion with EGR and a minimum air fuel ratio of 24:1. The model does not predict particulate emissions, which may be extremely high.

- NO_x aftertreatment or fuel modifications will most likely be required to meet the SOP research goal of 1.0 g/hp-hr over the transient cycle.

- Homogeneous Charge Compression Ignition (HCCI) combustion is one method to achieve extremely low engine-out NO_x emissions; a 98 percent reduction in NO_x was measured compared to conventional diesel combustion.

- Future diesel engines may operate with a dual-mode combustion system. The engine may start as a conventional diesel engine and then switch over to HCCI combustion mode for predefined speed and load ranges. The dual-mode combustion diesel engine will have emissions that are lower than the conventional diesel engine. The dual-combustion mode diesel engine may be able to meet the SOP research goal of 1.0 g/hp-hr NO_x.

- A "complete HCCI engine" has the potential to eliminate the direct injection fuel system and replace it with a relatively inexpensive, port fuel injection system.

ACKNOWLEDGMENTS

Appreciation is expressed to the following companies for supporting the Clean Heavy-Duty Diesel Engine (CHDDE) project at SwRI during the period 4/1/90 - 4/1/93.

Caterpillar, Chevron, Cummins, Deere and Company, Detroit Diesel, Garrett Automotive, Hino Motors, Isuzu, Iveco Motorenforschung, Lucas Diesel Systems, Mack, Mitsubishi Motors, Navistar International, Nissan Diesel, Renault Vehicles Industriels, Robert Bosch, Volvo Truck, and Zollner Pistons.

REFERENCES

1. Dodge, Lee G., Leone, Douglas M., Naegeli, David W., Dickey, Daniel W., and Swenson, Kendall R., "A PC-Based Model for Predicting NO_x Reductions in Diesel Engines," SAE Paper No. 962060.

2. Tullis, S., and Greeves, G., "Improving NO_x Versus BSFC with EUI 200 Using EGR and Pilot Injection for Heavy-Duty Diesel Engines," SAE Paper No. 960843

3. Tow, T. C., Pierpont, D. A., and Reitz, R. D., "Reducing Particulate and NO_x Emissions by Using Multiple Injections in a Heavy Duty D.I. Diesel Engine," SAE Paper No. 940897

4. Gray, Allen W.,III, (Bill), and Ryan., Thomas W.,III "Homogeneous Charge Compression Ignition (HCCI) of Diesel Fuel," SAE Paper No. 971676.

5. Dickey, Daniel W., "Method to Reduce Emissions Using Dual Combustion Mode Diesel Engine" Patent Pending (June 9, 1997)

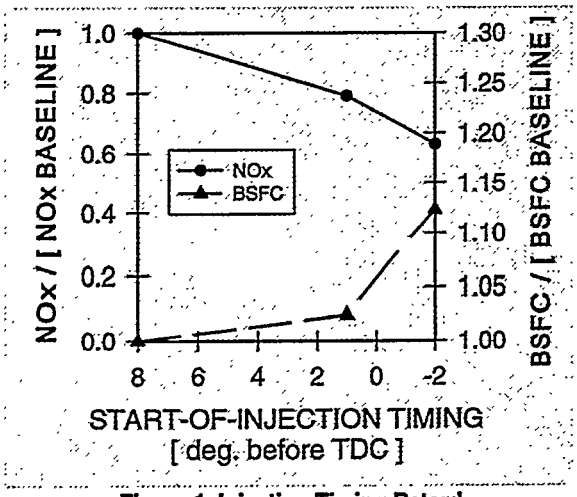


Figure 1. Injection Timing Retard

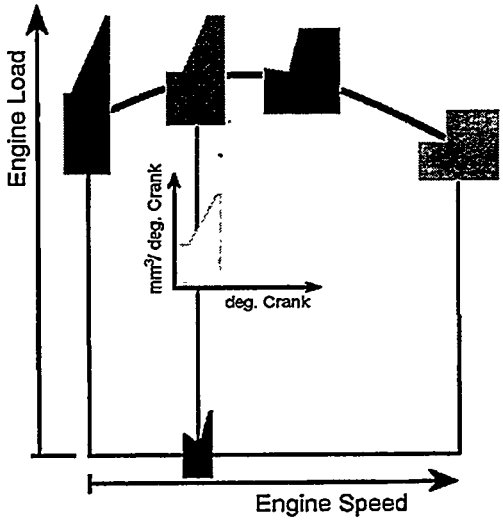


Figure 2. Advanced Injection Rate Shape

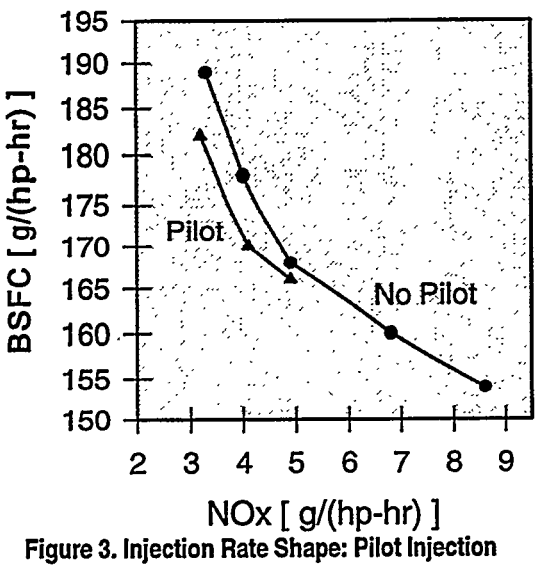


Figure 3. Injection Rate Shape: Pilot Injection

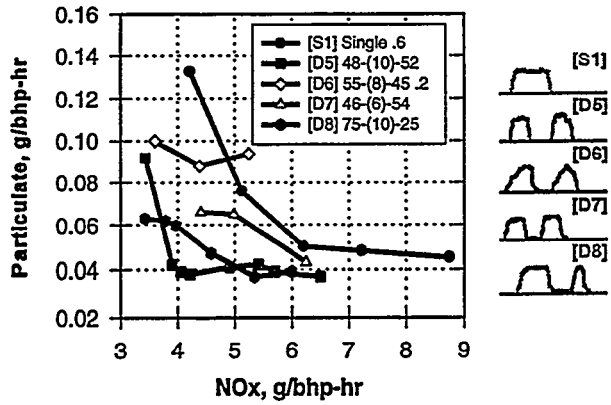


Figure 4. Injection Rate Shape: Split Injection

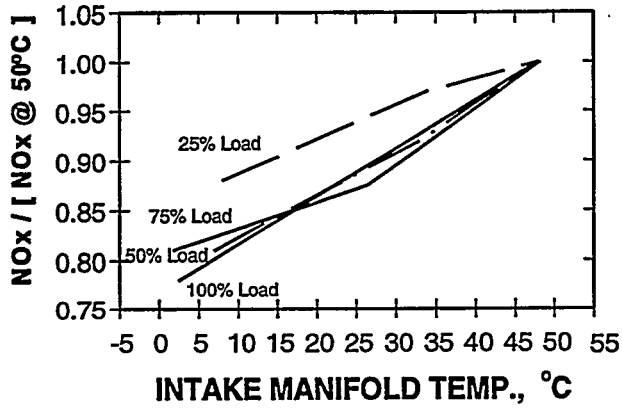


Figure 5. Charge Air Chilling

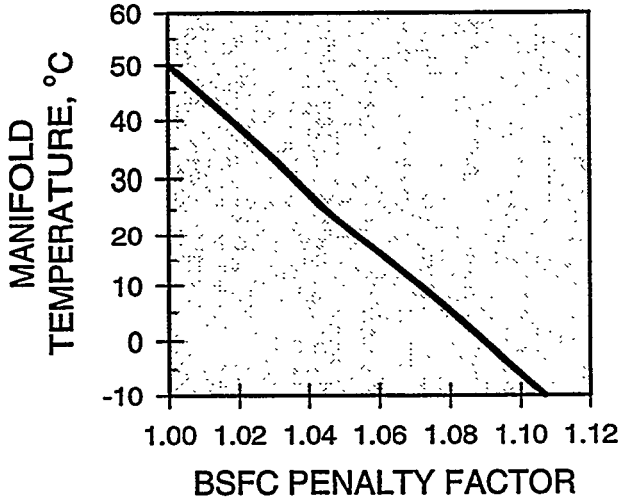
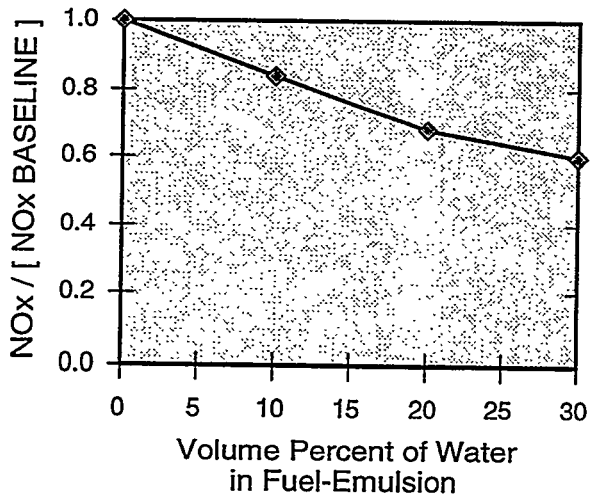


Figure 6. Vapor Cycle Chilling Cost



6 Liter, 2000 rev/min, 80% Load

Figure 7. Water Fuel Emulsion

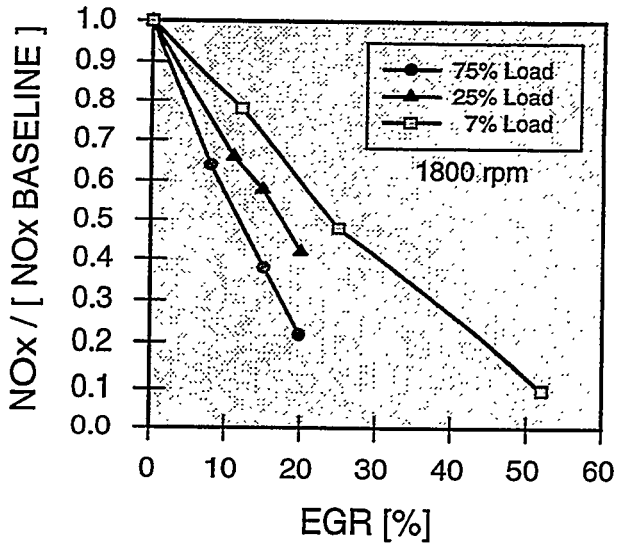


Figure 8. Exhaust Gas Recirculation (EGR)

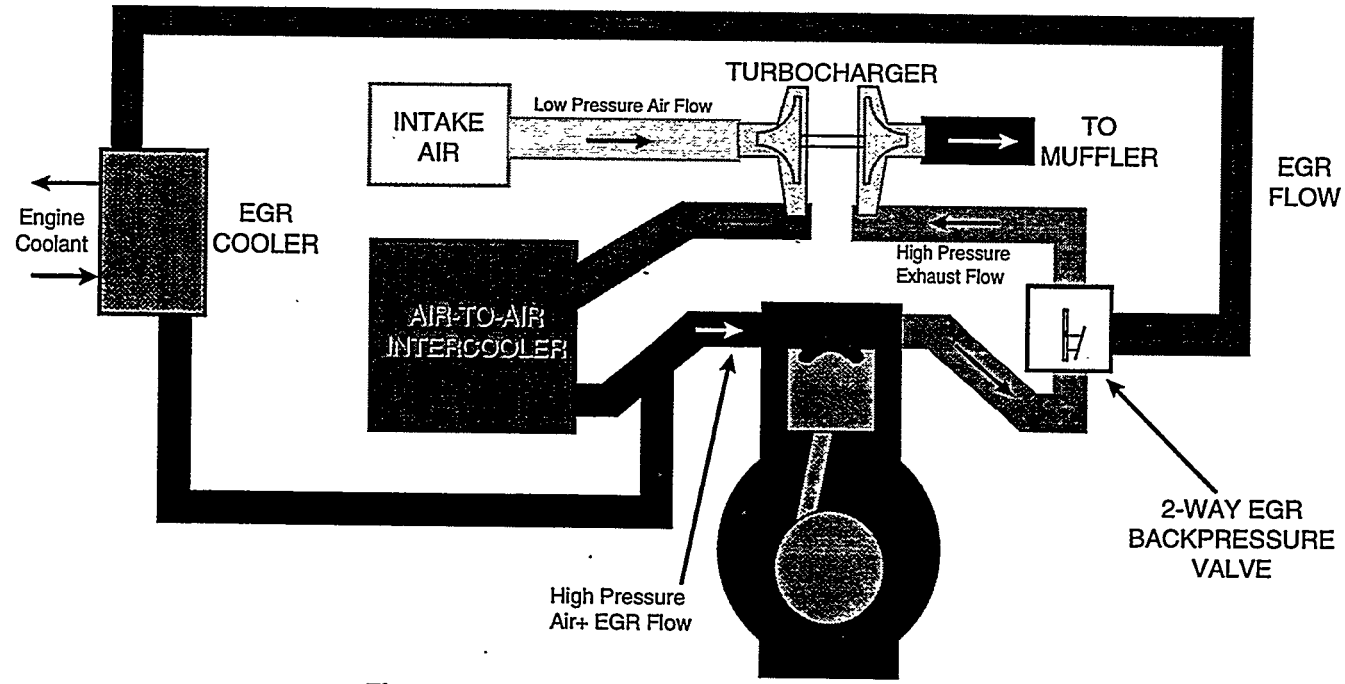


Figure 9. High Pressure Loop (HPL) EGR System

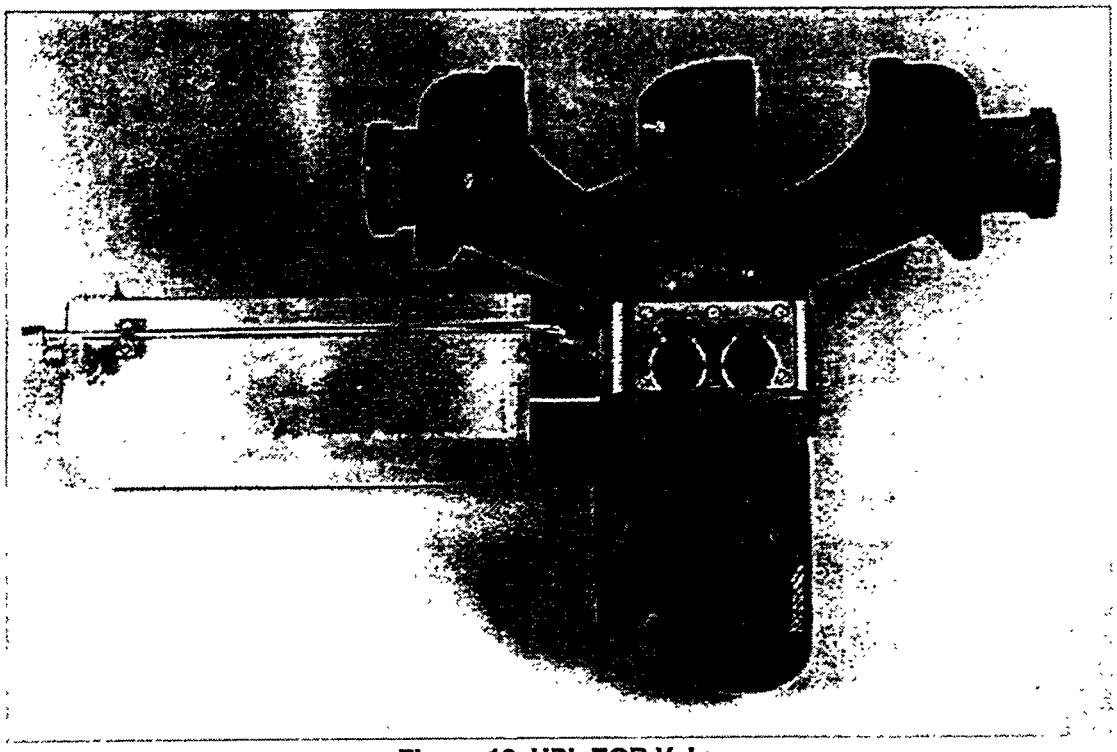


Figure 10. HPL EGR Valve

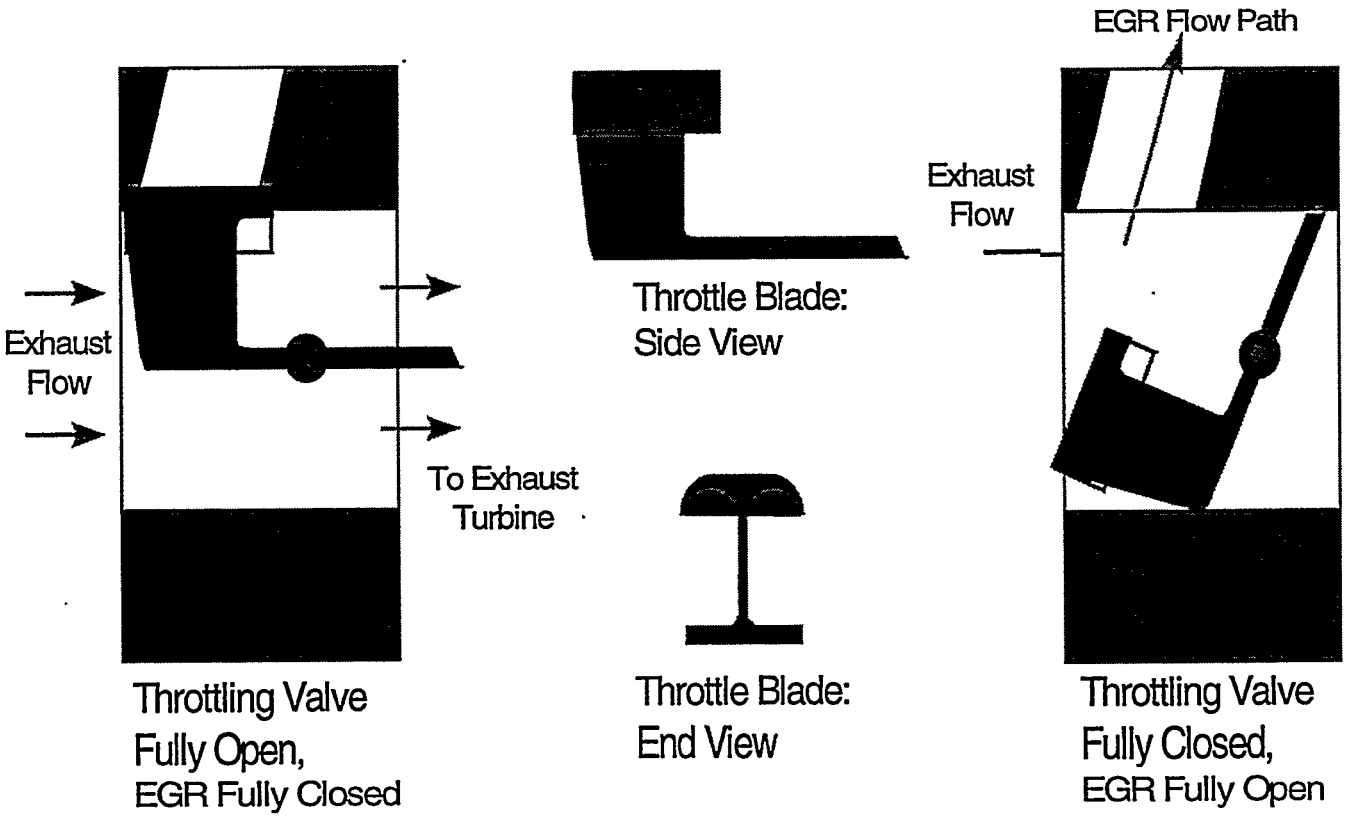


Figure 11. HPL EGR Valve

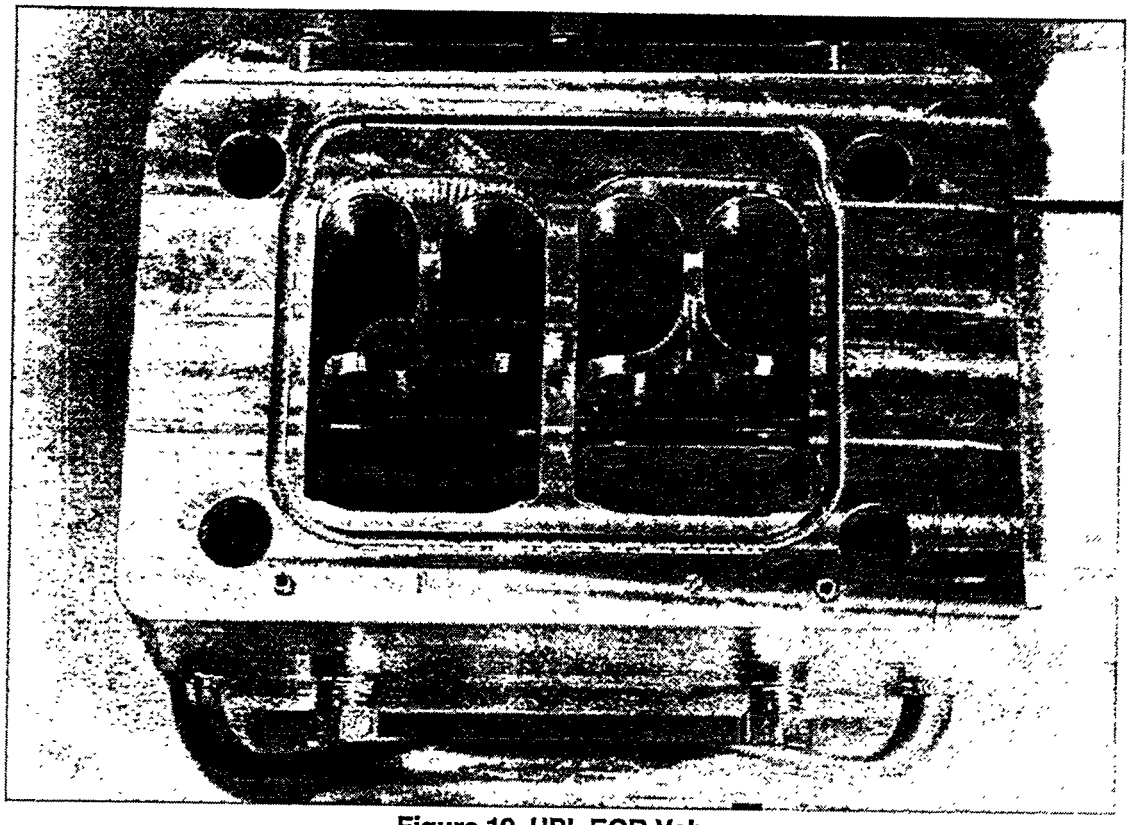


Figure 12. HPL EGR Valve

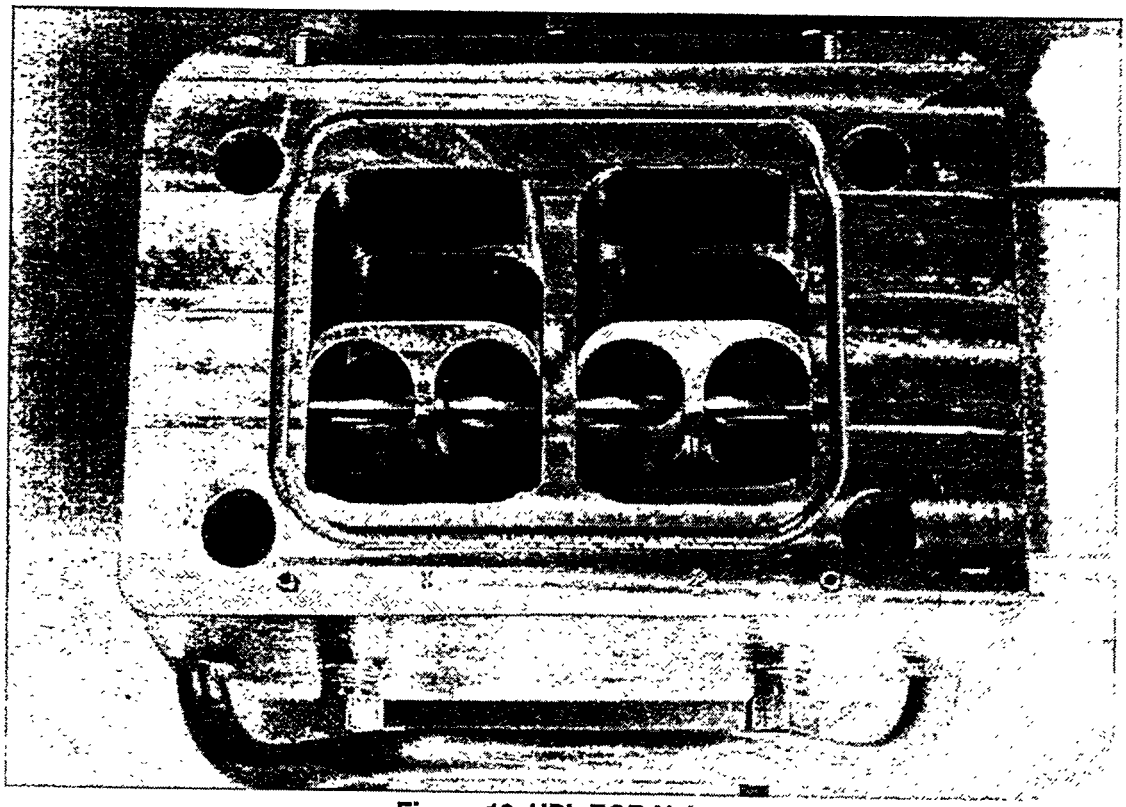


Figure 13. HPL EGR Valve

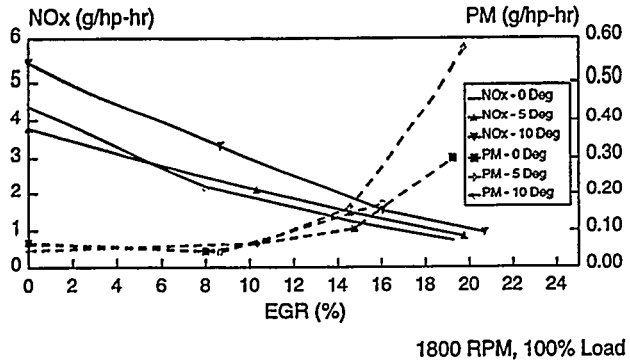


Figure 14. NO_x & PM vs. EGR Rate

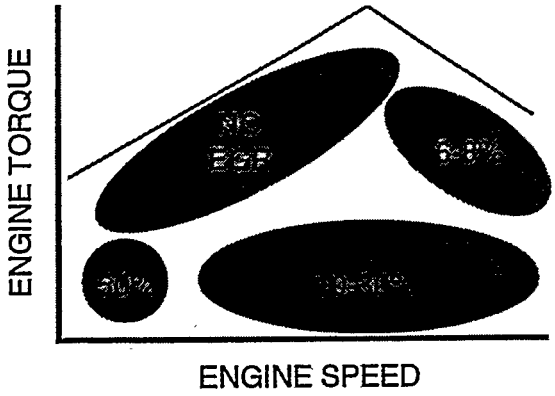


Figure 15. EGR Strategy to Optimize NO_x-PM Tradeoff for U.S. FTP

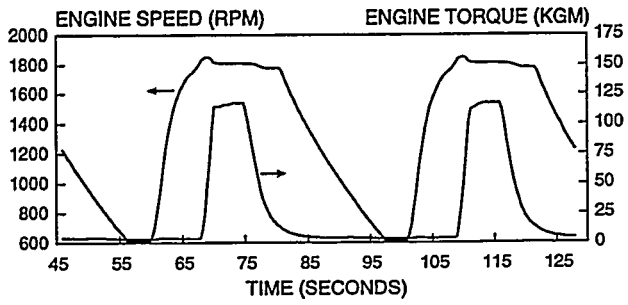


Figure 16. Engine Speed and Load for Step Transient

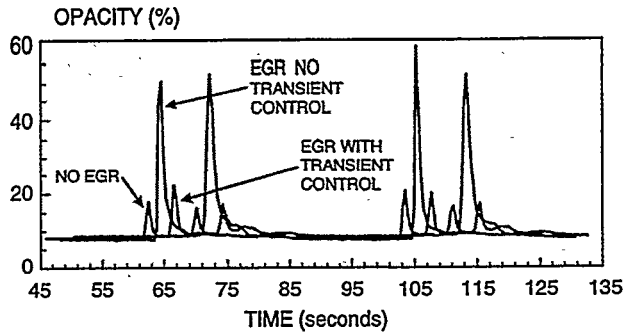


Figure 17. Effect of Step Transient on Opacity

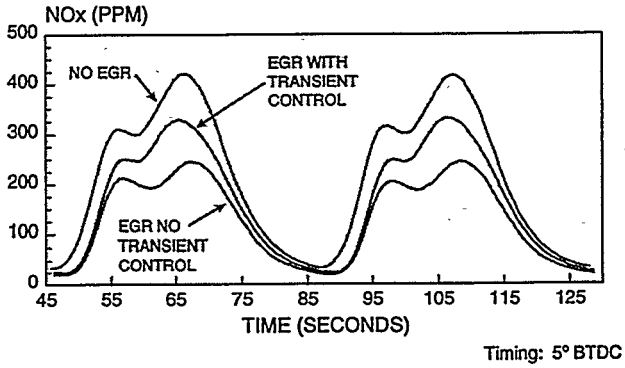


Figure 18. Effect of Step Transient on NO_x

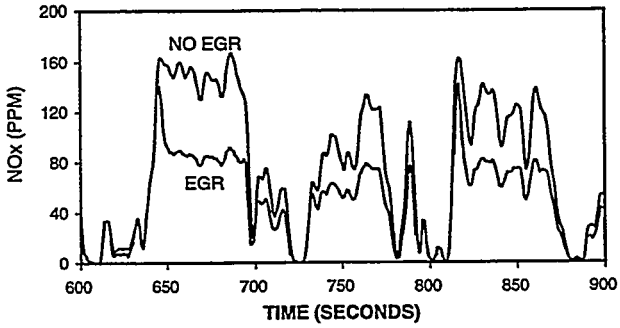


Figure 19. U.S. FTP Transient NO_x

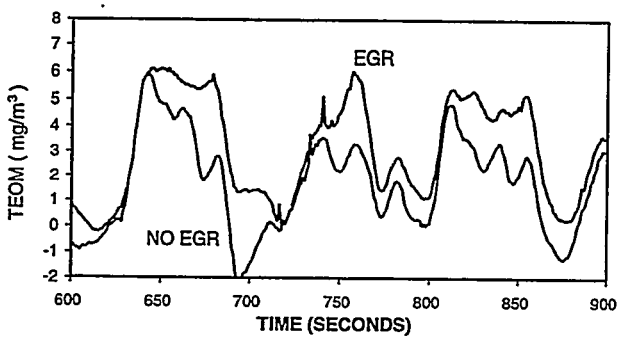


Figure 20. U.S. FTP Transient Particulates

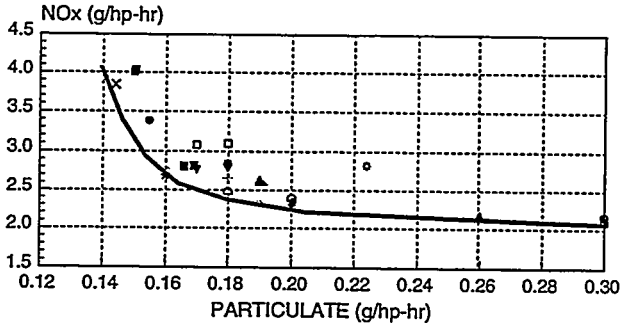


Figure 21. Effect of EGR Strategies
U.S. FTP Transient Test Results

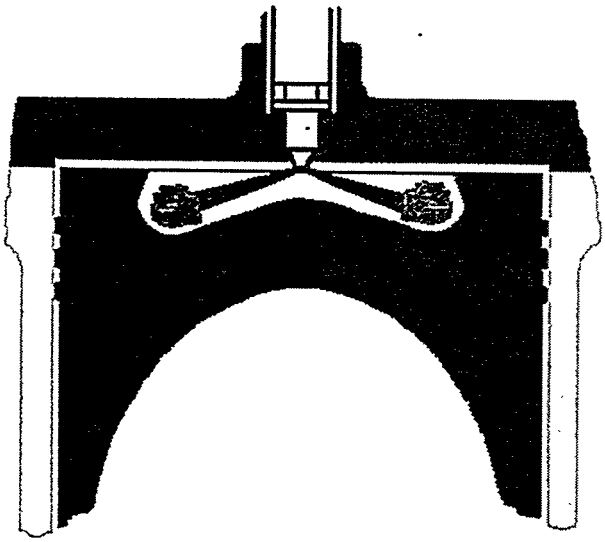


Figure 22. Diesel Engine Combustion

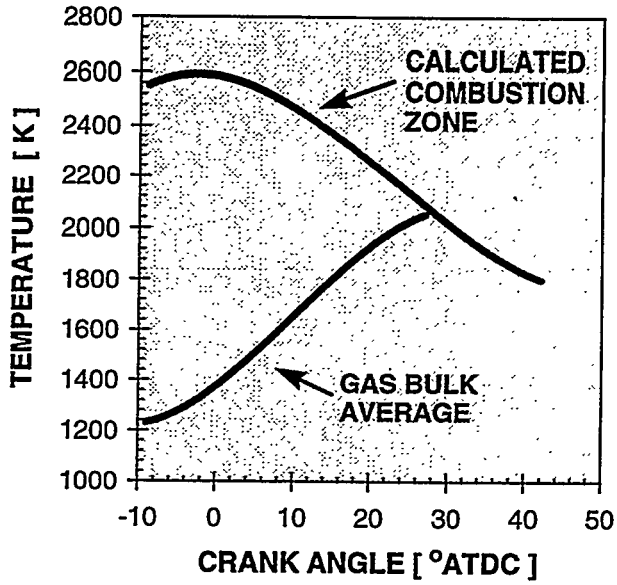


Figure 23. NO_x Formation (Diesel Combustion)

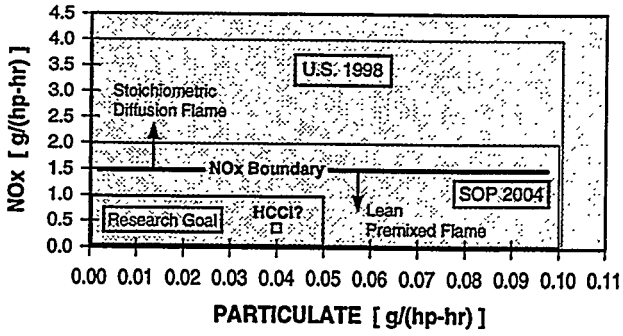


Figure 24. NO_x Boundary

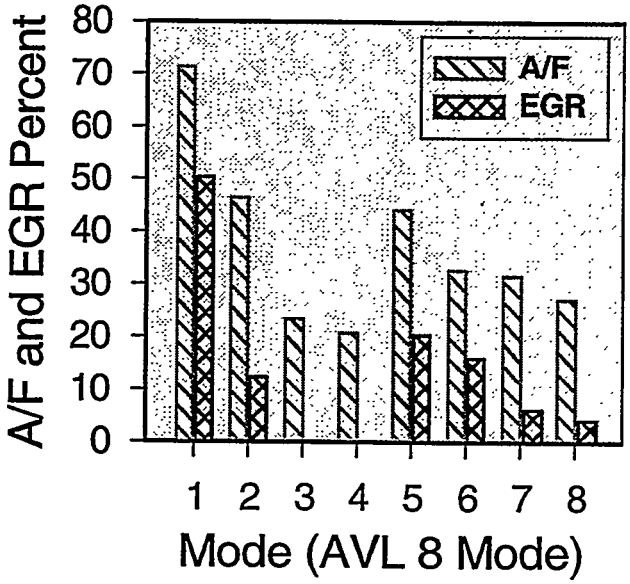


Figure 25. Measured EGR, Air/Fuel, and No_x
(Measured NO_x = 2.73 g/hp-hr and
Modeled NO_x =2.88 g/hp-hr)

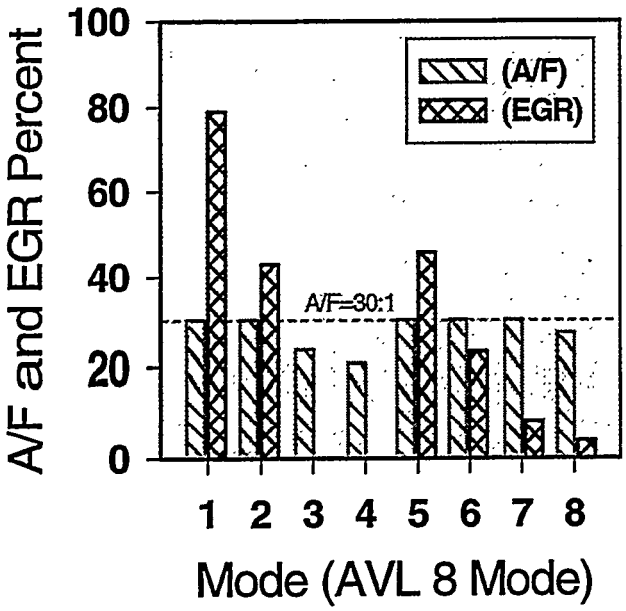


Figure 26. Modeled NO_x (NO_x= 2.3 g/hp-hr)

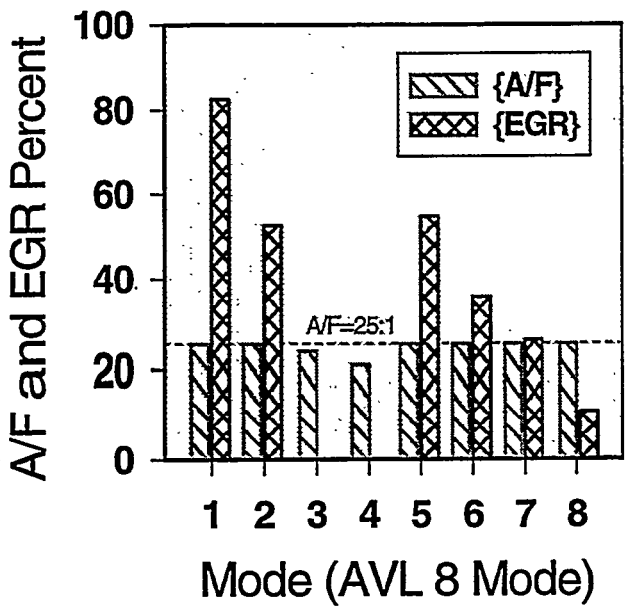


Figure 28. Modeled NO_x (NO_x= 1.4 g/hp-hr)

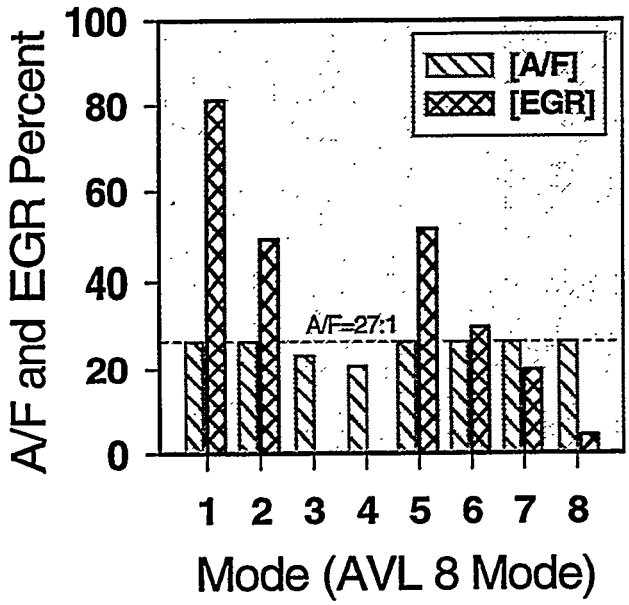


Figure 27. Modeled NO_x (NO_x = 1.9 g/hp-hr)

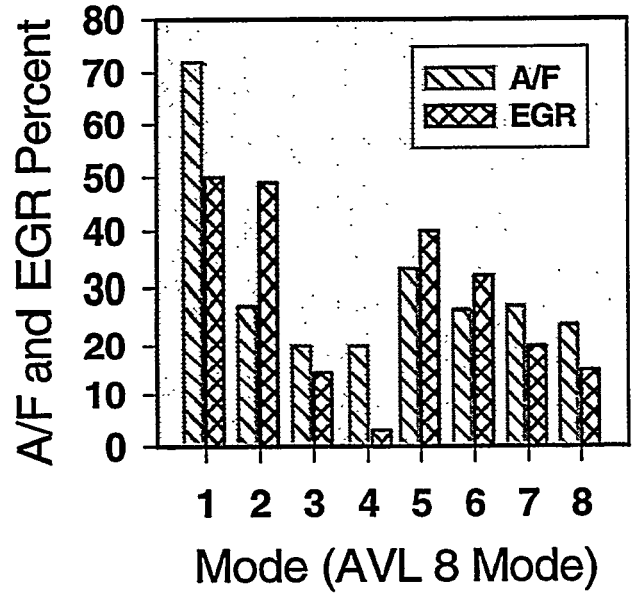


Figure 29. Modeled NO_x (NO=1.2g/hp-hr)

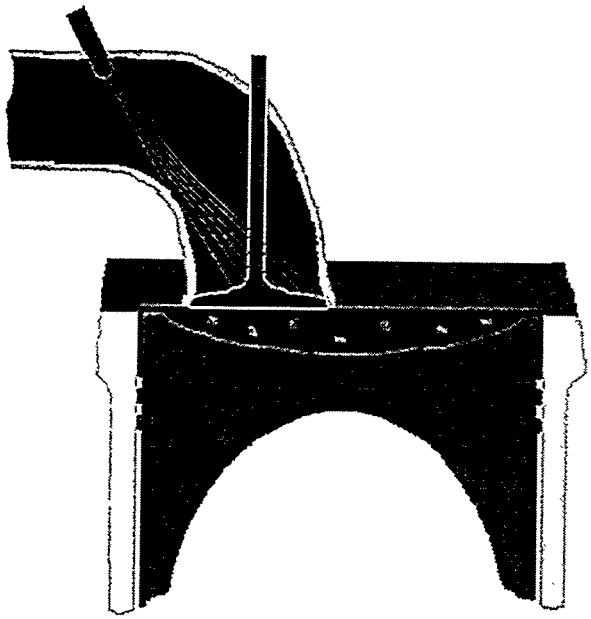


Figure 30. Homogeneous Charge Compression Ignition (HCCI) Combustion

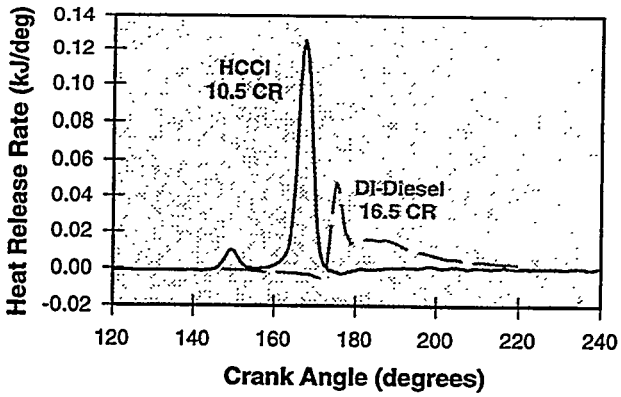


Figure 32. DI-Diesel vs. HCCI Heat Release Rate Comparison

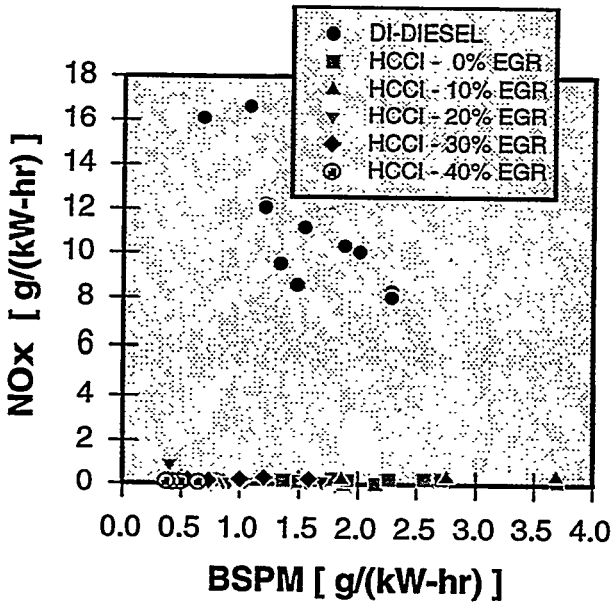


Figure 31. Emissions Comparison: DI-Diesel vs HCCI

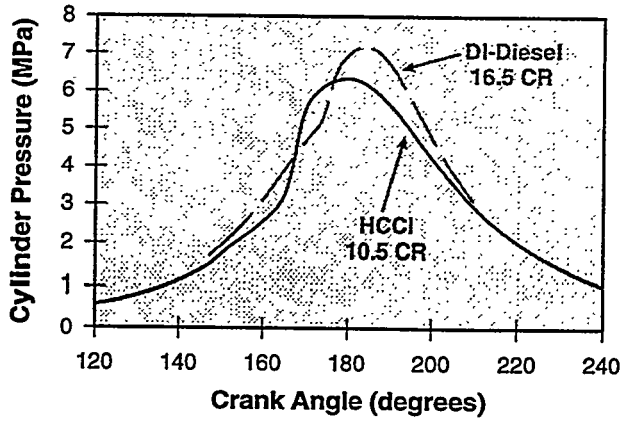


Figure 33. Cylinder Pressure Comparison

DIESEL ENGINE EMISSION CHALLENGES

A. Chanda
Caterpillar Inc.

While the diesel engine remains the most efficient power source for transportation work, it can benefit from significant new technologies developed in the future. On-road regulations for both heavy duty and light duty engines will likely remain the pace setters for the technol-ogy selection process.

The future challenges for the diesel create opportunities for new approaches, as well as continued refinement of fuel, air, and combustion technologies. The very nature of combustion, from direct-injection heterogeneous burn to lean homogeneous combustion, lean NO_x aftertreatment systems, rapid-response NO_x sensor technology, along with fuel formulation will need to be researched and developed for suitable application.

As the end-user expectation of engines becomes more demanding relative to reliability, durability, fuel efficiency, and operational costs, the engines will also need to produce lower emissions over a longer useful life. The challenges are significant for the selected and necessary technologies to be well-proven and cost-effective, while remaining customer-accept-able. Partnerships will be needed between engine and oil companies, along with DOE sponsorship.

DIESEL REGULATION
TRUCK

> 1998 (4.0 NOx, 0.10 PM)
- field, preproduction engines started

> 2004 (~ 2.0 NOx, 0.10 PM)
- technology/feasibility research underway

> 2007 / 8
- what new regulation may apply ?
- investigate potential
  - PRODUCTION- VIABLE
  - END-USER ACCEPTABLE technologies

CUSTOMER INPUT

IN ORDER OF PRIORITY

> RELIABILITY

> DURABILITY
- 1 million mile engine
- improved service intervals

> FUEL ECONOMY

>.

>

> *EMISSIONS*
- legal engines, but function the same as before

2004 DIESEL EMISSIONS

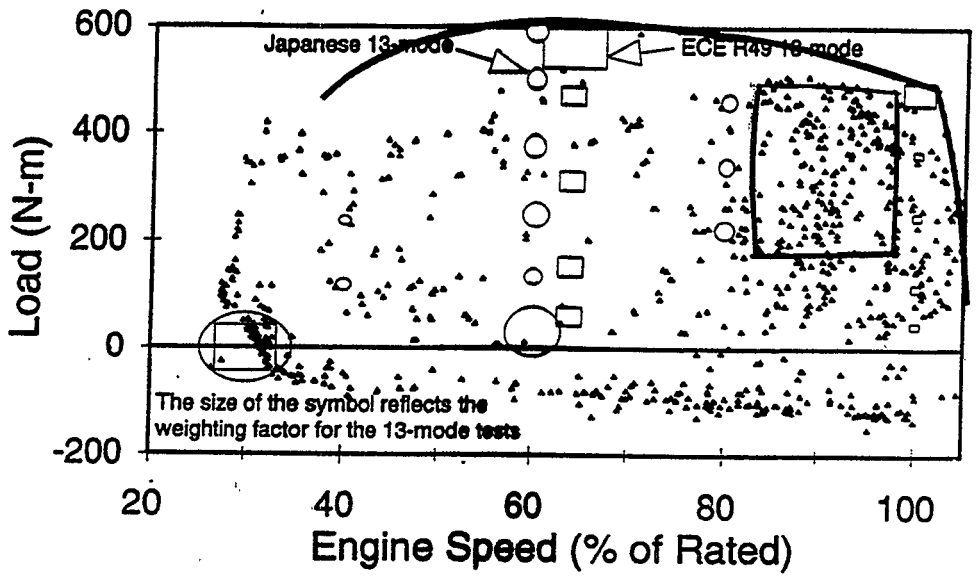
HEAVY & MEDIUM DUTY TRUCK ENGINES

2.0 g/hp.hr NOx, 0.10 Particulates

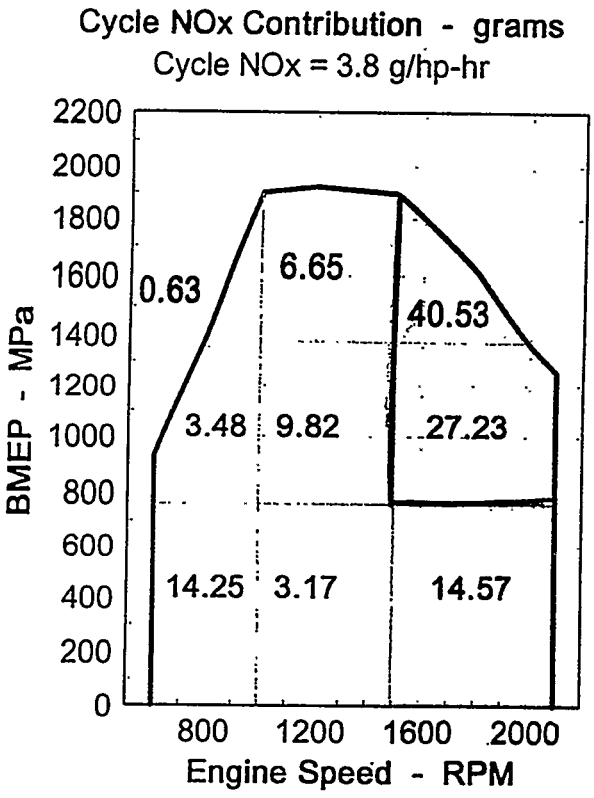
> EGR CONSIDERED KEY TECHNOLOGY
(transient control, durability, cooler efficiency and wear iss
> EUI / HEUI WITH INJECTION RATE SHAPE
(high peak injection pressures)
> SINGLE STAGE TURBOCHARGING (possible VGT)
> PISTON RINGs FOR REDUCED OIL-PARTICULATEs
> AFTERTREATMENT (probably limited to 2-way, medium duty)

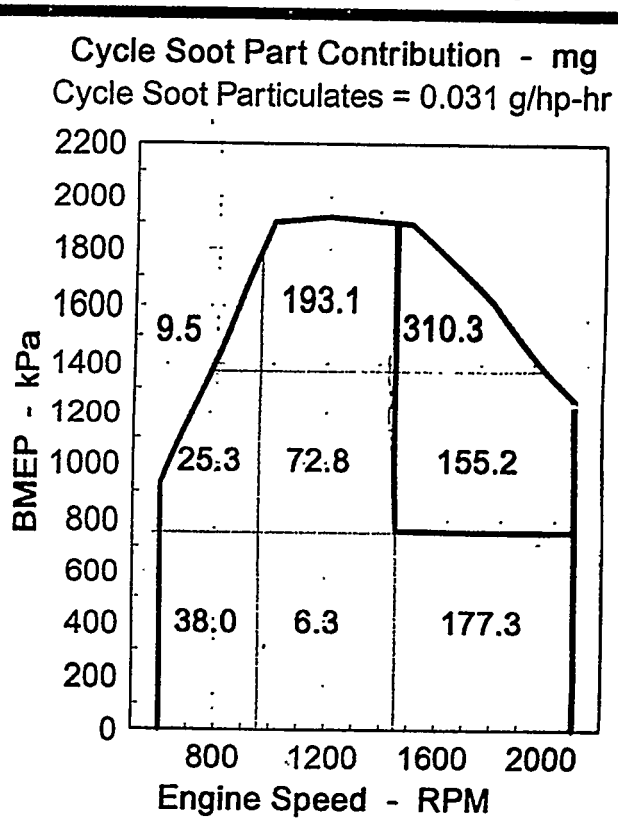
COMPARISON OF EMISSIONS CYCLES

Japanese 13, ECE R49, US FTP Cycles



Speed and Load Distribution of NOx and Particulates Formed During Transient Test Cycle





EGR - 2004

HEAVY & MEDIUM DUTY MOBILE APPLICATIONS

> EGR KEY TECHNOLOGY
> EFFECTIVE NOx REDUCTION TO 2004 LEVELS
> INTERNAL OR EXTERNAL LOOP
> 10 - 50% EGR THROUGH OPERATING RANGE
> COOLING BENEFICIAL

EGR - 2004 ISSUES

> CONTROL THROUGH TRANSIENT CYCLE
> AIR/FUEL RATIO CONTROL (may need vgt)
> BSFC
> PARTICULATES CONTROL (higher inj. press.)
> COOLER EFFICIENCY / SERVICE LIFE
> TURBOCHARGER WEAR (external loop)
> COMPONENT WEAR (short-hour tests encouraging)
> OIL DEGRADATION / SERVICE INTERVAL

> SYSTEM COST

FUEL INJECTION

> INJECTION RATE SHAPE

> PROGRAMMABLE ENTIRE OPERATING RANGE

> ELECTRONICALLY CONTROLLED FUEL SYSTEM

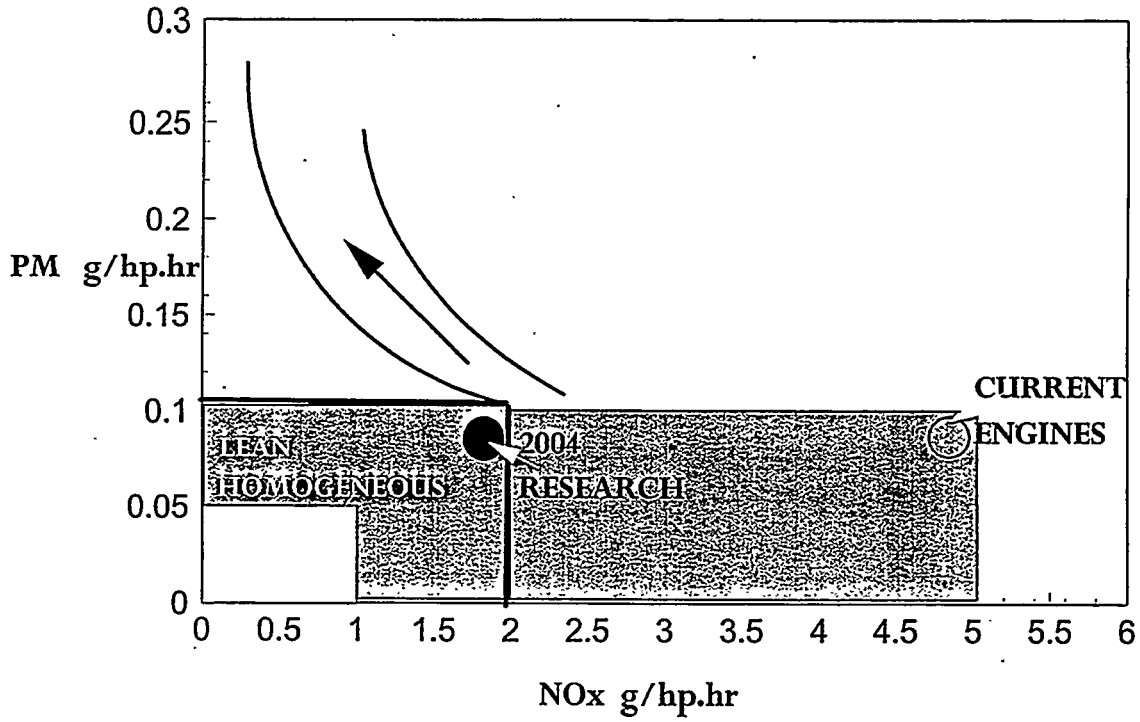
IN-CYLINDER EMISSIONS CONTROL

> NO APPARENT PRODUCTION VIABLE TECHNOLOGY FOR NOx & PM CONTROL

> IN-CYLINDER CATALYSIS
- concerns: available surface area, residence time
- recommending program to Oak Ridge

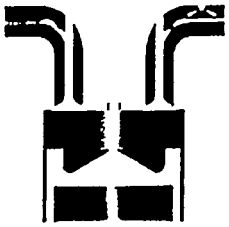
> COMBUSTION
- lean homogeneous

2007/8 DIESEL EMISSIONS COMBUSTION

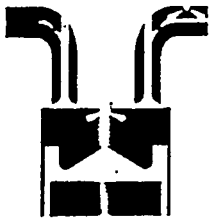


Lean Homogenous Combustion

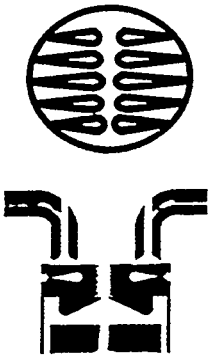
Experimental Configurations



Port Injected Diesel



PI Gas, DI Diesel



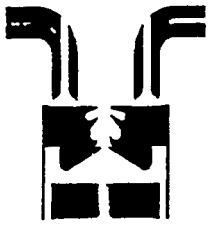
Multiple Side Injectors



Early Injection



Impingement Plate



Early Pre-Mix/Pilot Ignition

AFTERTREATMENT

> NOx AFTERTREATMENT SYSTEMS
  - scr, storage, denox, plasma
  - parasitic load/effectiveness

> NON-THERMAL PLASMA
  > DOE /CAT SUPPORT
    - NOXTECH, TECOGEN
    - 1997 ASSESS MERITS/POTENTIAL

> PROMISE OF ENGINE THERMAL EFFICIENCY

TOOLS

> PREDICTIVE ANALYSIS CODES
  - NOx, PM
  - KIVA, CHAD, OTHER COMMERCIAL

> NEED TO BE QUANTITATIVELY ACCURATE

> JOINT EFFORT DOE/INDUSTRY

> REDUCE ENGINE DEVELOPMENT, CYCLE

FUEL(S)

> ENGINE COMPANIES HAVE SIGNIFICANT R & D PROGRAMS FOR 2004 AND BEYOND

> BUT *CI FUEL MUST ALSO IMPROVE*
  - sulfur, cetane, aromatics, restructured h-c bonds?

> PARTNERSHIP DOE/ ENGINE/ FUEL COMPANIES NEEDED FOR BETTER CI FUEL

2007 / 8 EMISSIONS

> IN-CYLINDER NOx CONTROL
- NO DEFINED PRODUCTION VIABLE TECHNOLOGY

> IN-CYLINDER CATALYSIS
- proposing program to Oak Ridge

> LEAN HOMOGENEOUS COMBUSTION
- in regimes needed, ignition/comb. control challenges

> LEAN NOx AFTERTREATMENT
- maintain thermal efficiency

> SENSOR(s)
- nox

> DIESEL FUEL PROPERTIES

SUMMARY

> DIESEL ENGINE POWER PLANT OF CHOICE (medium, heavy..)
- efficiency, durability, owning/operating costs

> KEY TECHNOLOGIES WILL NEED ADDITIONAL FIELD-TIME
- more so if fuel, oil changes occur

> EMISSIONS CONTROL TECHNOLOGIES SELECTED
- COST-EFFECTIVE
- IMPROVE FUEL ECONOMY (fleets running 2-3% margin)
- END-USER ACCEPTED
- INCREASED EMISSIONS USEFUL LIFE (> 435,000 miles)

MICROWAVE REGENERATED PARTICULATE TRAP

A.C. McDonald, Jr. and T.M. Yonushonis, Cummins Engine Company, Inc.
W.C. Haberkamp, Fleetguard, Inc.
F. Mako, L.K. Len, R. Silberglitt, and I. Ahmed, FM Technologies, Inc.

INTRODUCTION

Since 1988 particulate matter (PM) emitted by diesel engines has decreased in excess of 80% from 0.60 g/BHp-Hr to 0.1 g/BHp-Hr. Diesel engine manufacturers continue to invest in technology to produce diesel engines that are environmentally sociable and compatible with the EPA legislated limits. Engine manufacturers have employed several methods to achieve the legislated EPA requirements listed in Table 1 including; advanced fuel injection systems, combustion and air handling technology and exhaust aftertreatment, e.g., catalysts, soot filters and particulate traps.

Table 1. Legislated Diesel Emission Requirements, g/BHp-Hr by year.

Year	Automotive HD	Urban Bus
Pre 1988	---	---
1988	0.6	0.25
1991	0.25	0.1
1994	0.1	0.05
2004	0.1	0.025

The diesel oxidation catalyst represents the single exhaust aftertreatment device equipped on production volume diesel engines. Although diesel particulate filters benefit from nearly thirty years of extensive research and evaluation many technical barriers remain unresolved including:

1. Extracting at least 90% of the particulate matter without degrading engine performance due to excessive exhaust restriction;

2. reducing thermal stresses produced by thermal gradients;

3. eliminating the catastrophic exothermic reaction that occurs when non-combusted particulate matter accumulates over several cycles suddenly ignites, melting the filter media; and

4. demonstrating system durability and reliability that are comparable to other engine components.

Previous efforts to develop a diesel exhaust particulate filter used an extruded cordierite wall flow filter that is heated by resistive or a fossil fuel burner [1, 2]. This effort focuses on developing a novel technology to reduce the particulate matter (PM) emitted by diesel engines while addressing the previous issues. This technology involves using a ceramic fibrous filter to collect the PM and microwaves to combust the collected PM or "regenerate" the filter. Compared to previous systems, a microwave filter offers the following potential advantages:

1. the porosity of the fibrous filter is inherent to the structure and not created from fugitive materials as with wall flow filters. This produces a structure without closed porosity that weakens the structure without participating in the filtration of the PM;

2. the filters are produced using current industry practices that can be readily automated; and

3. microwave heating produces rapid and uniform heating that reduces ther-mal gradients minimizes the resulting ther-mal stresses.

It has been demonstrated that microwaves can

heat filters and combust particulate matter [3, 4]. However, it has not been adequately demonstrated that a microwave system possesses the robustness necessary for the diesel environment. In addition to evaluating filter performance, this paper also examines the robustness of the magnetron in a simulated diesel truck environment.

FILTER DEVELOPMENT AND TESTING

FILTER DEVELOPMENT - The fibrous particulate filter is a composite structure comprised of aluminum oxide (Al2O3) fibers with a chemical vapor infiltrated (CVI) silicon carbide coating (SiC). The filter preform is produced from a paper manufacturing process that combines inorganic Al2O3 fibers with organic constituents to improve green strength. After the preform is cured a silicon carbide coating is applied. A report completed for the California Energy Commission contains a detailed description of filter design and development [5].

HEATING CHARACTERISTICS - After application of the silicon carbide coating the heating characteristics are evaluated using a laboratory bench test at the facilities of FM Technologies. Testing is conducted by wrapping an insulating sheet around the filter and placing the wrapped filter into a stainless steel cavity that is connected to a microwave source. Thermocouples are inserted into the filter at several radial locations and power is initiated to the magnetron. Temperature data are recorded as well as visual observations while the filter is heating. Extensive investigations and analysis by FMT have determined that microwaves are not adversely impacting the temperature measurements. Several tests were conducted where power was terminated and the temperature data does not show an abrupt change in slope. After reinstating the power the heating rate resumed at the initial rate.

A filter that has sufficient coating will display a dull glowing within 30 to 300 seconds and within 600 seconds the entire filter will demonstrate an orange glowing. The plot in Figure 1 depicts the rapid heating rates and the minimal thermal gradients that can be achieved using microwaves. A filter that is not coated properly will not demonstrate uniform heating or display the orange glow. Results of scanning electron microscopy, spectral analysis and a high temperature heat treatment suggest that filters that exhibit nonuniform heating do not contain sufficient silicon carbide on the interior. The filter in Figure 2 has completed a high temperature heat treatment and displays grayish regions devoid of structural rigidity. Elemental analysis indicates these regions are comprised primarily of aluminum with lesser amounts of silicon. Unlike silicon carbide the alumina fibers do not heat as readily in the presence of microwaves.

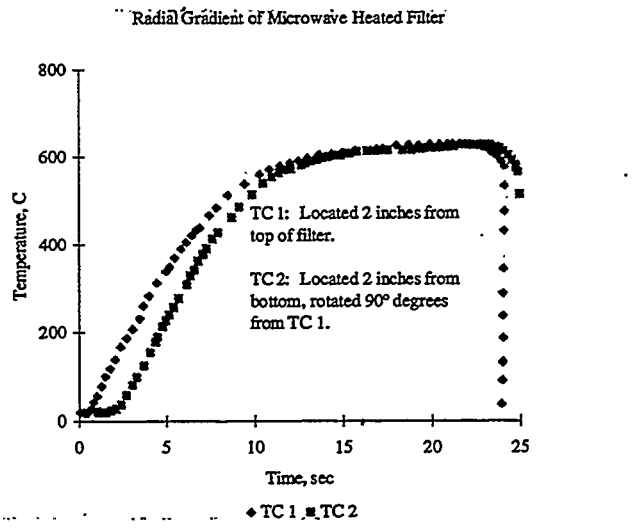


Figure 1. Plot of heating rate and thermal gradients for tibrous filter.

ENGINE TESTING - Engine tests have been completed using the silicon carbide coated fibrous particulate filter to evaluate particulate reduction and back pressure. Particulate emission reduction was evaluated using the transient emissions cycle and back pressure results were obtained using bench test evaluation.

Particulate reduction measurements were completed on two filters (81 D and 85M) by the Emissions Measurement Laboratory at the Cummins Technical Center (CTC). Both filters were evaluated over the transient emission

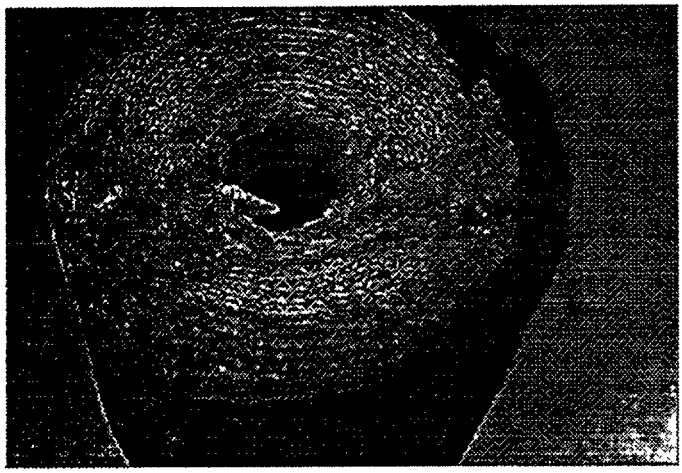


Figure 2. Photograph showing damaged regions on the Interior that were not fully coated and do not possess adequate structural rigidity.

cycle using production engines. Filter 81 D was canned by Nelson and installed in the test cell behind a 175 Hp B 5.9 liter engine. The filter was subjected to four hot cycles and one cold cycle. A review of the data indicated that the particulate levels increased compared to the baseline configuration (engine with catalyst).

After removing the filter from the test cell visual inspection revealed the exhaust pressure displaced and fractured the center core into smaller sections (Figure 3). It is likely that the small sections from the damaged core collected on the filter patch producing the apparent particulate increase. Before submitting filter 85M to the CTC emissions laboratory the core was sealed with a ceramic adhesive to prevent it from being displaced. It was canned by Nelson and then installed into the test cell behind a 215 Hp B5.9 liter engine. The results from this testing provided more encouragement than the first emissions test. Although visual inspection revealed that the core (the entire core remained in the can) was also displaced during testing, the data showed that a fifty percent reduction in particulate matter was achieved. Absence of the core resulted in an eleven percent increase in open frontal area that does not contribute significantly to exhaust filtration. Alternative methods of sealing the center are being evaluated. This filter was repaired and submitted for bench test evaluation.

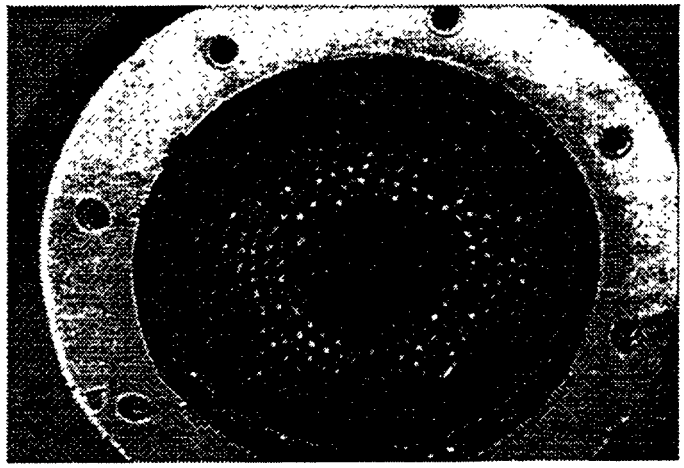


Figure 3. Photo of filter 81D without center core after completing transient emissions testing.

BENCH TEST EVALUATION - The bench test evaluation is used to evaluate the performance of new filter designs under a controlled environment and to compare the results with historical data. Bench testing consists of a typical test cell with dynamometer and engine; however, a by pass loop has been installed that restricts exhaust flow between thirteen and twenty two percent of full exhaust flow. This allows testing smaller units that would otherwise be incapable of withstanding the full exhaust flow and maintaining space velocities. Generally it is easier to fabricate smaller prototype filters in the range of six inches in diameter. The bench test evaluates characteristics such as, loading rates, balance point and engine back pressure. The balance point may be defined as the temperature at which the rate soot loading and combustion are equivalent.

After filter 85M was removed from the emissions test laboratory it was installed for bench test evaluation. The core was replaced with a sheet of kaowool insulation that was rolled to the correct diameter and inserted. The sheet was then trimmed to correspond to the filter length.

Figure 4 shows the results of the bench evaluation and comparison to a dense cordierite filter. Compared to the cordierite filter the

fbrous filter demonstrated extremely low engine back pressure. The slope of the fibrous filter curve indicate that particulates may be collec-ting at a faster rate or more effectively than the cordierite filter.

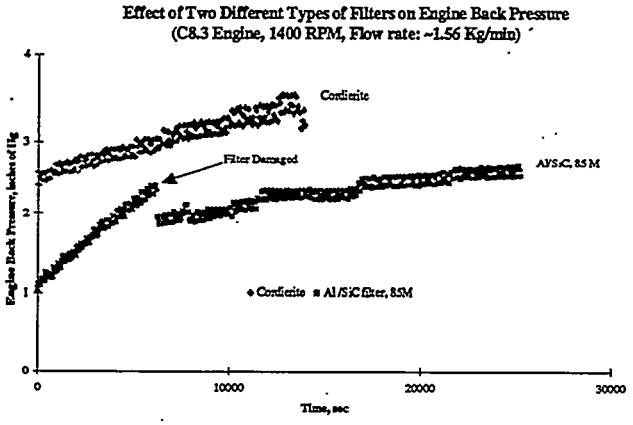


Figure 4. Effect of engine back pressure for fibrous and wall flow filters.

MAGNETRON DURABILITY

During the development of the microwave particulate filter significant process has been made on how to deliver or "port" microwaves to the filter. Previous researchers [3, 4] have demonstrated that it possible to heat particulate filters and combust particulates using microwaves instead of resistive or fossil fuel burners. In fact our work has repeatedly demonstrated that microwave heating of a filter is readily accomplished; however, the robustness of the components associated with producing microwaves (magnetron) has not been evaluated. This is an important consideration since development of the diesel oxidation catalyst [6, 71 required extensive research, design and testing to ensure durability and reliability. Notwithstanding, the Environmental Protection Agency (EPA) legislated durability requirements of 8 years/290,000 miles for exhaust aftertreatment devices, customers expect all engine components to exhibit durability comparable to the engine. In the case of diesel engines today one million miles is not unrealistic.

Cummins has extensive knowledge and experience assessing the durability of electronic components, many of our engines incorporate electronics in the fuel injection systems. A first step to understanding the durability is to expose the component to a simulated diesel operating environment, including road and cab vibration, severe thermal conditions, and salt and humidity.

VIBRATION TESTING - Initial screening of magnetron robustness was assessed by conducting vibration testing for twenty hours on three mutually perpendicular primary axes (x, y, z).

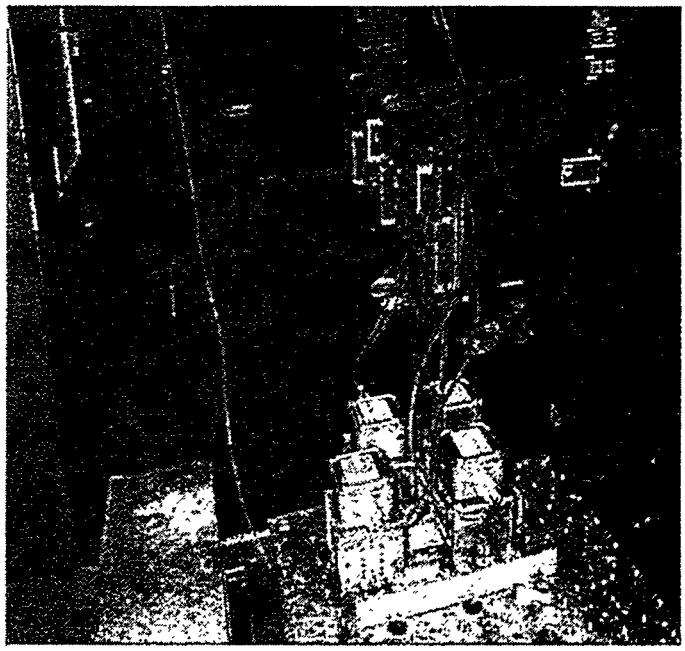


Figure 5. Photograph of magnetrons Installed on vibration stand prepared for "hot" testing.

Figure 5 shows the magnetrons being installed for vibration testing. The spectrum used to complete the testing was acquired from vehicles during operation. Before proceeding to production, new electronic components must demonstrate an ability to complete this testing without incident.

There were four sets of testing completed on three groups of magnetrons. Post test inspection evaluated mechanical damage and electrical characteristics. Initially the magnetrons were tested without current supplied

to the filament (referred to as "cold" testing). Once cold testing was successfully completed, electrical current was connected to evaluate the robustness of a "hot" filament.

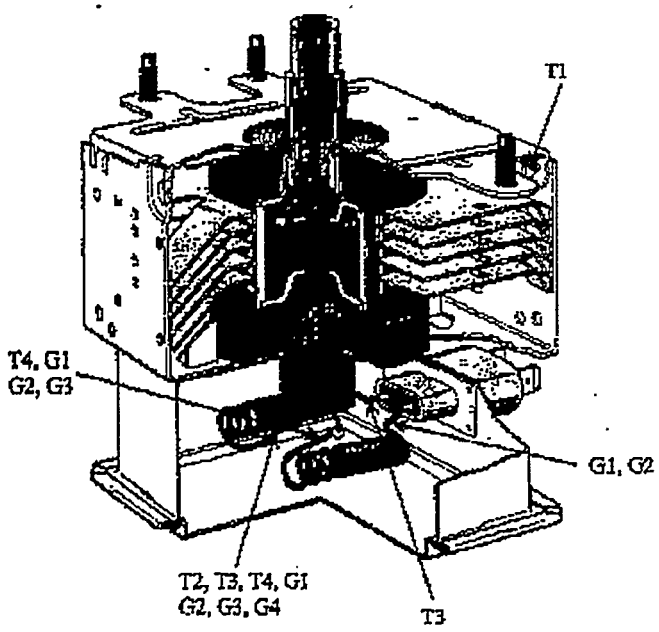


Figure 6. Schematic of magnetron Indicating location of failures.

During the cold tests nine out of the ten magnetrons incurred damage at the inductor and the remainder at the housing tab (Figure 6). After analyzing the failures it was determined that by reinforcing the "weak" spots the components would survive the test. The inductors were reinforced by applying a silicone based adhesive and allowing it to cure at ambient temperature. The reinforced magnetron's were then subjected to a cold test and all completed the test without incident. Next the same set of reinforced magnetrons were connected to power supplies that would allow current to flow without generating microwaves. The current output was monitored during testing to determine when a failure occurred. One of the magnetrons suffered a fatigue failure on a mechanical tab during the first twenty hours; however, the remainder completed the test without incident.

ON BOARD POWER

All testing previously presented was conducted by powering the magnetrons using 110 V from a standard power outlet. However, on-board operation requires using the power available from the vehicle's electrical system. To investigate the feasibility of operating the magnetron using on board power a bench test was developed consisting of a 5 horsepower engine, a 150 amp alternator, a battery, and an inverter (Figure 7). The engine operated the alternator at 8325 RPM which produced 150 A with a 0.1 ohm load. The system was then connected to the inverter which generated 110 V used to power the magnetron's, 143 amps went to the load and 7 amps went to the battery. The magnetron was successfully powered by the setup and the filter heated up.

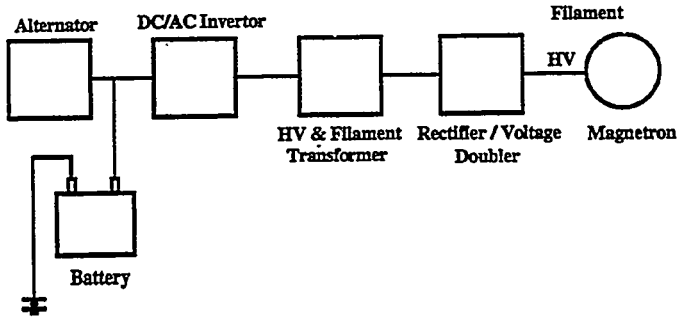


Figure 7. Schematic of circuit designed to operate a microwave power on-board a diesel truck.

SUMMARY

It has been demonstrated that a fibrous particulate filter can extract particulate matter from the diesel exhaust. However, additional engineering efforts remains to achieve the design target of 90%. It has also be shown that with minor modifications magnetrons produced for home ovens can endure a simulated diesel operating environment.

Much work remains to develop a robust product ready to complete extensive engine testing and evaluation. These efforts include,

1. additional environmental testing of magnetrons;

2. vibration testing of the filter in the housing;
3. evaluating alternative methods/ designs to seal the center bore: and

4. determining the optimum coating thickness that provides sufficient structural integrity while maintaining rapid heating rates.

ACKNOWLEDGMENTS

The authors gratefully acknowledge the support of John Fairbanks and Ron Graves of the Department of Energy and Jim Patten of Cummins Engine Company. The authors also acknowledge the contributions of Dave Stinton of the Oak Ridge National Laboratory, Dick Nixdorf of ReMaxCo., Darren Welson of B.F. Goodrich, the Cummins State Street Laboratory, and Mike Goble, Shouxian Ren and Monty Green of the Cummins Engine Company.

REFERENCES

1. McDonald, J. S. and Simon, G. M.; "Development of a Particulate Trap System for a Heavy -Duty Diesel Engine," SAE 880006.

2. Kojetin, P.; Janezich, F.; Sura, L. and Tuma, D.; "Production Experience of a Ceramic Wall Flow Electric Regeneration Diesel Particulate Trap," SAE 930129.

3. Garner, C. P.; and Dent, J. C.; "Microwave Asisted Regeneration of Diesel Particulate Traps," SAE 890174.

4. Walton, F. B.; Hayward, P. J. and Wren, D. J.; "Controlled Energy Deposition in Diesel Particulate Filters During Regeneration by Means of Microwave Irradiation," SAE 900327.

5. The Cummins Engine Company, Inc.; "Microwave Regenerated Particulate Trap for Diesel Engines," California Energy Commission Consultant Report; Contract 500-92-047; June 1995.

6. Clerc, J. C.; Miller, R. K.; McDonald, Jr., A. C. and Schlamdinger, H.;"A Diesel Engine/Catalyst System for Pick-up and Medium-Duty Trucks," SAE 932892.

7. Miller, R. K.; McDonald, Jr., A. C. and Gulati, S. T.; "Systems Design for Ceramic LEA Substrates for Diesel/Natural Gas Flow-Through Catalysts," SAE 950150.

COMMERCIAL INTRODUCTION OF THE ADVANCED NOxTECH SYSTEM

B. C. Sudduth
NOxTECH. iNC.

INTRODUCTION

NOxTECH, Inc. is commercializing emissions control systems for combustion equipment. The first commercial product is the Advanced NOxTECH system for diesel engine exhaust. This system reduces NO_x emissions more than 90% and controls emissions rates below 0.25 g NO_2/hp-hr. These emissions reductions are achieved without NH_3 slip which is characteristic of other chemical aftertreatments such as selective catalytic reduction (SCR).

The Advanced NOxTECH system replaces the exhaust silencer for diesel engines. This simple, compact design was developed as an improvement to the commercial NOxTECH systems which are Best Available Control Technology (BACT) for diesel electric generators. Advanced NOxTECH uses a liquid chemical which reduces equivalent to powdered cyanuric acid. Like cyanuric acid powder, the liquid chemical is non-hazardous and innocuous, but it is handled more simply and conveniently than powder.

Southern California Edison Company (Edison) is using a NOxTECH system daily to operate a 2.8 MW diesel generator in compliance with their operating permit for a new major NO_x emissions source in the Los Angeles Air Basin. Also, a 150 kW Advanced NOxTECH system is operating at the NOxTECH test facility in Irvine, CA. Based on this successful development plan (Sudduth, et. al. 1995), NOxTECH, Inc. is introducing commercial systems as described below.

NOxTECH ESTABLISHED AS BACT

A first commercial NOxTECH system was installed on a 1.5 MW generator at the Edison Pebbly Beach Generating Station. This system demonstrated compliance with Rule 1110.2 of the South Coast Air Quality Management District (AQMD). Based on these results, the AQMD permitted Edison to construct a new 2.8 MW generating unit using the NOxTECH system for exhaust aftertreatment. The NOxTECH system was supplied to Edison with a guarantee for 95% NO_x reduction meeting the BACT requirement for major emissions sources.

This NOxTECH system (Picture 1) started operating in October 1995. By December 1995, the system was reliably reducing NO_x as much as 98% at 1400° F. During this period, the reactor startup procedure was modified for unexpectedly low engine exhaust temperatures of only 500-600°F. The modified procedure enabled the NOx-TECH system to startup within about 45 minutes while the engine exhaust slowly warmed up to normal operating temperatures in the range of 500-600° F.

The NOxTECH control system was upgraded in early January 1996 to implement the modified startup procedure automatically. As soon as the 4,000 hp engine switches from idle to run status, the burner firing rate is controlled to maintain an exhaust gas temperature of 1400° F in the NOxTECH reactor. This hot gas discharges into the NOxTECH heat exchanger for preheating the engine exhaust. After the engine warms up, the burner shuts down and the temperature is controlled by injecting diesel fuel directly into the preheated exhaust. The heat recovery and exhaust preheating minimize the consumption of diesel fuel to control the reactor temperature at 1400° F.

The final emissions source tests were conducted in late January 1996 following the successful automation of the modified start-up procedure. In addition to verifying compliance with the operating permit, the source tests also confirmed that the NOx-TECH system decreased particulate emissions by about 60% with negligible reaction by-products. Using powdered cyanuric acid to reduce NO_x, the system maintained CO below 50 ppm and NH_3 slip never exceeded 2 ppm. Extensive third-party testing detected no toxic reaction by-products.

These source test results established NOx-TECH as BACT for diesel electric generators. Since January 1996, continuous emissions monitoring has verified compliance with the new source operating permit for the 2.8 MW generator. These successful emissions controls have enabled Edison to expand their diesel electric power generating capacity on Catalina Island. Without this BACT performance, the emissions regulations would have required Edison to install combustion turbine generators at much greater expense.

ADVANCED NOxTECH SYSTEM

The Advanced NOxTECH system was developed to decrease the size, weight, and cost of equipment for BACT emissions reductions. In this system, the reactor and heat exchanger are integrated compactly together. Resembling an exhaust silencer, this configuration greatly improves heat recovery and accommodates thermal cycling to temperatures in the range of 1400-1550° F. At these conditions, the gas-phase NO_x reduction is completed in only 0.2-0.3 seconds, and less fuel is added to maintain the temperature.

NOxTECH, Inc. is operating a full-scale commercial prototype (Picture 3) of the advanced system at its test facility in Irvine, CA. This system replaces the silencer on a 150 kW generator. The engine exhaust discharges directly from the turbocharger to the Advanced NOxTECH system. The temperature and liquid chemical injection are controlled automatically as illustrated in Figure 1. NO_x reduction is monitored using stack gas emissions measurements.

In the Advanced NOxTECH prototype, the engine exhaust is first preheated within 120-150° F of the reaction temperature for NO_x reduction. After this heat recovery, the temperature is controlled by adding diesel fuel to the preheated exhaust, and the liquid chemical is injected to reduce NO_x. The gas-phase reactions require no solid catalytic surfaces. After NO_x removal, heat is recovered to preheat the engine exhaust and cool the treated stack gas.

The Advanced NOxTECH heat exchanger operates effectively throughout the normal load range for the diesel engine. The steady-state temperature measurements in Figure 2 show this performance in the range of 20-160 kW. The engine exhaust is consistently preheated to 1230-1370° F even though the turbocharger discharge varies between 600° F and 1080° F with generator load. No fuel is consumed for this exhaust preheating.

Diesel fuel is added only to control the reactor exit temperature. The preheated exhaust temperature increases by only 120-150° F. After NO_x reduction, the hot exhaust exits the reactor and enters the heat exchanger. The incremental heating enables countercurrent heat exchange between the hot treated gas and the engine exhaust. The stack gas temperature increases less than 120-150° F due to heat losses.

Heating the exhaust gas by 120-150° F increases fuel consumption less than 8% at full load. With Advanced NOxTECH, this small fuel penalty enables more than 90% NO_x reduction. Engine modifications cannot reduce NO_x equivalently, and they penalize fuel consumption more severely. The Advanced NOxTECH system reduces NO_x emissions more efficiently and cost-effectively than any engine modifications.

COST-EFFECTIVE EMISSIONS COMPLIANCE

The Advanced NOxTECH system enables diesel engines to operate most efficiently and cost-effectively. Higher baseline NO_x levels and lower exhaust temperatures do not increase the fuel consumption. BACT emissions levels are maintained while engines operate at maximum fuel efficiency, power production, and service reliability. This optimization of engine operations conserves fuel and offsets the small fuel penalty for Advanced NOxTECH which removes NO_x more selectively and less expensively than engine modifications.

The Advanced NOxTECH system reduces high NO_x levels in proportion to the liquid chemical injection. In Figure 3, this NO_x reduction is expressed stoichiometrically on a basis comparable to cyanuric acid which decomposes and forms HNCO. Emissions of about 6.0 g NO_2/hp-hr are reduced proportionately as much as 90%.

Chemical consumption increases more than stoichiometrically only when NO_x levels are reduced below 1.0 g NO_2/hp-hr. The NO_x emissions are reduced 95% or more to levels below 0.25 g NO_2/hp-hr by injecting liquid chemical in excess of stoichiometric amounts. The Advanced NOxTECH system maintains NH_3 slip below 2 ppm despite 50% excess chemical injection.

With the low-cost liquid chemical and the high-efficiency heat exchanger, NO_x removal costs are generally lower than $700/ton (basis NO_2 removed). This operating cost for fuel and chemical corresponds to a baseline NO_x level of 6.0 g NO_2/hp-hr. Since the gas-phase NO_x reactions do not deteriorate like catalysts, emissions are always reduced reliably using the same fuel and chemical injection.

NOxTECH, Inc. is quoting costs of about $100/kW for the Advanced NOxTECH system in prime power applications. These costs for introductory units depend on the performance guarantees in specific applications. Production units with standard performance guarantees are expected to cost $30-60/kW after about one-year of introductory unit operations.

In standby applications, the Advanced NOxTECH system costs about half as much as for prime power units. The heat exchanger is not needed when the startup burner is operated continuously to preheat the engine exhaust. If units are operated infrequently, the exhaust is preheated less expensively using the burner rather than the heat exchanger.

Less stringent emissions reductions lower both the equipment and operating costs for Advanced NOxTECH. For example, a 1.8 g NO_2/hp-hr engine is controlled below 1.0 g NO_2/hp-hr by treating 50% of the exhaust with 90% NO_x reduction. Then, Advanced NOxTECH costs only half as much as a standard application requiring 90% NO_x reduction overall, and the fuel consumption is increased no more than 4% because only half of the exhaust is heated to reaction temperatures. The liquid chemical consumption remains proportional to the NO_x removed when NO_x reduction does not exceed about 90%.

EMISSIONS CONTROL ADVANTAGES

The Advanced NOxTECH system uniquely controls exhaust temperature. The burner quickly establishes the reactor temperature after engine startup. As the engine warms up, the burner modulates to maintain the reactor temperature. After the engine is warmed up, the burner or a heat exchanger can preheat the engine exhaust. In either case, the exhaust is heated continuously to an optimum temperature for NO_x reduction.

This unique temperature control enhances emissions control in comparison with other exhaust aftertreatments. In standby applications, the Advanced NOxTECH system operates effectively before the engine exhaust is warm enough for catalytic NO_x removal. Soon after startup, the Advanced

NOxTECH system is removing CO, particulates, and ROG's.

Advanced NOxTECH does not trade off one pollutant for another. The NOxTECH temperature control reliably maintains NH_3 slip below 2 ppm even when NO_x is reduced by 95% or more. In SCR systems, NO_x emissions are reduced more than 90% only by greatly increasing NH_3 slip or catalyst volume. The catalyst accumulates poisonous contaminants and represents a hazardous waste similar to excess NH_3 slip.

Even engine modifications cannot generally remove NO_x concurrently with CO, particulates, and ROG's. Engine modifications typically result in tradeoffs between the different pollutants which can damage SCR catalysts by plugging their pores with soot or poisonous contaminants. Only Advanced NOxTECH removes all criteria pollutants concurrently, and no exhaust contaminants are detrimental to the gas-phase thermal reactions.

These inherent advantages enable NOxTECH systems to control emissions reliably without continuous emissions monitoring. Advanced NOxTECH can maintain emissions compliance using feedforward control of the liquid chemical injection. Only a feedback temperature control is needed to ensure effective reduction of all criteria pollutants. NOxTECH, Inc. is testing various methods for verifying NO_x reduction without measuring NO_x specifically.

OTHER NOXTECH APPLICATIONS

With its inherent advantages, NOxTECH is suited to a wide range of commercial and industrial applications. The Advanced NOxTECH system can compactly replace the exhaust silencers for mobile diesel engines, especially in fleet applications including trucks, buses, and locomotives. NOxTECH, Inc. is also planning to test equipment for applying the technology to industrial and utility boilers.

The Advanced NOxTECH system is especially well-suited for coal-fired utility boilers. A boiler retrofit requires only the installation of an injection grid and control system. The boiler operations already preheat the exhaust gas and recover waste heat. Such boiler retrofits are projected to cost less than half as much as SCR systems. Advanced NOxTECH is expected to enhance flyash properties substantially, decreasing unburned carbon. In this case, flyash is upgraded from a hazardous waste to a valuable cement component.

SUMMARY AND CONCLUSIONS

NOxTECH is BACT for diesel electric generators. Emissions of NO_x are reduced 95% or more with substantial concurrent reductions in CO, particulates, and ROG's. No engine modifications or other exhaust aftertreatments can remove all criteria pollutants as effectively as NOxTECH. The NOxTECH system reliably maintains NH_3 slip below 2 ppm. Unlike other emissions controls, NOxTECH does not generate hazardous by-products.

The Advanced NOxTECH system reduces the size, weight, and cost for BACT emissions reductions. Based on the operation of a 150 kW prototype, NOxTECH, Inc. is quoting commercial units for diesel electric generators. Advanced NOxTECH equipment costs about half as much as SCR systems, and NOx reduction can exceed 95% with guarantees for emissions compliance.

REFERENCES

Sudduth, B.C., M. Addy, M. Ramavajjala, V. Palekar, S. Ren, and R. Slone, "Advanced NOxTECH System for Exhaust Aftertreatment", Proceedings of the 1995 Diesel Engine Emissions Reduction Workshop, July 24-27 (1995).

ACKNOWLEDGEMENT

NOxTECH, Inc. has developed the Advanced NOxTECH system with assistance from the U.S. Department of Energy.

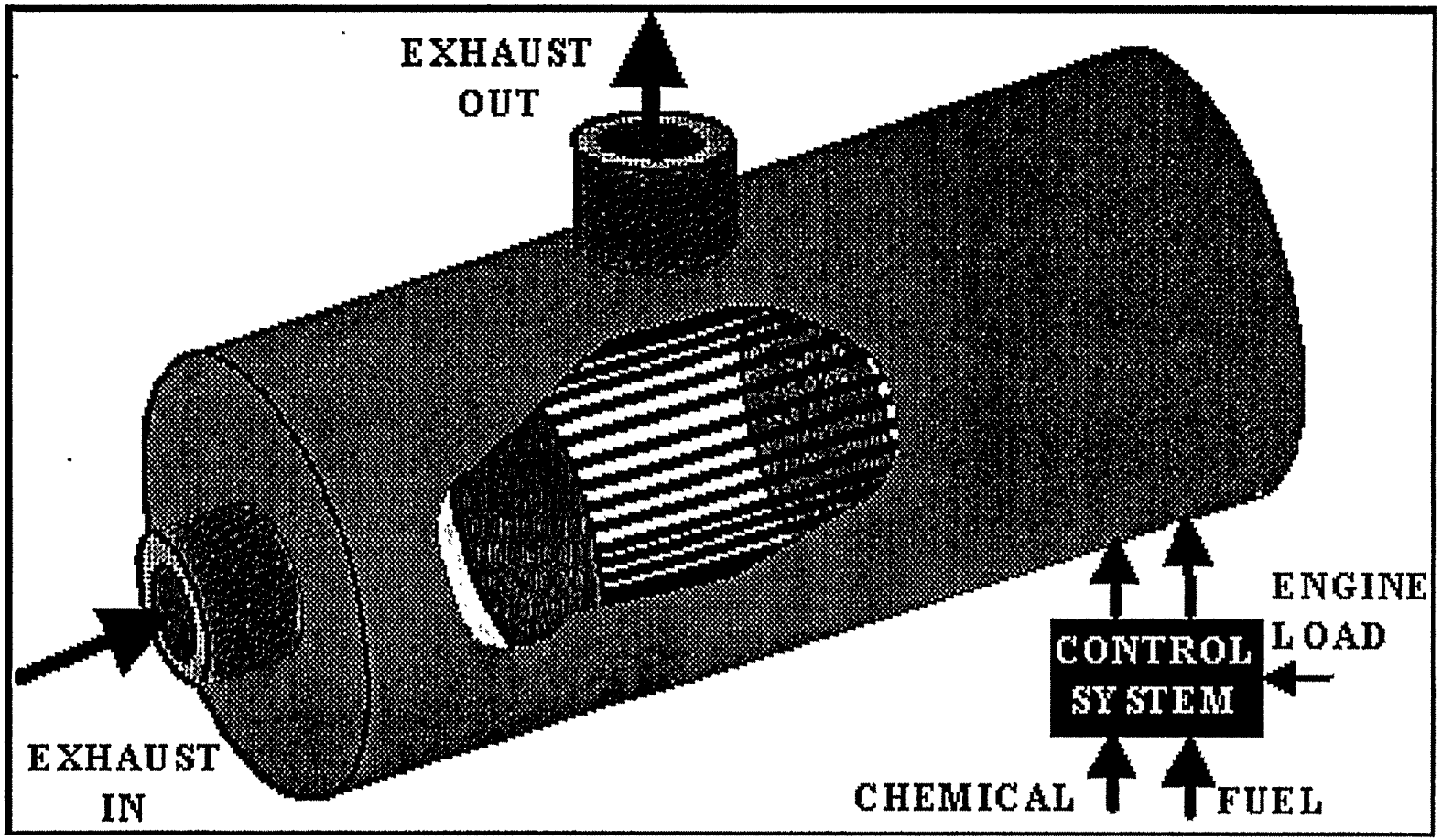


Figure 1 Controlled Fuel and Chemical Injection for Exhaust Aftertreatment

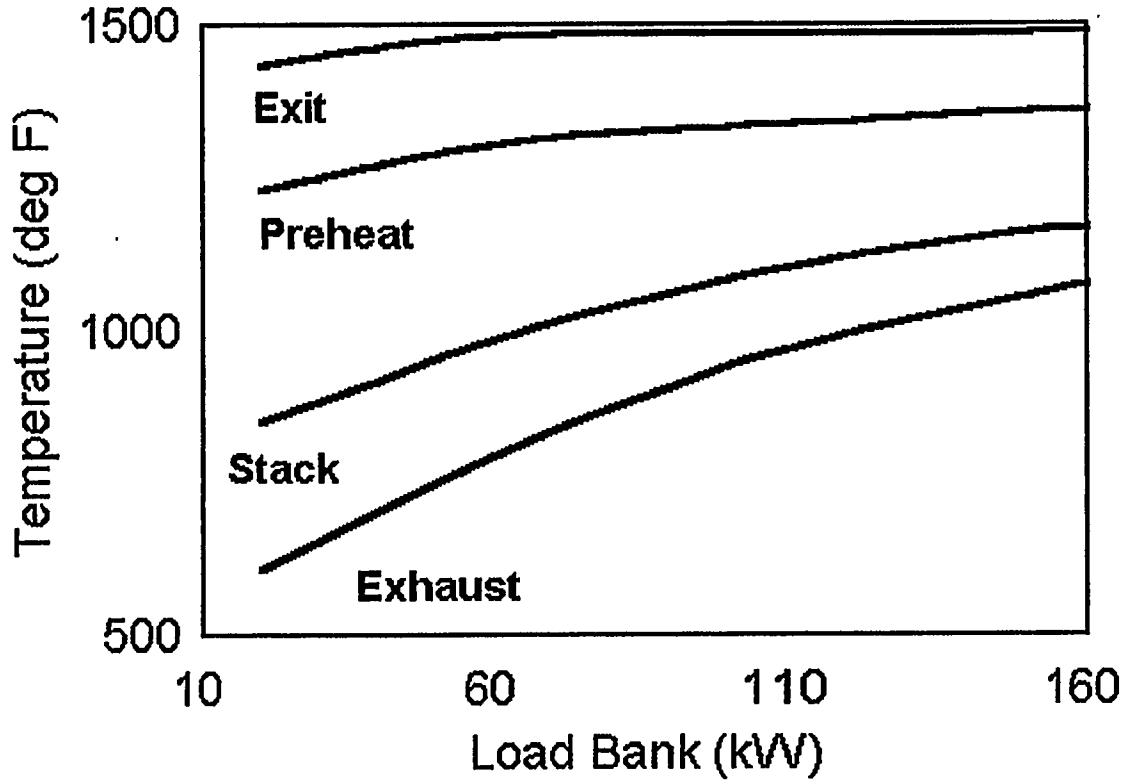


Figure 2 Uniform Exhaust Preheating Over Load Range

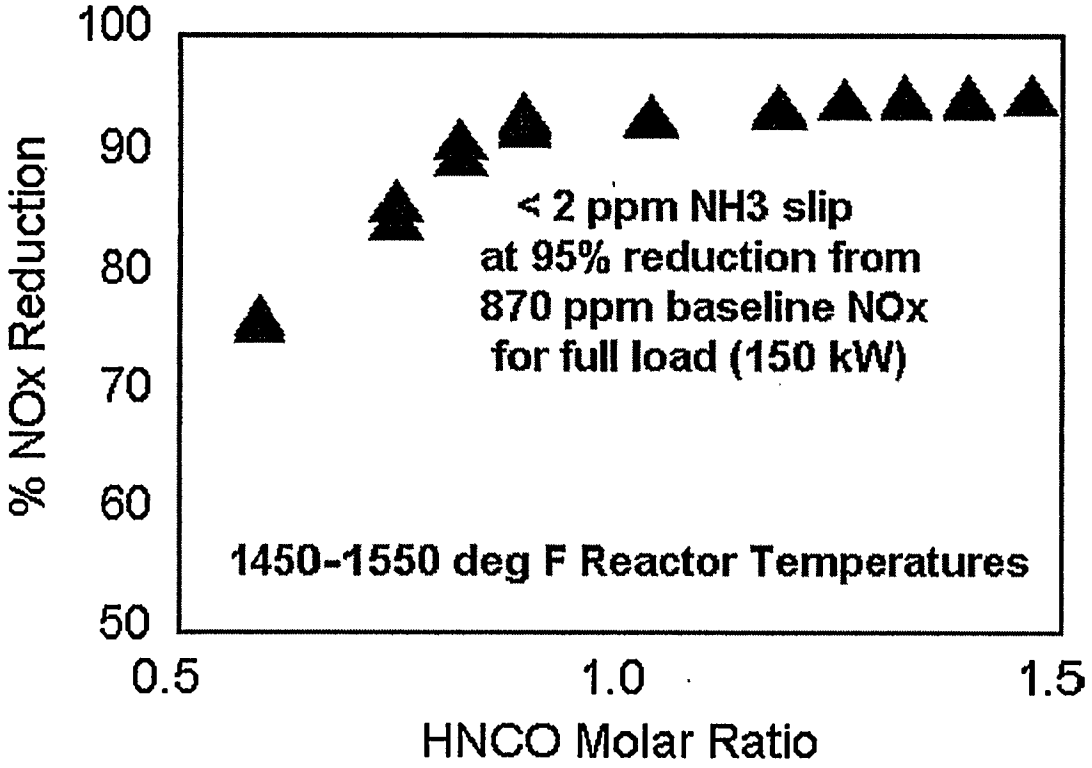
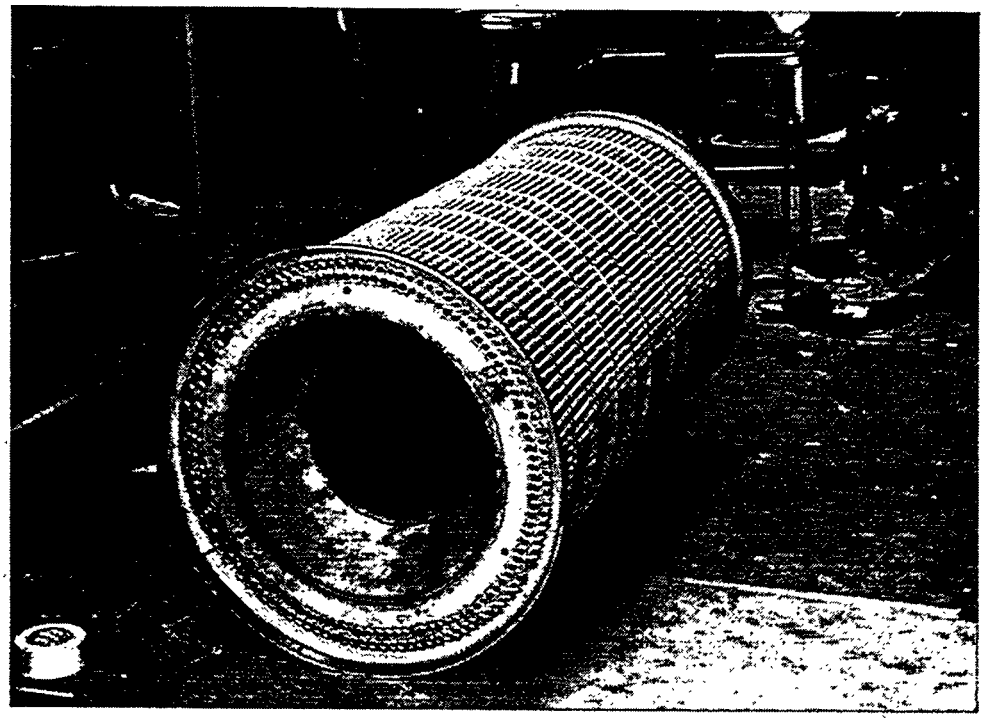


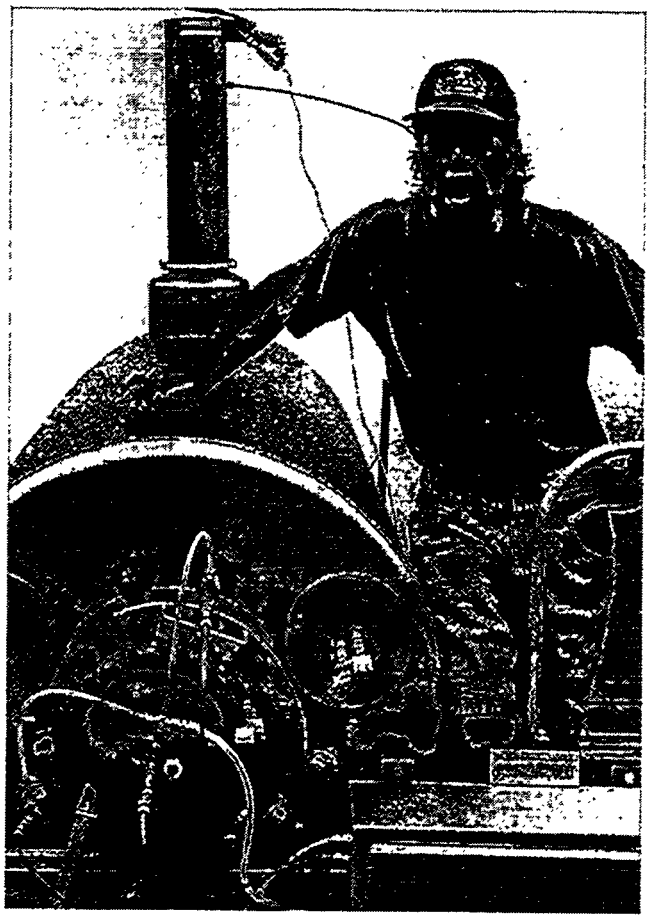
Figure 3 Liquid Injection Equivalent to Cyanuric Acid



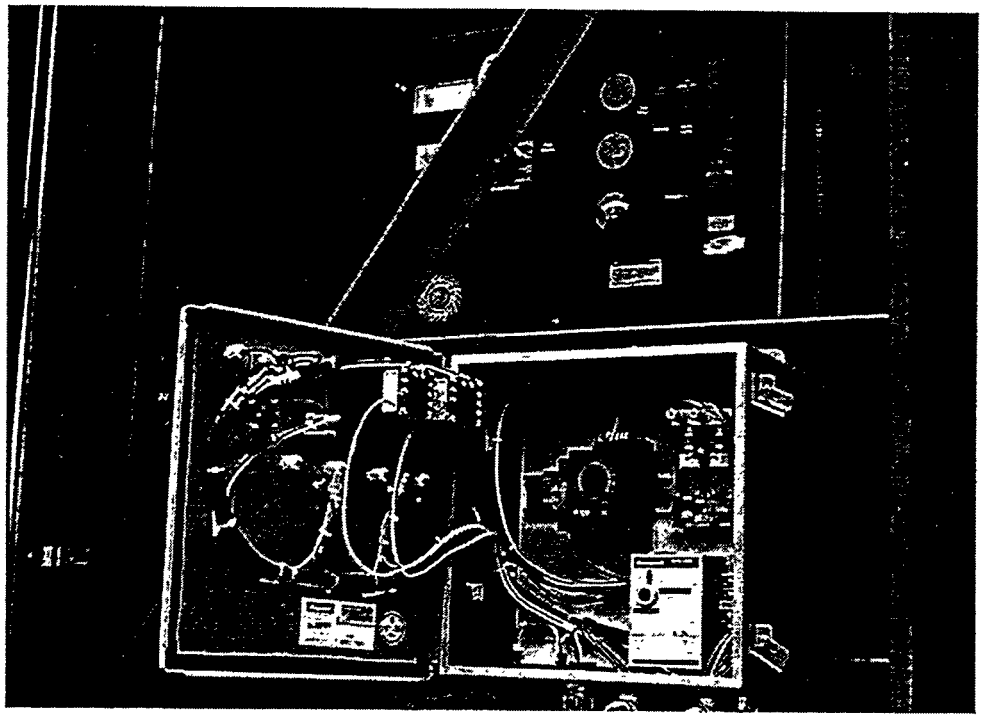
2.8 MW system established NOxTECH as BACT for diesel generators



Advanced NOxTECH heat exchanger surrounds open reaction chamber



. Commercial NOxTECH protoype resembles and replaces exhaust silencer



NOxTECH temperature control ensures removal of all criteria pollutants

SESSION V

Combustion, Fuel, and Air Management

Chairman: Mike Osborne
U.S. Naval Sea Systems Command

DIESEL COMBUSTION AND EMISSIONS FORMATION USING MULTIPLE 2-D IMAGING DIAGNOSTICS

J.E. Dec
Sandia National Laboratories

INTRODUCTION

Understanding how emissions are formed during diesel combustion is central to developing new engines that can comply with increasingly stringent emission standards while maintaining or improving performance levels. Laser-based planar imaging diag-nostics are uniquely capable of providing the temporally and spatially resolved information required for this understanding.

Using an optically accessible research engine, a variety of two-dimensional (2-D) imaging diagnostics have been applied to investigations of direct-injection (DI) diesel combustion and emissions formation. These optical measurements have included the following laser-sheet imaging data: Mie scattering to determine liquid-phase fuel distributions, Rayleigh scattering for quantitative vapor-phase-fuel/air mixture images, laser induced incandescence (LII) for relative soot concentrations, simultaneous LII and Rayleigh scattering for relative soot particle-size distributions, planar laser-induced fluorescence (PLIF) to obtain early PAH (poly-aromatic hydrocarbon) distributions, PLIF images of the OH radical that show the diffusion flame structure, and PLIF images of the NO radical showing the onset of NO_x production. In addition, natural-emission chemiluminescence images were obtained to investigate autoignition.

These imaging diagnostics have been used to map out the processes occurring in the cylinder of an operating diesel engine from the start of injection, through autoignition, the premixed burn, and the first part of the mixing-controlled burn (*i.e.* until the end of injection). Each diagnostic provides important information on the corresponding aspect of diesel combustion; however, combining the results of the individual measurements provides an even greater understanding of the combustion and emissions formation processes. This more complete understanding leads to a description or "conceptual model" of diesel combustion [1].

In the following sections the experimental setup is described, and the image data showing the most relevant results are presented. Then the conceptual model of diesel combustion is summarized in a series of idealized schematics depicting the temporal and spatial evolution of a reacting diesel fuel jet during the time period investigated. Finally, recent PLIF images of the NO distribution are presented and shown to support the timing and location of NO formation hypothesized from the conceptual model.

EXPERIMENT DESCRIPTION

A schematic of the optically accessible engine used for the imaging measurements is shown in Fig.1. The engine is a single-cylinder, direct-injection, 4-stroke diesel engine based on a Cummins N-series production engine. The N-series engine is typical of heavy-duty size-class diesel engines, with a bore of 140 mm and a stroke of 152 mm. These dimensions are retained in the optical-access engine, and a production Cummins N-series cylinder head is used so that the production engine intake port geometry is also preserved.

The design of this engine utilizes a classic extended piston with piston-crown window. Additional windows located around the top of the cylinder wall provide the orthogonal optical access required for the two-dimensional (planar) laser imaging diagnostics. These

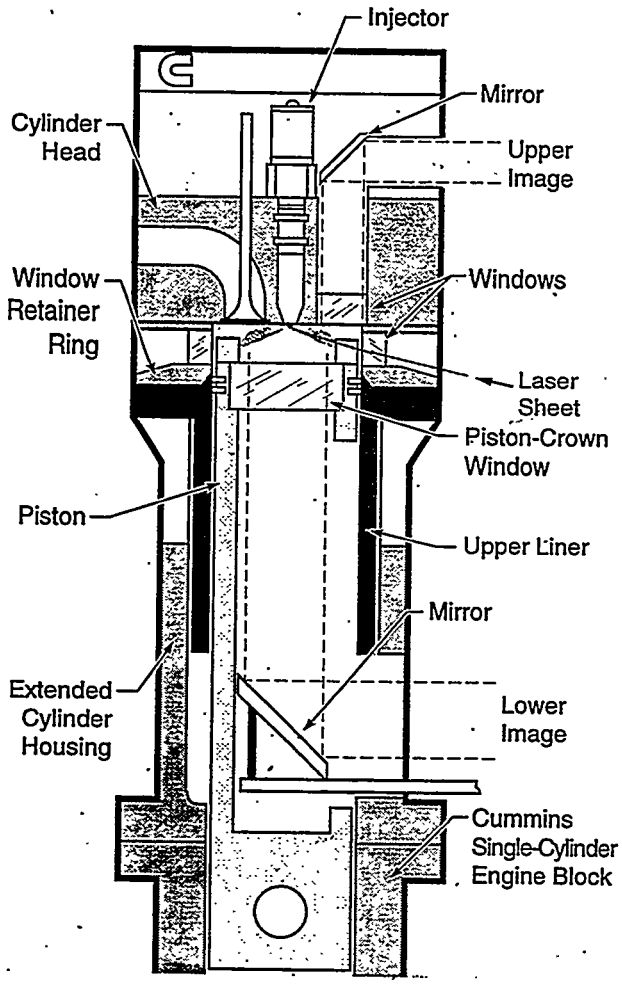


Figure 1. Schematic of the optical-access diesel engine showing the laser sheet along the fuel jet axis. Images were obtained through both the cylinder-head window (upper image) and the piston-crown window (lower image).

windows allow the laser sheet to enter the cylinder along the axis of the fuel jet (see Fig. 1) or horizontally. A window in the cylinder head replaces one of the two exhaust valves to obtain a view of the squish region and the outer portion of the combustion bowl. A complete description of the engine may be found in Ref. [2].

The experiments were conducted at a medium speed (1200 rpm) operating condition with a motored TDC (top dead center) temperature and pressure of 992° K and 5.0 MPa, which are representative diesel-engine conditions. Before conducting the experiments the engine was heated to 368° K (95°C) by means of electrical heaters on the "cooling" water and lubricating oil circulation systems. To minimize the rate of window fouling and to avoid overheating, the engine was fired once every 10th or 20th engine cycle, at which time the data were acquired. A complete discussion of the operating conditions and fuels used for the experiments may be found in Ref. [1].

Figure 2 presents a typical plot of the cylinder pressure, injector needle lift, and apparent heat release rate. As is typically found in diesel combustion, the apparent heat release rate curve in Fig. 2 first goes negative just after the start of injection as fuel vaporization cools the in-cylinder air. Then, after a few degrees, the combustion energy release exceeds that required for vaporizing the fuel, and the apparent heat release rises rapidly. The heat release rate curve then goes up through a local maximum and drops back down before rising again more slowly through a second local maximum. The initial sharp rise and fall is due to the rapid combustion of fuel that has premixed with air during the ignition delay period, and it is commonly referred to as the "premixed burn" or the "premixed burn spike". The second, broader hump in the curve is due to the mixing-controlled combustion and is commonly referred to as the "mixing-controlled burn".

Several different lasers, laser-sheet configurations, and camera setups were used for the various imaging data presented in this article. The laser sheets were typically about 25 mm wide and 250 to 300 mm thick at the probe volume. As shown in Fig.3, the laser sheet entered the combustion chamber through one of the windows at the top of the cylinder wall which was in line with one of the fuel jets. The laser sheets were oriented either horizontally or along the fuel jet axis, and images were acquired through both the piston-crown and cylinder-head windows with either one or two gated, intensified CCD video cameras. Various lens and filter combinations were used as appropriate. For some experiments, the piston bowl rim was cut out in line with

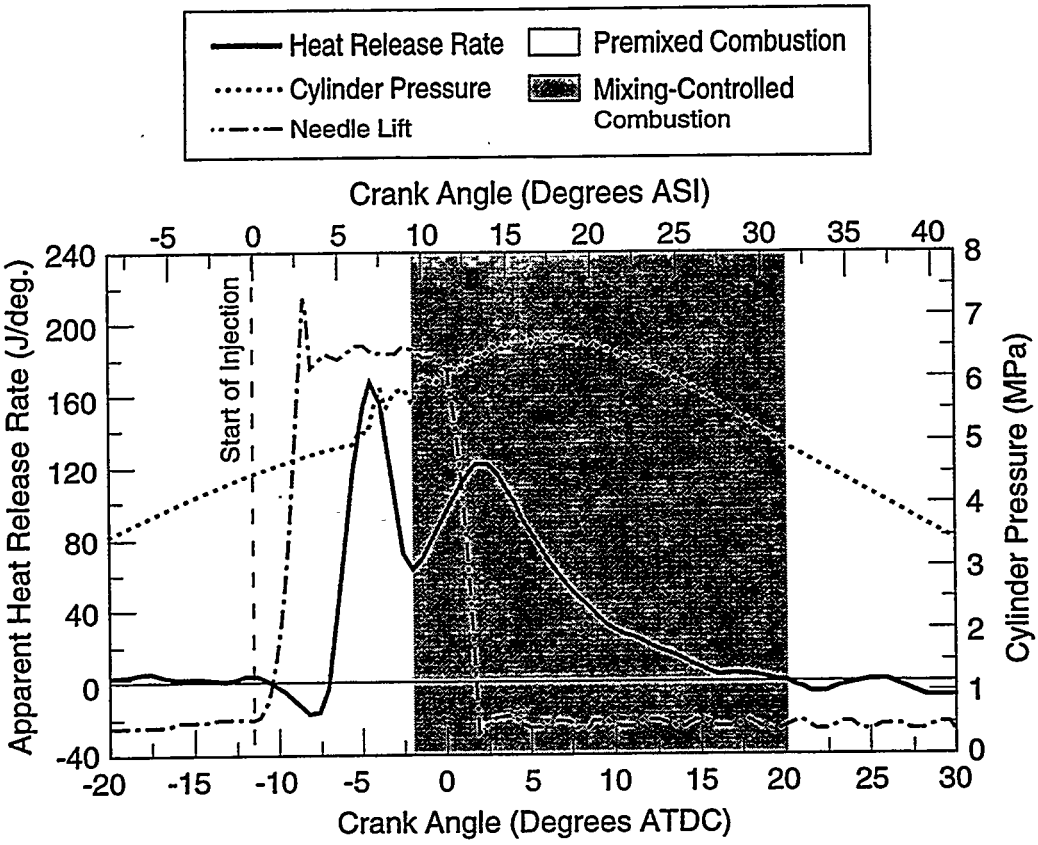


Figure 2. Apparent heat release rate, cylinder pressure, and injector needle lift for the low fuel loading (ϕ=0.25) at the base operating condition (TDC temperature = 992 K, TDC density = 16.6 kg/m^3). The engine speed is 1200 rpm, and the data are ensemble-averaged over 20 cycles.

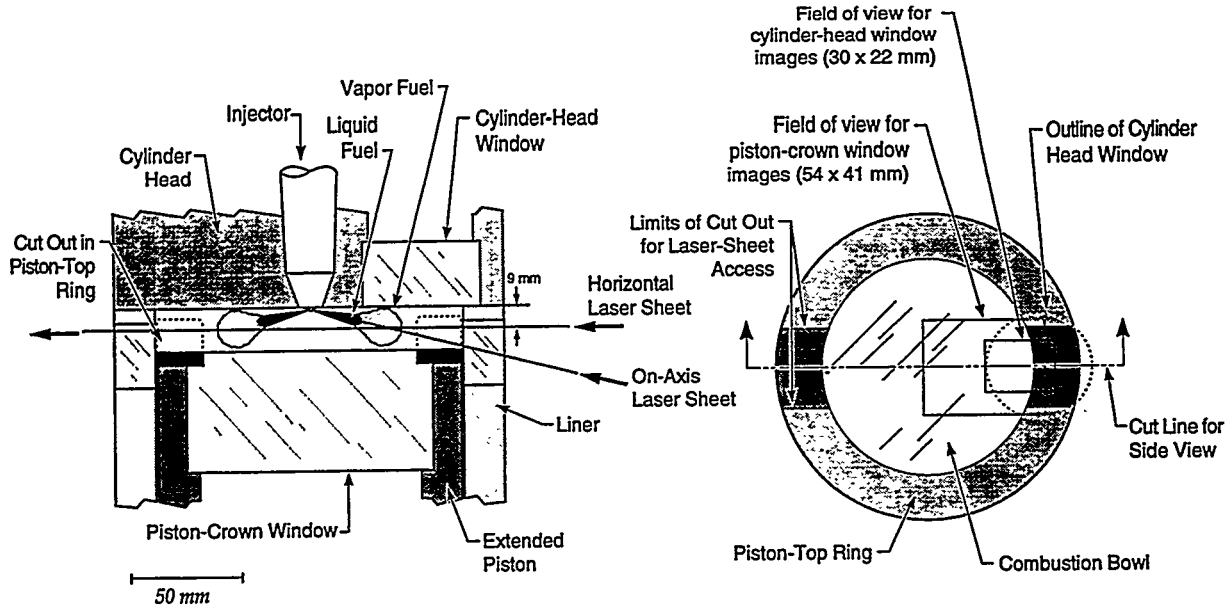


Figure 3. Geometry and optical configuration of the combustion chamber with cut outs in the rim for laser access. The schematic at the left shows a side view of the combustion chamber and the two laser-sheet orientations. At the right is a top view of the piston and typical fields of view for images obtained through both piston-crown and the cylinder-head windows. The piston is shown at the TDC position.

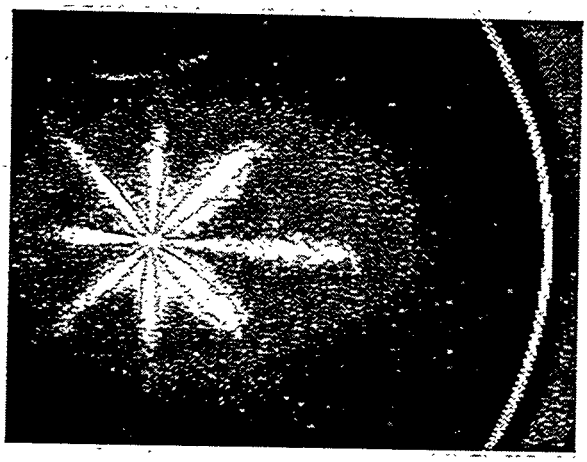


Figure 4. Liquid-phase fuel images show that all the fuel vaporizes within a characteristic length (~25 mm for the base operating condition) from the injector. See Ref. [3].

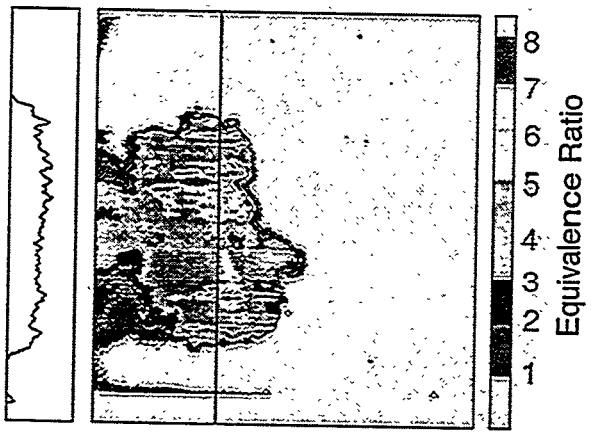


Figure 5. Quantitative vapor fuel images show that downstream of the maximum liquid penetration, the fuel and air are mixed to and equivalence ratio of 2 to 4. This relatively uniform mixture is separated from the surrounding air by a sharp transition as shown in the plot at the left. See Ref. [4].

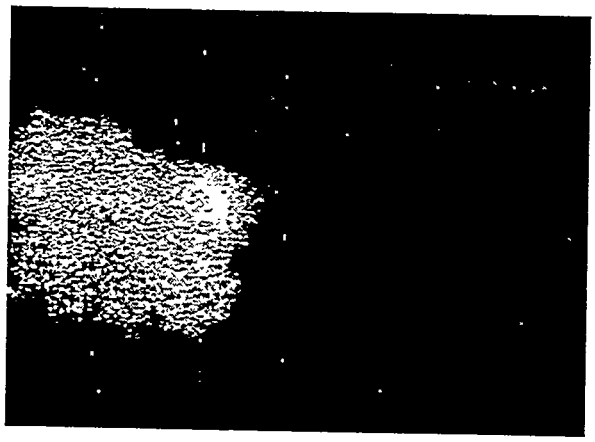


Figure 6. Chemiluminescence imaging shows auto-ignition occurring across the downstream portion of the fuel jet. See Ref. [5].

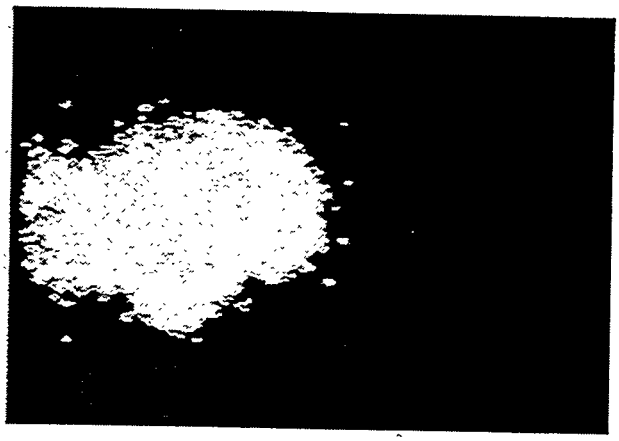


Figure 7. PAHs form throughout the cross-section of the downstream portion of the fuel jet immediately following fuel breakdown at the start of apparent heat release. See Ref. [1].



Figure 8. LII soot images show that soot forms throughout the cross-section of the fuel jet beginning just downstream of the liquid-fuel region. See Refs. [1,5].

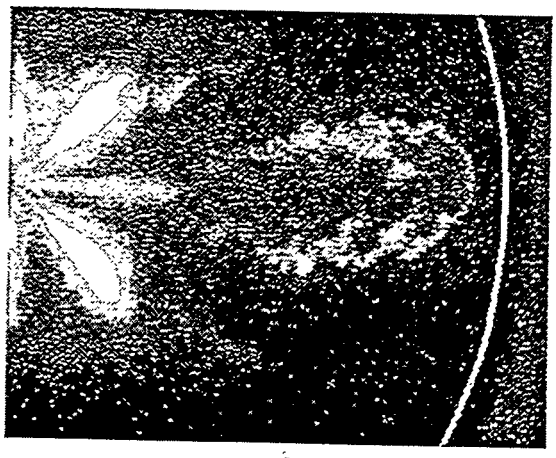


Figure 9. OH radical images show that the diffusion flame forms at the jet periphery subsequent to an initial fuel-rich premixed combustion period. See Ref. [6].

the laser sheet to permit the laser sheet to enter the combustion chamber near TDC. The intake-air temperature and pressure were adjusted to maintain the same TDC conditions despite the reduction in compression ratio resulting from the cutouts.

LASER SHEET IMAGING DATA

As mentioned above, the conceptual model of diesel combustion presented in the next section has been derived by combining the results from a variety of 2-D imaging diagnostics. Because the imaging data have been described in detail elsewhere, only a summary will be presented here. Figures 4 - 9 show typical images of most of the data types along with a brief descriptions of the most significant findings. Additional information may be found in the references given the figure captions.

Although Figs. 4 - 9 show images at only a single instant during the combustion event, temporal sequences of images were actually acquired with each of the diagnostics. An example of this is given in Fig. 10. This figure shows a temporal sequence of soot images from 7° to 17° after the start of injection (ASI) for three different imaging diagnostics, as noted at the left. These images show how the soot volume fraction and particle-size distribution develop within the reacting fuel jet in a diesel engine [1,7].

CONCEPTUAL MODEL OF DI DIESEL COMBUSTION

This section presents a series of schematics that combine the information from the individual imaging measurements into a comprehensive picture of DI diesel combustion.

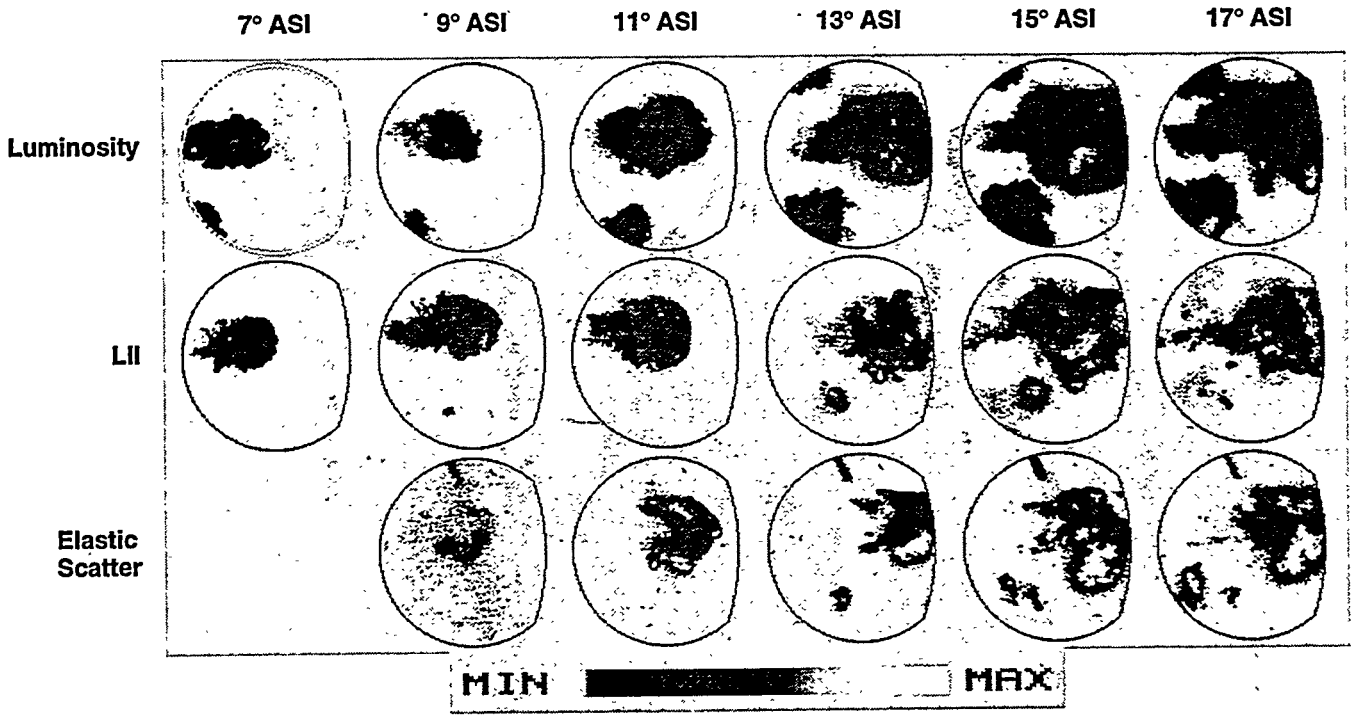


Figure 10. A temporal sequence of natural soot luminosity, laser-induced incandescence (LII), and elastic-scatter images. The crank angle degree ASI is given at the top of each set. The average equivalence ratio is 0.43, and the engine speed is 1200 rpm.

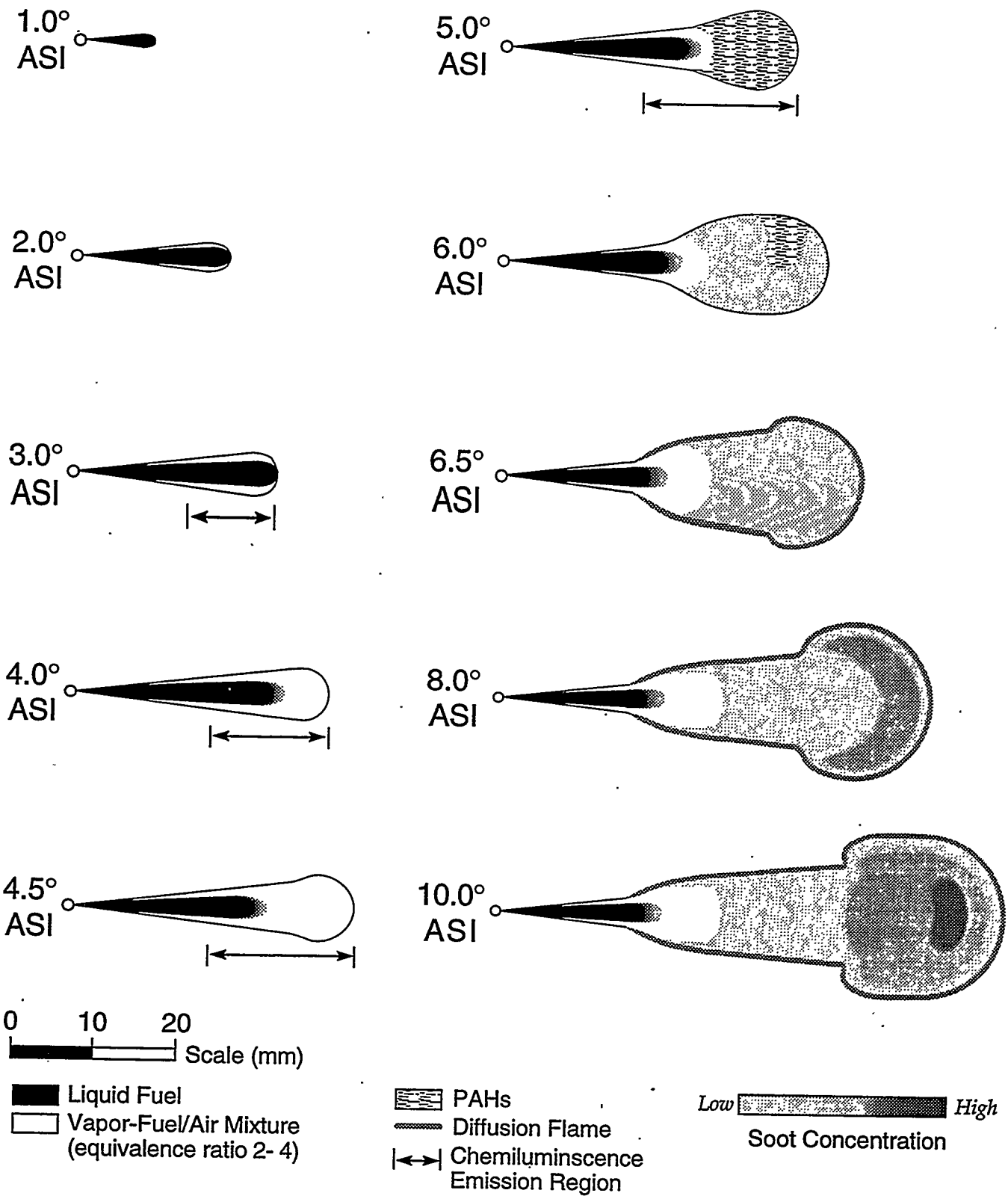


Figure 11. A temporal sequence of schematics showing how DI diesel combustion evolves from the start of injection up through the early part of the mixing-controlled burn. The temporal and spatial scales depict combustion for the base operating condition (a typical diesel engine condition) with an injection duration extending beyond the sequence shown. The crank angle degree ASI (after the start of injection) is given at the side of each schematic (1° = 139 μs).

These composite schematics represent idealized cross-sectional slices through the midplane of the jet, and they show conceptually how DI diesel combustion occurs in the absence of wall interactions and swirl. These schematic images depict the typical operating condition described above. For production engines the amount of turbocharger boost, intercooling, and injector characteristics can vary greatly, affecting both the temporal and spatial scaling (see for example Refs. [3, 8]).

Figure 11 gives a temporal sequence of schematics showing the development of a diesel fuel jet from the start of injection, through the premixed burn, and into the first part of the mixing-controlled burn. Initially, liquid fuel penetrates across the chamber, entrains hot in-cylinder air, and begins to vaporize. By 3.0° ASI, the tip of the fuel jet has penetrated about 25 mm from the injector, and sufficient air entrainment has occurred so that all the fuel is vaporized beyond this characteristic length (Fig. 4). The vapor-fuel/air mixture then penetrates on across the chamber, and a head vortex eventually develops as is typical of penetrating gas-phase jets. By 4.5° ASI, the leading portion of the jet contains a "relatively uniform" fuel/air mixture with equivalence ratios ranging from about 2 to 4 (Fig. 5).

The exact point of autoignition is not well defined either temporally or spatially. Some weak chemiluminescence occurs over the downstream portion of all the jets as early as 3.5° ASI. (This is indicated by the black arrows in Fig. 11.) As the jet penetrates, the chemiluminescence region grows and the signal becomes brighter. By 4.5° ASI, which coincides with the start of the rapid rise in the apparent heat release rate (see Fig. 2), most of the chemiluminescence is coming from the large region of vapor-fuel/air mixture in the leading portion of the jet (Fig. 6). Then, within 70 μs (5.0° ASI) the planar images show that the fuel breaks down across the cross section of the vapor-fuel/air mixture at the front of the jet, and PAHs (poly-aromatic hydrocarbons) form throughout this region (Fig. 7). These planar imaging measurement

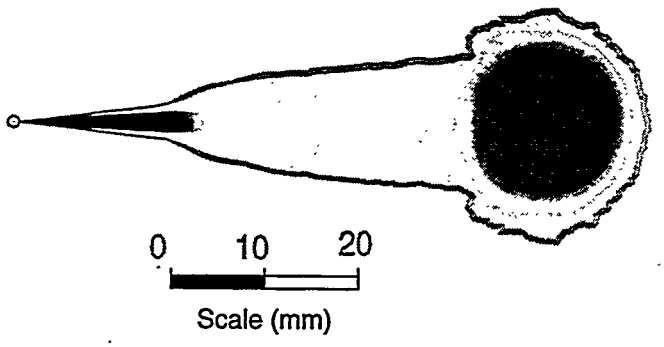


Figure 12. A schematic showing the conceptual model of DI diesel combustion derived from laser-sheet imaging for a typical time during the first part of the mixing controlled burn (*i.e.* prior to the end of injection). The color coding is the same as that given in Fig. 11.

indicate that the majority of the premixed burn occurs volumetrically in the fuel-rich (equivalence ratio 2 - 4) mixture in the leading portion of the jet.

At 6.0° ASI, small soot particles appear throughout large portions of the cross-section of the downstream region of the fuel jet at locations that vary from cycle to cycle. These small soot particles are arising from the fuel-rich premixed burn. By 6.5° ASI, soot is found throughout the cross-section of the downstream region of the jet.

Also at 6.5° ASI, a diffusion flame forms at the jet periphery between the products of the fuel-rich premixed burn (which contain a significant quantity of unconsumed fuel) and the surrounding air. This thin diffusion flame (see Fig. 9) completely encircles the downstream portion of the jet (as indicated in the schematic) just prior to the midpoint of the premixed burn spike in the apparent heat release rate. In addition, the soot particles become larger in a thin layer around the jet periphery (not shown in the schematic), due to some effect of the diffusion flame. However, it is important to note that there is no indication of a corresponding increase in soot concentration (volume fraction) at the jet periphery with the formation of the diffusion flame.

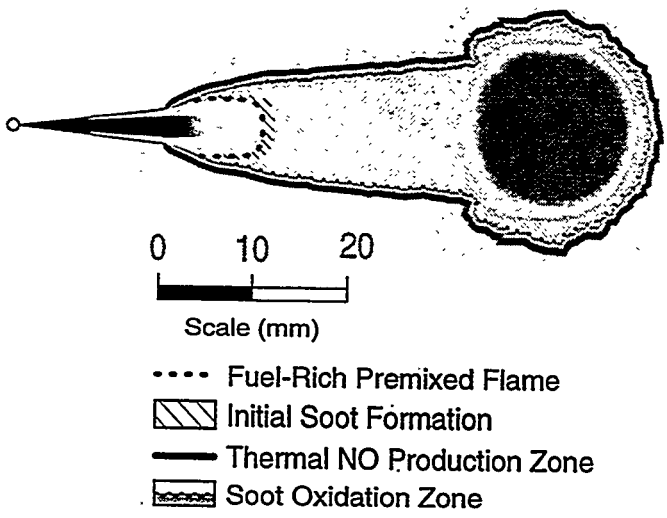


Figure 13. A schematic of the conceptual model from Fig. 12 with additional features (fuel-rich premixed flame, initial soot formation, soot oxidation, and NO formation zones) that are indicated by the data but have not yet been verified. The color coding is the same as Figs. 11 and 12 except for the additional colors given in the legend at the bottom.

Through the remainder of the premixed burn, the jet continues to grow and penetrate across the chamber, and the soot concentration continues to increase. By the end of the premixed burn (9.0° ASI) small soot particles are present throughout the jet cross section beginning approximately 27 mm from the injector. Soot particle size and concentration both increase moving down the jet with the largest soot particles and highest concentrations appearing in the head vortex.

As the combustion transitions to being purely mixing-controlled, the overall appearance of the jet shows only moderate changes, as seen in the 10° ASI schematic of Fig. 11. In fact, the jet appearance remains approximately the same up through the end of fuel injection, except that it grows larger and the soot concentrations increase. Figure 12 presents a typical schematic of the conceptual model during the mixing-controlled burn, prior to the end of fuel injection. No attempt has been made to extend the model beyond the end of fuel injection, because data are insufficient. Temporally, the schematic in Fig. 12 follows the last one in the sequence in Fig. 11; however, the size is only "representative," since a real jet grows across the time period represented. In addition, the jet boundaries in Fig. 12 have been drawn with a ragged appearance to suggest the turbulent nature of a real diesel jet.

The schematics in Figs. 11 and 12 show only the features of the reacting diesel fuel jet that have been verified by experiment. Figure 13 is a reproduction of Fig. 12 to which additional expected (hypothesized) features have been added. These additional features include: 1) a fuel-rich premixed reaction zone that leads to the onset of small soot particles throughout the jet cross section at about 27 mm from the injector; 2) a soot oxidation zone at the diffusion flame; and 3) an NO formation zone on the lean side of the diffusion flame. A complete discussion of this conceptual model of DI diesel combustion and the reasons for these additional expected features may be found in Ref. 1.

NO IMAGING DATA

Subsequent to developing the conceptual model of DI diesel combustion presented in Figs. 11 - 13, PLIF images have been obtained of the NO molecule distribution in the reacting diesel fuel jet. Figure 14 presents a temporal sequence of NO PLIF images (right) along with elastic-scatter images (left) during the early stages of DI diesel combustion. The elastic-scatter images provide a reference to determine how the combustion is proceeding. The images were obtained through the cylinder-head window using a horizontal laser sheet as shown in Fig. 3. Because of the limited field of view, only the leading portion of the fuel jet can be seen at the left in the images.

In the elastic-scatter images the bright region across the center and at the right of the field of view is Rayleigh scattering from the in-cylinder air. In the first two elastic-scatter images, the tip of the fuel jet is entering the field of view at the left and is evident as a darker region because the premixed burn is

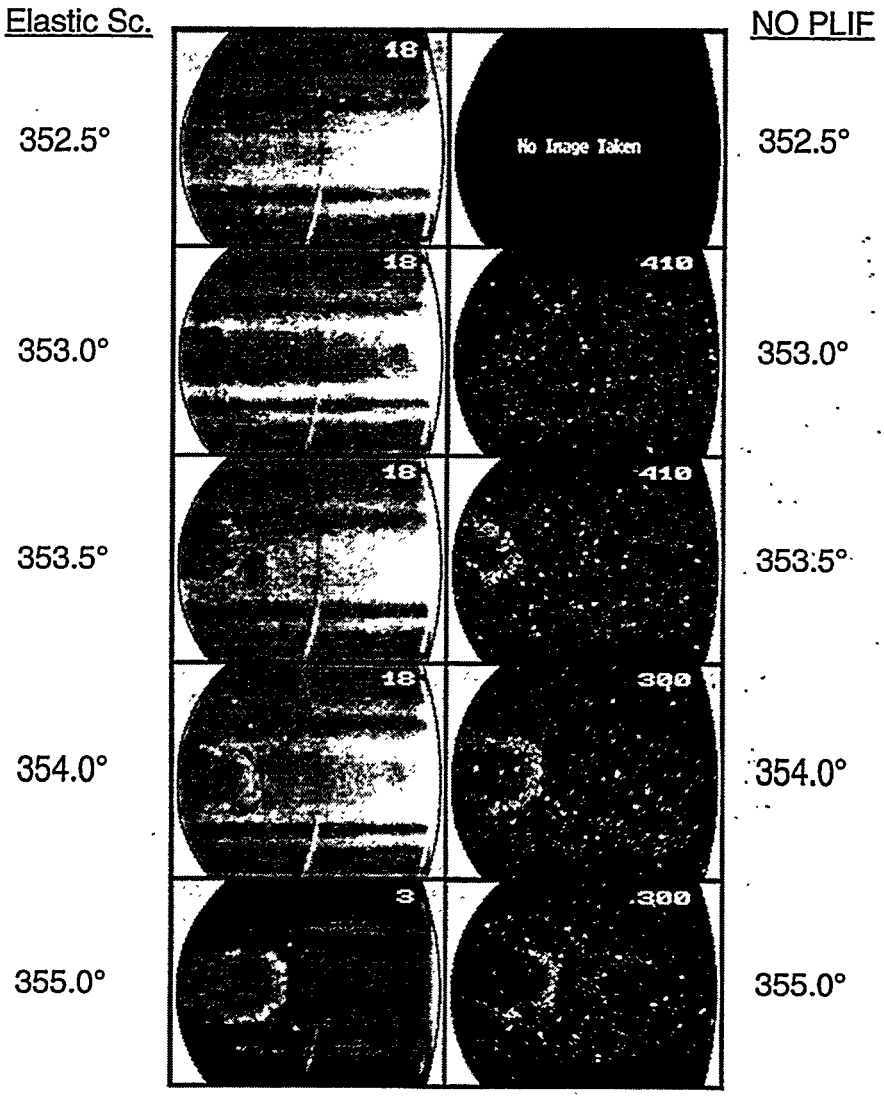


Figure 14. NO PLIF (right) and elastic-scatter (left) images in the plane 10 mm below the cylinder head. The crank angle after TDC exhaust is given at the side of each image, and the field of view is 43 by 33 mm. The number at the upper right of each image is a relative camera gain.

underway and the gases within the fuel jet are less dense than the surrounding air. During this initial portion of the premixed burn there is no signal in the corresponding NO images at the right. Then, at 353.5°, the elastic scatter image shows a signal in the central region of the jet indicating the presence of soot particles, with a very black (low-density) region around the jet periphery where the diffusion flame has just formed. This image corresponds to the 6.5° ASI schematic in Fig. 11. At this crank angle, the NO image now shows a signal in a horseshoe-shaped region around the jet periphery. This same general NO distribution remains through the rest of the sequence presented.

These NO image data strongly support the conceptual model of diesel combustion presented above. As discussed in the description of the model above, the initial premixed portion of diesel combustion is fuel rich (equivalence ratio of 2 - 4). This results in combustion temperatures that are too low to produce NO by the thermal mechanism. Also, oxygen levels are so low that even the "prompt" mechanism does not produce NO at these equivalence ratios [9]. In agreement, the images in Fig. 14 show no NO signal from the premixed combustion area. The conceptual model indicates that the only location for significant NO production up through the end of fuel injection is at the jet periphery on the

lean side of the diffusion flame as shown in Fig. 13. It is at this location, where temperatures are high and oxygen is available, that the images in Fig. 14 show a signal from NO beginning with the onset of diffusion combustion.

CONCLUDING REMARKS

The results presented in this article show that laser-sheet imaging diagnostics have added considerably to our knowledge of DI diesel combustion and emissions-formation. By combining the data from multiple diagnostics a fairly complete picture or "conceptual model" of diesel combustion has been developed. This model covers the diesel combustion process from the start of injection through the first part of the mixing-controlled burn (*i.e.* until the end of injection). It correlates all of the data of the author and coworkers and virtually all the other data in the literature. However, additional work is needed to extend this conceptual model to the late stages of diesel combustion and to determine the effects of walls, swirl, and changes in operating conditions on the reacting diesel fuel jet.

The recent NO imaging results are in full agreement with the conceptual model as presented, and they extend the model by verifying some of the features that were previously hypothesized.

ACKNOWLEDGMENTS

The author would like to acknowledge the contributions of Christoph Espey who has been a co-author on many of the supporting papers referenced here. I am also grateful to Eldon Porter for maintaining the experimental apparatus and for help with the data acquisition. The author would also like to express his gratitude to Patrick Flynn and Roy Primus of the Cummins Engine Co. for their continual strong support of this project.

This work was performed at the Combustion Research Facility, Sandia National Laboratories, Livermore, CA. Support was provided by the U.S. Department of Energy, Defense Programs Technology Transfer Initiative through a cooperative research and development agreement (CRADA) with the Cummins Engine Co. and by the DOE Office of Transportation Technologies through a CRADA with Cummins Engine Co., Caterpillar, and Detroit Diesel Corp.

REFERENCES

1. Dec, J. E., " A Conceptual Model of DI Diesel Combustion Based on Laser-Sheet Imaging," SAE paper no. 970873, 1997.

2. Espey, C. and Dec, J. E., "Diesel Engine Combustion Studies in a Newly Designed Optical-Access Engine Using High-Speed Visualization and 2-D Laser Imaging," *SAE Transactions*, Vol. 102, Sec. 4, pp. 703-723, paper no. 930971, 1993.

3. Espey, C. and Dec, J. E., "The Effect of TDC Temperature and Density on the Liquid-Phase Fuel Penetration in a D.I. Diesel Engine," *SAE Transactions*, Vol. 104, Sec. 4, pp. 1400-1414, paper no. 952456, 1995.

4. Espey, C., Dec, J. E., Litzinger, T. A. and Santavicca, D. A., "Planar Laser Rayleigh Scattering for Quantitative Vapor-Fuel Imaging in a Diesel Jet," *Combustion and Flame*, Vol. 109, 65-86, 1997.

5. Dec, J. E. and Espey, C., "Ignition and Early Soot Formation in a D.I. Diesel Engine Using Multiple 2-D Imaging Diagnostics," *SAE Transactions*, Vol. 104, Sec. 3, pp. 853-875, paper no. 950456, 1995.

6. Dec, J. E. and Coy, E. B., "OH Radical Imaging in a DI Diesel Engine and the Structure of the Early Diffusion Flame," SAE paper no. 960831, 1996.

7. Dec, J. E., "Soot Distribution in a D.I. Diesel Engine Using 2-D Imaging of Laser-Induced Incandescence, Elastic Scattering, and Flame Luminosity," *SAE Transactions*, Vol. 101, Sec. 4, pp. 101-112, paper no. 920115, 1992.

8. Naber, J. D. and Siebers, D. L., "Effects of Gas Density and Vaporization on Penetration and Dispersion of Diesel Sprays," SAE paper 960034, 1996.

9. Miller, J. A. and Bowman, C. T., "Mechanism and Modeling of Nitrogen Chemistry in Combustion," *Prog. Energy Combust. Sci.*, Vol. 15, pp. 287-338, 1989.

CHEMICAL KINETIC CHARACTERIZATION OF MODEL FUELS USED FOR DESCRIBING COMBUSTION OF DIESEL

R. Seiser and K. Seshadri
University of California - San Diego

INTRODUCTION

Recent environmental legislations require the automotive industry to significantly reduce emissions from engines burning diesel. Diesel comprises several aliphatic and aromatic compounds and its exact content varies between different refineries and countries. Several laboratories are currently conducting experiments on test engines to characterize their performance and to determine the influence of various parameters on the rates of pollutants formed. The results will clearly depend on the fuel used in these studies. It is useful to develop model fuels of known chemical composition which can reproduce the physical and chemical char-acteristics of diesel. These model fuels can then be used in test engines as well as in numerical simulations of engine performance and rates of pollutant formation.

To develop model fuels for diesel, experiments were conducted on a simple and weliknown geometry, a laminar non-premixed flame in a counterflow configuration. Although a diesel engine uses turbulent spray combustion at high pressures, the flame on the surface of a tiny droplet can be considered as a laminar non-premixed flamelet [1].

EXPERIMENT

An apparatus, as described in [2],[3] or [4]. is used to produce the counterflow flame at atmospheric pressure shown in Figure 1. An oxidizer stream, consisting of air and nitrogen, is directed towards a pool of liquid fuel. A flat thin flame is established between the upper duct and the liquid pool. The heat transferred from the flame to the surface of the pool vaporizes the liquid.

For each oxygen concentration in the oxidizer stream, a certain strain rate can be found to extinguish the flame. The strain rate is directly proportional to the total oxidizer flow:: $a = 2V/l$ (1)

V is the velocity of the oxidizer stream at the duct exit, l the separation distance between the oxidizer duct and the liquid pool surface. Figure 2 shows the oxygen concentration vs. the strain rate, and gives a first characterization of the reactivity of diverse fuels.

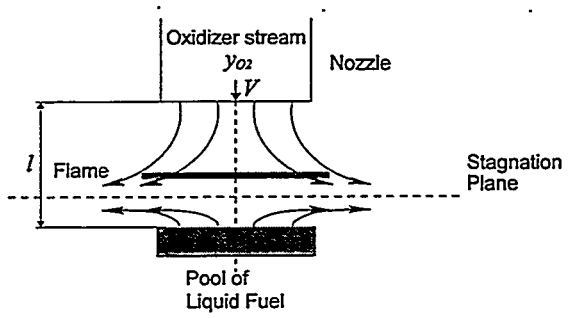


Fig. 1: Schematic illustration of liquid fuel counterflow diffusion flame.

THEORETICAL FORMULATION OF EXTINCTION

One of the first to analyze the structure of a non-premixed flame in a stagnation-point flow was Fendell [5]. Assuming incompressible and invis-cid flow, he used a numerical integration to plot the maximum temperature as a function of the Damköhler number, and achieved the char-acteristic S-shaped curve; its corners identifying the critical conditions of extinction and ignition. For the limit of large activation-energies, Linan [6] achieved analytical results for extinction and ignition conditions for a nonpremixed flame in an inviscid counterflow configuration of two gaseous streams. Krishnamurty et al. [7] extended this analysis to predict extinction of a non-premixed flame

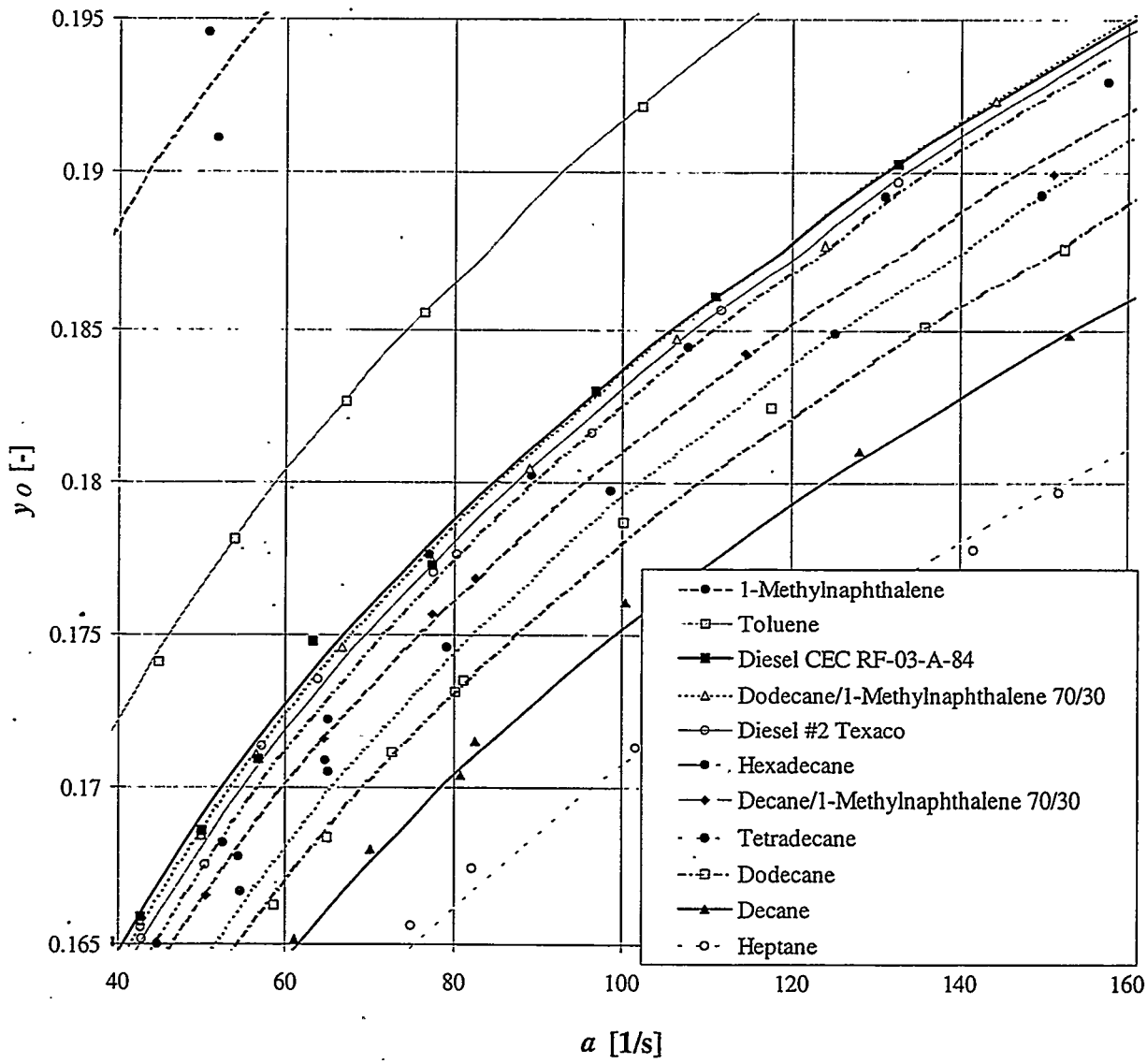


Fig. 2: Extinction data for hydrocarbon fuels.

in the stagnation point boundary layer of a condensed fuel.

Basis for calculation of kinetic parameters from extinction criteria is a one-step overall reaction

$$fuel + \nu_o\ oxygen \rightarrow products, \qquad (2)$$

ν_o being the stoichiometric molar ratio of oxygen to fuel. Further approximations are that the Lewis numbers for fuel and oxidizer in the gas are unity, that the Prandtl number is constant, and that the product $\mu\rho$ = constant (μ = coefficient of viscosity, ρ = density).

The Damköhler number is defined as a diffusion time divided by a chemical reaction time and given by [7]

$$D = \rho B_o/[M_F k(du_o/dr)] \qquad (3)$$

where B_o is the pre-exponential factor of consumption of oxidizer, M_F the molecular weight of fuel vapor, and (du_o/dr) the stagnation point velocity gradient, which is for rotational flow [8]:

$$(du_o/dr) = V/l. \qquad (4)$$

The geometry factor k is 1 for a two-dimensional and 2 for the present axisymmetric flow.

Using the extinction criteria found by Linan [6] and adopted by Krishnamurty et al. [7], and assuming extinction occurring in the diffusion flame regime, the Damköhler number at extinction is given by:

$$D_E = F \cdot \left(\frac{E}{R \cdot T_f} \right)^3 \cdot \exp \left(\frac{E}{R \cdot T_f} \right). \quad (5)$$

E is the activation energy for the reaction (2). and R the universal gas constant. The factor F is a correction factor taking into account the viscous flow in the stagnation-point bound-ary layer. It can be found as result of a parametric study in Krishnamurty et al. [7], F being a function of T_f, T_∞, $y_{f,stoich}$, and the fuel properties. T_f is the adiabatic flame temperature calculated by the oxygen and nitrogen concentration of the oxidizer stream and the corresponding stoichiometric fuel concentration $y_{f,stoich}$. For this theo-retical flame temperature it is assumed, that the products are only carbon dioxide and water. T_∞ is the temperature of the oxidizer stream.

Combining the two expressions for the Damköhler number and using the assumptions $\rho B_o = \rho_f B_{of}$ and $\rho_\infty T_\infty = \rho_f T_f$ (ideal gas), one single equation can be formulated describing the extinction condition:

$$\underbrace{\ln\left(\frac{F \cdot a}{\rho_\infty \cdot T_f^2}\right)}_{Y} = \underbrace{\ln\left(\frac{B_{Of} \cdot T_\infty \cdot R^3}{M_F \cdot E^3}\right)}_{A} \underbrace{-\frac{E}{R}}_{B} \cdot \underbrace{\frac{1}{T_f}}_{X}. \quad (6)$$

All experimentally measured variables enter through X and Y. A plot of Y over X yields an Arrhenius-plot, where a linear least-square fit can be determined. Its intercept and slope are the parameters A and B, from which B_{of}, and E can be found. Expressing the pre-exponential factor for the molar consumption of fuel:

$$B_F = B_{of} / V_o \quad (7)$$

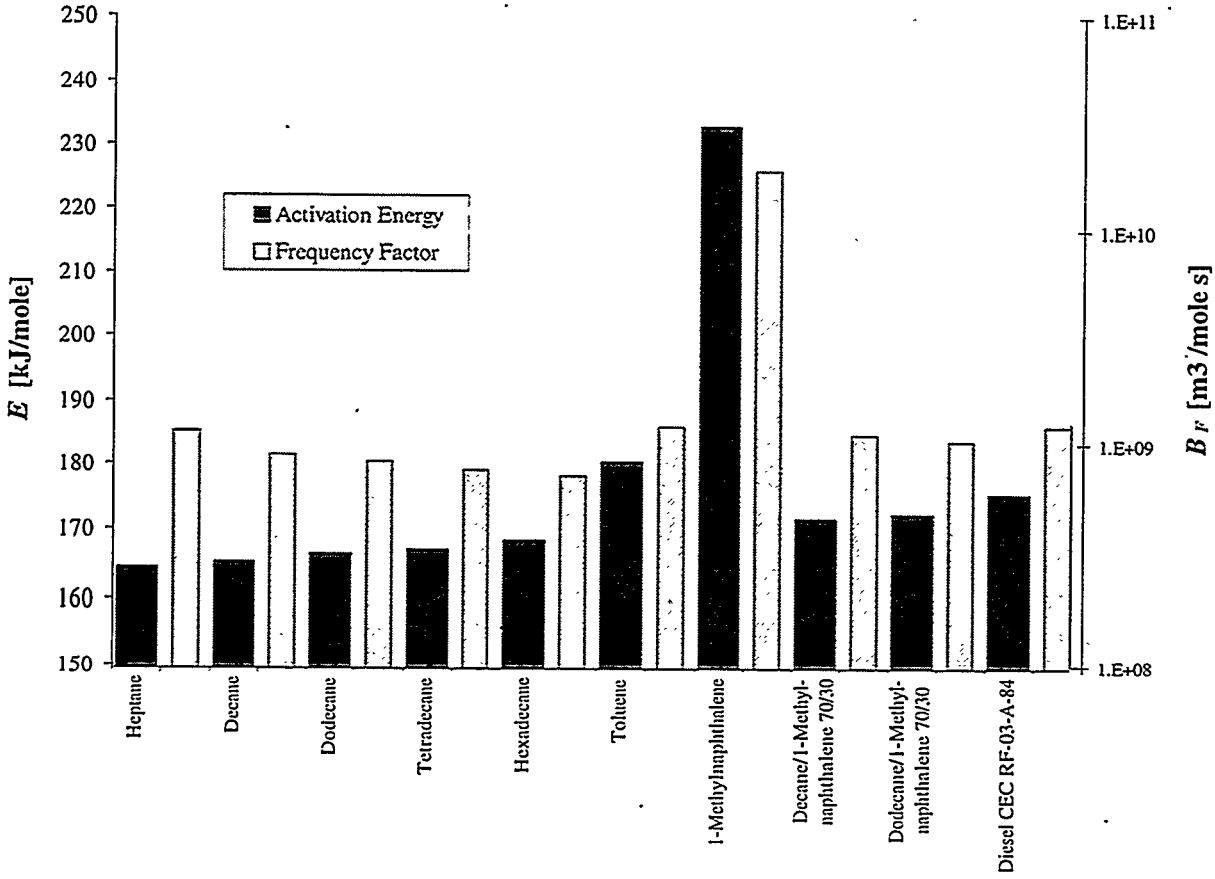


Fig. 3: Activation energies and frequency factors of hydrocarbon fuels

RESULTS AND CONCLUSION

Figure 3 shows the frequency factors and activation energies for the tested fuels. The kinetic parameters for diesel #2 were not calculated due to its unknown composition. The results can be used to describe the molar reaction rate of the fuels:

$$\omega_F = c_F \cdot c_O \cdot B_F \cdot \exp\left(-\frac{E}{R \cdot T}\right). \quad (8)$$

The molar concentrations of fuel and oxidizer, c_F and c_o appear with an exponent of 1 in this equation.

Reviewing the extinction data and activation energies, the mixture dodecane/1-methylnaphthalene (70/30 m%) resembles the results of the CEC-diesel very closely. This was expected, because they have the same amount of aliphatic/aromatic content (70/30). Further study of ignition behavior and pollutant formation is planned, to confirm the proposed fuel as a model fuel for diesel. In this case it is intended to gen-erate a detailed chemical-kinetic mechanism.

List of Symbols

a	[1/s]	strain rate
A, B	[-, K]	constants
B_F	[m^3/kmole s]	pre-exponential rate factor for molar fuel consumption
B_O	[m^3/kmole s]	pre-exponential rate factor for molar oxidizer consumption
c	[kmole/m^3]	molar concentration
D	[-]	Damköhler number.
E	[J/kmole]	activation energy
F	[-]	flow factor relating kinetic parameters to extinction conditions
k	[-]	geometry factor (1, two-dimensional; 2, axisymmetric)
l	[m]	distance between oxidizer duct and fuel surface
M	[kg/kmole]	molecular weight
r	[m]	radial direction
R	[J/kmole K]	universal gas constant
T	[K]	temperature
u	[m/s]	velocity in radial (r-) direction
V	[m/s]	axial velocity at exit of oxidizer duct.
X, Y	[1/K, -]	diagram coordinates

Greek

μ	[kg/ms]	coefficient of viscosity
ν_O	[-]	stoichiometric ratio of oxygen to fuel
ρ	[kg/m^3]	density
ω	[kmole/m^3s]	molar reaction rate

Subscripts

E	extinction
∞	oxidizer stream
F	fuel
f	equilibrium diffusion flame
O	oxidizer

References

[1] **N.Peters**, Laminar diffusion flamelet models in non-premixed turbulent combustion. Institut für Allgemeine Mechanik, RWTH Aachen, Germany, 1983.

[2] **J.H.Kent and F.A.Williams**, Extinction of laminar diffusion flames for liquid fuels, Fifteenth Symposium (International) on Combustion, The Combustion Institute, Pittsburgh, Pennsylvania, 1974, pp. 315-325.

[3] **A.Hamins and K.Seshadri**, Prediction of overall kinetic rate parameters for extinction of diffusion flames above multicomponent fuels. Combust. Sci. and Tech., 38:89-103, 1984.

[4] **D.Trees**, Chemical inhibition of diffusion flames, Dissertation RWTH Aachen, Shaker Verlag Germany, ISBN 3-8265-1922-1, 1996.

[5] **F.E.Fendell**, Ignition and extinction in combustionof initially unmixed reactants, J. Fluid Mech. 21 281-303 (1965)

[6] **A.Liñán**, The asymptotic structure of counterflow diffusion flames for large activation energies. Acta Astronautica, 1(7-8):1007-1039, July 1974.

[7] **L.Krischnamurthy, F.A.Williams, and K. Seshadri**, Asymptotic theory of diffusion flame extinction in the stagnation-point boundary layer. Combustion and Flame, 26:363-377, 1976.

[8] **K.Seshadri and F.A.Williams**, Laminar flow between parallel plates with injection of a reactant at high Reynolds number. Int. J. Heat Mass Transfer 21, 251, 1978.

NOx REDUCTION IN DIESEL FUEL FLAMES BY ADDITIONS OF WATER AND CO_2

S.C. Li
University of California - San Diego

INTRODUCTION

Natural gas, composed mostly of methane, CH_4, has been called the 'prince' of hydrocarbon fuels [1]. Global natural gas reserves have kept on increasing rapidly. For example, global reserves of natural gas increased from 40 billion tons in 1970 to 130 billion tons in 1992 while global oil reserves increased from 70 billion tons to 140 billion tons in the same time period. This means that natural gas will remain cheap and abundant in the future. Natural gas has the highest heating value per unit mass (50.1 MJ/kg, LHV) of any of the hydrocarbon fuels (e.g., butane, liquid diesel fuel, gasoline, etc). Since it has the lowest carbon content per unit mass, combustion of natural gas produces much less carbon dioxide, soot particles, and oxide of nitrogen than combustion of liquid diesel fuel. In view of anticipated strengthening of regulations on pollutant emissions from diesel engines, alternative fuels, such as compressed natural gas (CNG) and liquefied natural gas (LNG) have been experimentally introduced to replace the traditional diesel fuels in heavy-duty trucks, transit buses, off-road vehicles, locomotives, and stationary engines [2]. In the 1997 SAE Future Transportation Technology Conference, there were more than 12 papers which addressed the possibility of natural gas as a major fuel for future diesel engines. To help in applying natural gas in Diesel engines and increasing combustion efficiency, the emphasis of the present paper is placed on the detailed flame chemistry of methane-air combustion. The present work is our continued effort [3] in finding better methods to reduce No_x. The goal is to identify a reliable chemical reaction mechanism for natural gas in both premixed and diffusion flames and to establish a systematic reduced mechanism which may be useful for large-scale numerical modeling of combustion behavior in natural gas engines.

NUMERICAL COMPUTATION AND MODELING

1. Numerical Integrations

We confine our attention to the neighborhood of the axis in an axisymmetric counterflowing configuration, as shown in Figure 1, where the axial velocity, and state variables depend on the axial coordinate only and the radial velocity is linear in radial coordinate and the pressure p depends on both coordinates in a special manner so that all the governing equations can be reduced to ordinary differential equations as discussed by Smooke et al. [4]. The numerical integrations apply to laminar flames with potential flow in the outer streams. Only the radiation from CO, CO_2 and H_2O is taken into account in the energy equation.

The integrations with detailed chemistry and transport included are performed employing a numerical code developed at RWTH, Aachen, Germany [5]. This code was modified locally to include the effects of droplet vaporization in the energy equation. In the present paper, we report results for a strain rate of $50s^{-1}$ at atmospheric pressure. The equivalence ratio is varied from $\Phi = 1.5$ to $\Phi = 3.0$. For diffusion flame, $\Phi = \infty$.

2. Chemical Reaction Mechanism

The reaction mechanism used in the numerical computations starts with $H_2/0_2$ combustion and is constructed by subsequently incorporating wet-CO oxidation and CH_4 flame chemistry, including formation and oxidation of C_2 and C_3 species. Reaction mechanisms in $H_2/0_2$ and $H_2/0_2/CO$ combustion systems have been thor-oughly evaluated earlier [6, 7, 8] and the resulting compilation is adopted here without modification. Oxidation mechanisms for methane and No_x chemistry are compiled and validated by the experiments of freely propagating flames and by our recent work on two-stage partially premixed

methane flames [9]. This detailed reaction mechanism consists of 224 elementary reactions among 50 species which are:

CH_4, O_2, CO, CO_2, H_2, H_2O, H, OH, O, HO_2, H_2O_2, CH, CHO, CHCO, $^1CH_2$, $^3CH_2$, CH_2O, CH_3, CH_3OH, CH_3O, CH_2OH, C_2H, C_2H_2, C_2H_3, C_2H_4, C_2H_5, C_2H_6, HCCO, CH_3CO, C_3H_3, C_3H_4, C_3H_5, C_3H_6, i-C_3H_7, n-C_3H_7, C_3H_8, N, NH, NH_2, NH_3, NO, HNO, HCN, HNCO, NCO, CN, NO_2, N_2, N_2H, N_2O.

EXPERIMENT

1. Two-Phase Counterflow Burner

The burner, which has two coaxial ducts placed one above the other, is shown in Figure 1. The single-phase methane-air gas mixture flows through the upper duct and the water spray with air through the lower duct. The separation distance between the upper and lower duct exits is 18 mm. The upper duct has an exit diameter of 45 mm and flow straighteners are installed to produce a uniform gas flow at the exit plane. The lower duct is a long contoured tube with the same exit diameter. An atomizer is located at the bottom of the lower duct to produce water spray. The air enters the duct below the spray nozzle and carries the spray upward to meet the gas flow from the upper duct. Since some droplets are lost to the walls or to the bottom of the lower duct, a liquid-fuel drain pipe is installed to discharge the accumulated liquid. The mass flow rate of water in the counterflow is obtained as a function of the flow rate of the carrier gas by metering the water flowing into the atomizer and out of the drain. In order to increase the amount of water added in the air stream, water vapor is introduced to coflow with the air.

2. Two-Stage Methane Air Flame

As described in our previous work and as shown in Figure I, this two-phase laminar counterflow configuration exhibits a green premixed flame, a blue diffusion flame, and a vaporization plane. All three are flat and parallel. The separation distances between them decrease with increasing equivalence ratio and strain rate. Since the distance between the two flames is as large as 6 mm, it is easier for probes to obtain reliable experimental results with good spatial resolution.

3. Measurements

The species H_2, O_2, N_2, CH_4, CO, CO_2, C_2H_2. C_2H_4 and C_2H_6 are measured by a Varian 3600 gas chromatograph. Centerline temperature pro-files in the present two-stage flame are measured by a Pt-6%Rh vs. Pt-30%Rh thermocouple. Velocity fields and spray structure are measured by the PDPA. The measured small droplet velocity is used to determine the strain rate in air side. By regulating the total flow rates of the two streams, the strain rate in the present experiment is adjusted to be about $50s^{-1}$ based on the PDPA measurement. All details for these measurement techniques were discussed in our previous publications [10, 11].

A No_x analyzer (Model 955, Rosemount Analytical Inc.), is employed for measuring concentrations of NO andNo_x. The analyzer can be operated at a low flow rate of sample so that the disturbance to flame structure can be reduced to a negligible level. The quartz micro-sampling probe for the analyzer is a standard type as described by Saito et al. [12], and it is mounted on a two-dimensional positioner to fix the probe at the desired location. The inner diameter of the probe tip is smaller than 0.I mm. Samples are withdrawn from the flame by the analyzer continuously at a flow rate of approximately 0.4 cc/sec. Because the sample flow rate is low, the response time of the analyzer is about three minutes at a given probe position. The analyzer is calibrated before the experiment and is checked by the calibration gas once every hour during the measurement to ensure that the analyzer performs accurately.

RESULTS

1. The Reaction Pathways

Figure 2 shows the reaction path for $\Phi = 3$ and $a = 50\ s^{-1}$ without water addition at normal atmospheric pressure. While specific information in the figure is associated with this condition, the general scheme applies over a wide range of conditions for which two-stage flames exist. The fractions(in parentheses) are obtained by

integrating consumption rates over the entire field, including both flames. It is seen here that H_2 68.9%, 25.5%, and 5.5% of the methane is consumed by H, OH, and O, respectively to form CH_3. The CH_3, the first product of methane, goes to C_2H_6, CH_3H_5, CH_2O $^1CH_2$, $^3CH_2$, CH_2OH, and CH_3O which eventually are oxidized to CO_2. The CH radical, which is the primary source for prompt No_x, is formed by the reactions of $^3CH_2$ with H and OH while the $^3CH_2$ is produced from CH_3, $C2H_2$ and $^1CH_2$. This is true not only for methane but for higher hydrocarbons. The CH radicals are mainly consumed by H_2O, CO_2 and O_2. In this example, 67%, 20%, and 9% of the CH are oxidized to form CO, CHO, and C H_2O by H_2O, CO_2 and O_2, respectively, and only about I% of the CH is consumed by N_2 to form N and HCN. It is clear that the concentration of the CH radicals can be reduced by increasing the concentrations of H_2O, and CO_2 in the region where the CH radicals are produced.

2. Flame Structure

Figures 3a and 3b for Φ = 1.5 and Figures 4a and 4b for Φ =2.5 show both measured and computed profiles of temperature and concentrations. We see from Figures 3a and 4a that methane and oxygen in the rich mixture react very rapidly to form CO and H_2, and their mole fractions reach maxima as methane disappears. This occurs in the green flame as shown in Figure 1. The further oxidation of CO and H_2 to form CO_2 and H_2O occurs in the diffusion flame which is characterized by the blue emission as shown in Figure 1. The C_2 species, such as C_2H_2, C_2H_4, and C_2H_6 are produced rapidly in the front of premixed flame as shown in Figures 3b and 4b. However these species have very short lives, and they cannot be found experimentally in the diffusion flame. Figures 3b and 4b clearly show that the concentrations of C_2 species strongly depend on the equivalence ratio; the richer the flame is. the higher is the concentration of C_2 species, consistent with observed soot emissions in fuel-rich methane-air flames. The agreement between experiment and prediction is very good for temperature and most of species.

There are some quantitative disagreements for H_2 and C_2H_2 and C_2H_4. The measured concentrations are always lower than the predicted. This is especially true for lower equivalence ratio. Further work is needed on this issue.

Since radicals such as H, OH, O, and CH play dominant roles in hydrocarbon flames, knowledge of their distributions in the flame should help in under-standing flame structure andNo_x formation. Figures 3b and 4b also show predicted profiles of their concentrations. These figures indicate that the concentrations of C_2 species peak in the premixed flame, the cooler flame, while the radicals H, OH, and O have the highest concentrations in the diffusion flame, the hotter flame. The CH concentration peaks between the premixed and diffusion flames. It is noted that there are two peaks for the concentration profiles of CH, H,and OH for the lower equivalence ratio as shown in Figure 3b, while those radicals have only one peak for the higher equivalence ratio as shown in Figure 4b. This is a very important character for the two-stage combustion.

3. Influence of Water and CO_2 on the Concentration of CH

As shown in Figure 2, the concentrations of CH radicals are directly controlled by the reactions

$$1 \quad CH + H_2O \rightleftharpoons CH_2O + H$$

$$2 \quad CH + O_2 \rightleftharpoons CHO + O$$

$$3 \quad CH + CO_2 \rightleftharpoons CHO + CO$$

$$4 \quad {}^3CH_2 + H \rightleftharpoons CH + H_2$$

$$5 \quad {}^3CH_2 + OH \rightleftharpoons CH + H_2O$$

where the first three consume CH and the last two produce it. It is clear that when the water and CO_2 are added to the region where CH radicals are produced the CH concentration can be significantly reduced. Computation results shown in Table 1 indicate how additions of water, CO_2, N_2, and Argon influence the maximum concentrations of CH radicals in two-stage combustion. For comparison, results of zero addition are also listed. It is found that both water and CO_2 are much more effective in reducing CH than nitrogen and Argon and that, for a given mass percentage of addition, water is the most effective agent for large Φ. For instance, addition of 10% water in the flame with

Φ = 3 can change the maximum of CH from 8.3×10^{-7} to 3.9×10^{-7}, more than 50%. The concentration of the CH is insensitive to additions of nitrogen and Argon. It is also found that additions of water and CO_2 become less effective in reducing CH when fuel concentration decreases in the methane-air stream. For example, additions of water and CO_2 have only minor influence on the maximum values of CH in the flames with Φ = 1.5. This means that the added agents in the air stream are not able to get into the region where the CH radicals are produced when the two flames are separated far apart.

4. Influence of Water Addition on No_x Formation

The experimental measurements as in Figures 5-8 have shown that the maximum concentrations of NO are always found near the blue diffusion flame and that they can be significantly reduced by adding water in the pure air stream. For example, the measured maximum NO concentrations were 69, 89, 100, 90 ppm for Φ = 1.5, 2.0, 2.5 and 3.0, respectively, at $a = 50\ s^{-1}$. On the other hand, by adding 5% of water into the pure air stream, these maximum NO concentrations were reduced to 60, 70, 50, and 40 ppm, respectively, without changing other conditions. In general, the agreements between experimental measurement and numerical prediction are reasonably good.

5. Influence of Water Addition on the Emission Index

The NO emission index is defined as

$$E_{NO} = \frac{1000 \int_{-L_s}^{L_s} M_{NO}\, \dot{\omega}_{NO}\, dz}{-\int_{-L_s}^{L_s} M_{CH_4}\, \dot{\omega}_{CH_4}\, dz} \quad \left(\frac{g}{kg - CH_4}\right),$$

where $-\dot{\omega}CH_4$ is the total consumption rate of methane and $\dot{\omega}_{NO}$ is the total production rate of NO, and M_{NO} and M_{CH_4} are the molecular weights of NO and CH_4, respectively. Figure 9 plots the predicted E_{NO} as a function of Φ at a strain rate of $50\ s^{-1}$ with adding 0, 5%, and 10% water, CO_2, N_2 and Argon in the air stream. It can be seen that water is the most effective agent in reducing NO emission. The effect of agent types on emission of NO varies as

$H_2O > CO_2 >> N_2 > Ar$.

The latter two agents reduce No_x emission through reducing flame temperature while the former two reduce No_x emission through reducing not only flame temperature but also prompt No_x. Another feature shown in Figure 9 is that the additions of water and CO_2 are always more effective in reducing No_x when Φ is large. All these are consistent with the data shown in Table 1.

CONCLUSIONS

Well-defined two-stage flames in counterflowing streams have been employed in testing a chemical-kinetic data base for H-C-N-O combustion systems recently compiled and validated. Both experimental and numerical prediction have indicated that the water vapor added in the air stream helps to increase the water concentration in the flame zone and thus reduce the concentration of CH radicals. The present work reveals that prompt NO in the present two-stage counterflow combustion plays a dominant role in No_x formation and that the No_x emission index strongly depends on the flame structure and on the mass fraction of water and CO_2 added in the air stream. The No_x emission index can be substantially reduced by adding water and CO_2 in the region where CH radicals are produced.

ACKNOWLEDGMENT

This research was supported by the Department of Energy, Office of Basic Energy Sciences, Division of Engineering and Geosciences under contract DE-F003-87ERI3685 and BKM, Inc. and South Coast Air Quality Management District under contract AB2766/97006.

REFERENCES

1. Langston, L., "Market drivers for electric power gas turbines: Reasons for the revolution." *Global Gas Turbine News,* Vol. 36, No.3, pp.7-10, 1996.

2. Bogdanoff, M.A.,"Diesel Engines and Emission Reduction Programs," *Proceedings of the 1995 Diesel Engine Emissions Reduction Workshop,* pp.I31-I39, University of California-San Diego, La Jolla, July 24-27, 1995,

Sponsored by Office of Transportation Technologies of U.S. Department of Energy.

3. Ilincic, N. and Li, S.C., "Influence of Water and CO_2 Addition on NO_x formation in Partially Premixed Flames," Western States Section/The Combustion Institute, 1995 Fall Meeting.

4. Smooke, M.D., Crump, J., Seshadri, K. and Giovangigli, V., "Comparison between Experimental measurements and Numerical Calculations of the Structure of Counterflow, Diluted, Methane-Air, Premixed Flames," Twenty-Third Symposium (International) on Combustion, The Combustion Institute, Pittsburgh, 1990, pp.463-470.

5. Pitsch, H., *Entwicklung eines Programm paketes zur Berechnung eindimensionaler Flammen am Beispiel einer Gegenstormdiffusionsflamme.* Masters thesis, RWTH, Aachen, Germany, 1993.

6. Balakrishnan, G. and Williams F.A. "Turbulent Combustion Regimes for Hypersonic Propulsion Employing Hydrogen-Air Diffusion Flames," Journal of Propulsion and Power 10, 434 (1994).

7. Rightley, M.L. and Williams, F.A., "Analytical Approximations for Structures of Wet CO Flames with One-Step Reduced Chemistry," *Combustion and Flame* 101, 287 (1996).

8. Rightley, M.L. and Williams, F.A., "Structures of CO Diffusion Flames Near Extinction " to appear in *Combustion Science and Technology,* (1997).

9. Li, S.C., Williams, F.A., and Ilincic, N., "Experimental and Numerical Studies ofNo_x Formation in Two-Stage Methane Flames," work in Progress, 1997.

10. Li, S.C., Ilincic, N., and Williams, F.A., " Reduction of NO_x Formation by Water Sprays in Strained Two-Stage Flames," presented at ASME TURBO-EXPO'96, Birmingham, England, UK, June 10-13, 1996, ASME Paper 96-GT-545 and to appear in *ASME Journal of Engineering for Gas Turbines and Power.* October, 1997.

11. Li, S.C. and Williams, F.A., "Experimental and Numerical Studies of Two-Stage Methanol Flames," *Twenty-Sixth Symposium (International) on Combustion, Naples* Italy, July 28 - August 2, 1996, pp. I0I7-I024.

12. Saito, K., Williams, F.A., and Gordon, A.S., "Structure of Laminar Coflow Methane-Air Diffusion Flames," *J. Heat Transfer,* 108, 640 (1986).

Table1: Maximum mole fraction of CH radical uder different additions of water, CO_2 and nitrogen.

Φ	Zero	H_2O		CO_2		N_2		Ar	
	Addition	5%	10%	5%	10%	5%	10%	5%	10%
1.5	1.5×10^{-7}	1.4×10^{-7}	1.4×10^{-7}	1.5×10^{-7}	1.5×10^{-7}	1.5×10^{-7}	1.5×10^{-7}		
2.0	3.7×10^{-7}	3.0×10^{-7}	2.4×10^{-7}	3.6×10^{-7}	3.4×10^{-7}	3.6×10^{-7}	3.6×10^{-7}		
2.5	6.5×10^{-7}	4.9×10^{-7}	3.6×10^{-7}	5.9×10^{-7}	5.4×10^{-7}	6.3×10^{-7}	6.0×10^{-7}		
3.0	8.3×10^{-7}	5.9×10^{-7}	3.9×10^{-7}	7.4×10^{-7}	6.4×10^{-7}	8.0×10^{-7}	7.5×10^{-7}		
∞	2.0×10^{-6}	1.1×10^{-6}	4.5×10^{-7}	1.5×10^{-6}	9.9×10^{-7}	1.8×10^{-6}	1.4×10^{-6}	2.0×10^{-6}	1.8×10^{-6}

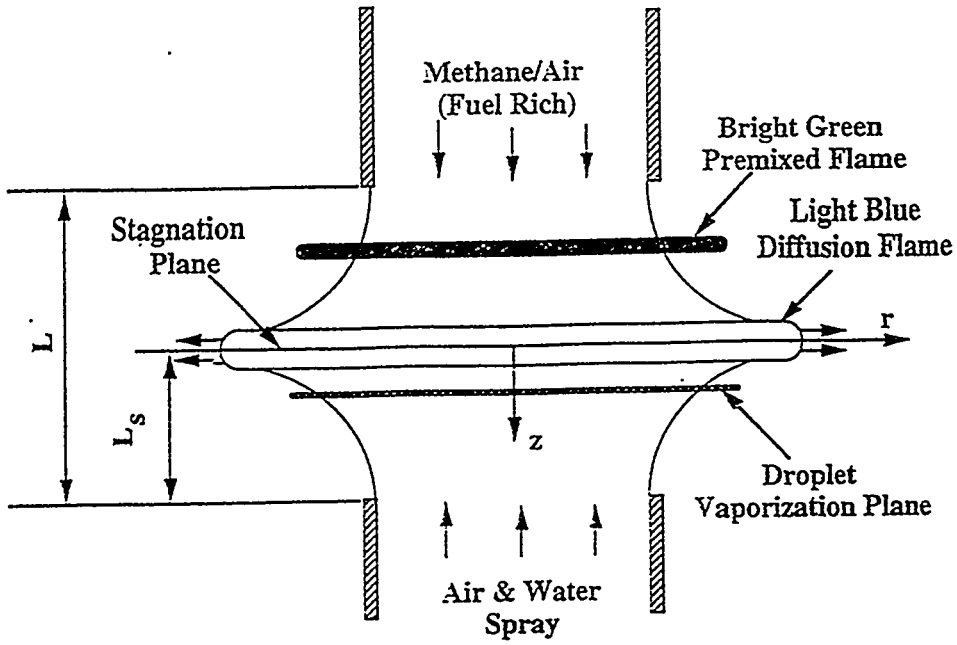


Fig.1: Sketch of a two-stage methane-air flame in water spray counterflow streams.

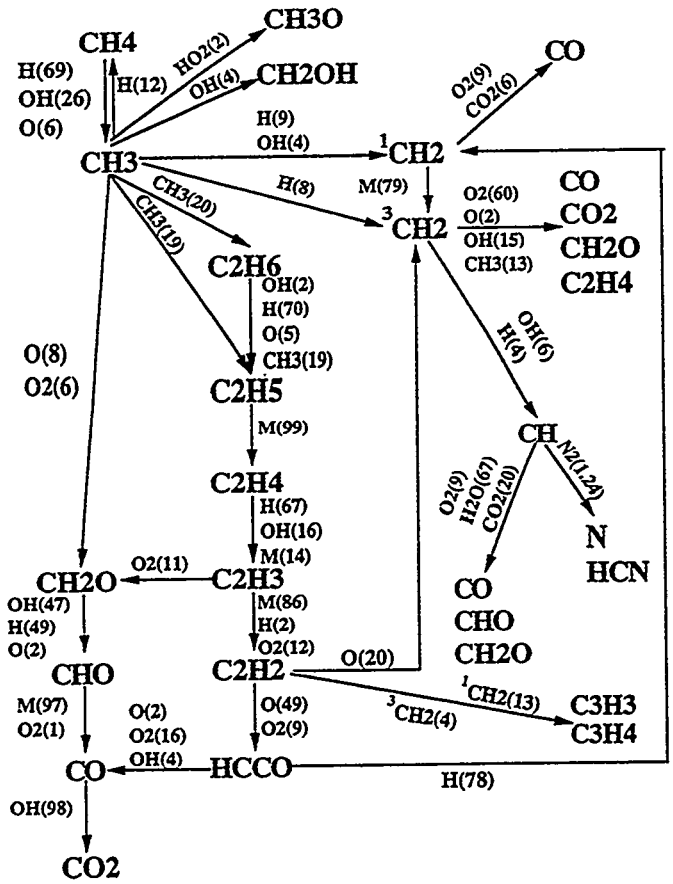


Fig.2: Reaction path of methane in two-stage methane-air flame with Φ= 3.

Fig.3a: Comparison between measurement and prediction for concentration profiles for Φ=1.5 and a = 50 s^{-1}.

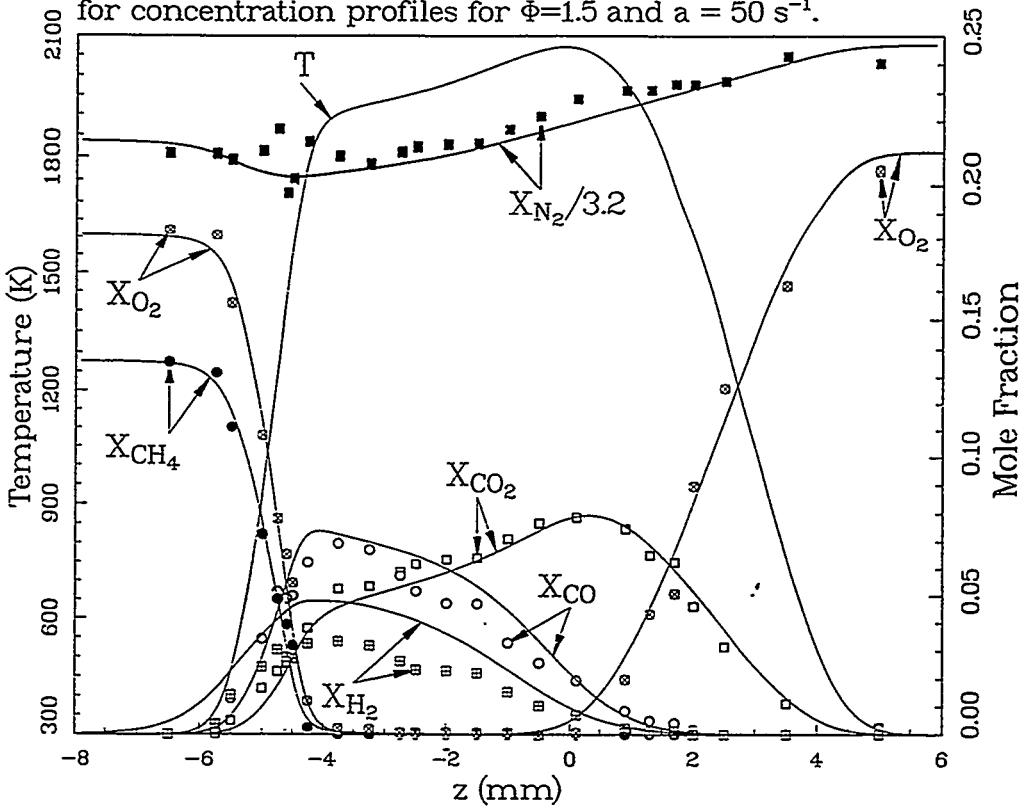


Fig.3b: Comparison between measurement and prediction for profiles of temperature and concentrations of radicals and C_2 species for Φ=1.5 and a = 50 s^{-1}.

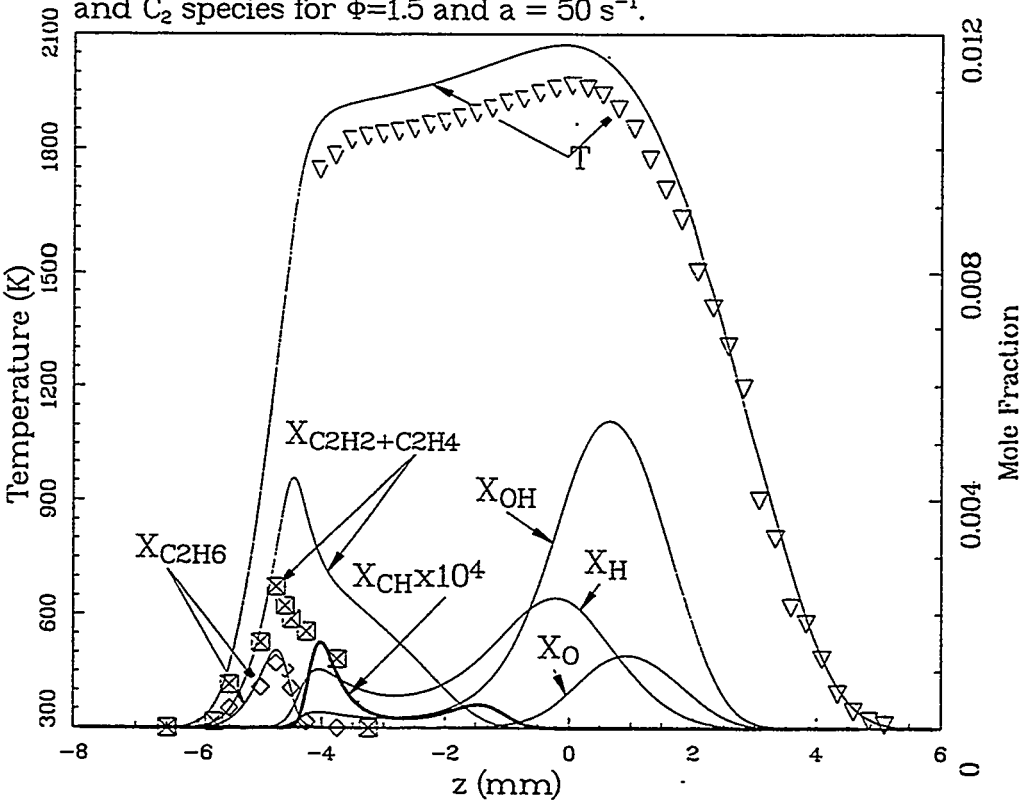


Fig.4a: Comparison between measurement and prediction for concentration profiles for Φ=2.50 and a = 50 s^{-1}.

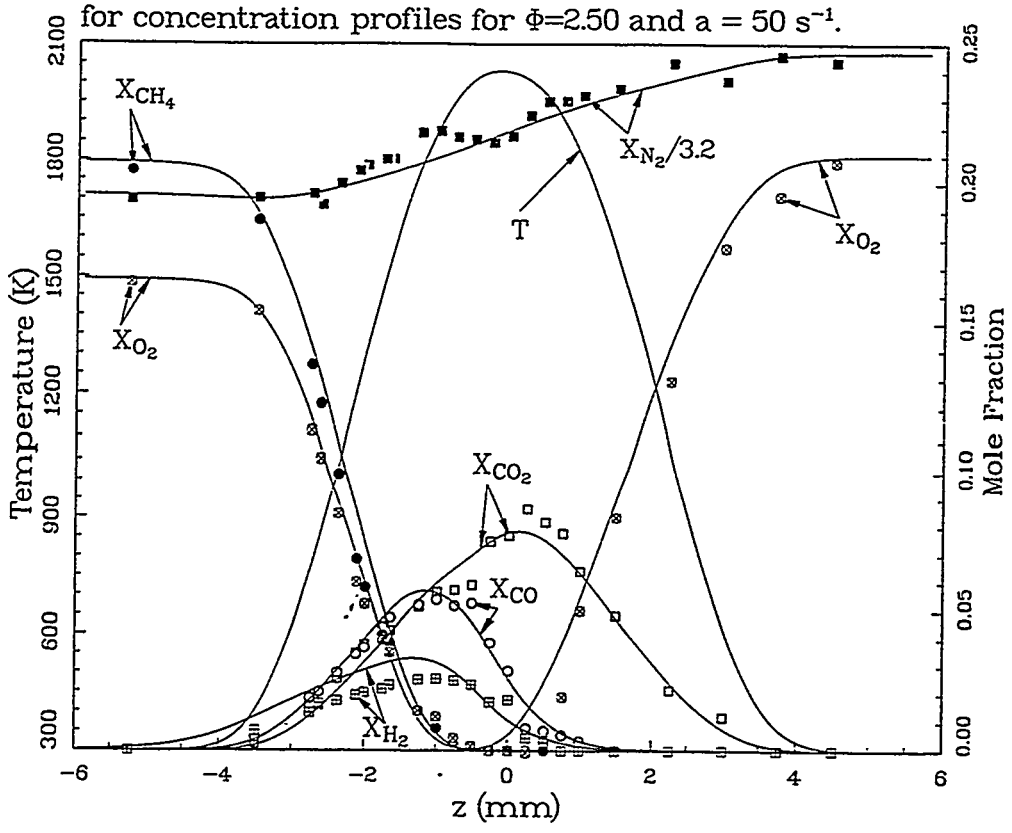


Fig.4b: Comparison between measurement and prediction for profiles of temperature and concentrations of radicals and C_2 species for Φ=2.5 and a = 50 s^{-1}.

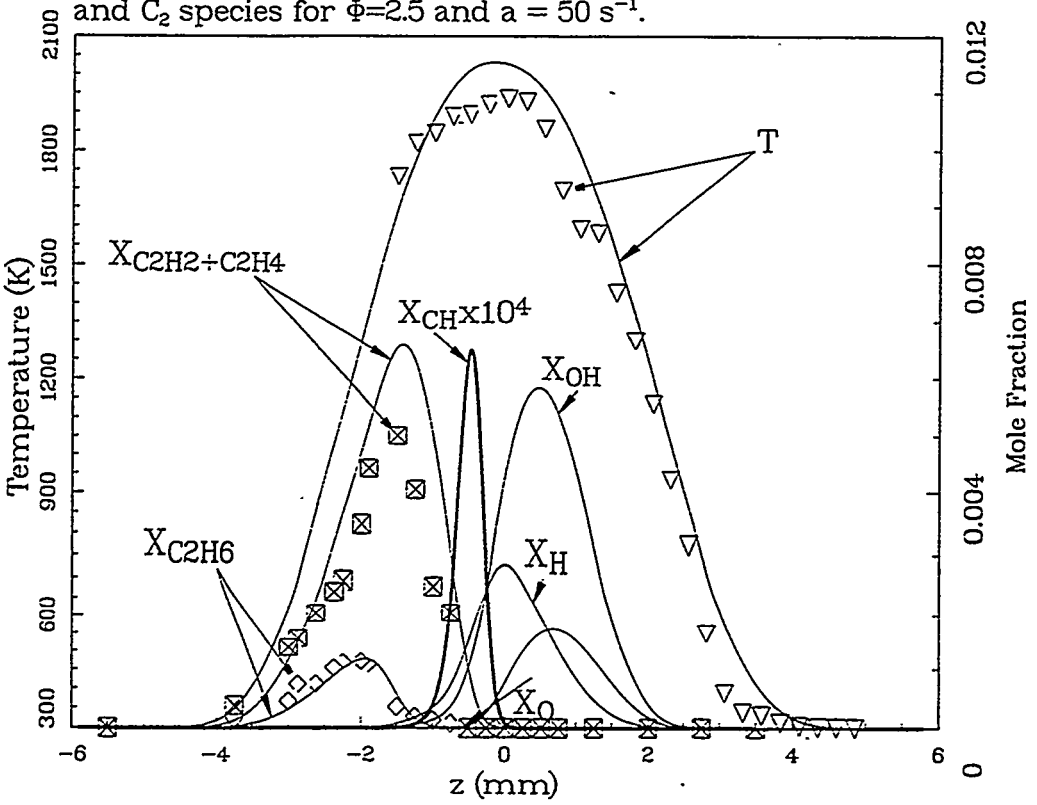


Fig.5: Comparison between measurement and prediction for profiles of NO concentration and temperature on the axis with Φ= 1.50 and strain rates of 50 s^{-1}.

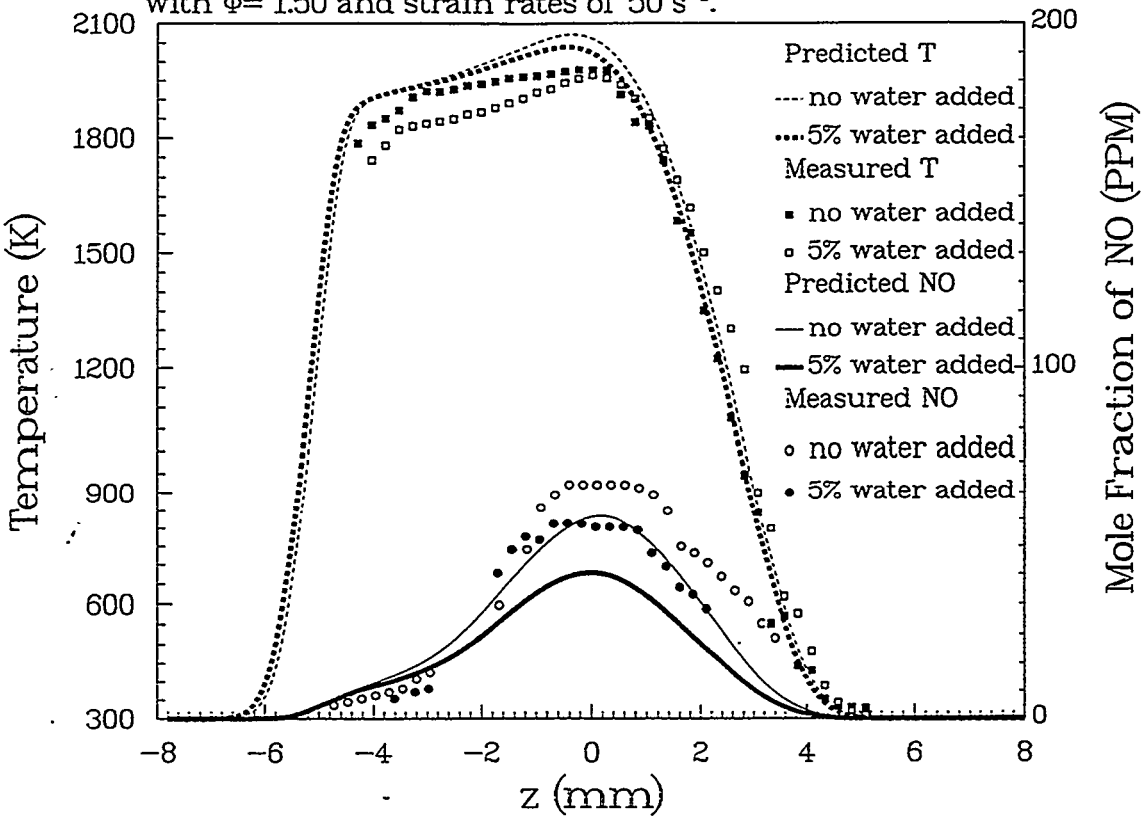


Fig.6: Comparison between measurement and prediction for profiles of NO concentration and temperature on the axis with Φ= 2.00 and strain rates of 50 s^{-1}.

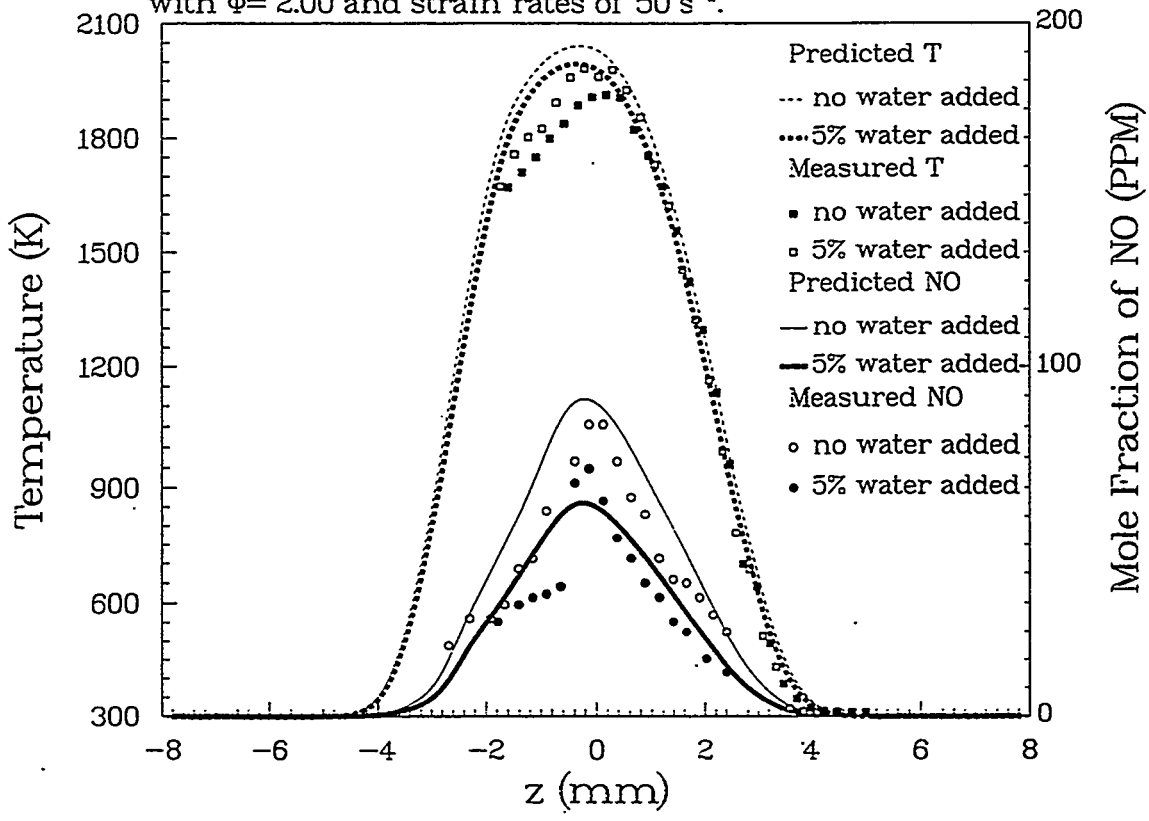


Fig.7: Comparison between measurement and prediction for profiles of NO concentration and temperature on the axis with Φ= 2.50 and strain rates of 50 s^{-1}.

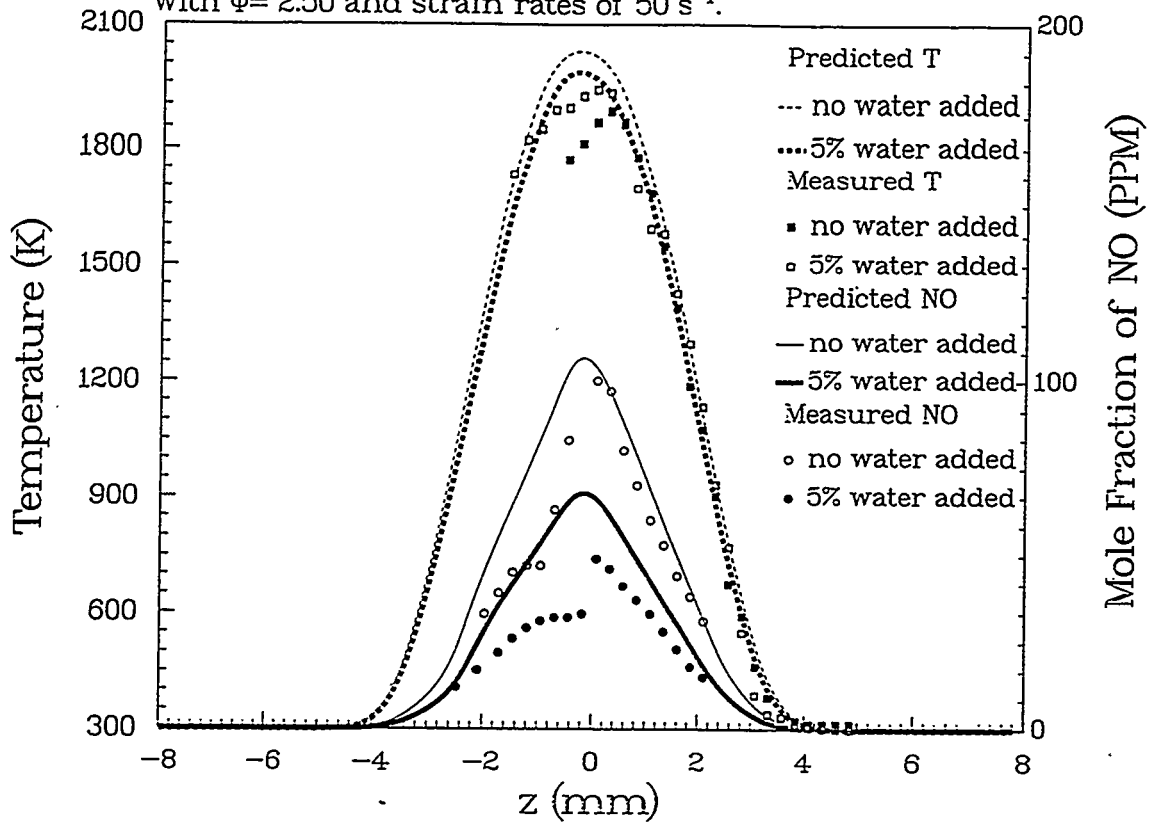


Fig.8: Comparison between measurement and prediction for profiles of NO concentration and temperature on the axis with Φ= 3.00 and strain rates of 50 s^{-1}.

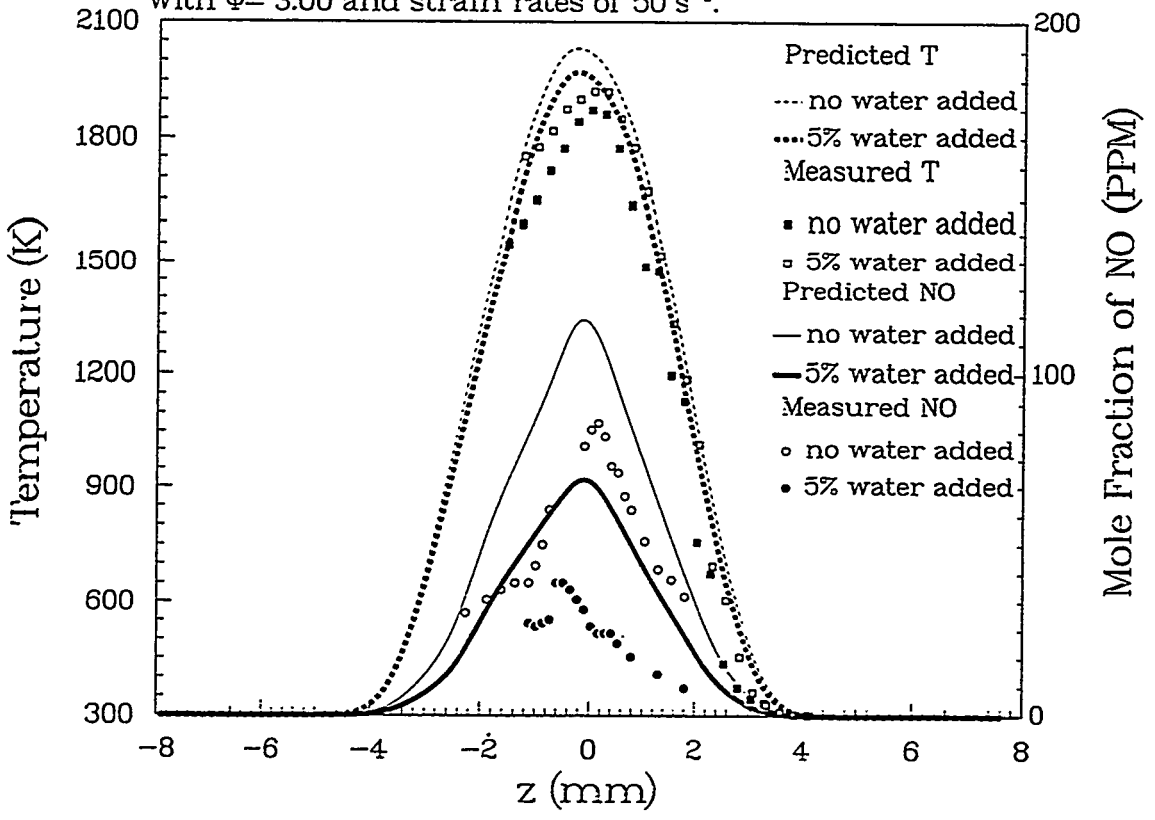
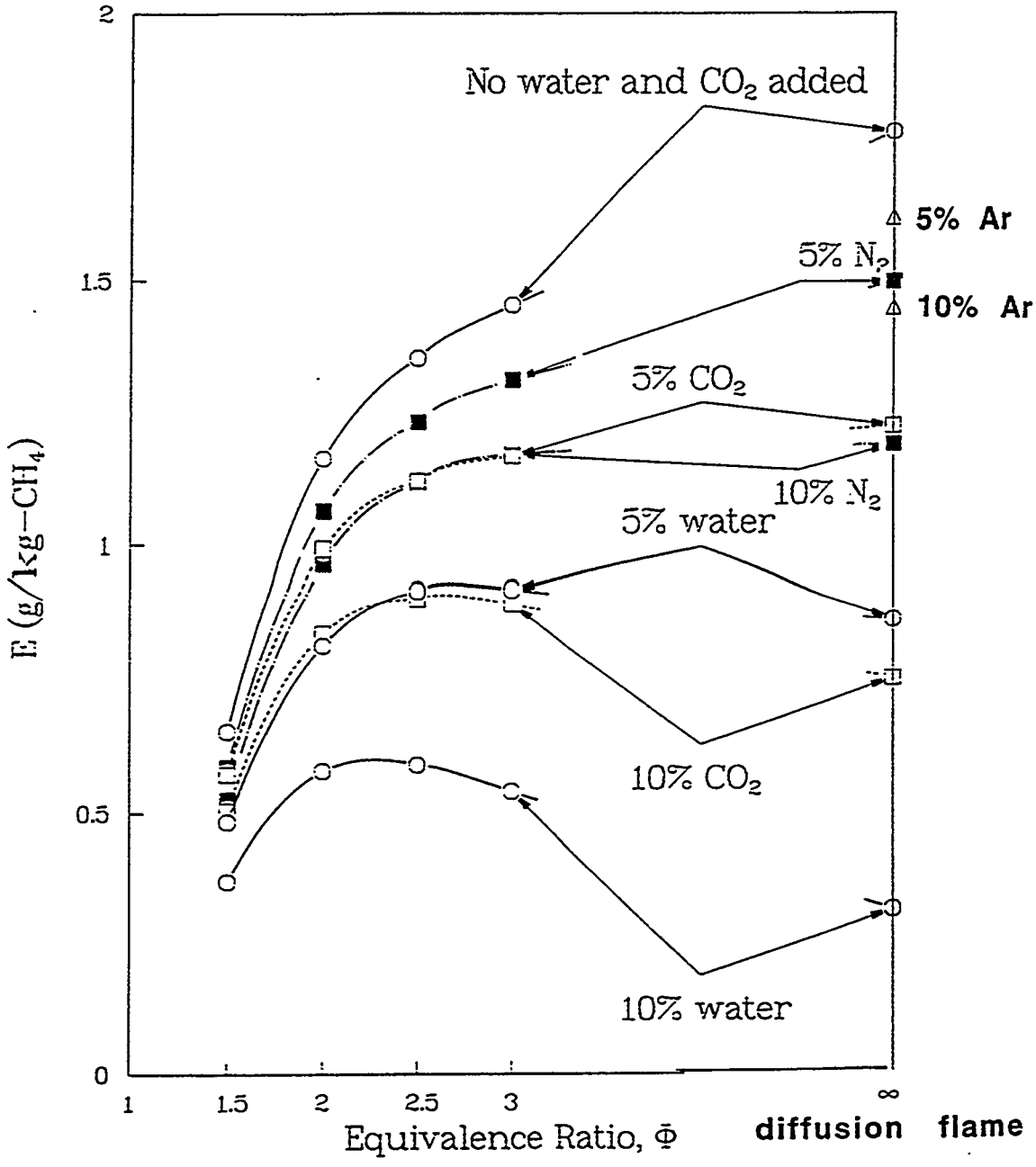


Fig.9: Predicted NO emission index as a function of equivalence ratio with water and CO_2 added to the air stream.



NEURAL NETWORK-BASED INTELLIGENT ENGINE CONTROL FOR REDUCING NO_x AND PM EMISSIONS FROM CIDI ENGINES

C. Atkinson
West Virginia University

INTRODUCTION

A neural network-based engine performance, fuel efficiency and emissions prediction system has been developed for both spark-ignited (SI) and compression ignition (CI) engines. The neural network (NN) system is able to predict real-time engine power output, fuel consumption and emissions using readily measured engine parameters. The system consists of a predictive engine model that is designed to run on a microprocessor in parallel with the engine in real time, taking input signals from the same sensors as the engine itself. The NN model of the engine is able to make highly complex, time-variant, non-linear and multi-dimensional associations between pre-selected engine input parameters and outputs in real-time. This allows the accurate prediction of engine performance (real-time torque output), engine emissions (HC, CO, NO_x, CO_2 and PM in diesel engines) and fuel consumption across the full range of engine operation. During limited dynamometer testing, the NN model learns in real-time and on the fly the precise relationship between all designated inputs and outputs. Once in the field or when operating in a vehicle, the model is able over time to update those relationships and to adapt to allow for engine or component wear, subtle changes in fuel composition or extreme combinations of operating or environmental variables.

This system, which allows for virtual emissions sensing, is equally well applicable to SI or CI engines, and has been demonstrated in both engine applications. Uses of this system include emissions prediction for engine control, on-board diagnostics and virtual emissions measurement for light and heavy-duty vehicles, stationary engines and marine, off-highway and locomotive diesels. Further applications include engine modeling, both for reducing the time required to develop engine control algorithms, and for light and heavy-duty vehicle emissions inventory prediction.

MOTIVATION

Ever increasingly stringent emissions requirements and rising fuel costs place an important premium on close control of combustion in internal combustion engines for all applications. For the foreseeable future, CI engines will continue to be used in fuel cost-sensitive applications such as in heavy-duty buses and trucks, power generation, locomotives and off-highway applications, as well as having application in light trucks and hybrid electric vehicles. Close control of combustion in these engines will be essential to achieve ever-increasing efficiency improvements while meeting increasingly stringent NO_x and PM standards. Future direct injection CI engines will utilize increasingly higher combustion and injection pressures with exhaust gas recirculation (to offset the higher NO_x levels produced by the elevated combustion pressures), variable geometry turbocharging and possibly infinitely variable valve timing, while being truly low emissions and fuel-flexible.

Close control of combustion in future SI and CI engines will be of overriding concern for both efficiency and emissions. As an example, in an ultra low emissions vehicle or ULEV, operation through one day with a failed engine sensor or control system may well produce a higher contribution to the emissions inventory than operation for a year with a fully functional system. Advanced on board diagnostic capability (OBD) and the ability to reconfigure control "on the fly" following fault detection will be an indisputable requisite in the future. These engines of the future will require significantly more complex control, having very many more degrees of freedom than those of today.

Standard classical "one-dimensional" or map-based control, in which fueling, boost and EGR are controlled somewhat independently, will prove woefully inadequate in dealing with the multiple independent degrees of freedom presented by injection rate shaping, EGR, boost and valve control. Future CIDI engines will require truly simultaneously optimized, multidimensional control. Moreover, the costs, time required and complexity associated with engine development, performance mapping, and control system development and calibration, are increasing significantly.

What is required is a truly multidimensional, adaptive, learning control system that does not require the laborious development of an engine model, while having excellent performance and emissions prediction capabilities across the full life of the engine, for all engine operating conditions. Neural network-based engine modeling offers all of these capabilities. The excellent generalization capabilities achieved through on-line learning means that the engine control system designer need make no assumptions about the governing equations dictating the engine performance and combustion characteristics. The virtual sensing system automatically develops the engine control laws by learning the engine behavior over time. This allows a truly optimized and adaptive engine prediction and control system to be developed with a minimum of effort.

OPERATION OF THE VIRTUAL SENSING SYSTEM

The system consists of a predictive engine model that is designed to run on a microprocessor in parallel with the engine in real time, taking input signals from the same sensors as the engine itself. The neural network (NN) model of the engine is able to learn the highly complex, non-linear and multi-dimensional associations between the pre-selected input parameters and outputs in real-time. Once the system has been trained to mimic the performance and emissions of the engine, it permits the accurate prediction of engine performance (real-time torque output), engine emissions (unburned hydrocarbons, carbon monoxide and oxides of nitrogen) and fuel consumption across the full range of engine operation.

LEARNING

During limited dynamometer testing, the NN model learns in real-time and on the fly the precise relationship between all designated inputs and outputs. The NN model assigns global or general weights between all designated inputs (engine operating parameters) and corresponding outputs (torque, fuel consumption and regulated emissions) on the basis of results learned during engine dynamometer testing. A further (local) set of weights is allowed to vary in time across the life of the engine in the field, thereby providing a true learning, adaptive prediction system. As a result the NN model is able to provide to the driver, to a smart diagnostic system or to an engine controller, the apparent results from a virtual suite of sensors. These virtual sensor results may either be unmeasured or unmeasurable engine parameters, or duplicate estimation of already measured variables. One immediate application is in the virtual measurement of engine-out NO_x emissions for on-board diagnostics (OBD) in both spark-ignited and compression ignition engines.

VIRTUAL SENSOR ARCHITECTURE

The neural network architecture used is that of a partially recurrent net, which is found to have more accurate mapping than a multi-hidden layer net [1]. Figure 1 shows the schematic of the neural network architecture, and the online learning or training configuration. The input vector includes instantaneous engine parameter values as well as a receding history window of 5-10 seconds of the same data (depending on engine type). Including this sliding window has been found to be necessary to capture the full dynamics of transient engine operation, including turbocharger spool-up in diesel engines and the emissions arising from transient fueling variations in CI engines. All raw engine measurements, either obtained from a fully instrumented engine on a dynamometer during training or obtained from an engine in the field during normal operation, are captured at a regular 20 Hz data-sampling rate. This rate can be increased or decreased depending on the balance between desired accuracy and

computational effort required. The data are filtered on-line through an infinite impulse response filter to provide smoothing while retaining their integrity. The transport delays and finite response times inherent in the existing engine sensors are taken into account in the virtual sensor modeling.

APPLICATION TO DIESEL ENGINES

Virtual sensing has been applied to the prediction of engine-out emissions, fuel efficiency and power output of three engines, including a 300 hp heavy-duty diesel engine, certified to 1994 US EPA heavy-duty emissions standards. In predicting the real-time performance of this compression ignition heavy-duty diesel engine (described in Table 1), the NN-based prediction model uses the real-time values of:

- intake manifold air temperature,
- intake manifold boost pressure,
- fuel rack position,
- engine coolant temperature,
- exhaust gas temperature,
- engine speed, and
- fuel rail temperature and pressure.

Using instantaneous values of these input parameters as well as a sliding, weighted window of their most recent values (extending 10 seconds back in time to capture turbocharger dynamics), the NN model is able to predict:

- instantaneous engine torque or power output,
- fuel consumption (and carbon dioxide emissions),
- exhaust gas temperature, and
- engine exhaust emissions (carbon monoxide, unburned hydrocarbons, oxides of nitrogen and smoke, as measured by whole exhaust opacity).

A limited set of emissions data was obtained from the engine described in Table 1, to conduct a proof of concept study (the data had previously been deskewed to remove the effect of variable response and delay times in the measurement of each of the emissions). The first 300 seconds of the data set were included in the engine training data, due to the limited total amount of data available, while the last 50 seconds of each data set shows the NN predictions on data on which the net had not been trained. In either case, the predictions are blind, implying no on-line learning or reinforcement. Figures 3 to 8 show the predicted versus measured engine torque, HC, CO, No_x, CO_2 and smoke emissions. All emissions have been non-dimensionalized with respect to the maximum value of that constituent found in the complete data set. These figures show the results of a blind prediction, although in this CI engine study alone, the difference between the measured and predicted exhaust gas temperature gives the local NN weights limited authority in modifying the prediction in an on-line adaptive fashion.

PROOF OF CONCEPT CIDI VIRTUAL SENSOR DEMONSTRATION

Table 1: CI Demonstration Engine Parameters.

Engine Type	10 liter, in-line 6 cylinder DI
Fuel	diesel (D2)
Compression Ratio	15:1
Turbocharger	150 kPa gauge maximum boost
Fuel Injection System	mechanical cam-driven jerk-type
Maximum Power	300 hp (224 kW) (at 2200 rpm)

VIRTUAL SENSING PREDICTION ACCURACY

In the case of CI engine prediction, the virtual sensor prediction model is able to predict these engine performance and emissions parameters to within 5-10% of their instantaneous values, given approximately 30 minutes of highly transient hot engine dynamometer training, and to well within 5% on an integrated basis. It should be borne in mind that this is achieved within 30 minutes of training, and that more training will reduce the instantaneous and integrated error significantly. Moreover, it should also be remembered that the virtual sensing system is calibrated (through training) to predict emissions in real, measurable units, as opposed to merely providing emissions trends. Finally, it should also be noted that a significant further benefit of the system is the fact that it provides relatively high accuracy predictions of all regulated emissions and CO_2, simultaneously. In the case of engine emissions, further testing of the system

on a SI engine has shown that the accuracy of the prediction can be improved to the point that it is of the same order as the accuracy of the measurements provided by the emissions analyzers used to provide the training data, integrated across a transient engine cycle.

VIRTUAL SENSING SYSTEM TRAINING

For the diesel engine described above, it was not necessary to vary all input parameters individually in a multi-dimensional test matrix, but rather to exercise the engine (as a system) through a wide cross-section of its expected performance envelope. By this is meant that it is not required to vary manifold air temperature, manifold boost pressure, commanded fuel rack position, engine coolant temperature, exhaust gas temperature, engine speed and load, and fuel rail pressure individually and independently, but rather to provide the NN with as wide a range of engine performance data as is feasible. The NN-based system has excellent generalization capabilities, provided that a wide range of representative engine performance has been used in generating the training data. Modeling of cold-start engine performance and emissions is quite feasible and could be accomplished through obtaining data from several cold starts at various initial engine and ambient air temperatures.

REAL-TIME COMPUTATIONAL REQUIREMENTS

Typical virtual sensing computational power requirements for running the NN model described above in real-time with data rates of 20 Hz are easily met by an Intel Pentium 100 MHz microprocessor-based personal computer. Running the NN on a dedicated RISC processor would reduce its computational requirements significantly, allowing for the use of a far cheaper dedicated computational processor, for on-board vehicle use. Efforts in reducing computational overhead and effort are continuing.

APPLICATIONS OF VIRTUAL SENSING

The virtual sensing system described here has immediate application in

- engine diagnostics,
- engine control, and
- engine or vehicle modeling.

ENGINE DIAGNOSTICS

In terms of engine diagnostics, a virtual sensing system may be integrated into a smart OBD system to give immediate warning of emissions exceedances. Moreover, the NN system can provide real-time values of unmeasured or difficult to measure parameters (such as NO_x emissions or PM emissions for diesel engines), from which the engine can be controlled. Virtual sensing can form the basis of a diagnostic information system, and can provide significantly more information on engine or vehicle performance and emissions than is presently available, while still using an existing sensor suite. Virtual sensing also allows the development of virtual O2,NO_x, HC, CO and PM sensors, from which the engine can be controlled in real time [2,3]. Real time fuel consumption and torque measurement for on and off-highway CI engines is also made feasible through this approach, as is the real-time prediction of emissions from stationary or marine engines for continuous emissions measurement (CEM) purposes.

By developing multiple NN performance prediction systems, each employing a sub-set of the full suite of available engine sensors, failure in a single sensor can be detected by comparing the results generated by each NN. Redundant prediction of the same engine output variable in this fashion could aid in the identification and isolation of both sensor and integral engine component failure. Virtual sensor prediction also provides a high level of redundancy albeit without additional sensor cost or hardware complexity. As an example, the instantaneous fuel consumption of the diesel engine is calculated by the NN based on the engine speed, rack position, manifold boost pressure and temperature, engine temperature and (perhaps) measured air flowrate into the engine. The fact that several of these input parameters are interrelated and dependent on each other, provides a significant level of in-built redundancy in the event of the failure of one of the engine sensors in that set.

The additional input to the NN system of output from further exhaust emissions sensing devices

(such as a viable NO_x sensor, when developed) would serve to strengthen the prediction capabilities of the virtual sensing method. The virtual sensor suite provides a true learning capability, and could allow for reconfigurable control to be used in the event of the failure of such a sensor or an integral engine component.

ENGINE CONTROL

Spark ignited engines enjoy the benefit of a remarkably powerful fueling feedback control parameter in exhaust gas oxygen sensing. CI engines on the other hand, suffer from the lack of readily available feedback parameters. This research seeks to redress that. The real-time NN prediction of engine performance and emissions allows for effectively "closed loop" control on the basis of virtual sensing of NO_x, CO, HC, or PM emissions, without requiring any additional engine sensors [2,3]. It can be used to control specific actuators or devices, such as EGR valves, fuel injection, ignition, boost control, or can be used for the full multidimensional control of fueling, ignition, EGR and variable valve timing (VVT) in SI engines, or fueling, boost, EGR and variable geometry turbocharger (VGT) devices in DI engines. Moreover, using the NN system in a predictive fashion will allow an engine to be operated at any pre-selected optimum, such as the lowest emissions level or the best power or best efficiency limit. Figure 2 shows a schematic implementation of a neural network-based engine control system.

The addition of measured in-cylinder pressure as an extra input into a CI engine emissions prediction model, will, it is believed, allow the prediction of NO_x emissions (specifically) on a cycle-to-cycle basis. Exhaust gas temperature (chosen for its robustness and ease of measurement) has been explored as a surrogate feedback parameter for CI engines, with some success.

ENGINE MODELING

Once developed on an existing or prototype engine, NN engine predictive models can be used to provide engine mapping data to reduce the time required for controller development. Instead of requiring extensive dynamometer time to establish full transient engine performance and emissions, the fully trained NN model of an engine can be used as a computational surrogate of the engine itself. In this way, engine control laws can be developed and optimized computationally, rather than requiring large amounts of dynamometer time.

While the work presented here describes the development of NN-based engine models, this technique can be used to develop combined engine and transmission models, or engine and exhaust gas aftertreatment device models in which stack-out (as opposed to engine-out) emissions are predicted. Likewise, a vehicle model can be developed, either for light or heavy duty vehicles, that includes transmission and drive-line effects, using both chassis dynamometer measurements of vehicle performance and emissions, and engine dynamometer measurements of engine-only performance.

A fully predictive engine model can also be used in a strategy-based vehicle control algorithm, such as in determining how to merge and combine energy from two sources in a hybrid electric vehicle. The model can also be used in a forward-looking strategy, limited only by the computational capability resident on the vehicle.

FUTURE APPLICATIONS

Further applications, such as engine and vehicle modeling for emissions inventory gathering are also feasible [4]. For example, once a NN model of the emissions characteristics of a vehicle has been established through limited testing on a chassis dynamometer, a computational model of the vehicle can be derived. This computational emissions model of the vehicle can then be "driven" across any driving cycle, or given topographic data, across any road. Integrating the fully predictive emissions model with a traffic simulation model or real-time data from a GPS-equipped vehicle, could allow the prediction of emissions from the vehicle under a wide range of vehicle operating conditions, driver behavior and traffic conditions.

Many such applications of virtual sensing and this method of neural network-based engine performance and emissions modeling remain to

be explored.

REFERENCES

1. T.W. Long and E.L. Hanzevack, "Hierarchical Competitive Net Architecture", Neural Network Engineering in Dynamic Control Systems, K.J. Hunt, G.R. Irwin and K. Warwick eds., Springer-Verlag, London 1995.

2. C.M. Atkinson and T.W. Long, "Neural Network-based Intelligent Engine Control for Reducing NO_x and PM Emissions from CIDI Engines", Proceedings of the US DOE Diesel Engine Emissions Reduction Workshop, San Diego, CA, July 1997.

3. E.L. Hanzevack, T.W. Long, C.M. Atkinson and M.L. Traver, "Virtual Sensors for Spark Ignition Engines Using Neural Networks". Proceedings of the American Control Conference, Albuquerque, NM, June 1997.

4. C.M. Atkinson, N.N. Clark, T. Long and E. Hanzevack, "Virtual Sensing: A Neural Network-based Emissions Prediction and Modeling System for Inventory Applications". Proceedings of the 7th Coordinating Research Council On-Road Emissions Conference, San Diego, April 1997.

Figure 1: Neural Network Architecture, showing Dynamometer-based Training to develop full Input-Output Parameter Association and Weights.

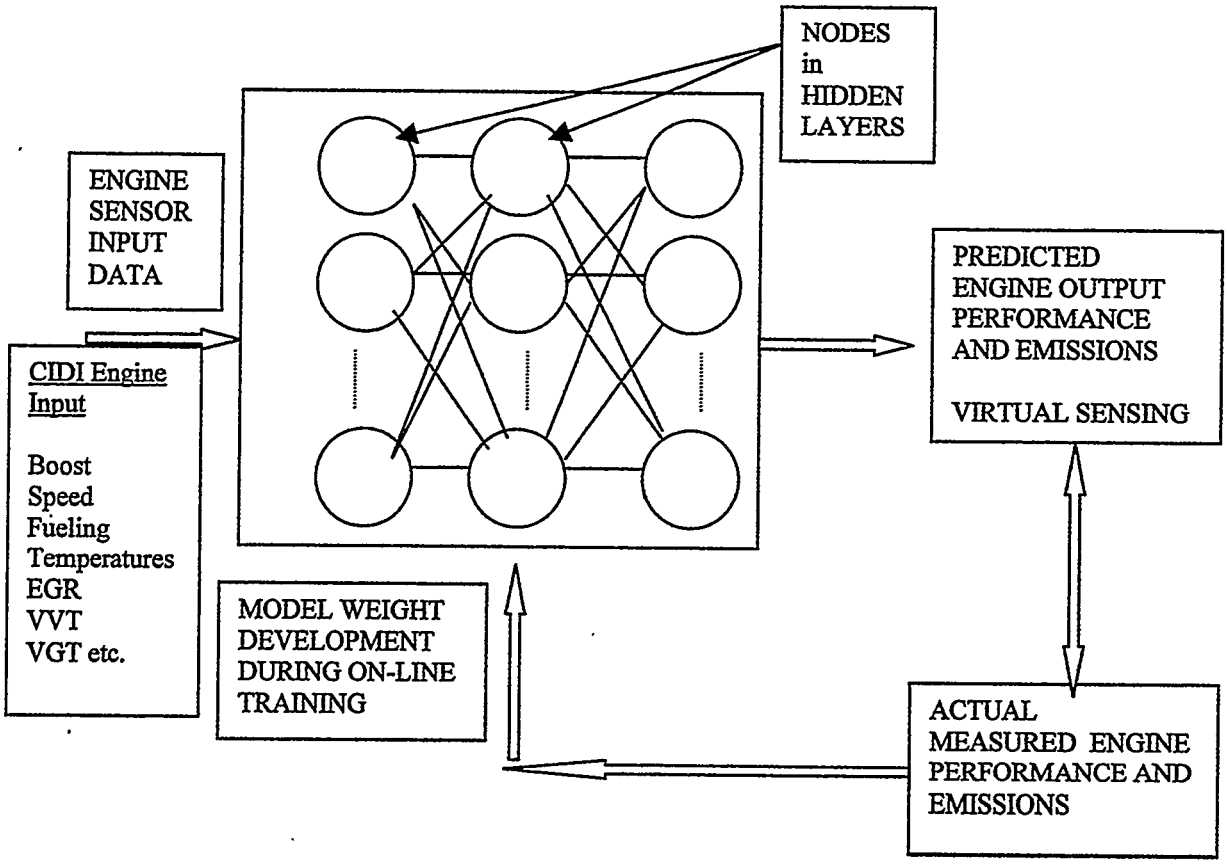


Figure 2: Engine Control using Neural Network-based Engine Modeling.

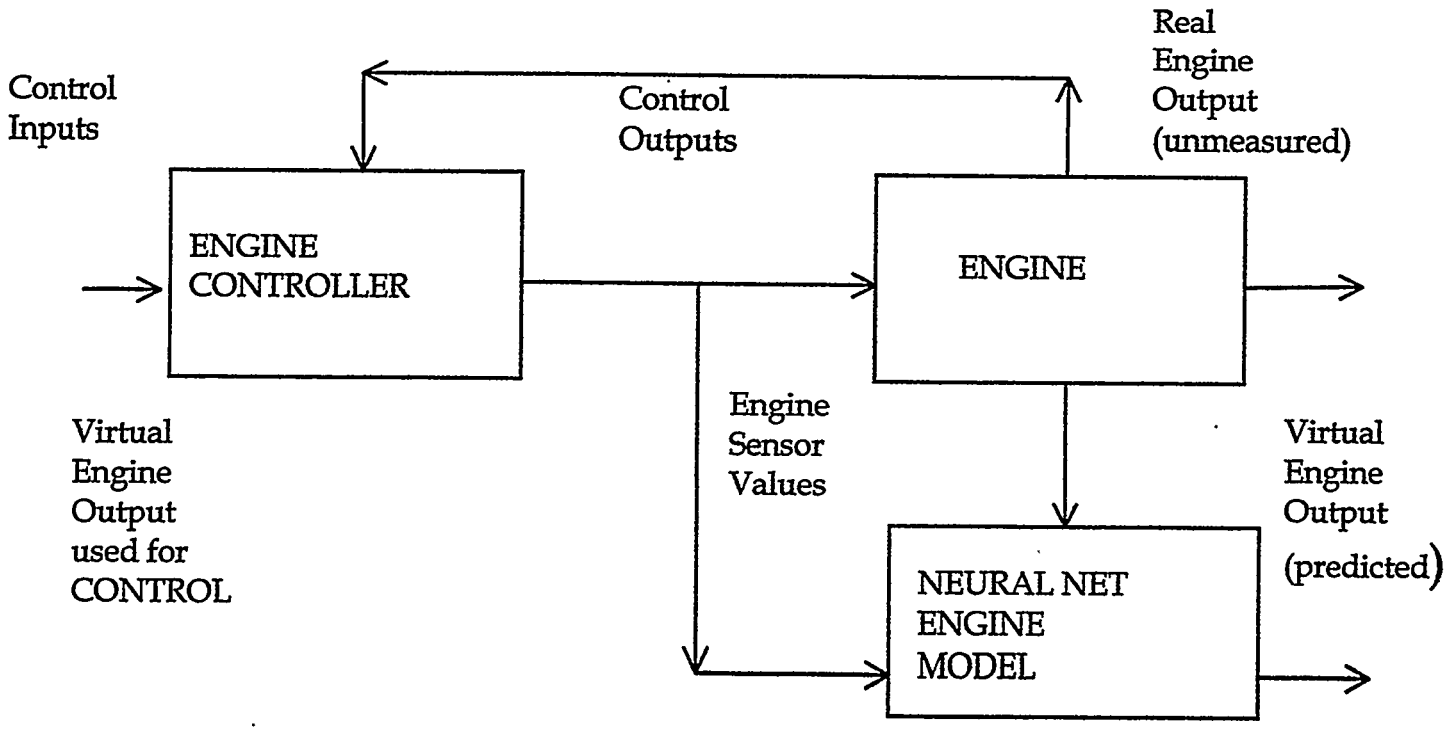


Figure 3: Measured versus Predicted Engine Torque for CI Engine NN Model Validation

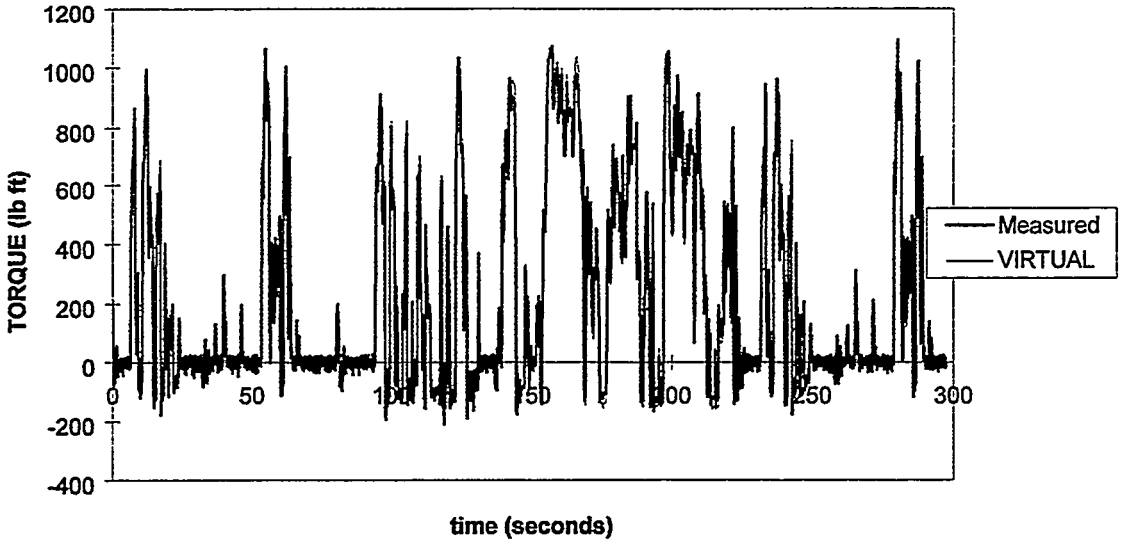


Figure 4: Measured versus Predicted Hydrocarbon Emissions for CI Engine NN Model Validation

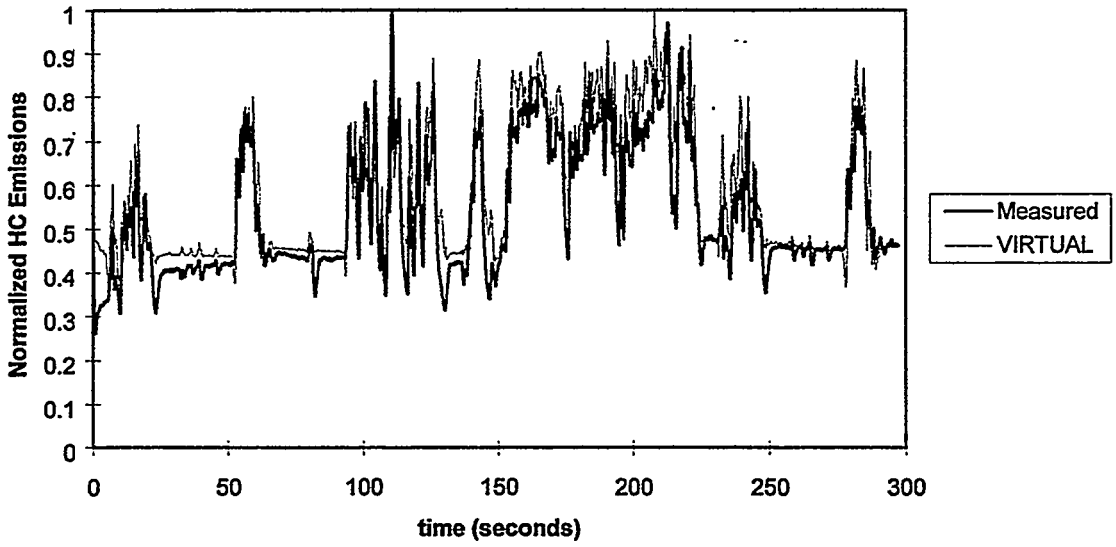


Figure 5: Measured versus Predicted Carbon Monoxide Emissions for CI Engine
NN Model Validation

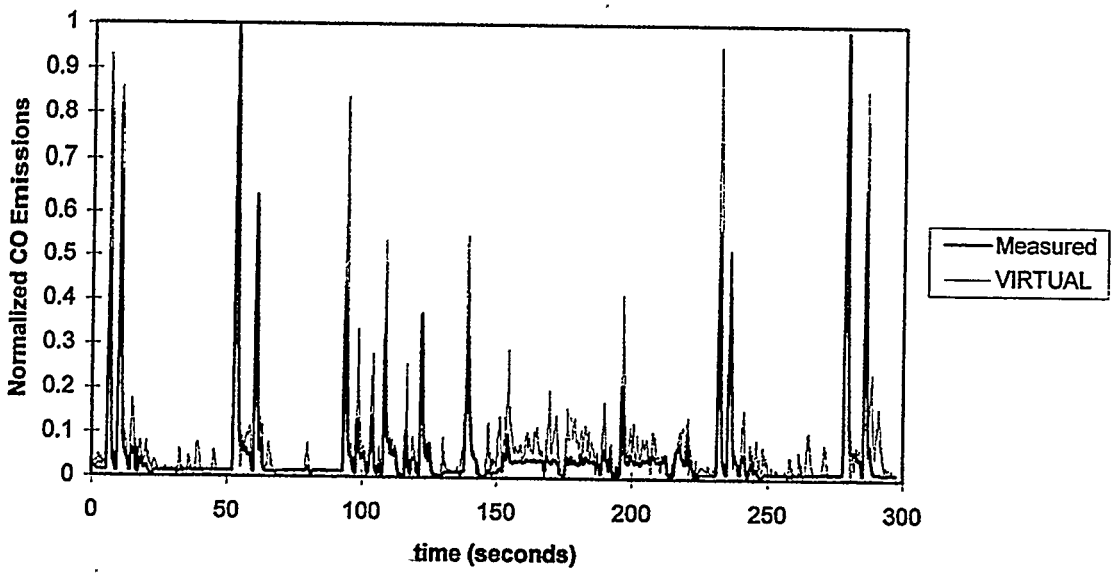


Figure 6: Measured versus Predicted Oxides of Nitrogen Emissions for CI Engine
NN Model Validation

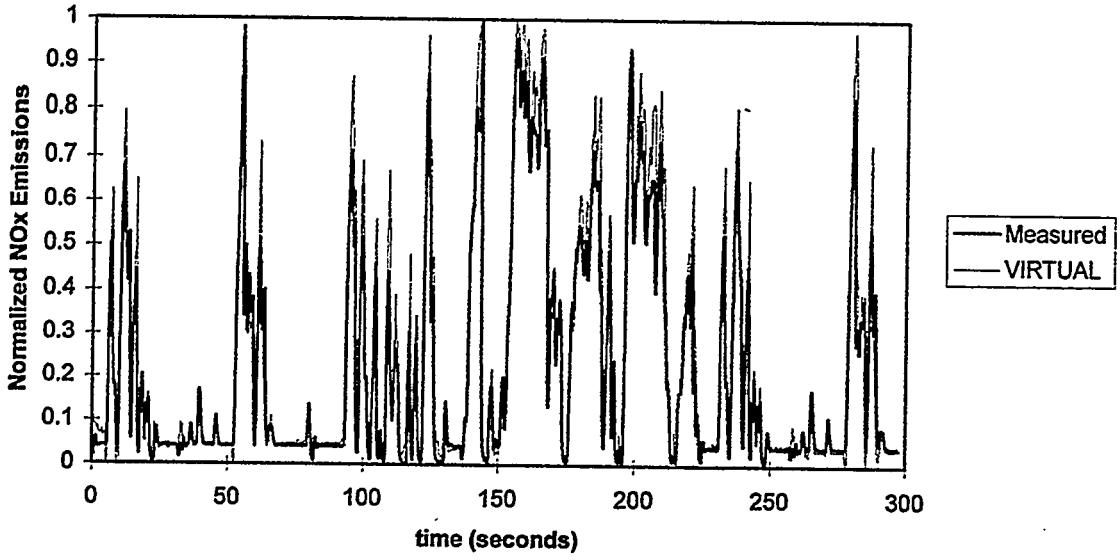


Figure 7: Measured versus Predicted Carbon Dioxide Emissions for CI Engine NN Model Validation

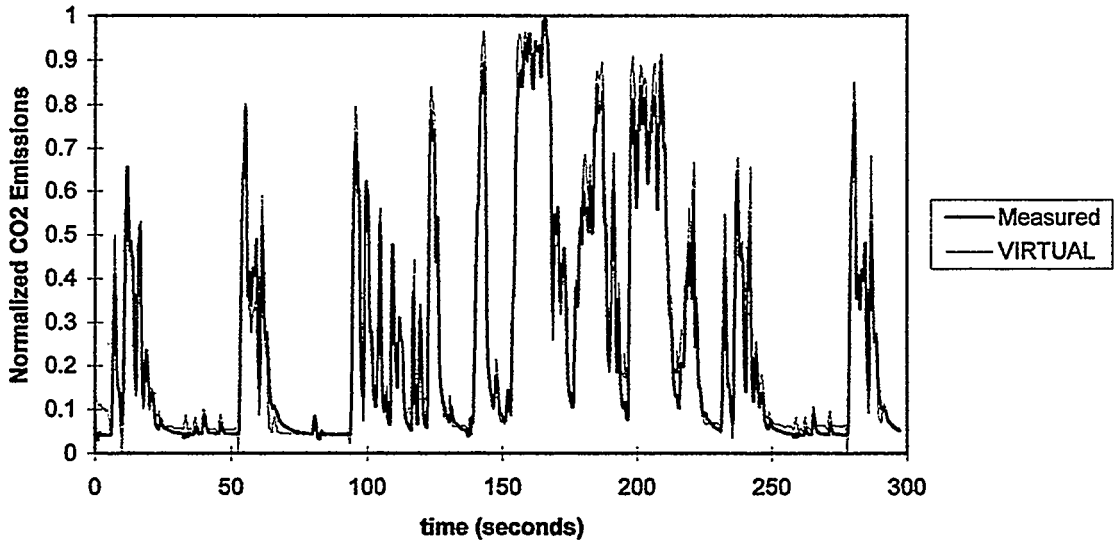
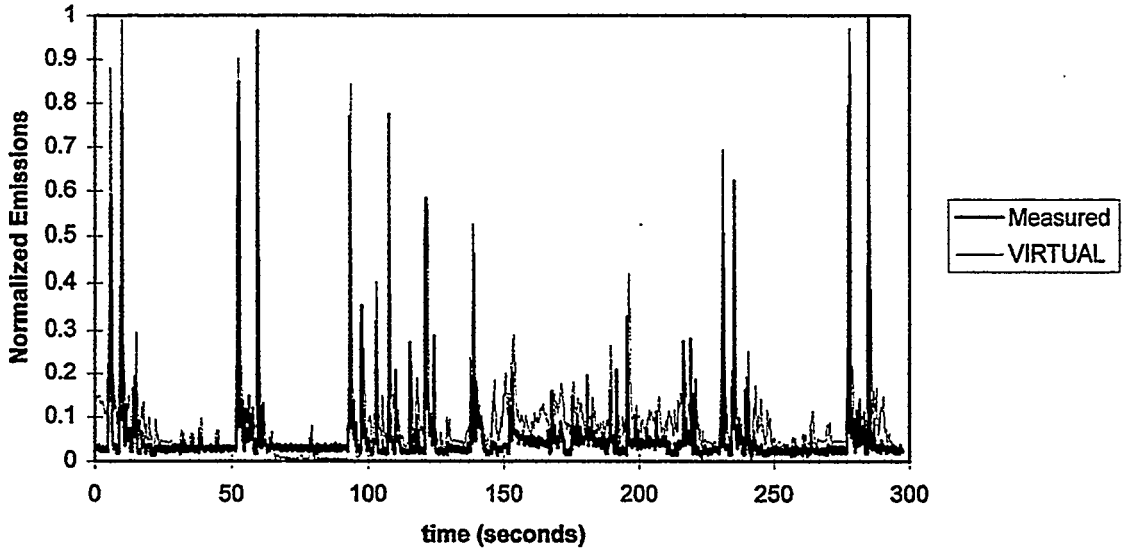


Figure 8: Measured versus Predicted Smoke Emissions for CI Engine NN Model Validation



THE PASSIVE TRAP, A MEANS FOR MEETING HEAVY DUTY DIESEL EMISSIONS BEYOND 2004

P. K. Das

Navistar

The future emissions standards are very challenging. The Heavy Duty engine Manufacturers, US Environmental Protection Agency (EPA), and California Air Resources Board (CARB) have agreed to a potential legislative standard for 2004 emissions. The agreement calls for a 50 percent reduction in NO_x levels from an already low value for 1998 with no easing off on particulate. The NO_x level in 2004 will be controlled to 2.0 gms/bhp.hr while particulate level will be maintained at 0.1 gms/bhp.hr. It, however, allows for NO_x and hydro-carbon emissions to be merged into a combined value of 2.5 gms/bhp.hr.

There are also continuing discussions on ambient air quality standards beyond 2004. The regulation will likely lead to more stringent particulate levels. It becomes important to explore technologies having potential for low particulate emission.

NO_x and particulate emissions are usually linked by a tradeoff relationship. It becomes particularly difficult to drastically reduce NO_x with no sacrifice in particulate. In addition, for the solution to be practical, the system must have long life, be reliable, have little to no fuel economy loss, and be affordable. It thus becomes a major challenge.

With these goals in mind, Navistar and Rhone Poulenc embarked on an innovative approach. The strategy was to employ extensive EGR (exhaust gas recirculation) for large reduction in NO_x. Navistar has an electronically controlled experimental EGR system which was found useful. EGR would increase particulate. However, Rhone Poulenc had an EOLYS technology which was highly efficient in reducing particulate. It employed a cerium additive to the fuel as a catalyst along with a passive trap for particulate filtering. The trap was self regenerating with no additional system.

The work was carried out in Navistar's 7.3 liter V8 engine in current production. The strategy not only accomplished a NO_x level of below 2.0 gms/bhp.hr. but also reduced particulate to an unheard of level of 0.01 gms/bhp.hr. The particulate level achieved is a 90% reduction from the 2004 standard.

A concern whether or not cerium would generate any new harmful emissions was recognized from the beginning. Rhone Poulenc has done extensive work in this area and is collaborating with EPA. While the evaluation is not complete, no harmful emissions have been identified so far. This is quite encouraging.

The technology shows good potential for lowering emissions in heavy duty diesel engines. It also offers production feasibility with further development.

EMISSION CHARACTERISTICS OF A TURBOCHARGED MULTI-CYLINDER MILLER CYCLE DIESEL ENGINE

R. Kamo and N.S. Mavinahally, Adiabatics, Inc.
W. Bryzik and M. Reid, U.S. Army Tank-Automotive Command

INTRODUCTION

In an effort to leave no stone unturned in the investigation of exhaust emissions characteristics in the various forms and versions of the compression ignition engine, the short compression-extended expansion concept "Miller " cycle diesel engine was investigated. The Miller cycle diesel engine was studied in the turbocharged form and also in the Low Heat Rejection (LHR) form by applying ceramic coating on the combustion chamber. The ceramic coated combustion chamber improved the performance of the conventional standard metal engine and thus was selected for the Miller cycle engine.

The extended expansion cycle in conjunction [2] with a short compression stroke is one of the few remaining engine concepts that is available for improving engine performance and reducing fuel consumption. The short compression stroke is achieved by: 1) closing the intake valve early in the cycle before BDC, or 2) by closing the intake stroke late after BDC. When the various engine breathing processes are considered such as emptying and filling, gas dynamics, the late intake valve closing displays some practical volumetric efficiency over the early intake valve closing. Better heat transfer is also achieved with late valve closing. These engines with extended expansion stroke and short compression stroke were known as the Atkinson Cycle and the later version as the Miller cycle [5].

The advantages of an extended expansion cycle are many and offer many ramifications for an improved engine cycle of the future. A phase 1 study of the Miller Cycle Advanced Military Engine resulted in the identification of a simple concept of closing the intake poppet valve late or early and pressurizing the intake air charge more to make up for the reduced inlet charge. Reduced specific fuel consumption and increased power output without increasing the peak cylinder pressure are some of the benefits [3]. The principle of operation is based on a low effective compression ratio and high expansion ratio. Because of the thermodynamic advantage of the Miller Cycle, the emissions such as NO_x are lowered.

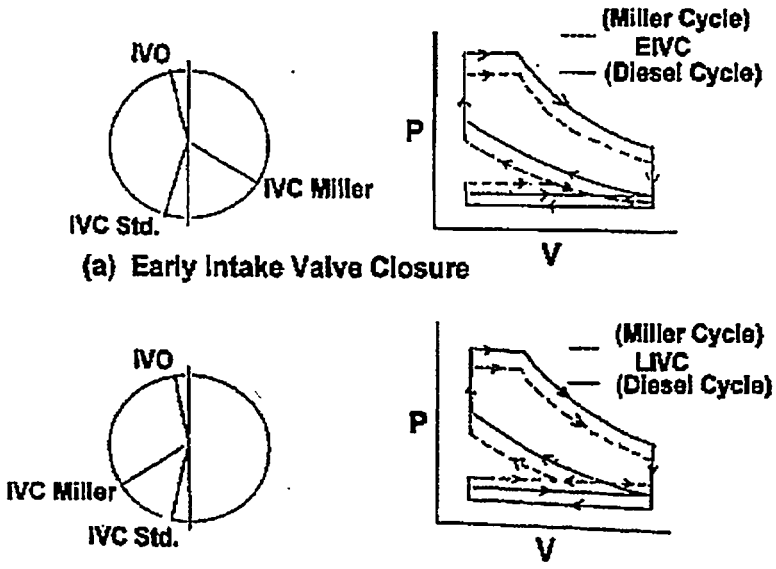
Finally, the incorporation of an insulated low heat rejection engine [4] with the Miller Cycle is shown to provide engine performance benefit nearly equal to the Miller Cycle alone. Application to military and commercial engines can be used to improve engine fuel efficiency, increase power output, improve durability, increase responsiveness, reduce heat rejection, and reduce the cost of power upgrading.

THE MILLER CYCLE

To illustrate the various aspects of the Miller Cycle engine [5], an early intake valve closing and a late intake valve closing cycle are shown. Figure 1(a) shows the valve timing diagram and a P-V diagram of the early intake valve closing cycle. Figure 1(b) shows the valve timing diagram and a P-V diagram of the late intake valve closure.

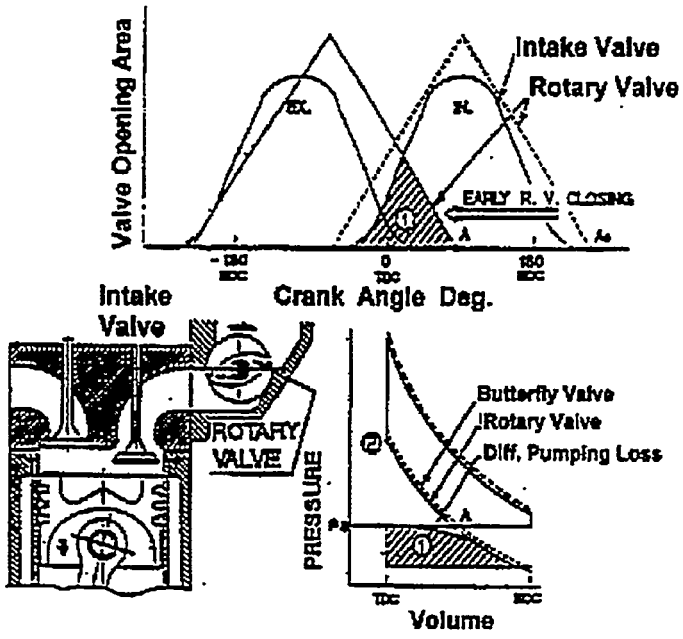
In both cases, the thermodynamics of the difference between the area below the expansion and compression curves is the network which is larger than the conventional engine. Conceptually and thermodynamically the early intake valve closure and the late intake valve closure are identical. The means to obtain a variable inlet valve closure will usually differ.

Another means of achieving variable inlet valve timing is to place another valve in series with the engine intake valve. Most notable of this type of valve timing is the K-Miller [1,2] Cycle in which a rotary valve is driven by the camshaft and is timed through a sliding mechanical helical gear set. This K-Miller concept has a dead volume



Two Methods of Obtaining Extended Expansion Cycle With
(a) Early Valve Closure and (b) Late Intake Valve Closure

Figure 1



Effect of Early R.V. Closing for Gas Engine

Figure 2

Engine Type	Miller 80				Standard (IVCT = 30)			
Load (%)	100	75	50	25	100	75	50	25
Exhaust Enthalpy (kW)	19.79	14.48	10.39	5.78	15.5	13	8.89	5.53
Air / Fuel Ratio	21.6	23.08	24.9	28.73	29.5	34.6	41.5	50
Compression Work	4.56	3.04	1.92	0.74	3.5	3.51	2.51	1.47
Turbine Work	8.51	5.65	3.54	1.33	7.3	6.4	4.28	2.45
Net Indicated Efficiency (%)	43.5	43.28	43	42.5	41.6	41.2	40.2	38.8
Peak Pressure (psi)	2,220	1,741	1,360	887	2,340	2,150	1,710	1,310
Fuel Input (kW)	81.6	63	48	30	64.8	55.2	40.2	27.6
ISFC (lb/HP-hr)	0.32	0.32	0.32	0.32	0.33	0.33	0.34	0.35
BSFC (lb/HP-hr)	0.37	0.39	0.42	0.53	0.41	0.43	0.51	0.7
Improvement in Indicated Efficiency (%)	4.54	5.13	6.99	9.42	-	-	-	-
Brake Power (kW)	30.6	22.37	15.7	7.85	21.7	17.5	10.9	5.46
Compression Ratio (GCR)	15	15	15	15	17.5	17.5	17.5	17.5
Effective CR (ECR)	10.3	10.3	10.3	10.3	16.72	16.7	16.7	16.72
Ratio of ECR to GCR	1.46	1.46	1.46	1.46	1.05	1.05	1.05	1.05
IMEP (kPa)	1714	1316	996.4	615.3	1302	1097	780	517.3
IMEP (psi)	248.6	190.9	144.5	89.24	188.9	159	113	75.02
Actual Boost Pressure Ratio	3.09	2.55	2.09	1.51	2.3	2.3	2.01	1.66

Figure 3: Performance of Miller Cycle, Standard

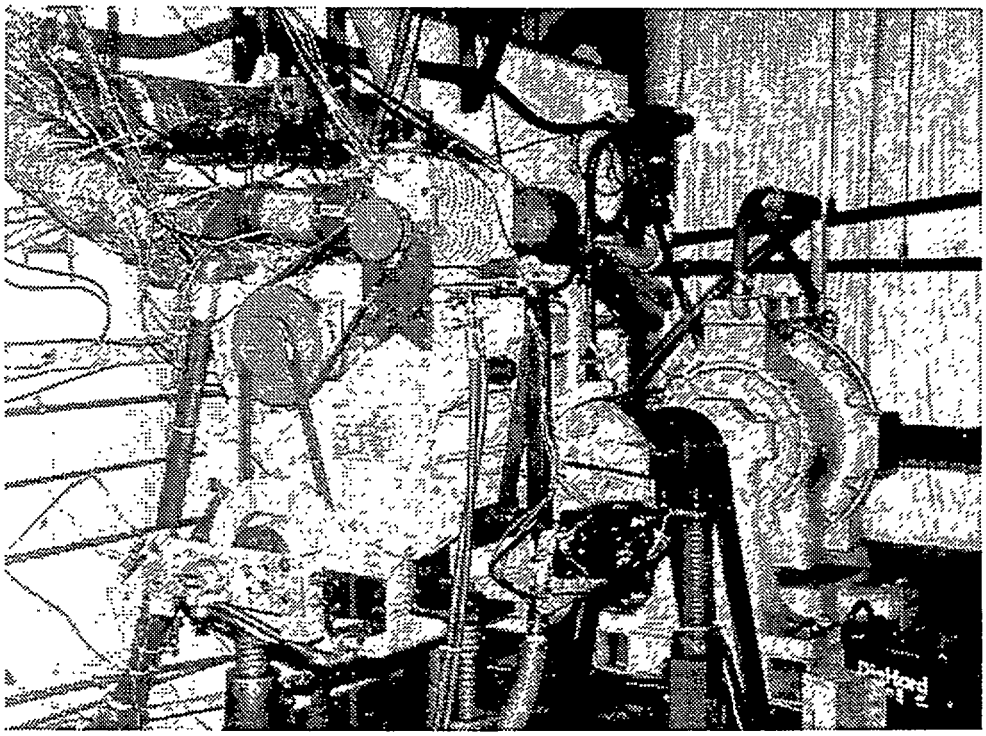
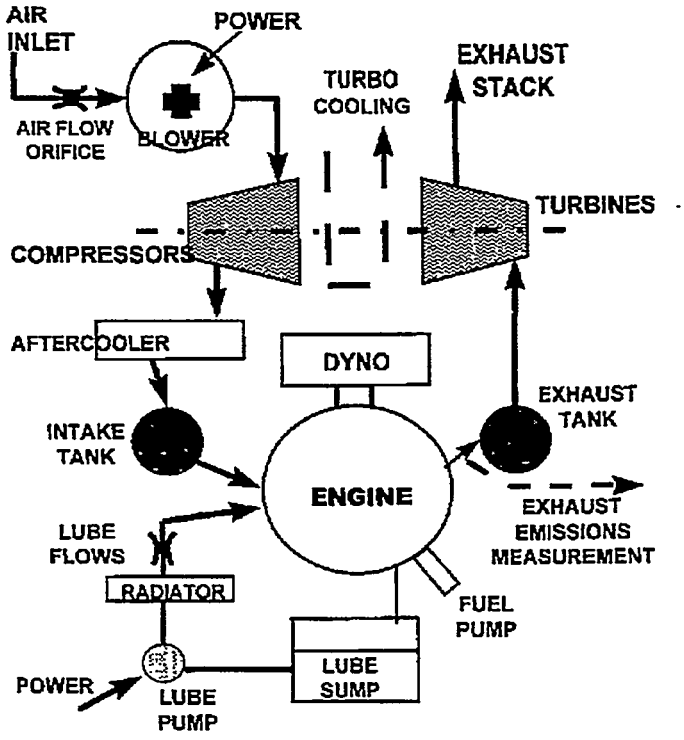


Figure 4: Engine Test Set Up in the Laboratory With Supercharger and Miller Cycle Modifications.



Test Set Up for Engine Emissions Measurements
Figure 5

between the engine and the rotary intake valve which is detrimental from the thermodynamic standpoint. The K-Miller concept, P-V diagram and valve events are shown in Figure 2 [1].

The advantages of an extended expansion cycle are many, aside from more power and efficiency over the conventional powerplant. From the P-V and T-V diagrams it can be shown that the following advantages are present:

1. Lower compression temperature for lower cylinder component stress, fuel knock deterrent, i.e. natural gas, lower emission.
2. Lower peak pressures - advantageous from stress standpoint and engine sizing.
3. Lower exhaust pressure.
4. Lower compression work.
5. Greater expansion work.

CYCLE SIMULATION

Before starting on engine modification and testing, a cycle simulation of the Miller cycle and the standard engine was performed. Figure 3 shows a summary of the simulation. It compares the Miller cycle with 80 degrees aBDC intake valve closure at four load conditions of 100%, 75%, 50% and 25%. With a single stage equipped turbocharger, the Miller cycle at 75% and 100% load is running at Air/Fuel of 23.08 and 21.6, respectively. These Air/Fuel (A/F) conditions are too rich for optimum combustion and emissions.

SUPERCHARGER

A better turbocharger or two stage supercharger-turbocharger will be desirable. For this reason an EATON M112 Supercharger was selected in this study to boost the intake air and raise the A/F ratio.

This approach is undesirable because the supercharger will take engine shaft power and increase the brake specific fuel consumption (BSFC). However, the engine response will be excellent [1]. The M112 Supercharger is coupled to the engine crankshaft and operates at 13000 rpm maximum giving up to 35 KPa boost pressure. The power required is 30 Kw.

TEST SETUP

Figure 4 shows the laboratory setup of the 6.6 liter engine rated at 2600 rpm. The bore x stroke is 107 mm x 127 mm. The engine is equipped with an Eaton M112 supercharger with a 5.1 speed booster.

Figure 5 is a schematic of the test setup. The first stage intake pressure booster is the M112 supercharger. The first stage boosted air from the supercharger is fed into the turbocharger compressor and through an aftercooler to the intake tank and to the engine. Part of the engine exhaust is then measured for exhaust emissions. The remaining exhaust gases are released to the exhaust tank and turbocharger exhaust turbine before being released to the exhaust stack.

The single-cylinder engine test cell had an automated microcomputer-based data acquisition system for recording various engine data-temperatures, pressures, flow rates, engine speed, load, emissions, etc. In addition, a National Instruments 8 channel high speed microcomputer data acquisition system for on-line acquisition of cylinder pressure data was available. This system is capable of acquiring hundreds of thousands of engine cycles, averaging, analysis of cylinder pressure diagrams, and computation of heat release rates.

The laboratory also had emissions capabilities for the engine tests. In addition to the sample handling system, the emissions setup consists of the following analyzers:

- Beckman model 955 Chemiluminescent NOx analyzer
- Beckman model 400A FID Hydrocarbon analyzer
- Beckman model 870 NDIR CO analyzer
- Beckman model 8P70 NDIR CO_2 analyzer
- Beckman model 7003D Polarographic oxygen analyzer
- In Line Particulate Measuring System Developed at M.I.T.

The particulate matter measurements were obtained to simulate the atmospheric dilution

process [6]. A mini-dilution funnel was patterned after development by M.I.T.

For smoke measurement, an AVL smoke filtering equipment was used. The mass fuel flow rate and laminar air flow rates were measured with the usual modern automotive laboratory equipment. A Kistler cylinder pressure indicator was used to determine peak pressures.

TEST RESULTS

Since presentation of all data for all loads and speeds was not possible within the context of this paper, a full 2600 rpm speed and 93% load conditions were presented. Some 25% load conditions are shown for comparison purposes only.

The factory performance curves of the original engine are shown in Figure 6. The tests were conducted on 93% load at various engine speeds (1600, 1800, 2000, 2200, 2400 and 2600 rpm). Some tests are shown for 25% load at various speeds. Figure 6 shows the points where tests were conducted.

Tests were conducted on the following engine builds:

- Standard metal engine (IVC @ 30 degrees aBDC)
- Standard Miller 100 (IVC @ 100 degrees aBDC)
- LHR Miller 100 (IVC @ 100 degrees aBDC) S/C OFF
- LHR Miller 100 (IVC @ 100 degrees aBDC) S/C ON
- Standard LHR Engine (IVC @ 30 degrees aBDC

#

Flexibility in testing engine builds was limited because once the thermal coating (LHR version) was applied, it was difficult to remove the thermal coatings to come back to the standard metal to check points.

Figures 7 to 18 are presented to display the emissions and performance characteristics for primarily 2600 rpm and 93% engine load conditions. The figures are adequately labeled for identification. Some data at 25% load are shown for comparison purposes.

Figure 7 shows the performance and brake specific fuel consumption for a standard metal engine with IVC of 35 degrees aBDC. The standard Miller cycle with 80 degrees aBDC intake valve closure and LHR (low heat rejection) are all plotted against engine speed at 93% torque conditions. The LHR Miller 80 displayed consistently about 5% improvement in BSFC. Thus, all future Miller cycle builds were insulated (LHR) [7].

Figure 8 shows the same brake specific fuel consumption curves with LHR Miller 100 degrees. Again the LHR 100 S/c OFF displayed better BSFC than the standard engine.

Since all data of insulated (LHR) Miller becomes the focal point, the standard engine was also coated and shown as Standard LHR. Figure 9 shows the comparison of smoke between LHR Standard and LHR Miller 100. The standard engine with insulation (LHR) did better than the LHR Miller 100 with and without the supercharger.

The superior NO_x emissions characteristics are shown in Figure 10 at full load for the LHR Miller 100 with S/C on or off. This is to be expected as the compression temperature is lower for the Miller cycle because of its short compression stroke [5].

Figure 11 shows the NO_x emissions from the engine at 25% load. Both the LHR Miller 100 with S/C on and the Standard LHR were equal. The LHR Miller 100 is penalized for lack of air with the S/C off.

Figure 12 shows the full load HC emissions at full load. The LHR Miller 100 with and without S/C did better than the LHR Standard @ 93% load. At 25% load the HC from the LHR Miller 100 with S/C on is better than the LHR Standard. The LHR Miller 100 with S/C is the worst offender.

Regarding total particulate emissions, including absorbed organic at full load, Figure 14 shows comparable results. The best is the LHR standard engine and the worst is LHR Miller 100 with the S/C on. However, the particulates at 25% load show the LHR Miller 100 with S/C off is

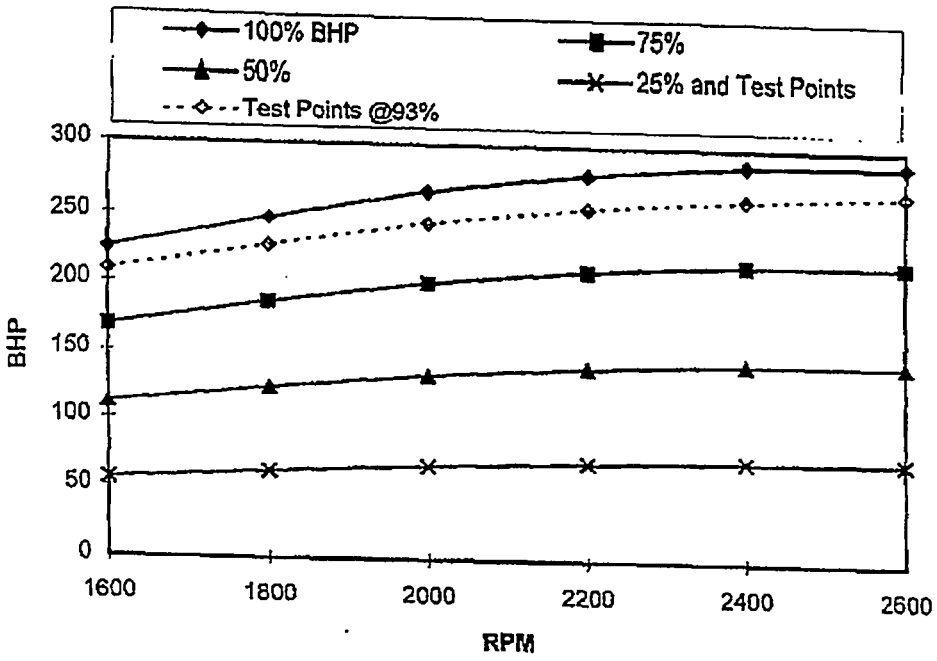


Figure 6. Brake Power vs. RPM

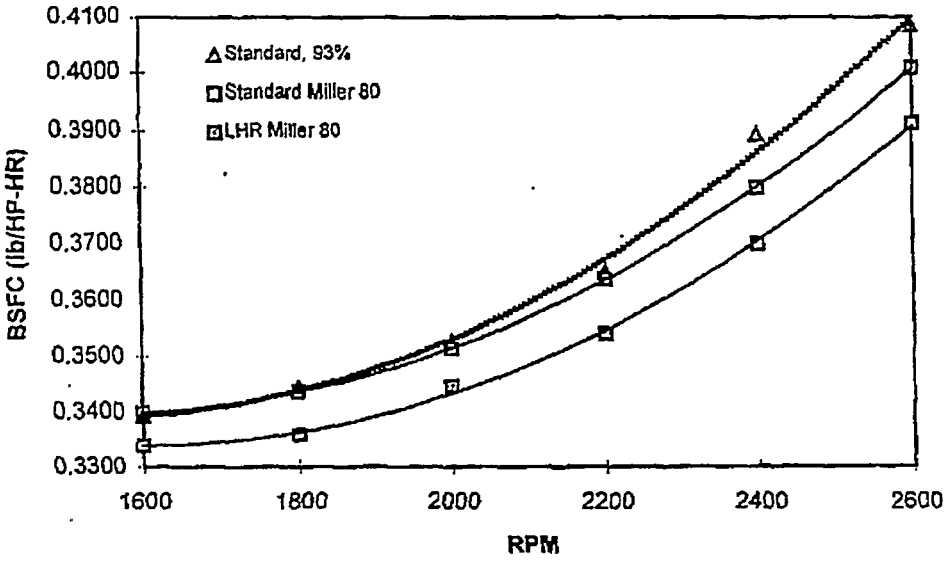


Figure 7. Comparison of BSFC Between Standard, Std Miller 80, and Insulated Miller 80 Engines at 93% Torque

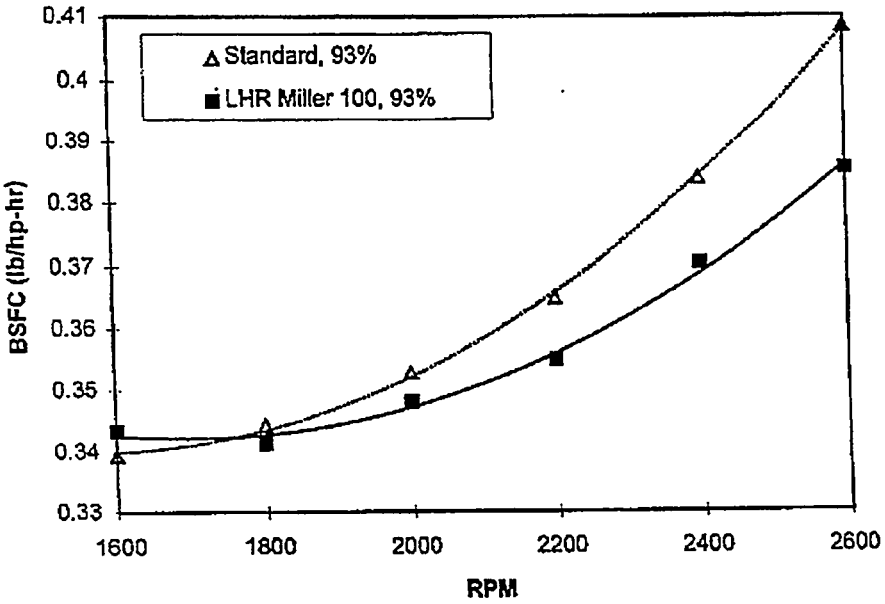


Figure 8. Comparison of BSFC Between Standard and LHR Miller 100 Engines at 93% Torque

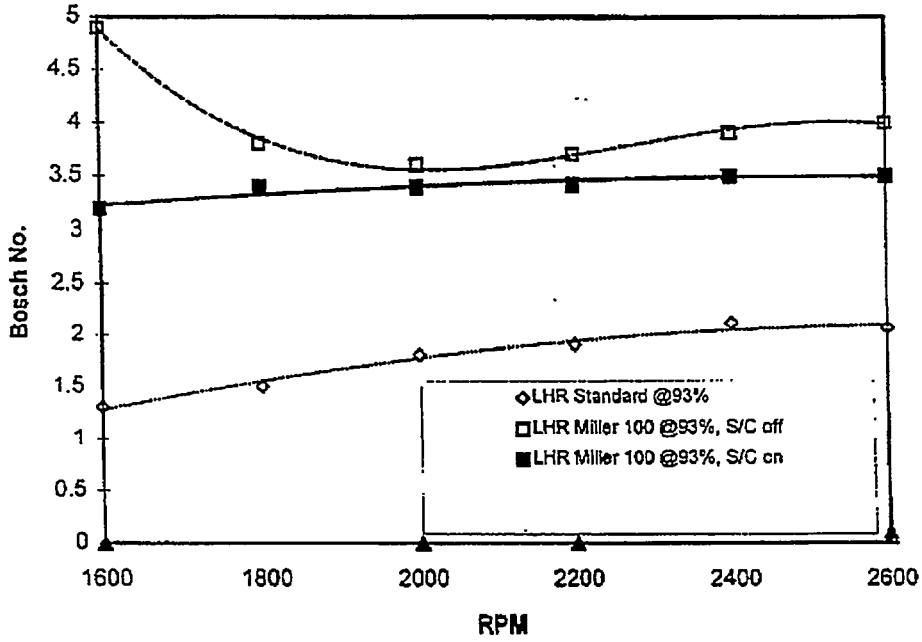


Figure 9. Comparison of Smoke Between LHR Standard and LHR Miller 100 at 93% and 25% Torque

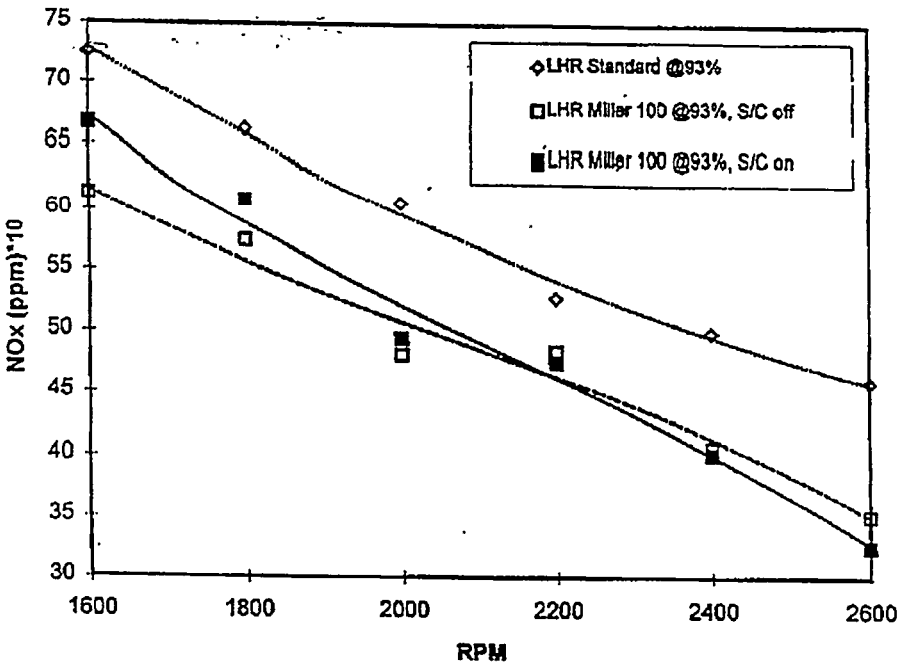


Figure 10. Comparison of NOx Between LHR Standard and LHR Miller 100 Engines at 93% Torque

best. The LHR Miller 100 with S/C on is the worst. The LHR Standard takes the middle road. These results are plotted in Figure 15.

In order to understand what is going on in the engine, it would be useful to know what the Air/Fuel ratio going into the engine is. Also the CO_2 out of the exhaust can indicate the completeness of combustion. For this purpose Figure 16 shows the full load Air/Fuel ratio for the various engines' tests. Figure 17 shows the comparison of CO_2 in the exhaust between LHR Std and LHR Miller 100 engines with and without S/C. Figure 17 is for 25% load and Figure 18 is for 93% load.

CONCLUSIONS

A conventional contemporary turbocharged diesel engine was converted to a late intake valve closure and extended expansion Miller Cycle turbocharged engine. A two-stage supercharger-turbocharger air handling system was employed. The supercharger could be used or cut out in the system. The exhaust emissions were measured to determine the emissions characteristics from a turbocharged Miller cycle diesel engine. The following can be concluded from the data presented:

1. The LHR Miller 100 offers superior BSFC over the LHR Standard engine.
2. LHR Standard engine has demonstrated better smoke characteristics than the LHR Miller 100 engines.
3. The LHR Miller 100 shows better lower NO_x emissions than the LHR Standard engine.
4. The LHR Miller 100 with supercharger offers lower HC emissions than the LHR Standard engine at all speeds and load conditions.
5. Total particulate matter, which includes absorbed organics at 93%, load is lowest for the LHR Standard engine. However, at 25% load, the LHR Miller 100 demonstrates lower particulates than the LHR Standard engine.
6. At 93% load, the air/fuel ratio is too low for good combustion at 1600-1800-2010 engine rpm

REFERENCES

1. Kanesaka, H. and Sakai, H, "The K-Miller Cycle for High Output Engine," Kanesaka Technical Institute, Tokyo, Japan (1993).

2. Mavinahally, N., "Experimental Investigation of Extended Expansion Concept Applied to Four Stroke S.I. Engine, "PhD Thesis, Indian Institute of Technology, Madras, India (1991).

3. Ishizuki, Y., Shimizu, Y., Hikino, H., Kawashima, Y., "A New Type of Miller Supercharging Systems for High Speed Engine, Part 2 , Realization of High BMEP Diesel Engines", Engine Research Division and Technical Center, Komatsu Ltd., SAE Paper 851523 (1985).

4. Mavinahally, N., Kamo, R., Bryzik, W., Reid, M., "Insulated Miller Cycle Diesel Engine," SAE Paper 961050, Detroit, Mi. (1996).

5. Miller, R. H., "Supercharging and Internal Cooling Cycle for High Output," Transactions, ASME, 69, 1947.

6. Laurence, R.B., Wong, V.W. and Brown, A.J., MIT, "Effects of Lubrication System Parameters on Diesel Particulate Emission Characteristics," San Diego Workshop, July, 1997.

7. Wong, V.W., Yu, M.L., Mogaka, Z.N., and Shahed, S.M., "Effects of Catalytic Wire-Mesh Traps on the Level and Measurement of Heavy-Duty Diesel Particulate Emissions," SAE Paper 840172, 1984.

ACKNOWLEDGMENT

Lloyd Kamo and May Kamo are acknowledged for their assistance in preparation of this manuscript.

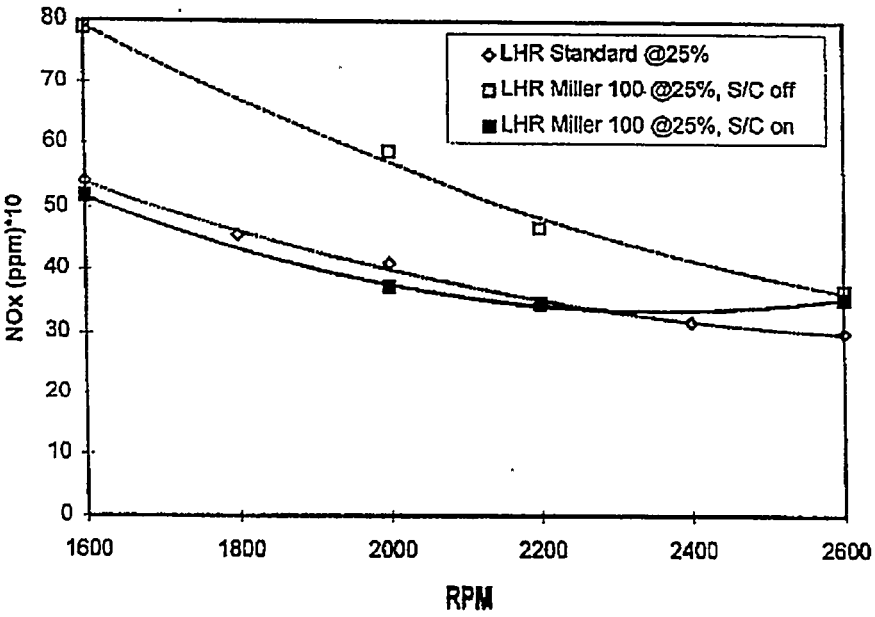


Figure 11. Comparison of NOx Between LHR Standard and LHR Miller 100 Engines at 25% Torque

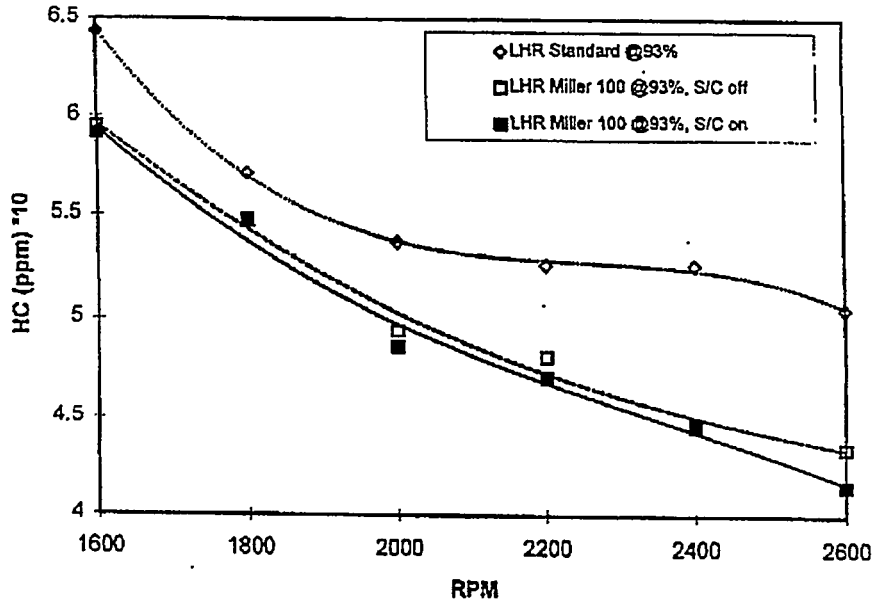


Figure 12. Comparison of HC Emission Between LHR Standard and LHR Miller 100 Engines at 93% Torque

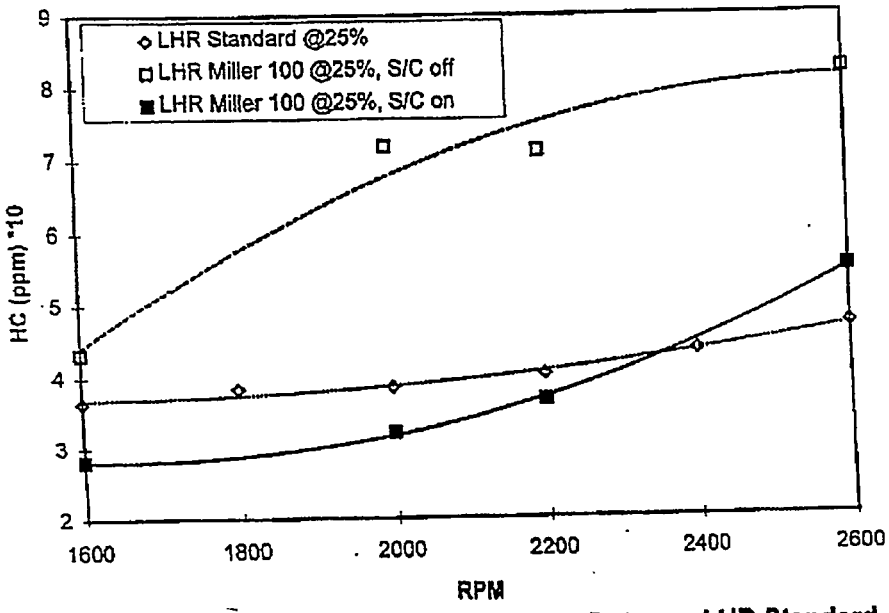


Figure 13. Comparison of HC Emission Between LHR Standard and LHR Miller 100 Engines at 25% Torque

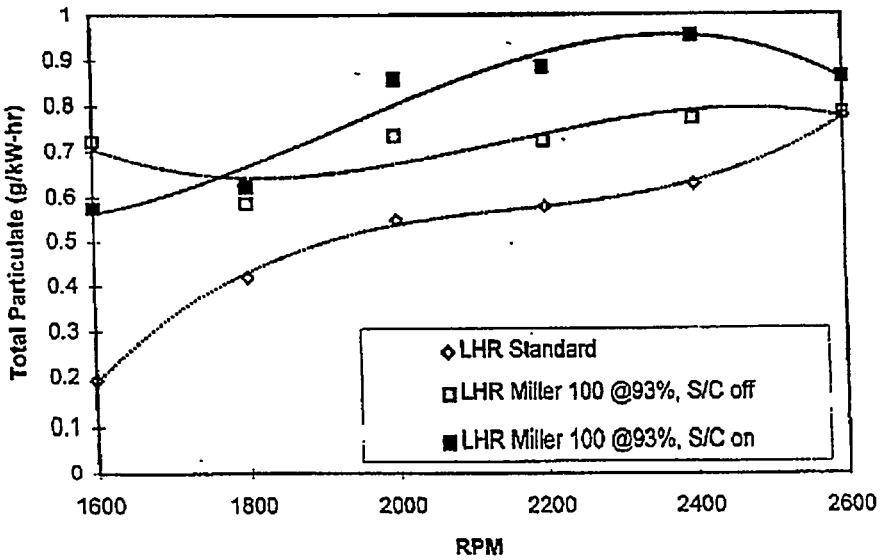


Figure 14. Comparison of Total Particulate (includes absorbed organic) Between LHR Standard and LHR Miller 100 Engines at 93% Torque

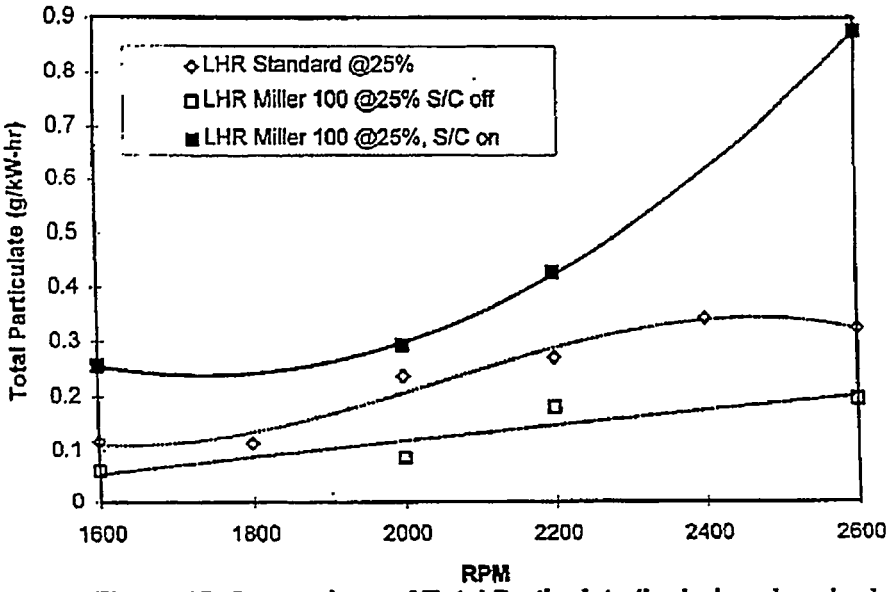


Figure 15. Comparison of Total Particulate (includes absorbed organic) Between LHR Standard and LHR Miller 100 Engines at 25% Torque

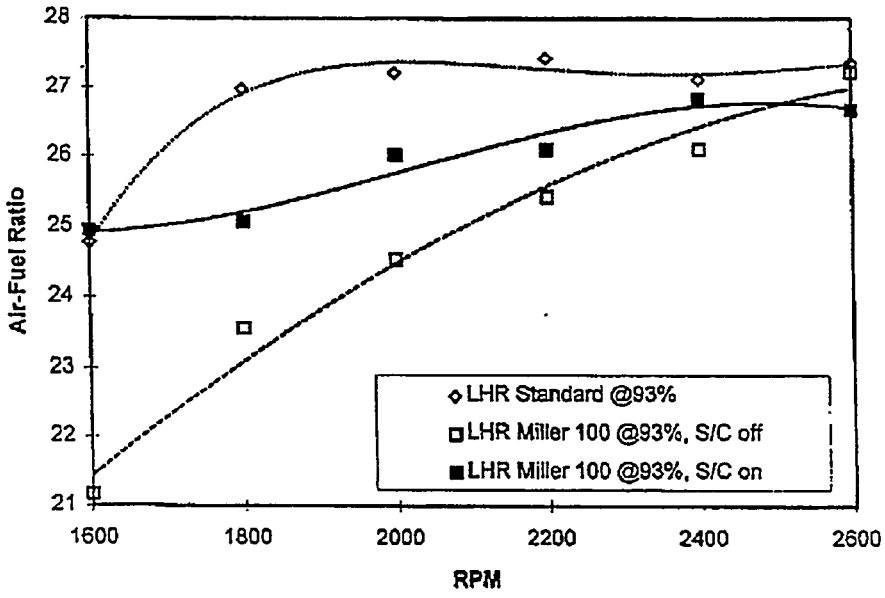


Figure 16. Comparison of Air-Fuel Ratio Between LHR Standard and LHR Miller 100 Engines at 93% Torque

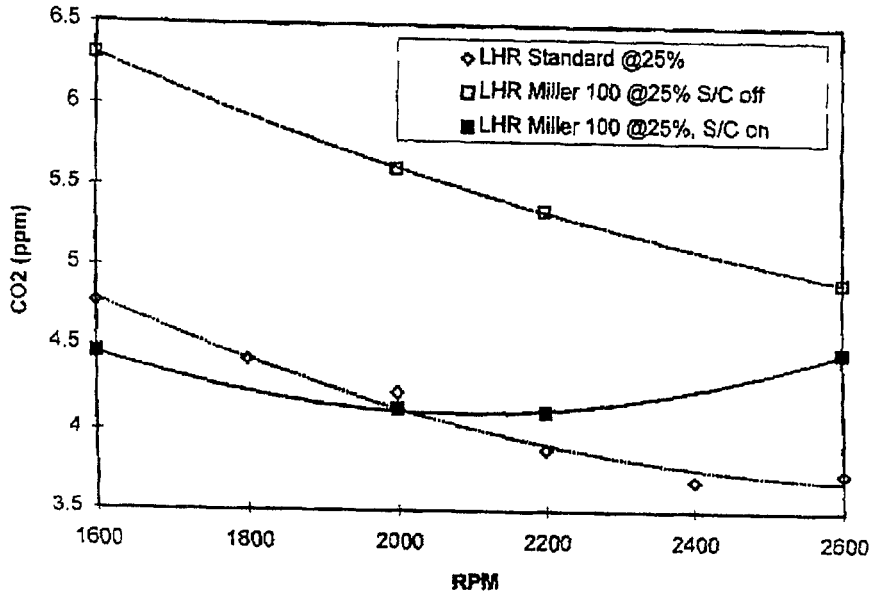


Figure 17. Comparison of CO2 Emission Between LHR Standard and LHR Miller 100 Engines at 25% Torque

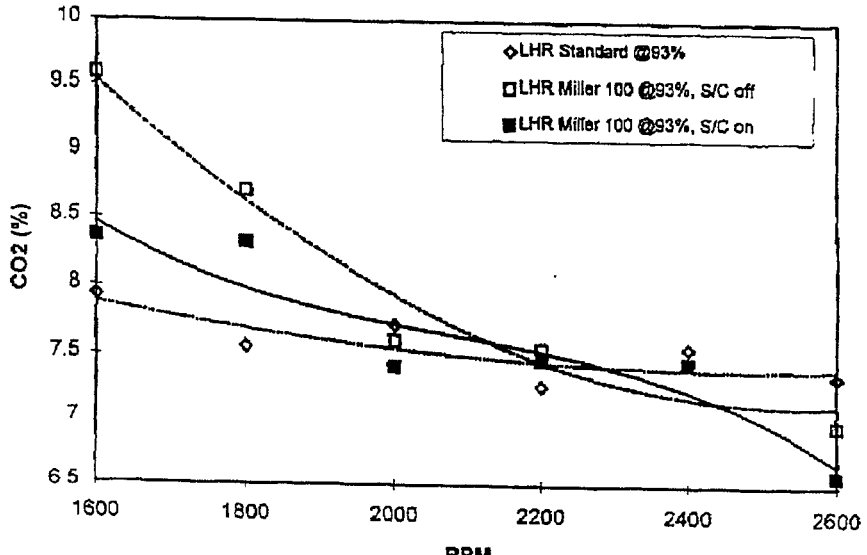


Figure 18. Comparison of CO2 Emission Between LHR Standard and LHR Miller 100 Engines at 93% Torque

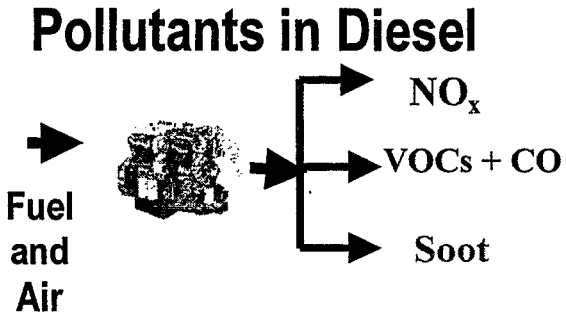
INDIRECT MICROWAVE TREATMENT OF DIESEL EXHAUST GASES FOR NO_x CONTROL

C.Y. Cha and C. Carlisle
CHA Corporation

INTRODUCTION

As shown in Figure 1, diesel exhaust gases contain a number of combustion products that have attracted considerable attention during the past couple of decades. Soot and VOCs, generated by all diesel engines, have been linked to cancer and lung disease in humans[1]. Equally NO_x, emissions contribute to smog formation and acid-rain[2].

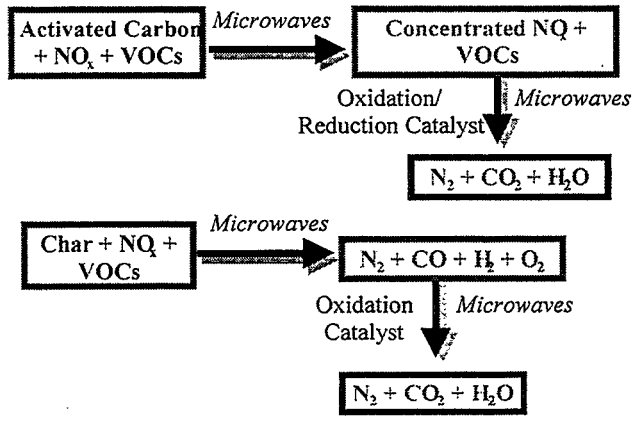
Figure 1



The CHA Corporation has been employing 2450 MHz microwave energy to drive various chemical reactions for several years[3,4]. We have found that NO_x and VOCs can be adsorbed by carbon and subsequently decomposed via chemical reduction by introd-ucing microwaves. Reaction temperatures are surprisingly low starting from 200 to 300 degrees Fahrenheit. We have also looked at various ways to utilize these reactions to abate NO_x and VOCs in diesel engine exhaust gases. The following group of reactions, shown in Figure 2, depict two schemes we have investigated. In the top set of reactions, the NO_x and VOCs are adsorbed on commercial activated carbon and the carbon is regenerated with microwave energy. In the second scheme the NO_x and VOCs are adsorbed on a less expensive carbon adsorbent labeled as char.

Figure 2

Interaction of Microwaves and Pollutants Adsorbed on Carbon



With the activated carbon scheme, the adsorbed pollutants are when microwave energy is introduced. The concentrated stream of NO_x and VOCs leaving the carbon is passed through an oxidation/re-duction catalyst bed where the pollutants are converted to harm-less gases. In the char scheme, a quite different sequence of reactions occur. In the presence of microwave energy, the adsorbed NO_x is reduced by the char to nitrogen and carbon monoxide. The VOCs are also reduced to hydrogen and carbon monoxide. Which gases are subsequently oxidized to carbon dioxide and water in an oxidation catalyst bed or monolith.

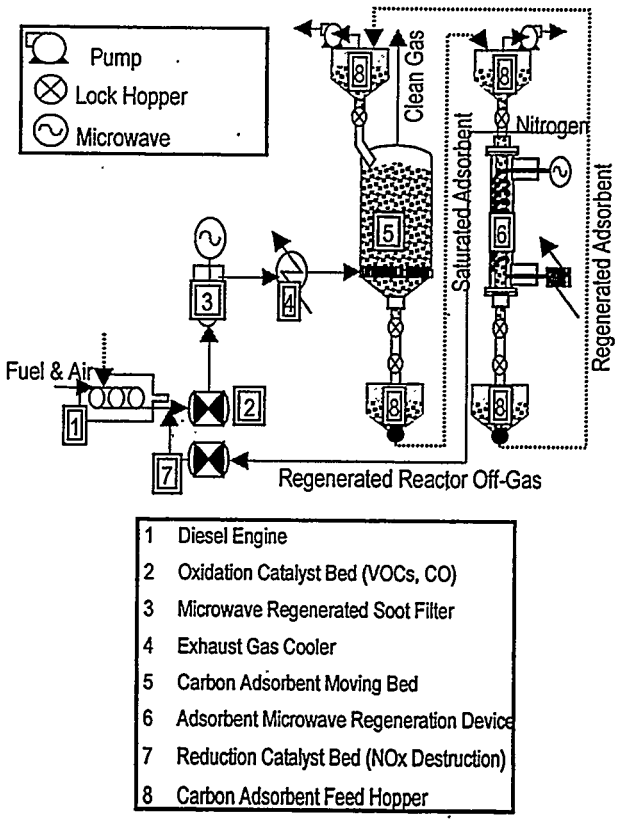
The process flow diagram for both schemes is shown in Figure 3.

Raw diesel exhaust gas is passed through a soot filter (3), heat exchanger (4), and carbon contactor (5), before release to the atmosphere. Activated carbon or char is an excellent adsorber for NO_x and VOCs. A NO_x capacity as high as 5.5% by weight can be achieved at gas temperatures below 175 degrees F. The NO_x adsorption capacity dominates saturation time since VOC concentrations are in the range of 150 to 400 ppm and NO_x concentrations are in the range of 500 to 2000 ppm. The carbon's adsorption ability is temperature dependent. No NO_x adsorption occurs above 300 degrees F and significant NO_x adsorption is not seen until the gas is cooled below 200 degrees F. Equally, the dew point of diesel exhaust is about 125 degrees F. This places the operating temperature range at 125 to 200 degrees F. Figure 4 shows NO_x breakthrough time as a func-tion of temperature for activated carbon. Since the gas leaving the exhaust manifold is about 1,000 degrees F., the gas must be cooled before NO_x can be removed via carbon adsorption. The air cooled heat exchanger (4), which has small passages to accommodate good heat removal performance, is vulnerable to soot plugging. The purpose of the soot filter (3) is to prevent plugging in the heat exchanger.

In the contactor (5) a 1.5 to 2 second residence time is needed to remove all of the NO_x from the exhaust gas. The speed of this NO_x removal step is dependent on a reaction that occurs in the carbon bed. The NO_x leaving the diesel engine is comprised primarily of NO, nitric oxide. Nitric oxide will not adsorb onto carbon in the process operating temperature range. However, in the presence of oxygen and carbon, nitric oxide converts to NO_2, nitrogen dioxide. Nitrogen dioxide is readily adsorbed by carbon. The long residence time is needed to facilitate the conversion of NO to NO_2. Interestingly, when activated carbon desorbs NO_x, the desorbed species is primarily NO.

Figure 3

CHA Corporation Diesel Exhaust Treatment Process Flow Diagram

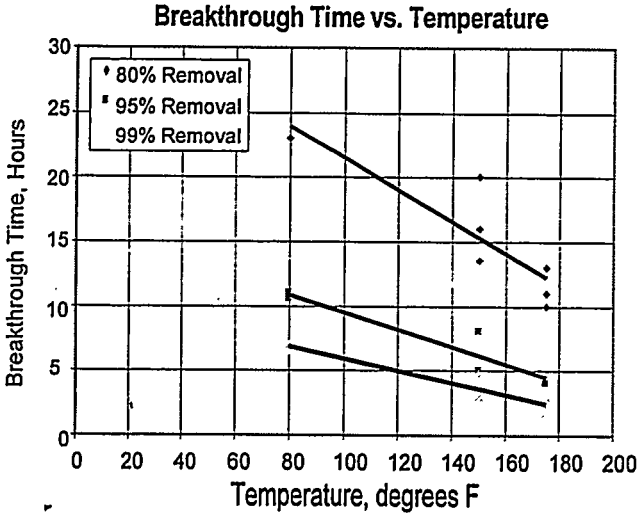


A moving bed contactor has been incorporated into the process to avoid NO_x breakthrough. Carbon is gravity fed through the bed and periodically lifted to the reactor feed hopper through a pneumatic lift system. In a similar fashion, spent carbon is gravity fed through the microwave reactor and pneumatically conveyed to the contactor feed hopper.

To size the prototype contactor and microwave regeneration reactor, we conducted a number of moving bed experiments using a 4.75 inch round contactor.

Diesel exhaust gas was passed through various carbon bed heights at various carbon feed rates and NO_x removal efficiency was determined for each configuration. Figure 5 shows a series of experimental results from this.

Figure 4

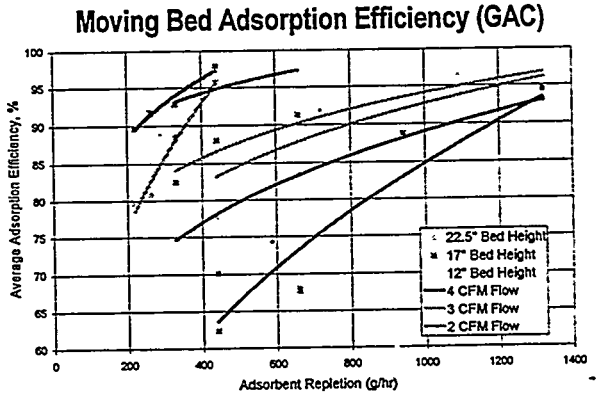


The contactor can be small in size and the carbon moved through at a high feed rate, or the contactor can be larger in size with a smaller carbon throughput rate. To continuously remove more than 90% of NO_x from a 100 SCFM gas stream carrying 1000 ppm NO_x, a square shaped contactor 30 inches in diameter is needed. A 22 inch tall carbon bed is needed to facilitate the NO to NO2 conversion and NO2 adsorption. Shorter beds (lower gas residence times) can be used if lower NO_x removal efficiency can be tolerated. For this size contactor, an activated carbon throughput of 15 pounds per hour is needed.

The microwave regeneration reactor was designed to match the 15 pounds of carbon per hour throughput of the contactor. Microwaves are applied through a 2.5 inch diameter 20 inch high helix wrapped around a 2.375 inch diameter quartz reactor tube at four wraps per foot. The quartz tube is held vertical in the reactor and the carbon is continuously gravity fed through the reactor tube. Microwave power level is constant at 1200 Watts. Carbon residence time in the reactor is 5.5 minutes. Nitrogen gas is purged through the reactor from top to bottom at 5 SCFH. The purge gas removes steam, desorbed pollutants and reaction products from the reactor and directs them to catalytic converter (7) in Figure 3, where desorbed pollutants are reduced. Microwave energy is 2,450 MHz. The source of the microwaves is two magnetrons identical to the ones used in a home microwave oven.

To test the process, we designed and constructed a prototype-integrated system to accommodate a 100 SCFM diesel exhaust stream. The prototype was matched to our 58 hp diesel test engine which is coupled to an alternator and load bank. This system is currently being evaluated at our laboratories and is scheduled for demonstration in March 1998.

Figure 5

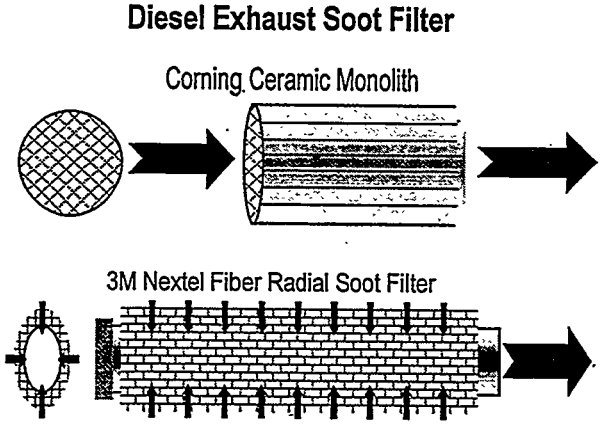


SOOT FILTER

Removing soot from the exhaust gases of a diesel has been a formidable task. Our need for a soot filter is limited to protecting the heat exchanger in the above mentioned process. As we

are interested in applying microwaves to various chemical processes, we were drawn to the idea of using microwaves to burn the soot from the surface of a filter material. Two materials were tested. One was a fiber based filter[5] manufactured by 3M and the other is a ceramic monolith[6] made by Corning, Inc. Figure 6 illustrates each of these soot filter materials. Samples of each soot filter were received from their respective manufacturers and suitable holders were prepared to pass diesel exhaust through the filter and subsequently apply microwave power to regenerate the filter.

Figure 6

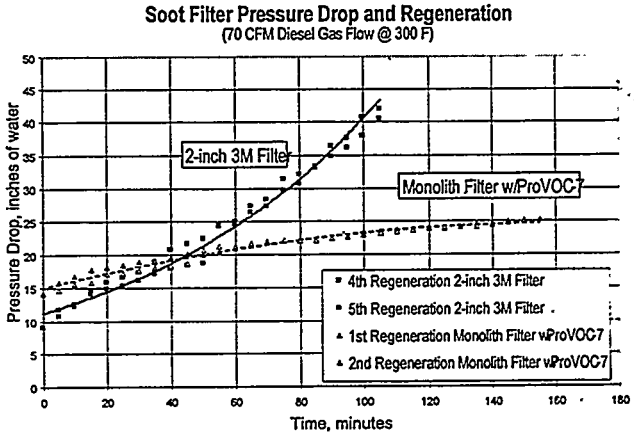


During regeneration, the filters were taken off line and a small flow of air was passed through the filter to supply oxygen. Microwave power levels used to regenerate the filters were in the range of 500 to 1500 Watts. Figure 7 shows the pressure buildup across each of these filters as a function of time. Two microwave regenerations are shown for each filter. Each ma-terial was successfully regenerated using microwaves. However, the filter material loaded with soot after two hours to a point where regeneration was needed. We are currently scaling up the size of these filters to increase the time between regenerations.

SUMMARY AND CONCLUSIONS

Diesel exhaust gases can be cleaned free of NO_x and VOCs by using activated carbon or char

Figure 7



that adsorb the pollutants. The carbon's ability to adsorb pollutants has been understood for some time. This work offers a method for regenerating the carbon adsorbent in a device operating in parallel to the absorber. The use of microwaves to desorb or destroy NO_x and VOCs on the surface of the carbon adsorbent is intriguing. The reaction proceeds quickly and reactor temperatures are low throughout carbon regeneration. Once tested and furhther developed, this process shows promise as a viable option for stationary diesel applications. The soot filter work shows that microwaves can be used to regenerate soot filters used to remove soot.

ACKNOWLEDGEMENT

This work was co-funded by the California Air Resources Board under the Innovative Clean Air Technologies program, The Sacramento Municipal Utility District, McClellan Air Force Base, Gerling Applied Engineering and the CHA Corporation. The authors wish to express their appreciation to each of these groups for their support and guidance.

AIR MANAGEMENT FOR DIESEL ENGINES

D.L. Page
Consultant

INTRODUCTION

Beginning in the 1970's, diesel engine manufacturers have developed technological approaches in response to increasingly stringent air quality regulations. The characteristics and performance requirements of heavy-duty diesel engines, however, have prevented them from achieving emission levels commensurate with light-duty gasoline vehicles. Despite the fact that diesel engines provide significant advantages in fuel efficiency, reliability and durability, control of PM and NO_x emissions have presented a conoid-enable challenge.

An advanced engine air enhancement device has been designed to meet these stringent egis-Zion standards while indicating performance increases not normally associated with emission reduction technologies. The technology improves air management within the internal combustion engine, which results in increased combustion efficiency and the resultant improvemeats in emissions, fuel economy and engine performance. The component, named the Electronic Demand Charger or TDC (trademark "Turbofan™"), is applicable to both naturally aspirated gasoline engines as well as diesel en-gins. The TDC works on the principle of adding air to the combustion chamber in order to im-prove the air/fuel ratio during combustion processes. This paper will focus on testing conducted with the TDC on heavy-duty diesel engine applications at Southwest Research Institute in San Antonio, Texas as well as tests conducted at Original Engine Manufacturer (OEM) transient test facilities. Test results indicate significant improvements that meet or exceed fuel management techniques designed to improve combustion efficiency, fuel economy, engine performance and emission reductions.

TRADITIONAL APPROACHES

Emission reduction approaches such as retarding injection timing have traditionally increased fuel consumption. Charge-air cooling, turbocharging and improved fuel injection seek to offset this penalty. Uncontrolled emissions of NO_x from heavy duty diesels range from 12 to 21 grams per kilowatt-hour (9 to 16 grams per brake horsepower hour) when measured using U.S. transient test cycles. PM emissions typically range from 1 to 5 g/kWh (0.75 - 3.7 g/bhp-hr). Engines that are tampered with or have been poorly maintained often emit higher PM emissions in the form of black smoke.

Moderate control of NO_x (8 g/kWhr or 6 g/bhphr) and PM (0.7 g/kWhr or 0.5 g/bhphr) requires further optimization of the overall combustion system. While traditional approaches such as variable fuel injection timing, high pressure fuel injection and charge air cooling are suitable approaches, it is combustion optimization that will correspond to U.S. Federal emission standards for PM and NO_x. This is particularly true for PM, with tighter U.S. standards (0.13 g/kwh or 0.10 g/bhphr) effective in 1994. Despite the requirement not to further limit PM in light of the NO_x requirements, in March of 1993 the EPA (Environmental Protection Agency) published a ruling reducing PM to 0.05 g/bhphr. In 1995 the EPA, California Air Resources Board (CARB) and automotive engine industry signed a Statement of Principles outlining their joint understanding of the actions required to meet a 2 g/bhphr NO_x limit by year 2004. This standard is expected to tighten once again upon further technological developments. In the U.S., urban buses are currently required to meet a 0.1 g/bhphr (0.13 g/kwh) PM standard under certification standards set by the EPA.

COMBUSTION AND EMISSIONS

Controlling NO_x and particulate emissions have proven a particularly difficult challenge for diesel engine manufacturers throughout the years. This is due to the effect of NO_x control approaches having the tendency to increase particulates, as well as particulate reduction technologies having an adverse effect on NO_x. This PM/NO_x tradeoff remains the subject of much research and debate.

Particulate matter, or black smoke, is the most visible pollutant attributable to diesels. These emissions are the combination of three phases: solids, liquids, and gases. The combination of solids and liquids comprise the Total Particulate Matter (TPM) or Particulate Matter (PM). PM is composed of dry carbon (soot), inorganic oxides (primarily as sulfates), and liquids. The liquids are composed of unburned fuel and lubricating oils, termed the soluble organic fractions (SOF) or volatile organic fractions (VOF). When diesel fuel is burned, a portion of the sulphur is oxidized to sulphate, which, when reacting with moisture in the exhaust, becomes H_2SO_4. The gas phase is composed of gaseous hydrocarbons, carbon monoxide, oxides of nitrogen, and sulfur dioxide. The dry soot comprises the insoluble fraction of the engine-out emissions.

The popularity of diesels is a result of their fuel efficiency relative to the gasoline engine. Diesels operate very lean with air-to-fuel ratios greater than approximately 22.

For an air-fuel mixture, stoichiometric conditions are often referred to as 100 percent theoretical air. Since actual oxidation reactions are incomplete, many combustion systems operate on excess air. For example, 150 percent theoretical air is equivalent to 50 percent excess air. A lean mixture ($\lambda>1$) contains more air; a rich mixture ($\lambda<1$) less air. The A/F ratio decisively affects the engine's operating characteristics. However, an insufficient quantity of excess air results in increased emissions of particulate matter, carbon monoxide, and hydrocarbons, as well as an increase in brake specific fuel consumption. Diesels generally produce good fuel economy and have an engine life approximately ten times that of a gasoline engine. For these reasons, much effort is placed on achieving PM/NO_x reductions.

The retrofitting of diesel engines with oxidation catalysts has been the most common approach to reducing the soluble fraction of diesel particulate emissions. The general idea surrounding diesel oxidation catalysts was for the catalyst to oxidize the SOF without oxidizing the SO_2 to sulphate. To function, the dry soot had to be further reduced to eliminate plugging of the system. The engine design parameters that had to be modified to allow for a reduction in the dry soot resulted in an increase in the SOF, which could then be oxidized by the catalyst. Catalysts containing precious metals such as Pt and Pd were the best candidates as they exhibited low-temperature activity for hydrocarbon conversions. Different catalysts provide different reductions for different engines. Some diesel engines exhibit a SOF fraction of 30 percent, whereas others are as high as 40 percent. It is necessary to further reduce the insoluble fraction to achieve the maximum benefit of the catalyst.

The Electronic Demand Charger, described more fully below, offers the opportunity to significantly reduce the insoluble fraction of the particulate matter formation. A brief understanding of the correlation between the A/F ratio and emissions formation is necessary in order to understand this effect. NO_x formation in diesels occurs due to a complex relationship of gas temperatures and non-uniform fuel distribution. The critical formation period exists when unburned gas temperatures are at a maximum between the start of combustion and just after peak cylinder pressure. Local NO_x concentrations rise to a maximum at $\lambda = 1$ and decrease as the mixture becomes leaner since formation becomes much slower as dilution occurs.

Particulate emissions (PM) are the solid and liquid particles resulting from the incomplete combastion of the fuel, wear particles, and dirt that escape the air filters and become airborne with the gaseous emission. Smoke consists primarily of visible particulate matter (the insoluble fraction) Most particulate material results from incomplete combustion of fuel hydrocarbons. The composition of the particulate material depends on the conditions in the engine exhaust and the

existing reduction technology. The TDC addresses overall emission formation by increasing the A/F ratio at low-end operating conditions in order to decrease emissions of HC, CO, and PM. The system introduces additional air to the engine manifold via a simple valving mechanism. This additional air not only leans the A/F ratio, but provides additional boost to the engine, which also improves engine performance by eliminating turbolag.

THE ELECTRONIC DEMAND CHARGER

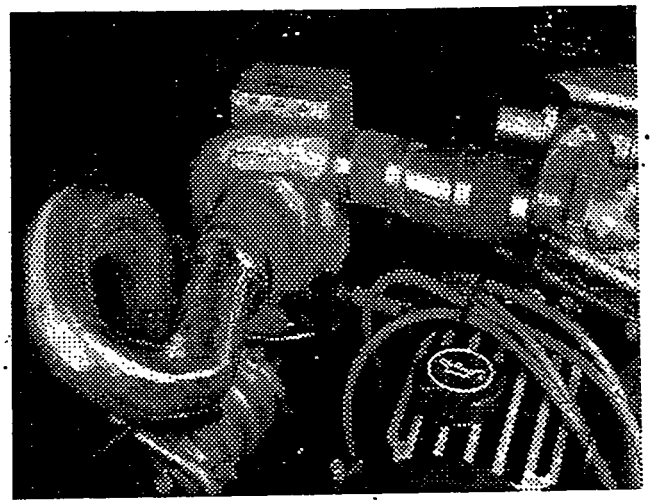
The application of a motor-assisted device, such as the electronically actuated TDC, provides a means of supplying air to the engine cylinder at low idle or low loads in preparation for the next acceleration of the engine before an increased amount of fuel is injected. When used in series with a standard turbocharger, the TDC supplies boost pressure to the engine until there is enough energy in the engine exhaust to accelerate the turbocharger. When the turbocharger is capable of supplying sufficient air, the unit is de-energized, thus eliminating the power drain from the vehicle batteries.

In diesel applications, the TDC is an inlet air compressor installed independently of the turbocharger between the air intake and the engine manifold. The system is comprised of a compressor housing, compressor wheel, a brushless electric motor, a motor controller, an engine interface controller, and simple valving mechanism (See Figure 1). This system can be installed on both gasoline and diesel applications. On turbocharged diesels it is installed in series with the turbocharger. In this instance, the assembly is comprised of a compressor assembly, a motor controller in a separate housing, a 5 inch (12.7 cm) diameter check valve, associated intake tubing and connecting sleeves, a manifold pressure shutoff switch, a throttle switch and bracket, a throttle switch actuation arm, and a wiring harness.

For the diesel, combustion processes inside the engine cylinder dictate engine power, efficiency and emissions. Following compression, burning proceeds as air and fuel mix to the composition necessary for combustion to take place. In the diesel engine, fuel is injected in the cylinder into high pressure and temperature air. The engine has less time to form the air-fuel mixture, which is less homogenous as a result. This creates periods during the combustion phase where the air to fuel relationship is non-optimized. This is particularly apparent during lowend operating cycles. Traditionally, efforts to reduce engine-out emissions have concentrated on fuel management. The TDC focuses instead on air management with the optimization of this relationship of air to fuel. In turbocharged diesel engines, the turbocharger provides the engine with more air than it can induce through natural aspiration. This increased air supply allows more fuel to be burned, thereby increasing power and torque obtainable from a given displacement engine.

In turbocharged engines, there is very little energy in the engine exhaust and this prevents the turbocharger from providing a significant level of boost in the engine intake air system. When the throttle is opened to accelerate the engine, there is a time lag before the exhaust energy level rises sufficiently to activate the turbocharger rotor. This time lag is traditionally termed "turbolag" and, over the years turbochargers have been made smaller and lighter in order to minimize this lag period.

The TDC can be installed on both turbocharged and non-turbocharged vehicles. In non-turbocharged vehicles it is installed between the air intake system and the engine manifold. In this application, the TDC provides benefits similar to retrofitting a turbocharger on the vehicle.



TDC INSTALLATION ON NONTURBOCHARGED ENGINE

A standard passenger car (1.9L) will realize a thirty to forty percent increase in low-speed torque in addition to fuel economy benefits and reduced pollutants. For the purposes of this paper, however, these benefits will not be quantified and the focus will remain on turbocharged heavy duty diesel applications.

On diesel, turbocharged vehicles, the compressor and check valve are configured in parallel, and together they feed in series with the existing turbocharger inlet. The check valve is oriented so that intake air will be drawn through the valve and the TDC during periods of high intake air demand. During periods of low intake air flow, the check valve will close and the TDC will pressurize the turbo inlet. All components are designed to mount directly onto the engine, whereas the controller should be mounted on the vehicle body or chassis in a clean environment where temperatures will not exceed 150° F (65.5° C). For heavy duty diesel applications, the unit requires a 24V DC power supply capable of 250 amps for 1 second and 150 amps at a 50 percent duty cycle. The three sensor switches are connected in series and control the engagement and disengagement of the TDC.

The unit utilizes a high speed boughless electric motor and an electronic controller for the purpose of electronically commutating the D.C. electric power into a three-phase power supply and a feedback circuit. The motor is activated by remote sensors that monitor the demand for power and boost. Using remote sensors, the EDC interface controller constantly monitors engine parameters such as throttle position and boost pressure. In configurations which utilize a pre-existing electronic engine controller, the unit can be integrated into the existing controller system. The interface controller then activates the EDC during predefined engine operating modes indicated by the sensors. The electronic control module can also interface with engine management systems in similarly equipped vehicles.

ENGINE PERFORMANCE AND EMISSIONS

A number of bench, steady state, and transient dynamometer tests were performed on the EDC under a variety of conditions. The following represents results achieved on various engines under varying operating conditions.

BENCH TESTING

The EDC compressor must accelerate rapidly to effectively reduce turbolag and PM. This acceleration is accomplished by means of a brushless permanent magnet motor which produces high torque, accelerating the compressor shaft to over 100,000 revolutions per second. To further reduce the time lag, the compressor "idles" at 10,000 rpm, waiting for the command to accelerate to 40,000 rpm. To verify the rapid pressure rise, the compressor discharge pressure was monitored on a digital oscilloscope. The results indicated that the compressor was able to produce 80 percent of its final pressure in 250 milliseconds, corresponding to 2.5 engine revolutions at a 600 rpm engine idle speed.

ENGINE PERFORMANCE RESULTS

An EDC was installed on a 225 kW turbocharged diesel engine to evaluate its effect on engine performance. The installation was discharging directly into the inlet of the turbocharger. A bypass check valve was used to prevent excessive inlet restriction at high engine speeds. BMEP improves up to 40 percent at low engine speeds. At 13 engine rpm and above, with the bypass valve opened, no improvement was indicated. The BMEP improvement is the result of additional airflow and a corresponding increase in fuel flow. Manifold Pressure Comparison indicates the intake manifold pressure for both baseline and EDC equipped engines. A portion of the increase in manifold pressure is a result of compounding the output of the EDC compressor and the turbocharger compressor. The additional pressure increase is the result of higher exhaust energy, thereby increasing turbocharger speed.

The EDC also improved brake specific fuel consumption by approximately 5 percent. The fuel consumption improvement can be accounted for by the increase in indicated torque, while the friction remains relatively constant, thus increasing the mechanical efficiency.

The low speed torque improvement is important

to many truck and bus applications, permitting lower clutch engagement speeds, lower stall speed torque converters, and better throttle response. Future research will be conducted to evaluate the effect of the EDC as a cold start aid. The EDC increases inlet air temperature by 15° C due to compression heating. The effective compression ratio also increases by 20 percent. The cranking compression ratio of a nominal 17:1 compression ratio engine would increase to 20:1, thereby promoting faster startup. The increase in effective cranking compression ratio also allows a lower mechanical compression ratio and a means to lower NO_x emissions.

EFFECT ON EMISSIONS

An EDC was installed on a 206 kW Detroit Diesel 6V92TA engine with mechanical unit injectors. The engine was installed on an engine dynamometer at Southwest Research Institute and the engine was tested for emissions using the EPA Heavy Duty Engine Transient Test Procedure. No adjustments to the fuel control governor or injector timing were made.

The reduction in PM was a direct result of the enhanced air supply to the engine during low speed accelerations. It was notable that there was no increase in No_x. This is particularly relevant in light of the previous discussion on the PM/NO_x tradeoff inherent in many emission reduction strategies aimed at heavy duty diesel engines. Additional research is currently underway to further enhance this possible simultaneous reduction in PM and NO_x while utilizing the EDC in a "dual use" format.

The EDC provided 20 KPa intake manifold pressure within 0.25 seconds after the throttle moved from idle position. Without the EDC, the turbocharger required 2-3 seconds to provide the same boost level. The EDC was programmed to run at high speed for 8 seconds after the throttle was moved from idle position. This was sufficiently long for the engine exhaust driven turbocharger to spool up to provide the remainder of the air requirement.

POWER CONSUMPTION

The battery voltage and current were monitored during the FTP transient testing to determine the power and energy requirements of the EDC. It was determined that the EDC consumed 13.8 Amp hrs of battery energy at 24 volts during the 20 minute test. The energy consumption was 330 watt-hrs. The total energy requirement from the engine during the FTP was 14.8 kW-hr, thus the energy required to drive the EDC was 2.2 percent of the total engine power. If the vehicle alternator efficiency is assumed to be 60 percent, this would be the equivalent of 1.6 kW average mechanical power. Reducing the high speed time period from 8 seconds to 5 seconds will have a corresponding reduction on the EDC power consumption.

CONCLUSIONS

Enhancing the air supply to diesel engines has proven to result in significant improvements in engine low speed torque, efficiency, and exhaust emissions. An EDC has demonstrated that this improvement can be made in a device retrofitted to existing engine configurations and is an effective alternative to traditional approaches that are associated with decreased engine performance, turbolag, fuel penalties and PM/NO_x tradeoffs.

There is a definitive need for improved emission control systems in the diesel industry. The ability to improve the air/fuel ratio and subsequent emissions formation emphasizes the need for combustion optimization during certain operating conditions. This is especially true of low-end, fuel rich mixture conditions on turbocharged diesel engines. As combustion processes dictate engine power and efficiency, they also directly influence emission formation. Development and testing of the EDC/"Turbopac™" has resulted in a system that generates significant additional air and is capable of optimizing this air to fuel relationship under low-end operating conditions, thus enhancing combustion efficiency and engine operation.

The impact of enhanced air supply will also ultimately result in smaller engines, reduced vehicle weight, improved fuel economy and lower operating expenses. Future research and development are moving forward on these efforts.

ACKNOWLEDGEMENTS

Grateful thanks are extended to Magdi Khair, Chris Sharp, and the scientists and staff at Southwest Research Institute for their invaluable expertise.

REFERENCES

1. Page, D. L., "Optimization of the Air/Fuel Ratio for Improved Engine Performance and Reduced Emissions", SAE Technical Paper Series 961714, Future Transportation Technology Conference, August, 1995.

2. Heywood, J. B., Internal Combustion Engine Fundamentals, McGraw-Hill, Inc., New York, New York, 1988.

3. Keating, E.L., Applied Combustion, Marcel Dekker, Inc., New York, New York, 1993.

4. Khair, M. K., "Progress in Diesel Engine Emission Control", 92-ICE-14 ASME, New York, New York, 1992.

5. Bosch GmbH, Automotive Handbook, 3rd Edition, Robert Bentley Publishers, Cambridge, Massachusetts, 1993.

6. Heck, R.M., Farrauto, Robert J.. "Catalytic Air Pollution Control"Von Nostrand Reinhold, 1995.

SESSION VIA

Fuels and Associated Technology

Chairman: Bob Beyerlein
DOE/Texas A&M University

A REVIEW OF CURRENT FUELS, FUEL CHEMISTRY, AND FUEL TRENDS

J.M. Perez, J.L. Duda, and H.H. Schobert
The Pennsylvania State University

INTRODUCTION

Current light duty and heavy duty engine fuels include a wide range of alternative, petroleum and synthesized fuels. Current trends in research on fuels include biodiesel, catalytically reformed fuels, alcohol and synthesized fuel supplements. Major factors affecting the fuel trends include the supply and demand for petroleum, environmental concerns, government regulations, consumer satisfaction and economics. Regulations around the world are established that tighten emissions regulations and impact global fuel compositions. In addition, growing global environmental concerns have lead to demands for more environmentally friendly hydraulic fluids and other lubricants. Minimizing the environmental impact of fuels and lubricants continues to be a challenge for OEM's, additive, and lubricant manufacturers.

Current research on fuels includes a variety of synthetic fuels derived from petroleum by-products, natural gas, coal, and natural resources. Studies have shown that the use of alternative fuels also requires consideration of the lubricants and tribology of the engine. Studies have shown that methanol, ethanol, and M-85 can cause lubricant related problems. Deterioration of lubricant additive packages exposed to the fuels reduces the performance properties of the lubricant. Removal of sulfur from diesel fuels resulted in engine problems related to the tribology of the system components and changes in the physical characteristics of the fuel. The separation of additive packages can be fuel selective and corrected through formulation changes in the lubricants.

This review will consider some of the types of fuels, their origin or processing, some advantages and disadvantages of the fuels. The current availability and the future trends related to fuels, lubricants, and environ-mental issues will be discussed. The types of fuels and their origin will be reviewed. Then, the processing and chemistry of the fuels will be briefly discussed and the trends and the possible scenarios affecting the trends will be summarized.

TYPES OF FUELS. A list of today's fuels and the primary source of the fuels are found on Figure 1.

PETROLEUM:	NATURAL GAS:
GASOLINE	METHANE
DIESEL FUEL	LPG
AVIATION FUELS	MeOH
COAL:	**AGRICULTURE:**
METHANE	MeOH (WOOD)
GASOLINE (SASOL)	EtOH (CORN)
METHANOL (MeOH)	BIODIESEL

SHALEOIL&TAR SANDS: OIL PRODUCTS

FIG.1 - FUELS AND SOURCES

The major sources of the current fuels are fossil fuels made from petroleum and coal. Trends on energy consumption and sector usage are well documented in the literature [1-3] and will not be covered in detail. However, the industrialized world is now consuming over 130 Quads of oil per year, about half of the total amount of crude produced. The developing countries consumed only about 20% of the total but their consumption has increased by a factor of 4 over the past thirty years. At this rate of consumption our finite supply of oil may last another 50 years.

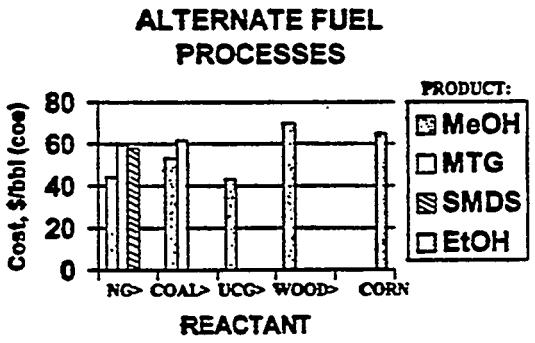


FIG. 2 - CRUDE OIL EQUIVALENT $

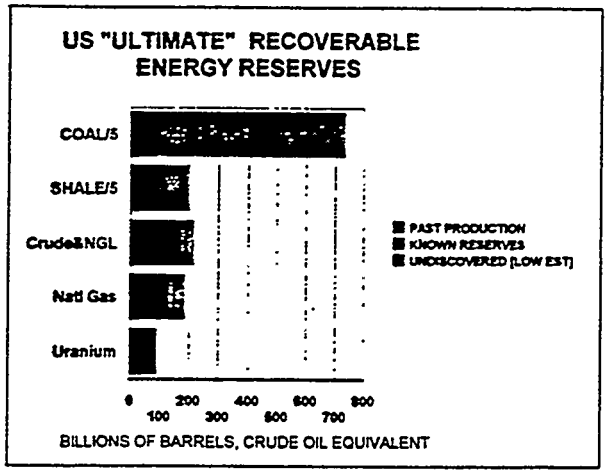


FIG.3 - U.S. OIL RESERVES (1980)

In 1992, the U.S. used about 17 million bbl/day [2]. The amount of petroleum used by various sectors in the US in 1992 ranges from over 60% for the transportation sector to about 3% for the electric utilities. Residential use was 7.6 % and industrial use was 27.9%. Comparing all energy sources, transportation used some 40% compared to 25% for industry. In comparison, Japan uses 50% for industry and a little over 20% for transportation. Considering third world countries, India uses about 55 % for industry and about 25% for transportation. In China about 65% of all energy consumed is used for industry and less than 5% is used for transportation.

There is also a discrepancy in how efficiently we use energy. China is one of the least efficient users of energy because of its dependence on coal and relatively ineffective technology. However, China's energy efficiency is improving rapidly. China has also started to exploit some of its large petroleum re-serves in the South China Sea as well as on the mainland. An interesting comparison is that of energy intensity or the amount of energy it takes different countries to produce US$1 of gross domestic product (GDP). UN researchers found the Japanese industry used only 5 megajoules to produce US$1 of GDP while the US required 12 megajoules. China used 66, India used 33, and Mexico 23 megajoules.

In 1992, the U.S. consumed more than one-quarter of the world's petroleum consumption [2]. Imports accounted for 46.1% of this use. Yet the cost of gasoline in the U.S. remains lower than it was in 1989. The current cost of a barrel of crude oil is around $17 dollars per barrel (1990 Dollars), a drop of $3 from 1990.

This makes the economics for most of the alternative fuels unacceptable and unlikely to make significant gains, unless other factors are involved. The price per barrel of crude needs to be over $40 per barrel for most alternative fuels to be competitive, Figure 2. In 1981, cost predictions were as high as $80/bbl by the year 1985 [4]. This was based on the oil crisis crude prices. The cost of crude increased from $3/bbl to $32/bbl from 1973 to 1980.

ORIGINS OF THE BIG THREE

When considering energy sources, petroleum, natural gas, and coal are the big three energy sources. The 1980 U.S. estimate of the reserves for these energy sources are shown on Figure 3. Two obvious observations are that there are considerably more coal and shale reserves in the world than any other source, billions of crude equivalent barrels and the amount remaining is less than the reserves remaining. Natural gas and petroleum are about equivalent. We have continued to find new sources of petroleum and the 25 year estimate in 1980 is now 25 to 50 years.

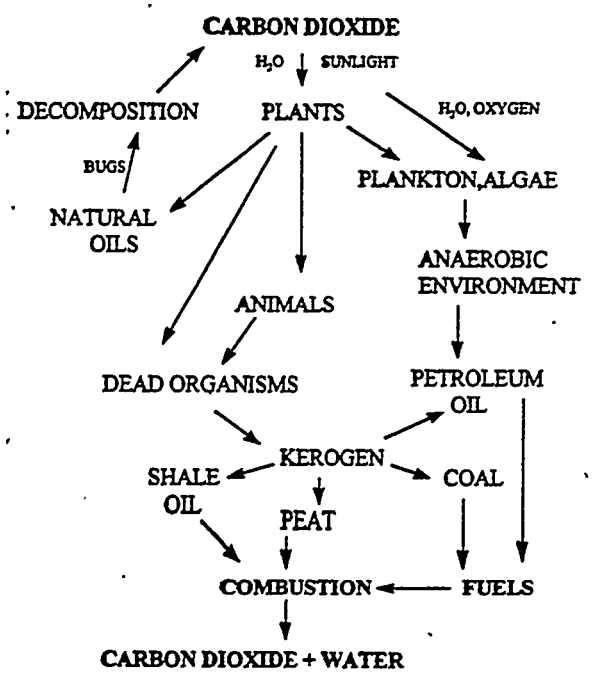


FIG. 4 - ORIGINS OF PETROLEUM

The link between these fossil fuels is carbon. The origin of petroleum is graphically shown on Figure 4. Sea plants and animals were processed by nature in an anaerobic environment for billions of years. The same car-bon cycle resulted in the formation of all carbon containing energy sources.

The first part of this process is called diagenesis and leads to the formation of Kerogen. The diagenesis process is documented in detail in reference [5].

Kerogen is the precursor to a number of fuel products through a process called categenesis. The chemical reactions are driven by temperature and pressure conditions inside the earth In the final step in the cycle. these fuels are combusted and return CO_2 and water to the earth's atmosphere. The type of product formed from Kerogen by the categenesis process depends on whether the hydrogen content is increased or decreased under anaerobic conditions. The process has been going on since time began and is a continuous process.

Depending on the time period, the crude composition differs: California Crudes are relatively new crudes formed during the Cenozoic Era some 60 million years ago. Arkansas, Oklahoma, and Texas crudes were formed some 150 million years ago in the Mesozoic Era, and the oldest crudes, the Pennsylvania and Appalachian, were formed 420 million years ago during the Paleozoic Era. The beginning of the Geological Age was 650 million years ago, the Poterozoic Era Formation of crudes was definitely a slow chemical process. The crudes as a result have different compositions.

This is part of the overall fuel problem since all crudes do not yield the same distribution of straight run products. The Pennsylvania crudes are paraffinic, low in sulfur, produce good quality lubricant distillates but low quality gasoline (RON 49-59). The California crudes tend to be aromatic, high in sulfur, produce little lube stock, but yield a good quality of gasoline (RON 66-73). The refineries take the crudes and optimize the process to produce the desired fuel products, Figure 5.

DIESEL FUEL

During a crisis, the economics dictate the product produced. The approximate fuel distillation ranges are shown on Figure 6. The distillation ranges of gasoline, jet fuel, kerosene, and diesel fuel fractions overlap significantly. During the past oil crisis, the gasoline and jet fuel yields were optimized, resulting in less and lower quality diesel fuels. The European problem was not as severe. They have a higher percentage of vehicle dieselization and their diesel final distillate covers a wider boiling range. This tends to yield better quality (higher octane number) diesel fuel.

More recently, environmental concerns have resulted in low sulfur diesel fuel. The low sulfur fuel results in improved engine emission levels that affect air quality. Initial use of the fuel was not without problems. Engine wear and filter problems, especially at low ambient temperatures occurred. These have been resolved but the low sulfur diesel fuel is a good

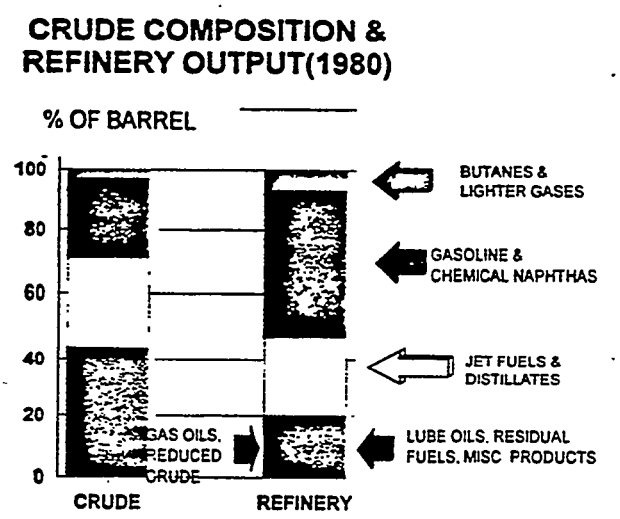


FIG. 5 - CRUDE OPTIMIZATION.

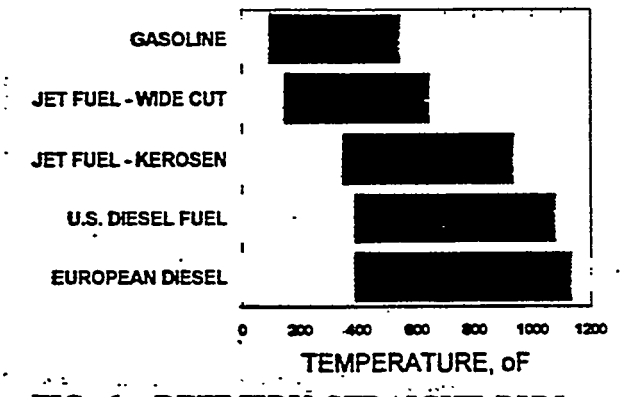


FIG. 6 - REFINERY STRAIGHT RUN DISTILLATION FRACTIONS.

example of the need for adequate research prior to dictating fuel changes.

Biodiesel - a diesel fuel area aimed at reducing the dependence on imported crude and reducing emissions is biodiesel fuel. Use of vegetable oils as diesel fuels is not new. The original use in diesels involved precombustion chamber engines [6]. These engines could tolerate almost any fuel. In the 1970's, these engines were replaced by more efficient direct injection engines. Vega-table oil fuel studies in the 1970's resulted in injector and piston deposits. Methylesters of the fuels performed somewhat better but cost was a factor.

Biodiesel is used in Europe but has not been widely accepted in the U.S. By definition [7], biodiesel fuel is the monoalkyl esters of long chain fatty acids derived from renewable lipid feedstocks, such as vegetable oils and ani-mal fats, for use in diesel engines. It is registered with the EPA as a fuel and fuel ad-ditive in the U.S. The usual mixture of bio-diesel fuel contains 20% methylated vege-table oil and 80 % diesel fuel. Research is needed to optimize the use of the fuel which can impact petroleum diesel fuel use. Diesel trucks used about 15 % of the total trans-portation energy consumption in 1992.

GASOLINE

Gasoline processing has seen a number of changes over the past 40 years. The elemination of lead resulted in the need for additives to maintain the octane rating required to run automobile engines efficiently. This is done by adding oxygenates to the base fuel. The current oxygenates include alcohols and ethers, Figure 7. The net heat content for the fuels is also shown. The difference between the gross (higher) and net (lower) values is the amount of heat required to vaporize the water of combustion and would be about 5-8%.

Alcohols:	Net BTU/gal (10^3)
MeOH	56.8
EtOH	76.0
IPA	87.4
TBA	94.1
Mixed C1- C5 Alcohols	-----
Ethers :	
MTBE	93.5
TAME	100.6
ETBE	>90
Mixed Ethers	----
Gasoline(C4-C12)	100

FIG.7 - CURRENT OXYGENATES

Some fuel additives such as methanol and ethanol are also used as alternative fuels. Others such as methyl tertiary butyl ether are used strictly as additives. Ethanol is used at levels up to 10% in gasoline (gasohol). Methanol is used at volume levels up to 5% plus 2.5% cosolvents (ethanol, butanol) and corrosion inhibitor. Up to 15% MTBE is used (3.5% oxygen) as a gasoline additive.

Currently, the most commonly used gasoline additives are methanol and MTBE. MTBE is one of the more cost effective additives, made from refinery byproducts. However, some recent health effect concerns have been raised in California where MTBE levels arc accumulating in some lakes and water reservoirs.

ALTERNATE FUELS

Pros and cons of some fuels are shown on Figure 8. Other potential fuels such as tar sands, shale oil products, electricity, hydrogen, and fuel cells are not included at this time. Although considerable progress has been made on these fuels, additional technology development and incentives are re-quired to make these prime candidates. Of the fuels shown, natural gas has the best potential to displace gasoline from petroleum imports in the next 25 years, especially if you consider some of the recent fuel process advancements.

The processing and manufacturing of alternative fuels varies significantly. One of the more exciting developments is the con-version of methane to gasoline. There are two processes well developed to convert methane to gasoline. The SASOL, (Fischer -Tropsch) process and the Zeolite-Socony-Mobil (ZSM-5) process. The first has been used for years to produce gasoline from coal. The second is well developed and is under-going large scale commercialization evalua-tions in New Zealand.

A brief comparison of some of the processing required to produce fuels will further demonstrate some of the advantages and disadvantages of the alternative fuels and the variations used to reformulate gasoline.

Methanol can be made from coal, wood, or other carbonaceous materials. However, it is usually made from cheap, imported, abun-dant natural gas using a highly selective catalyst:

$$CH_4 + 0.5O_2 \rightarrow CO + H_2$$
$$CO + 2\,H_2 \rightarrow CH_3OH$$

Higher alcohols such as ethanol and butanol can also be produced if a less selective catalyst is used:

$$2\,CO + 4\,H_2 \rightarrow C_2H_5OH + H_2O$$
$$4\,CO + 8H_2 \rightarrow C_4H_9OH + 3H_2O$$

Tertiary butanol (IDA), a cosolvent for rnethanoL, is produced by an oxidation process using isobutane and propene.

Ethanol is usually produced by hydration of ethylene, a cheap refinery byproduct:

$$CH_2 = CH_2 + H_2O \rightarrow C_3H_2OH$$

This requires mixing the ethylene with steam at 60-70 atmospheres at ~300°C over a phosphoric acid catalyst supported on a substrate. It can also be made by fermentation of biomass, a process that is being exten-sively researched by USDOE [7].

MTBE, TAME, and ETBE are all widely used ethers in gasoline blending. They are produced from methanol and other refinery products such as isobutylene or isopentene. The downside on all of these from a conservation viewpoint is that they are all made from petroleum. The upside is that they all can be used to upgrade the quality of non-leaded gasoline.

RECENT CONVERSION PROCESSES AND DEVELOPMENTS

To round out the overview on alternative fuel processes, some of the newer more promising developments [7] include:

Shell Middle Distillate Synthesis

A Fischer-Tropsch catalysis process to convert

FIGURE 8

Developed Alternative Fuels

FUEL	ADVANTAGES	DISADVANTAGES
METHANOL	-Vehicles Developed. -Flexfuel Vehicles Available -Organic emissions less reactive than gasoline. -Less toxic pollutants -Less flammable - Made from Coal, Wood, Natl Gas, Corn -Abundant Natl Gas	-Range 1/2 less gasoline, - High costs. -Formaldehyde emissions, Cold start problems. -More toxic than gasoline. -Non-visible flame, explosive in closed tanks. -Greenhouse problems if made from coal, Corn supply limitations. -Probably imported
ETHANOL	-Flexfuel vehicles available -Emissions, lower reactivity -Improved engine efficiency -Domestic supply source - Enzyme prodn from wood	- Range 1/3 less gasoline, high cost - Cold start problems -Flame - safety -Limited supply form corn -Technology cost, development needed
NATURAL GAS	-No.Amer. moderate supply -Excellent emissions -Gas abundant world-wide -Modest greenhouse advantage -Can be made from coal -1mmbd gasoline displaced	-Imported -Possible higher NOx -Distribution system -Limited range (LNG = MeOH) -Greenhouse problem - coal -Vehicles, fueling needs research
REFORMULATED GASOLINE	-No infrastructure change -Engine modif. not required -Applicable to entire fleet -Economics	-Emissions benefits uncertain -Costs uncertain but significant -No greenhouse advantage -No energy security

[Source: USDOE Office of Technology Assessment, 1990]

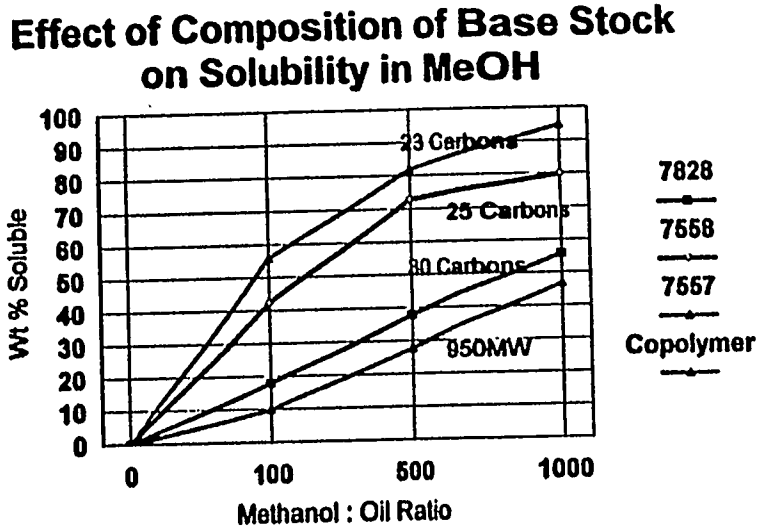
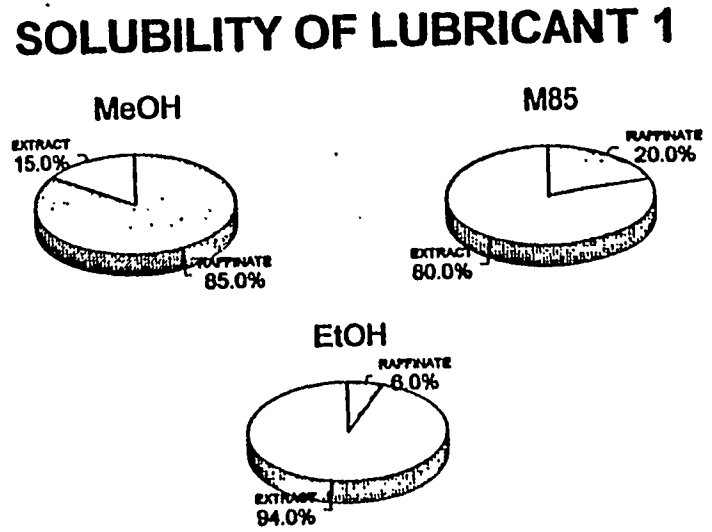


FIG. 9 - BASE STOCK EFFECT.



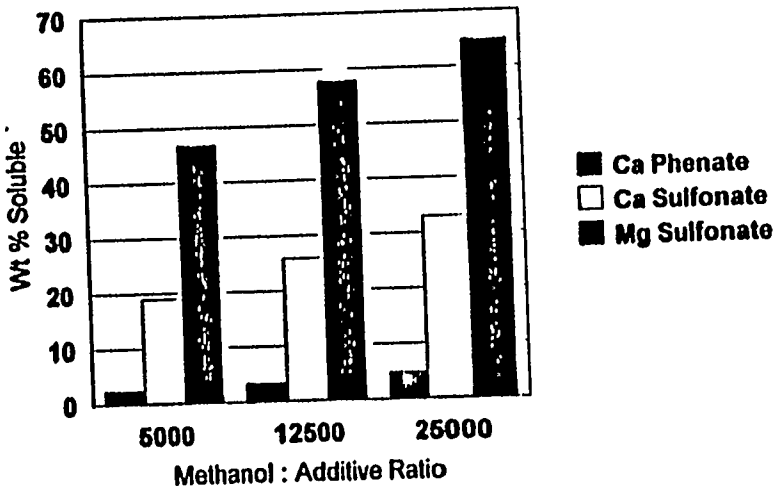


FIG. 10 - SOLUBILITIES OF DETERGENTS.

ADDITIVES EXTRACTED:

	ORIG	MeOH	M85	EtOH
Mg	1150	1100*	550*	<50*
Zn	1100	1000*	700*	0*

* ppm in Extract Phase

FIG. 11 - EFFECT OF FUEL TYPE.

Natural Gas into Transportation Fuels.

The process combines a well proven conversion process with new heterogeneous catalyst technology. The process converts Natur-al Gas into Synthesis Gas and then com-bines the hydrogen and CO in a molar ratio of 2:1. SMDS is technically proven and commercially viable. A pilot plant is opera-ting in Bintulu, Malaysia.

Dimethyl Ether (DME) from Coal

NKK Corporation, Tokyo, Japan, reportedly has developed a DME process. Production is at the stage where NKK claims DME can become a practical energy source for home use, electrical power generation, and transportation.

Synthesis of Fuel alcohols and MTBE from Syngas

Union Carbide has reported development of a catalyst system for the synthesis of near equal mixtures of methanol and isobutanol from syngas. These products are then used to synthesize MTBE, a preferred gasoline octane booster.

Liquid Phase Methanol (LPMeOH™).

Air Products and Chemicals, Inc., have a commercial scale (150,000 g/d) demonstration plant for Integrated Gasification Combined Cycle (ICGG) power generation applications. Technology yields methanol at $0.50/gallon. The process can use syngas from coal gasification process and is a once-through catalyst system

Natural Gas to Synthetic Petroleum Liquids via the Syntroleum Process

The Syntroleum Process is a proprietary method for converting natural gas into liquid hydrocarbons (GTL), reportedly competitive with current oil prices. It is a modification of the Fischer-Tropsch process and uses a autoreforming step using air to partially oxidize the natural gas.

LUBRICANTS

One last area that should be considered in researching alternate fuels is that the entire system needs to be considered. Lessons learned from the conversion of the use of methanol in both gasoline and diesel engines should be remembered. Not all lubricants and fuels are compatible. Studies at Penn State University [8,9] have shown extraction of additives occurs readily with methanol ethanol and M85. The solubility of both the base stock, Figure 9, and the additive pack-age need to be evaluated, Figure 10. In addition, the extraction of the lubricant is close-ly tied to the type of fuel, Figure 11. The lubricant must be designed to function in a system where fuel contamination can result in appreciable depletion of the functionality of the additive package.

SUMMARY AND CONCLUSIONS

FUTURE TRENDS

The major factors that can significantly affect the rate of change to alternative fuels are shown on Figure 12.

RATE OF CHANGE CAN BE AFFECTED BY:

1. **CRUDE OIL PRICES**
2. **NATIONAL SECURITY**
3. **ENVIRONMENTAL CONCERNS**
4. **VEHICLE TECHNOLOGY**
5. **ECONOMICS/PRODUCT SELECTION**

FIG. 12 - MAJOR FACTORS

They are listed in order of influence in the current climate. The price of crude is stable. As long at it stays this way there is little incentive to accelerate current production. Price supports or tax incentives for new fuels

and infrastructure are not the long term answer.

The life blood of U.S. industry is petroleum. Any. threat to national security will affect prices and result in increased reactivity. Continued efforts to establish alternative fuel strategies will soften any future crisis affecting petroleum irnports.

Environmental concerns are a constant is-sue. Controversy over the impact of diesels, alternate fuels, and reformulated gasoline continue. Health effects of diesels are still unresolved and are not without controversy. Foreign dieselization is significantly ahead of the U.S. and a positive approach to energy conservation. Coal processed fuels are very high in aromatic compounds. This improves the octane rating of the products which is significantly undesirable if looked at from a health effects issue. The impact of the alternate fuels on air quality are positive but not without problems. The aldehydes produced by alcohol fuels on cold startup or in poorly maintained catalysts are still issues to be resolved.

New engine technology including electric, hydrogen and fuel cell vehicles has made some progress but is not readily available technology. The improvements in the combustion efficiency of current SI and CI engines have made significant impact on fuel economy and engine emissions. The re-search on advanced diesels requires additional support.

Most chemical processing to produce alternative fuels is not economically competitive with petroleum at the current time. The research, especially to convert natural gas and methane to gasoline and diesel pro-ducts, needs to continue to search for better processes. As petroleum availability decreases, prices will go up and economic is-sues should dissolve.

Lubricant research on the tribological aspects of the new fuels needs additional effort.

SCENARIOS

The following scenarios could have a significant impact on petroleum conservation and use:

1. If oil prices increase rapidly or national security factors occur, development of alterative fuels will accelerate along with the cost of petroleum.

2. If oil prices remain stable, then environmental concerns and considerations, and advanced technology will be driving factors in use of alternative fuels.

3. Decreasing crude quality will result in poorer fuel quality. This will result in more interest in additives, such as surfactants, and cetane improvers.

4. Biomass and coal become more important as the reserves decrease and processing economics become more favorable. This will take some 25 years or another oil crisis.

5. Renewable resources will make inroads as lubricant base stocks and diesel fuels as economics improved. The technology is demonstrated. However, the use volume of lubricant products is so large, current production of vegetable oils could not meet the requirements. The use of these lubricants could impact the dependence on imported oil. It could also help third world countries whose economies now depend on petroleum. Further inroads could be made if technology is developed to significantly extend drain periods for alternative fuels and lubricants. Recycling technology is another need.

The main competition to renewable fuels and lubricants resources will be the need for food as the earth's population continues to expand uncontrollably. Research to achieve better crop yields and better quality vegetable oils is needed.

REFERENCES

1. Global Trends in Environment and Development Presentation, World Resources Institute 1709 New York Avenue, NW, Washington, DC 20006,

2. USDOE Transportation Energy Data Book, Edition No. 14, May 1994, ORNL-6798.

3. World Resources 1992-93, Oxford University Press, NY, 1992).

4. Energy. A Special Report, National Geographic, February 1981.

5. H.H. Schoebert, The Chemistry of Hydrocarbon Fuels, Butterwort Heileman, Ltd. Linacre House, Jordon Hill, Oxford OX2 6DP (1991)

6. S. Howell, "Biodiesel Fuel Standard Making Progress," ASTM Standardization News, pp I6-19, April 1997

7. Clean Fuels, ACS Division of Fuel Chemistry Preprints, Volume 42, No.2, April 13-17, 1997

8. USDOE Biomass workshop, Golden, Colorado, 1994

9. Raj Shah, Development Of A Bench Test To Evaluate Lubricants For Use With Alternative Fuels, PhD thesis, The Pennsylvania State University, University Park, PA (August 1995).

GAS TURBINE LOW NO_x EVALUATION

A. Jung, Texaco Inc.
J. Gore and L.Tseng, Purdue University
T. Risley, JJMA
M. Osborne, NAVSEA

INTRODUCTION

On and off-road engine exhaust regulations have focused principally on new diesel and gasoline engines. There has not been much emphasis on regulating existing diesel engines or gas turbines used in mobile applications. However, off-road gas turbines and existing diesel engines may some day also be impacted by air pollution (NO_x, SO_x, CO, CO2, particulates, UHC, etc) regulations.

Two problems arise when considering the possible regulation of existing and new marine engines in military use. The first is cost. Projected retrofit cost for emission controls on all of the Navy's existing engines would be high. The second deals with balancing power density against the emission of air pollutants. Navy marine applications, like most mobile applications thrive on high power densities (in both weight and volume). However, high power densities will typically be accompanied by high firing temperatures. In turn, high firing temperatues are a precusor to high emissions of thermal NO_x. Thus the challenge is to improve power density without increasing NOx generation to the environment.

The injection of ammonia (or related chemicals) in the exhaust stream of gas turbines or diesel engines is a very effective means for removing NO_x before it is released into the environment. This method can reduce NO_x emissions up to 90 percent in fossil-fueled power plants if the chemicals are applied within a critical temperature window. For mobile engines as those on ships, additional equipment and retention of chemicals for the processes are sometimes inconvenient, if not impractical.

One solution is to add the NO_x-removing chemicals directly to the fuel to avoid the need for carrying extra equipment or chemicals. The challenge with this approach is to protect the chemical additive as it passes through the combustion flame zone so that it can reduce NO_x in the exhaust stream. The Texaco Researh Center in Beacon, New York has been working on such an approach for diesel engines. Texaco Inc. has produced some experimental fuels additives that have shown promise in reducing NO_x in diesel engines, but had not been evaluated in gas turbines.

The fuel (NATO F76) used by U.S. Navy ships must be suitable for both their diesels and gas turbines engines. This would also be a requirement for any fuel additives used by the Navy. Since previous fuel additive work has focused on diesel engines, a Navy program was initiated to explore the potential for these additives in gas turbines. The development of an additive suitable for both gas turbines and diesel engines was recognized as an unexplored research area, however it the Texaco fuel additive proves successful in all engines, then the challenge of power density vs NO_x generation would be met successfully.

PARTICIPANTS

This program was sponsored by the Office of Naval Research (ONR) with NAVSEA serving as principal investigator. The program manager was Mr. Michael E. Osborne of NAVSEA. John J. McMullen Associates, Inc. (JJMA) provided consulting and program coordination, with Mr. Tom Risley serving as the program coordinator. Texaco Inc.'s Mr. Al Jung developed the test additives, provided the additized and baseline fuels as well as, information about the chemistry of the fuel additives. The combustion tests were conducted at Purdue University with Dr. J. P. Gore serving as the lead research scientist with his assistant

Doctoral candidate Li-ken Tseng.

ADDITIVE TECHNOLOGIES

The purpose of the fuel additive, NOx-reduction program was to assess whether certain fuel additive technologies that demonstrated NO_x reduction in compression ignition (diesel) engines could also reduce NO_x in turbine engine applications using F76 fuel combustcd under simulated turbine conditions.

Three specific technology approaches were chosen:

1. Improve the burn characteristics of the fuel using a "combustion modifier".

2. Improve the dynamics of the fuel injector spray and diffusion using a "spray modifier".

3. Attempt to scavenge NO_x post-combustion using a "Rapranox-like" additive.

These technologies were chosen for the initial phase of this program since they demonstrated very favorable NO_x reduction results when evaluated in compression ignition tests using standard diesel fuels (Figure 1). The differences between the Navy's F76 fuel and the diesel used by Texaco were judged to be minimal. Thus, any change in NO_x formation between the diesel and gas turbine was postulated to result primarily from differences in the mode of combustion between the two engines and in differences in combustion temperatures.

F76 fuel was additized at the Beacon Research Labs of Texaco and NO_x emissions were evaluated at Purdue University in a simulated gas turbine combustor. Unadditized F76 fuel was used to generate baseline NO_x data; these data were compared with data generated from fuel containing the experimental additives. All additives evaluated at Purdue under simulated turbine conditions were first tested at Texaco under compression ignition conditions in diesel fuel. Only those additives that demonstrated a net reduction in NO_x under compression ignition were tested at Purdue. The additives investigated contain only carbon, hydrogen, oxygen, and nitrogen. Additives containing metals or metal salts were not included in the study because of possible environmental hazards.

The specific samples of F76 fuel evaluated at Purdue are listed below:

Identification	Description
R96-1041.00	F76 baseline fuel
R96-1041.10	F76 fuel w/combustion modifier
R96-1041-20	F76 fuel w/combustion modifier
R96-1041.30	F76 fuel w/spray modifier
R96- 104 1.40	F76 fuel w/Rapranox-like additive

COMBUSTION MODIFIERS

Combustion modifiers are used to alter burn and time characteristics of the combustion process by chemically modifying the onset of ignition and the number of ignition kernels in the fuel spray.

In the first case, conventional combustion modifiers tend to advance the onset of diesel ignition, resulting in longer burn times and eliminating pressure spikes during the cycle. In turn, this decreases maximum in-cylinder combustion pressure and lowers maximum combustion temperature. Since NO_x generation is a direct function of combustion temperature, the lower temperature results in lower NOx emissions in diesels. There appears to be no power loss associated with the use of combustion modifiers despite the change in both maximum pressure and rate of pressure increase compared to the base fuel.

In the second case, the modifier is thought to promote combustion not only in the premixed portion of the fuel spray, but also in the diffusion zone. Facilitation of combustion in the diffusion portion of the flame could also lead to a more controlled pressure increase and avoidance of pressure and temperature spikes.

Another explanation for the reduction of NO_x using combustion modifiers involves their interaction with the Zeldovich and/or the Prompt mechanisms of NO_x formation. Zeldovich and Prompt describe the formation of NO_x via the generation and reaction of

radicals with nitrogen, oxygen, and fuel under combustion conditions. Combustion modifiers are also thought to work via radical mechanisms. It can be postulated that the radicals formed by the modifier could interact with the Zeldovich and Prompt mechanisms in such a way as to suppress the formation of NO_x. The latter explanation is being investigated further for maximizing NO_x reduction.

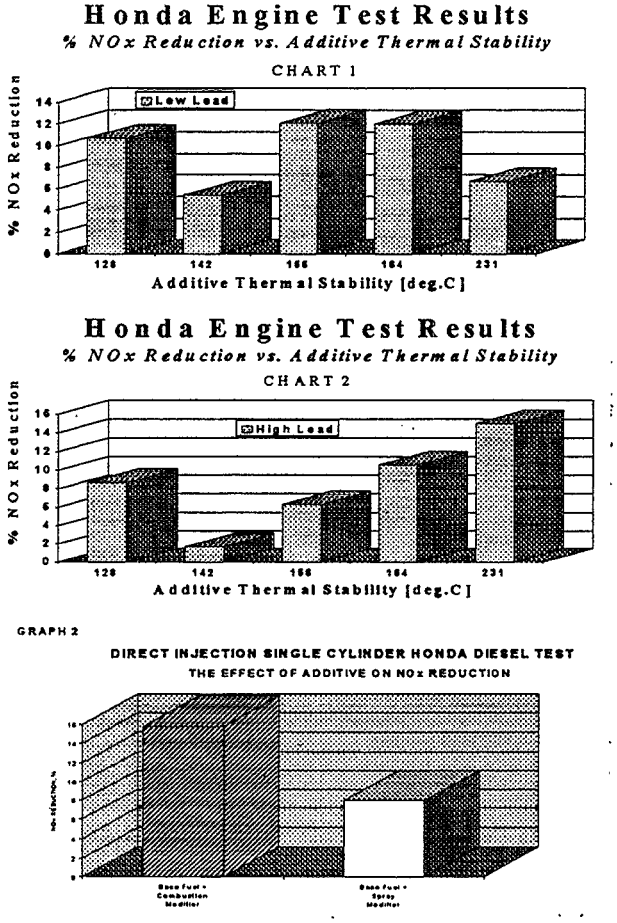


Figure 1: Effect of Rapranox-Like Additive (Top and Center) Combustion Modifier and Spray Modifier Additives on NO_x Reduction

The fuels referred to as R96-1041.10 and R96-1041.20 are F76 fuels that contain different combustion modifiers. In previous Texaco diesel engine tests, each additive decreased NO_x approximately 15 percent over that of the base fuel in diesel engine tests run at Texaco. These samples were submitted for NO_x testing under simulated turbine conditions at Purdue.

SPRAY MODIFIERS

Spray modifiers are used to physically alter the fuel injector spray patterns over those of the base fuel. In diesel engines these additives may have the same effect on combustion and emissions as increasing fuel injector pressure. Spray modifiers are expected to produce smaller droplet sizes (higher surface area to volume ratio) and increase swirl or turbulence of the fuel spray.

In diesel engine tests run at Texaco, spray modifiers have been shown to reduce NO_x emissions without increasing the cetane value of the fuel. Prcssure/time curves, however, show similarities to cetane-improved fuels (Figure 2). In effect, spray modifiers advance the onset of ignition and can change the volume ratios of the premixed and diffusion portions of the fuel charge, resulting in longer burn times with lower pressure spikes during diesel combustion. A lower pressure spike produces lower maximum combustion temperatures and lower NO_x emissions. Typically, a 12 percent reduction in NO_x is observed in diesel combustion when comparing fuel containing a spray modifier with the base fuel (Figure 2).

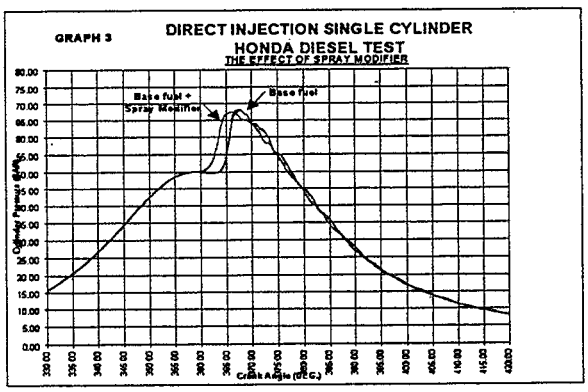


Figure 2: Effect of Spray Modifier on Nox Reduction

Spray modifiers are temperature-sensitive, so it is necessary to match combustion temperatures with the modifier decomposition- temperature. Diesel combustion temperatures are generally lower than those in turbine engines,

and a modifier that reduces NO_x in diesels might not show equivalent performance in turbines. A quantity of F76 fuel with a spray modifier (R96-1041.30) was submitted for NO_x testing in this program.

RAPRANOX-LIKE ADDITIVE
(Fuel-Soluble Cyanuric Acid Derivative).

Cyanuric acid has been shown to effectively reduce NO_x emissions from diesel engines when used in an "after treatment" mode. The cyanuric acid is presumed to decompose initially to isocyanate, which further reacts with NO_x to form innocuous byproducts such as nitrogen and water. Cyanuric acid is not soluble in hydrocarbon fuels, however, and this shortcoming has limited the investigations of this technology in-situ, that is, generating isocyanate in a cylinder directly from dissolved cyanuric acid. It is understood that even if the cyanuric acid could be dissolved in the fuel, its decomposition must be timed to coincide with the production of NO_x during combustion. Timing is critical since the lifetime of the reactive isocyanate intermediate is short.

The additive solubility problem in hydrocarbon fuels was solved by attaching hydrocarbon chains to the cyanuric acid portion of the molecule. The hydrocarbon chains sufficiently modify the polarity of the cyanuric acid to promote solubility.

Previous diesel emission studies at Texaco showed that the NO_x-reducing ability of a specific additive depended on in-cylinder temperature. Incylinder temperature can vary depending on engine load, suggesting that it is unlikely that one additive will maintain its NOx-reducing power over a wide range of engine loads. The data suggest that a combination of additives may be more effective over a wide temperature range than any single additive. One sample, R96-10414O, was submitted for evaluation in the current program.

TEST FACILITIES

Low and high pressure combustion tests were carried out at the Thermal Sciences and Propulsion Center of the School of Mechanical Engineering, Purdue University, West Lafayette, Indiana.

The test facility for the low-pressure tests is shown in Figure 3. The low pressure air supply system is used as the preheated air source. Pressure and temperature of the air are monitored by a pressure gauge and a stainless steel, shielded, K-type thermocouple before the air is directed into the combustor through a diverging section. Five different fuel tanks were built, one for each of the experimental fuels and the baseline fuel. The individual fuel tanks were designed for specific fuel blends and were not interchanged in order to prevent contamination. Each fuel tank has an independent fuel filter to prevent unwanted material from entering the fuel line. A nitrogen gas cylinder was used to pressurize the fuel tanks to obtain enough upstream pressure for fuel delivery. Fuel flow rate is monitored by a rotameter, which was calibrated for each test fuel to ensure flow rate accuracy within 5 percent. A pressure gauge mounted be-tween the rotameter and the fuel injector monitors the pressure drop across the fuel injector. This is essential to ensure the quality of atomization of the fuel spray. A shutoff valve located in the fuel line just before the combustor is a safety feature. The outside diameter of the fuel line decreases from 0.25 to 0.125 inch upstream of the fuel wafer, which encloses the 0.125-inch fuel line to minimize heat transfer from the preheated air stream. The fuel injector is mounted directly on top of the fuel wafer. The air supply system used for low-pressure, lowflow tests could deliver air flow rates up to 45 g/s (as measured by a subsonic differential pressure orifice plate and a water manometer) at temperatures up to 750°F and pressures up to 2 atmospheres. Pressure swirl atomizers with 60-degree hollow cone angles were used throughout the tests. A miniature thermocouple was fed into the fuel line up to the entrance of the fuel injector to monitor the temperature of the fuel before injection into the combustor.

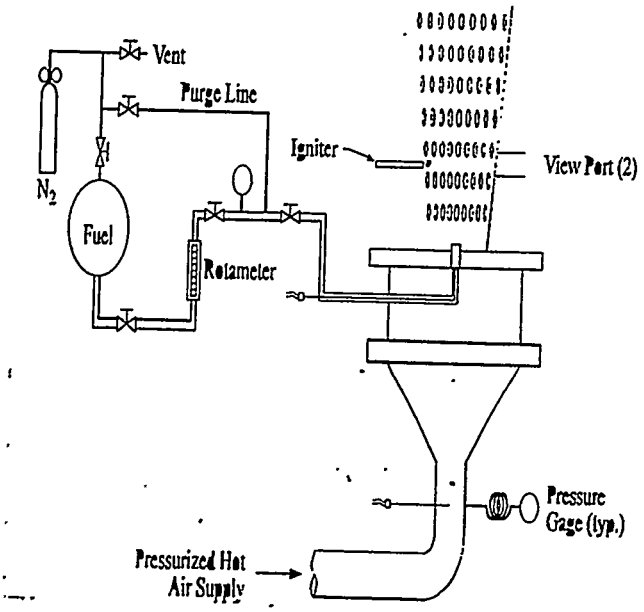


Figure 3: Experimental Apparatus

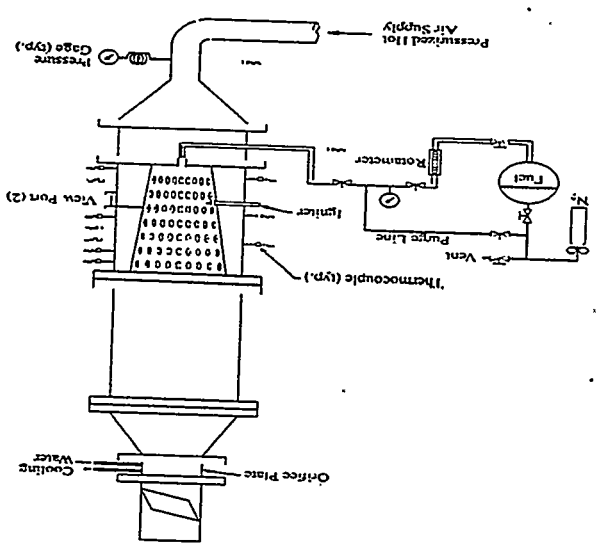


Figure 4: Schematic of High-Pressure Experimental Apparatus

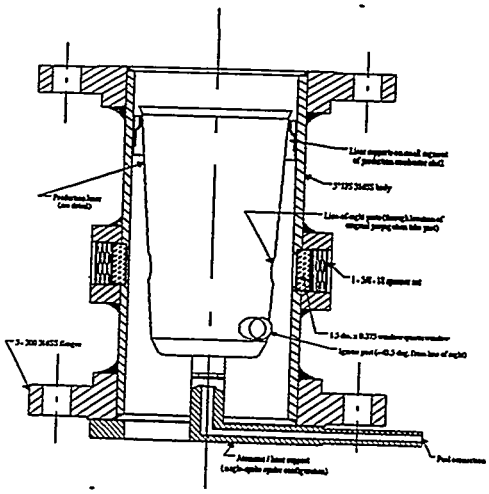


Figure 5: Schematic of Combustor

The facility used for the high-pressure tests is shown in Figure 4. A high-pressure air supply system was used as the preheated air source. Air pressure and temperature are monitored upstream of the combustor by a pressure gauge and a stainless steel, shielded, K-type thermocouple. The fuel supply system included a highpressure (up to 800-psi operating pressure) rotameter, which was calibrated for each tested fuel to ensure accuracy in fuel flow rate. The combustor was modified and reinforced to have an operating pressure up to 15 atmospheres, and a transparent plastic safety shield was added around the combustor section. A tail pipe with a diffuser plate was added to the system to provide a uniform subsonic exhaust stream from the system. Ten K-type thermocouples were welded to the outside surface of the combustor casing to monitor casing temperature during the high-pressure tests. The high mass-flow, high pressure air system could supply air at flow rates up to 9 lb/s at temperatures up to 750°F and pressures up to 2000 psi. The mass flow rate could be controlled with both subsonic and choked orifice plates, but for these tests a choked orifice plate was used, controlling mass flow by adjusting pressure upstream of the plate.

Figure 5 shows a detailed sketch of the combustor liner for a Boeing Gas Turbine Model 502-2E built for the Naval Bureau of Shipping (now the Naval Sea Systems Command). The diameter of the combustor is the same as the casing of the turbine engine so that a liner support segment from the original turbine engine could be fitted perfectly into the inside wall of the combustor. The fuel supply wafer is designed so that a minimum length of fuel line is exposed to the preheated air. A special

igniter was built to fit the igniter port of it c lincr. Two quartz windows are positioned at the exact location of the propagation port on the liner to provide visual access to the combustor. This design deviates slightly from the original combustor, but it provides necessary access for measurements and allows fuel emission properties to be examined under gas turbine conditions representative of naval engines.

TEST PROTOCOL

The procedure for each test involved purging the fuel line after the appropriate fuel tank was connected to the fuel supply system. The air heaters were started after the air flow rate was adjusted to the desired test conditions. This heating process generally took about 2 hours since a large thermal mass was involved in the air supply system. During the heatup process, gas analyzers were warmed up and calibrated. After the preheated air was stabilized at the desired flow and temperature test conditions, the fuel supply system was pressurized and fuel injection and ignition in the combustor were initiated. The igniter was turned on before the fuel injection, and could be turned off after the fuel flow rate was adjusted to the desired value. The combustor was kept running at each test condition for about 15 minutes to reach steady-state conditions before global emission data were measured. Gas samples were taken continuously at the exit of the test apparatus. The sampled gases were delivered to NO_x, CO, and UIHC analyzers so that the concentrations of these pollutants could be measured simultaneously.

A schematic of the exhaust gas analysis system is shown in Figure 6. A water-cooled stainless-steel probe was used to draw samples from the exhaust into the gas analysis system. Concentrations of NO/NO_x were measured using a chemiluminescence-based analyzer (Thermo-Enviromental Instruments Model 10) with an accuracy as derived from the nitrous oxide (NO) or NO_2 calibration gas of 1 percent of full scale. Concentrations of CO and carbon dioxide (CON were measured using a nondispersiveinfrared (NDIR) analyzer (Horiba MEXAGE 311) with a repeatability within 0.04 percent for CO measurements and within 0.3 percent for CO2. The lowest (or least) count of the CO/CO2 analyzer was 0.01 percent (100 ppm). This analyzer was calibrated using calibration gases of 5 percent CO_2, 2 percent CO, and 25 ppm NO. Dried nitrogen of 99.995-percent purity was used as the zero gas. A chiller-trap was used to condense water out before the sample entered the NO/NO_2 and CO/CO_2 analyzers. Since a CO analyzer with a lowest count of 0.01 percent is unsuitable for measuring of sub100 ppm CO levels, a gas-filter-correlation CO analyzer (Thermo-Enviromental Instruments Model 42) was used to measure CO concentrations in the 0- to 100-ppm range in some of the experiments. An HO analyzer, using a flame ionization detector (Rosemount Model 400A), was used to measure UHC concentration measurements in some of the experiments. The sampling line to the UHC analyzer was heated to prevent condensation.

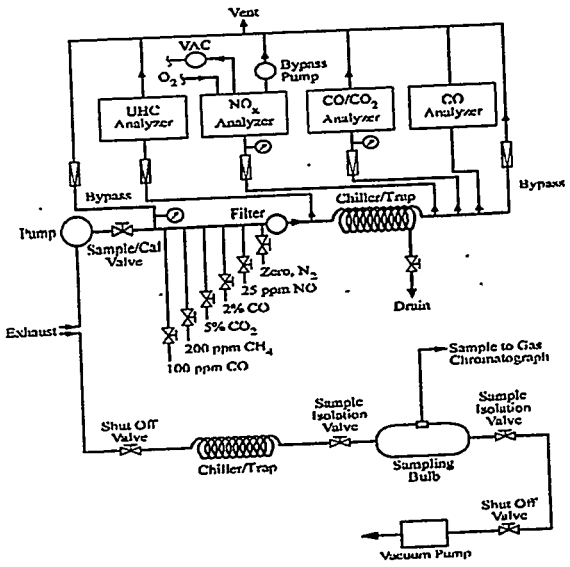


Figure 6: Schematic of Exhaust Gas Analysis System

TEST OBSERVATIONS

The test matrix included atmospheric pressure, 2-atmosphere pressure, and 15-atmosphere pressure tests. Tests at atmospheric pressure

were first conducted for the experimental fuels to examine their atomization, vaporization, and combustion stability performance. The more promising experimental fuels were then tested at a combustor pressure of 2 atmospheres. Finally, one of the experimental fuels and the baseline fuel were tested at 15 atmospheres

Flame temperatures at atmospheric pressure for the baseline, R96-1041.30, and R96-1041.40 fuels were measured. Of these fuels,the additized R96-1041.40 had higher peak flame temperatures, particularly at higher equivalence ratios. Peak temperatures for the R961041.30 fuel were lower than those for the baseline fuel at lower equivalence ratios, but were similar at higher equivalence ratios

The R96-1041.10 fuel did not yield stable flames under most operating conditions. Under conditions that resulted in apparently stable flames, flameout would occur unexpectedly and erratically. Further testing of this additized fuel, therefore, was not pursued. The R96-1041.20 fuel yielded stable flames but caused significant precipitation of a solid powder in the fuel lines and on the fuel filter, eventually clogging the filter. Further examination revealed that this fuel also caused significant precipitation at room temperature in the fuel tank. The cause for the precipitation was not investigated, instead it was decided that tests with the R96-1041.30 fuel should be abandoned since precipitation of the additive could not be prevented. Stable flames and repeatable data were obtained for experimental fuels R96-1041.30, R96-1041.40 and the baseline fuel

The next phase of atmospheric pressure tests included fuels R96-1041.00, R96-1041.30, and R961041.40. Thermal stability tests were conducted for all three fuels up to 400°F. Fuel precipitation was not observed. This ensured that clean fuels were injected into the combustor since the fuel temperature before the fuel injector typically was about 175°F.

The additized fuel, R96-1041.30, when tested at 15 atmospheres reached stable condition, but a sudden change in emission readings and combustor casing peaking temperature was observed. The peak temperature of the combustor casing increased to 580°C and, as a result, the test was terminated. During the combustor checkout after disassembling, it was discovered that the combustor liner had burned through in several locations during the high fuel-flow rate tests for R96-1041.30 fuel. After installing a new liner, high pressure tests were continued with a medium fuel-flow rate using the same test matrix and protocol as for the low flow rate tests. The flame still covered all the viewing area for both the baseline and the additized fuel. Emission data were obtained throughout the test matrix and the liner was not damaged when checked after posttest disassembly.

A second series of tests was conducted at 15 atmospheres with the same test conditions used for the middle firing rate case. When R96-1041.30 was tested, it produced a much shorter flame than the baseline and the combustor wall temperatures rapidly increased near the dome of the combustor liner. A visual examination of the combustor liner showed slight damage to its inner surface. Surface roughness increased near the dome of the combustor liner, indicating that the flame was either impinging on or very close to the liner.

R96-1041.40 was tested next. The observations of the flame appearance and chamber temperature showed results similar to those of the previous high pressure tests of the same fuel under similar conditions, indicating that combustor performance had not been affected by the slight damage to the liner caused by the R96-1041.30 fuel.

RESULTS AND DISCUSSION

Two types of tests were conducted to cover the operating envelope of practical combustors. In the first type, the equivalence ratio was adjusted by changing the air flow rate while keeping the Fuel flow rate constant. Under these conditions the equivalence ratio and the residence time varied simultaneously and significantly. The second type of tests involved varying the fuel flow rate to obtain

different equivalence ratios. Since residence time in the combustor is determined primarily by air flow rate, the results of these tests allowed the effects of equivalence ratio variations to be delineated

Figure 7 shows a comparison of Emission Index (EI) for the baseline fuel, R96-1041.00, and experimental fuel R96-1041.30 plotted as a function of equivalence ratio. The test conditions for Figure 7 were constant Fuel flow rate. Different fuel equivalence ratios were obtained by varying the air flow rate. This type of operation provides a wide range—at least a factor of three—of flow velocities inside the combustor. The characteristic residence time, therefore, also varies by more than a factor of three. It can be seen that the EINO and $EINO_x$ for R96-1041.30 are consistently higher than those of the baseline fuel, R96-1041.00. Both EINO and $EINO_x$ decreased as the fuel equivalence ratios increased for both experimental and baseline fuels. The reduction in available air reduces recirculation by changing the swirl number and causes jet-like luminous flames with higher equivalence ratios. The changes in flame structure lead to lower NO_x emissions with increasing equivalence ratio under these test conditions. The EINO and $EINO_x$ data for the two baseline fuel tests, one before testing experimental fuel R96-1041.30 and one after, are consistent. The differences in the EINO for the two tests of baseline R96-1041.00 fuel might have been caused by the fuel coking inside the combustor liner that was found after disassembling the combustor. This coking might have had a slight influence on CO and UHC measurements, but it would not have affected EINO and $EINO_x$ since the emissions they represent were produced in the flame zone.

To obtain comparable residence times, tests also were conducted with constant air flow rates, but fuel flow rates were varied to obtain a range of fuel equivalence ratios. One limitation of the tests with variable fuel flow rates is that three different nozzles had to be used to cover a reasonable range of equivalence ratios. Figures 8 and 9 show graphs of EI vs. fuel equivalence ratio for R961041.00

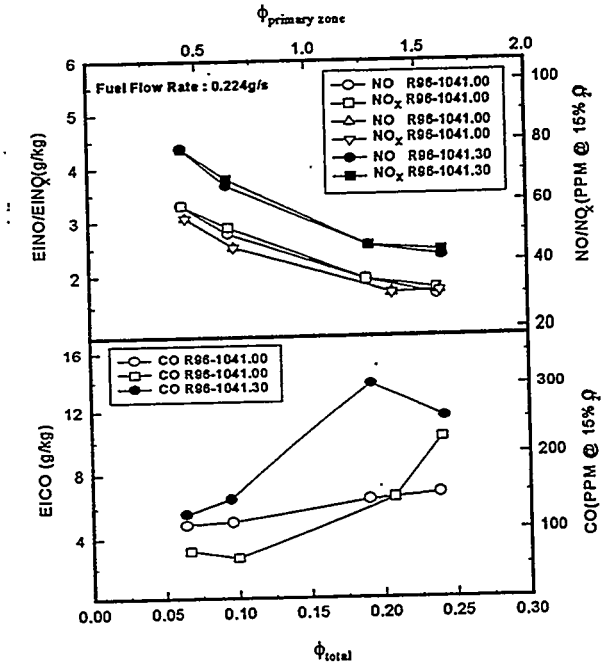


Figure 7: Pollutant Emissions for R96-1041.30 and Baseline Fuels at Constant Fuel Flow Rate Test Conditions Under Atmospheric Pressure

R96-1041.30, and R96-1041.40 feels under constant air flow rates. The EINO has the same values as the $EINO_x$ over these test conditions, so only the $EINO_x$ is shown. The flow field inside the combustor liner is relatively unchanged over the small range of fuel equivalence ratios for the constant air flow rate test conditions. The EI over this range of fuel equivalence ratios are relatively free from flow effects. Figure 8 shows that the $EINO_x$ slowly increases as the fuel equivalence ratio increases. This is because the product temperature also increases as fuel equivalence ratio increases. One can see that the EINOX remains about the same over each range except for the conditions at which larger droplets were created by the atomizers and EICO increased. As shown in Figure 9, the experimental fuel R96-1041.40 has higher $EINO_x$ at all test conditions.

In the first series of high-pressure tests, the baseline fuel and experimental fuel R96-1041.40 were tested with one air flow rate and three fuel flow rates at a combustor pressure of 15 atmospheres. The results

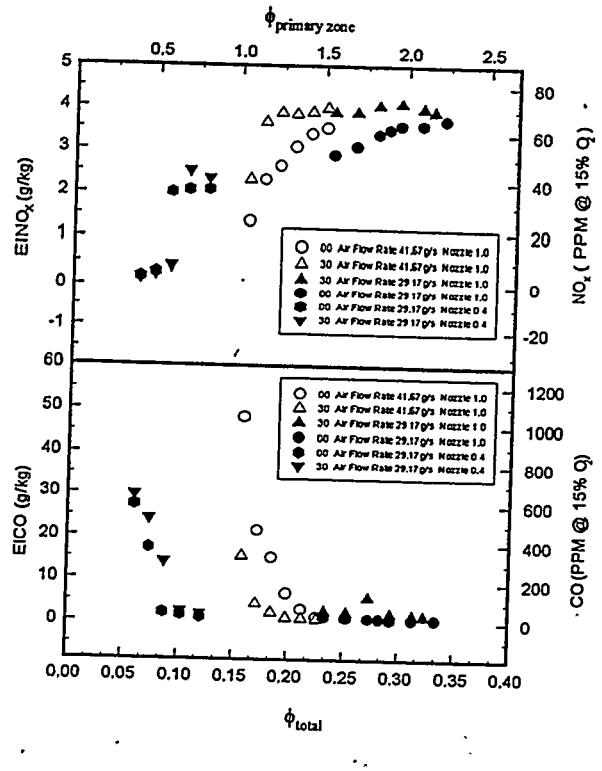


Figure 8: Pollutant Emissions for R96-1041.30 and Baseline Fuel at Constant Air Flow Rate Test Conditions Under Atmospheric Pressure

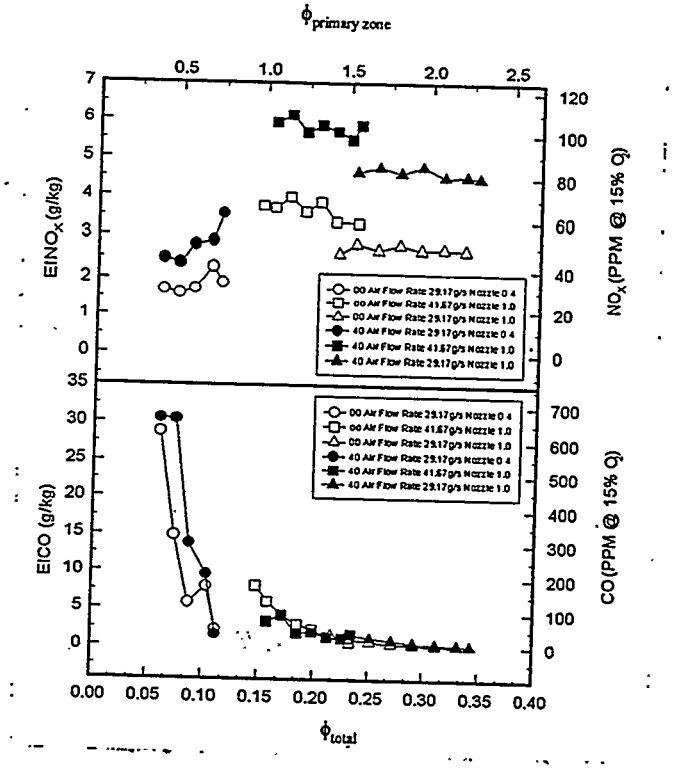


Figure 9: Pollutant Emissions for R96-1041.40 and Baseline Fuels at Constant Air Flow

show that at these conditions R96-1041.40 still produces more NO_x than does the baseline fuel. Differences between the $EINO_x$ of the two fuels, however, decrease at this higher pressure, although the overall NO_x emissions increased for both fuels. This decrease in the difference between NO_x emissions for the baseline fuel and the experimental fuel may be due to a change in chemical reactions, change of combustor characteristics, or simply a decrease in the percentage of the extra NO_x produced by the fuel additives.

Figure 10 shows the EINO and $EINO_x$ as a function of fuel equivalence ratios for all 15-atmosphere tests, with open symbols representing data from the earlier tests and solid symbols representing data from the second series of tests. The baseline fuel F76 produces the lowest NO and NO_x emissions for all test conditions. The difference between NO_x emissions of the R961041.40 fuel and the baseline fuel is similar for the earlier and present tests except for the data obtained at the high firing rate, high fuel-equivalence ratio, where flame impinging on the combustor liner could be the cause of the small difference. The flame impingement also caused a burn-down of a combustor liner during the earlier tests. The fuel mixture, an equal volume mixture of R96- 1041.30 and R96- 1041.40 fuels, shows EINO and EINOX similar to those of the R96-1041.40 fuel. The EINO and $EINO_x$ produced by R96-1041.30 fuel have a value between the baseline F76 fuel and the R96-1041.40 fuel. The R96-1041.30 fuel, however, also caused a dramatic change of temperature distribution in the combustor liner, which resulted in minor damage to it.

The effects of the R96-041-30 (spray-modifier) fuel additive (microexplosive) were further examined in a spray flame in a co-flow air configuration. A pressure swirl atomizer with a flow rate of 0.4 gallon per hour was used as the fuel injector for the spray flames. The fuel injector was placed in an axisymmetric co-flow of air with a duct diameter of 3 inches. The velocity of the co-flow air was kept constant

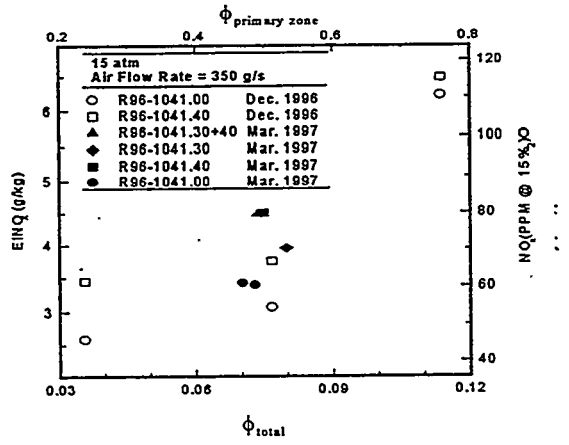


Figure 10: NO_x Emissions at 15 Atmospheres at 3 meters per second.

The fuel supply pressure was also kept constant at 110 psig during the test. Two different fuels baseline F76 (R96-1041.00)) fuel and the R96-10)41.30) fuel. were tested under identical test conditions.

Figure 11 shows photographs of the two spray flames under identical operating conditions. The spray flame shown on the bottom is fueled by baseline F76 fuel and the one on the right is fueled with the R96-1041.30 fuel. One can see that the F76-fueled spray name has a flame height about twice as long as the spray flame fueled with the R96-1041.30 fuel. This is because the F76-fueled spray name has a larger fuel droplet size and. therefore. longer evaporation time is needed to vaporize these larger fuel droplets. The spray-modifier fuel additive in the R96-1041.30 fuel causes the larger spray droplets produced by the pressure atomizer to experience a microcxplosion and reduces them to smaller droplets. The lifetime of the smaller droplets is much shorter and so the height of the spray flame fueled by the R96-1041.30 fuel is much shorter. The angle of the F76-fueled spray flame is smaller than that of the R96-1041.30-fueled spray flame.

Two possible mechanisms contribute to this phenomenon:

1. The microexplosion caused by the spray modifier additives in the R96-1041.30 fuel increases the spray angle

2. The momentum transfer for the smaller droplets in the R96-1041.30 fuel spray flame is much more effective than that for the larger droplets in the F76-fueled spray flame.

Although the spray-modifier led to an increase in NO_x in the present combustor configuration. advanced combustor concepts such as lean direct injection (LDT) would benefit significantly from the use of this additive.

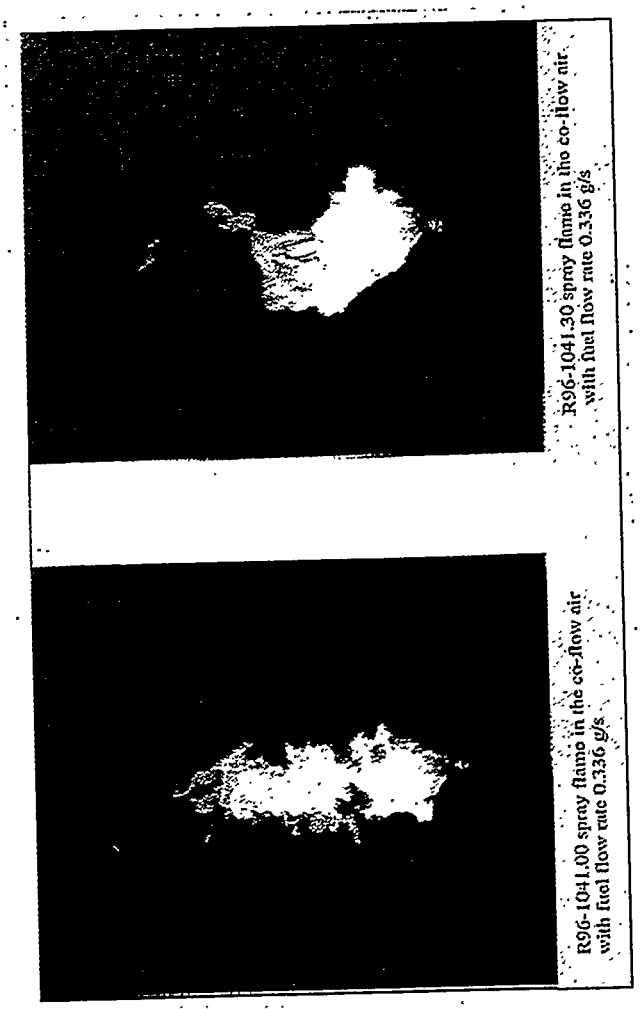


Figure 11: Spray Flames

CHEMICAL REACTION MODEL

The effects of adding the nitrous oxide-(NO_x-) reducing chemicals were studied computationally using an opposed-flow nonpremixed flat-flame code with methane as the fuel. This

one-dimensional flame provides an opportunity to conduct a detailed study of the chemical reac-tion mechanism within the current computation capacity. The most recent reaction mecha-nism developed by the Gas Rcscarch Institute, GRIMECH. was used for this study. The mechanism considers 49 chemical species and 279 reversible reactions.

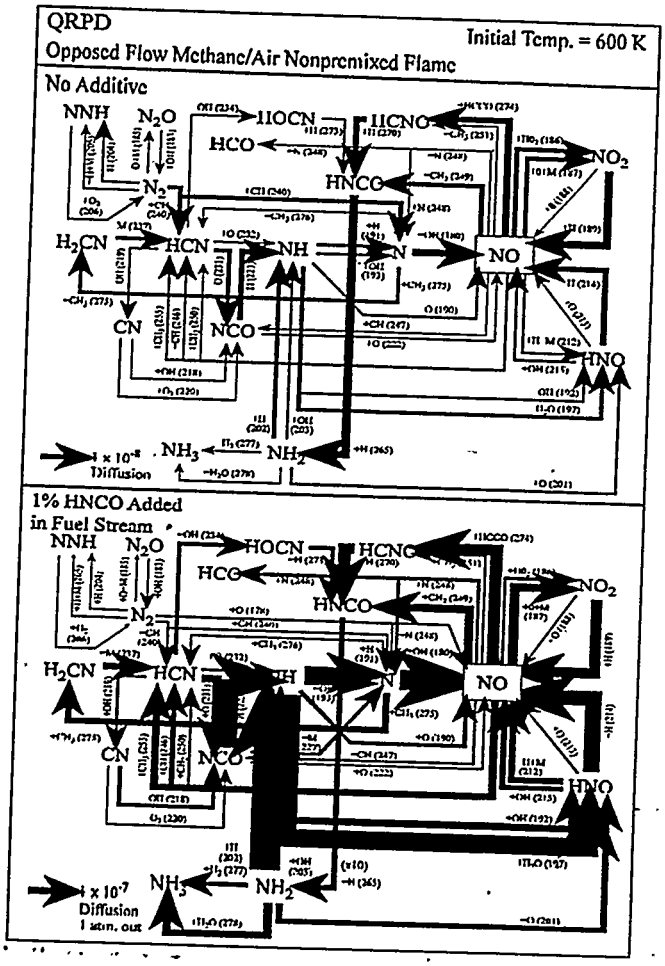


Figure 12: QRPD for Methane/Air Flames With Initial Temperature = 600°K

Figure 12. shows the QRPD of important NO_x emissions-related reactions for the nonad-ditized and the HNCO-added flames with an initial temperature 600°K. Each line in the QRPD represents a chemical reaction. The line thickness representing the value of the integrated reaction rate of this specific reaction over the entire flow field. The direction of reaction is indicated by the arrows. The reac-tion is producing or consuming a species if the arrow is pointing into or away from the species respectively. It can be seen that the additive HNCO is mainly involved in the reactions with HCNO, NO, and NH_2. A comparison of the upper panel and the lower panel of Figure 12 shows that the reaction rate of many NO-related chemical reactions are drastically augmented. Reaction number 265 was plot-ted in one tenth of the scale to fit into the plot. Adding HNCO not only increases the con-sumption rate of NO but also increases the production rate of other species such as NH, HNO, and nitrogen (which all lead to more NO), and so results in a net increase of NO produc-tion.

CONCLUSIONS

Measurements of pollutant EI at three different pressures for baseline F76 and four additized fuels were attempted. Of the four additized fuels, R96-1041.10 did not yield stable flames under gas turbine conditions and R96-1041.20 fuel showed solid precipitation at room tem-perature in the fuel line and in the fuel filter. The reasons for these unexpected results were not pursued, thus it is possible that the addi-tives may have been incorrectly formulated.

R96-1041.30 and R96-1041.40 fuels showed approximately a 30- to 50-percent increase in NO_x emissions over the baseline fuel index at combustion pressures of 1 and 2 atmospheres. At 15 atmospheres pressure, the $EINO_x$ for R96-1041.40 fuel is 30 percent higher than the $EINO_x$ baseline fuel under low and medium fire conditions. The $EINO_x$ for the two fuels are almost identical for the high fire conditions, but flame impingement on the liner may have affected these data.

The results from present tests suggest that the fuel additives may become more effective at pressures higher than 15 atmospheres, but this is conjecture and needs to be verified directly. Therefore, tests in the pressure range of 18 to 30 atmospheres should be explored.

Despite the higher NO_x emissions with the additzed fuels, the fact that the emissions were affected would indicate that tailoring of the additive for a gas turbine combustor may be more successful.

The fuel additives appear to affect the atomization performance, so the surface tension and viscosity changes that they may cause need to be examined. The atomization characteristics need direct experimental investigation.

The reductions in NO_x emissions caused by the fuel additives were in the 10- to 20-percent range based on diesel engine tests at Texaco Inc. This was the first time these additives were evaluated in a gas turbine combustors. The results of this evaluation points out the complexity in using fuel additives in two different combustion processes.

Lean Direct Injection (LDI) combustor concepts may find value in the additives similar to R96-1041-30 since this additive seems to promote a more rapid combustion.

COMMERCIALIZATION OF HEAVY DUTY NATURAL GAS ENGINES

J. Wiens
California Energy Commission

INTRODUCTION

The purpose behind the participation of California energy and air quality agencies in the creation and expansion of alternative fuel low emission vehicle markets is to support public policy goals for fuel diversity in the transportation market and improved air quality. Remarkable advances in commercializing natural gas vehicles have occurred in some heavy-duty market segments, but the levels of future market growth needed to achieve the public policy goals will require improved economics for truck purchasers. These improved economics seem to require a combination of more efficient engines, economic return from reduced emissions, and lower equipment and fuel prices.

Fuel efficiency is very dependent on driving patterns. Available Otto cycle spark-ignited and throttled natural gas engines yield lower fuel economy at low load and idle operating on congested urban streets and freeways than the diesel engines that they compete with. This means that long haul and any other trucking sectors that can minimize low load and idle operation become preferred target markets where the fuel economy disadvantages of spark-ignited natural gas engines can be minimized. However, this will require widespread natural gas availability servicing the principal corridors used by long-haul trucking.

•There are some fundamental conflicts that can frustrate attempts to create large and sustainable markets for heavy-duty natural gas vehicles. The long-haul truck market typically operates at 10,000 miles per month or higher with medium- to high-load duty cycles. The duty cycles that characterize this market allow current spark-ignited natural gas engines to operate at their best fuel efficiency, although this is at best 15 percent lower than typical diesel efficiency. Theoretically, the large quantities of relatively inexpensive natural gas fuel consumed could result in a large enough fuel cost savings to amortize the current high engine and vehicle differential prices. Unfortunately, this long-haul market also requires a dense network of CNG or LNG fuel stations outside of the major air quality challenged urban areas. It is very difficult to economically justify the large investments necessary to create such a dense and widespread fueling network when there are only very limited numbers of near-term customers (the chicken and egg problem so familiar to alternative fuel supporters). Natural gas fueling stations also require high utilization to be able to amortize their high capital costs and dispense fuel that will be inexpensive enough to compete effectively with diesel fuel despite less efficient engines.

Heavy duty diesel sources have been targeted by California air quality districts as the last major source of photochemical oxidant air pollution (principally NO_x as a precursor to Ozone) with the potential for relatively low cost control. Inventories of mobile source nitrogen oxide (NO_x) emissions in California's South Coast and Sacramento Air Basins show about half or more comes from heavy duty diesel trucks. This reflects considerable success in achieving up to 98 percent reductions in NO_x emission levels with improved emission control technology in light duty vehicles. A large portion of the heavy duty truck emissions is not controllable by regulation of locally-based sources, because it comes from long-haul trucks that are often not based in the local district and thus difficult to control with local regulation. Indeed, there is real concern that tougher regulations can force relocation of trucking firms that are economically important to the local community. The size of the targeted heavy duty market segments is also

large enough to support both the commercialization of heavy duty natural gas vehicles and the necessary widespread natural gas (primarily LNG) fueling station network.

This paper will describe the major types of heavy duty natural gas engine technologies, current results of demonstrating several examples in trucks, and the results of economic payback analysis. It will discuss the need for improved fuel efficiency (in actual duty cycles typical of major market segments) along with a reduction in federal highway fuel excise taxes for LNG and a return on the purchaser's investment in lower emission engine technology in order for heavy duty natural gas engines to achieve their economic potential in trucking markets.

ENGINE TECHNOLOGIES

There are three basic types of heavy duty natural gas engines currently available: spark-ignited stoichiometric, spark-ignited lean bum, and pilot-ignition dual fuel.

Spark-ignited stoichiometric engines provide the lowest NO_x emissions, as low as 1/5 that of modern diesels, but at the cost of the lowest fuel economy, perhaps half that of modern diesels in typical truck duty cycles. Examples of these engines are:

- The Caterpillar G3306 engine, a 10 liter engine based on a widelymarketed mechanical diesel engine, includes an oxygen sensor and closed loop computer feedback technology to control the air/fuel ratio at stoichiometric to allow a three-way catalyst to effectively control NO_x in addition to HC and CO. This engine is certified at 0.7 g/bhp-hr NO_x, the lowest available. This engine has received only very limited commercial market acceptance, likely due to both low fuel economy and high heat rejection.

- The Tecogen (ThermoPower) 7000 and 7000T engines are converted Chevrolet 427 CID (7 liter) gasoline engines. They include a three-way catalyst, but are open loop without an oxygen sensor and computer feedback system to precisely control the air-fuel ratio at stoichiometric.

Spark-ignited lean burn engines: the majority of the current market offerings, provide intermediate fuel economy, perhaps 2/3 of modem diesels in typical truck duty cycles, with NO_x emissions as low as 1/3 that of modern diesels. Examples of these engines are:

- The Cummins natural gas engines use this principle. The latest generations of L10, C8.3, and B5.9 series natural gas engines incorporate advanced oxygen sensor and closed loop computer feedback technology with central fuel metering systems to maintain lean air/fuel ratios near the lean limit.

- The John Deere 6081 (8.1 liter) and 6068 (6.8 liter) engines and the Mack E-7G (12 liter) engine utilize advanced lean bum oxygen sensor and closed loop computer feedback technology.

- The Detroit Diesel Series 50G (8.5 liter) (currently available for trasit markets without oxygen senso feedback control) and 60G (12.7 liter) engines are projected to become available for automotive marketrs in 1998 with advanced lean burn oxygen senso and closed look computer feedback technology.

A more sophisticated type of oxygen sensor and computer feedback technology is required to measure the oxygen *quantity* at lean air/fuel ratios rather than the more common stoichiometric sensor and feedback systems (in gasoline passenger cars and light trucks) that merely monitor the *presence or absence* of oxygen.

Pilot-ignition dual fuel: engines provide NO_x emissions from 1/2 to equal that of modern diesels, with fuel economy nearly equal to modern diesels. An example of this type of engine is:

- The Clean Air Partners/Power Systems Associates/ Caterpillar dual fuel engines use this principle. The technology developed by Clean Air Partners and

produced by Power Systems Associates (a major Caterpillar dealer) involves modifications to a range of Caterpillar diesel engines that maintain the Caterpillar warranty. The technology includes automotive type port fuel injectors for natural gas with the conventional diesel fuel direct injection system injecting just enough diesel fuel to ignite the natural gas intake charge. Improved versions of Caterpillar 3126 (7.2 liter 190 and 250 hp), C10 (10 liter 275 and 350 hp), and C12 (12 liter - 350, 400, and 425 hp) dual fuel engines are expected to be certified this year to the ARB optional NO_x emission standards of 2.5 g/bhp-hr.

EARLY SUCCESSES

The most notable early successes of natural gas heavy duty engines have been in the transit bus market. The Federal Transit Agency (FTA) provides funds from gas tax revenues to pay for 80 - 85 percent of the purchase price of transit buses for public transit districts. Transit agencies have been able to obtain FTA funding to cover the higher capital costs of alternative fuel engines, fuel storage systems, and to some extent the necessary fueling infrastructure. Transit districts thus do not need to amortize the higher capital costs with fuel cost savings or economic return from emission bene fits.

Cummins has been notably successful in taking advantage of this public support for natural gas to enter the transit market previously dominated by Detroit Diesel Corporation (DDC) with their two stroke diesel engines. Over 135 million cumulative miles experience have been achieved on over 1,500 natural gas Cummins L10G engines, initially the L10-240G, later the L10-260G, and most recently the L10-300G (280 hp transit rating), primarily in the transit market[1].

DDC responded to the Cummins market challenge with a Series 50 four stroke diesel engine that is a four cylinder, 8.5 liter version of the very successful six cylinder Series 60 12.7 liter truck diesel engine. DDC also developed a natural gas version, the Series 50G, that is available in 250 and 275 hp transit ratings. The previously market-dominating DDC two stroke diesel engines have not been certified to California transit emission standards (without particulate traps) since 1990[2].

There have also been substantial sales of heavy duty natural gas engines in municipal refuse collection service and schoolbuses. Engines include the Cummins C8.3G and L10G series, the DDC Series 50G, the Mack E-7G, the Tecogen TecoDrive 7000 and 7000T, and the John Deere 6081.

DEMONSTRATION EXAMPLES

The California Energy Commission has cosponsored several demonstrations of heavy duty natural gas engines in a variety of truck applications. Cosponsors include the South Coast Air Quality Management District, Southern California Gas Company, the U. S. Department of Energy, the National Renewable Energy Laboratory (NREL), the American Trucking Associations Foundation's Trucking Research Institute, Ventura County APCD, and Santa Barbara County APCD.

The relative fuel efficiencies of the demonstration spark-ignited lean burn engines described below are remarkably consistent. The 25 - 40 percent loss of efficiency that appears to characterize these engines in typical truck duty cycles needs to be recognized as a formidable barrier to their commercialization in trucking markets. The Caterpillar and Detroit Diesel engines are prototypes that may not include potential fuel efficiency improvements. Some recent engine improvements in other engines may show improved relative fuel efficiency, but reliable data confirming this is not yet available.

- Vons Caterpillar G3406LE (14 liter - 350 hp) - 30 percent lower BTU fuel economy compared to a mechanical 3406B diesel in the same service[3]. The duty cycle was relatively high load, pulling high gross weights over Grapevine pass. Caterpillar decided not to commercialize this engine due to both

the lack of sufficient market demand to justify significant further development efforts and the availability of the dual fuel engine option.

- L.A.. Times DDC S60G (12.7 liter -370 hp) - 35 to 40 percent lower BTU fuel economy compared to electronic DDC S60 diesels in the same service 4. The duty cycle is medium load, pulling medium gross weights in frequently congested roadways primarily on the Los Angeles regional freeway system.

- Wal-Mart DDC S60G (12.7 liter -370 hp) - 29 to 33 percent lower BTU fuel economy compared to electronic DDC S60 diesels in the same servic[5]. The duty cycle was relatively high load, pulling medium gross weights over various open road highways including the Grapevine pass.

- Jack B. Kelley Cummins LIO-30OG (10 liter - 300 hp) - 25 percent lower BTU fuel economy compared to diesels in the same service [6]. These are high load operating vehicles hauling LNG and other cryogenic gases on rural highways. This is a private commercial demonstration with some NREL fundng.

- City of Long Beach Cummins L10260G (10 liter - 260 hp) - 30 perent lower BTU fuel economy compared to mechanical Cummins LI0 diesels in the same service [7]. These are refuse packer trucks that collect municipal waste from homes and deliver to a central solid waste recovery facility. This demonstration of three natural gas trucks is funded by a DOE Grant.

ECONOMIC ANALYSIS OF NATURAL GAS TRUCKS

The author performed an analysis of natural gas truck economics to determine the ability of currently available engines and fuel systems to amortize higher vehicle prices with lower cost fuel and emission incentives. The payback analysis for natural gas trucks illustrated in the Appendix includes a range of assumptions for duty cycle efficiencies, monthly mile age accumulation, emission benefits, and incentives for emission benefits. The analysis presented assumes a$35,000 capital cost increase for natural gas engines and fuel systems, 2 g/bhp-hr NO_x emission levels in comparison to 4 g/bhp-hr for diesels (required for trucks in 1998), a 10 percent annual cost of capital (hurdle rate), $1.50 per gallon diesel and $.50 per gallon LNG retail price, and either no value for NO_x emission reductions or a $10,000 per ton of NO_x emission credit.

At 10,000 miles per month, common in long-haul trucking, and the 30 percent efficiency loss typical of current engines (in demonstration fleets), nearly 14 years is required for payback without emission credits. This can be reduced to 2.4 years with emission credits. For a fleet that can achieve 15,000 miles per month, with a 30 percent efficiency loss, payback ranges from nearly 7 years without credits to about a year and a half with credits. For a fleet that can achieve 20,000 miles per month, with a 30 percent efficiency loss, payback ranges from about 5 years without credits to about a year with credits. Obviously, different efficiency and fuel price assumptions lead to different results, but these assumptions appear to reflect future possibilities with some optimism for low LNG prices and stable diesel prices. The $0.50 per gallon LNG price could represent fuel from a nearby liquefaction plant with the Federal Excise Tax (FET) reduced to CNG levels as proposed in pending Federal tax legislation. Although other assumptions can be modeled, it is difficult to project economic competitiveness without improvements in engine efficiency and emission incentives.

LNG price forecasts incorporate three elements for discussion: location, tax rates, and utilization. LNG is transported by cryogenic truck tanker from production plants to fuel stations, and production locations are not generally located close to fuel stations needed for California demonstrations. Siting new production plants to minimize the haul distance to needed fuel stations will be a critical element in achieving competitive pricing.

Federal fuel excise taxes are currently at a level that penalizes LNG (and LPG and methanol) compared to CNG, diesel, gasoline, and ethanol on a BTU content basis. There are efforts underway in the U.S. Congress to either normalize the tax rate per BTU or establish rates for alternatives that would initially be lower than conventional fuels (potentially zero since electricity currently has no excise tax). The present varied tax rate structure for different fuels appears to reflect the relative political strength of various alternative fuel constituencies and the failure of alternative fuel proponents to work together for mutual benefit.

Lastly, the price of LNG and any other alternative will be somewhat sensitive to fuel station utilization. The higher the fuel station investment per BTU delivered, the more sensitive that station's economics is to utilization. LNG fuel station investment is lower than CNG, but higher than the other liquid fuels, giving it an intermediate sensitivity to utilization.

Attainment of the necessary market growth to accomplish fuel diversification goals will be delayed until sufficient economic improvements occur to meet the needs of the targeted heavy duty natural gas truck customers.

ECONOMIC INCENTIVES FOR NO_x REDUCTION

The opportunity to achieve an economic return from lower emissions is also a critical element in projecting a successful economic basis for trucking industry investment in natural gas vehicles. Currently, purchasers of lowemission heavy duty natural gas engines do not receive any direct economic benefit from the lower emissions. Some trucking companies may be able to justify the higher prices in return for image improvement (sometimes called "green marketing"), but it is difficult to see this occurring on a large enough scale to achieve the necessary air quality improvement without commensurate direct economic benefits.

Some pioneering air quality agencies have pursued establishment of market mechanisms for emission credit trading to provide the needed direct economic benefits, but difficulties in providing the necessary accurate documentation of actual emission benefits have prevented achievement of effective market success.

Another approach is to provide public funding to purchase emission benefits. This has been proposed in AB 1368 to the California Legislature that would provide funds to pay the additional purchase cost of low emission heavy duty vehicles up to a value of $12,000 per ton of NO_x reduced. Since major reductions in NO_x from heavy duty vehicles are required by the California State Implementation Plan, the bill would essentially pay for the emission reductions needed for attainment. Tougher emission standards for 2004 are not projected to be sufficient or in time to achieve attainment, particularly in the Sacramento area where attainment is required by 2005 (the South Coast Air Basin has until 20 10). Attainment is projected to require early adoption of all possible alternative fuel and low emission technologies and the bill would encourage such early adoption.

IMPROVING TECHNOLOGY

In recognition of the need to improve the efficiency of heavy duty natural gas engines, the American Trucking Associations Foundation's Trucking Research Institute (TRI), with funding by the U. S. Department of Energy, the South Coast Air Quality Management District, and the Gas Research Institute, has initiated a program to cost-share the development of improved fuel efficiency engines with original equipment manufacturers. The California Energy Commission, the California Air Resources Board, and other organizations are considering cofunding of the TRI administered program.

Proposals from original equipment manufacturers (Caterpillar, Cummins, John Deere, and Mack) include some very interesting and pioneering fundamentally new future technologies, in addition to substantial near-term improvement of existing technologies. Technologies proposed include direct injection compression ignition (diesel like) technology,

improved feedback control for SI engines, electronic fuel metering for each cylinder to reduce maldistribution and facilitate skip fire, improved high-energy ignition for leaner mixtures, and camless valve actuation for complete timing flexibility.

CONCLUSIONS AND RECOMMENDATIONS

1. Currently available heavy duty natural gas engines are significantly less fuel efficient than the diesel engines they are competing with in representative truck duty cycles with substantial idle and light load operation.

2. Natural gas, primarily LNG, will not become economically competitive in heavy duty truck markets until some combination of improved engine efficiency in customer duty cycles, lower engine and fuel system prices, lower fuel prices, and emission credits becomes available. Lower engine and fuel system prices can be anticipated when scale economics and competitive pressures occur. Lower fuel prices can come from reduced FET and from local LNG facilities that can provide shorter haul distances.

3. Organizations with responsibility for attaining air quality standards that are significantly impacted by emissions from heavy duty trucks should pursue ways to improve the economics of natural gas trucks by finding ways to provide economic benefits to truck purchasers in return for emission benefits.

4.Organizations with responsibility to improve fuel diversity in transportation markets should pursue ways to improve the economics of natural gas trucks by finding ways to increase the fuel efficiencies of heavy duty natural gas engines and reduce natural gas, principally LNG, prices and FET rates.

LEGAL NOTICE

The views and conclusions expressed in this document are those of the author and should not be interpreted as necessarily representing the official policies of the Energy Commission or the State of California.

REFERENCES

1. Vinod Dugal, Cummins, Personal Communication, July 24, 1997.

2. Jerry Hunt, Detroit Diesel, Personal Communication, July 22, 1997.

3. Acurex Environmental Corporation Final Report FR-94-123, "Alternative-Fueled Truck Demonstration Natural Gas Program: Caterpillar G3406LE Development and Demonstration," January 31, 1995.

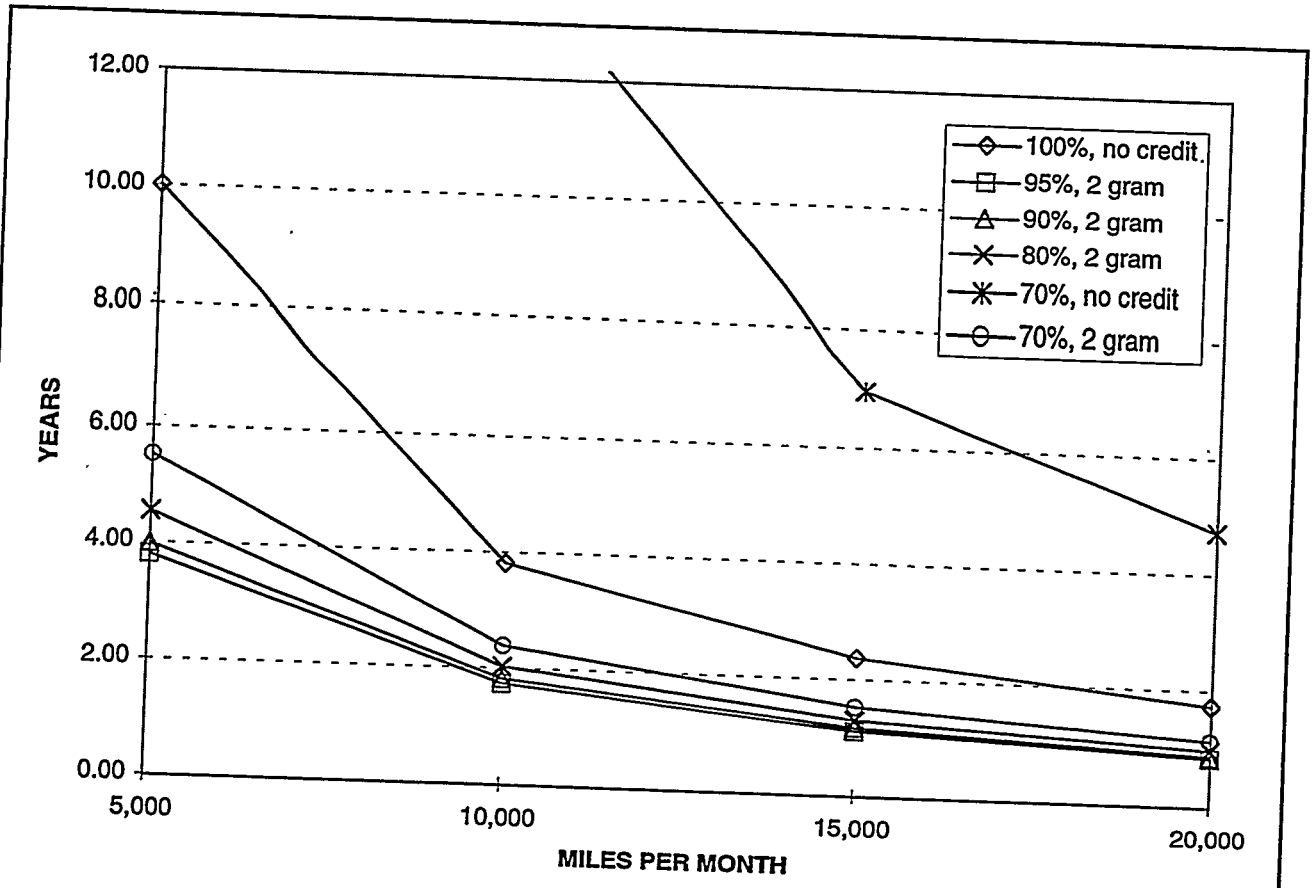
4. Acurex Environmental Corporation Draft Final Report FR-97-101, "Alternative-Fueled Truck De-monstration: Natural Gas Program," March 21, 1997 and Monthly Progress Reports.

5. Acurex Environmental Corporation Final Report FR-96-110,"LNG Heavy Duty Truck Demonstration Program," September 27, 1996 and Monthly Progress Reports.

6. Jack B. Kelley, Inc., Monthly Technical Progress Reports.

7. City of Long Beach, Federal Grant DE-FG51-94R900029, Monthly operating data reported to the NREL Alternative Fuels Data Center.

APPENDIX - NATURAL GAS TRUCK AMORTIZATION



MILES/MO	100%, no credi	95%, 2 gram	90%, 2 gram	80%, 2 gram	70%, no credit	70%, 2 gram
5,000	10.01	3.80	3.99	4.54		5.51
10,000	3.81	1.72	1.80	2.01	13.90	2.38
15,000	2.37	1.11	1.16	1.30	6.96	1.52
20,000	1.72	0.82	0.86	0.96	4.72	1.12
Efficiency % of diesel	100%	95%	90%	80%	70%	70%
NOx g/bhp-hr LNG	2	2	2	2	2	2
NOx g/bhp-hr DSL	4	4	4	4	4	4
CF-LNG (mi/bhp-hr)	4.1	4.1	4.1	4.1	4.1	4.1
CF-DSL (mi/bhp-hr)	4.3	4.3	4.3	4.3	4.3	4.3
NOx g/mi LNG	8.2	8.2	8.2	8.2	8.2	8.2
NOx g/mi DSL	17.2	17.2	17.2	17.2	17.2	17.2
NOx $/ton	$0	$10,000	$10,000	$10,000	$0	$10,000
Diesel mpg	6.9	6.9	6.9	6.9	6.9	6.9
LNG mpg	4.002	3.8019	3.6018	3.2016	2.8014	2.8014
Diesel price	$1.50	$1.50	$1.50	$1.50	$1.50	$1.50
LNG price	$0.50	$0.50	$0.50	$0.50	$0.50	$0.50
Interest rate	10.00%	10.00%	10.00%	10.00%	10.00%	10.00%
LNG gal	0.58	0.58	0.58	0.58	0.58	0.58
Cap. Cost Differential	$35,000	$35,000	$35,000	$35,000	$35,000	$35,000

U.S. DOE INDIRECT COAL LIQUEFACTION PROGRAM: AN OVERVIEW

J. Shen, E. Schmetz, J. Winslow, and R. Tischer, U.S. Department of Energy
R. Srivastava, Burns and Roe

INTRODUCTION

Coal is the most abundant domestic energy resource in the United States (U.S.). The Fossil Energy organization within the U.S. Department of Energy (DOE) has been supporting a coal liquefaction program to develop improved technologies to convert coal to clean and cost-effective liquid fuels to complement the dwindling supply of domestic petroleum crude. The goal of this program is to produce coal liquids that are competitive with crude at $20 to $25 per barrel. Indirect and direct liquefaction routes are the two technologies being pursued under the DOE coal liquefaction program.

In indirect liquefaction, coal is gasified in the presence of steam and oxygen to produce a synthesis gas (syngas) containing mostly carbon monoxide and hydrogen. This syngas, after being cleaned of impurities and adjusted to the desired H_2/CO ratio (if required), is converted in the presence of catalysts. A unique feature of the indirect liquefaction is its ability to produce a broad array of sulfur and nitrogen free products including motor fuels, methanol, mixed alcohols, dimethyl ether (DME), and chemicals with the use of different combinations of catalysts and process conditions. The conversion of syngas to liquid hydrocarbon fuels is known as Fischer-Tropsch (F-T) synthesis. In addition to coal, other carbonaceous feedstock also can be used in indirect liquefaction applications, including natural gas, petroleum/oil sands coke, petroleum resid, biomass, and municipal/refinery wastes.

Commercial indirect liquefaction plants to produce motor fuels have been in operation since 1955, including coal based plants in South Africa, and natural gas based plants in New Zealand, Malaysia, and South Africa. All these plants use F-T technology, with the exception of the New Zealand plant which uses a Mobil MTG (methanol to gasoline) technology. In addition, a coal to methanol plant has been in operation in U.S. since 1983. In all these plants, the syngas is converted in gas phase reactors. Because of the high exotherm (heat release) associated with the reactions, it has long been known that a liquid phase reactor could offer both cost and operational flexibility advantages over gas phase reactors due to its superior heat transfer capability and simpler reactor design. Earlier work in liquid phase reactor technology after World War II was suspended because of the cheap petroleum crude price. Interests in this technology was revived in the late 1970s with the rise in crude price. Scoping economics study supported by DOE and Electric Power Research Institute (EPRI) indicated that the capability of a liquid phase reactor to process a lean syngas (low H_2/CO ratio syngas) produced from advanced coal gasifiers could offer substantial cost advantages over the gas phase reactors (Gray et al., 1980; Brown et al. 1982). In the early 1980s, DOE began to support a R&D program to advance the liquid phase reactor technology aimed for coal based applications under joint efforts with the industries. In 1989 liquid phase methanol technology was successfully demonstrated at the proof-of-concept (POC) unit at LaPorte, Texas under cost shared contracts with Air Products and Chemicals, Inc. (Air Products). Subsequent efforts have been directed at extending the know-how to the development of liquid phase dimethyl ether (DME) and slurry phase F-T technologies. Recent publications indicate that other industrial companies also have been active in the area of slurry phase F-T technology development (Fourie 1995; Eisenberg et al. 1993). Liquid phase reactor also is known as slurry phase reactor and the two terms are considered interchangeable in this paper.

This paper will give an overview of the DOE indirect liquefaction program. More detailed discussions will be given to the F-T diesel and

DME fuels which have shown great promises as clean burning alternative diesel fuels. We also will briefly discuss the economics of indirect liquefaction and the hurdles and opportunities for the early commercial deployment of these technologies. Our discussions will be preceded by two brief reviews on the liquid versus gas phase reactors and the natural gas versus coal based indirect liquefaction.

LIQUID PHASE VERSUS GAS PHASE SYNGAS CONVERSION REACTORS

A schematic drawing of the liquid phase and the two commercial Sasol gas phase reactors now in operation in South Africa is shown in Figure 1. In a liquid phase reactor, the fine catalyst particles are suspended in a liquid medium by a syngas stream on the shell side of the reactor. In a gas phase reactor, the catalysts are packed inside the tubes in a fixed bed gas reactor, and are circulated around the loop by the syngas stream on the shell side of a fluidized bed Synthol reactor. In addition to higher transfer capability, liquid phase reactor also has the advantage that it can process a sub-stoichiometric hydrogen to CO ratio syngas, partially because of the higher hydrogen to CO ratio on the catalyst surface than the bulk gas phase due to the differences in the solubility and diffusivity between hydrogen and CO in the liquid medium. A recent publication indicates that the current know-how has deemed it feasible to design a 10,000 barrels per day slurry phase F-T reactor (Sasol 1997).

NATURAL GAS VERSUS COAL BASED INDIRECT LIQUEFACTION

Natural gas is richer in hydrogen than coal, and thus produces a syngas with a higher hydrogen to CO ratio. Depending on the technology used, natural gas can be converted to a syngas with a hydrogen to CO ratio in the 1.8 to 5.4 range. In the Shell F-T plant in Malaysia, the syngas is produced by a combination of partial oxidation (POX) and steam reforming which leads to a hydrogen to CO ratio close to the stoichiometric value of 2. Recent publications indicate that other F-T developers have opted to use a catalytic autothermal reforming technology to produce syngas from natural gas (Agee 1997). Cobalt catalyst is the choice for F-T synthesis with natural gas based syngas, partially because it does not have a concurrent water gas shift (WGS) activity which would convert CO and water to hydrogen and carbon dioxide.

Advanced POX gasifiers are now the choice for coal gasification because of the higher thermal efficiency. In these gasifiers, coal is converted to a syngas with a H_2/CO ratio in the 0.5 to 0.9 range. At the Eastman Chemical Company (Eastman) coal to methanol plant, the syngas from a Texaco gasifier is first shifted in a separate step to increase the hydrogen to CO ratio to the stoichiometric value of 2. In the Sasol coal based F-T plants in South Africa, syngas is produced from the first generation Lurgi gasifier which yields a syngas with hydrogen to CO ratio of 1.9. F-T synthesis is carried out over an iron catalyst which has a concurrent WGS activity. No separate WGS step is installed in the Sasol plants.

DOE INDIRECT LIQUEFACTION PROGRAM

The DOE indirect liquefaction program is aimed to develop a liquid phase reactor/catalyst system which can convert syngas from advanced POX gasifiers to various clean liquid fuels and chemicals without a prior WGS step. This technology has the advantage that it can be readily integrated into an Integrated Gasification Combined Cycle (IGCC) for power, fuels, and chemicals coproduction.

LIQUID PHASE METHANOL REACTOR TECHNOLOGY

Liquid phase methanol is the first technology developed under the DOE indirect liquefaction program. Its feasibility is demonstrated in a 120 day run conducted in 1989 at the LaPorte POC facility using a commercial methanol catalyst in a once-through mode with a 0.67 hydrogen to CO ratio syngas simulating that from a Texaco coal gasifier. The methanol from this technology has a water content less than 1%, and meets the fuel grade methanol specifications. For comparison, the methanol from commercial gas phase reactor would have a water content of 10% because of the hydrogen rich environment in the reactor. More details on the development

highlights of the liquid phase methanol technology can be found elsewhere (Shen et al. 1996).

Liquid phase methanol is now undergoing commercial demonstration under a cost-shared contract jointly supported by the industry and DOE Clean Coal Technology program. This demo plant is located at the Eastman complex in Kingsport, TN, and uses a syngas produced from a Texaco coal gasifier on the site. Its construction began in October 1995 and was completed in December 1996. The plant initiated operation in April 1997 and achieved the design rate of 260 tons of methanol per day on the third day after the startup. This represents a successful 26-fold scale up from the 10 tons per day proof-of-concept (POC) scale plant. Chemical grade methanol produced from this demonstration plant has met the specifications and now accepted by Eastman for captive chemical feedstock uses in the complex.

The demonstration project is managed by the Air Products Liquid Phase Conversion Company, L.P., which is a joint venture between Air Products and Eastman. The funding mix between the joint venture and DOE is 43%/57%. It will be operated for four years to demonstrate the reactor operability over a wide range of process conditions and syngas compositions, as well as to prove out the important features which will enable the integration of this technology into an IGCC facility for power/methanol co-production. Fuel grade methanol produced from a low hydrogen to CO ratio syngas will be collected and used in a concurrent product testing program to demonstrate its various commercial applications, including fuels for transportation use and power production.

The opportunity for the commercial deployment of liquid phase methanol technology for power and methanol coproduction has recently been reviewed (Osterstock et al. 1997).

LIQUID PHASE DIMETHYL ETHER (DME) TECHNOLOGY

DME (CH_3-O-CH_3) is manufactured today by the dehydration of two molecules of methanol. In the liquid phase DME technology, the methanol synthesis and the subsequent methanol dehydration to DME are carried out in a single reactor by using a binary physical mixture of catalysts for these two separate activities. Again, this technology is aimed for coal based syngas coproduction applications. It is being developed under joint efforts between Air Products and DOE. There have been considerable industrial interests in this one-step synthesis gas-to-DME technology, which would offer cost advantages over the conventional two-stage process. DME is now primarily used as precursors for chemicals, but has shown potential as a super clean diesel fuel (Fleisch et al.1995). Haldor-Topsoe recently has reported the technology of a single step gas phase reactor to convert natural gas based syngas to DME (Hansen et al. 1995).

Feasibility of liquid phase DME technology for a 0.67 hydrogen to CO ratio syngas was first demonstrated by Air Products at the LaPorte POC unit in 1991. Continued work since then at the bench scale unit has led to the development of modified methanol dehydration catalysts with substantial improvement in activity and life maintenance over the earlier versions (Peng et al. 1996). Discussions are underway between Air Products and catalyst manufacturing companies to scale up the production of these newly developed dehydration catalysts. A demonstration run to prove out the superiority of the new binary catalyst system at the LaPorte POC unit is tentatively planned for 1998.

Recent research by Air Products shows that the DME molecules can be coupled to form a mixture called "DME soup" which would have boiling point range comparable to that of a conventional diesel. Preliminary data indicates this coupled DME mix have a cetane number over 100 and could be used as a blending component for the conventional diesel. .

SLURRY/LIQUID PHASE F-T TECHNOLOGY

F-T Synthesis Chemistry: Unlike methanol synthesis, products from F-T synthesis are a mixture of hydrocarbons with carbon number ranged from C_1 to C_{40} or higher, which can be predicted by the Anderson-Flory-Schulz distribution developed for the polymerization

reactions using a single parameter called "alpha" (probability of chain growth). The basic building block, $-CH_2-$, is formed from Reaction (1). The chain growth terminates when a molecule disassociates from the catalyst surface. The probability of chain termination is defined as (1-alpha). The value of alpha in F-T synthesis is controlled by the catalyst composition and process conditions. The fraction of F-T products, which has a carbon number greater than 20, is called wax. It can easily be refined to produce gasoline and distillate. Thus, the product slate selectivity from F-T synthesis can be varied by F-T catalyst alpha, the F-T wax refining conditions, or a combination of the two. For the Shell F-T plant in Malaysia which uses a high alpha cobalt catalyst, the following product slate selectivity has been reported (Tijm et al. 1995).

Product slate % wt	Diesel mode	Kerosene mode
Naphtha	15	25
Kerosene	25	50
Diesel	60	25

For F-T iron catalyst which also has WGS activity, Reaction (2) occurs in parallel with Reaction (1). A combination of Reactions (1) and (2) yields Reaction (3), indicating that F-T synthesis could proceed with a syngas having a 0.5 hydrogen to CO ratio in case an iron catalyst is used. The feasibility of processing a 0.67 hydrogen to CO ratio syngas in a slurry phase F-T reactor with an iron catalyst was successfully demonstrated at the bench scale unit by Mobil under cost-shared contracts with DOE. More detailed review of the Mobil work can be found elsewhere (Shen et al. 1996). It should be noted that the wax fraction of the F-T products would remain in the slurry phase reactor and has to be removed after separation from the catalysts.

$$2\,H_2 + CO \rightarrow -CH_2- + H_2O \quad (1)$$

$$H_2O + CO \rightleftharpoons H_2 + CO_2 \quad (2)$$

$$H_2 + 2\,CO \rightarrow -CH_2- + CO_2 \quad (3)$$

Slurry Phase F-T Operations at LaPorte POC Unit: Three slurry phase F-T runs have been made at the LaPorte POC unit between 1992 and 1996, with costs shared by different industrial consortiums headed by Air Products. The first two runs used iron catalysts and their results have been reviewed in details (Bhatt et al. 1995a, 1995b, 1995c). The third run used a cobalt catalyst and its data workup is now in progress. All three runs indicate that catalyst/-wax separation remains to be a challenging problem for slurry phase F-T reactor technology development.

F-T Catalyst Development: In the F-T catalyst development area, the Kentucky Center for Applied Energy Research (CAER), in conjunction with the United Catalyst, Inc., has reported successful results at bench scale unit of a low alpha iron catalyst with improved activity and life maintenance using a 0.67 hydrogen to CO ratio syngas (O'Brien et al. 1996). Our immediate future effort is to modify this catalyst to increase its alpha value to an intermediate value to produce straight chain alpha olefins in the C_5 to C_{15} range. This represents our continued effort to improve the iron catalyst versatility to produce a broader array of high value chemicals in addition to fuels to further enhance the profitability of plants based on this technology.

Synthesis Gas to Oxygenates and Chemicals : Novel catalyst R&D cost shared with industry and universities has been underway to explore the use of synthesis gas as an alternative feedstock to produce oxygenate octane enhancers and oxygenate based chemicals which would offer cost advantages over the conventional technologies. The products include mixed alcohols including isobutanol (Xu et al. 1996), vinyl acetate monomer (Tustin et al. 1996), methyl methacrylate (Spivery et al. 1996), and dimethyl carbonate (Hagen 1996). The industrial participants in this effort include Air Products, Eastman, and Amoco.

Slurry-Phase Bubble Column Reactor (SBCR) Hydrodynamics: A five-year engineering development study for the SBCR system has been underway since 1995 under a cost-shared contract with Air Products. The two sub-contractors are: Ohio State University and Washington University (St. Louis, MO). Sandia National Lab, through a separate contract with DOE, also is a participant to this project. The expertises of these participants will be joined to

develop an improved SBCR design data base by combining the know-how gained from the hydrodynamics studies conducted in the non-reacting and reacting systems under the commercially prevalent conditions. A second objective of this study is to gain a better fundamental understanding of the SBCR hydrodynamics. More detailed descriptions of the proposed contract work can be found elsewhere (Degaleesan et al. 1996; Jackson et al. 1996). Separately, an in-house research group at the DOE/Federal Energy Technology Center has been developing new diagnostic techniques to aid the SBCR hydrodynamics studies (Soong et al., 1995)

ENVIRONMENTAL PREMIUMS FOR DME AND F-T DIESEL

DME and F-T diesel, which are free of sulfur and aromatics and have high cetane number, are both known to have potential as a cost-effective, super clean diesel fuels. Engine testing with DME supported by an industrial consortium shows that the emissions from DME fuels would meet the California Ultra Low Emissions Vehicle (ULEV) regulations for medium-duty vehicles (Fleisch et al.1995). In a separate study funded under cost-shared contracts with DOE, emissions from F-T diesel are reduced by up to 40% when compared with a conventional petroleum diesel (Montalvo1995). More recent data indicate that the emissions from a F-T diesel used in advanced diesel engines also would meet the ULEV regulations (Starr 1997). Review of the earlier diesel engine testing with blends of petroleum and F-T diesel fuels can be found elsewhere (Shen et al. 1996).

ECONOMICS OF INDIRECT LIQUEFACTION

A DOE supported study by Bechtel indicates that indirect coal liquefaction is competitive with conventional crude oil production and refining at a crude cost of $34 per barrel based on the current status of slurry F-T technology. The conceptual commercial plant, which is located at an Illinois #6 coal mine site, produces 50,000 barrels/day of gasoline and diesel fuels meeting and/or exceeding market specifications. This product cost represents a value in reference to a crude used by a typical refinery in the local area, and is called crude oil equivalent (COE) price. Subsequent studies show that this cost could be reduced to $27 per barrel with continued R&D in both slurry phase F-T synthesis and the upstream syngas production steps. In special cases where the F-T plant is located adjacent to an existing refinery, the COE price could be reduced to the $20-25 per barrel range (Gray et al. 1995; Gray et al. 1996). A schematic drawing of the COE prices for different cases is shown in Figure 2.

HURDLES AND OPPORTUNITIES FOR THE COMMERCIAL DEPLOYMENT OF INDIRECT LIQUEFACTION TECHNOLOGY

The DOE liquid phase reactor technology development has been focused on its integration into an IGCC plant to coproduce power, fuels, and chemicals. Our analysis shows this mode of operation offer the best promise for the early commercial deployment of this technology in the U.S. One of the main hurdles for this deployment strategy is the technical risks inherent in the individual gasification and F-T synthesis steps, and also in the system integration. The technical risks associated with the gasification step should be greatly reduced with the ongoing commercial demonstration of several advanced gasification technologies in the IGCC projects supported by the DOE Clean Coal Program (DOE 1996a, 1996b, 1996c). Because of the current federal budget constraints, financing for the commercial demonstration of slurry phase F-T technology could pose a challenging problem. We have explored the concept of a pioneer plant which would employ a single commercial train slurry phase F-T reactor and located adjacent to a facility with existing infrastructures. We feel that the formation of an industry led consortium would be an appropriate vehicle to undertake this pioneer plant project. We also feel that financial incentives would be needed for the first few pioneer plants to compensate for the technical and market risks associated with these projects. One of the important features of these pioneer plants will be their capability to process feedstock beyond coal to include other carbonaceous materials like petroleum coke, wastes, and biomass. We are considering joining with industry to conduct a preliminary feasibility study for this pioneer plant which would include site

selection, a financial plan, the types of incentives needed, and additional R&D support required. More discussions on this subject can be found elsewhere (Gray et al., 1997; Schmetz et al. 1996; Schmetz et al. 1997). Results have been reported on several case studies which deploy the indirect liquefaction technologies in commercial applications to coproduce power and fuels (Osterstock et al. 1997; Gray et al. 1997; Tam 1993).

Recent publications also indicate that the deployment of IGCC for power, hydrogen and syngas production has received more commercial commitments and/or interests with choices of feedstock including natural gas, petroleum coke, refinery wastes, and petroleum residue (Chemical Week 1996; Rhodes 1996; Aalund, 1996; Oil & Gas Journal 1997). These projects are case specific and have been undertaken for a variety of reasons including the needs to dispose byproducts, to reduce plant emissions in com-pliance with environmental regulations, and to meet the niche market demands in the local areas. With more and more IGCC systems in place and/or under considerations, the opportunity to add an indirect liquefaction component to coproduce premium transportation fuels and chemicals in addition to power could offer the best prospects for the early commercial deployment of the indirect liquefaction technologies. With the learning experience gained from these early entrant operations, a transition to a coal based indirect liquefaction could be underway with greatly reduced technical risks between 2010 and 2015 when coal liquids would become competitive with crude.

CONCLUSIONS

We have presented an updated summary of the work performed under the DOE indirect liquefaction program since 1994. We also have summarized the recent diesel engine emission data with DME and F-T diesel as the test fuels. Finally, we have discussed the prospects for the early commercial deployment of indirect liquefaction in an IGCC facility to coproduce power, fuels, and chemicals. We feel that the appeal for coproduction concept would be enhanced with continued R&D to develop more versatile iron catalysts to produce a broad array of high value chemicals in addition to fuels.

REFERENCES

1. Aalund, L.R., "Italian Refinery Gasification Project to Make Electricity, Steam, and Hydrogen from Tar", Oil & Gas Journal, P. 33, October 21, 1996

2. Agee, M.A. 1997 "Economic Conversion of Natural Gas to Synthetic Petroleum Liquids", Paper Presented at the ACS National Meeting, San Francisco, CA, April 14-17, 1997

3. Bhatt, B.L., R. Frame, A. Hoek, K. Kinnari, V.U.S. Rao, and F.L. Tungate 1995a "Catalyst Processing Scale-up for Fischer-Tropsch Synthesis", Topics in Catalysis 2 (1995) 235-257.

4. Bhatt, B.L. 1995b, "Liquid Phase Fischer-Tropsch (II) Demonstration in the LaPorte Alternative Fuels Development Unit", topical Research Report, Prepared by Air Products and Chemicals for the US. DOE, contract No. DE-AC22-91PC90018, September, 1995

5. Bhatt, B.L., D.M. Brown, E.C. Heydorn, Hoek, A., and G.J. Stiegel 1995c "Productivity Improvements for Fischer-Tropsch Synthesis", 14th North American Meeting of the Catalysis Society, Snowbird, Utah, June 11-16, 1995

6. Brown, R.E., et al. 1982. "Economic Evaluation of the Co-Production of Methanol and Electricity with Texaco Gasification-Combined-Cycle Systems", EPRI AF-2212, Project 239-2, Final Report, January 1982

7. Chemical Week 1996. "Texaco and Praxair in syngas Venture", Pg. 15, March 27, 1996

8. Degaleesan, S., S. Kumar, M.P. Dudukovic, B.A. Townsend, and B.L. Bhatt 1996 "Progress in Understanding the Fluid Dynamics of Bubble Column Reactors", Paper Presented at the DOE First Joint Power and Fuels Systems Contractors Conference, July 9-11, 1996

9. DOE Clean Coal Technology Topical Report 1996a "The Tampa electric Integrated Gasification Combined-Cycle Project", Topical Report No.6, October 1996

10. DOE Clean Coal Technology Topical Report 1996b "The Wabash River Coal Gasification Repowering Project", Topical Report No.7, November 1996

11. DOE Clean Coal Technology Topical Report 1996c "The Pinon Pine Power Project", Topical Report No.8, December 1996

12. Eisenberg, B., G.C. Lahn, R.A. Fiato, and G.R. Say 1993 "Exxon AGC-21 Advanced Gas Conversion Technology", Paper Presented at the at the Council on Alternate Fuels' Alternate Energy '93, April 27-30, 1993

12. Fleisch, T., C. McCarthy, A. Basu, C. Udovich, P. Charbonneau, W. Slodowske, S. Mikkelsen, and J. McAandless 1995. "A New Clean Diesel Technology: Demonstration of ULEV Emissions on a Navistar Diesel Engine Fueled with Dimethyl Ether", SAE Paper Series No. 950061, February 27-March 2, 1995

13. Fourie, J.H., 1995 "Sasol Update 1995", Paper Presented at the Council on Alternate Fuels 15th Annual Spring Conference, May 1-4, 1995

14. Gray, D., et al. 1980 "The Impact of Developing Technology on Indirect Liquefaction", MTR-80W326, Mitre Corp., November, 1980

15. Gray, D. and G. Tomlinson 1995 "Rationale for Continuing R&D in Indirect Coal Liquefaction", Proceedings for the Coal Liquefaction and Gas Conversion Contractors Review Conference, Pittsburgh, PA, August 29-31, 1995

16. Gray, D. and G. Tomlinson 1996 "Rationale and Proposed Strategy for Commercial Deployment of Coal-Derived Transportation Fuels", MP 96W0000209, Mitretek Systems, June 1996

17. Gray, D., and G. Tomlinson 1997 "Opportunities for Early Commercial Deployment of Indirect Liquefaction", Paper Presented at the American Chemical Society Meeting, San Francisco, CA, April 13-17, 1997 .

18. Hagen, G.P. 1996 "Synthesis of Oxygenate Products for High Volume Fuels Applications", Paper Presented at the First Joint Power & Fuel Systems Contractors Conference, Pittsburgh, PA, July 9-11, 1996

19. Hansen, J.B., B. Voss, F. Joensen, and I.D. Siguroardottir 1995. "Large Scale Manufacture of Dimethyl Ether - a New Alternative Diesel Fuel from Natural Gas", SAE Paper Series No. 950063, February 27-March 2, 1995

20. Jackson, N., J.R. Torczynski, K.A. Schollenberger, T.J. O'Hern, and D.R. Adkins 1996 "Sandia Support for PETC Fischer-Tropsch Research: Experimental: Characterization of Slurry Phase Bubble Column Reactor Hydrodynamics", Paper Presented at the DOE First Joint Power and Fuels Systems Contractors Conference, July 9-11, 1996

21. Montalvo, D.A. 1995 "Engine Evaluation of Fischer-Tropsch Diesel Fuel, Phase I", Final Report, Prepared for Bechtel Group by Southwest Research Institute under DOE Contract DE-AC22-93PC91029, October 1995

22. O'Brien, R.J., Raje, A., R.L. Spocer, L. Xu, S. Bao, R.A. Keogh, S.H. Lambert, S. Liaw, S. Chokkaram, D.J. Houpt, and B.H. Davis 1996, "Technology Development for Iron Fischer-Tropsch Catalysts", Paper Presented at the DOE First Joint Power and Fuels Systems Contractors Conference, July 9-11, 1996

23. Oil & Gas Journal 1997. "Cogeneration: Star Enterprises .....", April 7, 1997

24. Osterstock, E.R., J. Klosek, and K.W. Guy 1997. "Dispatchable IGCC Facilities: Flexibility through Coproduction", Paper Presented at the Power-Gen Europe 97, Madrid, Spain, June 17-19, 1997

25. Peng, X.D., G.E. Parris, B.A. Toseland, and R.P. Underwood 1996 "Some Advances in Catalysts for alternative Fuels", Paper Presented at the DOE First Joint Power and Fuels Systems Contractors Conference, July 9-11, 1996

26. Rhodes, A.K., "Kansas Refinery Starts Up Coke Gasification Unit", Oil & Gas Journal, P. 31, August 5, 1996

27. Sasol 1997. "Natural Gas to Liquids in Qatar", a Sasol Limited Media Reelease, March 19, 1997

28. Schmetz, E., J. Shen, and D. Gray 1996 "Coal Liquids: A Domestic Option for Liquid Transportation Fuels", Paper Presented at the Pittsburgh Coal Conference, September 4, 1996

29. Schmetz, E., J. Shen, G. Stiegel, and R. Tischer 1997 "DOE Indirect Coal Liquefaction Program - Hurdles and Opportunities for its Early Commercialization", Paper Presented at the American Chemical Society National Meeting, April 1997

30. Shen, J., G. Stiegel, and A.C. Bose 1996 "DOE Indirect Coal Liquefaction Program - An Overview". Fuel Sciences & Technology Int'l., 14(4), 559-576 (1996)

31. Soong, Y., I.K. Gamwo, F.W. Harke, A.G. Blackwell, and M.F. Zarochak 1995 "Fischer-Tropsch Slurry Reactor Modeling", Proceedings of Coal Liquefaction and Gas Conversion Contractors Review Conference, August 29-31, 1995

32. Spivery, J.J., M.R. Gogate, J.R. Zoeller, R.D. Colberg, G.N. Choi, and S.S. Tam 1996 "Synthesis of Methyl Methacrylate from Coal-Derived Syngas", Paper Presented at the First Joint Power & Fuel Systems Contractors Conference, Pittsburgh, PA, July 9-11, 1996

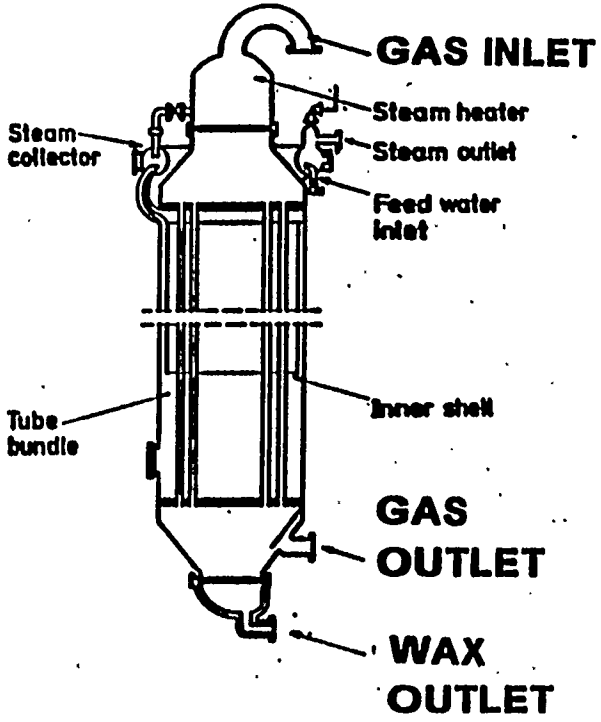
33. Starr, M.E. 1997. "Heavy-Duty Transient Emissions at Various Engine Timings Using Fischer-Tropsch Fuel", Final Report, Prepared for Bechtel Group by Southwest Research Institute under DOE Contract DE-AC22-93PC91029, April, 1997

34. Tam, S.S. 1993. "Indirect Coal Liquefaction Via Fischer-Tropsch Technology for the Baseload IGCC Plant", IEA Second International conference on the Clean and Efficient Use of Coal and Lignite: Its Role in energy, environment and Life", November 30-December 3, 1993

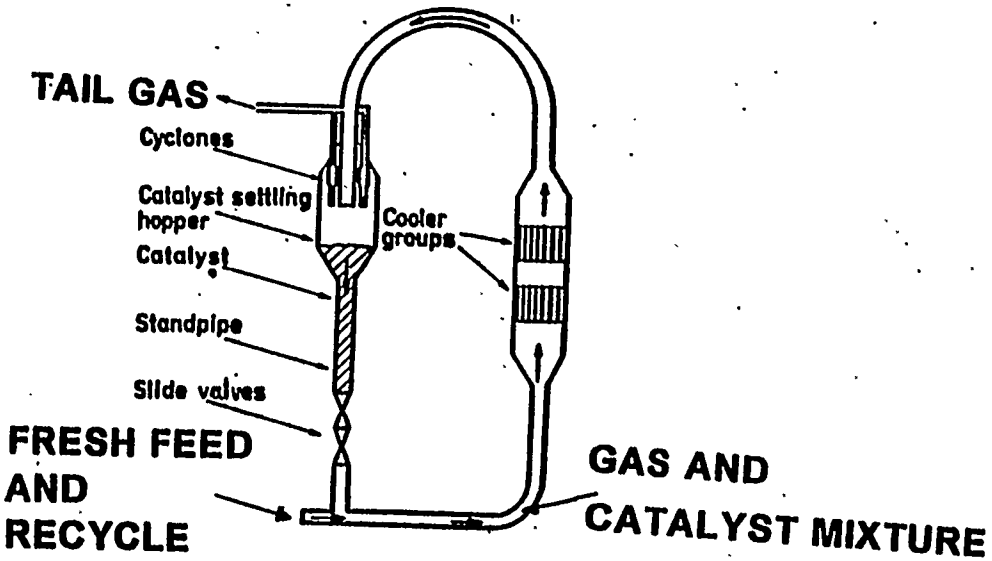
35. Tustin, G.C., J.R. Zoeller, and L. DePew 1996 "Synthesis of Vinyl Acetate Monomer from Synthesis Gas", Paper Presented at the First Joint Power & Fuel Systems Contractors Conference, Pittsburgh, PA, July 9-11, 1996

36. Xu, M., B.L. Stephens, M.J.L. Gines, and E. Iglesia 1996 "Reaction Pathways and Catalyst Requirements in the synthesis of Isobutanol from CO and Hydrogen", Paper Presented at the First Joint Power & Fuel Systems Contractors Conference, Pittsburgh, PA, July 9-11, 1996

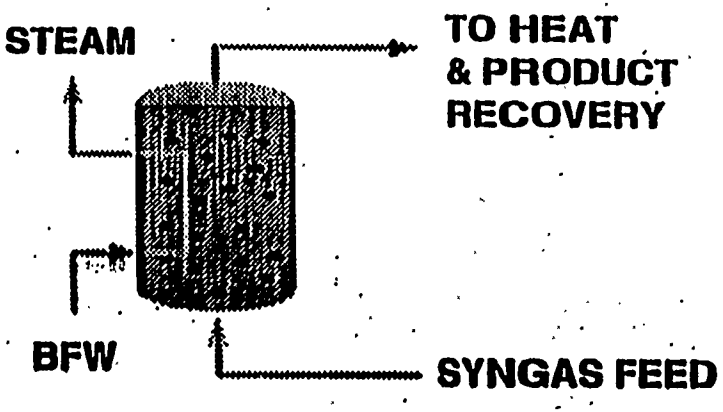
FIGURE 1 GAS AND LIQUID PHASE REACTORS



SASOL FIXED BED REACTOR



SASOL SYNTHOL REACTOR



LIQUID PHASE REACTOR

FIGURE 2 Continued R&D Can Significantly Reduce Fuel Cost and Time to Deployment

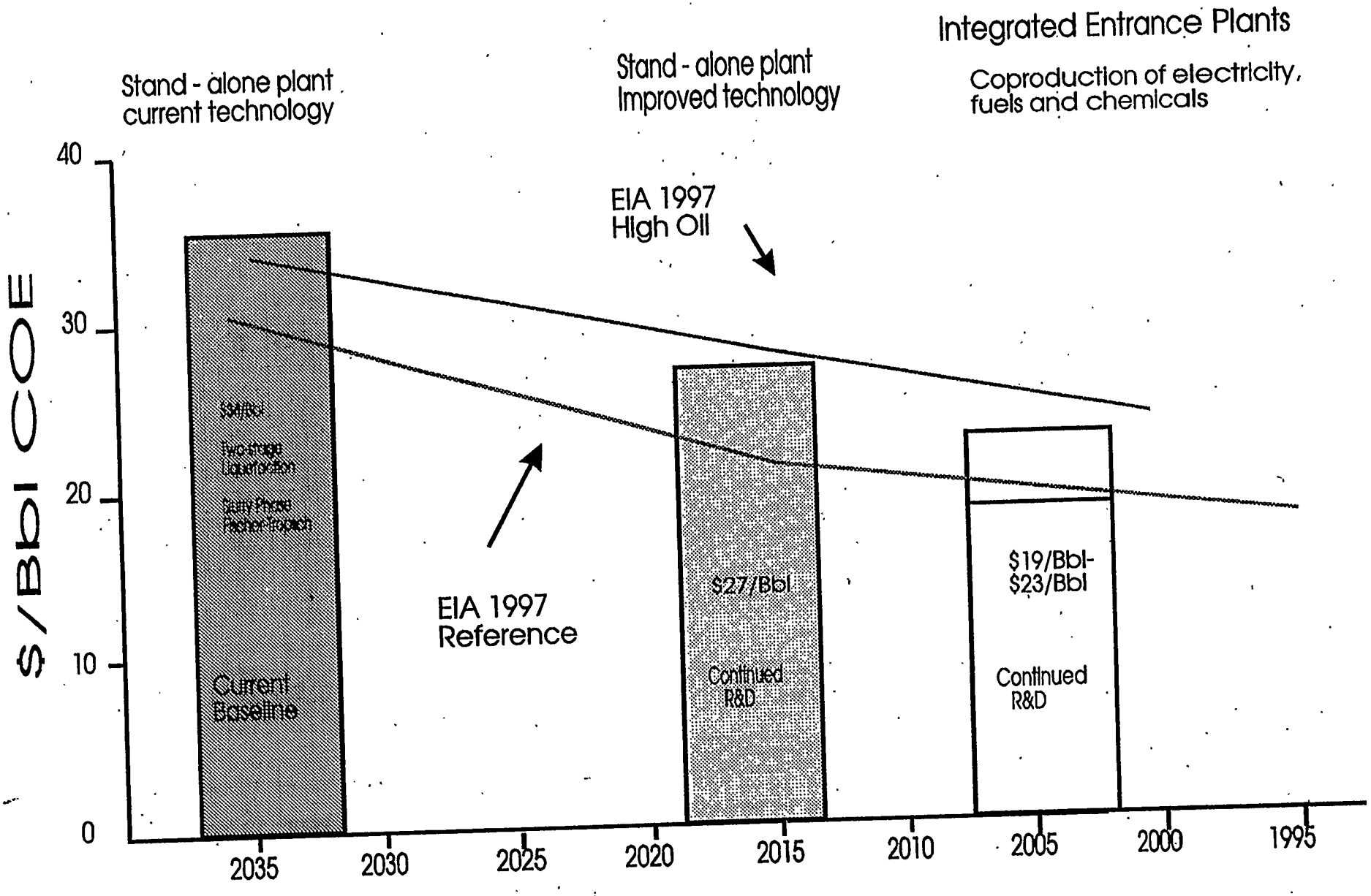


FIGURE 3: STATUS (INDIRECT LIQUEFACTION)

COMMERCIAL (GAS PHASE REACTOR)

- SOUTH AFRICA: SASOL (COAL TO MOTOR FUELS) & MOSSGAS (NATURAL GAS TO MOTOR FUELS)
- NEW ZEALAND: MOBIL MTG (NATURAL GAS TO GASOLINE)
- U.S.A. EASTMAN CHEMICALS (COAL TO METHANOL)
- MALAYSIA: SHELL (NATURAL GAS TO MOTOR FUELS)

UNDER DEMONSTRATION (LIQUID/SLURRY PHASE REACTOR)

- SOUTH AFRICA: SASOL (COAL TO MOTOR FUELS)
- U.S.A.: EXXON (NATURAL GAS TO MOTOR FUELS)
- U.S.A. : DOE/AIR PRODUCTS/EASTMAN (COAL TO METHANOL)

PRE-DEMONSTRATION/BENCH UNIT DEVELOPMENT

- NG BASED: SYNTROLEUM, RENTECH, SHELL, TEXACO, CONOCO/DUPONT, ENI
- COAL BASED: CHINA

FIGURE 4: INDIRECT LIQUEFACTION TECHNOLOGY PORTFOLIO

LIQUID PHASE METHANOL

- HIGHLIGHTS OF POC OPERATIONS
  - 0.67 H_2 TO CO RATIO SYNGAS (TEXACO GASIFIER)
  - RAW METHANOL MEET FUEL GRADE SPEC
  - ACHIEVED 10 TONS/DAY (TPD) RATE
- COMMERCIAL DEMONSTRATION UNDERWAY

LIQUID PHASE DIMETHYL ETHER (DME)

SLURRY PHASE FISCHER-TROPSCH (F-T)

ALL THREE TECHNOLOGIES AIMED FOR CO-PRODUCTION APPLICATIONS

FIGURE 5 FUTURE WORK AT LAPORTE

SLURRY PHASE F-T IV RUN

- PARTICIPANTS: DOE/AIR PRODUCTS/SHELL OIL
- PRODUCE F-T DIESEL FOR ENGINE EMISSION TESTING
- COBALT F-T CATALYST

LIQUID PHASE DME RUN

- PARTICIPANTS: DOE/AIR PRODUCTS/EASTMAN CHEMICALS
- PROVE OUT IMPROVED CATALYST SYSTEM
- EQUIPMENT UPGRADING UNDER CONSIDERATIONS TO ALLOW FOR DME PRODUCTS COLLECTED FOR ENGINE EMISSION TESTING

FIGURE 3: STATUS (INDIRECT LIQUEFACTION)

COMMERCIAL (GAS PHASE REACTOR)
- SOUTH AFRICA: SASOL (COAL TO MOTOR FUELS) & MOSSGAS (NATURAL GAS TO MOTOR FUELS)
- NEW ZEALAND: MOBIL MTG (NATURAL GAS TO GASOLINE)
- U.S.A. EASTMAN CHEMICALS (COAL TO METHANOL)
- MALAYSIA: SHELL (NATURAL GAS TO MOTOR FUELS)

UNDER DEMONSTRATION (LIQUID/SLURRY PHASE REACTOR)
- SOUTH AFRICA: SASOL (COAL TO MOTOR FUELS)
- U.S.A.: EXXON (NATURAL GAS TO MOTOR FUELS)
- U.S.A. : DOE/AIR PRODUCTS/EASTMAN (COAL TO METHANOL)

PRE-DEMONSTRATION/BENCH UNIT DEVELOPMENT
- NG BASED: SYNTROLEUM, RENTECH, SHELL, TEXACO, CONOCO/DUPONT, ENI
- COAL BASED: CHINA

FIGURE 4: INDIRECT LIQUEFACTION TECHNOLOGY PORTFOLIO

LIQUID PHASE METHANOL

- HIGHLIGHTS OF POC OPERATIONS
  - 0.67 H_2 TO CO RATIO SYNGAS (TEXACO GASIFIER)
  - RAW METHANOL MEET FUEL GRADE SPEC
  - ACHIEVED 10 TONS/DAY (TPD) RATE
- COMMERCIAL DEMONSTRATION UNDERWAY

LIQUID PHASE DIMETHYL ETHER (DME)

SLURRY PHASE FISCHER-TROPSCH (F-T)

ALL THREE TECHNOLOGIES AIMED FOR COPRODUCTION APPLICATIONS

FIGURE 5 FUTURE WORK AT LAPORTE

SLURRY PHASE F-T IV RUN
- PARTICIPANTS: DOE/AIR PRODUCTS/SHELL OIL
- PRODUCE F-T DIESEL FOR ENGINE EMISSION TESTING
- COBALT F-T CATALYST

LIQUID PHASE DME RUN
- PARTICIPANTS: DOE/AIR PRODUCTS/EASTMAN CHEMICALS
- PROVE OUT IMPROVED CATALYST SYSTEM
- EQUIPMENT UPGRADING UNDER CONSIDERATIONS TO ALLOW FOR DME PRODUCTS COLLECTED FOR ENGINE EMISSION TESTING

FIGURE 6: DME FUEL PROPERTIES

PROPERTY	DIESEL	DME	PROPANE /BUTANE
FORMULA	———	CH3COCH3	C3H8/C4H10
BOILING POINT RANGE, °C	191-344	-25	-42/-0.5
VAPOR PRESSURE @ 20°C, BAR	LOW	5.1	8.4/2.1
LIQUID DENSITY @ 20°C, G/ML	0.8-0.84	0.668	0.501/0.610
LOWER HEATING VALUE, MJ/kg	42.5	28.4	46.4/45.7
CETANE NUMBER	40-55	55-60	—/—
IGNITION TEMP, °C	—	235	470/365

FIGURE 7: DIESEL FUEL PROPERTIES

PROPERTY	2D DIESEL	PSEUDO CARB DIESEL	F-T DIESEL
DENSITY G/ML @15°C	0.845	0.842	0.780
DISTILLATION RANGE			
IBP, °C	191	210	201
EP, °C	344	344	358
SULFUR, PPM	330	345	N.D.
CETANE NO.	46	50	76
FLASH POINT, °C	71	82	88
AROMATICS, V%	30	9	N.D.
CLOUD POINT, °C	-17	-16	1
POUR POINT, °C	-26	N.A.	N.A.

N.D. = NOT DETECTABLE
N.A. = NOT AVAILABLE

FIGURE 8: PIONEER PLANT CONCEPT FOR COMMERCIAL DEMONSTRATION

- LIQUID PHASE DME AND SLURRY PHASE F-T TECHNOLOGIES REQUIRE COMMERCIAL DEMONSTRATION TO MITIGATE TECHNICAL RISKS
- PIONEER PLANT PROPOSED TO CARRY OUT COMMERCIAL DEMO
  - -- A SINGLE COMMERCIAL TRAIN
  - -- INDUSTRY LED EFFORTS (TEAMING ARRANGEMENT)
  - -- FEEDSTOCK FLEXIBILITY BEYOND COAL
  - -- DOE TO COFUND FEASIBILITY STUDY
    - ** DEFINE ISSUES RELATED TO TECHNICAL & MARKET RISKS
    - ** SITE SELECTIONS
    - ** FINANCIAL PLAN
    - ** SUPPORT R&D

FIGURE 9: COAL VS NATURAL GAS BASED INDIRECT LIQUEFACTION

	COAL/COKE	NATURAL GAS
ATOMIC H/C RATIO	0.5-0.8	4.0
H_2 TO CO RATIO IN SYNGAS	0.5-0.7	1.75 - 5
CATALYSTS (F-T)	IRON & COBALT	COBALT & IRON
IMPURITIES IN SYNGAS	USE GUARD BED	—
PRODUCTS	FUELS, WAX, CHEMICALS	FUELS, WAX, CHEMICALS

FIGURE 10: PARTNERSHIP BETWEEN INDIRECT LIQUEFACTION AND OTHER DOE PROGRAMS

POTENTIAL PARTNERS	RELATIONSHIP W. IND . LIQ.	AREAS OF JOINT WORK
FE/IGCC POWER	SYNGAS/POWER PRODUCER	■ POWER/FUELS COPRODUCTION ■ SYSTEM INTEGRATION
FE/GAS TO LIQUIDS	SYNGAS/ FUELS PRODUCER	■ FUELS PRODUCTION ■ SYSTEM INTEGRATION ■ FUELS EMISSION TESTING
EE/HEAVY VEHICLE TECHNOLOGIES	FUELS USER	■ FUELS PRODUCTION ■ FUELS EMISSION TESTING

FIGURE 11: POLICY ISSUES

CO2 EMISSIONS FROM INDIRECT LIQUEFACTIONS

- COAL BASED TECHNOLOGY
- NATURAL GAS BASED TECHNOLOGY
- ISSUES: BENCH MARKING FUELS, ENVELOPE OF LIFE CYCLE ANALYSIS

FIGURE 11: CONCLUSIONS

- THE 260 TONS/DAY COMMERCIAL DEMONSTRATION PLANT FOR LIQUID PHASE METHANOL WAS SUCCESSFULLY STARTED UP IN 4/97.
- LIQUID PHASE DME AND SLURRY PHASE F-T ARE SCHEDULED FOR PROOF-OF-CONCEPT (POC) SCALE DEMONSTRATION IN 1998.
- F-T DIESEL AND DME SHOW PROMISE AS CLEAN ALTERNATIVE DIESEL FUELS WHICH WOULD MEET ULEV EMISSION SPEC.
- AN INDUSTRY-LED PIONEER PLANT CONCEPT HAS BEEN PROPOSED TO UNDERTAKE THE COMMERCIAL DEMONSTRATION OF LIQUID PHASE DME AND SLURRY PHASE F-T TECHNOLOGIES.
- ACTIVITIES SUPPORTED BY THE PROGRAMS OF INDIRECT COAL LIQUEFACTION, NATURAL GAS TO LIQUIDS, AND HEAVY VEHICLE TECHNOLOGIES OFFER BROAD COMMON GROUND FOR COOPERATIONS.

A STUDY OF EMISSION INDICES WITH F76 AND FUEL ADDITIVES

M. Osborne
U.S. Naval Sea Systems Command

INTRODUCTION

On and off-road engine exhaust regulations have focused principally on new diesel and gasoline engines. There has not been much emphasis on regulating existing diesel engines or gas turbines used in mobile applications. However, off-road gas turbines and existing diesel engines may some day also be impacted by air pollution (NO_x, SO_x, CO, CO_2, particulates, UHC, etc) regulations.

Two problems arise when considering the possible regulation of existing and new marine engines in military use. The first is cost. Projected retrofit cost for emission controls on all of the Navy's existing engines would be high. The second deals with balancing power density against the emission of air pollutants. Navy marine applications, like most mobile applications thrive on high power densities (in both weight and volume). However, high power den-sities will typically be accompanied by high fir-ing temperatures. In turn, high firing temperatures are a precusor to high emissions of ther-mal NO_x. Thus the challenge is to improve power density without increasing NO_x generation to the environment.

The injection of ammonia (or related chemicals) in the exhaust stream of gas turbines or diesel engines is a very effective means for removing NO_x before it is released into the environment. This method can reduce NO_x emissions up to 90 percent in fossil-fueled power plants if the chemicals are applied within a critical temperature window. For mobile engines as those on ships, additional equipment and retention of chemicals for the processes are sometimes inconvenient, if not impractical.

One solution is to add the NO_x-removing chemicals directly to the fuel to avoid the need for carrying extra equipment or chemicals. The challenge with this approach is to protect the chemical additive as it passes through the combustion flame zone so that it can reduce NO_x in the exhaust stream. The Texaco Research Center in Beacon, New York has been working on such an approach for diesel engines. Texaco Inc. has produced some experimental fuels additives that have shown promise in reducing NO_x in diesel engines, but had not been evaluated in gas turbines.

The fuel (NATO F76) used by U.S. Navy ships must be suitable for both their diesels and gas turbine engines. This would also be a requirement for any fuel additives used by the Navy. Since previous fuel additive work has focused on diesel engines, a Navy program was initiated to explore the potential for these additives in gas turbines. The development of an additive suitable for both gas turbines and diesel engines was recognized as an unexplored research area, however if the Texaco fuel additive proves successful in all engines, then the challenge of power density vs NO_x generation would be met successfully.

PARTICIPANTS

This program was sponsored by the Office of Naval Research (ONR) with NAVSEA serving as principal investigator. The program manager was Mr. Michael E. Osborne of NAVSEA. John J. McMullen Associates, Inc. (JJMA) provided consulting and program coordination, with Mr. Tom Risley serving as the program coordinator. Texaco Inc.'s Mr. Al Jung developed the test additives, provided the additized and baseline fuels as well as, information about the chemistry of the fuel additives. The combustion tests were conducted at Purdue University with Dr. J. P. Gore serving as the lead research scientist

with his assistant Doctoral candidate Li-keng Tseng.

ADDITIVE TECHNOLOGIES

The purpose of the fuel additive NO_x-reduction program was to assess whether certain fuel additive technologies that demonstrated NO_x reduction in compression ignition (diesel) engines could also reduce NO_x in turbine engine applications using F76 fuel combusted under simulated turbine conditions.

Three specific technology approaches were chosen:

1. Improve the burn characteristics of the fuel using a "combustion modifier".

2. Improve the dynamics of the fuel injector spray and diffusion using a "spray modifier".

3. Attempt to scavenge NO_x post-combustion using a "RAPRENOX-like" additive.

These technologies were chosen for the initial phase of this program since they demonstrated very favorable NO_x reduction results when evaluated in compression ignition tests using standard diesel fuels (Figure 1). The differences between the Navy's F76 fuel and the diesel used by Texaco were judged to be minimal. Thus, any change in NO_x formation between the diesel and gas turbine was postulated to result primarily from differences in the mode of combustion between the two engines and in differences in combustion temperatures.

F76 fuel was additized at the Beacon Research Labs of Texaco and NO_x emissions were evaluated at Purdue University in a simulated gas turbine combustor. Unadditized F76 fuel was used to generate baseline NO_x data; these data were compared with data generated from fuel containing the experimental additives. All additives evaluated at Purdue under simulated turbine conditions were first tested at Texaco under compression ignition conditions in die-sel fuel. Only those additives that demon-strated a net reduction in NO_x under compres-sion ignition were tested at Purdue. The addi-tives investigated contain only carbon, hydrogen, oxygen, and nitrogen. Additives containing metals or metal salts were not in-cluded in the study because of possible en-vironmental hazards.

The specific samples of F76 fuel evaluated at Purdue are listed below:

Identification	Description
R96-1041.00	F76 baseline fuel
R96-1041.10	F76 fuel w/combustion modifier
R96-1041-20	F76 fuel w/combustion modifier
R96-1041.30	F76 fuel w/spray modifier
R96- 104 1.40	F76 fuel w/RAPRENOX-like additive

COMBUSTION MODIFIERS

Combustion modifiers are used to alter burn and time characteristics of the combustion process by chemically modifying the onset of ignition and the number of ignition kernels in the fuel spray.

In the first case, conventional combustion modifiers tend to advance the onset of diesel ignition, resulting in longer burn times and eliminating pressure spikes during the cycle. In turn, this decreases maximum in-cylinder combustion pressure and lowers maximum combustion temperature. Since NO_x generation is a direct function of combustion temperature, the lower temperature results in lower NO_x emissions in diesels. There appears to be no power loss associated with the use of combustion modifiers despite the change in both maximum pressure and rate of pressure increase compared to the base fuel.

In the second case, the modifier is thought to promote combustion not only in the premixed portion of the fuel spray, but also in the diffusion zone. Facilitation of combustion in the diffusion portion of the flame could also lead to a more controlled pressure increase and avoidance of pressure and temperature spikes.

Another explanation for the reduction of NO_x using combustion modifiers involves their interaction with the Zeldovich and/or the Prompt mechanisms of NO_x formation. Zeldovich and Prompt describe the formation of NO_x via the generation and reaction of radicals with

nitrogen, oxygen, and fuel under combustion conditions. Combustion modifiers are also thought to work via radical mechanisms. It can be postulated that the radicals formed by the modifier could interact with the Zeldovich and Prompt mechanisms in such a way as to suppress the formation of NO_x. The latter explanation is being investigated further for maximizing NO_x reduction.

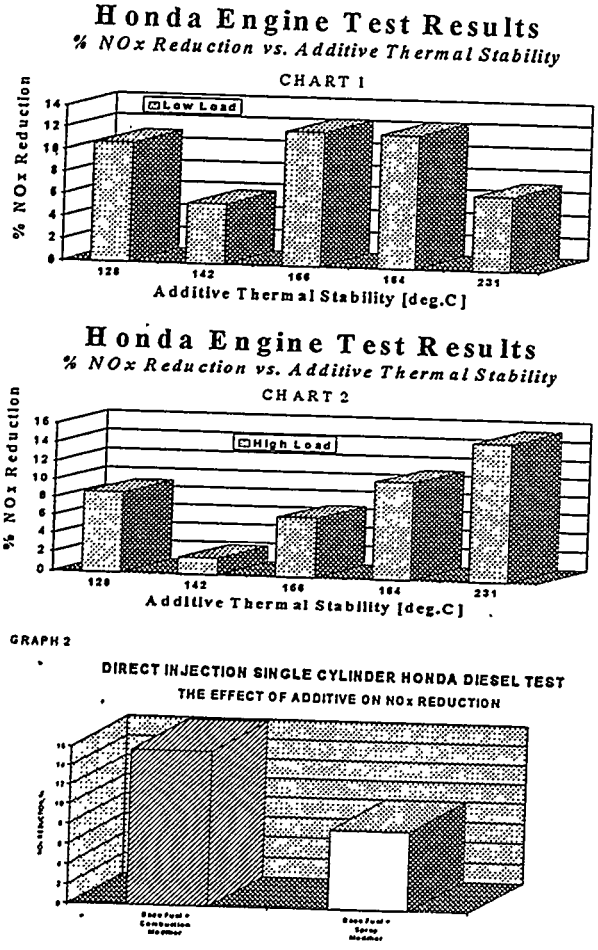


Figure 1: Effect of RAPRENOX-Like Additive (Top and Center) Combustion Modifier and Spray Modifier Additives on NO_x Reduction

The fuels referred to as R96-1041.10 and R96-1041.20 are F76 fuels that contain different combustion modifiers. In previous Texaco diesel engine tests, each additive decreased NO_x approximately 15 percent over that of the base fuel in diesel engine tests run at Texaco. These samples were submitted for NO_x testing under simulated turbine conditions at Purdue.

SPRAY MODIFIERS

Spray modifiers are used to alter physically the fuel injector spray patterns over those of the base fuel. In diesel engines these additives may have the same effect on combustion and emissions as increasing fuel injector pressure. Spray modifiers are expected to produce smaller droplet sizes (higher surface area to volume ratio) and increase swirl or turbulence of the fuel spray.

In diesel engine tests run at Texaco, spray modifiers have been shown to reduce NO_x emissions without increasing the cetane value of the fuel. Pressure/time curves, however, show similarities to cetane-improved fuels (Figure 2). In effect, spray modifiers advance the onset of ignition and can change the volume ratios of the premixed and diffusion portions of the fuel charge, resulting in longer burn times with lower pressure spikes during diesel combustion. A lower pressure spike produces lower maximum combustion temperatures and lower NO_x emissions. Typically, a 12 percent reduction in NO_x is observed in diesel combustion when comparing fuel containing a spray modifier with the base fuel (Figure 2).

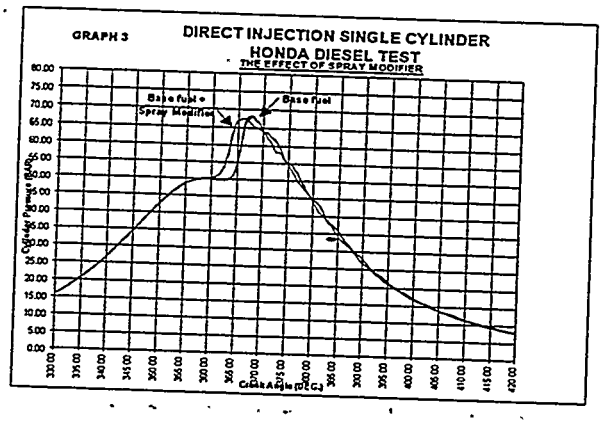


Figure 2: Effect of Spray Modifier on NO_x Reduction

Spray modifiers are temperature-sensitive, so it is necessary to match combustion temperatures with the modifier decomposition- temperature. Diesel combustion temperatures are generally lower than those in turbine engines,

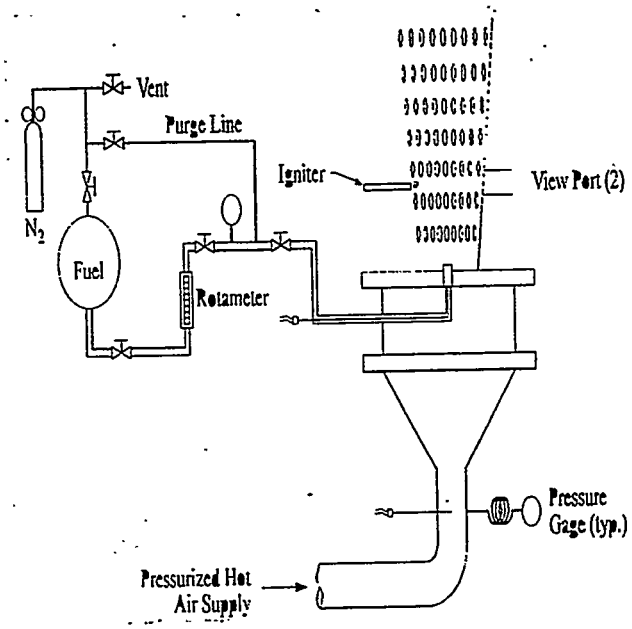


Figure 3: Experimental Apparatus

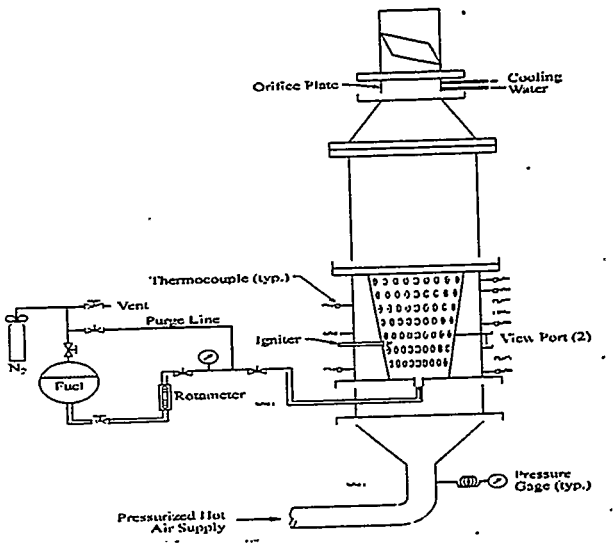


Figure 4: Schematic of High-Pressure Experimental Apparatus

The facility used for the high-pressure tests is shown in Figure 4. A high-pressure air supply system was used as the preheated air source. Air pressure and temperature are monitored upstream of the combustor by a pressure gauge and a stainless steel, shielded, K-type thermocouple. The fuel supply system included a high pressure (up to 800-psi operating pressure) rotameter, which was calibrated for each tested fuel to ensure accuracy in fuel flow rate. The combustor was modified and reinforced to have an operating pressure up to 15 atmospheres, and a transparent plastic safe-to shield was added around the combustor section. A tail pipe with a diffuser plate was added to the system to provide a uniform subsonic exhaust stream from the system. Ten K-type thermocouples were welded to the outside surface of the combustor casing to monitor casing temperature during the high-pressure tests. The high mass-flow, high pressure air system could supply air at flow rates up to 9 lb/s at temperatures up to 750° F and pressures up to 2000 psi. The mass flow rate could be controlled with both subsonic and choked orifice plates, but for these tests a choked orifice plate was used, controlling mass flow by adjusting pressure upstream of the plate.

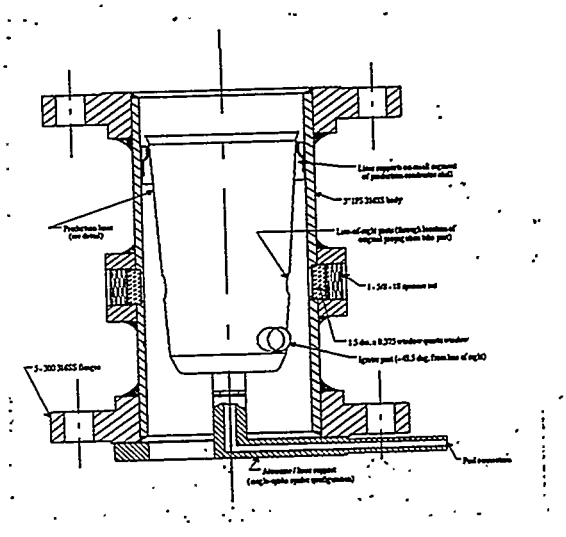


Figure 5: Schematic of Combustor

Figure 5 shows a detailed sketch of the combustor liner for a Boeing Gas Turbine Model 502-2E built for the Naval Bureau of Shipping (now the Naval Sea Systems Command). The diameter of the combustor is the same as the casing of the turbine engine so that a liner support segment from the original turbine engine could be fitted perfectly into the inside wall of the combustor. The fuel supply wafer is designed so that a minimum length of fuel line is exposed to the preheated air. A special igniter

was built to fit the igniter port. Two quartz windows are positioned at the exact location of the propagation port on the liner to provide visual access to the combustor. This design deviates slightly from the original combustor, but it provides necessary access for measurements and allows fuel emission properties to be examined under gas turbine conditions representative of Naval engines.

TEST PROTOCOL

The procedure for each test involved purging the fuel line after the appropriate fuel tank was connected to the fuel supply system. The air heaters were started after the air flow rate was adjusted to the desired test conditions. This heating process generally took about 2 hours since a large thermal mass was involved in the air supply system. During the heatup process, gas analyzers were warmed up and calibrated. After the preheated air was stabilized at the desired flow and temperature test conditions, the fuel supply system was pressurized and fuel injection and ignition in the combustor were initiated. The igniter was turned on before the fuel injection, and could be turned off after the fuel flow rate was adjusted to the desired value. The combustor was kept running at each test condition for about 15 minutes to reach steady-state conditions before global emission data were measured. Gas samples were taken continuously at the exit of the test apparatus. The sampled gases were delivered to NO_x, CO, and UIHC analyzers so that the concentrations of these pollutants could be measured simultaneously.

A schematic of the exhaust gas analysis system is shown in Figure 6. A water-cooled stainless-steel probe was used to draw samples from the exhaust into the gas analysis system. Concentrations of NO/NO_x were measured using a chemiluminescence-based analyzer (Thermo-Enviromental Instruments Model 10) with an accuracy as derived from the nitrous oxide (NO) or NO_2 calibration gas of 1 percent of full scale. Concentrations of CO and carbon di-oxide (CON were measured using a nondis-persiveinfrared (NDIR) analyzer (Horiba MEXAGE 311) with a repeatability within 0.04 percent for CO measurements and within 0.3 percent for CO_2. The lowest (or least) count of the CO/CO_2 analyzer was 0.01 percent (100 ppm). This analyzer was calibrated using calibration gases of 5 percent CO_2, 2 percent CO, and 25 ppm NO. Dried nitrogen of 99.995-percent purity was used as the zero gas. A chiller-trap was used to condense water out before the sample entered the NO/NO_2 and CO/CO_2 analyzers. Since a CO analyzer with a lowest count of 0.01 percent is unsuitable for measuring of sub100 ppm CO levels, a gas-filter-correlation CO analyzer (Thermo-Enviromental Instruments Model 42) was used to measure CO concentrations in the 0- to 100-ppm range in some of the experiments. An HO analyzer, using a flame ionization detector (Rosemount Model 400A), was used to measure UHC concentration measurements in some of the experiments. The sampling line to the UHC analyzer was heated to prevent condensation.

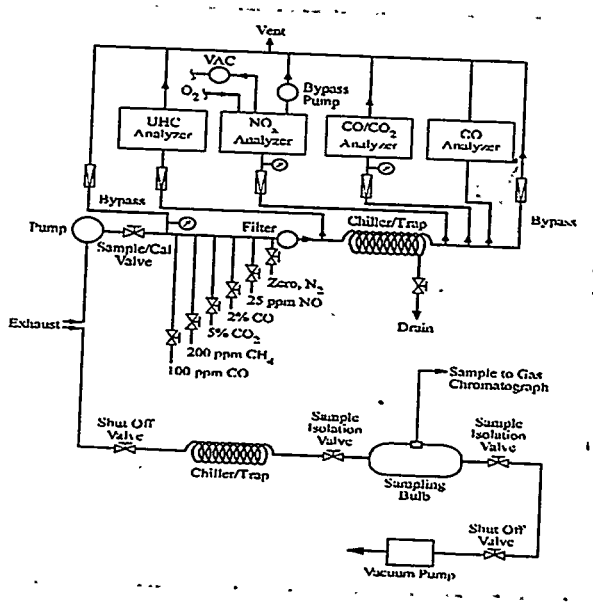


Figure 6: Schematic of Exhaust Gas Analysis System

TEST OBSERVATIONS

The test matrix included atmospheric pressure, 2-atmosphere pressure, and 15-atmosphere pressure tests. Tests at atmospheric pressure

were first conducted for the experimental fuels to examine their atomization, vaporization, and combustion stability performance. The more promising experimental fuels were then tested at a combustor pressure of 2 atmospheres. Finally, one of the experimental fuels and the baseline fuel were tested at 15 atmospheres

Flame temperatures at atmospheric pressure for the baseline, R96-1041.30, and R96-1041.40 fuels were measured. Of these fuels, the add-tized R96-1041.40 had higher peak flame temperatures, particularly at higher equivalence ratios. Peak temperatures for the R961041.30 fuel were lower than those for the baseline fuel at lower equivalence ratios, but were similar at higher equivalence ratios

The R96-1041.10 fuel did not yield stable flames under most operating conditions. Under conditions that resulted in apparently stable flames, flameout would occur unexpectedly and erratically. Further testing of this additized fuel, therefore, was not pursued. The R96-1041.20 fuel yielded stable flames but caused significant precipitation of a solid powder in the fuel lines and on the fuel filter, eventually clogging the filter. Further examination revealed that this fuel also caused significant precipitation at room temperature in the fuel tank. The cause for the precipitation was not investigated, instead it was decided that tests with the R96-1041.30 fuel should be abandoned since precipitation of the additive could not be prevented. Stable flames and repeatable data were obtained for experimental fuels R96-1041.30, R96-1041.40 and the base-line fuel

The next phase of atmospheric pressure tests included fuels R96-1041.00, R96-1041.30, and R961041.40. Thermal stability tests were conducted for all three fuels up to 400°F. Fuel precipitation was not observed. This ensured that clean fuels were injected into the combustor since the fuel temperature before the fuel injector typically was about 175° F.

The additized fuel, R96-1041.30, when tested at 15 atmospheres reached stable condition, but a sudden change in emission readings and combustor casing peaking temperature was observed. The peak temperature of the combustor casing increased to 580°C and, as a result, the test was terminated. During the combustor checkout after disassembling, it was discovered that the combustor liner had burned through in several locations during the high fuel-flow rate tests for R96-1041.30 fuel. After installing a new liner, high pressure tests were continued with a medium fuel-flow rate using the same test matrix and protocol as for the low flow rate tests. The flame still covered all the viewing area for both the baseline and the additized fuel. Emission data were obtained throughout the test matrix and the liner was not damaged when checked after post test disassembly.

A second series of tests was conducted at 15 atmospheres with the same test conditions used for the middle firing rate case. When R96-1041.30 was tested, it produced a much shorter flame than the baseline and the combustor wall temperatures rapidly increased near the dome of the combustor liner. A visual examination of the combustor liner showed slight damage to its inner surface. Surface roughness increased near the dome of the combustor liner, indi-cating that the flame was either impinging on or very close to the liner.

R96-1041.40 was tested next. The observations of the flame appearance and chamber temperature showed results similar to those of the previous high pressure tests of the same fuel under similar conditions, indicating that combustor performance had not been affected by the slight damage to the liner caused by the R96-1041.30 fuel.

RESULTS AND DISCUSSION

Two types of tests were conducted to cover the operating envelope of practical combusors. In the first type, the equivalence ratio was adjusted by changing the air flow rate while keeping the fuel flow rate constant. Under these conditions the equivalence ratio and the residence time varied simultaneously and significantly. The second type of tests involved varying the fuel flow rate to obtain

different equivalence ratios. Since residence time in the combustor is determined primarily by air flow rate, the results of these tests allowed the effects of equivalence ratio variations to be delineated

Figure 7 shows a comparison of Emission Index (EI) for the baseline fuel, R96-1041.00, and experimental fuel R96-1041.30 plotted as a function of equivalence ratio. The test conditions for Figure 7 were constant Fuel flow rate. Different fuel equivalence ratios were obtained by varying the air flow rate. This type of operation provides a wide range—at least a factor of three—of flow velocities inside the combustor. The characteristic residence time, therefore, also varies by more than a factor of three. It can be seen that the EINO and $EINO_x$ for R96-1041.30 are consistently higher than those of the baseline fuel, R96-1041.00. Both EINO and $EINO_x$ decreased as the fuel equivalence ratios increased for both experimental and baseline fuels. The reduction in available air reduces recirculation by changing the swirl number and causes jet-like luminous flames with higher equivalence ratios. The changes in flame structure lead to lower NO_x emissions with increasing equivalence ratio under these test conditions. The EINO and $EINO_x$ data for the two baseline fuel tests, one before testing experimental fuel R96-1041.30 and one after, are consistent. The differences in the EINO for the two tests of baseline R96-1041.00 fuel might have been caused by the fuel coking inside the combustor liner that was found after disassembling the combustor. This coking might have had a slight influence on CO and UHC measurements, but it would not have affected EINO and $EINO_x$ since the emissions they represent were produced in the flame zone.

To obtain comparable residence times, tests also were conducted with constant air flow rates, but fuel flow rates were varied to obtain a range of fuel equivalence ratios. One limitation of the tests with variable fuel flow rates is that three different nozzles had to be used to cover a reasonable range of equivalence ratios. Figures 8 and 9 show graphs of EI vs. fuel equivalence ratio for R961041.00

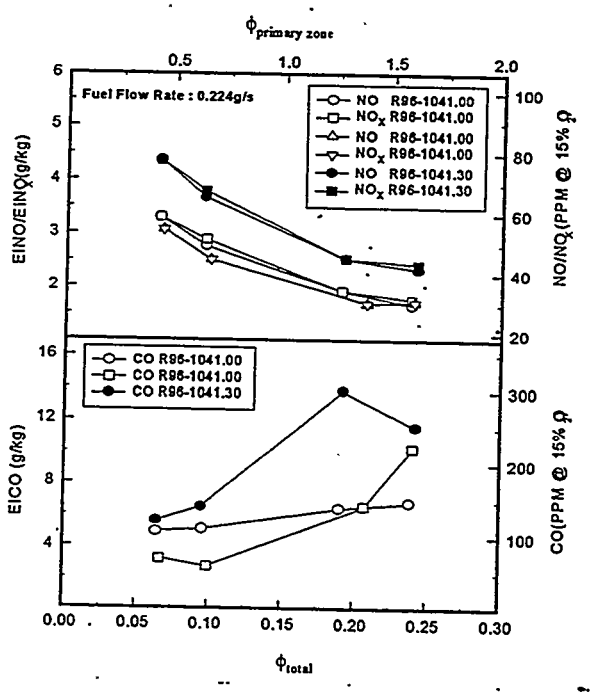


Figure 7: Pollutant Emissions for R96-1041.30 and Baseline Fuels at Constant Fuel Flow Rate Test Conditions Under Atmospheric Pressure

R96-1041.30, and R96-1041.40 feels under constant air flow rates. The EINO has the same values as the $EINO_x$ over these test conditions, so only the $EINO_x$ is shown. The flow field inside the combustor liner is relatively unchanged over the small range of fuel equivalence ratios for the constant air flow rate test conditions. The EI over this range of fuel equivalence ratios are relatively free from flow effects. Figure 8 shows that the $EINO_x$ slowly increases as the fuel equivalence ratio increases. This is because the product temperature also increases as fuel equivalence ratio increases. One can see that the $EINO_x$ remains about the same over each range except for the conditions at which larger droplets were created by the atomizers and EICO in-creased. As shown in Figure 9, the experimental fuel R96-1041.40 has higher $EINO_x$ at all test conditions.

In the first series of high-pressure tests, the baseline fuel and experimental fuel R96-1041.40 were tested with one air flow rate and three fuel flow rates at a combustor pressure of 15 atmospheres. The results show

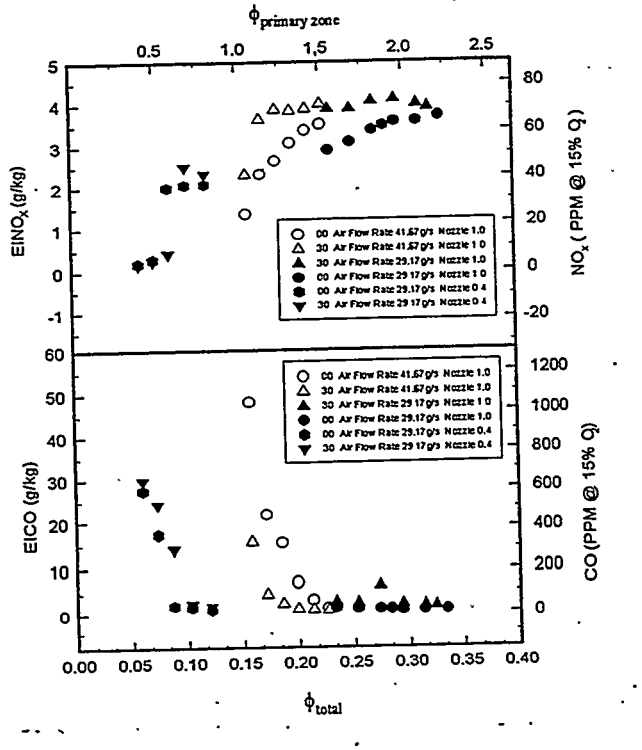


Figure 8: Pollutant Emissions for R96-1041.30 and Baseline Fuel at Constant Air Flow Rate Test Conditions Under Atmospheric Pressure

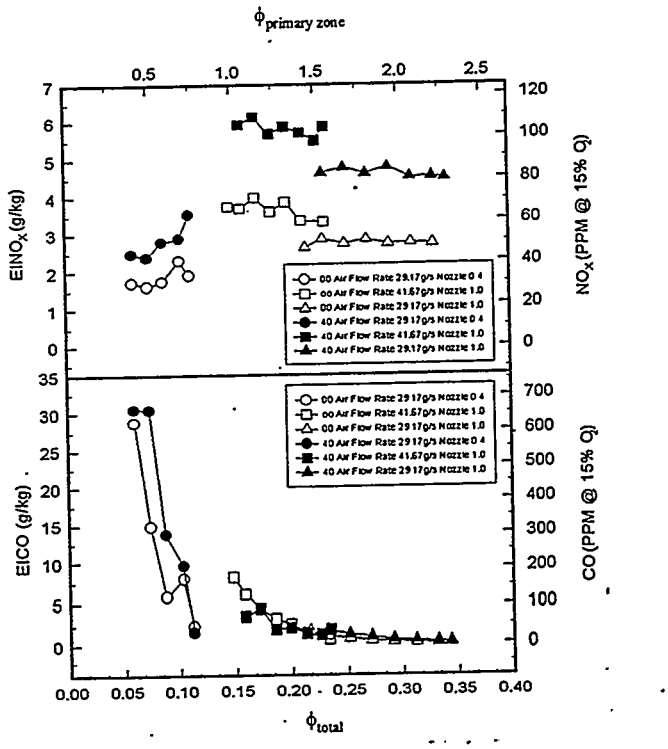


Figure 9: Pollutant Emissions for R96-1041.40 and Baseline Fuels at Constant Air Flow

that at these conditions R96-1041.40 still produces more NO_x than does the baseline fuel. Differences between the $EINO_x$ of the two fuels, however, decrease at this higher pressure, although the overall NO_x emissions increased for both fuels. This decrease in the difference between NO_x emissions for the baseline fuel and the experimental fuel may be due to a change in chemical reactions, change of combustor char-acteristics, or simply a decrease in the percentage of the extra NO_x produced by the fuel additives.

Figure 10 shows the EINO and $EINO_x$ as a function of fuel equivalence ratios for all 15-atmosphere tests, with open symbols representing data from the earlier tests and solid symbols representing data from the second series of tests. The baseline fuel F76 produces the lowest NO and NO_x emissions for all test conditions. The difference between NO_x emissions of the R961041.40 fuel and the baseline fuel is similar for the earlier and present tests except for the data obtained at the high firing rate, high fuel-equivalence ratio, where flame impinging on the combustor liner could be the cause of the small difference. The flame impingement also caused a burn-down of a combustor liner during the earlier tests. The fuel mixture, an equal volume mixture of R96-1041.30 and R96- 1041.40 fuels, shows EINO and EI NO_x similar to those of the R96-1041.40 fuel. The EINO and $EINO_x$ produced by R96-1041.30 fuel have a value between the baseline F76 fuel and the R96-1041.40 fuel. The R96-1041.30 fuel, however, also caused a dramatic change of temperature distribution in the combustor liner, which resulted in minor damage to it.

The effects of the R96-041-30 (spray-modifier) fuel additive (microexplosive) were further examined in a spray flame in a co-flow air configuration. A pressure swirl atomizer with a flow rate of 0.4 gallon per hour was used as the fuel injector for the spray flames. The fuel injector was placed in an axisymmetric co-flow of air with a duct diameter of 3 inches. The

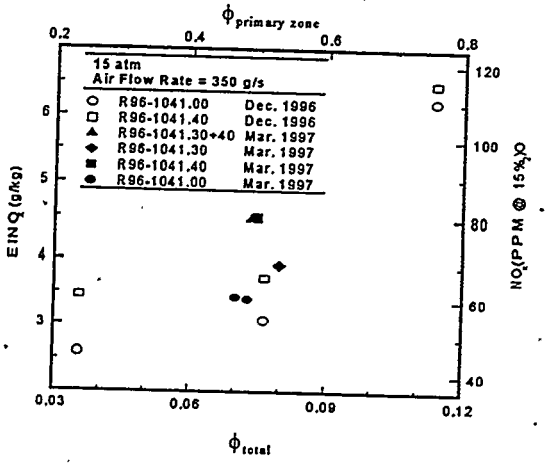


Figure 10: NO_x Emissions at 15 Atmospheres at 3 meters per second.

velocity of the co-flow air was kept constant.

The fuel supply pressure was also kept constant at 110 psig during the test. Two different fuels, baseline F76 (R96-1041.00)) fuel and the R96-10)41.30) fuel, were tested under identical test conditions.

Figure 11 shows photographs of the two spray flames under identical operating conditions. The spray flame shown on the bottom is fueled by baseline F76 fuel and the one on the right is fueled with the R96-1041.30 fuel. One can see that the F76-fueled spray name has a flame height about twice as long as the spray flame fueled with the R96-1041.30 fuel. This is be-cause the F76-fueled spray name has a larger fuel droplet size and. therefore. longer evapora-tion time is needed to vaporize these larger fuel droplets. The spray-modifier fuel additive in the R96-1041.30 fuel causes the larger spray droplets produced by the pressure atomizer to experience a microexplosion and reduces them to smaller droplets. The lifetime of the smaller droplets is much shorter and so the height of the spray flame fueled by the R96-1041.30 fuel is much shorter. The angle of the F76-fueled spray flame is smaller than that of the R96-1041.30-fueled spray flame.

Two possible mechanisms contribute to this phenomenon:

1. The microexplosion caused by the spray modifier additives in the R96-1041.30 fuel increases the spray angle

2. The momentum transfer for the smaller droplets in the R96-1041.30 fuel spray flame is much more effective than that for the larger droplets in the F76-fueled spray flame.

Although the spray-modifier led to an increase in NO_x in the present combustor configuration. advanced combustor concepts such as lean direct injection (LDI) would benefit significantly from the use of this additive.

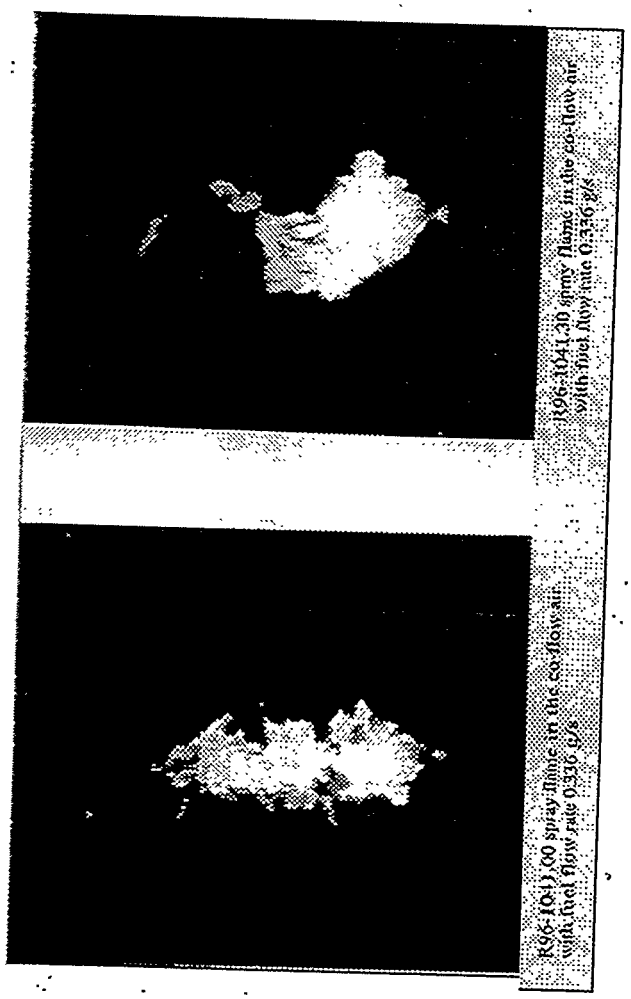


Figure 11: Spray Flames

CHEMICAL REACTION MODEL

The effects of adding the nitrous oxide-(NO_x-) reducing chemicals were studied computationally using an opposed-flow non-premixed flat-

flame code with methane as the fuel. This one-dimensional flame provides an opportunity to conduct a detailed study of the chemical reac-tion mechanism within the current computation capacity. The most recent reaction mechanism developed by the Gas Research Institute (GRIMECH) was used for this study. The mechanism considers 49 chemical species and 279 reversible reactions.

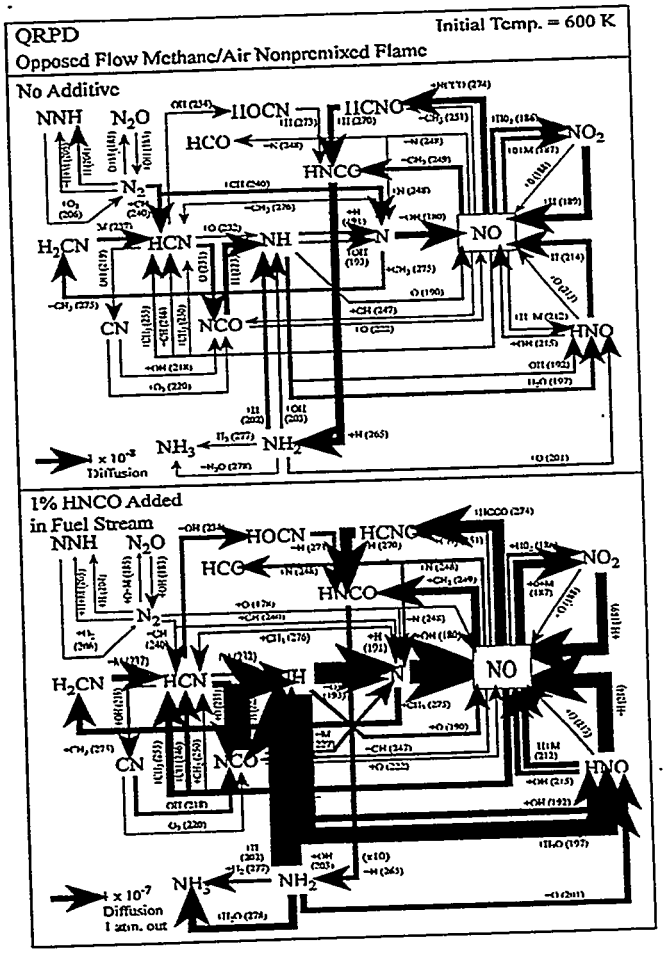


Figure 12: QRPD for Methane/Air Flames With Initial Temperature = 600° K

Figure 12. shows the QRPD of important NO_x emissions-related reactions for the nonadditized and the HNCO-added flames with an initial temperature 600° K. Each line in the QRPD represents a chemical reaction. The line thickness representing the value of the integrated reaction rate of this specific reaction over the entire flow field. The direction of reaction is indicated by the arrows. The reaction is producing or consuming a species if the arrow is pointing into or away from the species respectively. It can be seen that the additive HNCO is mainly involved in the reactions with HCNO, NO, and NH_2. A comparison of the upper panel and the lower panel of Figure 12 shows that the reaction rate of many NO-related chemical reactions are drastically augmented. Reaction number 265 was plotted in one tenth of the scale to fit into the plot. Adding HNCO not only increases the consumption rate of NO but also increases the production rate of other species such as NH, HNO, and nitrogen (which all lead to more NO), and so results in a net increase of NO production.

CONCLUSIONS

Measurements of pollutant EI at three different pressures for baseline F76 and four additized fuels were attempted. Of the four additized fuels, R96-1041.10 did not yield stable flames under gas turbine conditions and R96-1041.20 fuel showed solid precipitation at room temperature in the fuel line and in the fuel filter. The reasons for these unexpected results were not pursued, thus it is possible that the additives may have been incorrectly formulated.

R96-1041.30 and R96-1041.40 fuels showed approximately a 30- to 50-percent increase in NO_x emissions over the baseline fuel index at combustion pressures of 1 and 2 atmospheres. At 15 atmospheres pressure, the $EINO_x$ for R96-1041.40 fuel is 30 percent higher than the $EINO_x$ baseline fuel under low and medium fire conditions. The $EINO_x$ for the two fuels are almost identical for the high fire conditions, but flame impingement on the liner may have af-fected these data.

The results from present tests suggest that the fuel additives may become more effective at pressures higher than 15 atmospheres, but this is conjecture and needs to be verified directly. Therefore, tests in the pressure range of 18 to 30 atmospheres should be explored.

Despite the higher NO_x emissions with the additzed fuels, the fact that the emissions were affected would indicate that tailoring of the additive for a gas turbine combustor may

be more successful.

The fuel additives appear to affect the atomization performance, so the surface tension and viscosity changes that they may cause need to be examined. The atomization characteristics need direct experimental investigation.

The reductions in NO_x emissions caused by the fuel additives were in the 10- to 20-percent range based on diesel engine tests at Texaco Inc. This was the first time these additives were evaluated in a gas turbine combustor. The results of this evaluation point out the complexity in using fuel additives in two different combustion processes.

Lean Direct Injection (LDI) combustor concepts may find value in the additives similar to R96-1041-30 since this additive seems to promote a more rapid combustion.

FUEL ADDITIVES FOR IN-CYLINDER NO_x REDUCTION FROM DIESEL ENGINES

M. Ramavajjala, V. Palekar, and R. Slone, NOxTech, Inc.
G. Yowell, California Energy Commission

INTRODUCTION

Heavy-duty vehicles contribute a significant portion to California's air pollution with over 50% of the oxides of nitrogen (NO_x) and over 84% of the particulate matter (PM). Environmental and health concerns have resulted in stringent emission standards which require heavy-duty diesel engines to meet a 4.0 g/bhp-hr NO_x standard in 1998 and potentially a further reduction down to 2 g/bhp-hr NO_x in the year 2004. There is a critical need for cost effective technologies to meet these mandates and to clean the air we breathe. One promising approach towards meeting these standards with minimal changes in the present infrastructure of the transportation industry is the use of fuel additives that when injected into the cylinder, along with the diesel fuel, can result in substantial NO_x reduction.

Previous in-cylinder studies have utilized water in-fuel microemulsions to lower combustion temperatures (adiabatic flame temperature) resulting in moderate NO_x reduction. These microemulsions involve the use of a surfactant which forms a reverse micelle entrapping the water phase into a homogeneous water/fuel blend. The NO_x reduction ability of these microemulsions can be augmented by additives (referred to as NO_x scavenger additives). These additives are derived from the class of chemicals that have demonstrated greater than 90% NO_x reduction in aftertreatment processes such as the selective non-catalytic reduction of NO_x. These scavengers are soluble in the aqueous phase of the water/fuel microemulsion and when used with the water-in-fuel microemulsion as a carrier, offer the potential for significant NO_x removal from diesel engine exhaust.

The primary purpose of this project was the characterization of these microemulsion fuel blends for NO_x reduction and as carriers for scavenger additives. Thirty-one fuel formulations were tested for NO_x removal effectiveness on a 1988 Cummins 200 hp C8.3 L engine. The effect of varying scavenger concentration on exhaust emissions and engine combustion was characterized by studying the effect of the various microemulsion components on emissions performance. The success of this approach can result in substantial reduction in diesel engine NO_x emissions with minimal engine modifications and economic impact.

BACKGROUND

NO_x Scavenger Chemistry

The heterogeneous combustion in a diesel engine is a complex sequence of events. The fuel burns in a diffusion type flame which is characterized by local high-temperature combustion zones around a cloud of vaporizing fuel droplets. The NO_x-formed in the cylinder is mainly due to reactions (1) and (2), according to the Zeldovich mechanism, and is often referred to as thermal No_x. In a diesel engine, the NO_x is considered to be predominantly formed on the outside of the flame front where, the 0_2 concentration is the highest.

$$N_2 + O \Leftrightarrow NO + N \quad \text{.....(1)}$$
$$N + O_2 \Leftrightarrow NO + O \quad \text{.....(2)}$$

There are two approaches to reducing the NO_x in the engine exhaust: (I) inhibit its formation by affecting the kinetics of reactions (1) and (2), or (ii) reduce its concentration by reaction with another species after it is formed. The addition of water is an example of the former approach while the addition of scavenger additives to the fuel results in NO_x reduction due to reaction between the NO_x formed and the additive.

While a reduction in combustion temperature by water addition and a reduction in cetane

number of the fuel can be used to reduce NO_x formation, considerable fuel penalty is incurred. Hence the desired approach is the reduction of NO_x after it is formed without affecting the combustion characteristics of the engine.

The use of NO_x scavenger additives have been demonstrated to result in greater than 90% NO_x reduction at temperatures of 1400-15000 F and atmospheric pressure in aftertreatment processes such as the selective non-catalytic reduction (SNCR) of NO_x. Under these conditions, the scavenger molecules generate reactive species called free radicals which react with the NO to give N2. The reaction chemistry with one such scavenger additive, cyanuric acid (HNCO)3, is as shown in reactions (3)-(5).

$$(HNCO)_3 \Leftrightarrow 3HNCO \quad \text{.....(3)}$$
$$HNCO + OH \Leftrightarrow NCO + H_2O \quad \text{.....(4)}$$
$$NO + NCO \Leftrightarrow N_2 + CO + O \quad \text{.....(5)}$$

These water soluble scavenger additives can be injected in to the engine cylinder via the use of microemulsions; using less than 10 wt.% water, microemulsion fuel blends can serve as efficient carriers for these scavenger additives. Thus, this approach offers the potential to reduce NO_x with minimal changes to the fuel injection system.

Technical Challenges

Although the efficacy of scavenger additives in SNCR processes is well known, the behavior of these chemicals under the high temperature and pressure in the cylinder of a diesel engine is unknown. When injected with the fuel, the water encased scavenger needs to pass through the high temperature flame front and reduce NO_x in the oxygen rich exhaust stream. Limited data exists on the effect of scavenger and microemulsion concentration on NO_x reduction, fuel consumption, by-product formation and combustion characteristics across the engine load range. In addition, the shear, long-term stability and the pumping efficiency of the additized microemulsion needs to be characterized. Also, the effect on engine components such as gaskets, filters, fuel pump, piston rings and liners and fuel injectors needs to be examined to evaluate the suitability of this technology to present day engines.

Effect on Diesel Engine Combustion

Modern engines are optimized for fuel efficiency by careful control of air/fuel ratio, injection and cylinder pressures, fuel atomization, injection timing and ignition delay. These parameters are critically dependent on fuel quality. The addition of water, emulsifying agents and scavenger additives will likely result in the broadening of the pressure peak and a 'spreading out' of the combustion in the cylinder. These effects need to be examined in detail to achieve an understanding of the effect of the additized microemulsions on engine combustion characteristics.

Measurement of a number of critical combustion characteristics such as peak cylinder pressure, heat rise and rate, shape of injection and net mean crank angle point of heat rise envelope was planned but due to equipment hardware and hookup problems, these parameters could not be measured.

MICROEMULSIONS

An emulsion of water in fuel can be of two types: (I) microemulsion and (ii) macroemulsion. Microemulsion fuel blends consist of small droplets, usually 2 to 100 nanometers diameter of water as the noncontinuous phase dispersed in base diesel fuel. The water and fuel form a single phase by the use of a surfactant such as Emersol 315 (E315) with an alcohol such as methyl benzyl alcohol (MBA) added as a cosurfactant to increase stability. These surfactant/cosurfactant molecules form a reverse micelle structure with a polar core which entraps the water molecules and a lipophilic non-polar outer region which has affinity with the fuel. Macroemulsions fuel blends, on the other hand, consist of much larger droplets and approach more of a physical mixture of water with diesel fuel.

The formulation for the modified diesel fuel consisted of a base water-in-oil microemulsion with the secondary addition of NO_x scavengers as additives. A typical fuel composition was as follows:

- 70% D2 CARIB diesel fuel, * 10% water,
- Less than 10% surfactant that forms a reverse micelle structure entrapping the water,
- Less than 5% oxygenate to stabilize and increase the solubility of the surfactant,
- Less than 3 wt.% of an acid neutralizing agent.
- Desired amount of scavenger additive (dissolved in water).
- Required amount of cetane improver to bring the cetane value of the fuel to that of D2.

The microemulsions appeared as clear, one-phase solutions with minimal mixing and are thermodynamically stable towards phase separation once formed. The order of addition and mixing were not found to be critical. These fuel blends have certain desired properties: (I) flash point greater than 1400 F, (ii) temperature stability between -10 to +700 C, (iii) good shear stability in fuel handling system, and (iv) good long term storage stability (fuel tank storage).

EXPERIMENTAL

The engine used for the testing was a 1988 Cummins 200 hp, 8.3 L, with a turbocharger and an aftercooler. A fuel manifold system for injecting the microemulsions in the engine was constructed. This manifold system allows up to five different fuel blends at the same time without interrupting the engine steady state conditions. Microemulsions with different formulations were blended prior to the testing and stored in 30 gallon containers. Fuel consumption was measured by loss of weight using a Mettler weight balance. The test procedure included pre-blending of the fuels in thirty gallon containers which were mounted in the fuel manifold system. The engine rpm and the torque were set and CARIB D2 fuel injected to acquire an emissions baseline. Under steady state conditions, the fuel was switched to the desired fuel blend and the fuel consumption was measured. NO/NO_x were measured using a Thermo Environmental Chemiluminescence analyzer, CO by Teledyne NDIR analyzer, 0_2 by Teledyne electro-chemical cell and the hydrocarbons were measured using a Horiba FID analyzer. Ammonia measurements were made using Miran 1132 single beam IR instrument.

DISCUSSION

There are three primary methods of introducing water. These are (I) water/fuel emulsion, (ii) direct water injection into the cylinder, and (iii) fumigation of water into the air intake. In the first mode, water is introduced along the fuel side of the diffusion flame while the latter two modes result in water on the air side of the diffusion flame. The injection of water as an emulsion is preferred since it incurs minimal changes to the engine and also results in suppression of NO_x and particulate levels. It is believed that when water is introduced along with the fuel in a region which is O_2 deficient, there is an abundance of OH radicals which leads to particulate oxidation in addition to lower NO_x formation. If introduced via the air side, a reduction in the combustion temperature results in NO_x reduction but increases the soot in the exhaust.

Effect of Water Addition

Figure 1 shows the effect of water addition to diesel fuel on NO_x and CO concentrations at various engine loads. Water addition to the fuel results in a drop in the combustion temperature, resulting in a suppression of NO_x formation. However the fuel cetane number was lowered as a result of water addition. This resulted in an increase in the hydrocarbon levels (not shown in the figure). This effect could be controlled by advancing the engine timing. Water levels of 10% or less were selected for this study since the focus of this project was to provide a medium for transporting the NO_x scavenger.

Effect of Surfactant/Co-Surfactant

The surfactant serves as an interphase between two phases and is characterized by hydrophilic-lipophilic balance. A cosurfactant or compatibilizing agent is added to the blend to increase the solubility of the hydrocarbon phase, increase the hydrophilic-lipophilic balance of the surfactant phase and increase the stability of the microemulsion. The effect of surfactant concentration on the NO_x and CO reduction is shown in Figure 2. It is evident

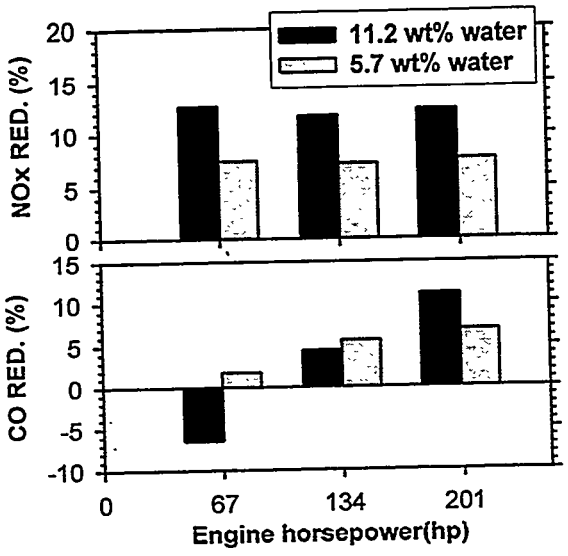


Figure 1: Effect of Water in Fuel on Exhaust Emissions at Various Engine Loads.

from the figure that the surfactant does not have any significant effect on the NO_x and CO levels in the exhaust, for the concentration levels tested. A similar set of experiments for the co-surfactant also revealed no effect on the NO_x and CO emissions. Based on these data it is clear that surfactant and cosurfactant do not participate in the NO_x reduction reactions.

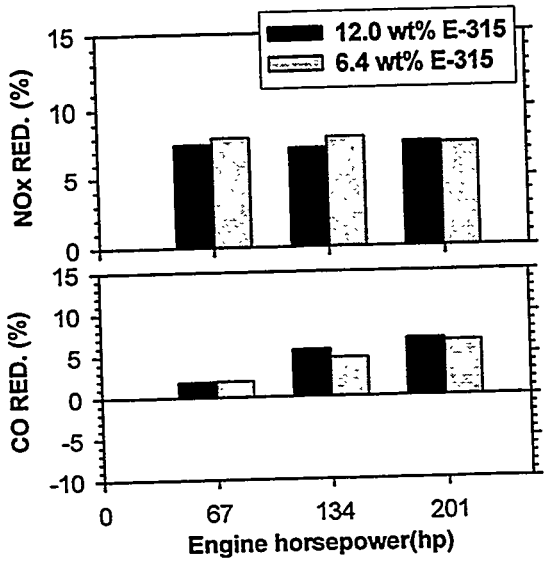


Figure 2: Effect of Surfactant on Exhaust Emissions at Various Engine Loads.

Effect of Cetane Improver

The effect of C1 as a cetane improver in both microemulsions as well as macroemulsions is shown in Figure 3. The improvement in the combustion characteristics of the fuel as a result of the cetane improver seems to lead to a small improvement in NO_x reduction in the case of the microemulsion fuel. The macroemulsion fuel showed a decrease in the NO_x reductions with increasing C11 concentration. The reason for this behavior is not clear, however, it is possible that the presence of nitrate compounds in C1 may have an influence on the formation or reduction of NO_x. The effect of C1 on other emissions such as CO, hydrocarbons and ammonia are plotted in Figure 4. It is clear from Figure 4 that there is no significant effect of the cetane improver on any of these emissions.

Effect of Scavenger Additive on NO_x reduction

All the data presented so far were obtained using microemulsions without the addition of a NO_x scavenger to enhance the NO_x reduction.

Figure 5 plots the results of the first series of tests at varying scavenger concentrations using

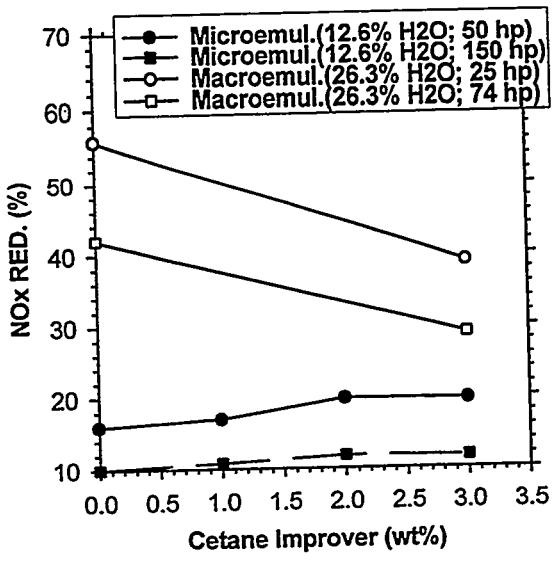


Figure 3. Effect of Cetane Improver C1 on No_x Reduction

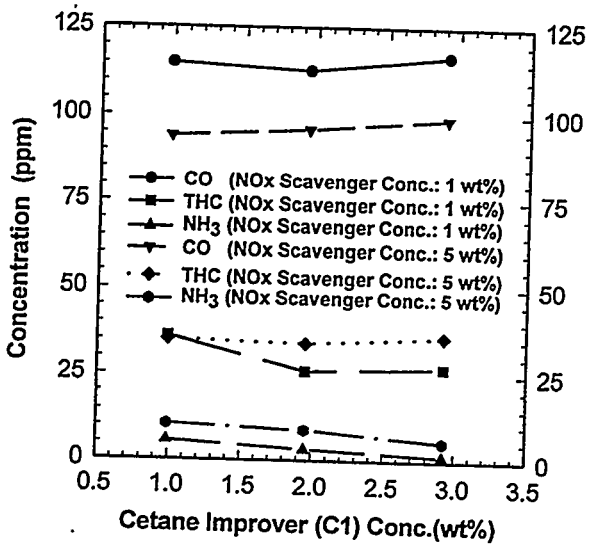


Figure 4: Effect of Cetane Improver C1 on CO and Hydrocarbon Reduction at Two Scavenger Levels

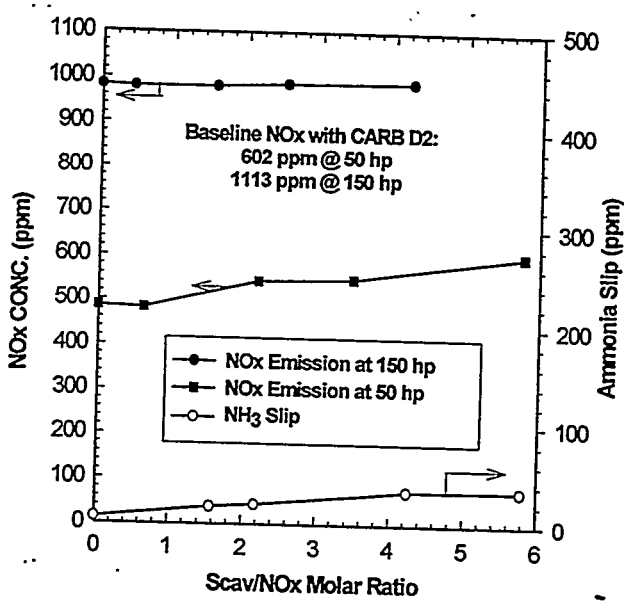


Figure 5: Effect of NO_x Scavenger Mole Ratio on NO_x Reduction. C1 as Cetane Improver

C1 as cetane improver. The scavenger concentration was varied between a scavenger/-NO_x molar ratio of 0 to 6 using 5 different fuel formulations. The scavenger concentration seemed to have little effect on the NO_x emissions and most of the NO_x reduction seemed to be a result of the microemulsion itself. However, up to 40 ppm unreacted ammonia (NI-13) slip was observed. One noteworthy feature is that although the exhaust NO_x concentration was not reduced, there was no substantial increase in NO_x in spite of the addition of large amounts of nitrogen containing additive. A possible explanation for this phenomenon could be that:

1 .the NO_x scavenger molecules were destroyed in the combustion process by pyrolysis in the fuel rich portion of the flame front with the survival of some residual NH_3 formed by a small amount of active scavenger only in cooler regions such as near the wall of the engine cylinders, or

2. the scavenger was indeed reactive but exhibited a low selectivity for NO_x reduction at the reaction conditions in the engine cylinder, i.e., possibly the formation of NO_x and its reduction proceeded at equal rates resulting in half the scavenger being responsible for re-during the NO_x formed by oxidation of the other half of the scavenger.

An additional complexity was the 41% decrease in cetane number of fuel, due to the addition of 3 wt.% of scavenger additive. The decrease in cetane number of fuel due to the addition of scavenger, possibly changed the nature of the combustion from that of a stratified charge, to premixed combustion. This makes it difficult to delineate the effect of scavenger from the effect of changing fuel cetane number. Moreover, the large drop in cetane number meant that large amounts of C1 had to be used to restore the cetane number, resulting in a possible influence of nitrates present in C1 on NO_x formation/reduction. Thus, to better understand the effect of additive concentration, its performance at constant cetane number of 50 was studied. To achieve this, the cetane improver was changed from C1 to C2 using the following criteria:

1 .The new cetane improver should have a substantially higher cetane value than 50 so that smaller quantities are sufficient to elevate the cetane value of the blend.

2..The molecular structure of the cetane improver should be similar to that of hydrocarbons present in diesel fuel so that the addition of which does not change the blend properties substantially.

2..The molecular structure of the cetane improver should be similar to that of hydrocarbons present in diesel fuel so that the addition of which does not change the blend properties substantially.

3. A cetane improver without any nitrates is preferable, so that there is no possible adverse effect on NO_x reduction.

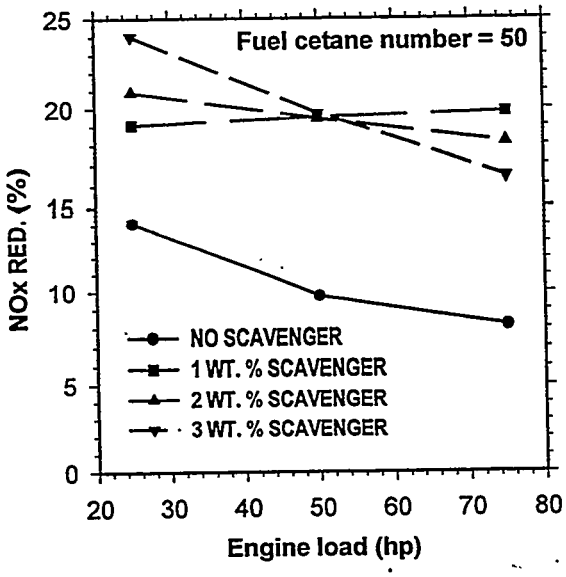


Figure 6: Effect of Scavenger Concentration on NO_x Reduction as a Function of Engine Load. C2 as a Cetane Improver.

Figure 6 shows the effect of varying scavenger concentration on NO_x reduction at a constant cetane number of 50. A considerable improvement in NO_x reduction is observed for the fuel with 1 wt.% scavenger in comparison to the fuel with no scavenger. This is in contrast to Figure 5 where the reduction seemed to be due to the microemulsion itself. Also, at low loads, there seems to be an improvement, with increasing scavenger levels, but this trend seems to reverse at the higher loads. The NH_3 levels in the exhaust were measured for the three scavenger concentrations and were found to be negligible. One possibility is that the improved cetane number of the fuel resulted in similar combustion characteristics in the cylinder and hence the scavenger survived the flame front and reacted with the NO_x formed downstream of the flame front. However, the addition of larger amounts of scavenger additive did not seem to linearly increase the amount of NO_x reduced.

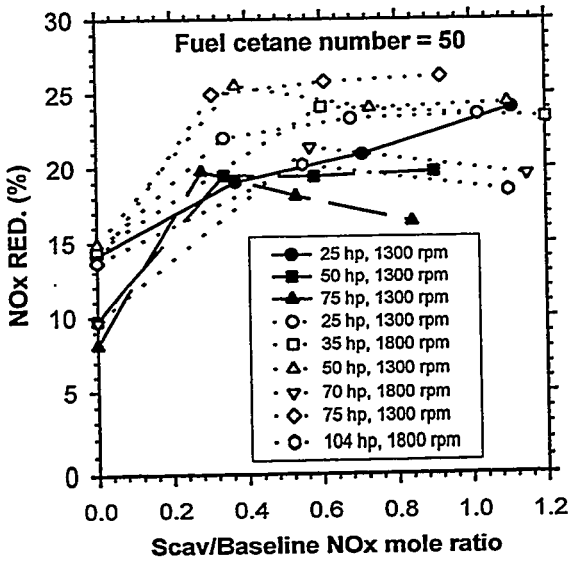


Figure 7: Effect of Scavenger to NO_x Molar Ratio on NO_x Reduction. C2 as Cetane Improver.

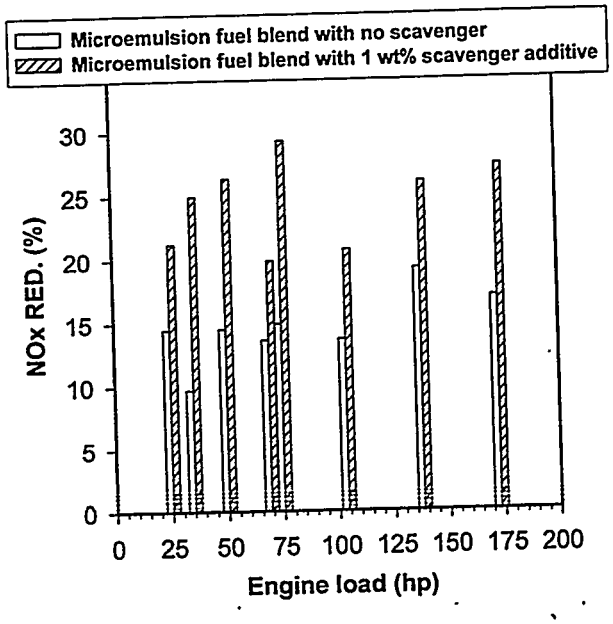


Figure 8: Summary of NO_x Reduction With and Without Scavenger at Various Loads. C2 as Cetane Improver.

The above results suggest that most of the scavenger is destroyed in the flame front and possibly a slightly larger amount compared to

leads to NO_x reduction downstream of the flame. This effect needs to be examined in greater detail under varying combustion and injection conditions. Figure 8 compares the NO_x reduction obtained with the 1 wt.% fuel with that of the microemulsion itself at various loads under steady state conditions. A maximum of 15% improvement in NO_x reduction was observed over that of the microemulsion itself. No clear trend was observed as a function of load, but the increase in NO_x reduction over that of the microemulsion itself seemed to vary between 7-15% across the load range of the engine. Thus, for a typical fuel blend, consisting of 10 wt.% water, less than 10 wt% emulsifying agents and 1 wt% scavenger, almost 30 % reduction can be obtained across the load range of the engine.

SUMMARY

The use of microemulsions containing scab-Engen additives offers potential for substantial reduction in NO_x. The addition of water was limited to 10 wt% as Microemulsions containing less than 10 wt% water were found to be effective in carrying scavenger additives. A typical composition containing 10 wt% water, less than 10 wt% surfactant/ cosurfactant/neutralizing agent and 1 wt% scavenger additive reduced NO_x by almost 30% across the load range of the engine.

The addition of quantities greater than 1 wt% of the scavenger additive did not have a beneficial effect on NO_x reduction. This may be due to the additive being destroyed in the flame and not making it past the flame front for reaction with NO_x.

The use of scavenger additives leads to a severe depression in the cetane number of the fuel. Selection of a cetane improver is critical from both cost and NO_x reduction perspectives. For possible commercial application, an effective low cost cetane improver would have to be developed to increase the cetane number of the resultant fuel blend.

Assuming a cost of $0.60 per gallon of D2 diesel and using the microemulsion components and the scavenger additive used in this study, this approach is likely to add a cost of 280 (46.5%) to the cost of diesel fuel (cost includes the cost of cetane improver). More work needs to be done to lower the fuel formulation cost and to examine its effect on the combustion characteristics and mechanical wear and tear of the engine.

ACKNOWLEDGMENTS

This project was partly sponsored by the Transportation Energy Technologies Advancement Program (TETAP) of The California Energy Commission, under contract # 500-91-028.

REFERENCES

1. Valdmanis and Wulfhorst, D.E. *The Effects of Emulsified Fuels and Water Induction on Diesel Combustion,* SAE Paper 700736, February 1970.

2. Greeves, Khan, I and Onion, G. *Effects of Water Introduction on Diesel Engine Combustion and Emissions,* 16th International Symposium on Combustion, Comb. Inst., 1976.

3. Loscutoff, Hooper, D. and Ettaro, J. E. *Feasibility Study of Using Water Injection to Reduce Exhaust Emissions in Diesel Engines,* Final report submitted to the California Energy Commission, Engineering Research Institute, California State University at Fresno, Fresno, California, July 1994.

4. Marshall, *Experiments with Novel Fuels for Diesel Engines,* Publication No. BERC/TPR-77/8, U.S. DOE, Bartlesville, 1978.

5. Broering and Holtman, L. W., *Effect of Diesel Fuel Properties on Emissions and Performance,* SAE Paper 740692, September 1974.

6. Gross and Murphy, K.E., Jr., *The Effects of Diesel Fuel Properties on Performance, Smoke and Emissions,* ASME 78-DGP-26, July 1978.

7. Griffith and Compere, A. L., Correlating *Microemulsion Fuel Composition, Structure and Combustion Properties,* Oak Ridge National

Laboratory Report, ORNL/TM11248, 1989.

8. Bowman, T., Hanson, R.K.., Schmidt, C.C. and Kemal, A., *Reduction of NOx and CO Emissions from Marine Gas Turbines and Diesel Engines using In-situ SNCR,* Proceedings of the 8th ONR Propulsion Meeting, edited by Roy, G.D. and Williams, F.A., University of California at San Diego, La Jolla, CA, October 1995.

EXPERIMENTAL AND NUMERICAL ASSESSMENT OF ON-ROAD DIESEL AND BIODIESEL EMISSIONS

B.H. West, J.M. Storey, S.A. Lewis, G.L. Devault, J.B. Green - Oak Ridge National Laboratory

C.S. Sluder, J.W. Hodgson, and B.L. Moore - University of Tennessee

INTRODUCTION

The Federal Highway Administration's TRAF-series of models use modal data to estimate fuel consumption and emissions for different traffic scenarios. A process for producing data-based modal models from road and dynamometer measurements has been developed and applied to a number of light-duty gasoline vehicles for the FHWA [1,2].

The resulting models, or lookup tables, provide emissions and fuel consumption as functions of vehicle speed and acceleration. Surface plots of the data provide a valuable visual benchmark of the emissions characteristics of the vehicles. Due to the potential fuel savings in the light-duty sector via introduction of diesels, and the concomitant growing interest in diesel engine emissions, the measurement methodology is been extended under DOE sponsorship to include a diesel pickup truck running a variety of fuels, including number 2 diesel fuel, biodiesel, Fischer-Tropsch, and blends.

EXPERIMENTAL

VEHICLE - The diesel test vehicle is a 1996 Ford F250 pickup truck with a direct-injection, turbocharged Navistar 7.3 liter engine. The Navistar engine has hydraulic electronic unit injectors (HEUI), with true "drive-by-wire" engine control. The accelerator pedal sensor (APS) is electronically sensed by the engine computer. This engine is emissions certified as a heavy-duty engine, and as such, is only available in vehicles over 8500 pound Gross Vehicle Weight Rating (GVWR), also known as heavy light-duty trucks.

ON-ROAD - Test vehicles are instrumented, tapping into as many on-board sensors as possible to minimize setup time. A Davit Lightspeed optical fifth wheel is used to sense vehicle speed, and all data are collected using an Advance Electronic Diagnostics Rough Ryder PC and VMS 1220 datalogger. After installation of the datalogger and optical fifth wheel, vehicles are road tested at steady speeds from 32 to 105 km/h (20 to 65 mph), in nominal 4 km/h (2.5 mph) increments on public roads with minimal grade. Since the East Tennessee area is somewhat hilly, all data are gathered in opposite directions on the same road to reduce grade (and wind) effects. Cruise control is used whenever possible during steady speed data collection.

Following steady speed road testing, vehicles are exercised on a 1.5 km (5000 ft) airport runway. The airport runway is used for very low and very high speed runs, and acceleration and deceleration runs which cannot be safely conducted on public roads. Acceleration runs are typically performed at 10 different throttle or rack settings ranging from 10% to 100%. All data on the runway are also gathered in both directions to reduce wind and grade effects, and typically two full sets of data are gathered. The runway has a maximum grade of 1%. Parameters typically collected on-road include vehicle speed, ambient, coolant and exhaust temperatures, manifold pressure, engine speed, throttle or accelerator pedal position, and fuel injection parameters.

DYNAMOMETER - Following on-road data collection, the vehicles are brought to the chassis dynamometer for emissions and fuel consumption measurements. The chassis dynamometer used is a twin-roll, eddy-current Sun Roadamatic. For transient testing, the dynamometer's discrete mass and drag coefficient times frontal area (C_dA) settings were adjusted to match on-road data. The C_dA was adjusted at high speed cruise until the engine condition matched that measured on-road at the same speed. Full power (100% APS) rolling acceleration runs were then used to set the inertia

weight that matched the on-road time required to accelerate from 32 to 97 km/h (20 to 60 mph). This process ensured that transients on the dynamometer most closely matched similar on-road conditions. During steady-state testing on the dynamometer, the load was manually adjusted to obtain the desired engine conditions.

Modal Testing - On the dynamometer, the same datalogger is used for collecting data similar to that collected on-road. In addition, fuel consumption and engine-out and tailpipe emissions constituents are measured and logged (HC, CO, NO_x, CO_2, O_2). The two parallel raw exhaust streams are pumped and cooled by a two-head ADI teflon/stainless steel diaphragm pump and a Baldwin Environmental thermoelectric chiller, respectively. Two identical emissions benches measure the exhaust species using Rosemount NGA 2000 gas analyzers. The analyzers include flame ionization detectors for hydrocarbons, non-dispersive infrared detectors for CO and CO_2, chemiluminescence detectors for NO_x, and paramagnetic detectors for oxygen. Heated FIDs are used for measuring diesel HC emissions.

The fuel consumption is measured using a Max Machinery 710 Fuel Flow Measurement System. The Max system contains a positive-displacement fuel flowmeter, heat exchanger, pumps, level controller, pressure regulators, and vapor eliminators to facilitate measuring the net fuel consumed by engines with high return flow. The fuel flow measurement system is accurate to ±0.5% with a turndown ratio of 200:1, however, it can take several seconds for it to respond to a transient event. As such, the flowmeter was used to measure flow under steady conditions on the dynamometer while recording other engine parameters. For spark ignition engines, the injector pulse width and frequency are measured. For the Navistar diesel reported on here, the fuel consumption is based on the accelerator pedal sensor position (APS) and the engine speed.

The on-road APS and RPM data were plotted to provide a guide or "roadmap" for dynamometer measurements, so that on-road engine conditions could be duplicated on the dynamometer. On-road APS vs RPM for the diesel pickup truck is shown in Figure 1. On the dynamometer, engine conditions were held steady for about 10 seconds while emissions data were recorded. Transient data were recorded between the steady set points. Data were gathered until the on-road APS vs RPM plot was adequately covered with steady-state dynamometer data. Transients were also recorded from idle to 120 km/h at various throttle settings, to ensure full coverage of the engine map, and to provide the resulting models with a composite of transient and steady-state data. Figure 2 shows the dynamometer APS vs RPM.

Driving Cycle Testing and Dilute Exhaust Sampling - The ORNL dilution tunnel consists of a positive-displacement pump (PDP) operating at 620 cfm with an eight inch stainless steel tunnel. A laminar flow element on the intake side as well as a rotation counter provide redundant measures of total volume. A 40 liter per minute

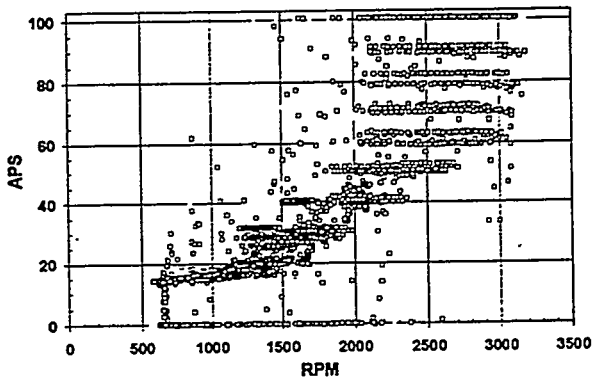


Figure 1. On-Road accelerator pedal sensor (APS) vs engine speed for diesel truck

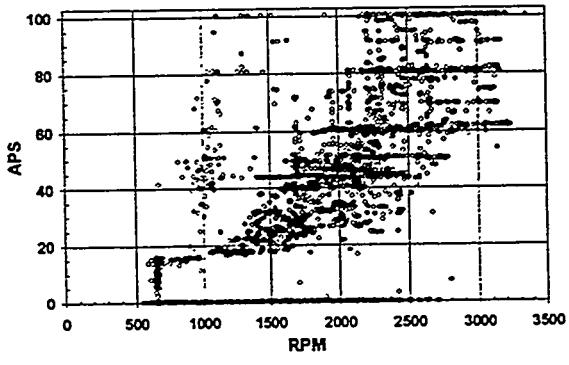


Figure 2. Dynamometer APS vs engine speed for diesel truck

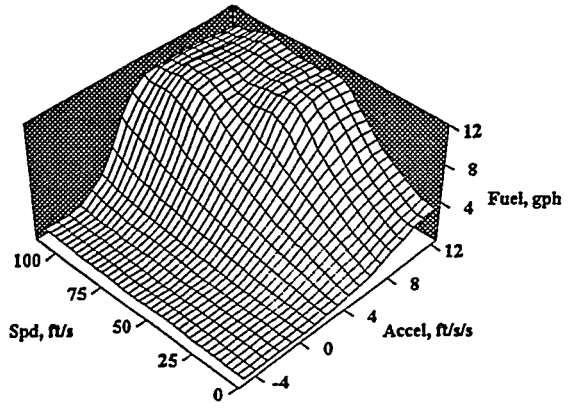


Figure 3. Gasoline composite vehicle fuel consumption

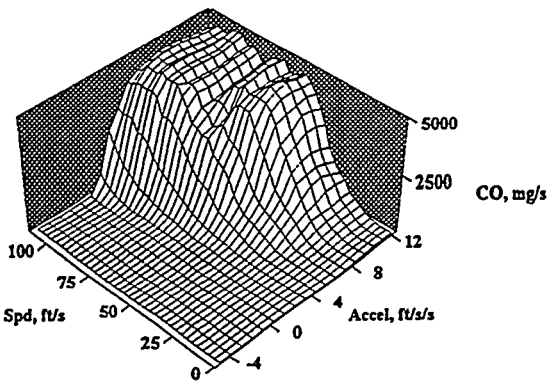


Figure 4. Gasoline composite vehicle CO emissions

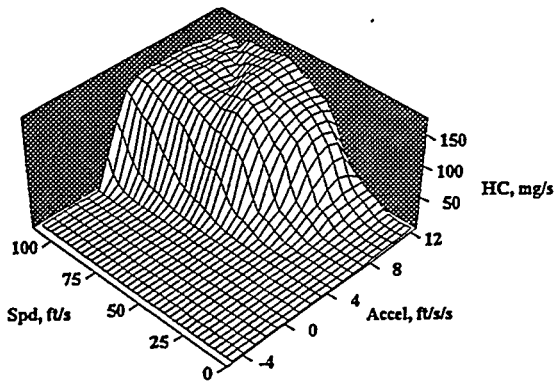


Figure 5. Gasoline composite vehicle HC emissions

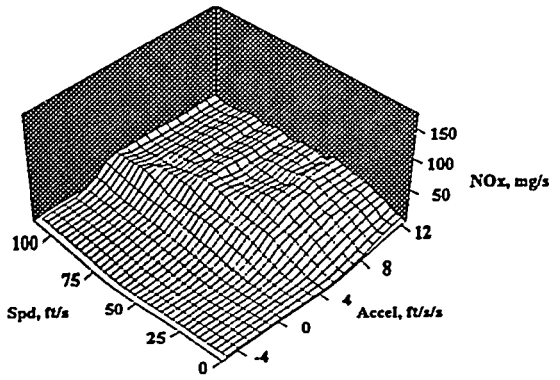


Figure 6. Gasoline composite vehicle NOx emissions

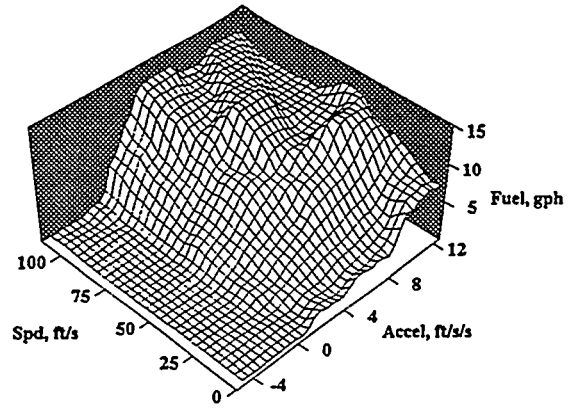


Figure 7. Diesel truck fuel consumption

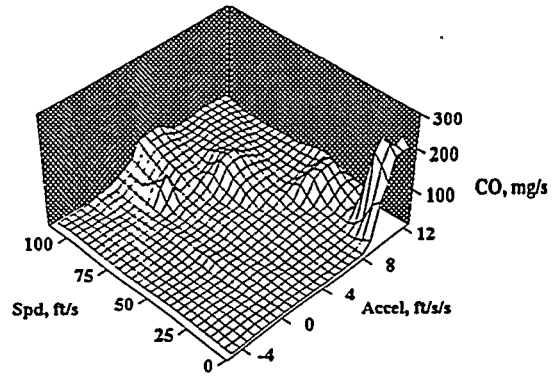


Figure 8. Diesel truck CO emissions

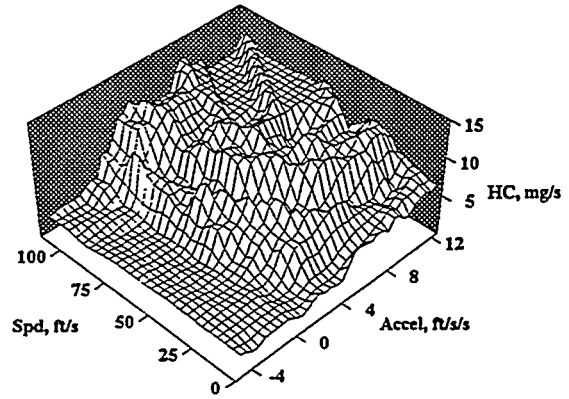


Figure 9. Diesel Truck HC emissions

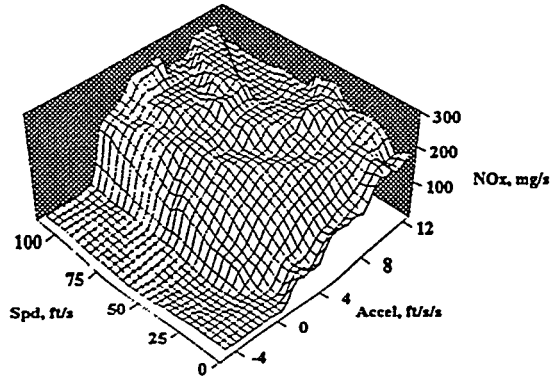


Figure 10. Diesel truck NOx emissions

(LPM) pump collects particulate samples through a 0.5 inch I.D. probe and dual 47 mm filter holders. Another smaller pump is used to fill the tedlar bags and provide samples for aldehyde and ketone analysis. The bag samples were analyzed for C_3-C_{12} hydrocarbons using a Hewlett Packard 5890/5970B GC/MS. Single point calibration with a standard mixture of exhaust HCs at ~ 1 ppm was performed. The aldehydes and ketones were collected on di-nitro phenyl hydrazine cartridges (Waters DNPH Sep-Paks), and analyzed with HPLC according to established methods [3]. Multipoint calibration using commercially-prepared DNPH standards was used for quantification.

The light-duty Federal Test Procedure (FTP) was modified to elevate the mass of particulate collected during testing. The FTP consists of a 505 second phase (Bag 1), an 867 second phase immediately following Bag 1 (Bag 2), a ten-minute soak, and finally a repeat of the first 505 seconds (Bag 3). Composite emissions are calculated with the assumption that the fourth phase (a repeat of the 2nd 867 second phase) results are identical to the Bag 2 results, so this phase is not normally repeated. To obtain a larger particulate sample, a modified FTP was used in which one filter and one bag were collected for the first two phases, and another filter and bag collected 10 minutes later, comprising a full repeat of the 1372 second cycle. Bag emissions were analyzed for CO, NO_x, and CO_2, as well as carbonyls and HC species.

A new "high-load" cycle will be added to the FTP for light-duty vehicles in the near future. This new cycle (called US06) demands much higher speeds and accelerations than the current FTP. The intent of the new cycle is to reduce emissions from enrichment events in spark ignition engines, although the higher engine loads could affect diesel emissions as well. It is not clear whether this cycle will apply to light-duty diesels, but with the possibility that it *will* apply, US06 driving cycle tests were also conducted on the diesel truck. For a thorough discussion of the development of the US06 cycle and its intent, the reader should consult the literature [4-7].

On-line particulate measurement - For a very short time, two on-line particulate instruments from Rupprecht and Patashnick Company were installed on the tunnel. The Tapered Element Oscillating Micro-balance (TEOM, model 1100) instrument provides near-real time information on PM emission rate. A sample is drawn at 2 LPM through a small filter which oscillates on the tip of a tapered element. The oscillation frequency is proportional to mass on the filter so a total mass as well as a rate-change of mass is recorded. The Diesel Particulate Measurement System (model 5100) measures volatile, semi-volatile, and elemental carbon fractions of PM based on thermal gravimetric analysis. A sample is drawn through a quartz filter held at constant temperature and then analyzed off-line by thermal oxidation followed by CO_2 analysis. The temperature ramp defines the volatile, semivolatile and elemental fractions. These instruments are particularly suited to rapidly comparing fuel effects under identical vehicle condi-tions, and although only a few tests were performed, some interesting comparisons between B100 and diesel fuel can be made.

RESULTS

MODAL TESTING - The on-road and dynamometer data were processed using desktop personal computers, and commercially available software. Custom FORTRAN programs were used to smooth the on-road data and put it into a more manageable size using a moving window average technique [8]. On-road data were collected at 10 Hz (10 samples per second), so it was not unusual for the aggregate on-road data file to contain over 30,000 lines of data. The smoothing routine reduced the file size to one fourth its original size.

The dynamometer data were collected at 2 Hz because the response of the gas analyzers and fuel flowmeter were on the order of seconds. Output from each gas analyzer was offset by a measured amount from realtime measurements of engine parameters to allow for transport of the gas and analyzer response time. Following computation of emissions rates (g/s), surface maps of emissions were generated as functions of RPM and APS.

On-road data were used to generate surface maps of RPM and APS as functions of vehicle

speed and acceleration. Using the RPM and APS surface maps, for any given speed and acceleration one can compute the engine condition. Given RPM and APS, one can then go to the dynamometer maps and compute the emissions. The resulting maps, or lookup tables, provide emissions and fuel consumption as functions of vehicle speed and acceleration. Graphical representations of the lookup tables for the light duty gasoline vehicles are shown in surface plots of the modal fuel consumption, CO, HC and NO_x emissions in Figures 3, 4, 5, and 6, respectively. These plots are for the average of the eight vehicles, or for a composite vehicle. The onset of enrichment is very clearly seen in the CO and HC plots, when the emissions increase drastically. The NO_x emissions are shown on the same scale as the HC emissions.

Graphical representations of the diesel truck's fuel consumption and emissions lookup tables are shown in figures 7, 8, 9, and 10. Note the differences in the general shape of the surfaces and the overall magnitudes as compared to the light duty composite maps. The CO and HC emissions are much lower, while the NO_x is much higher. Modal surface maps for the biodiesel fuel and blends have not yet been completed, but will be reported in a future publication.

It is important to point out that most vehicles cannot operate in every mode represented here. For almost any vehicle the maximum obtainable acceleration rate decreases at higher speeds. Since the lookup tables are provided on a rectangular matrix, the unobtainable cells are filled with their nearest neighbor. That is, the emissions or fuel consumption for that same speed.

DRIVE CYCLE TESTING - Results of FTP tests with Number 2 diesel fuel and B100 are shown in Figure 11. The use of B100 lowers CO, HC, NO_x, and PM at the expense of fuel economy. Similar results are seen in Figure 12 for the US06 cycle, except for an increase in NO_x emissions.

HC speciation - The amount of hydrocarbon in the bags was very low - most compounds were on the order of 100 ppb by mass, so accurate quantitation will require the use of a flame

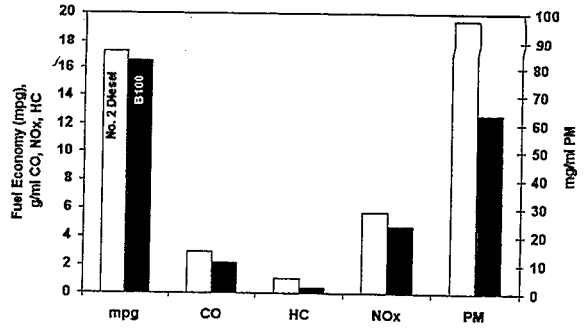


Figure 11. Diesel and Biodiesel results for light-duty FTP cycle

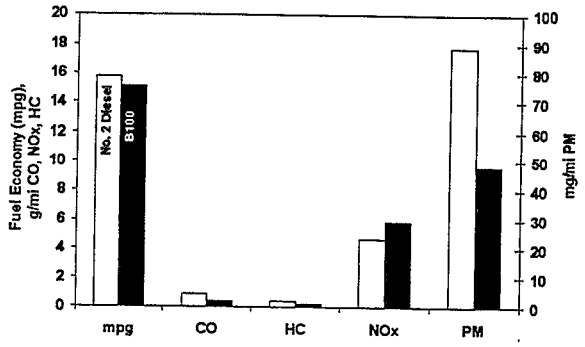


Figure 12. Diesel and Biodiesel results for light-duty US06 cycle

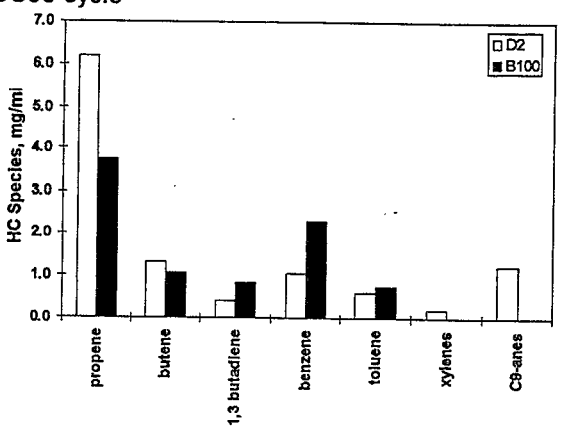


Figure 13. Select HC species for diesel and B100 on light-duty FTP cycle

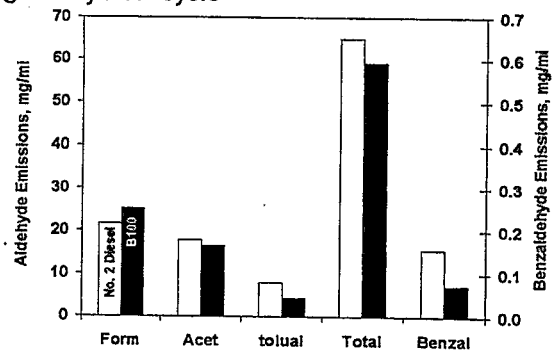


Figure 14. Select carbonyls for diesel and B100 on light-duty FTP cycle

ionization detector. Our interests included identifying what species were present; therefore, the mass spectrometer was used in this initial work. The preliminary results of the bag speciation for the FTP are shown in Figure 13. B100 reduced the overall HC emissions rate but some compounds, including the air toxics benzene and 1,3 butadiene were enhanced over that of diesel. The quantities are still very low, on the order of milligrams per mile. As expected, the heavier aromatic and aliphatic compounds were not present with the B100.

The carbonyls (aldehyde and ketones) analysis saw the majority of emissions from both fuels to be three compounds, formaldehyde, acetaldehyde, and tolu-aldehyde. Figure 14 shows that total aldehydes were reduced with the use of B100, although not significantly. Notably, benzaldehyde emissions from B100 were one half the level of the emissions from diesel. This is in contrast to the result for benzene which saw a twofold increase in concentration.

Real-time PM measurement - These results should be considered quite preliminary, as the instruments were only available for a few days. Nonetheless, some interesting observations and comparisons can be made between the two fuels. The TEOM data shown in Figure 15 follows the accumulation of particulate mass over the FTP cycle for B100 fuel. Note that the filter loses mass under some conditions; typically, load points followed by idle. This occurs on the regular 47 mm filters as well, when water and volatiles blow off the filter, but the integrated sample only measures net weight gain. The modal data in Figure 16 show the instrument response for a series of steady state conditions during the mapping activities with B100. For a given load and speed, the PM emission rate can be determined. Hopefully, this will allow mapping of PM for diesel vehicles in the same manner that the HC, NOx, CO and fuel consumption are mapped.

The data from the Diesel Particulate Measurement System show large differences in the fuel's effect on PM. For the FTP data, Figure 17 shows that the biodiesel lowers the semivolatile fraction (350°C - 650°C) by a factor of two and the elemental carbon (650°C-750°C) by a factor of 5 or more. Results from a heavier load steady-state test are shown in Figure 18, where all three fractions are greatly reduced with B100 fuel. The lower semivolatile and elemental fractions can be attributed to the lack of aromatics in B100. As catalyst temperatures were higher under the steady load condition, the "wetter" B100 particulate was probably more readily oxidized under these conditions. The average catalyst temperatures over the FTP rang-ed from 300-320°F with peaks less than 450°F, while the averages over the chosen steady-state condition (40% APS at 2000 RPM) were on the order of 700°F with peaks above 800°F.

SUMMARY AND FUTURE WORK

Data-based modal models provide a simple means to predict cycle emissions or make vehicle-to-vehicle, or fuel-to-fuel comparisons. Driving cycle tests of a heavy light-duty diesel truck have shown that neat biodiesel fuel can reduce cycle particulates, semi-volatile PM fraction, aldehydes, and some HC species. Future testing will include diesel and biodiesel blends, Fischer-Tropsch (FT) diesel, and F-T blends.

ACKNOWLEDGEMENTS

This work was conducted by Lockheed Martin Energy Research Corporation for the U.S. Department of Energy under contract number DE-AC05-96OR22464. The authors wish to thank the U. S. Department of Energy for funding this work, particularly Mr. Steve Goguen.

REFERENCES

1. West, Brian H., Ralph N. McGill, Jeffrey W. Hodgson, C. Scott Sluder, and David E. Smith, "Development of Data-Based, Light-Duty Modal Emissions and Fuel Consumption Models," Society of Engineers Paper No. 972910, October 1997.

2. McGill, Ralph N., John. N. Hooker, and Jeffrey W. Hodgson, "Fuel Consumption and Emissions Values for Traffic Models," U. S. Department of Transportation, Federal Highway Administration, Report No. FHWA/RD-85/053, May 1985.

3. Swarin, S. J., J. F. Loo, E. Chladek, M. S. Drouillard, and S. B. Tejada, "Advanced Emission Speciation Methodologies for the Auto/Oil Air Quality Improvement Research Program - II. Aldehydes, Ketones, and Alcohols," SAE Paper number 920321.

4. Haskew, Harold M., Kevin Cullen, Thomas F. Liberty, and William K. Langhorst, "The Execution of a Cooperative Industry/-Government Exhaust Emission Test Pro-gram," SAE Technical Paper 94C016, 1994.

5. Kishan, S., T. H. DeFries, and C. G. Weyn, "A Study of Light-Duty Vehicle Driving Behavior: Application to Real-World Emission Inventories," SAE Paper No. 932659, October 1993.

6. Environmental Protection Agency, "Federal Test Procedure Review Project: Preliminary Technical Report," May 1993.

7. Environmental Protection Agency, "Final Technical Report on Aggressive Driving Behavior for the Revised Federal Test Procedure Notice of Proposed Rulemaking," Office of Mobile Sources, January 1995.

8. Annino, Raymond, and Richard D. Driver, *Scientific and Engineering Applications with Personal Computers*, John Wiley and Sons, 1986.

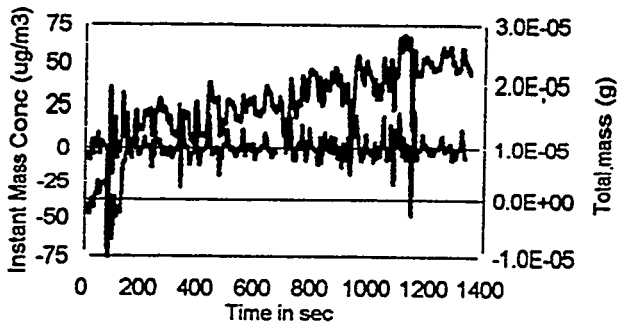


Figure 15. TEOM data for diesel truck on light-duty FTP, B100 fuel

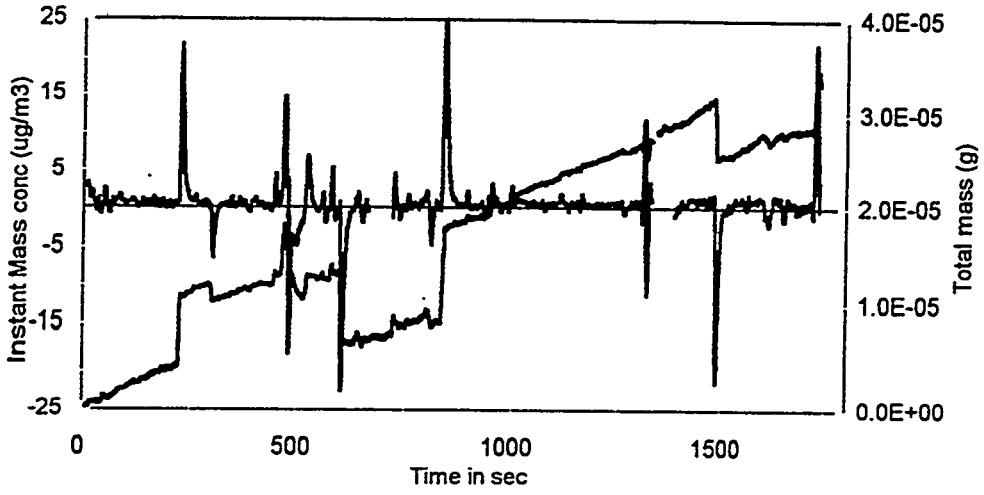


Figure 16. TEOM data for diesel truck during modal testing, B100 fuel

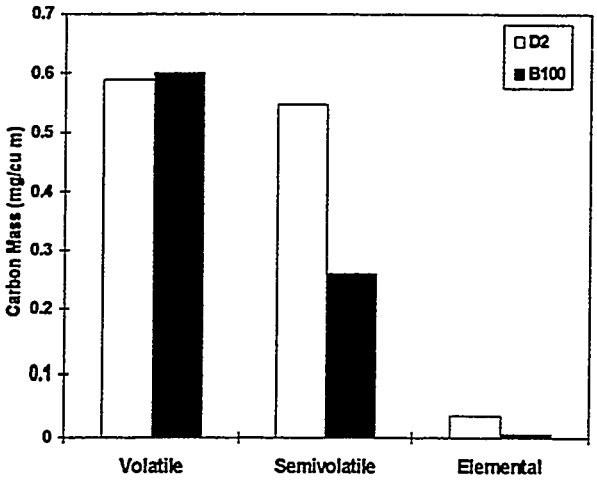


Figure 17. Particulate fractions for diesel truck on light-duty FTP for diesel and B100 fuels

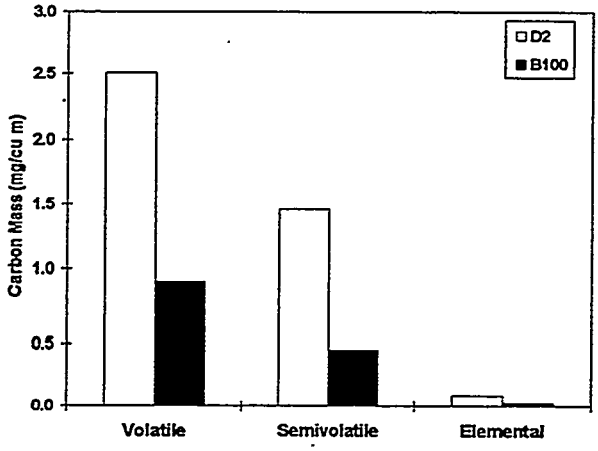


Figure 18. Particulate fractions for diesel truck under steady load for diesel and B100 fuels

SESSION VIB

Advanced Technology

Chairman: Rebecca Dyer
U.S. Department of Energy

DETAILS OF AN INJECTOR DEPOSITING TEST FOR EVALUATION OF DIESEL QUALITY

S.D. Whitacre
Cummins Engine Company, Inc.

Diesel engine emission control can be greatly improved by maintaining the integrity of the fuel injection system. While previous efforts have focused on mechanical design improvements, it is clear that fuel quality issues must also be addressed. Poor quality fuels promote deposit formation, corrosion, and inadequate lubrication, all of which deleteriously impact injector performance. Cummins' commitment to improved diesel fuel quality resulted in the development of an engine laboratory test to evaluate injector deposit formation. It is the only known test to measure diesel injector deposits and has been included in the EMA Premium Fuel Specification. The 125 hour test utilizes an '88 Cummins L10 engine alternating between powering and motoring cycles with injector deposits visually rated at the end of the test. Deposit levels and composition correlate well with field measurements with reasonable repeatability.

Details of an Injector Depositing Test for Evaluation of Diesel Fuel Quality

Shawn D. Whitacre
Cummins Engine Company
July 31, 1997

1997 Diesel Engine Emissions Reduction Workshop
University of California - San Diego

Introduction

- Diesel emission control improved by maintaining the integrity of the fuel injection system
- Fuel quality impacts:
  - deposit tendency
  - corrosivity
  - lubricity
  - filter plugging

→ Injector Performance

- Cummins Engine Company committed to improved diesel quality worldwide

Overview

- Injector deposits have long history of occurrence
- Impact:
  - Engine performance
  - Emissions
- Hardware changes driven by emission regulations
- New focus: Diesel fuel quality

Background

- Performance loss due to deposit formation noticed by fleets operating in hilly areas
- Problem attributed to duty cycles with frequent periods of high speed driving and motoring
- Design change on the injector plunger provided a fix
- Fuel quality still an issue however

Test Development

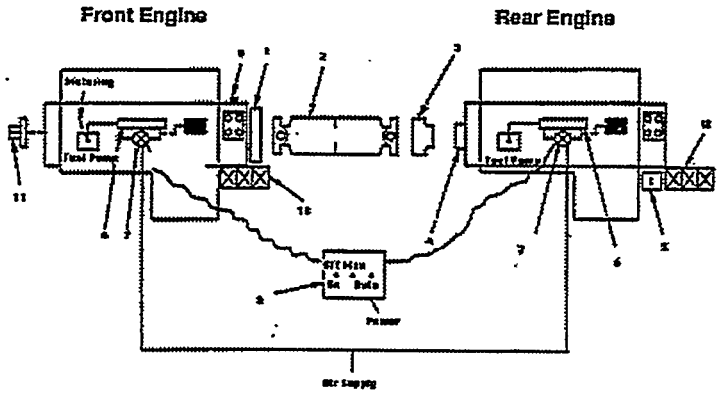
- In response, Cummins developed an engine test to mimic the 'problem' duty cycle
- Cummins '88 L10 engine (6 cyl, DI, 300 HP)

  Fixed time - PT fuel system
- Test cycle:

  2300 RPM/60 HP

  15 seconds driving/15 seconds driven (alternating)

  125 hours
- Tandem or dyno stand setup



Tandem Engine Schematic

L10 Injector Depositing Test

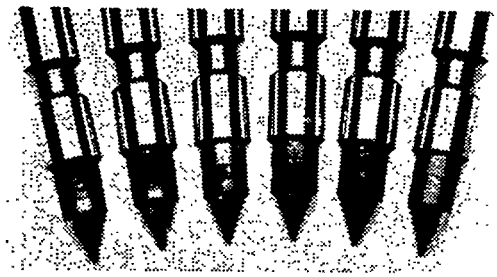
Injector Evaluation

- Deposit rating
  - Visual rating of carbon and lacquer/varnish
  - Modified version of CRC piston deposit rating
  - Digital imaging method under development
- Flow
  - Injector flow measured before and after test

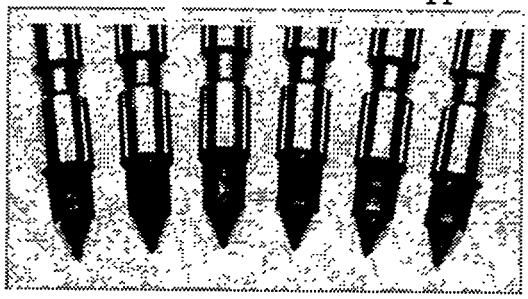


Test Stand Calibration

- Test stands referenced using specified fuel and additive
- Stands must reference within acceptance bands with a neat and additized fuel
- Neat fuel
  - Howell 0.4% Sulfur Diesel Test Fuel
  - Deposit rating: 21.2 - 28.6
- Additized reference fuel
  - Howell fuel with 200 ppm CRA-1



Reference Diesel Fuel Treated with 200 ppm CRA-1



Unadditized Reference Fuel

Test Stand Availability

- Qualified test stands established at five labs
  - 3 independent test labs
  - 2 additive suppliers
- 10 raters trained, workshops held periodically
- ASTM Surveillance Task Force formed
  - test standardization planned for '98
- Growing interest worldwide as test matures

Current Applications

- L10 IDT included in EMA's FQP-1
- Part of Cummins diesel fuel performance criteria
- Qualifying test for Thailand railroad diesel fuel
- Premium diesel increasingly prevalent in agricultural applications

Impact of Fuel Detergency

- Maintaining injector life means maintaining emission control capability and fuel economy
- Studies by Lubrizol, Paramins, Texaco demonstrate that prolonged use of treated fuels lowers:
  - fuel consumption
  - hydrocarbons
  - CO
  - particulates

  (as compared to fleets using untreated fuels)

Summary

- Cummins is devoted to improved diesel fuel quality worldwide
- An engine test is available to evaluate diesel detergency with reasonable precision
- Fuel detergency enhances the durability of the injection system...a positive for emission control and fuel economy

THE EFFECTS OF THERMAL BARRIER COATINGS ON DIESEL ENGINE EMISSIONS

A.L. Boehman, M. Vittal, J. Borek, and D. Marks - The Pennsylvania State University

D. A. Okrent, Rupprecht & Patashnick Co., Inc. and A.P. Bentz, JBL Associates, Inc.

INTRODUCTION

The major promises of thermal barrier coated (also known as low heat rejection, LHR) engines were increased thermal efficiency and elimination of the cooling system [1]. A simple first law of thermodynamics analysis of the energy conversion process within a diesel engine would indicate that if heat rejection to the coolant was eliminated, the thermal efficiency of the engine could be increased. However, due to a number of challenges posed by the presence of thermal barrier coatings within the engine, these particular promises have not been kept.

What instead appears to be the benefit of thermal barrier coatings is a change in smoke and particulate emissions [2-5]. The effect on NO_x emissions is not as clear, with some investigations showing increases in NO_x emissions and others showing no increase. Also, a fuel economy penalty can be expected with a thermal barrier coated diesel engine. But, as a strategy to reduce particulate emissions, thermal barrier coatings have proven to be effective, especially in some recent studies by Engelhard Corp. [4] and at Penn State [5-7].

In this paper, we summarize some our of recent work at Penn State that has been performed on behalf of the U.S. Coast Guard R&D Center, Groton, CT. This work has included collaboration with Rupprecht & Patashnick Co. (R&P Co.), Inc., Albany, NY. Here we will briefly describe the experimental configuration used, and some of the key results obtained thus far. The motivation for this work has been to determine whether rebuilding in-service marine diesel engines to include thermal barrier coated parts is a viable means of reducing emissions from Coast Guard vessels. Objectives of this work have been to characterize changes in emissions caused by thermal barrier coatings and to understand the reasons for any observed changes.

EXPERIMENTAL

Apparatus and Testing Procedure:

A schematic of the engine test cell is shown in Figure 1 and specifications of this engine are listed in Table 1. As seen in the figure, the engine was coupled to a Clayton water brake dynamometer. The dynamometer torque was measured using a strain gauge load cell and the speed was monitored using a 60-tooth gear assembly. The exhaust, lube oil and coolant temperatures were also measured to monitor engine operation. The temperature of the ex-haust gas was monitored with a type-K thermocouple mounted in the exhaust manifold. The data acquisition system was a Gateway 2000 P-5/100 MHZ computer with a DAS-8/PGA data acquisition and control board from Keithley Metrabyte. The computer was set up to log real-time engine speed, engine torque, engine power, and exhaust, lube oil and coolant temperatures.

The piston crown, cylinder head, and valves were given thin thermal barrier coatings (300 μm thick) by Turbine Components Corporation of Branford, CT. The parts were given a bond coat of NiCoCrAly, followed by a top coat of Metco pre-alloyed, yttria stabilized zirconia. No attempt was made to maintain a fixed compression ratio. Instead identical engine components were used where the only difference was the presence of the ceramic coating on the aforementioned surfaces. Assuming that the combustion chamber consists of a simple cylindrical surface, we estimate that the compression ratio changed from 19.5 to 21.6 between the baseline and ceramic coated configurations. However, the actual difference in compression ratio was most likely negligible. The baseline (uncoated) engine acquired a significant carbon deposit during the break-in period, which would increase the baseline compression ratio. The Coordinating Research Council considers a "trace to light" combustion chamber deposit to be of 200 to 400

μm thickness [8]. During the break-in period, the ceramic coated surfaces resisted formation of significant carbon deposits. So, the "in-use" compression ratios of the baseline and ceramic coated engines were probably similar. If the carbon deposit on the baseline engine increased to even a "medium" rating (1.59 mm), the ceramic coated engine could result in lower "in use" compression ratio.

The test procedure was chosen so as to match the typical duty cycle of a diesel engine for marine applications. The International Standard (ISO 8178, Part 4) was consulted for guidance. Table 2 shows the test matrix used in this work. It is based broadly on cycle E3 (Marine Applications, heavy-duty propulsion engines) described in ISO 8178, Part 4. There are four modes, a mode being a part of the test cycle with defined speed and torque.

A protocol was established to effect the changeover from the baseline (metal) configuration to the ceramic-coated configuration. The same piston rings and fuel injector were used for both configurations. However, for each changeover, the cylinder head gasket was replaced with a new (identical) gasket to ensure quality of the seal between the head and the cylinder block. The lube oil and coolant were also changed, although lubricant consumption was not monitored. The lube oil was SAE 10W30 Motor Oil from Valvoline and the coolant was Prestone Antifreeze/Coolant. Each time the lube oil was changed, the engine was run for 8 hours to break in the new oil. The oil temperature in the engine typically took up to an hour to reach steady state. Thus, an hour-long warm-up period was always used to prepare the engine for testing. A low-sulfur Diesel fuel from BP Oil was used in all tests.

The gaseous portion of the exhaust was analyzed using an ENERAC Model 3000E Integrated Emissions System and a NICOLET Magna-IR 550 Spectrometer. The ENERAC gas analyzer is based on electrochemical sensors and measures NO, NO_2, CO, combustibles, SO_2 and O_2 concentrations. The FTIR was used to quantify CO, NO, NO_2 and N_2O emissions.

Diesel exhaust particulates were collected on Pallflex TX40HI20WW filters using a Sierra Instruments Model BG-1 Micro-Dilution Test Stand. The total flow rate was set at 50.0 standard liters/minute (SLPM) and the dilution flow rate was set at 41.7 SLPM. These settings yield a sample flow rate of 8.3 SLPM and thus a dilution ratio of 5.0. Particulates were collected for ten minutes at each mode. The International Standard (ISO/DIS 8178-1.2) stipulates that the temperature of the collection filters should be below 52° C, a minimum of 2.3 mg of soot should be collected, the pressure drop increase during the test should not exceed 25 kPa, and the filters should not tear. The flow rates were adjusted by trial and error until these criteria were satisfied completely. All runs reported here complied with these requirements. Particulate was collected on the primary filter and the secondary filter served as a back up to collect any particulate that should pass through the primary filter. Before and after sampling, the filters were allowed to equilibrate in a humidity-controlled chamber and weighed using a Sartorius microbalance with an accuracy of ±2 μg.

Several methods were used to study the chemical and physical characteristics of the particulate matter collected from the baseline and ceramic coated engine over the four modes of the Type E3 test. These were scanning electron microscopy (SEM), electron dispersive spectrometry

Table 2. ENGINE TEST MATRIX

	Mode 1	Mode 2	Mode 3	Mode 4
Speed (RPM)	2200	2002	1760	1386
% Rated Speed	100	91	80	63
Power (HP)	12.26	8.77	5.32	2.03
% Rated Power	81.7	58.5	35.5	13.5

Table 1. ENGINE SPECIFICATIONS

Parameter	Type / Value
Make	Yanmar
Model	TS180C
Type	Prechamber
No. of cylinders	1
Bore * stroke (mm)	102*106
Displacement (l)	.866
Continuous rating output (kW/rpm)	11.2/2200
Specific Fuel Consumption (g/kWh)	275
Compression ratio	19.5

(EDS), thermal analysis, and GC, GC-MS, and HPLC analyses of the soluble fraction. At present, the chemical analyses of the SOF are only qualitative, and will not be discussed here. Efforts to complete a quantitative analysis procedure will likely make use of HPLC, since this provided superior sensitivity and peak identification for PAH compounds.

SEM and EDS Analyses:
An ISI SX 40-ABT SEM was used for energy dispersive X-ray analyses and a JOEL JSM-6300 FV SEM was used for microstructural analyses. The particulate laden Pallflex filters were dried for 1 hr. at 80°C under vacuum to remove moisture. This reduced the volatility of the particulate samples and enhanced the stability of the SEM probe and imaging system. Small quantities of particulate matter were placed on test stands to permit the SEM analysis. For the ISI SEM, a carbon test stand was used. For the JEOL SEM, an aluminum test stand was used. In both situations, a vacuum safe double-sided adhesive tape was used to mount the particulate samples on the test stands. In order to take photographs with the scanning electron microscopes, it was necessary to coat the samples with gold, a conducting medium, by using a sputter coater.

Thermal Analysis:
A Series 5100 Diesel Particulate Measurement System from R&P Co. was attached to the exhaust stack by means of a heated sample tube. The instrument cycle has two phases which are controlled by an instrument computer. During the collection phase, the system draws a sample of particulate-laden gas from the exhaust and routes it to a quartz filter. As the gas passes through the filter, particulate is trapped and filtered exhaust gas is vented out of the device. During the analysis phase, the collected sample is heated according to a user-defined temperature program. As the filter temperature increases, volatiles leave the filter, enter the gas stream, and travel to an afterburner set for 750° C. Oxidation of the carbonaceous materials produces CO_2, which is read by an NDIR CO_2 analyzer. The instrument computer converts the reading into a carbon concentration (mg of carbon per ml of exhaust gas collected).

The collection and analysis parameters used in this work were as follows: Particulate-laden exhaust gas was sampled at a rate of 8.0 liters/min for 60 sec at engine operating modes 1 and 2, and 120 sec at modes 3 and 4. The collection temperature was 75° C. After collection, the filter temperature was ramped from 200° to 750° C at a rate of 5° C/min. The CO_2 concentration data at each temperature were downloaded from the instrument to a PC for graphing.

RESULTS AND DISCUSSION

Emissions Measurements:
Emissions of CO and NO_x exhibited the same trends for both the baseline and ceramic-coated engines. As shown in Fig. 2, brake specific CO emissions decreased sharply from Mode 4 to Mode 3, and slightly thereafter. Brake specific NO_x emissions decreased with increasing power

as shown in Fig. 3. For all modes, CO emissions were higher for the ceramic-coated engine, while NO_x emissions were the same for both configurations. The exhaust temperature was higher for the ceramic-coated engine over the full range of power settings.

It was expected that CO emissions would be lower for the ceramic-coated engine since the higher temperatures of the combustion gas and chamber walls should increase the rate of oxidation reactions leading to the complete combustion product, CO_2 [9]. However, for all modes there was a slight increase in BSCO emissions for the ceramic-coated engine. Higher CO concentrations were also reported by researchers at the Southwest Research Institute [10] for an LHR engine at high loads. One explanation lies in the strong relationship between CO emissions and the air/fuel ratio. As the air/-fuel ratio decreases, CO emissions increase. Exhaust gas analysis showed that for all modes the air/fuel ratio was lower for the ceramic-coated engine, thus explaining the higher CO concentrations in the exhaust. However, the sharp increase in BSCO emissions at Mode 4 for both configurations is harder to explain. Since diesel engines always operate on the lean side of stoichiometric, CO emissions should vary little with air/fuel ratio. It is possible that combustion at this mode was highly degraded because of lower temperatures resulting in slower kinetics.

The thermal barrier coating caused no significant change in the brake specific NO_x emissions. There was a marked decrease in $BSNO_x$ as power was increased. It may be expected that the ceramic-coated engine would have higher NO_x emissions due to the higher combustion temperatures and indeed other researchers have found an increase in NO_x emissions for LHR engines [3]. However, NO_x emissions are a function of both temperature and pressure of the burned gas. On the one hand, NO_x formation is accelerated by the higher temperatures in the LHR engine. On the other hand, the shift from premixed to diffusion combustion in the LHR engine results in lower peak pressures [1]. Due to these two competing factors, there may be a trade-off between the temperature and pressure effects on the NO_x formation rate. The most likely explanation for the observed consistency in NO_x emissions from the baseline and ceramic coated engine arises from the IDI engine configuration. As noted by Heywood [12], most of the NO forms within the prechamber and is then transported into cylinder where the NO concentration is frozen through rapid mixing with the surrounding air. The prechamber was not given a TBC coating, and thus, with regard to NO_x emissions, the opportunity for differences to arise between the two engine configurations was reduced.

The EPA defines particulates as solid or liquid except for water that collects on a filter at or below 52o C [13]. Diesel particulates are made up primarily of carbonaceous soot with some adsorbed hydrocarbons. Particulate formation in diesel engines is a complex and not fully understood process. From what is known, soot formation can be considered to occur in four stages: nucleation, surface growth, agglomeration, and adsorption/condensation [12]. The mass of soot in the exhaust gas is a function of the relationship between formation and oxidation. Both formation and oxidation rates are increased in the coated engine due to the higher temperatures and improved air to fuel mixing [14]. In the case of most LHR engines, the increase in oxidation rate is greater than the increase in formation rate. The higher oxidation rate led to decreased BS particulates in the ceramic-coated engine as shown in Fig. 4. At light loads (Modes 3 and 4) the decrease in particulate emissions from the ceramic-coated engine relative to the baseline engine was greater than at high loads (Modes 1 and 2). This is because at light loads a greater fraction of the fuel energy is lost to the coolant [13]. Thus, the decrease in energy rejection to the coolant due to the ceramic coating is greater at lighter loads, and a larger decrease in particulate emissions is realized.

EDS Analysis of Particulates:
For the uncoated engine, the energy dispersive X-ray analysis showed that in addition to a large amount of carbon © in the particulate sample; there was evidence of sulfur (S) and oxygen (O). There were also other elements present that were less than approximately three weight percent. These trace or minor elements were protactinium (Pa), titanium (Ti), zinc (Zn), calcium

(Ca), tellurium (Te), barium (Ba), cesium (Cs), sodium (Na), aluminum (Al), potassium (K), polonium (Po), chlorine (Cl), molybdenum (Mo), iron (Fe), and lead (Pb). For the coated engine, the energy dispersive X-ray analysis showed traces of nickel (Ni), yttria (Y), chromium (Cr), and cobalt (Co) in addition to those elements observed in the analysis of the particulate matter from the uncoated engine. The emission of several of the observed elements was likely the result of different factors such as utilization of organo-metallic additives in the diesel fuel or lubrication oil, contamination of the diesel fuel by alkyllead compounds, wear and corrosion of engine, and exhaust system parts [12]. Sulfur and traces of calcium iron, silicon, and chromium are found in diesel fuel; zinc, phosphorus, and calcium compounds are frequently used in lubricating oil additives [15]. The concentration of elemental components in diesel soot generally varies with operating conditions, which affect fuel and oil consumption, combustion efficiency (soot production), and mechanical strain [12].

SEM Analysis of Particulate Morphology:
There were some very evident changes of the microstructure of the diesel particulate samples. The structures of the diesel particulates are apparent from the images shown in Figures 5 and 6 for the samples collected from the exhaust of the diesel engine. The samples are seen to consist of primary particles (soot) agglomerated into aggregates (particulate). The particles range in appearance from clusters of spherules to clusters of platelets. The clusters may contain as many as 100 spherules, which range in diameters between 30 and 150 nm. The clusters of spheres are considered to be solid carbon (soot). Particulate matter is a combination of solid carbon particles surrounded by insoluble as well as soluble hydrocarbons [16]. What is seen in Figures 6 (a)-(d) is mostly the carbon particles. Whereas in Figure 5(d), what is seen is the substantial agglomeration of the primary soot particles which are bound together by condensable hydrocarbons. In other words, Figure 5(d) shows particulate matter from an engine operating condition where the oxidation of condensable hydrocarbons is poor. Enhanced oxidation of the SOF during the combustion process would leave a more porous and less agglomerated particulate structure [17]. Furthermore, under the conditions of Mode 4 (see Figure 5(d)), the engine releases particulates in a form that is potentially harmful to the environment and human health, since it is known that the condensable (and mostly soluble) fraction of the particulate contains known and suspected carcinogens [16].

Thermal Analysis of Diesel Particulates:
Thermal analysis of diesel particulate matter yields the boiling point distribution of its volatile components. It is important to bear in mind that the R&P Series 5100 differs from a conventional TGA apparatus in that it does not weigh the sample as it is heated but measures the amount of CO_2 formed when carbonaceous materials are oxidized.

For comparative purposes, the data are plotted in Figure 7 (a)–(d). It can be seen that particulates from the ceramic-coated engine contain 13–60% less low-to-medium boiling hydrocarbons than do particulates from the baseline engine. The source of these hydrocarbons is believed to be unburned fuel [17]. The material evolved between 300-450° C consists of high-boiling components, likely from the lubricating oil, and does not seem to be affected very much by the ceramic insulation. The dry soot fraction of the particulate is much higher across all the operating modes for the ceramic-coated engine. It is clear that the particulates from the ceramic-coated engine have a lower volatile content. The lower volatile content reduces the degree to which soot particles agglomerate into larger structures [18]. The particulate carbon concentrations in the exhaust are also shown in Figure 4. It is clear that the ceramic coating caused a reduction in the total particulate emissions.

Thermogravimetric analysis of fresh and used SAE 10W30 lubricating oil was also performed using a Mettler TA4000 Thermal Analyzer. The analysis was done in air at 5°C/min with a sample weight of approximately 22 mg. It was found that a little over 10% of the oil volatilizes before 250°C. The cylinder liner temperature in a conventional diesel engine is about 150°C near top dead center (TDC) and decreases significantly with distance from the cylinder head [16]. The cylinder liner temperature in a ceramic-coated engine would have to be over 100°C

higher to result in greater consumption of lubricating oil relative to the baseline engine. Also, very little difference in thermal stability was found between the fresh and used oils. The used oil was collected after about 60 h of engine operation.

With an uncooled or insulated liner, the full load increase in cylinder liner temperature near TDC can be 100°C or higher. Higher liner temperatures frequently result in lubrication problems due to increased oil consumption and lower volumetric efficiency due to heat transfer to the intake air. For this reason, it is generally preferred to leave the liner cooled and uninsulated. Alkidas [14] found a significant increase in the volatile fraction of the particulates emitted by an uncooled engine with an air-gap insulated piston, fore deck, and exhaust ports. Sudhakar and Hunter [18] reported that the dry soot emission from an uncooled engine is lower, but the extractable mass is higher by as much as 50%. In both cases, increased lubricating oil consumption was suggested as the reason for the higher volatile content. Since both groups used an uncooled cylinder liner, the higher liner temperatures may indeed have resulted in increased evaporation of oil from the liner surface.

In this work, the cylinder liner was left cooled and uninsulated. The average coolant temperature was 110° C for both baseline and ceramic-coated engines. Across all the operating modes, the ceramic-coated engine produced particulates with more dry soot and fewer volatiles. The lubricating oil contribution was relatively unaffected, suggesting that the liner temperature did not change very much. The compositional differences between particulates from the two engines can be attributed to differences in the engine exhaust conditions [12]. At exhaust temperatures above 500° C, the particles are composed principally of carbon coated with some hydrocarbons. As the temperatures decrease below 500° C, the particles become increasingly coated with condensed and adsorbed high molecular weight hydrocarbons. Figure 8 shows the exhaust temperature at different powers for the baseline and ceramic-coated engine configurations. At Mode 1 (highest power), the exhaust temperature for the insulated engine is about 520° C – almost 70° higher than the baseline engine. The hotter exhaust results in less hydrocarbon condensation and increased post-cylinder (manifold) oxidation of hydrocarbons. Therefore, the decrease in the volatile portion of the particulate matter is attributed to the higher exhaust temperature. This result is in contrast to the observations of Voss et al., who saw an overall reduction in total particulates, but observed an increase in the volatile fraction of the remaining particulate matter (i.e., a decrease in the dry soot fraction) as a result of thermal barrier coated engine components [4].

CONCLUSIONS

A combination of particulate mass, microscopic, and thermal analyses suggest that ceramic insulation of the combustion chamber walls of an IDI diesel engine is effective in reducing the volatile portion of the particulate emissions. The hotter exhaust condition in the ceramic-coated engine decreases the tendency for vapor phase hydrocarbons to condense on the particulates, resulting in a lower volatile fraction and a lower total particulate mass. With a cooled cylinder liner, no increase in the lubricating oil contribution to the volatile fraction was found relative to the baseline engine. The results indicate that it may be desirable to maintain cooling of the liner to keep oil consumption to a minimum. Thus, the original concept of the low heat rejection engine (increased thermal efficiency by decreased heat rejection) may not have proven viable. But, the thermal barrier coated engine can prove useful as one route to cleaner burning diesel engines.

ACKNOWLEDGMENTS

The authors wish to thank the U.S. Coast Guard R&D Center for support of this work. Also, the authors wish to acknowledge in-kind support from Dr. Rafal Sobotowski of BP Oil Co., who supplied the fuel used in this study.

REFERENCES

1. Amann, C. A., "Promises and Challenges of the Low-Heat-Rejection Diesel, "J. *Engr. Gas Turbines Power,* 110:475-481 (1988).

2. Belardini, P., Bertoli, C., Corcione, F.E., and Police, G., "Thermal Barriers Adoption in D.I. Diesel Engines: Effect on Smoke and Gaseous Emissions," SAE Paper No. 840995 (1984).

3. Siegla, D. C. and Alkidas, A. C., "Evaluation of the Potential of a Low-Heat-Rejection Diesel Engine to Meet Future Heavy-Duty Emissions Standards," SAE Paper No. 890291 (1989).

4. Voss, K., Cioffi, J., Gorel, A., Norris, M., Rotolico, T., and Fabel, A., "Zirconia Based Ceramic, In-Cylinder Coatings and Aftertreatment Oxidation Catalysts for Reduction of Emissions from Heavy Duty Diesel Engines," SA EPaper No. 970469 (1997).

5. Marks, D.A. and Boehman, A.L., "The Influence of Thermal Barrier Coatings on Morphology and Composition of Diesel Particulates," SAE Paper No. 970756 (1997).

6. Boehman, A. L., Vittal, M., Borek, J. A., Marks, D. A. and Bentz, A. P., "The Effects of Thermal Barrier Coatings on Diesel Engine Emissions," to be presented at the 1997 Fall Technical Conference of the ASME Internal Combustion Engines Division, Madison, WI, Sept. 27-Oct. 1 (1997).

7. Vittal, M., Borek, J. A., Boehman, A. L. and Okrent, D. A., "The Influence of Thermal Barrier Coatings on the Composition of Diesel Particulate Emissions," to be presented at the 1997 Fall Fuels and Lubricants Meetings of the SAE, Tulsa, OK, Oct. 13-16 (1997).

8. Megnin, M. K and Choate, P. J., "Combustion Chamber Deposit Measurement Techniques," SAE Paper No. 940346 (1994).

9. Thring, R.H., "Low Heat Rejection Engines," SAE Paper No. 860314 (1986).

10. Dickey, D.W., "The Effect of Insulated Combustion Chamber Surfaces on Direct Injected Diesel Engine Performance, Emissions and Combustion," SAE Paper No. 890292 (1989).

11. Assanis, D., Wiese, K., Schwarz, E. and Bryzik, W., "The Effects of Ceramic Coatings on Diesel Engine Performance and Exhaust Emissions," SAE Paper No. 910460 (1991).

12. Heywood, John B., Internal Combustion Engine Fundamentals. McGraw-Hill, New York (1988).

13. Arnann, C. A., "The Low-Heat-Rejection Diesel (Also Called the 'Adiabatic Diesel')," in Advanced Diesel Engineering and Operation, ed. S. D. Haddad, Ellis Horworth, Chichester, UK, pp. 173-239 (1988).

14. Alkidas, A.C., "Performance and Emissions Achievements with an Uncooled Heavy Duty Single Cylinder Diesel Engine," SAE Paper No. 890144 (1989).

15. Amann, C. A. and Siegla, D. C. "Diesel Particulates - What They Are and Why," *Aerosol Science Technology,* 1:73-101 (1982).

16. Neeft, J. P. A., Makee, M., and Moulijn, J. A., "Diesel Particulate Control," *Fuel Processing Technology,* 47:1-69 (1996).

17. Ishiguro, T., Suzuki, N., Fujitani, Y., and Morimoto, H., "Microstructural Changes of Diesel Soot During Oxidation," *Combustion and Flame, 85:1-6* (199 1).

18. Sudhakar, V. and Hunter, G., "Transient Emissions from an Uncooled Diesel Engine." SAE Paper No. 860224 (1986).

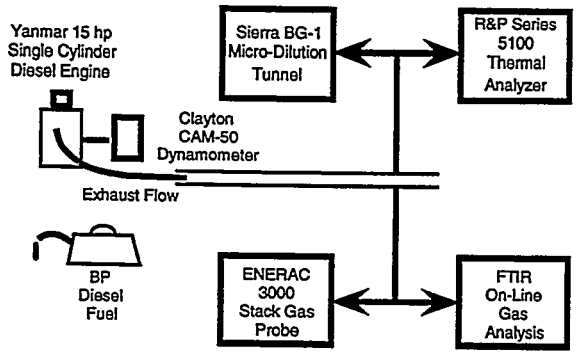


Fig. 1 Schematic of the single-cylinder engine test cell

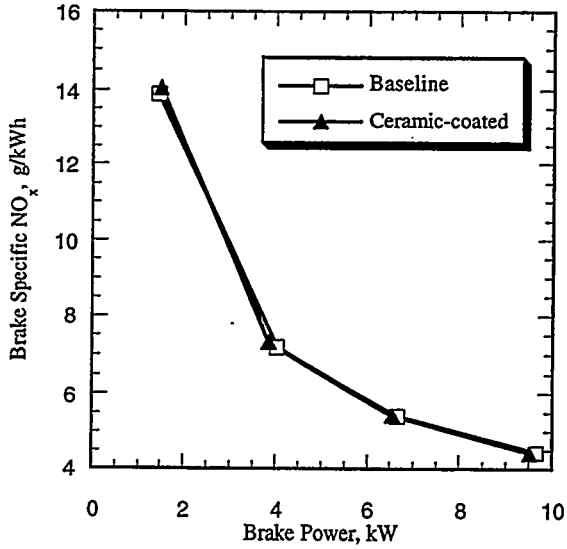


Fig. 3 Brake specific NO_x emissions for the baseline and ceramic-coated engine configurations.

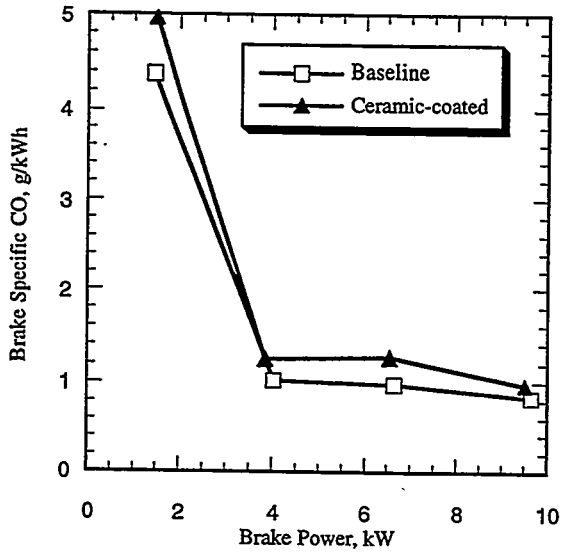


Fig. 2 Brake specific CO emissions for the baseline and ceramic-coated engine configurations.

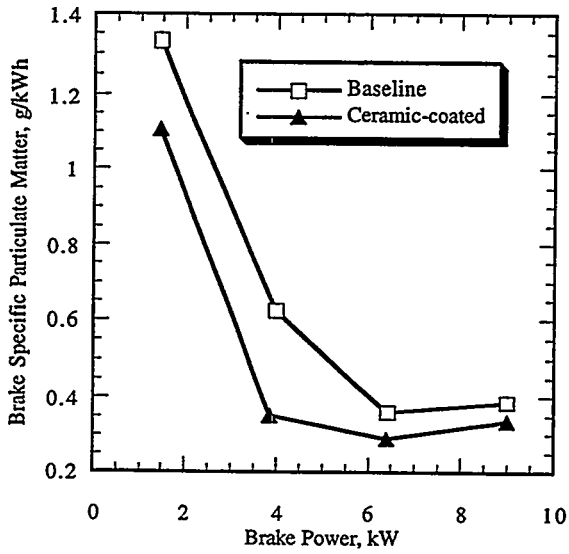


Fig. 4 Brake specific particulate matter emissions for the baseline and ceramic-coated engine configurations.

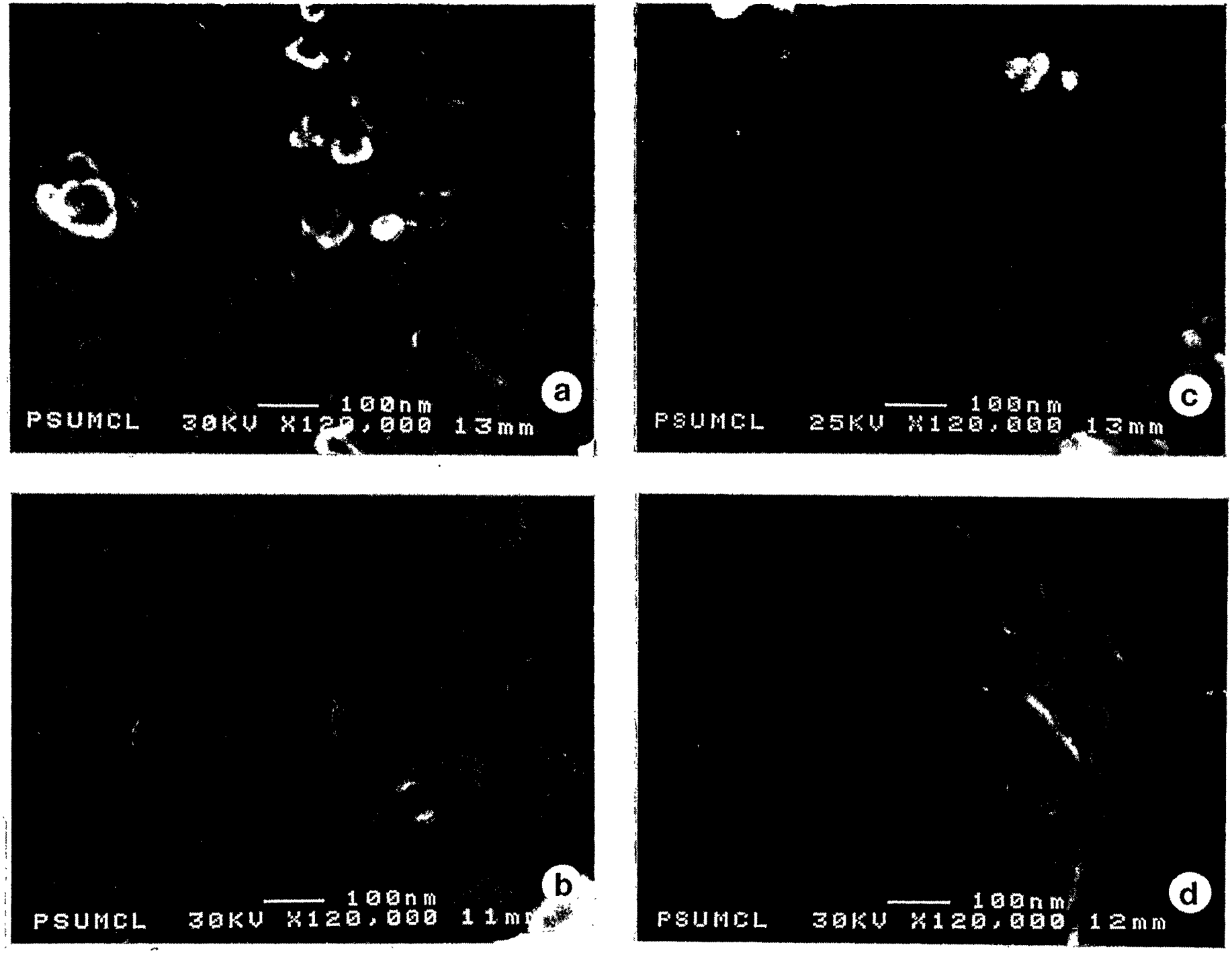


Fig. 5 SEM Micrographs at 120,000x magnification for the baseline engine configuration: (a) Mode 1; (b) Mode 2; (c) Mode 3; (d) Mode 4.

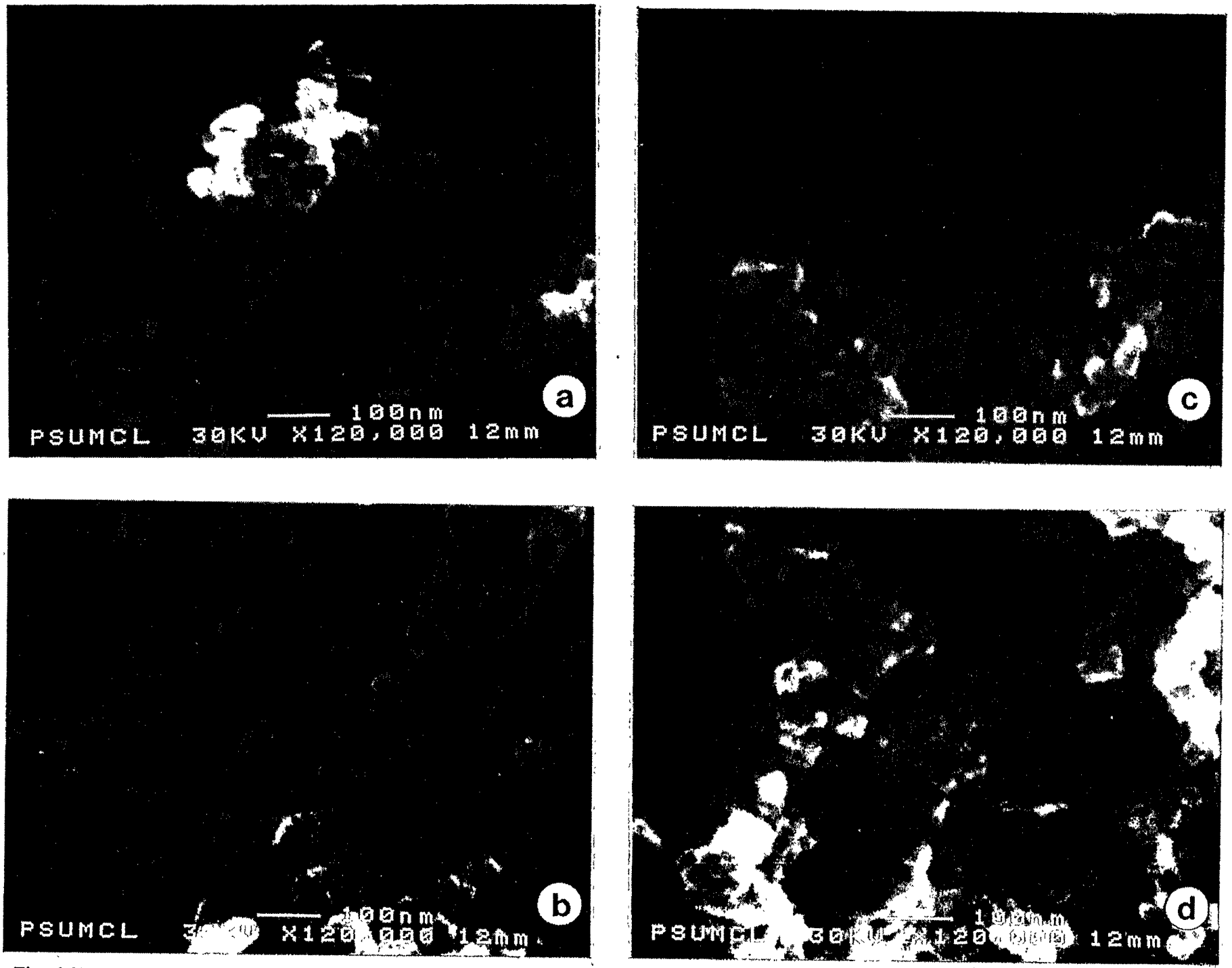
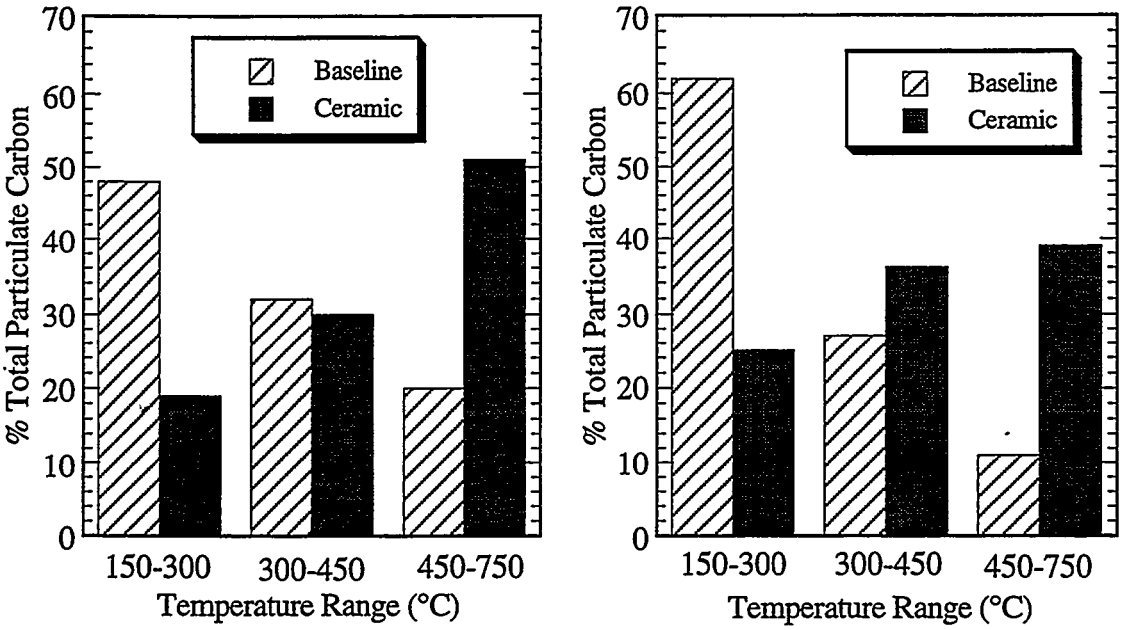
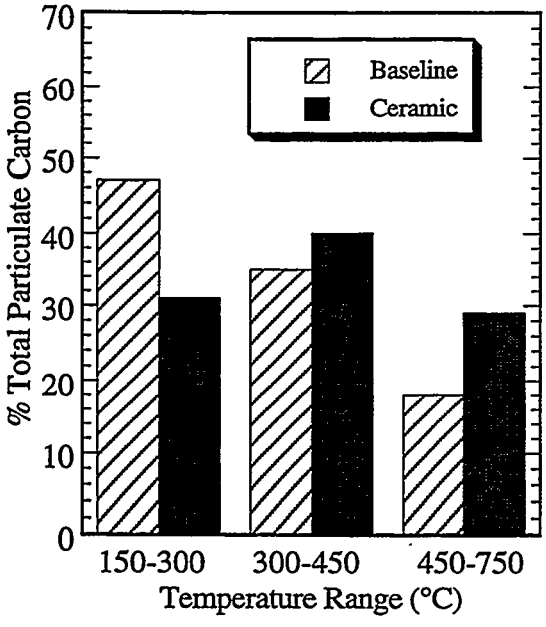


Fig. 6 SEM Micrographs at 120,000x magnification for the ceramic-coated engine: (a) Mode 1; (b) Mode 2; (c) Mode 3; (d) Mode 4.

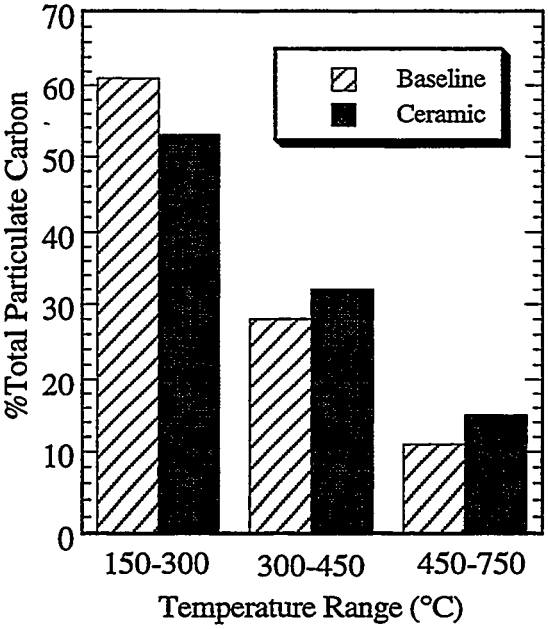


(a) Mode 1

(c) Mode 3



(b) Mode 2



(d) Mode 4

Fig. 7 Compositional changes between particulate matter determine by thermal analysis for the baseline and ceramic-coated engine configurations.

CHARACTERIZATION AND ASSESSMENT OF DIESEL ENGINE PARTICULATE EMISSIONS REDUCTION VIA LUBE-OIL CONSUMPTION CONTROL

T.C. Miller, M.A. Jackson, A.J. Brown, and V.W. Wong, Massachusetts Institute of Technology

DEFINITION OF THE PROBLEM

The motivation for this research stems from the engine community's interest in reducing particulate emissions from both land-based vehicles and marine vessels, sparked by regulatory activities of the U.S. Environmental Protection Agency (U.S. EPA), the California Air Resources Board (CARB), and the International Maritime Organization (IMO). To reach extremely low emission levels, reduction of particulates via lube-oil-consumption control is becoming an essential part of the total strategy. Important advances are being made through improvements in the combustion system, including changes such as higher fuel-injection pressures, combustion chamber and piston ring-pack designs, exhaust gas re-circulation and electronic controls, etc. In addition, engine manufacturers and suppliers are actively investigating control of particulate emissions contributed by the engine lubricant. In contrast to other major combustion system changes which are being incorporated in new engines, particulate reduction via lubrication system improvement also offers the potential of application to existing engines. However, much work remains to be done before it can be implemented. This strategy is the focus of this paper.

Studies dating back to the early 1980's have already shown that engine lubricant consumption (hereafter used interchangeably with "lube-oil consumption" or simply "oil consumption") contributes significantly to diesel exhaust particulate emissions [1]. For engines of older vintage, the lube-oil contribution to particulate alone far exceeds the current standard for the total particulate matter for new engines. The lubricant contribution will become increasingly important as the total particulate emission level continues to be reduced in the future. Conclusions in recent reports indicate that it is necessary to further reduce lube-oil consumption to reach mandated diesel particulate emission levels.

The relationship between particulate emissions and lube-oil consumption is believed to vary with the lubricant type, piston ring-pack configurations and operating conditions [2]. However, the detailed mechanisms relating to either parameter are largely unclear. This research attempted to address some of these issues, specifically the piston-ring and operating-condition effects on the correlation between engine lube-oil consumption and diesel-particulate emissions.

The relationship between the diesel particulate emission characteristics - quantity, composition, and lube-oil contribution - and engine lube-oil consumption was investigated. Experiments were conducted on a direct-injection single-cylinder diesel engine in the Sloan Automotive Laboratory at the Massachusetts Institute of Technology (MIT). The primary variables measured included instantaneous lube-oil consumption, particulate sample weight, sample composition and instantaneous lube-oil consumption.

TEST BED

A Ricardo Hydra single-cylinder, direct-injection, naturally-aspirated diesel engine purchased from Cussons Technology was utilized as the test bed for this research project. The engine specifics are listed in Table 1.

LUBE OIL CONSUMPTION MEASUREMENT SYSTEM

A sulfur dioxide-based diagnostic system was

fitted to the engine to measure real-time lube-oil consumption (RTOC). An exhaust sample was taken from the engine exhaust manifold. The output voltage, corresponding to the sulfur dioxide level in the exhaust was then converted to lube-oil consumption using the calculations in Reference [3]. Complete descriptions of the RTOC system operation can be found in the theses by Jackson, [5] and, Schofield [6].

Lubrizol 30W lubricating oil was used in the engine during testing. Lubrizol 30W possessed a consistent sulfur content throughout the distillation fractions with good material balance (sulfur recovery). This eliminated the potential for false measurement of the consumption by ensuring that sulfur components did not vaporize disproportionately [7]. Secondly, since it was important to maximize (in comparison with other sources) the sulfur content in the engine lube-oil, Lubrizol 30W with sulfur content ~ 1.27% sulfur by weight was excellent when used in conjunction with the ultra low sulfur fuel. The fuel and lube-oil properties are listed in Tables 2.

SAMPLING PROCEDURES AND ANALYSIS

Particulate Sampling System

Diesel particulate matter is composed of a carbonaceous core comprised of carbon particles formed in the cylinder during combustion. These particles adhere to one another forming agglomerates that form the core of the diesel particulate matter; this fraction is called solids (SOL) [1, 8]. A large fraction of the particulate matter formed in the engine cylinder is oxidized during the combustion process; the remainder leaves the cylinder with the exhaust. Once exhausted to the atmosphere, the exhaust gas is cooled and diluted by ambient air which initiates the adsorption and condensation processes. At this point, some of the many products of incomplete combustion of the diesel fuel and engine lube-oil adsorb onto the car-bonaceous material of the particulate. Figure 1, a reproduction from reference [1], displays the particulate formation process.

ENGINE DETAILS: RICARDO HYDRA - SINGLE CYLINDER DI DIESEL		
Type:	Standard DI Hydra	
Bore:	80.26 mm	
Stroke:	88.90 mm	
Number of Cylinders:	1	
Swept Volume:	.4498 liters	
Compression Ratio:	19.8:1	
Aspiration:	Natural	
Rated Speed:	4500 RPM	
Water Out Temperature:	85° C	
Lube-Oil Inlet Temperature:	85° C	
Tappet Clearances:	0.4 mm	
Valve Timing:	IO - 10° BTDC	IC - 41° ABDC
	EO - 58° BBDC	EC - 11° ATDC
Fuel:	Ultra-Low Sulfur Diesel (< 0.1ppm)	
Lube-Oil:	Lubrizol 30W (1.27% sulfur by weight)	

Table 1
Engine Details

ULTRA-LOW DIESEL FUEL PROPERTIES	
Sulfur Content (Weight ppm)	0.1

LUBRIZOL 30W PROPERTIES	
Brand	Lubrizol High Sulfur
Type	SAE 30W
Sulfur Content (% by weight)	1.27

Table 2
Diesel Fuel and Lubrizol 30W Properties

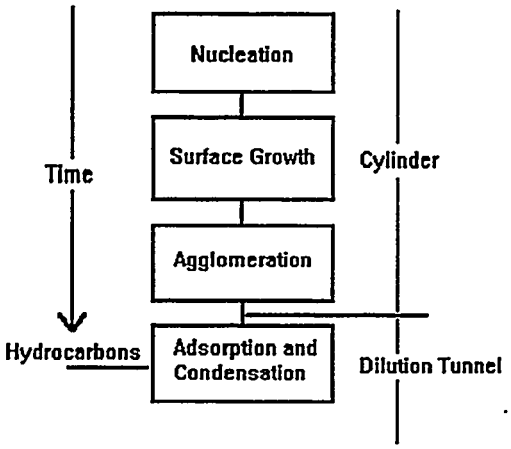


Figure 1
Particulate Formation Process

The intent of the dilution-tunnel sampling system is to simulate release of the exhaust gases to the atmosphere. The exhaust is cooled by ambient air to a temperature of 52°C or less [1], initiating adsorption and condensation, and completing the particulate formation process. Particulate samples are then collected by filtering the dilute exhaust gases.

System Description

A Mini-Dilution Tunnel was constructed by Laurence [2] and used to collect particulate samples. This system was a scaled down version of a Constant Volume Sampling (CVS) Dilution Tunnel constructed in accordance with Environmental Protection Agency (EPA) protocols, similar to the one described by Wong [9]. However, this dilution tunnel was modified to dilute either the entire or a fraction of the exhaust flow.

Particulate samples were collected simultaneously with lube-oil-consumption data during steady state operation of the engine at various speeds, loads, air intake pressures and with various piston-ring configurations. The exhaust was directed into the main stream of the dilution tunnel. Previously, Laurence [2] and Ford [10] had used the dilution air as a means of creating suction, through a venturi, to draw the sample into the dilution tunnel, and as a temperature stabilizer. However, due to the need for a specified flow through the RTOC system, all the exhaust was directed into the dilution tunnel in order to provide sufficient back pressure and generate sufficient flow through the SO_2 RTOC system. Therefore, the dilution air served as a temperature stabilizer for the exhaust stream. The dilution air was filtered to remove lube-oil and moisture from the air (the stated removal effectiveness of the filter is 93% [2]). Concentrations of carbon dioxide were measured in both the raw and diluted exhaust lines to determine the dilution ratio. A sample of the exhaust mixture was drawn through a Pallflex Teflon-coated 47mm glass-fiber filter.

Sampling Procedures

Sample times ranged from 5 to 20 minutes, dependent on the operating conditions. Close attention was paid to the sample line temperatures before and after the filter to ensure temperatures were below 52°C [1] throughout the duration of sample collection. Maintaining the filter face temperature below 52°C helped to ensure the proper adsorption and condensation of hydrocarbon on the carbonaceous fraction of the particulate [8]. It had been shown that dilution tunnel temperature has a greater effect on the process of adsorbing hydrocarbons onto solids (producing soluble organic fraction (SOF)) than does the actual hydrocarbon concentration in the tunnel. Also, more consistent data were obtained when the filter face temperatures were held constant [8]. Consequently, dilution tunnel and engine operating conditions were closely monitored and reproduced to obtain the constant filter face temperature between repeated test runs. A diagram of the dilution tunnel is shown in Figure 2.

Sample Analysis

A quantitative analysis was conducted by ORTECH Corporation, a service contractor, on specified samples to determine what percentage of the SOF was derived from the lubricating oil that had been consumed. The fractions of fuel and lubricant in the particulate samples were determined using a ratio of

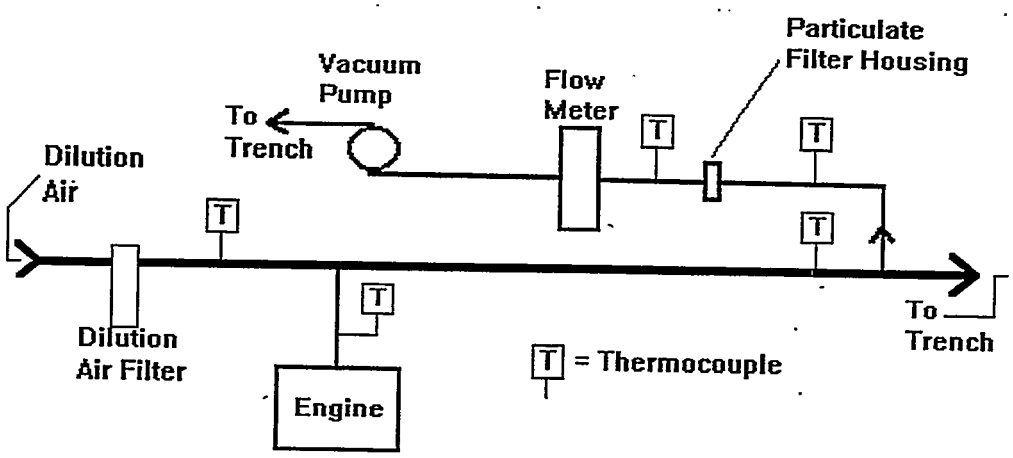


Figure 2
Particulate Sampling System

integrated areas (proportional to mass) obtained from chromatograms of three samples: 1) the extracted SOF, 2) the "topped" fuel, and 3) the new lube-oil. The precision of the lubricant derived portion of the SOF results is on the order of 0.001 g/bhp-hr. The data reduction steps for the particulate emission rate, as well as the calculations of the lube-oil consumption rate, are straight forward and are detailed in Reference [3].

Ring Pack Configurations

The standard ring-pack configuration was the standard as set by the manufacturer's specifications. The first ring, or compression ring, was chrome plated and slightly rounded in shape. The second ring, or scraper ring, was beveled. The third ring, or lube-oil control ring, was chrome plated wih two rails and a separate coil spring for tension control. Table 3 displays the ring-pack Specifications.

RESULTS AND ANALYSIS

Lube-Oil-Consumption Characteristics

The specific lube-oil-consumption (lube-oil consumption , rate per unit engine power output) characteristics for the standard ring-pack configuration are displayed below. The general trends observed are increasing specific lube-oil consumption (OC) with increases in speed at constant load, and decreasing specific OC with increasing load at constant speed, for the 2400 and 3200 RPM operating conditions. Figure 3 displays these trends.

Figure 4 displays the specific lube-oil consumption characteristics for the standard ring pack when the intake-manifold air pressure decreases. Specific OC increases as the air pressure is lowered from 101.3 kPa. The increase occurs as a result of additional lube-oil being drawn into the combustion chamber by the vacuum generated by the drop in air pressure [5].

RING	DIAMETER (mm)	COLD GAP (mm)	TENSION (newtons)		
			Std Ring Pack	Ring Pack 2	Ring Pack 3
Compression	80.25	0.43	9.3	9.3	9.3
Scraper	80.25	0.43	8.2	8.2	8.2 (Inverted)
Oil Control	80.25	0.51	53.8	28.01	53.8

Table 3
Standard Ring Pack Characteristics

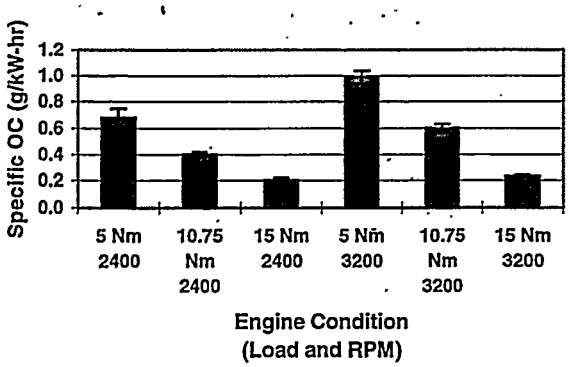


Figure 3
Specific OC Trends for the Standard Ring Pack

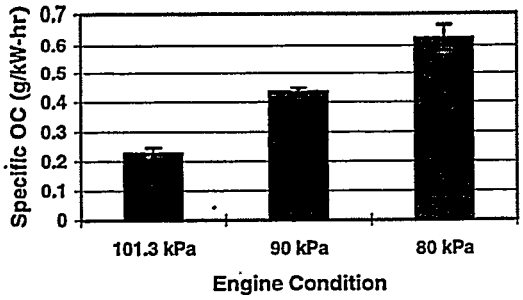


Figure 4
Specific OC Characteristics for Standard Ring Pack; Varied Intake Air Pressures (1200 RPM-Low Load)

Specific OC increases by a factor of ten between the standard ring pack and ring pack 2, and by a factor of 5.5 between the standard ring pack and ring pack 3. Significant increases were desired to provide a wide range of data points. In each case for the varied ring packs, the specific OC increases with increases in speed, and remains nearly constant for increases in load. See Figure 5.

Particulate Characteristics

The breakdown of the specific total particulate rate (TPR) for the standard ring-pack configuration at 2400 and 3200 RPM is displayed in Figure 6. The specific TPR is lowest at medium load, and approximately the same magnitude at low and high loads for each engine speed. The lube-oil-derived soluble organic fraction (SOF) follows the same trend between low and medium loads, but shows little to no increase between medium load and high load.

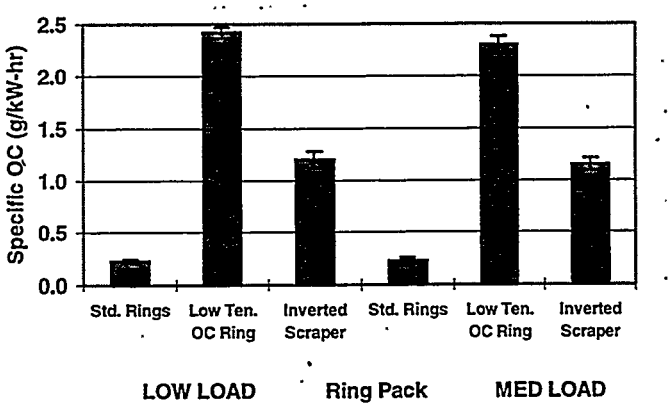


Figure 5
Specific OC Characteristics Comparison Among Ring Packs (1200 RPM-Low & Med Load)

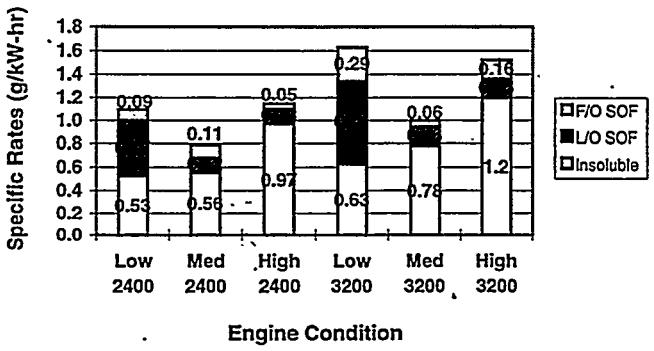


Figure 6
TPR Composition (2400 and 3200 RPM; Varied Loads)

Figure 7 displays the component breakdown for the varied intake air pressures at 1200 RPM-Low Load. The particulate rate increases as the intake air pressure is lowered. Note that the lubricant is the major contributor (over 87%) to SOF at all three conditions. Although only two repeat samples at each air-pressure condition were analyzed for the percentage of SOF contributed by the lube-oil (i.e., L/O SOF as percentage of SOF by mass), the results were very repeatable with standard deviations of 2.9%, 0.7%, 3.2% for the high, medium, and low air-pressure conditions respectively.

Soluble Organic Fraction (SOF)

The generation of the soluble organic fraction (SOF) takes place primarily in the dilution

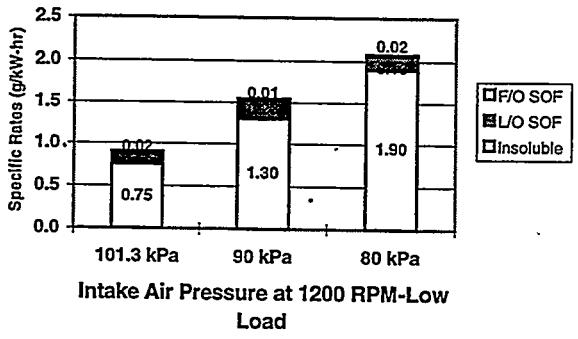


Figure 7
TPR Composition (1200 RPM-Low Load; Varied Intake Air Pressures)

process through adsorption and condensation. The bulk of the SOF is acquired after the exhaust gas is mixed with dilution air [1]. Once the exhaust gases are emitted from the cylinder, cooling from the dilution air initiates the adsorption and condensation processes. Over-fueling, over-leaning, and under-mixing all directly affect the level of hydrocarbons emitted from the cylinder due to incomplete combustion and therefore affect the fuel-derived SOF (F/O SOF). However, only the characteristics of the lube-oil-derived SOF (L/O SOF) are evaluated in this study.

The levels of SOF derived from the lube-oil, for this study, range from 33 to 99 percent of total SOF, indicating that the primary contributor to the SOF was the lube-oil. This suggests that condensation is the dominant process in the development of the SOF. Figure 8 shows that the fraction of the engine lube-oil consumption that contributes to the SOF follows the same general trend as the TPR. The decrease between low and medium loads may indicate that additional lube-oil is being oxidized due to the increase in combustion temperatures which resulted from increased loading. However, this alone does not explain the increase between medium and high load. Oxidation is also a function of the excess air present in the exhaust gases. The air-fuel ratio, and consequently the excess air, is highest at low load and lowest at high load. At low load, there is substantial excess air, but the exhaust temperatures were lower resulting in minimal lube-oil oxidation. Conversely, at high load, the exhaust temperatures were sufficient for oxidation, but the amount of excess air is lower, and therefore oxidation of the lube-oil was again minimal. This trend is observed for both 2400 and 3200 RPM. It is therefore possible that an optimal combination of excess air and exhaust temperature may exist around the medium load condition. Table 4 displays the exhaust temperature and air-fuel ratio behaviors and the resulting effects on the L/O SOF fraction of engine OC, for 2400 and 3200 RPM, as the load is increased.

Of interest at 1200 RPM, was the behavior of the lube-oil-derived SOF when the intake air pressure is decreased. The specific oil consumption is seen to increase (Figure 4) as intake air pressure decreases from 101.3 kPa to 90 kPa and then to 80 kPa. However, the results depicted in Figure 9 show that the fraction of OC that ends up as L/O SOF actually diminishes. This observed effect appears to be primarily a function of exhaust temperature. As intake air pressure decreases, exhaust temperature usually increases and the measured L/O SOF as a fraction of OC actually decreases. A plausible explanation is that the oxidation or combustion tendency of the consumed lube-oil is higher at the higher exhaust temperatures that are expected at the lower intake air pressure conditions.

TEMPERATURE EFFECT ON DEVELOPMENT OF SOF						
Speed	2400	2400	2400	3200	3200	3200
Load	5 N-m	10.7 N-m	15 N-m	5 N-m	10.7 N-m	15 N-m
Exhaust Temps.	243° C	359° C	468° C	299° C	412° C	580° C
Air-Fuel Ratio	71	52	42	71	50	31
L/O SOF Fraction of OC	.71	.31	.65	.72	.26	.69

Table 4

Temperature & Air-Fuel Ratio Effect on L/O SOF Fraction of OC

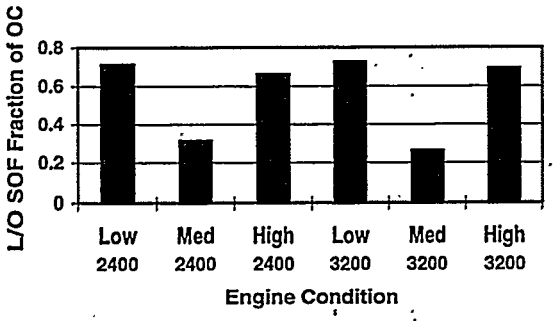


Figure 8
L/O SOF Fraction of Engine Lube-Oil Consumption

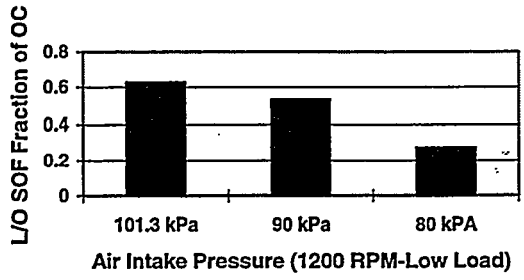


Figure 9
L/O SOF Fraction of Engine Lube-Oil Consumption

deviations from a straight-line relationship when specific data points are selected. A linear regression, conducted by the method of least squares, fit a curve to the aggregate data displayed below. The slope of the resulting curve is 0.641, and the intercept is zero. As shown in Figure 10, Essig's data [11] displays a survival rate of about 50 percent while the data from this study displays a survival rate of about 64 percent.

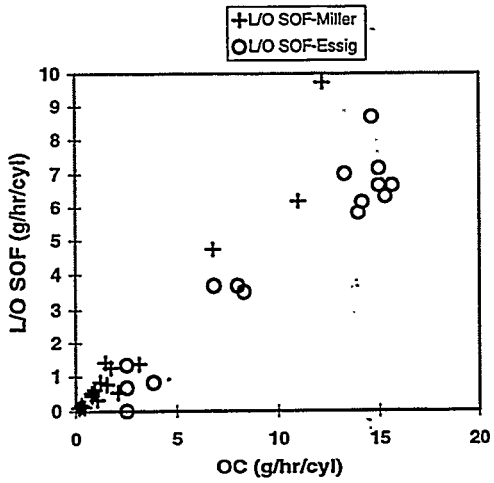


Figure 10
Lube-Oil Derived Soluble Organic Fraction (SOF) vs. Engine Lube-Oil Consumption (OC)

L/O SOF Analysis

Previous works [11] indicated that as specific lube-oil consumption increased, the lube-oil-derived portion of the SOF also increased. This trend was consistent with the data obtained for all testing conditions of this study, as shown below in Figure 10 by the data designated as "L/O SOF - Miller", from Miller's thesis [4].

The trend of increasing specific lube-oil-derived SOF with increasing specific OC is evident and appears to maintain a linear relationship. The overall data show a general trend of increasing L/O SOF with increasing OC when a wide range of OC values are considered. It should be noted that while the data in the aggregate did show a general linear trend, there are variations when specific engine speeds or loads are held constant and, there are

CONCLUSIONS

1. The lube-oil-derived soluble organic fraction (SOF) of the particulate matter increases and decreases with the corresponding change in engine lube-oil consumption. The lube-oil-derived soluble organic fraction is greatest at the high-speed (3200 RPM) - low-load (5 N-m) operating condition. This result agrees with the findings of Essig et al [11]. The agreement with previous work confirms that the dilution tunnel configuration, particulate sampling system, and analysis provide reliable and consistent results.

2. Overall, an approximately linear relation-ship exists between engine lube-oil consumption and the amount of lube-oil-derived soluble organic fraction - from both previous work and this study. The slope is calculated to be 0.64 for this study, and 0.47 for the data reported

by Essig et al [11]. The documented range for the amount of consumed lube-oil contributing to the SOF is between 30 and 80 percent [12]. Therefore, an average value of 64% obtained from this study seems reasonable.

3. The ratio of lube-oil SOF to lube-oil consumption is lowest at the medium-load condition. This may indicate an optimal operating condition for this particular diesel engine. The combination of the exhaust temperature (at least 300° C) and air-fuel ratio (~ 50) at the medium-load condition, for 2400 and 3200 RPM, appears to provide an environment highly suitable for the oxidation of the consumed lubricant. Therefore, the amount of lube-oil contributing to the SOF decreases substantially at this condition.

4. Lube-oil SOF and lubricant consumption (OC) did not behave in exactly the same manner as the intake air pressure was reduced from atmospheric. While OC increased steadily as the intake air pressure decreased, lube-oil SOF first increased between atmospheric pressure and 90 kPa. As intake air pressure further decreased to 80 kPa, lube-oil SOF decreased somewhat. This can be attributed to the increase in the burn-up of lube-oil from the 90 kPa to the 80 kPa condition.

ACKNOWLEDGEMENTS

This paper is the result of research sponsored by the Maritime Administration, under Corporate Agreement Number DTMA91-95-H00051, with support from the United States Coast Guard (USCG). Special thanks to Mr. Daniel W. Leubecker of MARAD and Dr. Alan Bentz of the USCG Research and Development Center for their guidance and support. This research was also supported by the Consortium of Lubrication in Internal Combustion Engines at Massachusetts Institute of Technology, whose members include Dana Corporation, Peugeot, Renault, and Shell Oil Company. The authors would like to thank several people who provided assistance to the completion of this research: Mr. John Lopatynski, ORTECH Corporation, Mr. Norbert Abraham, Sr., Mr. Richard Flaherty, Mr. Gordon Starr, Mr. Weibo Weng, Dr. Dana Richardson, Cummins Engine Company, and Mr. Dave Fiedler, Dana Corporation. This research is part of the U. S. Coast Guard / U.S. Maritime Administration Cooperative Research on Marine Engine Exhaust Emissions.

REFERENCES

1. Heywood, J.B., Internal Combustion Engine Fundamentals, McGraw-Hill Book Company, New York, 1988.

2. Laurence, R.B., "The Effect of Lubrication System and Marine Specific Factors on Diesel Engine Emissions," Masters Thesis, Departments of Ocean and Mechanical Engineering, 1994.

3. MARAD Report MA-ENV-820-96004, "Prevention of Air Pollution from Ships: Characterization and Assessment of Diesel Particulate Emission Reduction via Lube-Oil Consumption Control," U.S. Department of Transportation, Maritime Administration.

4. Miller, T.C., "Characterization of Lube Oil Derived Diesel Engine Particulate Emission Rate vs. Lube Oil Consumption," M.S. Thesis, Department of Ocean Engineering and Department of Mechanical Engineering, May 1996.

5. Jackson, M.A., "Assessment of a Sulfur Dioxide-Based Diagnostic System in Characterizing Real Time Oil Consumption in a Diesel Engine," Masters Thesis, Departments of Ocean and Mechanical Engineering, 1996.

6. Schofield, D.M., "Diesel Engine Instantaneous Oil Consumption Measurements Using the Sulfur Dioxide Tracer Technique," Masters Thesis, Departments of Ocean and Mechanical Engineering, 1995.

7. Ariga, S., et. al., "Instantaneous Unburned Oil Consumption Measurement in a Diesel Engine Using SO_2 Tracer Technique," SAE Paper 922196, 1992.

8. Waldenmaier, D.A., et. al., "The Influence of Sampling Conditions on the Repeatability of Diesel Particulate and Vapor Phase Hydrocarbon and PAH Measurements," SAE Paper 900642, 1990.

9. Wong, V.W., et. al., "Effects of Catalytic Wire-Mesh Traps on the Level and Measurement of Heavy-Duty Diesel Particulate Emissions," SAE Paper 840172, 1984.

10. Ford, E.J., "The Effects of Lubrication Parameters and Exhaust Aqueous Injection on Diesel Engine Oil Consumption and Emissions," Masters Thesis, Departments of Ocean and Mechanical Engineering, 1995.

11. Essig, G., et. al., "Diesel Engine Emission Reduction - The Benefits of Low Oil Consumption Design," SAE Paper 900591, 1990.

12. Farrar, J.R., et. al., "Quantitative Diesel Particulate Analysis using Gas Chromatography/Mass Spectrometry," Proc. Instn. Mechanical Engineers, Vol 207, 1993.

MODELING POLLUTION FORMATION IN DIESEL ENGINES

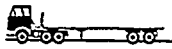
N. Brown
Lawrence Berkeley National Laboratory

Modeling combustion under conditions that prevail in a Diesel engine presents a great challenge. Lawrence Berkeley National Laboratory has invested Laboratory Directed Research and Development Funds to accelerate progress in this area. Our research has been concerned with building a chemical mecha-nism to interface with a high fidelity fluid code to describe aspects of Diesel combustion. The complexity of these models requires imple-mentation on massively parallel machines. Collaborators in this effort are Michael Frenklach, Phillip Colella, and John Bell.

The level of complexity of the chemical mecha-nism is dictated by combustion con-ditions and by the question being asked. For example, flame propagation can be described with five or less reactions and ignition with approxi-mately twenty. How-ever, describing pollutant formation and, especially, soot and NO_x, requires substantially more complex chemistry. We will describe our efforts concerned with building such a complex mechanism. We begin with C and CO2 chemistry and add sequentially higher hydrocarbon chemistry, aromatic production chemistry, soot chemistry, and chemistry describing NO_x production. The metrics against which this chemistry is evaluated are flame velocities, induction times, ignition delay times, flammability limits, flame structure measurements, and light scattering. We assemble a set of elementary reactions, kinetic rate coefficients, and themochemistry. Data are provided from experimental studies and theory. Tools used to build mechanisms of varying complexity are reaction path analysis, sensitivity, and principal component analysis. Reduction is achieved by using these tools, lumping portions of the chemistry, employing the method of moments, and invoking quasi-steady-state and partial equilibrium approxi-mations. We modify existing Sandia codes to be able to investigate the behavior of the mechanism in well-stirred reactors, plug flow reactors, and one-dimensional flames. The modified combustion code with a chemical mechanism at the appropriate level of com-plexity is then interfaced with the high fidelity fluids code. The fluids code is distinguished by its ability to solve the requisite partial dif-ferential equations with adaptively refined grids necessary to describe the strong variation in spatial scales in combustion.

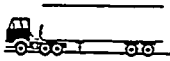
Diesel Collaboratory New Paradigm

- To make available electronically to members of the Collaboratory: Models, results, and tools
- To use Collaboratory computational infrastructure to make our models, results and tools, as well as those of others, available to the broader combustion community
- Team: Caterpillar, Cummins, Detroit Diesel, LBNL, LANL, LLNL, SNL, University of Wisconsin



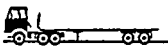
Collaborators

Michael Frenklach
Michael Koszykowski
Ken Revzan
Nigel Moriarty
Carmen Ortiz
John Bell
Phil Colella



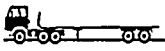
Modeling Diesel Combustion

- Complexity of Problem
- Modeling the Combustion
- Tools of the Trade
- Chemical Mechanisms
- The Diesel Collaboratory
- Conclusion



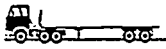
Complexity of Diesel Modeling

- High pressure and high temperatures
- Spray atomization of liquid fuels
- Radiation heat transfer
- Complex fluid flow
- Complex combustion chemistry

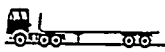


Drivers for Diesel Improvements

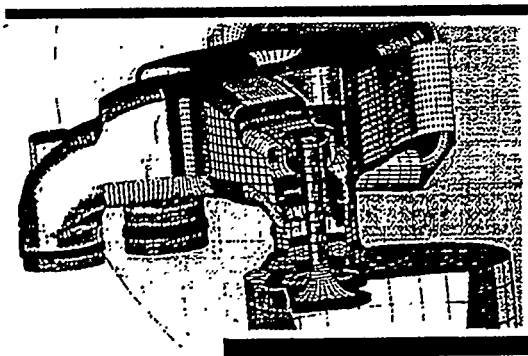
- **Technical Drivers**
  - higher pressures--greater efficiency
  - better atomization
  - new fuels
- **Regulatory Drivers**
  - more stringent regulations of criteria pollutants
  - new PM regulations
  - new fuels



Optimizing Diesel combustion performance criteria with respect to the technical and regulatory drivers presents a daunting task to a modeling team that requires teraflop computing resources

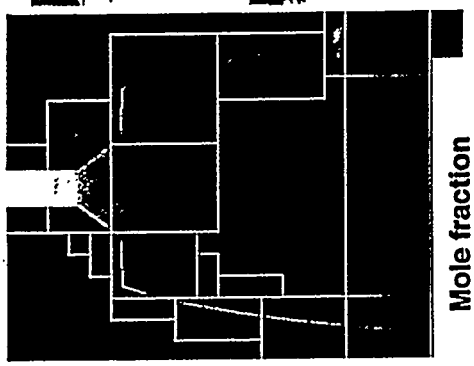


Computational Modeling of Diesel Combustion

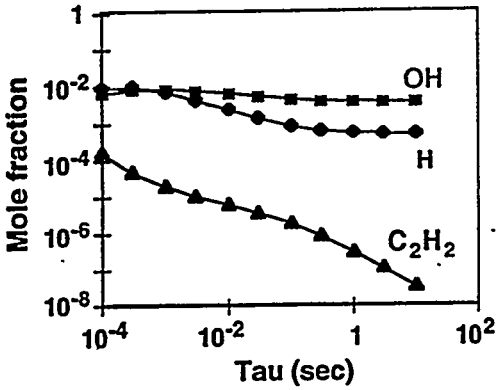


Engine model (Industry-Lab collaboration)

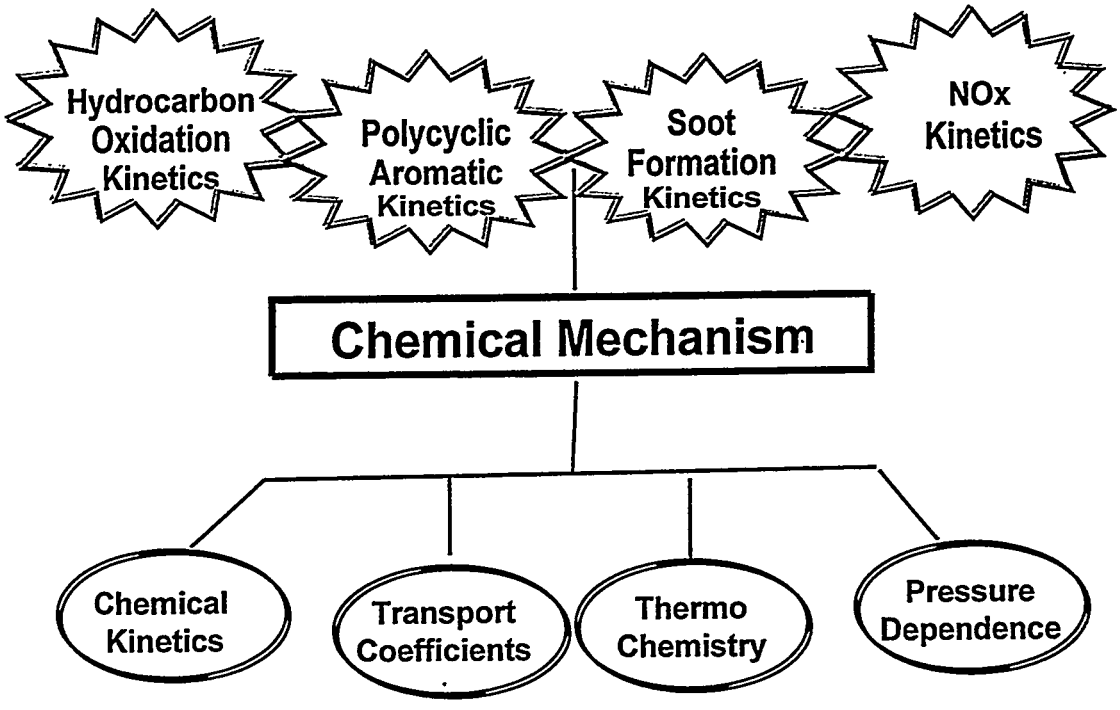
Adaptive griding of flow geometry

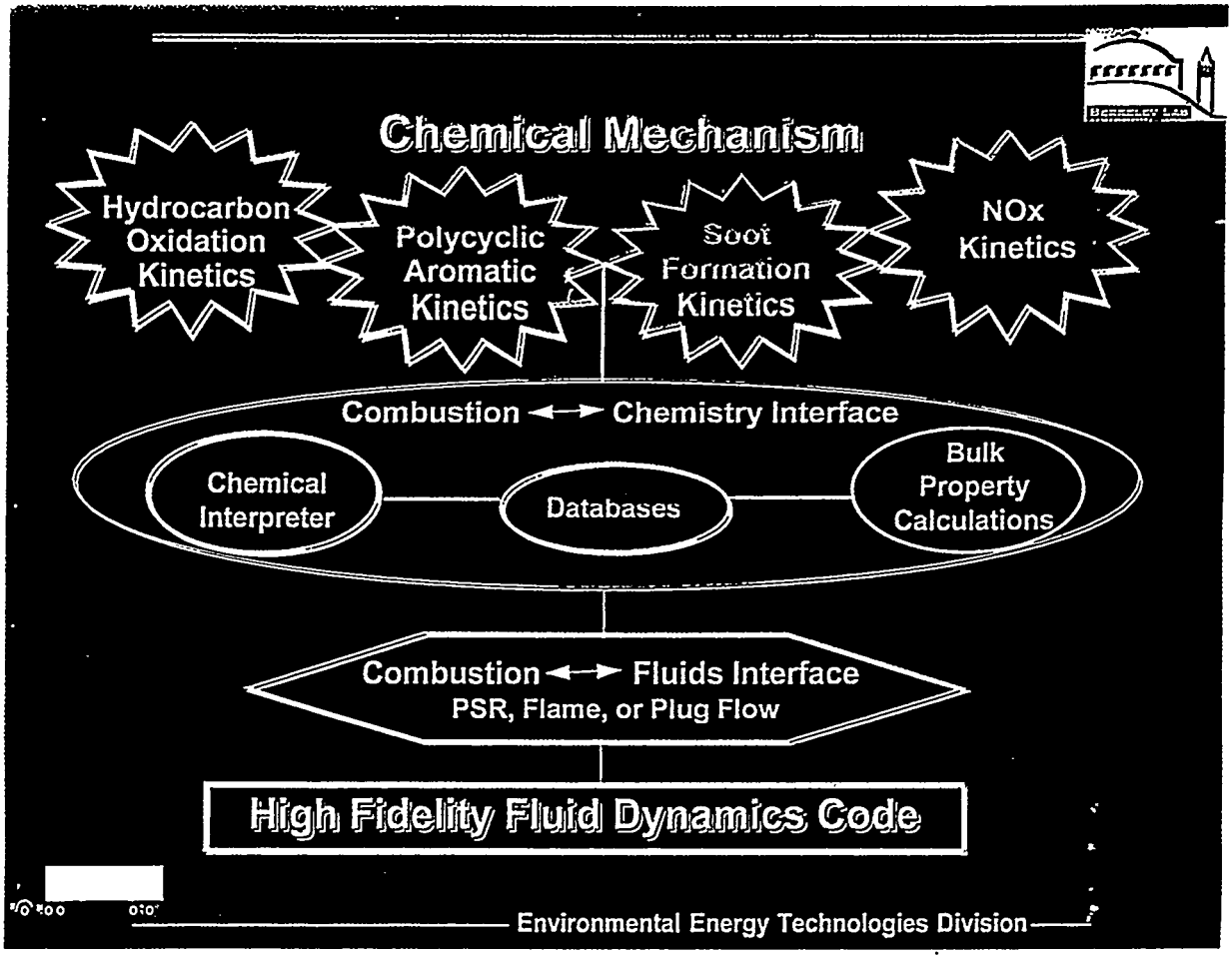


Nonequilibrium chemistry of soot precursors



• J. Bell, P. Collela, N. Brown

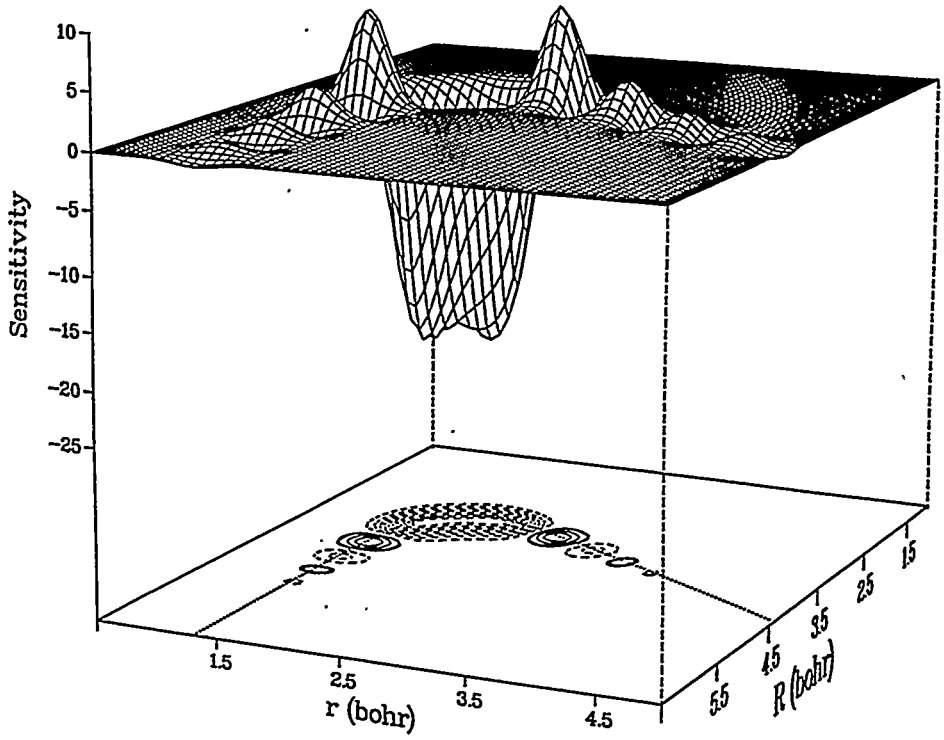




Tools of the Trade

- reaction path analysis
- sensitivity analysis
- mechanism reduction
- rate ratio asymptotics
- potential energy surface calculations
- rate coefficient calculations

Rate Coefficient Sensitivities



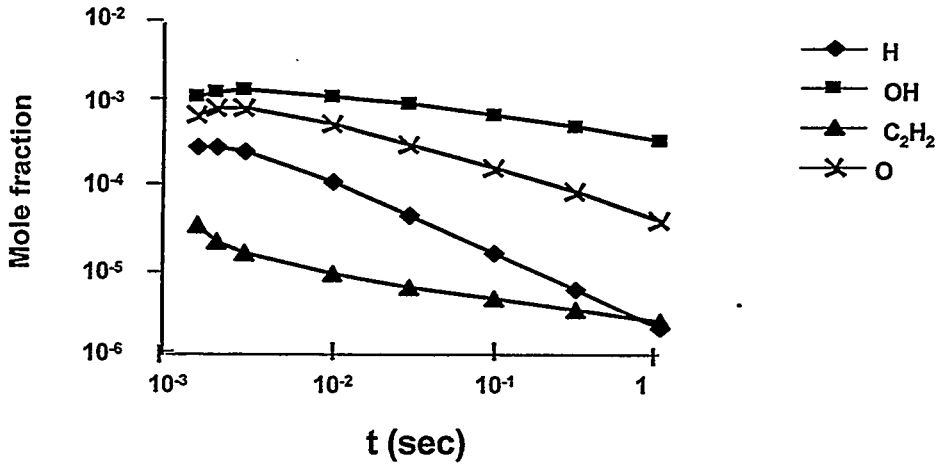
Hydrocarbon (HC) oxidation kinetics

- start with H_2, CH_4, C2 chemistry
- either add aromatics or continue to increase the C skeleton
  - both are useful and comparisons with experiments test different parts of the mechanism
- higher alkanes can be reduced to C1 and C2 chemistry
  - abstraction with H, OH, or OH
  - alkyl radical thermal dissociates via β scission

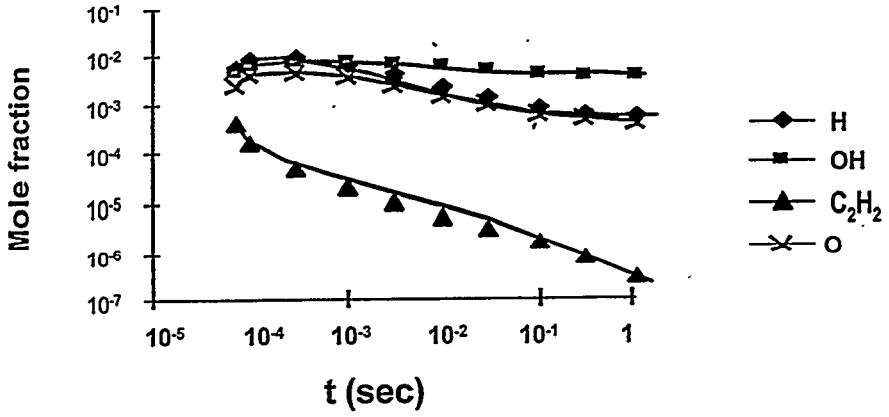
Higher alkanes

- **Dissociation and isomerization of R**
- **R + Y → R' + HY (Y= H, O, OH)**
- **R' → R" + R"'**
- **β scission -- governs decomposition of a complex HC radical:**
  - **bond most likely to break is one carbon removed from the site of radical attack-- C-C rather than C-H is usually broken**
- **Research need:** dearth of experiments must be rectified, need flame structure measurements, and theoretical development for kinetics, thermochemistry, and transport

Heptane Combustion in a Perfectly Stirred Reactor as a Function of Residence Time for Phi = 0.5

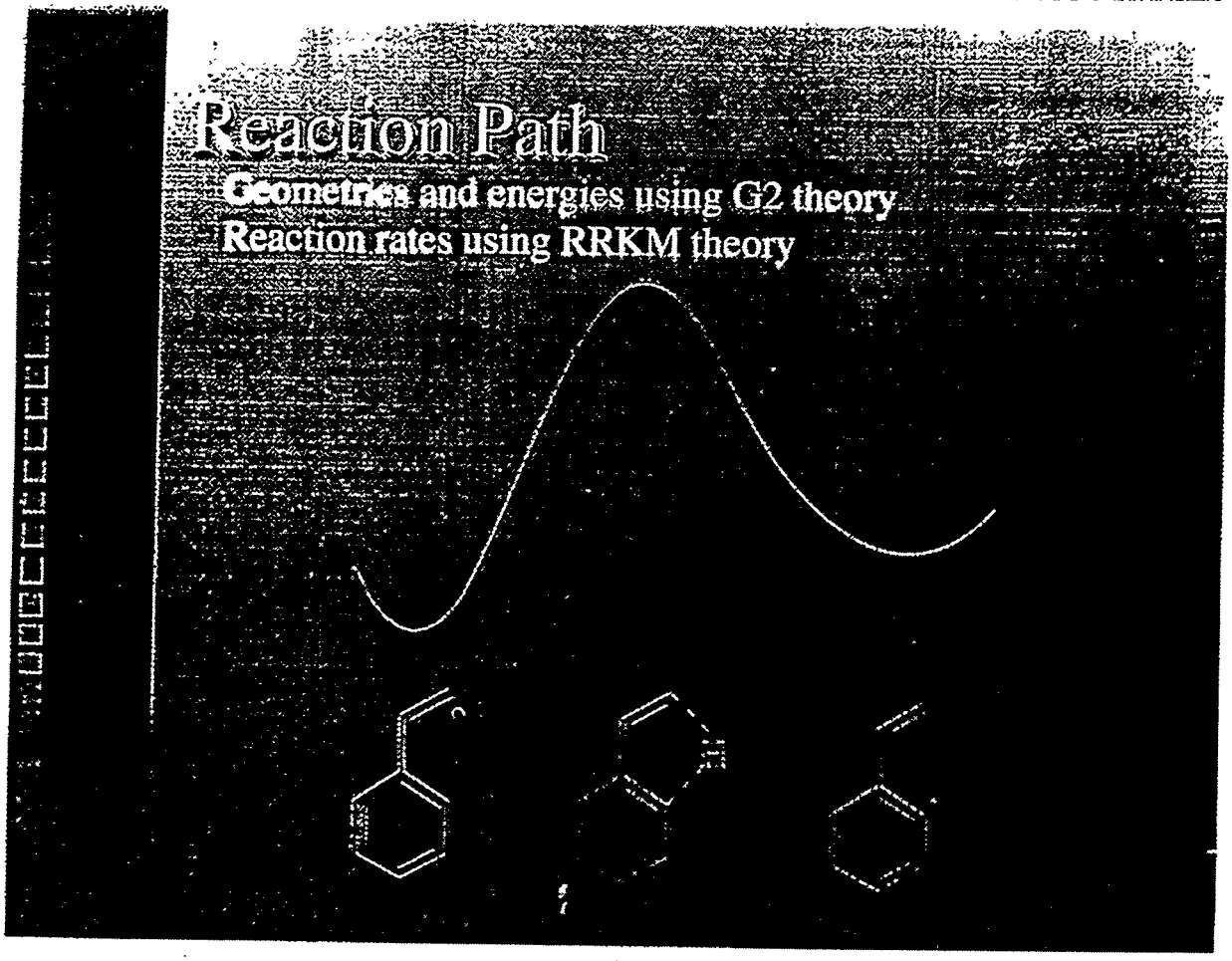


Heptane Combustion in a Perfectly Stirred Reactor as a Function of Residence Time for Phi = 1.0



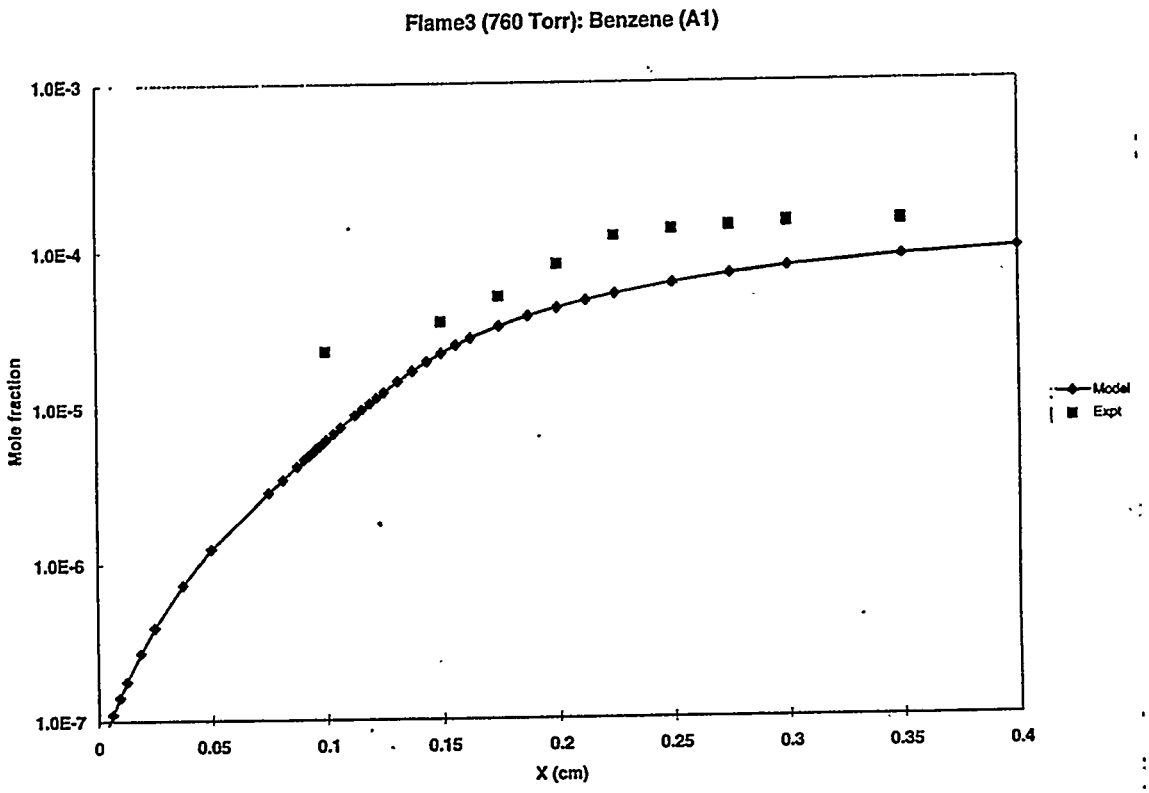
Aromatic chemistry

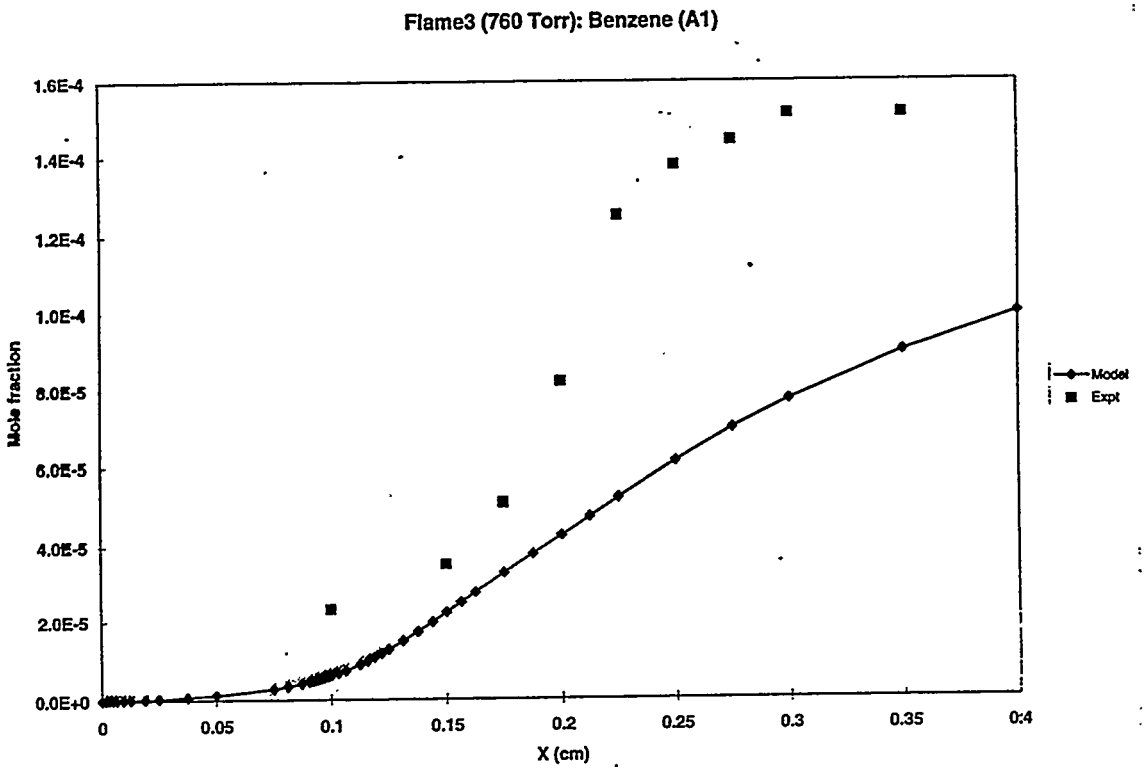
- Formation of first ring controversy
- Acetylene--standard model
  - $C_4H_3 + C_2H_2 \rightarrow C_6H_5$
  - $C_4H_5 + C_2H_2 \rightarrow C_6H_6$
- Propargyl
  - $C_3H_3 + C_3H_3 \rightarrow C_6H_5 + H$ or C_6H_6
- Large aromatics are formed from small by steps: H abstraction, acetylene addition, and cyclization
- Theory--very useful in estimating kinetics and thermochemisty



Wang-Frenklach Mechanism: Flame Conditions

Flame #	C_2H_2	C_2H_4	O_2	Ar	Pressure (Torr)	Tmax (K)	Velocity (cm/s)
	(concentration in mole fraction)						
1	0.465		0.485	0.05	20	1901	50
2	0.236		0.214	0.55	90	1988	20.4
3		0.165	0.179	0.656	760	1606	7.8

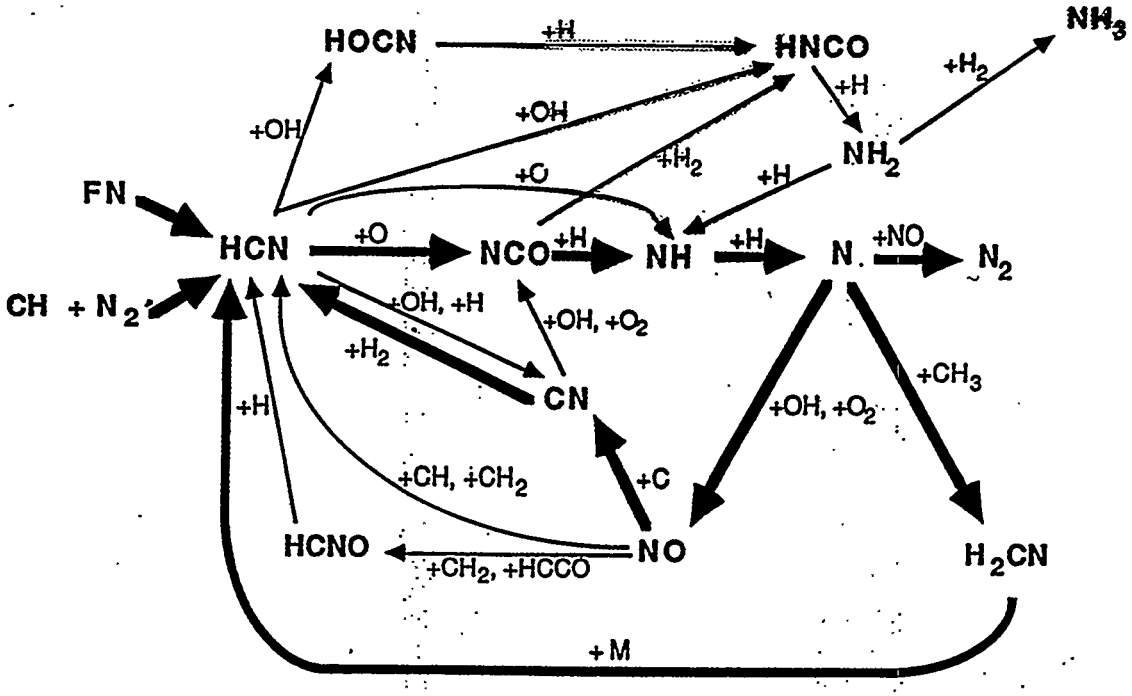

Flame3 (760 Torr): Benzene (A1)
1.0E-3
1.0E-4
1.0E-5
1.0E-6
1.0E-7
Mole fraction
0
0.05
0.1
0.15
0.2
0.25
0.3
0.35
0.4
X (cm)
Model
Expt


Flame3 (760 Torr): Benzene (A1)
1.6E-4
1.4E-4
1.2E-4
1.0E-4
8.0E-5
6.0E-5
4.0E-5
2.0E-5
0.0E+0
Mole fraction
0
0.05
0.1
0.15
0.2
0.25
0.3
0.35
0.4
X (cm)
Model
Expt

NOx Chemistry

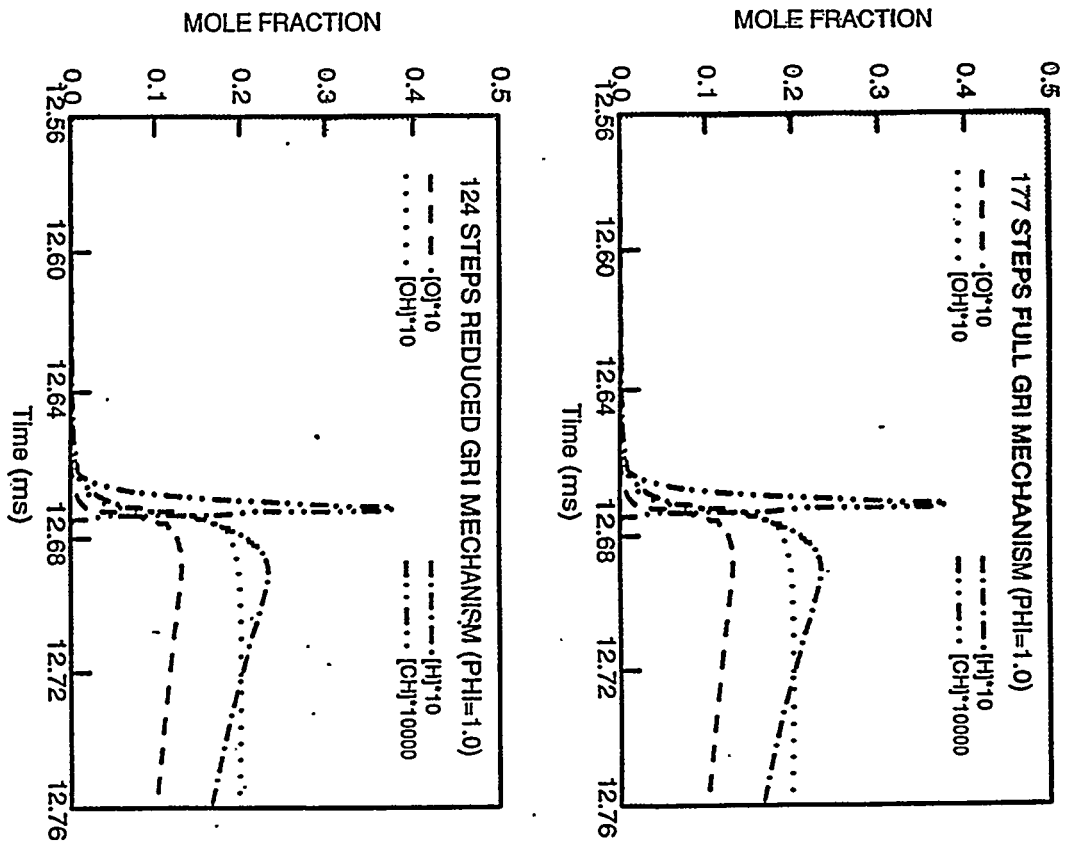
- Zeldovich kinetics-- $O + N_2 \rightarrow NO + N$, large E_a
- Prompt mechanism--$CH + N_2 \rightarrow HCN + N$
- N_2O mechanism--important at high pressures, N_2O reactions with H and O
- reburn mechanisms--NO is converted to N_2--reactions with NH and N are most important
- many reactions--not equilibrated, relative importance strongly influenced by ambient conditions

NITROGEN CHEMISTRY IN RICH FLAMES



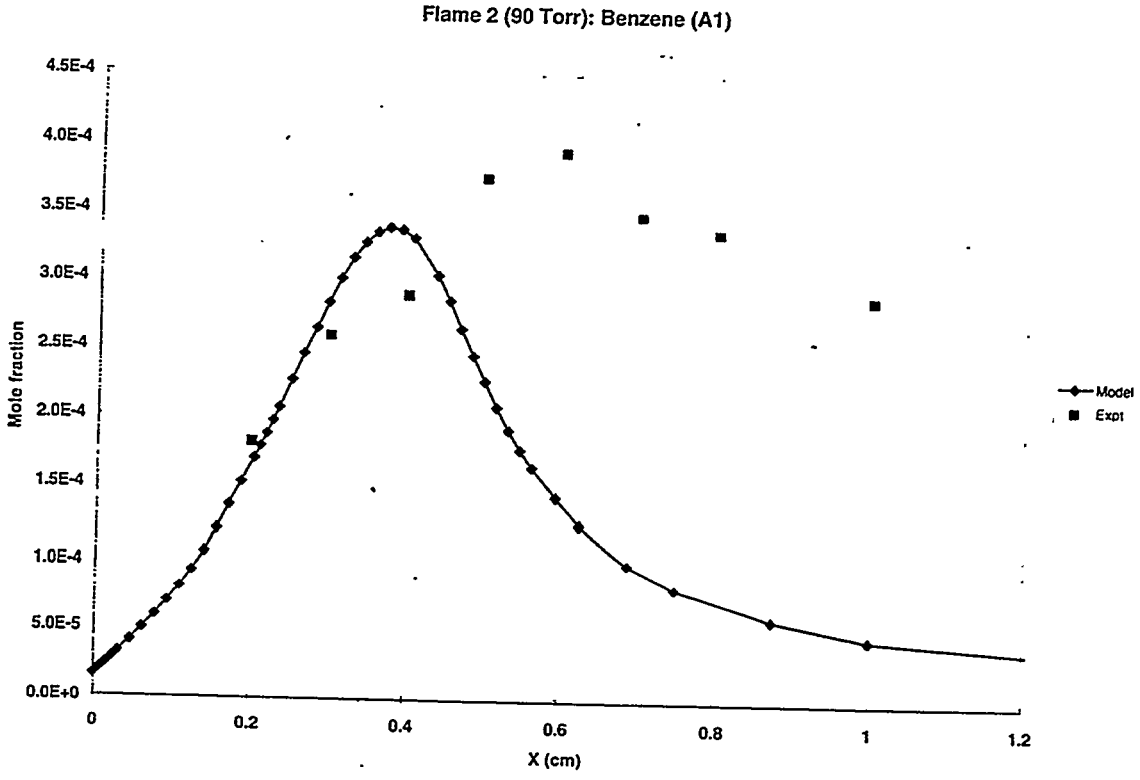
Mechanism reduction

- System reduction -- reduces number of parameters
- System lumping -- reduces number of species
- Mechanism reduction uses tools of the trade and a number of approximations

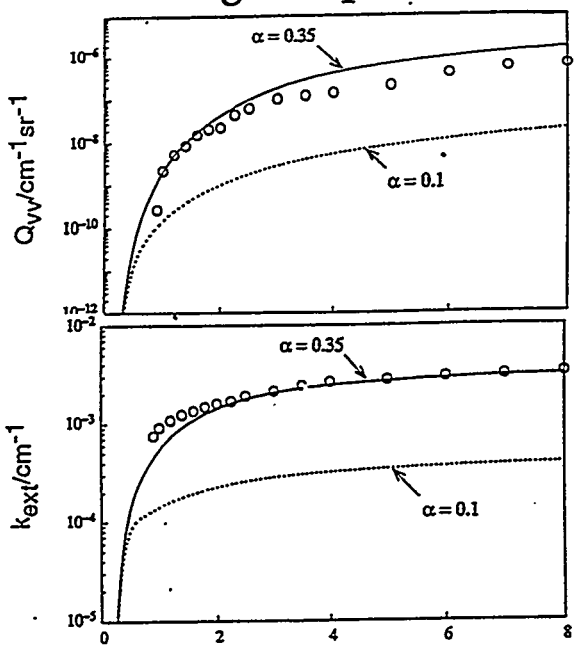


Modeling soot

- Evolution of soot particle size distribution is described by method of moments
- Describes 4 processes responsible for the formation, growth, and oxidation of soot particles
  - inception
  - PAH condensation
  - coagulation and surface growth



Experimental-Modeling Comparison of Light Scattering



Conclusions

- **Complexity of Problem**
- **Modeling the Combustion**
- **Tools of the Trade**
- **Chemical Mechanisms**

PARTICULATE MATTER EMISSION FROM ON-ROAD LIGHT DUTY VEHICLES

S. Cadle
General Motors Research and Development Center

INTRODUCTION

Mobile sources contribute to the atmospheric burden of particulate matter (PM) through three mechanisms: primary PM emissions; secondary PM formation, and fugitive emissions. Primary particles are those directly emitted by vehicles. They are emitted in the vehicle exhaust, and also are emitted via brake and tire wear. Secondary PM formation refers to the production of particles in the atmosphere from the reactions of gaseous emissions. Gases of concern are HC, NO_x, and SO_2. HC reacts in the atmosphere to form less volatile species that condense into the particle phase, thereby contributing to the carbonaceous particle burden. NO_x oxidizes to nitric acid which reacts with ammonia to form ammonium nitrate. The amount of ammonium nitrate in the particle phase is a function of temperature. SO_2 is oxidized to sulfuric acid, which exists primarily in the particle phase. Mobile sources are generally a major contributor to the HC and NOx burdens in urban areas, but are minor contributors to the SO_2 in most areas.

Fugitive emissions are PM that is re-suspended by the turbulence caused by vehicle traffic. The amount of dust generated is a function of the amount of fine particles (silt) on or near the roadway. This is a major source of PM-10 (particles with a diameter less than or equal to 10 μm), but will be less important for the new PM-2.5 (particles with a diameter less than or equal to 2.5 μm) standard since re-intrained dust is comprised mostly of large particles. The focus of this paper will be on the primary PM emissions from light-duty vehicles. The emphasis will be on exhaust emissions.

HISTORICAL PERSPECTIVE

Gasoline Vehicles: Exhaust particulate matter (PM) emissions have decreased dramatically in the last 25 years. Before 1975, gasoline vehicles were designed to operate on leaded fuel. The average lead content of fuel was 2 g/gal. Approximately 75% of the lead consumed was emitted as exhaust PM. This resulted in average PM emission rates of 200 to 250 mg/mi (Cadle et al, 1979). A few measurements of 1973 and 1974 vehicles operated on unleaded gasoline were reported as well. These vehicles had PM emission rates of approximately 25 mg/mi.

Leaded gasoline remained available, although at greatly reduced lead concentrations, until 1996. Average lead concentrations in gasoline were 1.4 g/gal in 1980, 0.5 g/gal in 1985 and less than 0.1 g/gal after 1985. As of 1996, no lead additives are allowed in gasoline in the United States. The actual rate at which lead PM emissions were phased out is a combination of three factors: fleet turnover to catalyst vehicles, misfueling of catalyst vehicles with leaded fuels, and the reduced concentrations of lead in gasoline. The phase out is dramatically reflected in the 1994 air quality data which show lead concentrations reduced by 97% since 1975, despite major increases in vehicle miles traveled (EPA, 1995).

Oxidation catalysts were introduced on vehicles in 1975. Since lead poisons these catalysts, the vehicles were required to operate on unleaded fuels. By 1977 all new cars were equipped with catalysts. Introduction on light-duty trucks was somewhat slower, with 7% of these vehicles being non-catalyst in 1978, and non-catalyst vehicles completely phased out by 1982.

The introduction of the oxidation catalyst raised a new concern, namely that vehicles would emit sulfuric acid particles. Sulfur is naturally present in crude oil, and is present in gasoline as a variety of organo-sulfur compounds. The national average sulfur content of gasoline in 1975 was approximately 0.03% by weight.

During combustion almost all of the sulfur is converted to sulfur dioxide, which remains in the gaseous state in the exhaust. These sulfur dioxide emissions are a very small portion of the total anthropogenic sulfur emissions inventory in most locations, and thus were of little concern. Oxidation catalysts, however, were capable of promoting the oxidation of a small fraction of the sulfur to sulfur trioxide (SO_3), which reacts immediately with water to form sulfuric acid. Typical sulfate emission rates from vehicles with oxidation catalysts with and without air pumps were 16 and 5 mg/mi, respectively, at an average speed of 19.6 mph (the average Federal Test Procedure speed) and 20 and 5 mg/mi, respectively, at higher speeds. These figures include the mass of the water associated with the sulfuric acid. Changes in catalyst tech-nology and improved A/F control have greatly reduced sulfuric acid emissions, although few measurements have been reported for late-model vehicles. Furthermore, reductions in fuel sulfur content will reduce the sulfate emission rate. Thus, in California, which has adopted the use of low sulfur fuels (<0.005% S), the sulfate emissions will be considerably lower than the values stated above.

Improvements in vehicle emission control tech-nology have continued to reduce exhaust PM emission rates. For example, Mulawa and Dasch (1995) reported average FTP PM emission rates from 12 1987-1990 light-duty gasoline vehicles of 7 mg/mi. A more recent study, discussed later in this report, shows that PM emission rates have been reduced further.

Diesel Vehicles:. Light-duty diesel vehicles remain a very small fraction of the on-road light-duty vehicle fleet (<1%). However, their relatively high PM emission rates may make their contribution to the light-duty vehicle exhaust particulate inventory significant. Cadle et al. (1979), reported that 1978 and 1979 production light-duty diesels had PM emission rates of 700-850 mg/mi. Similarly, Energy and Environmental Analysis (1985) reported that pre-1981 light-duty diesels averaged 700 mg/mi. Post-1987 diesels were reported to have emission rates of 200 - 260 mg/mi. All Federal Tier 0 vehicles had to meet a PM standard of 200 mg/mi, while Federal Tier 1 vehicles must meet a PM standard of 80 mg/mi. While they apply to all light-duty vehicles, these standards were set to control diesel emissions. Thus, considerable progress has been made in controlling diesel PM emissions as well as gasoline PM emissions.

Tires and Brakes: Particle emissions from tires are dominated by very large particles that are produced under high-wear driving modes (cornering, braking, accelerating). It was estimated in 1978 that the average tire wear rate was 140 mg/mi per tire. Most of the particles formed, however, were found to be very large. Tire wear rates have improved, but there have not been any additional comprehensive emission characterization studies. Brake wear emissions have also been studied. Most of the studies, however, focused on asbestos brake pads. Since asbestos has been largely eliminated from the brake pads used on new vehicles, the current fine particle emission rate from brakes is not well known.

EMISSION MODELS

PART5 is the U.S. EPA's official model for projecting PM emissions from on-road motor vehicles. Most of the elements of this model are included in the California EMFAC model as well. PART5 uses the same vehicle classes and activity data as the MOBILE5 model, and estimates PM emissions from both light-duty and heavy-duty vehicles. However, the algorithms for PM are much simpler than those used for other emissions. For example, there is no separation of cold start from other operating modes, no effect of ambient temperature, and no consideration of the vehicle's accumulated mileage. This is largely because there is little data on which these effects can be based. Despite these limitations, and those discussed above regarding tire and brake emissions, it is worth while examining the model predictions.

The PART5 estimated in-use, light-duty vehicle fleet average PM-10 emissions using the default fleet age distribution for 1995 are 14 mg/mi for exhaust, 13 mg/mi for brake wear, 8 mg/mi for tire wear, and 36 mg/mi for fugitive emissions, for a total emission rate of 57 mg/mi. PART5 projects no change in brake or tire wear in the future. Exhaust and fugitive PM are predicted to

decrease to 12 and 35 mg/mi, respectively by the year 2010 (Rykowski, et al, 1996).

Exhaust PM emissions from different classes of vehicles can be compared as well. For example, the EMFAC7G model predicts Southern California PM-10 emissions of 1.65, 0.67, 0.84, and 15.8 tons/day from light-duty gasoline, medium-duty gasoline, light-duty diesel and medium- and heavy-duty diesels, respectively, for the year 1995. These change to 1.45, 0.19, 0.12, and 7.48 tons/day for the year 2005, reflecting a major improvement from the diesel vehicles. Finally, the exhaust emissions can be combined with the brake and tire wear emissions to give the comparison shown in Figure 1. This figure shows that tire and brake wear emissions dominate the PM-10 from light-duty vehicles in the year 2005 and that together these emissions are similar to those from the diesel trucks. It should be emphasized, however, that there are major uncertainties in all of the model projections. Given the model uncertainties, it is best to examine recent studies of PM emissions from light-duty vehicles.

RECENT LIGHT-DUTY VEHICLE EXHAUST PM STUDIES

Environmental Research Consortium Study. The Environmental Research Consortium (ERC) project was conducted by Chrysler, Ford Motor Co., and General Motors Corporation. The purpose was to determine exhaust PM emission rates from late-model, high-production-volume gasoline vehicles at both low and high mileage. Vehicles were tested on chassis dynamometers using the Federal Test Procedure (FTP) Urban Dynamometer Driving Schedule (UDDS). Filter samples of the particulate were collected for each of the three FTP phases. The vehicles were operated on California Phase II fuel. Preliminary work indicated that it was necessary to collect PM on the same set of filters over four FTP tests in order to obtain enough mass to weight reliably. Results of the study are summarized in Table 1.

When examining the results in Table 1 it should be noted that the emission rates for HC, CO, and NO_x are given in grams per mile while those for PM are in milligrams per mile. All of the vehicles were operating properly and met the applicable emission standards, as evidenced by the average regulated emission rates given in the table. PM emission rates were very low for both the cars and trucks, and increased only slightly with mileage. The average PM emission rate for these vehicles, approximately 1 mg/mi, can be compared to the average rate of 14 mg/mi predicted by PART5. One difference is that these vehicles were operated on a low sulfur fuel, while the PART5 prediction is based on a national average fuel. This, however, is not expected to have a large impact. These results suggest that the current model greatly overestimates PM exhaust emission rates for properly-functioning, light-duty gasoline vehicles in future years.

Off-cycle and In-use PM Emission Rates: Two additional factors need to be considered when estimating the light-duty vehicle PM emission rate. The first is that not all driving occurs under FTP conditions. Thus, studies need to be conducted that determine the effect of other driving cycles, ambient temperature, altitude, and fuel on PM emission rates. Currently, no data are available for PM emission rates on high-speed, high-load driving cycles such as the US06. Studies are underway to address this deficiency. The next study discussed has some information on the effects of fuel and temperature, and the Coordinating Research Council study discussed

Table 1. Summary of Results from the ERC Study

Vehicle	Number	Mileage	HC, g/mi	CO, g/mi	NOx, g/mi	PM, mg/mi
Car	6	7,000	0.13	1.28	0.18	0.60
Car	3	93,000	0.19	1.75	0.43	0.81
Truck	7	9,500	0.18	1.91	0.27	1.22
Truck	3	95,000	0.31	2.86	0.38	1.60

later is generating data at low temperature at altitude. The second factor that must be considered is the effect of vehicle condition on PM emission rates. Studies conducted over the last ten years have demonstrated that in-use vehicle emissions from the on-road fleet are dominated by the emissions from a small percentage of vehicles that are poorly maintained. The situation is expected to be the same for PM emission, since casual observation confirms that there are still a few gasoline vehicles in the in-use fleet that emit visible smoke during operation. Thus, to determine the in-use contribution of gasoline vehicles to the PM inventory, it is necessary to measure emissions from a representative sample of the in-use vehicle fleet.

Effect of Ambient Temperature and E-10 Fuel. During the winter of 1994-95, the State of Alaska Department of Environmental Conservation conducted a study in Fairbanks to evaluate the impact of switching from regular grade gasoline to an E-10 fuel (gasoline with 10% ethanol). The U.S. EPA and the GM R&D Center were participants in that study. As part of that program, 10 vehicles were tested on a chassis dynamometer at temperatures of 20°, 0°, and -20° F. Three of the vehicles were retested in the EPA facilities at Research Triangle Park, NC, under the same conditions and at the standard FTP temperature of 75° F. Vehicles were tested using the FTP and PM-10 emission rates were determined. Results have been published (Mulawa et al, 1997). Figure 2 shows the results for the three vehicles tested at EPA.

The three vehicles in Figure 2 were a 1994 Ford Aspire, a 1989 Chevrolet Celebrity, and a 1987 Plymouth Voyager. PM emission rates at 75 °F on gasoline were similar to those discussed above, with the Aspire, Celebrity, and Voyager having PM emission rates of 1.2, 1.6, and 7.5 mg/mi, respectively. PM emission rates clearly increase with decreasing temperature. Thus, at -20° F, the PM emission rates were 24, 45, and 64 mg/mi., respectively. The one exception was that the PM emission rate for the Aspire did not increase between 75 and 20° F. This may be because this vehicle was designed to meet the low temperature CO emission standard, whereas none of the other vehicles were designed to this standard. The increase in PM emission rate with decreasing temperature was primarily a cold-start effect. For these three vehicles, the average emission rates for the three phases of the FTP at -20° F were 203, 0.5, and 7.4 mg/mi., respectively. Figure 2 also shows that the use of E-10 fuel reduced the PM emission rate in most instances. It is likely that this is due to an increase in A/F ratio during the cold start portion of the FTP. Overall, the results demonstrate that modeling PM emissions from light-duty vehicles should separate cold-start emissions from hot stabilized emissions, and that the impact of oxygenated fuels should be considered as well.

CAWRS Study:. The Clark and Washoe Remote Sensing Study (CAWRSS) was conducted in 1994 in the Clark and Washoe Counties (Reno and Las Vegas) of Nevada. Participants were the GM R&D Center, the Desert Research Institute, and the U.S. EPA. The primary purpose of the study was to determine the emission rates of HC and CO from the local in-use light-duty vehicle fleet. Vehicles were screened by infrared remote sensing and high-emitting vehicles were pulled over and asked to volunteer for a roadside I/M test. The remote sensing selection criteria were approximately 4% CO or 0.3% HC. The U.S. EPA operated a portable chassis dynamometer at the site that was equipped with a dilution tunnel. This setup afforded an opportunity to conduct a screening program to determine if in-use vehicles had significant PM emission rates. A dual PM-10 sampling system was added to the dilution tunnel for this purpose. The system permitted the simultaneous collection of a Teflon filter for mass determination and a quartz filter backed up by a PUF-XAD trap. The quartz filter was used to determine the organic and elemental carbon content of the PM as well as the non-volatile PAH (polyaromatic hydrocarbon) compounds. The PUF-XAD trap was analyzed for the volatile PAH compounds. The purpose of examining the PAH compounds was primarily to develop a light-duty gasoline PM fingerprint that could be used in source-apportionment studies. Results of the study have been published (Sagebiel, et al., 1997).

The 23 recruited vehicles had an average age of 10.5 years and an estimated average odometer reading of 99,800 miles. The average regulated

emission rates were 3.5, 45.0, and 1.72 g/mi for HC, CO, and NO_x, respectively. The average PM-10 emission rate was 183 mg/mi. This average rate is biased high by the specific recruitment of 5 vehicles that were observed to have visible smoke emissions. The average PM-10 emission rate for these five vehicles was 558 mg/mi. The average PM-10 emission rate of the remaining 18 vehicles was 51 mg/mi. Analysis of the filter samples indicated that most of the PM was carbonaceous material. The organic carbon content of the carbonaceous material was 77%, on average, with a wide range (35 - 95%). Sulfate emissions were also measured and were found to be very low, averaging 0.12 mg/mi, with one high emitter omitted. Twenty-four PAH compounds were measured and it was determined that there were significant differences in the PAH profiles between the smoking and other vehicles. Overall, it was concluded that there is a set of in-use, on-road vehicles with relatively high PM emission rates, and that further studies would be needed to characterize these vehicles further.

Orange County Study: An opportunity to obtain additional information on in-use vehicle PM emission rates occurred in 1995 with a South Coast Air Quality Management District sponsored study (Program for the Use of Remote Sensing Devices to Detect High-Emitting Vehicles). Participants were the Environmental Research Consortium, the U.S. EPA, and the Desert Research Institute. The study was similar to the CAWRS Study in that remote sensing was used to identify high emitting vehicles which were subsequently pulled over and tested on a chassis dynamometer using the IM240 driving cycle. An additional aspect to this program was that vehicles were repaired after the initial test and then returned to the roadside site for a retest to determine repair effectiveness.

PM-10 IM240 emission rates were determined on 103 high-emitting vehicles. Filter samples were analyzed for organic and elemental carbon and trace elements. Figure 3 shows a histogram of the pre-repair PM-10 emission rates. Each bar gives the number of vehicles within the emission rate bin. PM-10 emission rate bins start with a range of 0 to 0.049 g/mi and increase to the last bin which is all vehicles with a rate greater than 0.5 g/mi. The mean PM-10 emission rate was 138 mg/mi. Vehicles that had been identified as having visible smoke emissions averaged 395 mg/mi, while those without visible smoke average 96 mg/mi. The fleet of vehicles tested was older than those in Nevada, averaging 12.3 years old, and had an average estimated odometer reading of 125,564 miles.

Vehicles were retested after repair. While HC and CO were greatly reduced, the average PM emissions were approximately the same. This result, however, is confounded by preconditioning effects. During the repair, the vehicles experienced extended idle time. They were not reconditioned for test upon their return, and it is likely that PM emission rates were elevated. In this regard, when 10 vehicles were given back-to-back IM240 tests after recruitment, nine had significantly lower PM-10 emission rates on the second test. The average decrease was 32%. It was concluded that further work is needed to study preconditioning effects.

Analysis of the filter samples showed, again, that most of the PM was carbonaceous material. The carbonaceous material was 71% organic carbon, on average. The organic content ranged from 19 to 97%. Elements were determined by X-ray fluorescence analysis. Fourteen elements were routinely detected above the detection limit. These were, sulfur, lead, zinc, phosphorous, calcium, magnesium, copper, iron, aluminum, silicon, chlorine, and bromine. Altogether, they comprised 3.5% of the PM-10 mass. Their mass contribution ranged from 0.4% to 12.3%, being highest for the lower emitting vehicles. Oil consumption was clearly a major source of many of these elements.

Overall, it was concluded on the basis of this study that there is a population of older, high-mileage vehicles in the current in-use fleet whose PM-10 emission rates are higher than those of new vehicles. Since the vehicles recruited in this study and the CAWRS Study were not randomly recruited, the data can not be used to estimate the in-use fleet emission rate. Therefore, it was recommended that a study be conducted that measures PM emission rates from a random selection of vehicles. Further, it was recommended that the study conduct the

tests using the FTP so that the effect of cold start versus other operating modes could be investigated. The Coordinating Research Council has undertaken the recommended study.

Coordinating Research Council Study: The Coordinating Research Council (CRC) Project E-24, Measurement of Exhaust Particulate Matter Emission from In-Use Light-Duty Motor Vehicles, is being performed by contractors at three locations: Denver, Colorado; Riverside, California; and San Antonio, Texas. At all three locations in-use, light-duty gasoline and diesel vehicles are recruited for FTP emission testing. Vehicles are tested as received on a chassis dynamometer and PM-10 emission rates are measured along with the regulated pollutants. In addition, filter samples and PUF/XAD cartridges are collected for subsequent analysis for organic and elemental carbon, elemental composition, sulfate and nitrate, PAHs, and hopanes and steranes.

The Denver portion of the study is sponsored by the CRC, General Motors Corp., the National Renewable Energy Laboratory (NREL), and Total Petroleum Co. The contractors are the Colorado Department of Public Health and Environment (CDPHE), General Motors Corp., U.S. EPA, and Colorado State University. This study measured emissions from 174 light-duty gasoline vehicles and 22 light-duty diesel vehicles. The study was conducted in two segments, one during the summer of 1996 and one during the winter of 1996/1997. During the winter portion of the study, vehicles were tested both indoors on the CDPHE chassis dynamometer and outdoors on the EPA portable dynamometer. The Riverside portion of the study is being conducted by the CE-CERT which is part of the University of California at Riverside. Sponsors are the CRC, the South Coast Air Quality Management District, and NREL. They will test 100 light-duty gasoline vehicles and 19 light-duty diesel vehicles. The San Antonio study is being conducted by the Southwest Research Institute under CRC, NREL, and the Texas Natural Resources Conservation Commission sponsorship. They will test 60 light-duty gasoline vehicles and 8 light-duty diesel vehicles. All programs are expected to be completed by the end of 1997.

At this time, preliminary data is available from the Denver study only.

Table 2 gives the number of vehicles tested during both the summer and winter segments of the Denver program. Vehicle selection was weighted more heavily towards the older vehicles in anticipation that they would have higher PM emission rates than the newer vehicles, and thus would be more important in determining the total in-use vehicle exhaust emissions PM inventory. The vehicles were binned into model year categories based on emissions-control technology. Thus, 1981-85 vehicles are predominantly the first generation of vehicles with closed-loop catalyst systems. The smoking vehicles are vehicles that were specifically recruited because they had been observed to emit visible smoke. Their average age in the summer and winter were 13.8 and 17.4 years, respectively. The diesels covered a broad range of model years. Their average ages in the summer and winter were 7.3 and 15.2 years, respectively. The average age was older during the winter because most late-model diesels are in large trucks which could not be tested on the EPA chassis dynamometer.

Table 2. Vehicles Tested in the Denver Program

Vehicle Category	Summer	Winter
Pre-1981	25	17
1981-1985	26	16
1986-1990	22	14
1991-1996	20	10
Smokers	9	15
LD Diesels	10	12

Table 3 gives the average PM emission rates for the summer as well as the range in PM emission rates by vehicle category. Results should be considered preliminary at this time since data analysis for the program is not complete. As anticipated the average rate for the older vehicles is much higher than that for the new vehicles. The range in emission rates is very large, with some of the older vehicles having low PM emission rates and some of the pre-1991 vehicles having high rates. No post-1990 model

Table 3. PM-10 Emission Rates for the Denver Summer Segment

Vehicle Category	Average, mg/mi	Maximum, mg/mi	Minimum, mg/mi
Pre-1981	95.5	278	7.0
1981-1985	47.4	271	1.1
1986-1990	44.4	442	0.8
1991-1996	2.8	9.6	1.1
Smokers	225	551	39
LD Diesels	811	3988	113

year gasoline vehicle had a PM emission rate greater than 10 mg/mi.

Table 4 gives the average PM emission rates measured indoor and outdoors during the winter segment of the Denver study. PM emission rates indoors during the winter averaged lower than those observed during the summer for vehicles in the same categories. The actual vehicles tested were not the same. This may be due to oxygenated fuel use, which is mandated for the winter in Denver, but not for the summer. The outdoor emission rates were higher than indoors due to increased PM emissions during the cold-start portion of the FTP. Overall, the emission rates are in agreement those seen in the other studies.

CONCLUSIONS

Changes in fuel composition and vehicle technology have greatly reduced the PM exhaust emission rate from light-duty vehicles over the last 20 years. However, there remains a population of older, in-use vehicles with elevated PM exhaust emission rates. Fleet turnover and smoking vehicle regulations should reduce this population of high PM emitters in the future. Current mobile PM source emissions factor models need to be updated with new information on the performance of current in-use vehicles taking into account factors such as vehicle age, driving mode, and fuel use. Results of the studies discussed above will help in that regard.

Table 4. PM-10 Emission Rates for the Denver Winter Segment

Vehicle Category	Outdoors	Indoors
Pre-1981[2]	78.3	54.2
1981-1985	46.7	35.9
1986-1990	28.3	11.4
1991-1996[2]	24.9 (12.6)[1]	3.4
Smokers	434	380
LD Diesels	487	460

[1]one high emitter removed from the average
[2]not all matching vehicles between outdoors and indoors

The source profiles generated in this study will be used in the Northern Front Range Air Quality Study to make a top-down estimate of the contribution of light-duty vehicles to the ambient PM burden. In addition, the data will be used to modify the PM emission estimates in PART5 to generate an improved bottoms-up inventory of the light-duty PM emissions.

REFERENCES

1. Cadle, S. H., P. A. Mulawa, J. Ball, C. Donase, A. Weibel, J. Sagebiel, K. Knapp, and R. Snow, *Particulate and Speciated HC Emission Rates from In-Use Vehicles Recruited in Orange County, CA*. Accepted for publication. Environ. Sci. and Technol. 1997.

2. Cadle, S. H., G. J. Nebel, and R. L. Williams, *Measurement of Unregulated Emissions from General Motors' Light-Duty Vehicles.* Society of Automotive Engineers, Paper 790694, 1979.

3. Energy and Environmental Analysis, Inc., *Size Specific Total Particulate Emission Factors for Mobile Sources.* Environmental Protection Agency Report EPA 460/3-85-005, 1985.

4. Environmental Protection Agency, *National Air Quality and Emissions Trends Report, 1994.* U.S. Environmental Protection Agency, Report EPA 454/R-95-014, 1995.

5. Mulawa, P. A., S. H. Cadle, K. Knapp, R. Zweidinger, R. Snow, R. Lucas, and J. Goldbach, *Effect of Ambient Temperature and E-10 Fuel on Particulate Matter Emissions from Light-Duty Vehicles.* Environ. Sci. and Technol. 31, 1302-1307, 1997.

6. Mulawa, P. A. and J. M. Dasch, *Characterization of Exhaust Particulate Matter from 1986 Through 1990 Model Year Light-Duty Gasoline Vehicles.* General Motors Research Publication 8456, 1995.

7. Sagebiel J., B. Zielinska, P. Walsh, J. Chow, S. H. Cadle, P. A. Mulawa, K. Knapp, R. Zweidinger, and R. Snow. *PM-10 Dynamometer Exhaust Samples Collected from In-Service Vehicles in Nevada.* Environ. Sci. and Technol., 31, 75-83, 1997.

8. Rykowski, R. A., T. L. Darlington, and J. Heuss, *Exhaust Particulate Emissions from Gasoline-Fueled Vehicles.* Proceedings of the World Car Conference '96, Center for Environmental Research and Technology, University of California, Riverside, 1996.

Figure 1. EMFAC7G Estimates of On-Road PM-10 Emissions for 2005

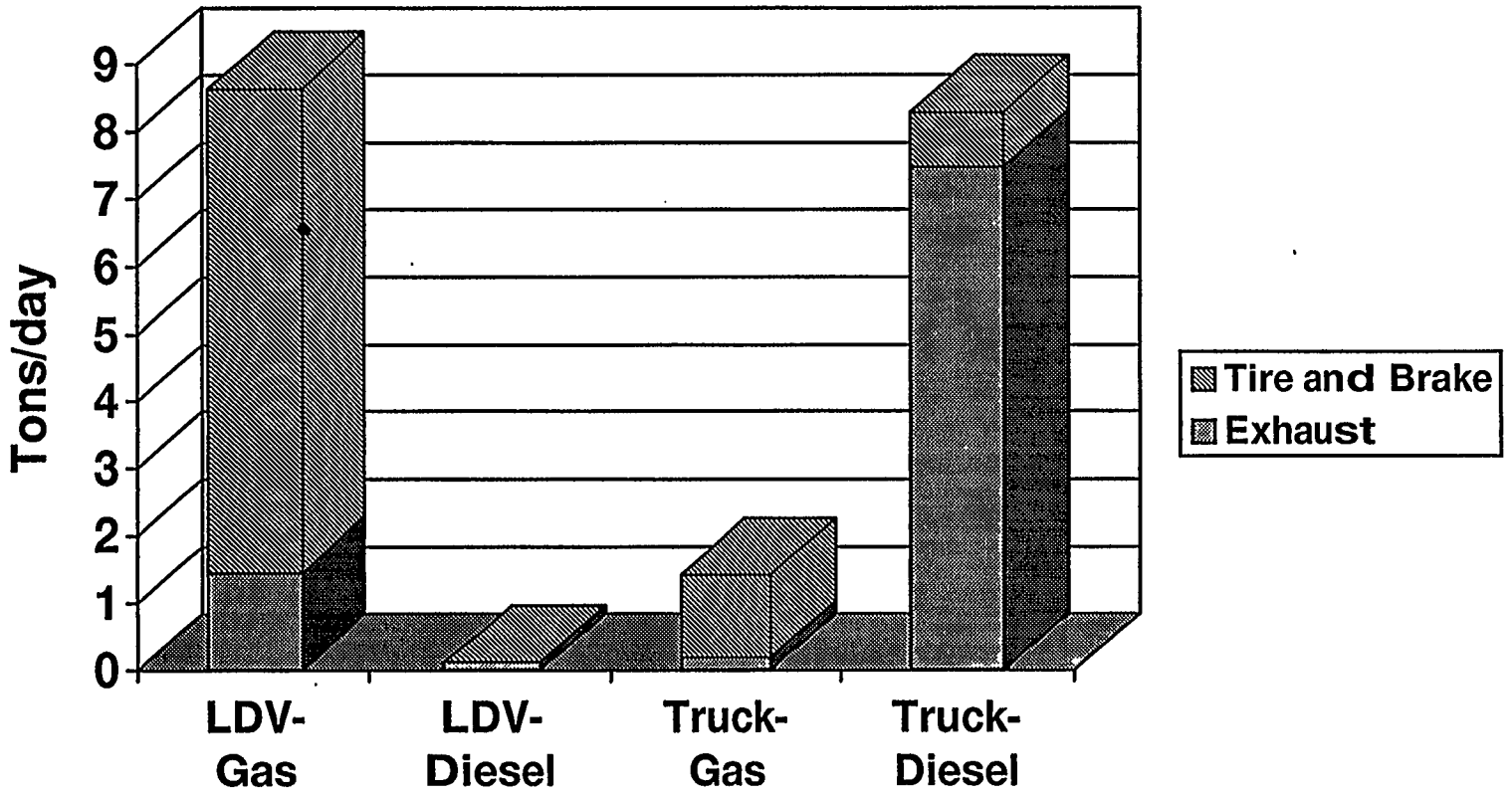


Figure 2. Effect of Ambient Temperature and E-10 Fuel on PM Emission Rates (mg/mi)

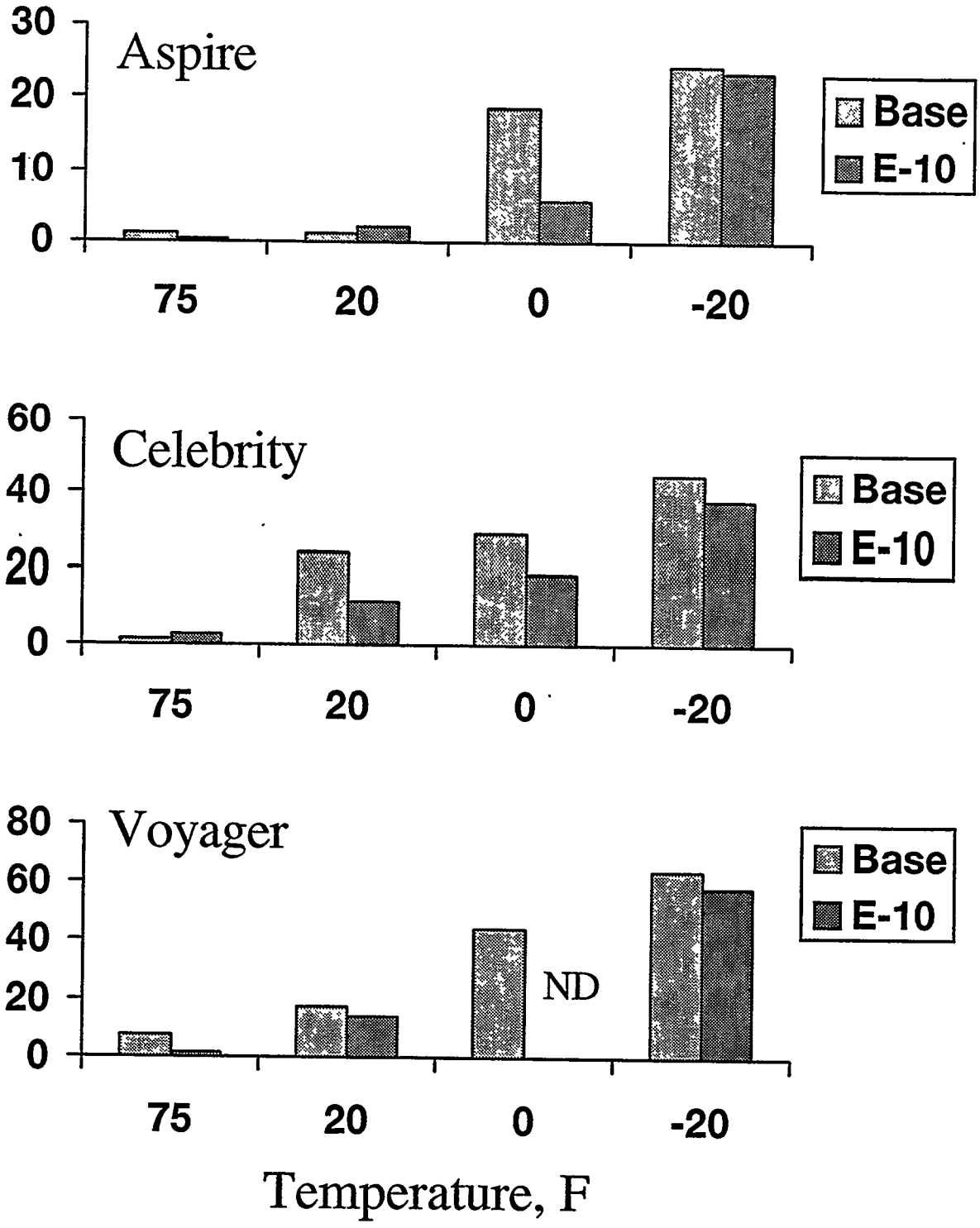
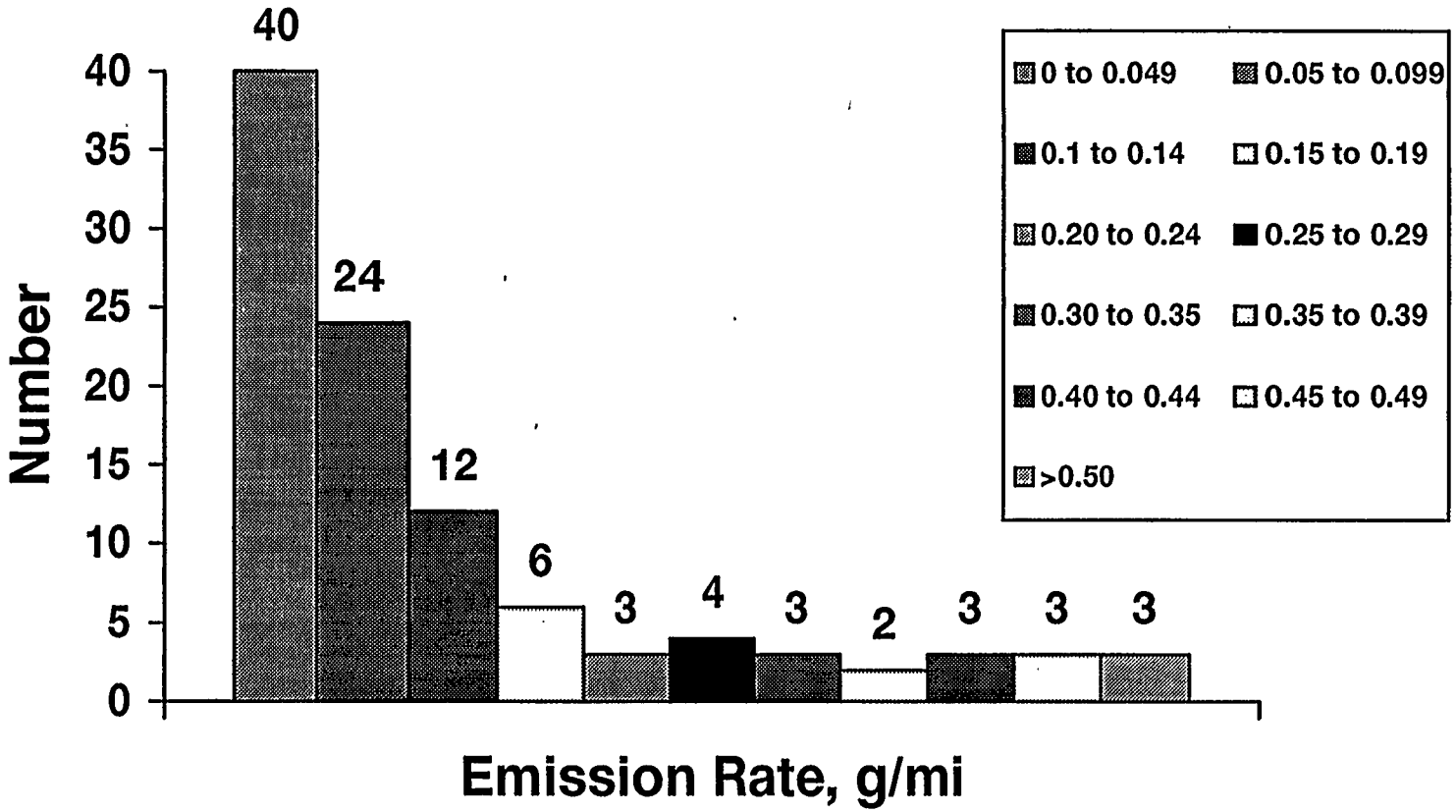


Figure 3. IM240 PM-10 Emission Rates From In-Use, High HC and/or CO Emitting Vehicles



DIESEL ENGINES VS. SPARK IGNITION GASOLINE ENGINES - WHICH IS "GREENER"?

J.W. Fairbanks
U.S. Department of Energy

Most of us have been behind heavy duty diesel powered trucks accelerating in traffic and emitting large clouds of black smoke. This exhaust smoke looks bad and intuitively it must have an adverse effect on health. However, the heavy particles comprising the black smoke quickly deposit on the ground or on the sides of buildings. Spark ignition (SI) gasoline engine powered automobiles equipped with catalytic converters appear to have clean exhausts. But then so do diesel trucks and buses built since 1994 as the human eye cannot detect smoke or carbon particles exhausted by these vehicles. It is emissions we can't see that are a concern from the human health perspective.

The fuels currently used for highway vehicles or that are viable candidates have some Cx Hy molecular structure. If we apply a carbon balance to the engine, carbon will be in the exhaust gas as either particulates (PM), hydrocarbons (HC), carbon monoxide (CO), or carbon dioxide (CO_2), the primary man made "greenhouse gas." We can either eliminate carbon and use pure hydrogen as a fuel or we can use highly efficient engines to minimize carbon in the exhaust.

Hydrogen as a fuel has widespread availability if produced from water. Unfortunately, this is a very expensive conversion. Roughly 90 percent of hydrogen used today is obtained from natural gas and used in petroleum refineries. Hydrogen is not an energy source and it will take more energy for its production than will be recovered in its use. Hydrogen costs $6 to $9 per million BTU's made from natural gas and roughly $2 to $25 per million BTU's made by electrolysis of water. About 7 gallons of diesel fuel and 8 gallons of gasoline provide a million BTU's at pre-taxed costs of about $4.20 and $4.80 per million BTU's respectively. Emissions related to hydrogen production could be substantial and so would the cost of the fuel and the supporting infrastructure. Safety concerns with hydrogen include hydrogen embrittlement which is a concern if existing pipelines are used. Leakage of hydrogen can be expected to be a factor of 3 greater than natural gas systems leakage. The energy density of hydrogen is about 1/3 that of methane, so the total energy release would be about the same. However, hydrogen leakage in a confined space will reach explosive proportions approximately 4 times faster than natural gas. Outdoors it would be safer than natural gas (1).

If hydrogen were available as an economically competitive fuel, reciprocating engines would challenge fuel cells on the basis of efficiency, cost, durability and existing field support, and manufacturing infrastructure.

What would the cost be to train `Mr. Goodwrench" to support fuel cell powered vehicles nationwide? If H is extracted from gasoline onboard the vehicle, where is the carbon going? And how much energy is consumed by this extraction? Fuel cell advocates talk about high efficiency conversion of fuel to electricity but tend to gloss over the losses in extracting H from fuel, electric power conditioning, and motor losses. Fuel cell technology will undoubtedly improve, but in 1997 on a fuel to drive train basis, fuel cells are roughly equivalent in efficiency to production gasoline cars with very low emissions and roughly 6 times the cost of a comparable SI gasoline powered automobile.

The consensus of the fuels and engine communities is that gasoline and diesel fuel will be primary fuels well into the 21st century. Reformulations of both fuels to further improve emissions are highly probable. Engine

efficiency is the best way of reducing carbon emissions based on a carbon balance. As an example, the diesel engines being developed to replace spark ignition gasoline engines for light truck applications will reduce both fuel consumption and CO_2 emissions by about 50 percent! Diesel engines have a relatively flat fuel use characteristic from idle to full power whereas gasoline engines and gas turbines have relatively high fuel use at low power and idle. Thus, the greater the extent of urban driving, the greater the advantage for diesel engine powered vehicles.

Virtually all Class 7-8 trucks worldwide are diesel engine powered. In Europe, diesel engine power is dominant thru all classes of trucks and constitutes about 30 percent of car sales. Light vehicles and cars are predominantly gasoline powered in the U.S. A meaningful comparson of diesel vs gasoline powered cars and light vehicles should include some of the European experience. VM Motori, a division of the Detroit Diesel Corporation, advertises that its diesel engine is better than the best gasoline engine with catalytic converter for the five primary emissions which are oxides of ntrogen (NO_x), particulate (PM), hydrocarbons (HC), carbon monoxide (CO), and carbon dioxide (CO_2). Let's consider these emissions:

Oxides of Nitrogen (NO_x)

SI gasoline engine powered cars are now equipped with a 3-way catalyst that reduces NO_x as long as the operating témperature is achieved and combustion is stoichiometric. Cars are equipped with as many as 4 oxygen sensors which are used in controlling the fuel/air mixture to stoichiometric conditions. Catalytic converters degrade with use and take increasingly longer to lift off. Consider the life of an automobile, which now averages about 130,000 miles. Over the last 110,000 miles, or 85 percent of the life of the car, the NO_x + HC emissions from gasoline powered cars are more than that from the diesel engine car. At the end of life there are 2.3 times the NO_x + HC out of the gasoline car as compared with the diesel engine as shown in Figure 1. Thus, NO_x emissions from the gasoline engine cars are higher than diesel engine cars over 85 percent of the life of the vehicle.

The catalytic converters currently used in cars have made a considerable contribution to cleaning up the air. Their use was stimulated by efforts of the California Air Resources Board (CARB) in 1974. These 3-way catalysts reduce levels of CO, HC, and NO_x. They typically use platinum, rhodium, or palladium deposited on ceramic or metallic substrates. The catalytic converters require stoichiometric combustion for NO_x reduction. If the engine runs rich (I. e., excess fuel) the CO and HC emissions will increase. If the engine runs lean, (i.e., excess air) then there is very little NO_x reduction. This restriction of the fuel/air ratio to 1, i.e., stoichiometric combustion, prevents achieving several points in efficiency that could be obtained with lean burn engines. Also, the oxygen sensors degrade with time (they are typically warranted for 2 years or 24,000 miles.)

Catalytic converters do not function until they reach their operational temperature. A car with a catalytic converter must be driven for about 7 miles in an urban area for the catalytic converter to reach operational temperature. In Great Britain, about 40 percent of the car trips are less than 3 miles. So the catalytic converter never lights off in these vehicles. In testing done in Great Britain on comparable cars, the gasoline powered car with 3-way catalyst over the first kilometer produced 83.9 grams of pollution (72.9 g/km of CO, 10.0 g/km of volatile organic compounds [VOC's], and 1.0 g/km of NO_x) while the diesel car produced 9.0 gms of pollution (5.3 g/km of CO, 1.9 g/km of VOC and 1.8 g/kmNO_x)

The new U. S. diesel engine fuel systems using microprocessor control, high fuel injection pressures, rate shaping, and pilot injection plus cooled EGR (exhaust gas recirculation) will dramatically reduce NO_x even lower. The NO_x and HC levels for the light vehicle (i.e., Sport Utility Vehicles (SUVs) vans, pickup trucks) diesel engines being developed at Cummins, Caterpillar, and DDC are projected to be

equivalent or lower than those from new gasoline powered vehicles. NO_x levels from these diesel engines in development would not deteriorate as they do with catalytic converters. Nonthermal plasmas could further reduce NO_x and PM to near zero levels! Nonthermal plasma devices replacing 3-way catalysts in S.I. gasoline engines would eliminate the cold start engine and allow lean burn operation with consequent improved efficiency without the degradation of the catalytic converter and oxygen sensors. Early work suggests non-thermal plasmas are self-cleaning.

Carbon Monoxide

Spark ignition (SI) gasoline engines with functioning catalytic converters emit at least 10 times as much CO as comparable diesel engines. CO is a product of incomplete combustion of a carbon containing fuel. Catalytic converter operation requires the stoichiometric ratio wherein there is just enough air oxygen to completely burn all the gasoline. As the mixture of fuel/air becomes richer, i.e., more fuel than air, the concentration of CO increases rapidly. This happens during vehicle operation. However, in the diesel engine with its very lean fuel/air mixture, the excess oxygen introduced into the combustion chamber fully oxidizes the carbon to carbon dioxide (CO_2) with only a small amount of CO. The level of CO emitted from gasoline engine powered cars is very high during cold start, i.e., before the catalytic converter lights off, and during acceleration enrichment.

CO emissions may become an increasing concern. In a recent study at Stanford University, CO levels 2 to 14 times greater were measured inside cars than in the air 150 feet away from the highway. Low CO levels induce drowsiness and headaches. These low CO levels are also dangerous to pregnant women and those with heart disease. High levels of CO can cause death. There are 2,850 deaths annually attributed to exhaust from gasoline engine cars. This is not the case with a diesel engine powered vehicle.

Another source of CO emissions is the programmed fuel/air enrichment during hard acceleration. During this hard acceleration excess fuel is introduced to prevent thermal damage to emission control parts as well as in-cylinder components under warranty. General Motors Research tested a 1989 3.8L V-6 gasoline powered car for 350 miles in Los Angeles with aggressive driving but with the fuel/air mixture maintained near stoichiometric most of the time. Compared with the Urban Dynamometer Driving Schedule there were 2,500 times more CO and 40 times more HC emissions measured. This test was considered representative of three-way catalyst equipped SI gasoline engines.

The only production cars that have eliminated acceleration enrichment are the Mercedes Benz C Class cars. This is achieved in these cars by using larger catalysts relative to engine displacement, an electric air pump to oxygenate exhaust manifolds, and electrically heated elements in the cylinder head. These technologies are costly. Acceleration enrichment cannot be achieved by reprogramming engine control components (3)

Particulate Matter (PM)

Particulates that are respirable by people are at the environmental center stage in mid-1997. Particulates that have an aerodynamic diameter of 10 microns or less are respirable. Most of the PM which are under 10 microns but over 2.5 microns are comprised of tire and brake wear debris, soil, and other crustal material. The PM 2.5 microns and below that typically result from combustion of fossil fuels in transportation, manufacturing and power generation, are referred to as fine particles. Ultra-fine PM are below 0.10 microns. The smaller the particle size, the greater the probability is that it will deposit in the lung.

The Harvard Six Cities Study, which involved 8,111 adults in 6 U.S. cities covering a 14 to 16 year period, showed a nearly linear relationship between the level of fine-particle pollution and mortality (4). A followup study with a larger cohort but shorter time period

produced similar results.

Heavy duty diesel engines manufactured before 1994 powering trucks and buses. characteristically belch large plumes of black smoke during acceleration. The human eye can't detect smoke from a post-1994 diesel engine powered heavy vehicle. The problem is that the Environmental Protection Agency (EPA) specified the mass levels of particulates in emission standards not particle size and distribution. Human health concerns suggest particle size and distribution as well as attached chemicals.

PM exhausted from spark ignition gasoline engine powered automobiles is typically smaller in diameter and lower in quantity than that from diesel engines. However, driving patterns strongly influence PM emissions. Cold start PM can be 2 orders of magnitude greater than PM emitted driving at engine operating temperatures. Rapid acceleration also produces significant PM which is not detected in current EPA tests for spark ignition (SI) gasoline powered automobiles.

Results of testing in the United Kingdom (UK) of comparable SI gasoline powered cars with 3-way catalysts compared with turbocharged diesel engine powered cars are shown in Figures 2 and 3. Note that the quantity of PM from the diesel car is larger with a distribution peak about 0.10 microns while the quantity from the SI gasoline auto is considerably smaller but the peak of the distribution is 0.030 microns, or 1/3 the diameter of the peak of the diesel car distribution. Figure 4, published by the Harvard School of Public Health, shows the relative deposition in the human pulmonary track of PM as a function of size. The peaks of the UK data are superimposed on this chart showing that the PM from the gasoline car has about twice the deposition factor of that from the diesel car.

Carbon Dioxide (CO_2)

If one does a carbon balance with a heat engine fueled with a hydrocarbon fuel, the exhaust gas will have the carbon as either particulates (PM), hydrocarbons (HC), carbon monoxide (CO), or carbon dioxide (CO_2). Since the particulates resulting from the combustion of hydrocarbon fuel are typically less than 2.5 microns in diameter, the least harmful to human health of carbon in exhaust is CO_2. While CO_2 is not a pollutant, it is a "greenhouse gas." Every breathing creature emits CO_2 which plants absorb then release oxygen into the atmosphere. Only about 4 percent of CO_2 in the atmosphere is manmade, essentially from the combustion of hydrocarbon fuels. Improving engine efficiency is the best near term technical answer to man-made CO_2 reduction. The new DOE light vehicle diesel engine will use 50 percent less fuel for combined city/-highway driving than the current gasoline engines; this also reduces CO_2 by 50 percent for each gasoline engine replaced with a diesel engine in these vehicles. This could be a meaningful contribution to the US commitment to the Global Warming issue.

Onhighway Emission Measurements

Emissions from primarily gasoline powered vehicles are being measured during regular onhighway use by portable remote sensing systems. Infrared beams are used to measure CO and HC and an ultraviolet beam is used for NO_x Calibrations are done with CO_2 absorption. Over two million cars in several countries have been tested this way. In California testing, a consistent pattern emerged. Emissions levels have gone down steadily as new and better emission control technology is introduced. However, for every vehicle model year, 10 percent of the vehicles contribute half of the total fleet's CO and HC emissions. These high emitters are found in all model year vehicles(5). It is not just the older vehicles that are the high emitters.

Evaporative Emissions From Gasoline

The levels of HC evaporation from automobiles is comparable to HC in the exhaust. Evaporation of HC from the vehicle fuel system can be classified into 3 categories: diurnal emissions, hotsoak emissions, and running losses. Diurnal emissions refer to those that occur in a parked vehicle as it draws in air at night as it cools down and expels air and gasoline vapor as it heats up during the day. This "diurnal breathing" of the fuel tank can produce

evaporative HC emissions of about 50 g/day. Hot soak emissions occur after the engine is shut off and the residual thermal energy heats the fuel system. Running losses occur as gasoline vapors are expelled from the fuel system when the car is driven and the fuel becomes hot. In addition, gasoline vapors can escape from the fuel system during fueling at the gas station. Regulations have required evaporative controls for over 20 years. However, these systems have been very ineffective in service. (5) These evaporative emissions contribute to photochemical ozone. Diesel powered vehicles have insignificant evaporative emissions.

The relative volatility of diesel fuel and gasoline has another human safety aspect. During a question and answer session at the SAE 1995 meeting in Detroit, Cayot of Lucas, responded to a human health related question by saying that in France, where 40-50 percent of new car sales since 1989 have been diesel engine powered cars, there have been about 5,000 people burned to death in collisions involving gasoline engine powered cars. However, there were no deaths reported in collisions involving diesel engine cars caused by burning. This is due to the high volatility of gasoline and low volatility of diesel fuel.

Benzene

Benzene is defined by the World Health Organization as a known human carcinogen. It is a proven cause of leukemia. The recommended limit of benzene in the atmosphere is currently 5 ppb, which will soon be reduced to 1 ppb. There is a minimal amount of benzene in diesel fuel (0.05%) because it reduces the cetane number. However, it is added to gasoline (about 1.0%) to increase the octane rating. Thus, there is more than 1 pint of benzene, a known carcinogen, in a 14 gallon tank of gasoline. EPA's National Air Pollution trends in October 1996 indicated that 97 percent of the benzene in the atmosphere came from gasoline engines and 3 percent from diesel engines in a highway study (7). Curiously benzene from gasoline has not been a candidate for Proposition 65 in California but has been identified as a toxic substance in diesel exhaust (8).

MTBE Gasoline Oxygenate

Methyl tertiary butyl (MTBE) is by far the most extensively used of the gasoline oxygenate required by the US Environmental Protection Agency (EPA). Gasline with 1 percent MTBE reduces CO by 20 percent, H_2 by 6 percent, and NO_x by 8 percent, but increases aldehydes, which are a precursor of ozone. MTBE is a potential carcinogen. The big problem with MTBE is that it mixes thoroughly with water, travels great distances through water, and is very difficult to remove from water. A significant number of wells in the Santa Monica area are contaminated with MTBE. The water is described as having a bad taste and odor. Water contamination with MTBE has been reported by the U. S. Geological Survey nationwide. Sources of MTBE are gasoline spills, leaks from underground tanks, and motorboat gasoline engines. Water contamination by MTBE as a result of a gasoline spill in North Carolina has resulted in a judgement against the oil company involved. The investment by the oil companies in MTBE is large. It is roughly a ten billion dollar a year business. Additional legal suits by residents encountering MTBE in their water should be anticipated. MTBE is not a diesel fuel additive (6).

Nitrous Oxide (N_2O) - Greenhouse Gas

Nitrous oxide (N_2O) is a greenhouse gas that is more commonly known as "laughing gas" as used by dentists. N_2O has about 300 times the infrared absorbing capability of CO_2. It is this infrared absorption along with, reflection and radiation back to earth by water vapor, CO_2, , and methane that provide the greenhouse effect. Solar energy, which is primarily the ultraviolet and visible part of the spectrum, is fairly well transmitted through the earths's atmosphere to the earth's surface. However some solar energy is reflected back to space by the atmosphere. The earth's surface absorbs incident solar energy and radiates some of it to deep space as thermal energy in the infrared wavelength. The transparent shield of tropospheric greenhouse gases absorbs some of this infrared radiation and radiates it back to earth, resulting in increased warming. With these greenhouse gases the average temperature of the earth is 59°F; without the

greenhouse gases the average temperature of the earth would be -4° F. The source of N_2O from highway vhicles is primarily the catalytic converter. EPA reports 99 percent of the on-road vehicle emissions of N_2O come from SI gasoline engine powered cars (7). N_2O emissions are not regulated. About 200,000 tons of NO are emitted worldwide per year. On a CO equivalent basis, N_2O contributes only a few percent to the global warming potential. Conversion of NO_x to N_2O by non-thermal plasma or lean NO_x catalyst should be (and can be) avoided. Early work with lean NO_x catalysis suggests considerable N_2O generation.

Greener Engines

Technology is emerging at the laboratory scale that suggests diesel and gasoline engine emissions can be further reduced to very low levels. Extensive engineering development is necessary to bring this technology into production. The question is becoming how low do we want to reduce onhighway emissions and how much are we willing to pay to do it?

SI gasoline engines are limited in efficiency by the necessity of stoichiometric air/fuel combustion to enable NO_x reduction by the catalytic converters. Stoichiometric combustion is maintained by using as many as 4 oxygen sensors controlling combustion. The problem is that both the catalytic converters and oxygen sensors degrade with use requiring replacement and the older cars typically wind up with drivers with low income levels. Many low income people are not in a position to pay $100 per oxygen sensor and several hundred more for a replacement catalytic converter. The State of California is considering paying the cost of oxygen sensor and catalytic converter replacement for California's low income vehicle owners up to some cap. This is probably a better approach than the earlier CARB sponsored cash for "clunkers" to get the older cars off the road. Public transportation is inadequate in Southern California and cars are a necessity for most residents. The other states will probably watch how well this works in California.

Non-thermal plasma devices are still in the development stage but early testing suggests 70 percent simultaneous NO_x and PM reduction stages; they will be self cleaning, will allow lean burn combustion with its attendant increase in efficiency and since they operate essentially independent of temperature, the cold start problem with gasoline engine powered cars could be eliminated. Non-thermal plasma device cost and power requirements are main concerns. There are several approaches which could minimize the electrical power requirement. Device costs are projected to be under $500. PM reduction can be improved with soot catalytic traps that are now available or microwave regenerated particulate traps that should be available within 2 years. Reformulated fuels should provide further PM emission reductions as sulfur and aromatics are further reduced.

Diesel engine emission reduction for the Class 7 & 8 trucks since 1978 has seen NO_x reduced by 73 percent and PM by 93 percent as shown in Figure 4. The EPA-required transient tests for heavy duty truck diesel emissions measurements while the Europeans and Japanese require much easier 13 step steady state testing. This chart presents difficulties for those involved with the human health aspects of diesel engine emissions. Evaluation of human exposure over the years involves emissions from a domestic truck fleet that is becoming dramatically cleaner over the years. For example, detailed health studies of people exposed to diesel exhaust from 1960-1980 would be questionable contrasted to those exposed to diesel exhaust say from 1997-2017.

Environmentalists

"Watchdog" environmentalists can and do make worthwhile contributions. They are certainly attacking diesel engine exhaust as a toxic air contaminant. The California Environmental Protection Agency is in the process of identifying diesel exhaust as a toxic air contaminant with its legal ramification. A cornerstone of this approach are the rat studies of exposure to diesel exhaust greater than 2.5 mg/m3 for 24 month's exposure. This diesel exhaust produced cancer. However, the group that conducted this testing says it was a unique rat reaction not duplicated in other

animals and not extrapolative to humans. This test was reproduced in Germany with road dust that produced similar cancers. Even after the author of this work wrote to the people preparing this report, the diesel exhaust causal effect of cancer in rats is still in the report. Why isn't gasoline engine exhaust with its high level of benzene (97% to 3% from diesels), high NO_x, PM, and CO levels causing concern for impartial environmentalists? (the World Health Organization has identified benzene as a known carcinogen). There are also problems in diesel exhaust for health concerns. There are significant concerns for automobile gasoline engine exhaust that the environmental community for the most part ignores. Accurate technical identification of human health concerns will generally cause more attention to be focused on the problem.

Summary/Conclusions

Criteria emissions, i.e.; NO_x, PM, CO, CO_2, and H_2, from recently manufactured automobiles, compared on the basis of what actually comes out of the engines, the diesel engine is "greener" than spark ignition gasoline engines and this advantage for the diesel engine increases with time. SI gasoline engines tend to get out of tune more than diesel engines and 3-way catalytic converters and oxygen sensors degrade with use. Highway measurements of NO_2, H_2, and CO revealed that for each model year, 10 percent of the vehicles produce 50 percent of the emissions and older model years emit more than recent model year vehicles. Since 1974, cars with SI gasoline engines have uncontrolled emission until the 3-way catalytic converter reaches operating temperature, which occurs after roughly 7 miles of driving. Honda reports a system to be introduced in 1998 that will alleviate this cold start problem by storing the emissions then sending them through the catalytic converter after it reaches operating temperature. Acceleration enrichment, wherein considerable excess fuel is introduced to keep temperatures down of SI gasoline engine in-cylinder components and catalytic converters so these parts meet warranty, results in 2,500 times more CO and 40 times more H_2 being emitted. One cannot kill oneself, accidentally or otherwise, with CO from a diesel engine vehicle in a confined space. There are 2,850 deaths per year attributable to CO from SI gasoline engine cars.

Diesel fuel has advantages compared with gasoline. Refinery emissions are lower as catalytic cracking isn't necessary. The low volatility of diesel fuel results in a much lower probability of fires. Emissions could be improved by further reducing sulfur and aromatics and/or fuel additives. "Reformulated fuel" has become the term covering reducing the fuels contribution to emissions. Further PM reduction should be anticipated with reformulated diesel and gasoline fuels.

References

1. F.J. Edesbuty et al, "Critical Review and Assessment of Environmental and Safety Problems in Hydrogen Energy Systems", prepared for Dept. of Energy under Contract W-7405-ENE-36, Los Alamos National Laboratory, Los Alamos, New Mexico.

2. EPA AP-42, 4th Edition.

3. Ward's Engine and Vehicle Technology Update, Dec. 1993.

4. D.W. Dockney, et al, "An Association Between Air Pollution and Mortality in Six U. S. Cities," The New England Journal of Medicine, Vol. 329, No. 24, Dec. 9, 1993.

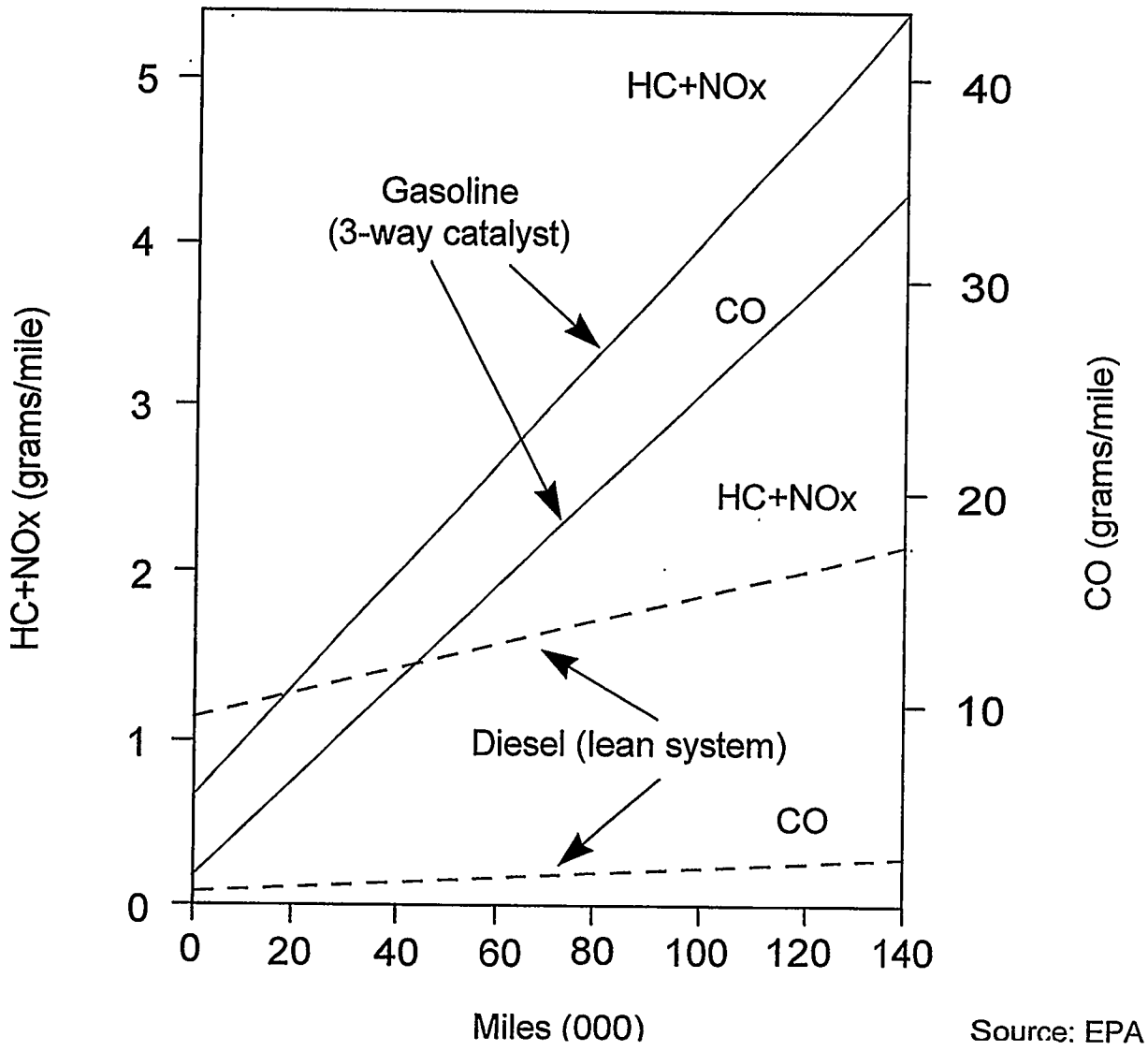
5. J.B. Haywood, "Motor Vehicle Emissions Control: Past Achievements, Future Prospects,"Combustion Engine Group Prestige Lecture presented at a Sponsored Lecture, London, 21 May 1996.

6. R. Brooks, personal communication - Ward's Engine Vehicle Technology Update contributor, August 1997.

7. National Air Pollutant Trends published by EPA, Oct. 1996.

8. Proposed Identification of Diesel Exhaust as a Toxic Air Contaminant, Executive Summary, California Environmental Protection Agency Public comment and SRP Version, May 9, 1997.

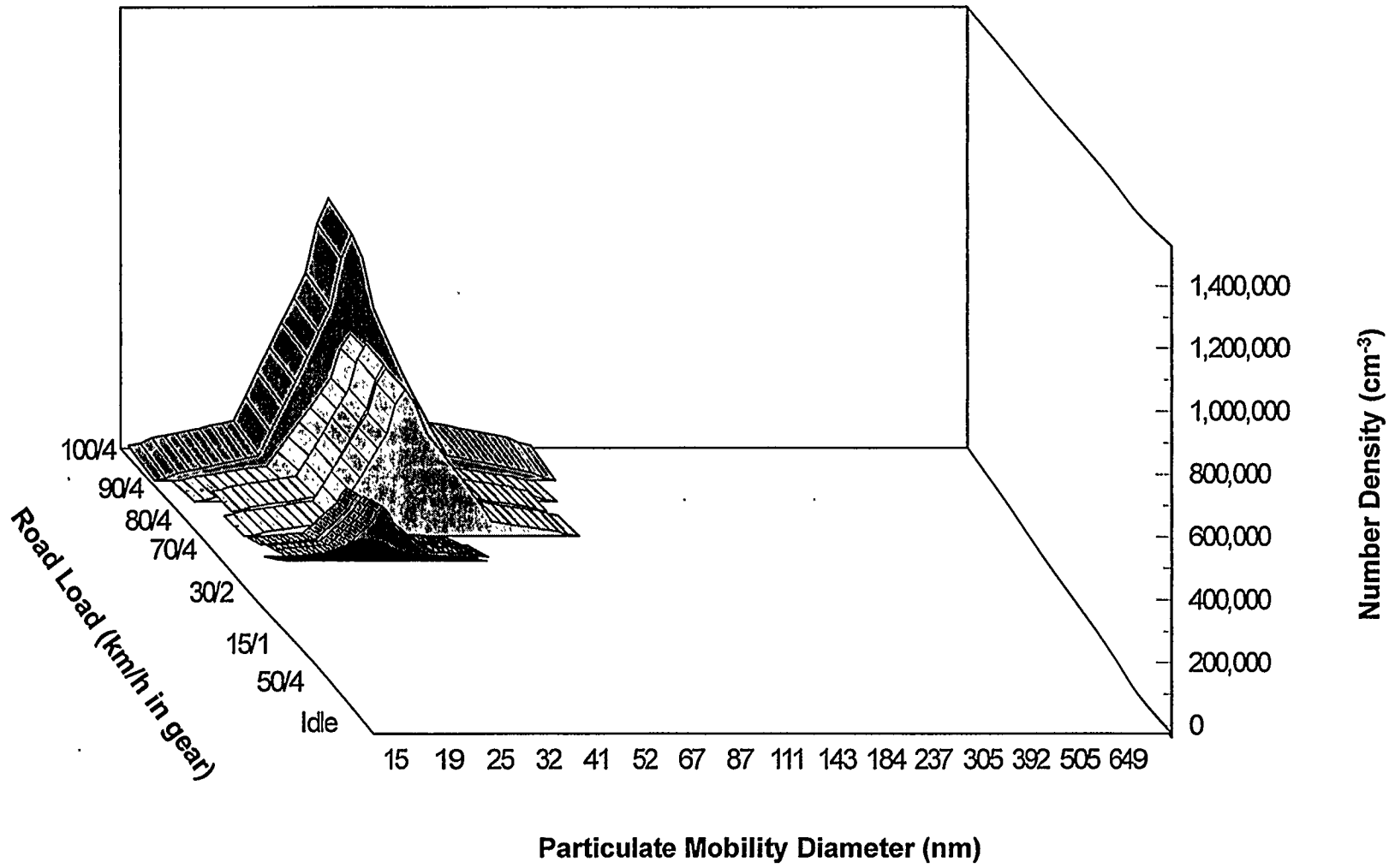
Projected Emissions of 1990 Light-Duty Vehicles



Source: EPA AP-42 4th Edition

Figure 1. EPA Projected Emissions of 1990 Light-Duty Vehicles

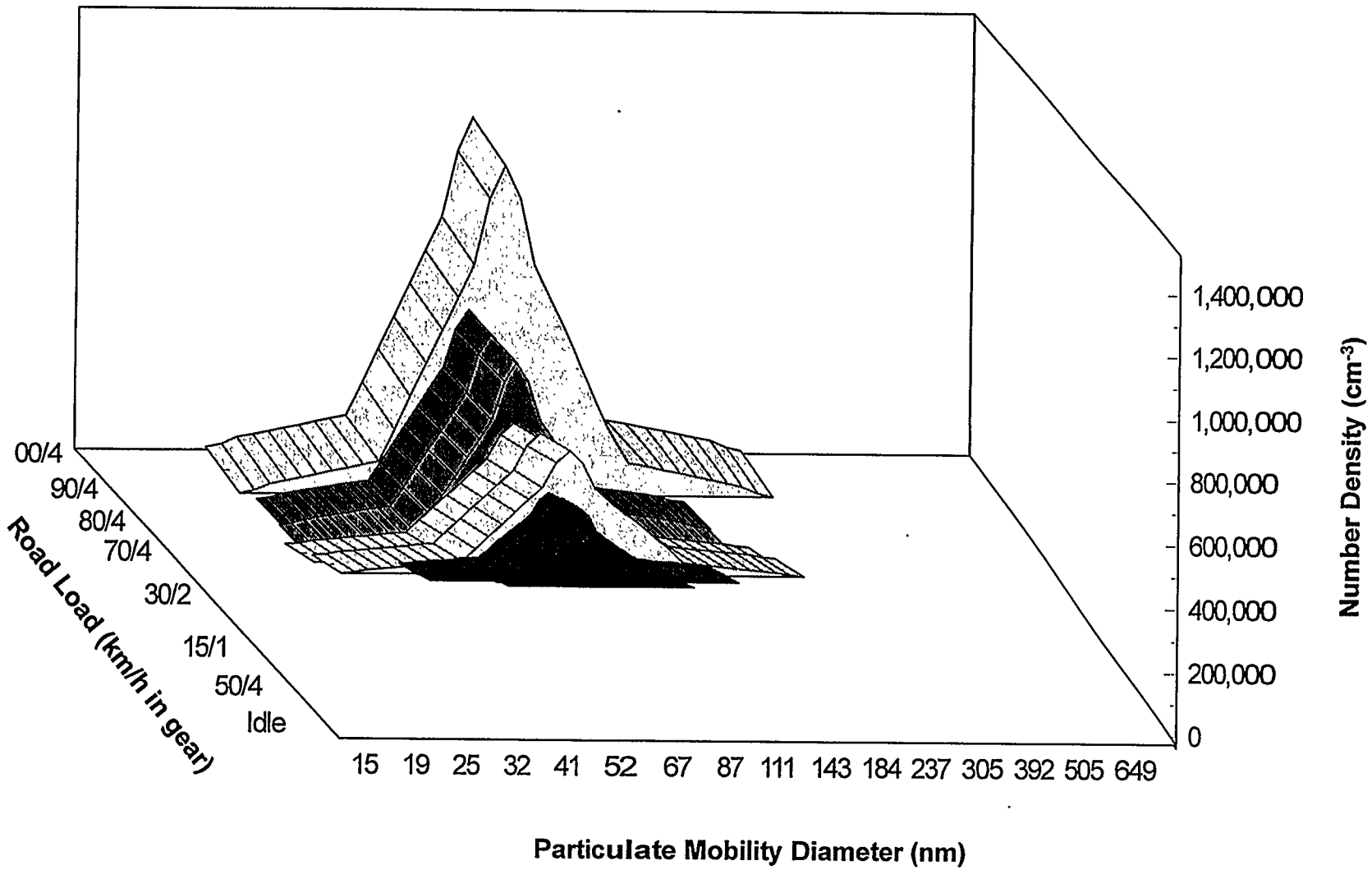
Particle Size Distribution from a 2.2 Liter Gasoline Vehicle (with Catalyst) at Constant Speeds



Report of the UK Particulate Group (Harwell)

Figure 2. UK Test Showing PM Distribution From 2.2 Liter Gasoline Vehicle With Catalysts

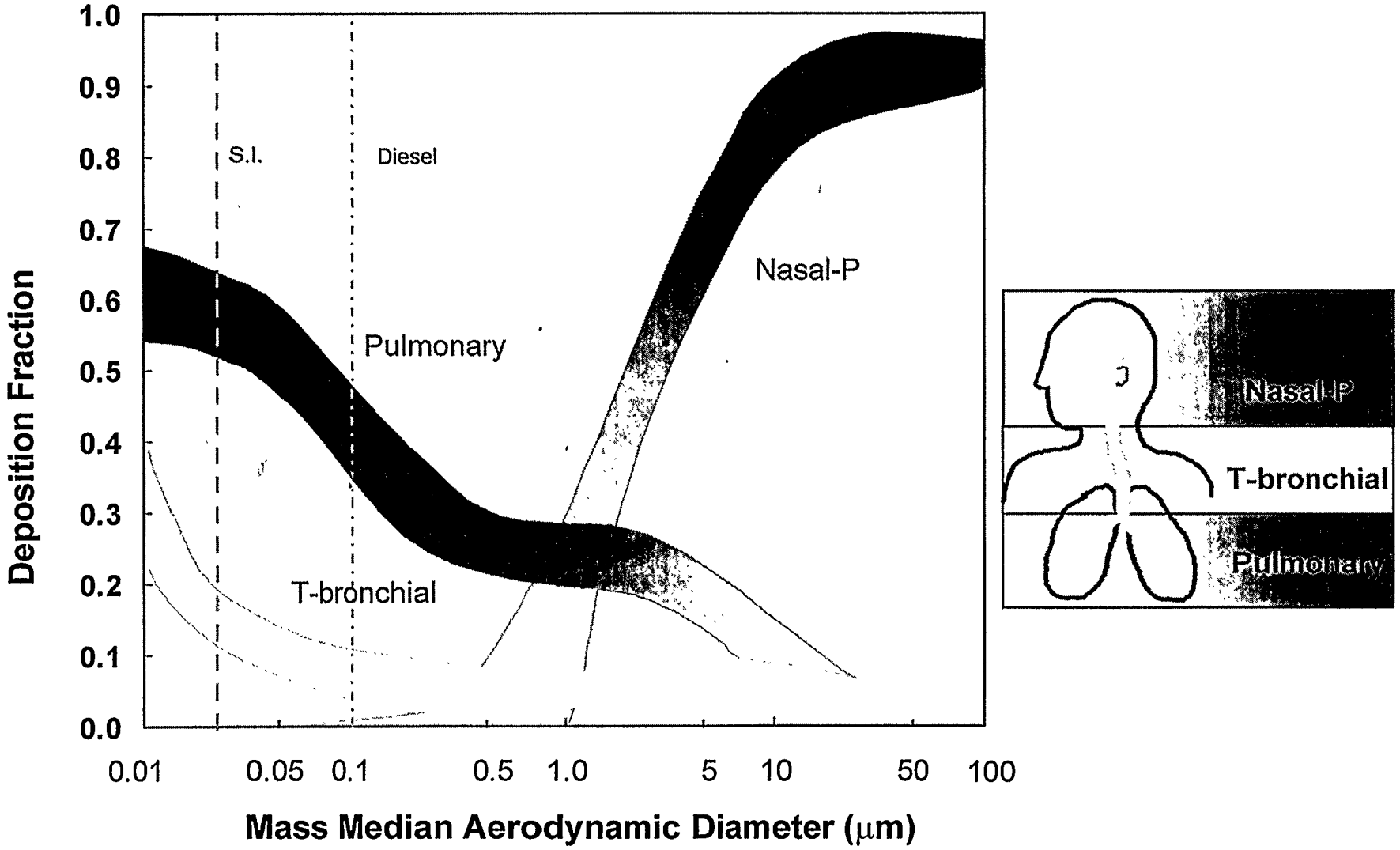
Particulate Size Distributions from a 1.9 Liter Turbocharged Diesel Vehicle at Constant Speeds



Report of the UK Particulate Group (Harwell)

Figure 3. UK Test Showing PM Distribution from a 1.9 Liter Turbocharged Vehicle

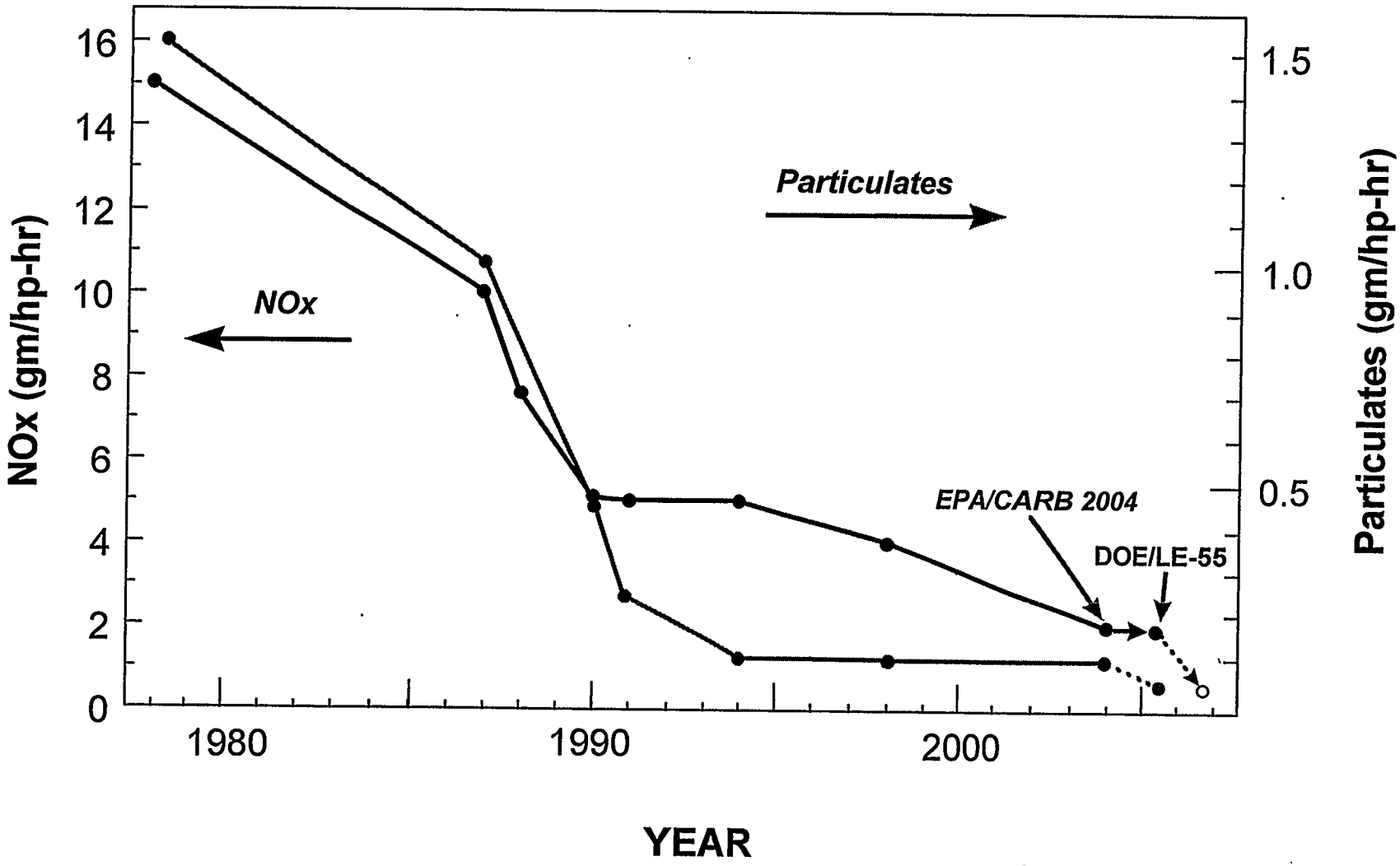
"Regional" Deposition of Particulates



Source: Particles in Our Air: Concentrations and Health Effects
1996 Harvard School of Public Health

Figure 4. Deposition of PM In The Human Respiratory Tract

Evolution of Heavy Duty Diesel Engine Emissions Control



Source: Cummins, modified by DOE

Figure 5. Evolution of Heavy Duty Class 7-8 Truck Diesel Engine Emissions Control

PARTICIPANTS

1997 DIESEL ENGINE EMISSIONS REDUCTION WORKSHOP

REGISTRATIONS

Dr. René B. Abarcar, Energetics. Inc., 7164 Gateway Drive, Columbia, MD 21046
Tony F. Andreoni, Air Resources Board, P.O. Box 2815, Sacramento, CA 95812
Alec C. Atanas, Engelhard Corporation, 9800 Kellner Road, Huntsville, AL 35824
Brian S. Ahern, Quantum Energy Technologies, 238 Main Street, Suite 201, Cambridge, MA 02142
Chris Atkinson, West Virginia University, Box 6106, Morgantown, WV, 26506-6106
Brent K. Bailey, National Renewable Energy Laboratory, 1617 Cole Boulevard MS 1633, Golden, CO 80401
Dr. Eric N. Balles, Clean Diesel Technologies Inc., 300 Atlantic Street, Suite 702, Stamford, CT 06901,
M. Lou Balmer, Pacific Northwest National Laboratory, P.O. Box 999, Battelle Blvd. MS K8-93, Richland, WA 99352
Marty Barris, Donaldson Company, Inc., P.O. Box 1299, Minneapolis, MN 55440-1299
John C. Bass, Hi-Z Technology, 7606 Miramar Road Drive, San Diego, CA 92126
N. John Beck, BKM, Inc, 5066 Santa Fe Street, San Diego, CA 92109
Frederick E. Becker, Thermo Power Corp., 45 First Avenue, Waltham, MA 02254-9046
Robert A. Beyerlein, ER-142, U.S. Department of Energy, 19901 Germantown Road, Germantown, MD 20874-1290
Avtar Bining, California Energy Commission, 1516 Ninth Street, MS-41, Sacramento, CA 95814-5512
David Biron, GM EMD, 9301 W. 55th Street, Dept. 870, LaGrange, IL 60525
Steven Bittenson, Thermo Power, 45 First Avenue, Waltham, MA 02254-9046
Rich Bloom, 3M Co, 3-M Center, Bldg 207 ISC-12, St. Paul, MN 55144-1000
André Boehman, Penn State University, 209 Academic Projects Building, University Park, PA 16802-2303
Brian Bolton, Detroit Diesel Corporation, 13400 Outer Drive West, Detroit, MI 48239-4001
Louis C. Broering, Exhaust Aftertreatment, Cummins Engine Company, 1900 McKinley Ave., Columbus, IN 47201
Nancy J. Brown, MS 70-1085, Lawrence Berkeley Lab, 1 Cyclotron Road, Berkeley, CA 94720
Lou Browning, Acurex Environmental, P.O. Box 7044, Mountain View, CA 94039
Dr. Walter Bryzik, Mail Stop 121, U.S. Army Tank-Automotive and Armaments Command, Warren, MI 48397-5000
Bruce Bunting, Cummins Engine Co., 1900 McKinley, MC 50183, Columbus, IN 47201
Chub Burgess, Parker Hannifin, 4112 Cambridge, Bakersfield, CA 93306
William A. Buscher, Jr., Texaco Inc., P.O. Box 509, Beacon, NY 12508
Steven H. Cadle, General Motors R&D Center, MS 480-106-269, 30500 Mound Road, Warren, MI 48090-9055
Charles C. Carlisle, CHA Corporation, 372 West Lyon, Laramie, WY 82073
Joshua L. Caron, SRD Corp. PO Box 191, Orono, ME 04473
Thomas F. Cash, Corning, Inc., HP-CB-031W, Corning, NY 14841
Professor Glen Cass, California Institute of Technology, Pasadena, CA 91125
Dick Cataldi, Association of American Railroads, 50 F Street, NW, Washington, DC 20001
Chang-Yul Cha, CHA Corporation, Box 1084, Laramie, WY, 82073
Ashop Chanda, Technical Center, Bldg. L, P.O. Box 1875, Caterpillar Inc., Peoria, IL, 309-578-2889
Derek A. Channing, Ford System Engineering, Suite 1300, 16630 Southfield Drive, Allen Park, MI 48154-5205
Gong Chen, GE Transportation Systems,.Bldg. 14-3, 2901 East Lake Road, Bldg. 14-3, Erie, PA 16531
A.S. "Ed" Cheng, University of California, Berkeley, 50B Hesse Hall, University of California, Berkeley, CA 94720
James J. Corbett, P.E., Carnegie Mellon University, 2301 Sherbrook Street 2nd Floor, Pittsburgh, PA 15217
Pranab Das, Navistar International, 10400 West North Avenue, Melrose Park, IL 60160
Jerome Davis, NOXTECH, INC, 1939 Deere Avenue, Irvine, CA 92606
Rich Daykin, 3M Co., 3M Center, Bldg. 223-IS-02, St. Paul, MN 55144-1000
John Dec, Sandia National Laboratory, P.O. Box 969, MS 9053, Livermore, CA 94551-0969
S. Paul Dev, D-Star Engineering, 4 Armstrong Road, Shelton, CT 06484
Robert Dibble, Dept. of Mech. Engrg. 6159 Etcheverry Hall, University of California, Berkeley, Berkeley, CA 94720
Daniel W. Dickey, Southwest Research Institute, P.O. Drawer 28510, 6220 Culebra Road, San Antonio, TX 78228
James P. Dunn, Center for Technology Commercialization, Inc., 1400 Computer Drive, Westborough, MA 01581
Rebecca R. Dyer, EE-33, Department of Energy, Washington, DC 20585
James J. Eberhardt, EE-33, Department of Energy, Washington, DC 20585
Brad Edgar, Thermatrix, Inc., 101 Metro Drive, San Jose, CA 95110
Norbert Elsner, HI-Z Technology, Inc., 7606 Miramar Road Drive, San Diego, CA 92126
John W. Fairbanks, EE-33, Department of Energy, Washington, DC 20585
E. Robert Fanick, Southwest Research Institute, 6220 Culebra, San Antonio, TX 78228-0510
Galen B. Fisher, Physics & Physical Chemistry Dept., GM R&D Center, MC #480-106-185, Warren, MI 48090-9055

Ralph D. Fleming, EFE Consulting Services, 17508 Clinton Drive, Accoceek, MD 20607-3404
Michael A. Flinn, Bldg. L, P.O. Box 1875, Caterpillar Inc., Peoria, IL 61656-1875
Nicholas E. Gallopoulos, General Motors R&D Center, Mail Code 480-106-2502, Warren, MI 48090-9055
John Garbak, OTT/EE-322, U.S. Department of Energy, Washington, DC 20585
Kresimir Gebert, BKM, Inc., 5141 Santa Fe Street, San Diego, CA 92109
Alan W. Gertler, Desert Research Institute, P.O. Box 60220, Reno, NV 89506
Jaal Ghandhi, University of Wisconsin, 1500 West Engineering Drive, Madison, WI 53706
Amarjit "Victor"Ghuman, Cummins Engine Co., MC 50160, 1900 McKinley Avenue, Columbus, IN 47201
Christina Gikakis, Energetics, Inc., 7164 Gateway Drive, Columbia, MD 21046
J.P. Gore, 1288 M.E. Building, Purdue University, West Lafayette, IN 47907
Madan R. Goyal, Advanced Products, Deere Power Systems Group, P.O. Box 8000, Waterloo, IA 50704-8000
Dr. Ronald L. Graves, Auto Propulsion, Box 2009, MS 8087, Oak Ridge National Laboratory, Oak Ridge, TN 37831
Daniel S. Greenbaum, Health Effects Institute, 955 Massachusetts Avenue, Cambridge, MA 02139,
E. W. Gregory, II, 9404 Park Hunt Court, Springfield, VA 22153-1351
Gary W. Grimes, Newport Associates, 224 Via Eboli, Newport Beach, CA 92663
John B. Grutzner, Dept. Of Chemistry, Purdue University, West Lafayette, IN 47907-1393
Prof. Martin Gundersen, Dept. of EE & Physics, Univ.of Southern California., Los Angeles, CA 90089-0484
Michael Gurevich, EE33, Department of Energy, Washington, DC 20585
Dr. Nabil S. Hakim, R&D, Detroit Diesel Corporation, 13400 Outer Drive, West, Detroit, MI 48239-4001
Jack Hale, Department of Energy EE30, 1000 Independence Avenue, Washington, DC, 20585
Ed Halimi, Turbodyne Systems, Inc., 6155 Carpinteria Avenue, Carpinteria, CA 93013
Stephen Hall, AEA Technology plc, F7, 129,Culham Laboratory, Abingdon, Oxfordshire, UK, OX14 3DB
Josh Hanna, Corning Incorporated, 30 HP-CB-03-02, Corning, NY 14031
Norman Helgeson, Naval Facilities Engineering Service Center, 1100 23rd Avenue, Port Hueneme, CA 93043
Mark Hemingway, MS-485-220-010, Delphi Automotive Systems, 1300 North Dort Highway, Flint, MI 48556
Professor Richard Herz, Chemical Engrg., MC 0310, Univ. of California-San Diego, San Diego, CA 92093-0310
John Hoard, Scientific Research Laboratory, Ford Motor Co., Mail Drop 3083, P.O. Box 2053, Dearborn, MI 48121
Mark Hsaio, Lawrence Livermore National Laboratory, P.O. Box 808 L-369, Livermore, CA 94550
Gary L. Hunter, Cummins Engine Co.,Mail Code 50180, P.O. Box 3005, Columbus, IN 47202-3005
Julian A. Imes, Jr., Exhaust Engineering, Donaldson Company Inc., P.O. Box 1299, Minneapolis, MN 55440
Scott Jensen, Energy Conversions, 6411 Pacific Highway East, Tacoma, WA 98424
Bill Johnson, BKM, Inc., 5141 Santa Fe Street, San Diego, CA 92109
D. Ray Johnson, Oak Ridge National Laboratory, P.O. Box 2008, Oak Ridge, TN 37831-6066
Professor John H. Johnson, Michigan Technological University, Dept. ME-EM, Houghton, MI 49931
Dr. Ashok V. Joshi, CERAMATEC, 2425 South 900 West, Salt Lake City, UT 84109
Al Jung, Texaco Inc., P.O. Box 509, Beacon, NY 12533
Roy Kamo, Adiabatics, Inc., 3385 Commerce Drive, Columbus, IN 47201
Dr. James Kelly, Canimet Energy Technology Center, 1 Haanel Drive, Nepean, Ontario/Canada KIA IMI
Karl Kharas, ASEC Manufacturing, P.O. Box 580970, Tulsa, OK 74158-0970
Richard Korzekwa, Los Alamos National Laboratory, P.O. Box 1663, MS-E525, Los Alamos, NM 87545
Jack Kracklauer, Econalytic Systems, Inc., 3450 Penrose Place, Suite 160, Boulder, CO 80301-1800
Harold H. Kung, Department of Chemical Engineering, Northwestern University, IL 60208-3120
David Lafyatis, Johnson Matthey, 436 Devon Park Drive, Wayne, PA 19087
Professor Ming-Chia Lai, Mech. Engrg. Dept., Wayne State University, 65050 Anthony Wayne, Detroit, MI 48202
L. K. Len, F.M. Technologies, Inc., 10529-B Braddock Road, Fairfax, VA 22032
Kenneth Levin, Seaworthy Systems,, 50 Vashell Way, Suite 201, Orinda, CA 94563
S.C. Li, Dept. of Appl.Mech. and Engrg. Sciences, University of California-San Diego, MC 0411, La Jolla, CA 92093
Dr. C. Y. (Eric) Liang, Caterpillar Inc., P.O. Box 610, Mossville, IL 61552-0610
Jan-Roger Linna, Arthur D. Little, Inc., Acorn Park MA 02140-2390
Chung Liu, South Coast Air Quality Management District, 21865 E. Copley Drive, Diamond Bar, CA 91765
Robert P. Lucht, University of Illinois, Dept. Of Mech and Ind Engr., 1206 W. Green St., Urbana, IL 61821
Wayne Lundy, U. S. Coast Guard, 2100 2nd Street, SW, Washington, DC 20593-0001
Frederick M. Mako, F.M. Technologies, Inc., 10529-B Braddock Road, Fairfax, VA 22032
Hector Maldonado, Air Resources Board, P.O. Box 2815, Sacramento, CA 95812
Hermann Mannshatz, Corning Inc., HP-CB -031W, Corning, NY 14841
Jason Mark, Union of Concerned Scientists, 2397 Shattuck Avenue, Suite 203, Berkeley, CA 94704
Christopher L. Marshall, Argonne National Laboratory, 9700 South Cass Avenue, Argonne, IL 60439-4831

Dr. Peter Martin, Procyon Power Systems, 1889 First St., Bldg 20, Suite 138, Alameda, CA 94501
Dr. Richard Martin, 101 Metro Drive, San Jose, CA 95110
Dr. J. L. Mauderly, DVM, Lovelace Respiratory Research Institute, P.O. Box 5890, Albuquerque, NM 87185
Donald J. McAllister, Jr., Quantum Energy Tech., Inc. 238 Main Street - Suite 201 Cambridge, MA 02142
Dr. Ralph McGill, Oak Ridge National Laboratory, P.O. Box 2009 MS 8087, Oak Ridge, TN 37831
Robert O. McLean, Corning, Inc., HP-CB-031W, Corning, NY 14841
Dr. Bernard T. Merritt, Lawrence Livermore National Laboratory, 7000 East Avenue, Livermore, CA 94551-9900
Robert K. Miller, Corning Inc., Corning, NY 14831
Marla Mueller, Air Resources Board, P.O. Box 2815, Sacramento, CA 95812
John M. Mulloy, Cummins Engine Company, 1405 Locust Drive, Columbus, IN 47203
Michael J. Murphy, Battelle, 505 King avenue, Columbus, OH 43201
Martin J. Murtagh, Corning Incorporated, SPDVO2-1, Corning, NY 14831
Mike A. Nazemi, South Coast Air Quality Management District, 21865 E. Copley Drive, Diamond Bar, CA, 91765
Sidney G. Nelson, Sorbent Technologies Corp., 1664 East Highland Road, Twinsburg, OH 44087
Henry NG, Argonne National Laboratory, 9700 S. Cass Ave., 362 Room C229, Argonne, IL 60439
Robert L. Nguyen, California Air Resources Board, P.O. Box 2815, 2014 Capitol Avenue, Sacramento, CA 95812
C. William Nirmaier, Johnson Mathey, 460 East Swedesford Road, Wayne, PA 19087
Paul Norton, National Renewable Energy Laboratory, 1617Cole Blvd., Mail Stop 1633, Golden, CO 80401
Dr. Thomas Orlando, Mail Stop K2-14, Pacific Northwest Laboratory, Battelle Boulevard, Richland, WA 99352
David A. Okrent, Rupprecht & Patashnick, Co., Inc., Albany, NY 12203
Michael Osborne, Naval Sea Systems Command, Code 03X32, 145 South Barton St., Arlington, VA 22204
Dr. Dorriah L. Page, Consultant, 115 Conte Barrioso, Camarillo, CA 93110
Dr. Vishwesh Palekar, NOXTECH, Inc, 1939 Deer Ave., Irvine, CA 92606
Dr. James W. Patten, Cummins Engine Company, MC 50183, 1900 McKinley Avenue, Columbus, IN 47201
Shirley Pearson, Dames & Moore, 6 Hutton Centre Drive, Suite 700, Santa Ana, CA 92707
Jack Peckham, Fuels Group, Hart Publications, Inc., 6011 Executive Boulevard - Suite 200, Rockville, MD 20852
Dr. Bernie Penetrante, Lawrence Livermore National Laboratory, 7000 East Avenue, Livermore, CA 94551-9900
William E. Pepelco, U.S. EPA, 401 M Street, SW, Washington, DC 20460
Dr. Joseph M. Perez, 1762 Princeton Drive, State College, PA 16803
Gary Pope, Praxair, P.O. Box 57, Huntington Beach, CA 92648
Madhu Ramavajjala, NOxTECH, Inc., 1939 Deere Ave., Irvine, CA 92714
Dr. David Raybone, AEA Technology plc, Culham Laboratory, Abingdon, Oxfordshire, UK OX14 3DB
Rich Remillara, Acurex Environmental, PO Box 7044, Mountain View, CA 94039
Dr. Louis Rozocha, MS E525, Los Alamos National Laboratory, P.O. Box 1663, Los Alamos, NM 87545
Jules Routbort, Energy Technology Division, Bldg. 212, Argonne National Laboratory, Argonne IL 60439-4838
Dr. Gabriel Roy, Office of Naval Research, 800 North Quincy Street, Arlington, VA 22217-5660
Professor Robert Sawyer, PO Box 524, Berkeley, CA 94720-0424
Allen Schaeffer, Environmental Affairs, American Trucking Associations, 2200 Mill Road, Alexandria, VA 22314
Curt B. Scheppmann, Engelhard Corporation, 3902 Worchester Drive, Egan, MM 55123
R. Seiser, Department of Appl. Mech. and Engrg. Sciences, University of California, San Diego, La Jolla CA 92093
Kal Seshadri,, Dept. of Appl. Mech. and Engrg. Sciences, University of California, San Diego, La Jolla CA 92093
Dr. S. M. Shahed, Turbocharging Systems Allied Signal, 3201 West Lomita Boulevard, Torrance, CA 90505
John Shen, Dept. Of Energy, FE-24, Germantown, MD 20874-1290
James E. Sibley, Technical Center, Bldg. L, P.O. Box 1875,, Caterpillar Inc., Peoria, IL 61656-1875
Rich Silberglitt, F.M. Technologies, Inc., 10529-B Braddock Road, Fairfax, VA 22032
Ralph Slone,.NOXTECH, Inc., 1939 Deere Ave., Irvine, CA 92713
Frank Stodolsky, Argonne National Laboratory, 955 l'Enfant Plaza North, SW, Suite 6000, Washington, DC 20024
Alan Stout, U.S. Environmental Protection Agency, 2565 Plymouth Road, Ann Arbor, MI 48105
Bruce Sudduth, NOXTECH, Inc., 1939 Deere Ave., Irvine, CA 92714
Cindy Sullivan, South Coast Air Quality Management District, 21865 E. Copley Drive, Diamond Bar, CA 91765
George M. Sverdrup, Battelle, 505 King Avenue, Columbus, OH 43201-2693
Theodore J. Tarabulski, Clean Diesel Technologies Inc., 300 Atlantic Street, Suite 702, Stamford, CT 06901
Dr. David Timoney, Arthur D. Little, Inc., Acorn Park, Cambridge, MA 02140-2390
Ken Trbovich, JJMA, PO Box 18267, Pittsburgh, PA 15236-8435
Arjun Tuteja, GM Powertrain, Romulus Engineering Center, 37350 Ecorse Road, Romulus, MI 48174
J. T. Vachon, New Technologies Department, Caterpillar Inc., P.O. Box 1875, Peoria, IL 61656-1875
James M. Valentine, Clean Diesel Technologies, Inc., 300 Atlantic Street, Suite 702, Stamford, CT 06901

Michael VanDerwerken, GE Corporate R&D, Bldg Kw Rm C260, One Research Circle, Niskayuna, NY, 12309
Keith Vertin, National Renewable Energy Laboratory, 1617 Cole Boulevard MS 1633, Golden, CO 80401
Dr. Kenneth E. Voss, Engelhard Corporation, 101 Wood Avenue, Iselin, NJ 08830-0770
Bruce W. Wadman, Diesel Progress, P.O. Box 688, Solana Beach, CA 92075-0688
C.Z. Wan, Engelhard Corp., R&D, 101 Wood Avenue South, Iselin, NJ 08830
Jim Warren, Composite Innovations Corporation, 24300 Aetna Street, Woodland Hills, CA 91367
Lewis Watts, Texaco Inc., P.O. Box 4459, Houston, TX 77210
Brian West, Oak Ridge National Laboratory, PO Box 2009, Oak Ridge, TN 37831
John Whealton, Energy Technology/Oak Ridge National Laboratory, 9108/MS 8088, Oak Ridge, TN 37831-8088
Shawn Whitacre, Cummins Engine Company, 1900 McKinley Ave., Columbus, IN 47201
Robert E. Whiteley, Engelhard Corporation, 101 Wood Avenue, P.O. Box 770, Iselin, NJ 08830-0770
Jerry Wiens, California Energy Commission, 1516 9th Street - MS-41, Sacramento, CA 95814
Stephanie Williams, California Trucking Association, 1251 Beacon Boulevard, West Sacramento, CA 25691
Harold J. Wimette, Chrysler, 5814 Brace, Detroit, MI 48228
Hassan Windawl, Johnson Matthey, 3 Colonial Way, Malvern, PA 19355
Rich Winsor, John Deere Product Engineering Center, Deere & Company, P.O. Box 8000, Waterloo, IA 50701-9766
Dr. Victor W. Wong, Bldg. 31-155, Mass. Institute of Technology, 77 Massachusetts Avenue, Cambridge, MA 02139
Benjamin Yen, Cummins Engine Co., 1900 McKinley Avenue, M.C. 50160, Columbus, IN 50160
Tom Yonushonis, Cummins Engine Company 1900 McKinley Ave., MC 50183, Columbus, IN 47201
Gary Yowell, California Energy Commission, 1516 9th Street, Sacramento, CA 95814
Yvonne Zaslawska, AEA Technology plc, F7, 108, Culham Laboratory, Abingdon, Oxfordshire, UK, 0X14 3DB
Ziemin Zhu, Detroit Diesel Corporation, 13400 Outer Drive, West, Detroit, MI 48239-4001